AFIT/GSO/ENG/99M-02

ANALYSIS OF RADIO FREQUENCY INTERFERENCE EFFECTS ON A MODERN COARSE ACQUISITION CODE GLOBAL POSITIONING SYSTEM (GPS) RECEIVER

THESIS

Kenneth D. Johnston
Major, Canadian Forces

AFIT/GSO/ENG/99M-02

VOLUME 2

Approved for public release; distribution unlimited

REPORT DOCUMENTATION PAGE

Form Approved
OMB No. 0704-0188

1. AGENCY USE ONLY *(Leave blank)*

2. REPORT DATE
March 1999

3. REPORT TYPE AND DATES COVERED
Master's Thesis

4. TITLE AND SUBTITLE
ANALYSIS OF RADIO FREQUENCY INTERFERENCE EFFECTS ON A MODERN COARSE ACQUISITION (C/A) CODE GLOBAL POSITIONING SYSTEM (GPS) RECEIVER

5. FUNDING NUMBERS

6. AUTHOR(S)
Kenneth D. Johnston
Major, Canadian Forces

7. PERFORMING ORGANIZATION NAME(S) AND ADDRESS(ES)

Air Force Institute of Technology, WPAFB OH 45433-6583

8. PERFORMING ORGANIZATION REPORT NUMBER

AFIT/GSO/ENG/99M-02

9. SPONSORING/MONITORING AGENCY NAME(S) AND ADDRESS(ES)
Major S. Delory
Canadian Forces School of Aerospace Studies
Canadian Forces Base Winnipeg
Westwin, Manitoba, Canada

10. SPONSORING/MONITORING AGENCY REPORT NUMBER

11. SUPPLEMENTARY NOTES

12a. DISTRIBUTION AVAILABILITY STATEMENT

Approved for public release, Distribution Unlimited

12b. DISTRIBUTION CODE

13. ABSTRACT *(Maximum 200 words)*
The purpose of this thesis was to investigate the performance of a commercial-off-the-shelf twelve channel Standard Positioning Service (SPS) based Global Positioning System (GPS) receiver using an eight state Kalman filter in a hostile radio frequency (RF) environment and to develop instructional tools for teaching RF interference on GPS receivers. The two types of jamming signals generated included Continuous Wave (CW) and Swept CW. Actual GPS and jamming signals were used in the research.
The signals received from GPS satellites exhibit a Doppler shift which vary between approximately ± six Kilohertz. The Doppler shift frequency can be reasonably predicted for a given time of day, for a given satellite, and for a known receiver location using GPS satellite almanac or ephemeris data. Additionally, the Pseudorandom Noise (PRN) Coarse Acquisition (C/A) code for each satellite exhibits specific maximum amplitude spectral lines. By tailoring the jamming signals to match with the Doppler shifted satellite frequencies and offsetting the jamming to a maximum spectral line, it was shown that individual Navstar XR5-M receiver channels for specific satellites could be selectively jammed/spoofed.
Swept CW jamming resulted in pulling the XR5-M receiver tracking channels off frequency by up to 20 Kilohertz but resulted in a maximum position error of only 220 meters. The CW jamming of at least one of the XR5-M receiver channels resulted in position errors in the receiver in excess of 12 kilometers.

14. SUBJECT TERMS

GPS, Radio Frequency Interference, Jamming, C/A Code Receiver

15. NUMBER OF PAGES
415

16. PRICE CODE

17. SECURITY CLASSIFICATION OF REPORT	18. SECURITY CLASSIFICATION OF THIS PAGE	19. SECURITY CLASSIFICATION OF ABSTRACT	20. LIMITATION OF ABSTRACT
UNCLASSIFIED	UNCLASSIFIED	UNCLASSIFIED	UL

AFIT/GSO/ENG/99M-02

ANALYSIS OF RADIO FREQUENCY INTERFERENCE EFFECTS ON A MODERN COARSE ACQUISITION (C/A) CODE GLOBAL POSITIONING SYSTEM (GPS) RECEIVER

VOLUME 2

THESIS

Presented to the Faculty of the Graduate School of Engineering
of the Air Force Institute of Technology
Air University
In Partial Fulfillment of the
Requirements for the Degree of
Master of Science in Space Operations

Kenneth D. Johnston, B.Sc. (Applied)
Major, Canadian Forces

March 1999

Approved for public release; distribution unlimited

Table of Contents

VOLUME 2

List of Figures

Figure		Page

APPENDIX A - 1988 DOPPLER SURVEY OF AFIT BUILDING 640 ROOFTOP

DEFENSE MAPPING AGENCY
HYDROGRAPHIC/TOPOGRAPHIC CENTER
TERRESTRIAL COMPUTATIONS BRANCH
WASHINGTON, DC 20315-0030

PROJECT: ANTENNA SURVEY

LOCATION: WRIGHT-PATTERSON AFB, OHIO

DATUMS:
1. WORLD GEODETIC SYSTEM OF 1972 (WGS 72)
2. WORLD GEODETIC SYSTEM OF 1984 (WGS 84)
3. ELEVATION BASED ON WGS 84 DERIVED ELLIPSOID HEIGHT AND GEOID HEIGHT COMPUTED GRAVIMETRICALLY USING WGS 84 POTENTIAL COEFFICIENTS (H=h-N).

SURVEY DATE: JULY 1988.

1. GEODETIC POSITIONS, ELLIPSOID HEIGHTS AND DOPPLER DERIVED ELEVATIONS.

STATION	DATUM	NORTH LATITUDE DEG MIN SEC	WEST LONGITUDE DEG MIN SEC	ELLIPSOID HEIGHT METERS	ELEVATION* METERS
DOPP 32058	WGS 72	39 46 55.306	084 04 58.472	269.41	
	WGS 84	39 46 55.424	084 04 57.918	271.77	306.27
ALGN MARK	WGS 84	39 46 55.128	084 04 59.648	272.42	306.92
GPS ANT. (BOLT)	WGS 84	39 46 55.369	084 04 59.422	272.54	307.04
GPS ANT. (TOP OF BASE OF MOUNT)					311.84
LOADING DOCK					293.67

*ALTHOUGH ELEVATIONS ARE GIVEN TO 0.01 METERS, THEY ARE DOPPLER-DERIVED AND HAVE AN ACCURACY OF +/- 5 METERS DUE TO THE UNCERTAINTIES OF THE GEOID HEIGHT.

SUMMARY OF SATELLITE-OBSERVED STATION

STATION NAME/LOCAL NUMBER	LOCATION	DOPPLER NO.
WRIGHT-PATTERSON	DAYTON, OHIO	32058

STAMPING ON MARK: DOPP STA 32058 1988 GSGS

AGENCY (CAST IN MARK): DMA

TYPE OF STATION MARK: BRONZE DISK

DOPPLER OBSERVATIONS

EQUIPMENT/SERIAL NO.	HEIGHT OF TRACKING EQUIPMENT REFERENCE POINT ABOVE STATION MARK:	TRACKING EQUIPMENT REFERENCE POINT
MAG 1502-DS-688	2.412m	RED BAND ON ANTENNA
OBSERVED BY (AGENCY)	**SATELLITE(S) OBSERVED**	**PERIOD OF OCCUPATION**
DMAHTC/GSGS	30130 30200, 30240, 30480, 30500	07 - 10 JULY 1988

SATELLITE-DERIVED COORDINATES

PASSES ACCEPTED	DEGREES OF FREEDOM	RESIDUAL RMS	STATION SET	GRAVITY MODEL	ELLIPSOID	MINIMUM ELEV. ANGLE
48	1140	0.09m	WGS 84	WGS 84	WGS 84	5 DEG.

(Satellite-derived coordinates referred to station mark)

φ N 39 46 55.424	λ E 275 55 02.082	h 271.77m	ACCURACY 1.5 METERS IN EACH AXIS (90% LINEAR ERROR)
X 506 020.04m	Y -4 882 282.48m	Z 4 059 593.06m	

(Satellite-derived coordinates of station mark transformed to ~~local datum~~ WGS 72)

φ N 39 46 55.306	λ E 275 55 01.528	h 269.41m	DATUM WGS 72
X 506 006.82m	Y -4 882 282.76m	Z 4 059 587.68m	ELLIPSOID WGS 72
ΔX	ΔY	ΔZ	DATE OF TRANSFORMATION

GROUND SURVEY COORDINATES OF STATION MARK

φ	λ	DATUM (HORIZONTAL)	ELLIPSOID
DATE OF ADJUSTMENT / ORDER	SURVEY BY (AGENCY)	DATE	LOCATION OF SURVEY DATA
ELEVATION (H) H=h-N 306.3m	DATUM (VERTICAL)	GEOID HEIGHT (N) (WGS 84) -34.5m ± 5m(1σ)	ELLIPSOID HEIGHT (h)
ORDER (ELEV.)	ESTABLISHED BY (AGENCY) / DATE	SOURCE OF (N) COMPUTED GRAVIMETRICALLY USING WGS 84 POTENTIAL COEFFICIENTS	

CONNECTION TO LOCAL CONTROL

FROM	TO	( ) AZ FROM NORTH	DISTANCE
DOPP 32058	GPS ANTENNA (BOLT)	267 18 01.3	35.839m
DOPP 32058	ALGN MARK	257 30 53.4	42.159m

REMARKS

OTHER RELATED DATA FOR THIS STATION

DATA	AVAIL.	LOCATION/REMARKS
STATION OCCUPATION REPORT	X	DMAHTC
GEODETIC INFORMATION REPORT		
STATION DESCRIPTION	X	DMAHTC
SURVEY DIAGRAM		
STATION SITE SKETCH	X	DMAHTC
PHOTOIDENTIFICATION		
ASTRONOMIC COORDINATES		
STATION PHOTOS	X	DMAHTC

PREPARED BY/DATE	CHECKED BY/DATE	REVISED BY/DATE	CHECKED BY/DATE
DMAHTC/RBK/OCT 88	DMAHTC/BHS/OCT 88		

DMA FORM 8290-1-R
SEP 76

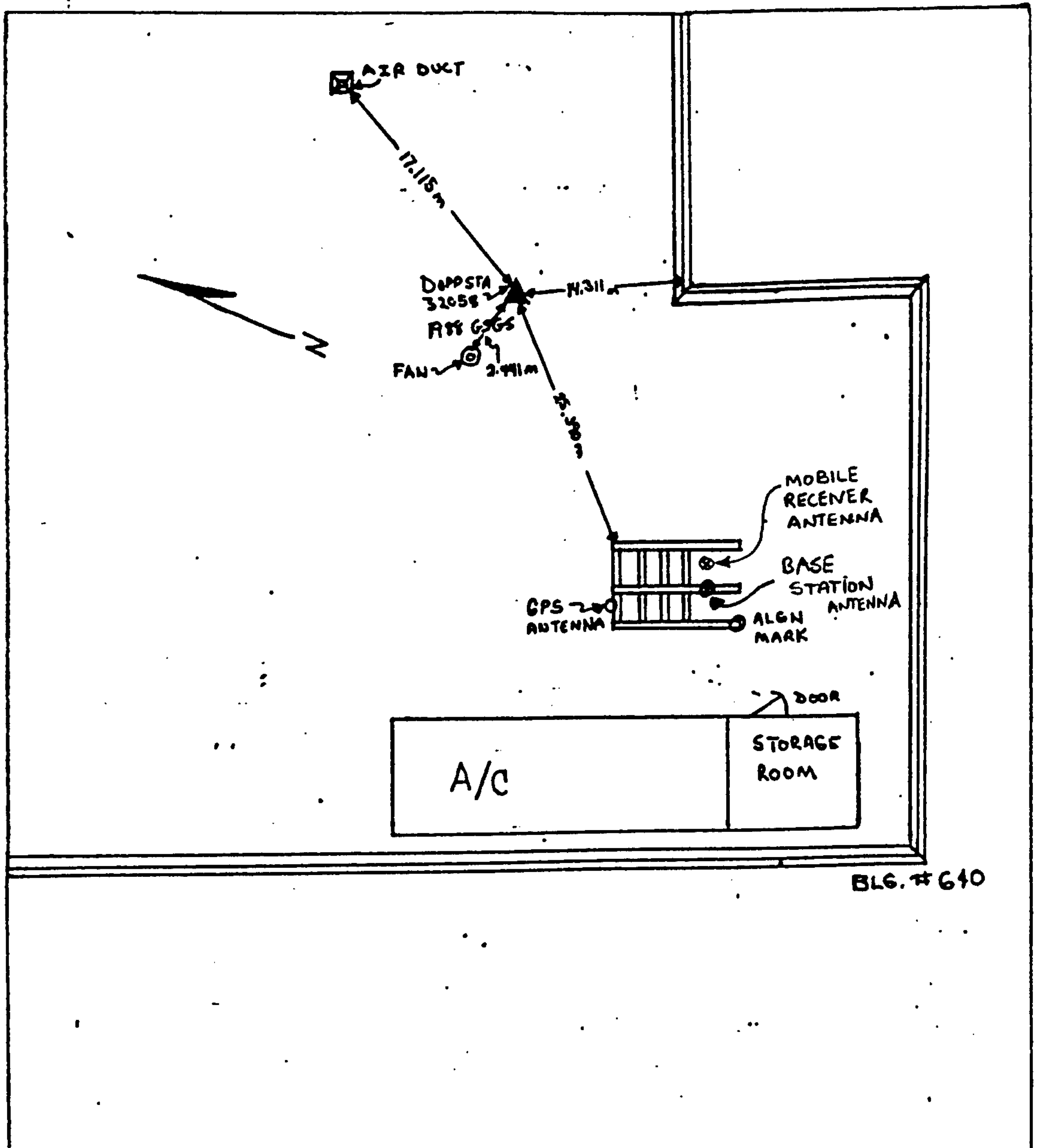

LEGEND

▲ - TRACKING STATION ■ - PHOTO POINT △ - GEODETIC STATION, RM'S & BM'

⊙ - SURVEY STATION —//— MEASURED DISTANCE

PREPARED BY	DATE	CHECKED BY	DATE
WOOTEN	9 July 88	CRAWFORD	18 July 88

GSGS 1-85 ATTACHMENT NUMBER 3

APPENDIX B -LATITUDE/LONGITUDE/ALTITUDE TO ECEF TRANSFORMATIONS

The Earth Center Earth Fixed (ECEF) coordinate system is commonly used in GPS calculations. In the ECEF system, the positive 'x' axis is oriented in the direction of zero degrees longitude, the positive 'y' axis points in the direction of 90 degrees East longitude. The x-y plane is coincident with the Earth's equatorial plane and rotates with the earth. The positive 'z' axis is normal to the x-y plane. For a detailed explanation of reference coordinate systems the reader is referred to [KAP96].

Satellite ephemeris data is provided in the Earth-Centered Inertial (ECI) coordinate system. These parameters are converted through transformation matrices to the ECEF coordinate system. Transformation from the ECEF system to latitude, longitude and altitude normally completes the process for the end user. For the purpose of this thesis, the ECEF position of the Mobile XR5-M receiver was compared to the ECEF position of the XR5-M Base Station.

One of the first challenges was to determine a reasonably accurate position for the Base Station. Since the primary measurement of interest was the relative difference between the Base Station antenna and the Mobile antenna, the Base Station was used in a relative/differential GPS configuration. By using relative/differential GPS, most of the position error attributed to Selective Availability (SA), ionosphere/troposphere, satellite perturbations, ephemeris prediction and satellite clock bias were removed. The major sources of position error between the Base Station and the Mobile receiver was a result of multipath, receiver measurement noise and RF interference. This setup was used to allow for a reasonable method to measure the effects of jamming. The Mobile receiver antenna was physically located 4.7 meters approximately east of the Base Station antenna. Position ECEF coordinates of the Mobile receiver antenna were corrected in MATLAB® software during post-processing back to the position of the Base Station antenna so that the antennas would be at the "same" position. Position error was determined by taking the difference between the corrected Mobile antenna location as measured by the Mobile receiver and the "ALGN MARK" position of the previous 1988 survey (Appendix A). No adjustment was made to correct the actual coordinates of the Base Station to the surveyed location of the "ALGN MARK" because the relative position between the two antenna was the measurement of interest.

The rooftop of Building 640 was surveyed by the Defense Mapping Agency in 1988; details of which are provided in Appendix A. Doppler Station 32058 was the main survey location and two additional surveyed sights were provided, "ALGN MARK" and "GPS ANTENNA (BOLT)." For the minimum cost and ease of antenna installation, the Base Station antenna was located approximately 8.2 meters east of the previous surveyed "ALGN MARK" position from the 1988 survey. The survey reported an accuracy of 1.5 meters in each axis (90 % linear error). Elevation was given as 306.92 meters but because the heights were Doppler derived the elevation measurement had an accuracy of ±5 meters.

The values for the "ALGN MARK" position were used as coordinates for the Base Station. The geodetic coordinates for "ALGN MARK" taken from the 1988 survey were determined to have the following properties:

Lat = 39 46 55.128 N
Long= 084 04 59.648 W
Ellipsoid Height = 272.42 meters, Altitude 306.92 meters.

On the XR5-M receiver, input of the above parameters on the computer display initialization page resulted in the following:

Lat 39 46 55.128 N was displayed as 39 46.9188 N
Long 084 04 59.648 W was displayed as 084 04.9941 W
Initial Altitude : 306.92 was displayed as 306.9

The XR5-M variable "npposn" provides the receiver's best estimate of position in ECEF coordinates. When the unit is configured as a Base Station the value input for latitude, longitude, and altitude is fixed to the values used in the initialization menu for the Base Station location. The coordinates in ECEF (meters) for "ALGN MARK" as converted by the XR5-M from the above input were (in meters):

X = 505979.8731834281
Y = -4882293.899751916
Z = 4059587.157385162

The 1988 survey did not provide ECEF coordinates for the "ALGN MARK" position. As a check on the XR5-M internal calculations, the coordinates for the "ALGN MARK" position from the 1988 survey were converted to ECEF using MATLAB® code and a more accurate set of transformation equations from [KAP96] (as compared to those presented in AFIT course EENG 533). The resulting ECEF coordinates (meters) for the "ALGN MARK" were as follows:

X = 505979.7386127784
Y = -4882293.041839992
Z = 4059586.447032988

The differences between the surveyed "ALGN MARK" ECEF coordinates as calculated by the XR5-M receiver compared to using the equations provided by Kaplan using MATLAB® to calculate ECEF position (in meters) were as follows:

X = -0.1345706497086212
Y = 0.8579119239002466
Z = -0.7103521740064025

A similar comparison was conducted using the transformation to ECEF coordinates provided in the 1988 survey for the "Doppler Station 32058." Values for ECEF coordinates for the Doppler Station provided in the survey, the XR5-M calculated ECEF coordinates, and the MATLAB® calculated ECEF coordinates using Kaplan's equations are summarized in Table B.1.

Latitude Longitude Ellipsoid Height for Doppler Station	ECEF Coordinates from 1988 Survey (x,y,z) in meters	ECEF transformation by XR5 (x,y,z) in meters	ECEF transformation using Matlab and Kaplan's equations (x,y,z) in meters
N 39 46 55.424	506020.04	506020.1624427695	506020.0340076035
E 275 55 02.082	-4882282.48	-4882283.308111367	-4882282.490429529
271.77	4059593.06	4059593.728202703	4059593.047042757

Table B.1 - Conversion of Latitude/Longitude/Altitude to ECEF Coordinates

Differences between the surveyed "Doppler Station 32058" ECEF position, the XR5-M calculated ECEF position and the MATLAB®/Kaplan calculated ECEF position (in meters) is provided in Table B.2. Based on the calculations in Table B.2 for ECEF position differences, the method of using MATLAB® and Kaplan's equations were more accurate than the XR5-M receiver calculations (assuming that the

Defense Mapping Agency calculations for ECEF coordinates were still accurate). Based on the results in Table B.2 the conversion process within the XR5-M receiver contributed to 3D position error on the order of 1.07 meters. The conversion process using MATLAB® code and Kaplan's equations contributed to 3D position error on the order of approximately 0.0177 meters.

Difference between ECEF Coordinates from 1988 Survey and XR5-M transformation (x,y,z) in meters	**Difference between ECEF Coordinates from 1988 Survey and Kaplan/MATLAB® transformation (x,y,z) in meters**
-1.224427695269696e-01	**-5.992396443616599e-03**
8.281113663688302e-01	**-1.042952854186296e-02**
-6.682027028873563e-01	**-1.295724278315902e-02**

Table B.2 Differences in Conversion to ECEF coordinates for Doppler Station

The position calculated by the XR5-M for the "ALGN MARK" was considered acceptable and was used with the knowledge that it could introduce calculation errors of one meter magnitude into final results data.

Any future research work using the Base Station receiver antenna location to measure absolute position should be aware of the 8.2 meter difference between the "ALGN MARK" coordinate from the 1988 survey and the actual Base Station antenna location.

APPENDIX C - XR5-M SYMBOL VARIABLES

A symbol file was generated using the Data Monitor program provided with the XR5-M software. Prior to using the symbol file <kdsymbl3.sy> it was necessary to load the main symbol file name <m1237.sy>. For further details the reader should refer to the XR5-M Control and Display Unit Software Manual, the XR5-M Power Users Data Monitor Toolkit Manual, and the data dictionary text file <datadic2.txt > provided with the XR5-M receiver software [NAV93, NAV96]. The variables in this Appendix were recorded during Test 12; previous tests consisted of a sub-set of these variables. The data were captured to a text file that was then opened in a text editor and stripped of the header and footer. The amended text file was then loaded into MATLAB® software for detailed analysis.

Variable ID		Col	Col # in Matrix	Description of Variable
1:	isid	12	1-12	SV(PRN) ID for raw measurements taken
2:	mestim	1	13	Local time of week (sec) when last 4 Hz measurements taken
3:	idopp	12	14-25	Measured satellite Doppler frequency (Hz)
4:	icno	12	26-37	Carrier to noise ratio (C/No) (dB-Hz)
5:	npclkb	1	38	Receiver clock bias (sec)
6:	npclkd	1	39	Receiver clock drift (seconds/sec)
7:	nplat	1	40	Current position latitude (radians)
8:	nplon	1	41	Current position longitude (radians)
9:	nkualt	1	42	User altitude (m)
10:	npposn	3	43-45	Receiver best estimate of position in ECEF coord frame (m)
11:	npvelc	3	46-48	Receiver best estimate of velocity in ECEF coord frame (m/sec)
12:	gdop	1	49	Geometric dilution of precision
13:	sltelv	12	50-61	Satellite elevation
14:	sltazi	12	62-73	Satellite azimuth
15:	satlist	5	74-78	Satellites used to calculate last position and velocity data
16:	sltsta	12	79-90	Channel status
17:	gpsfix	1	91	Fixing status of receiver (also see dfsoln)
18:	iqll	12	92-103	Measurement quality of pseudorange
19:	npugsp	1	104	User ground speed (m/s)
20:	npuvsp	1	105	User vertical speed (m/s)
21:	nknteh	1	106	Estimated horizontal accuracy (m)
22:	nkntev	1	107	Estimated vertical accuracy (m)
23:	nkntep	1	108	Estimated position accuracy (m)
24:	nkprrs	12	109-120	Kalman Filter pseudorange residuals (m)
25:	nkdprs	12	121-132	Kalman Filter delta range residuals (m/s)
26:	dfsoln	1	133	Flags navigation solution as differentially derived
27:	carlock	12	134-145	Number of measurements without cycle slips (4 Hz)

APPENDIX D - XR5-M TECHNICAL INFORMATION

This Appendix describes the basic technical characteristics and configuration of the two XR5-M receivers used in support of this thesis. Further details are provided in the XR5-M Control and Display Unit Software Manual, and the XR5-M Data Monitor Toolkit Manual [NAV93, NAV96]. Navstar/Navsymm Systems Limited is a subsidiary of Telecom Solutions Europe Ltd.

The XR5-M is a twelve channel GPS receiver which can be operated in either a standalone or a differential mode. The unit may also be configured as a base station receiver by providing real-time differential correction data to mobile GPS receivers. The receiver may also be configured to record data to a PC for subsequent post-processing.

The Special Committee 104 to the Radio Technical Commission for Maritime (RTCM) Services was established in 1983 to develop the standards for differential GPS corrections [KAL86]. The XR5-M receivers were equipped with version 3.7 software which operate with RTCM Type 1, Type 2, Type 3 and Type 9 Messages. The units are specified to provide differential corrections with position measurements better than 3 meter CEP. The latest upgrade to the software, version 4.9, supports RTCM message Types 20 and 21 and provides sub-meter position measurements.

The Control-Display Unit (CDU) software enables an operator to connect the receiver directly to a PC (using MSDOS version 3.3 or higher) in order to initialize and to control the functions of the GPS receiver. Communication between the PC and the

XR5-M is through either the COM1 or COM2 port. The XR5-M receiver has a comprehensive list of variables that may be accessed using the Data Monitor (DM) program. A master symbol file of all variables <m1237.sy> must first be loaded into the DM program before a subset of variables can be generated. A detailed description of all XR5-M variables is provided in the text file <datadic2.txt> provided with the receiver software. The master symbol file must also be loaded each time the DM program is used in order to execute the customized symbol variable file. The master symbol file is appropriately named for the number of receiver channels (12) and the software version (3.7). The DM program allows an operator to customize the data display, and to generate a subset of variables that may be captured to a data file. Several symbol files were written during the course of the thesis research. The list of variables used for the collection of data in Test 12 is provided in Appendix C and the associated symbol file name was <kdsymbl3.sy>.

During the preliminary testing phase, the first attempt to exit from the DM program back to XR5-M main menu using the command, <$e>, at the end of a data capture run locked up the PC and resulted in the loss of the data file. Subsequently using the command, <$q>, to stop data collection and save the data worked fine with no lockups over the six weeks of testing. This procedure was limited by the fact that it takes the user back to DOS prompt for the XR5-M directory, requiring the user to re-run the XR5-M executable file again to re-enter into the XR5-M main user menu.

One of the two XR5-M receivers was configured as a base station and was used to output differential corrections to the second receiver configured as a mobile system.

Normally, the differential corrections from the XR5-M base station receiver would be transmitted via a Navsymm DR5-96S Radio Modem. The RTCM port is a RS 232 interface connected using a Series 723 12 Pin Plug as shown in Figure D.1.

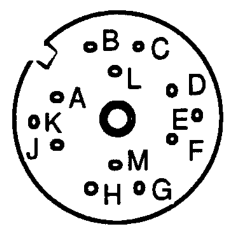

Figure D.1 Series 723 12 Pin Connector

For the purpose of this thesis research, the RTCM ports of each of the receivers were "hot-wired" directly together to enable the transfer of differential corrections from the base station to the mobile receiver. The base station receiver RTCM port Pin B (Radio Control, RC also known as Request to Send, RTS) was wired to the RTCM port Pin D (Clear to Send, CTS3) on the mobile receiver, and the base station receiver RTCM port Pin F (Transmit Data, TXD3) was wired to the RTCM port Pin H (Receive Data, RXD3) on the mobile receiver (see Figure D.1) [NAV96].

Confirmation of differential operation of the mobile receiver was verified by several methods. The receiver reports the method of calculating position fixes as three dimensional (3D), two dimensional (2D), and no valid fix. It also reports whether the position fix is based on non-differential or differential corrected measurements. The fixing status of the receiver is presented on the Receiver Measurement Report screen (keystroke "F3"), ie. three dimensional differential (3D-DIF); the actual differential corrections sent by the base station can be viewed on the View Differential Corrections Report screen (keystroke "F7") and the differential corrections received on the mobile receiver can be viewed using the same keystroke. Finally, the base station antenna position (from Appendix B) was entered as a waypoint into the mobile receiver using the Waypoint Setup Screen (keystroke "w"). The difference between the measured position and the waypoint measured by the mobile receiver was observed on the Waypoint Navigation screen (keystroke "n"). Prior to collection of data, the receiver was verified to be operating with a valid 3D differential position output.

The MSDOS based XR5-M receiver software provides access to a very large set of receiver variables which can be downloaded to an ASCII file and then opened in a text based word processor such as Microsoft™ Word® to strip off header and footer lines before being imported into MATLAB®. All automatic features such as spelling and grammar checking should be disabled to expedite the process of stripping off the header and footer (given that some of the file sizes were in excess of 2000 text pages/or 15 Megabytes). The data files were easily read into MATLAB® for data analysis. Overall, the numerous variables and the data monitor program in the XR5-M receiver make it an excellent receiver for education purposes.

The XR5-M volute antenna has a pre-amplifier with a 50 MHz filter centered on L1. Signals outside the filter bandwidth are reduced by 40 dB [BUT99]. The pre-amp is provided due to the cable length required between the AFIT building rooftop and the navigation laboratory. The volute antenna was designed for the dynamic pitch and roll of a maritime environment. For future testing purposes it may be preferred to use a choke ring antenna in order to reduce multipath effects. A single antenna shared by the two receivers may also reduce the multipath effects by using DGPS since the multipath effects would be common to both receivers.

The XR5-M has two intermediate frequency (IF) stages; the first IF stage is at 295 MHz and has a bandwidth of 20 MHz, the second IF stage is at 24.58 MHz and has a bandwidth of 8 MHz. The receiver uses a pre-correlation A/D and it has a 2 bit quantizer with 3 states (above a positive threshold, below a negative threshold, and in between thresholds). The receiver design does not incorporate a frequency lock loop (FLL) but does employ a phase lock loop (PLL). The minimum levels of C/N_o (plus or minus a few dB-Hz) for receiver operation are 32 dB-Hz for acquisition mode, and 30 dB-Hz for loss of lock [BUT99].

The variable "nkntep" provides the estimated position accuracy (1 sigma) and the variable "nknteh" provides a measure of horizontal position accuracy. A navigation solution is considered valid if:

i. there are at least 3 healthy satellites (for a 2D fix) with valid ephemeris;
ii. the estimated accuracy (1 sigma) is less than 1 nautical mile;
iii. the velocity is less than 515 m/s; and,
iv. the altitude is less than 60,000 feet.

For the installed CDU software version 3.7, GDOP calculations were based on the five satellites used in the navigation solution. The latest software version 4.9 (not installed) calculates an all-in-view solution and the DOPs are based on all satellites used in the solution.

Below are the equipment configuration settings recommended for anyone wishing to conduct similar testing using the XR5-M receivers. From the DOS prompt on the CDU, change directories to: >C:\cd xr5m12, typing <xr5m> will then execute the file <xr5m.exe> and launch the main CDU program.

The first step is to configure the two receivers via the CDU of each PC. Select keystroke "1" to enter the Initialization menu.

The following inputs were used:

Input date (d m y): enter current date ie. 17 12 1998
UTC time (h m s): enter UTC time(either 4 hrs or 5 hrs plus local time for AFIT)
Initial Lat: enter 39 46 55.128 N and it will automatically display it as 39 46.9188 N
Initial Long: enter 084 04 59.648 W and it automatically display it as 084 04.9941 W
Initial Altitude: enter 306.92 and XR5-M will automatically display it as 306.9

The operator should select "Ctrl s" to save the initialization settings to file; This research effort used <kdinit>. The file is automatically saved in the DOS directory >C:\xr5m12\xr5m\data. Any future initializations can be expedited by loading this file, simply type Ctrl l <filename>. The user then needs only to amend the date and time but initial position will remain valid unless antenna location is changed from the test location. Once the parameters are correct, the operator then needs to select "Ctrl x" to execute the settings. The XR5-M will reply with "Message Acknowledged" provided all the initialization steps are completed correctly. The initialization parameters can be checked by using the "F1" function key.

The Installation Settings are slightly different for the two receivers depending on whether the receiver is configured as a base station, or as a mobile receiver. Select keystroke "2" for the Installation Screen.

Set Receiver ID	0
Receiver dynamics	set to 5 for DGPS base station and set to 3 for mobile receiver
Cable Length (m)	10.0
Cable Delay (ns)	52.56
Elevation Mask (deg)	5
Timing Pulse Mode	Standard 1 PPS

The user should select "Ctrl s" to save the installation settings to file. This research effort used <kdinstal> for a file name. This file is automatically saved in >C:\xr5m12\xr5m\data directory. The user needs to select "Ctrl x" to execute the settings. The XR5-M will again reply with "Message Acknowledged".

The next step is to set up the two RTCM ports for each receiver. The RTCM settings are slightly different for the two receivers depending on whether the receiver is configured as a base station, or as a mobile receiver. Select keystroke "5" to enter the RTCM Setup Message Screen. Select the settings as follows:

Port Function :	RTCM
RTCM Function:	select "RTCM Output Single Frame" for the base station receiver
RTCM Function:	select "RTCM Input & Status Output" for the mobile receiver
Status Message Length:	Standard
Status Message Coordinates:	Lat/Lon
Status Message Units:	Knots/Nm
RTCM format:	6 of 8
Baud Rate:	4800
Parity:	ODD
Stop Bits:	1
Tx Output Interval:	1 s
Tx Output Offset:	0 s
Tx Output Offset:	100 ms
Authorization Code	0

The user should select "Ctrl s" to save the RTCM settings to file. This research effort used <kddiff> for a file name. This file is automatically saved in the

>C:\xr5m12\xr5m\data directory. The user needs to select “Ctrl x” to execute the settings. The XR5-M will again reply with "Message Acknowledged".

This completes the initialization, installation and RTCM setup. The user can then proceed to the Receiver Measurement Report Screen using the F3 function key. Detailed data capture is conducted using the Data Monitor program. Details for writing customized symbol variable files are provided in the CDU Software Manual and in the Data Monitor Toolkit Manual [NAV93, NAV96].

Overall the XR5-M receivers worked very well. Graphical presentation of real-time data using the XR5-M software was limited to position plots only. Ideally real-time graphical plots of any user-selected parameter would be desired, ie. Doppler tracking frequencies versus time, this would allow for the assessment of jamming effectiveness while capturing data. Also, saving files as XR5-M "log" files offer a very limited ability to view data as it is written to disk. The ability for the user to pre-program the data capture period in the Data Monitor program prior to data collection, ie. two hours, would be a desirable feature in a receiver designed for testing purposes.

APPENDIX E - HEWLETT PACKARD EQUIPMENT DESCRIPTION

The three main Hewlett Packard (HP) products used in the course of thesis work were an HP 8643A Signal Generator, an HP 8563A Spectrum Analyzer, and an HP Variable Attenuator Model # 394A.

The HP 8643A Signal Generator, Serial Number-3221A00164 was used to generate CW and swept CW signals. The signal generator operates over a range of 0.252 to 2060 MHz and was therefore suitable for generating jamming signals at GPS frequencies. The output was set at -10 dBm for the entire test period and the HP Variable Attenutator was used to adjust jamming levels. The accuracy of the frequency output by the signal generator was verified as being within specification by the spectrum analyzer; however, the frequency accuracy of the signal generator was 0.375 x 10^{-6} times the carrier in Hz and resulted in an accuracy of ±590 Hz [HEW92]. The XR5-M receiver was used to measure the approximate error bias in the signal output by the signal generator by observing the Doppler frequency offset at which channels were jammed. This bias was then adjusted for using the frequency selector panel on the signal generator. This was discussed further in Section 4.9.

The HP 8563A option 026 Serial Number - 3222A02089 was used to verify that the output of the signal generator was within specifications. The HP 8563A Spectrum Analyzer is capable of measuring signals from -119.9 dBm to +30 dBm over a frequency range of 9 kHz to 26.5 GHz. The unit was warmed up for at least five minutes before use. The accuracy of frequency measurement depends on several factors including the frequency readout, the aging of the analyzer, temperature stability, the frequency span, the resolution bandwidth plus an additional 10 Hz. Based on the above variables, the frequency accuracy of the spectrum analyzer was estimated at ±460 Hz at L1 [HEW91]. The HP 8563A provides the user with the ability to program and memorize various setups. This was useful for setting center frequency, frequency span, and resolution bandwidth to best measure the output of the signal generator. The settings could be recalled at a later date for various tests.

The HP Variable Attenuator Model # 394A is adjusted to provide 6 to 120 dB of attenuation and is optimized for a frequency range of 1000 to 2000 MHz. Attenuator settings of 120, 85, 80, 75, 70, and 65 dB were used during the tests. Although the unit is somewhat dated it was suitable for the purpose of the thesis research.

The following information was taken from technical specification sheet provided by HP (the sheet was retrieved from the HP archives and was last updated February 1, 1967 [HEW67]). Absolute accuracy was specified as ±1.25 dB or ±2.5 percent of the dial reading, whichever was greater. This would account for approximately ±2.1 dB of error for an attenuator setting of 85 dB. The attenuator handles up to 200 watts average depending on the terminations. Phase shift versus attenuation is negligible for values of attenuation above approximately 20 to 30 dB because the unit is of the waveguide-beyond-cutoff type of attenuator. The attenuator is basically free of phase shift with attenuation. Actual phase shift results from changes in input and output reflection coefficient that is virtually constant for attenuation above approximately 20 to 30 dB. During data capture testing the attenuator was not used below 65 dB attenuation. The reflection coefficient is specified as less than 0.23 between 15 and 120 dB of attenuation [HEW67].

The unit has dimensions of 140 mm wide, 305 mm long, and 70 mm deep and weighs 6 lbs. The unit had a list price in 1967 of $550 US. Hewlett Packard declared the unit obsolete in 1984. Newer designed models have subsequently replaced the 394A model.

APPENDIX F - MATLAB® SOFTWARE CODE

Appendix F is a sample listing of MATLAB® software code written for three files. The first file "appendt.m" was used to load and perform calculations on the applicable data file "da17adec.txt" for Test 12 on 17 Dec 98, for results plotted in Appendix T. The associated plotting file was "mplott.m". The last MATLAB® file "ll2ecef.m" was used to convert from geodetic latitude, longitude and ellipsoid height to ECEF coordinates.

```
% File name appendt.m
% Data captured on 17 December 98
% Times: 1430Z to 1705Z
% Sample Rate: One sample per second
% Summary of Test
% This was a data run with 10 periods duplicated for
% CW at 70 dB jamming on attenuator (J/S of 35.7) for ten minutes of
% jamming followed by five minute periods with no jamming
%
% Note: Correction of 4.7 meters in ECEF X direction applied
%
% Elevation mask angle set for 5 degrees in both XR5 receivers
%
% Load captured data from text file, set variables, and determine position
% errors. A list describing each of the XR5 variables is provided at
% Appendix C. The names of XR5 variables were maintained in the
% following Matlab code.
clear
fid=fopen('da17adec.txt');
[data]=fscanf(fid,'%f',[145,9300]);
fclose(fid);
data=data';
isid=data(:,1:12);
mestim=data(:,13);
idopp=data(:,14:25);
icno=data(:,26:37);
npclkb=data(:,38);
npclkd=data(:,39);
nplat=data(:,40);
nplon=data(:,41);
nkualt=data(:,42);
npposn=data(:,43:45);
npvelc=data(:,46:48);
gdop=data(:,49);
```

```
sltelv=data(:,50:61);
sltazi=data(:,62:73);
satlist=data(:,74:78);
sltsta=data(:,79:90);
gpsfix=data(:,91);
iql1=data(:,92:103);
npugsp=data(:,104);
npuvsp=data(:,105);
nknteh=data(:,106);
nkntev=data(:,107);
nkntep=data(:,108);
nkprrs=data(:,109:120);
nkdprs=data(:,121:132);
dfsoln=data(:,133);
carlock=data(:,134:145);
%
format long e
% Load  "ALGN MARK" ECEF coordinates used in XR5 Base Station receiver
afit=[5.059798731834281e+05 -4.882293899751916e+06
4.059587157385162e+06];
N=9300;
for i=1:N
    % calculate norm of 3D miss distance w/o correction
    miss=norm((npposn(i,1:3)-afit));
    miss1=((npposn(i,1:3)-afit))';
    % write 3D miss distance into colunm i
    miss1b(:,i)=miss1;
    % write 1D norm of miss into column i
    missb(:,i)=miss;
end
% set time for x axis to minutes
t=(1:N);
t=t';
t=t*1/60;
% transpose of matrix to get N by 1 for missb
% this is uncorrected position error vector
missb=missb';
% transpose of matrix to get N by 3 for miss1b
% this is uncorrected position error in x,y, z direction
miss1b=miss1b';
% create new matrix of 3D miss distance
miss2b=miss1b;
%
% subtract out actual distance between GPS antennas
```

```
% this was an approximation in ECEF X direction
% in fact the 4.7 meters could be broken down more
% precisely into a portion in the x,y,z direction
%
miss2b(:,1)=miss1b(:,1)-4.7;
for i=1:N
    % determine norm of miss distance after correction
    % for distance between GPS antenna
    miss3b(:,i)=norm(miss2b(i,1:3));
end
%  transpose of corrected miss distance
miss3b=miss3b';
%
% miss3b is the variable used to plot 3D position error in figures
% miss2b is the variable used to plot position error in X,Y,Z direction in figures
%
% mean of uncorrected position error
meanmiss1b=mean(miss1b)
% mean of corrected position error
meanmiss2b=mean(miss2b)
% mean of 3D position error
meanmiss3b=mean(miss3b)
% determine 2D ( X Y ) norm of miss distance after correction
% this was interest only for 2D errors not including height
for i=1:N
    miss5b(:,i)=norm(miss2b(i,1:2));
end
miss5b=miss5b';
meanmiss5b=mean(miss5b)
%
% open associated plotting program mplott.m to see Figures for test 12
% end of file
%%%%%%%%%%%%%%%%%%%%%%%%%%%%%%%%%%%%%%%%%%%%%%%%%%%%%%%%%%%%%%%%%
```

The MATLAB® file "mplott.m" was used for plotting the figures used in Appendix T. I have included additional comments on the plotting of figures in Appendix H. The MATLAB® code for mplott.m is provided below.

```
% Appendix T Plots for Test 12 Results
% for 17 Dec 98 1430Z to 1705Z
% Use Print position in Matlab of [.8  1  7  9.4]
% the print position can be modified to optimize plots/page layout
%
% plot of PRN # used in Nav solution
%
figure(3)
h=axes('Position',[0 0 1 1],'Visible','off');
axes('Position',[.2 .15 .7 .75])
plot(t,satlist);axis([0 155 0 31])
zoom
ylabel('PRN # Used In Nav Solution')
xlabel('Time(minutes)')
title('Start Time 1430Z 17 Dec 98')
str(1)={' '};
str(2)={'Figure T.3. PRN # Used In Nav Solution vs Time'};
str(3)={' '};
str(4)={' '};
str(5)={'                         T-3'};
str(6)={' '};
set(gcf,'currentaxes',h)
text(0.320,0.013,str,'FontSize',12)
hold off
%
% Plot of PRN # assigned to each tracking channel
%
figure(4)
h=axes('Position',[0 0 1 1],'Visible','off');
axes('Position',[.2 .15 .7 .75])
plot(t,isid);axis([0 155 0 31])
zoom
ylabel('PRN # Assigned to Each Tracking Channel')
xlabel('Time(minutes)')
title('Start Time 1430Z 17 Dec 98')
str(1)={' '};
str(2)={'Figure T.4. PRN # Assigned to Each Tracking Channel vs Time'};
str(3)={' '};
str(4)={' '};
str(5)={'                         T-4'};
```

```
str(6)={' '};
set(gcf,'currentaxes',h)
text(0.25,0.013,str,'FontSize',12)
hold off
%
% Plot of GDOP vs time
%
figure(5)
subplot(2,1,1)
plot(t(1:3000,:),gdop(1:3000,:))
title('Start Time 1430Z 17 Dec 98')
ylabel('GDOP')
xlabel('Time(minutes)')
subplot(2,1,2)
plot(t(3000:9300,:),gdop(3000:9300,:))
ylabel('GDOP')
xlabel('Time(minutes)')
h=axes('Position',[0 0 1 1],'Visible','off');
axes(h)
str(1)={' '};
str(2)={' '};
str(3)={'Figure T.5. GDOP vs Time'};
str(4)={' '};
str(5)={' '};
str(6)={'                T-5'};
str(7)={' '};
set(gcf,'currentaxes',h)
text(0.38,0.013,str,'FontSize',12)
hold off
%
% Plot of the idopp variable vs time
% over the entire period
%
figure(6)
h=axes('Position',[0 0 1 1],'Visible','off');
axes('Position',[.2 .15 .7 .75])
plot(t,idopp)
zoom
ylabel('Doppler Frequency Offset(Hz) by PRN #')
xlabel('Time(minutes)')
title('Start Time 1430Z 17 Dec 98')
str(1)={' '};
str(2)={'Figure T.6. Doppler Frequency vs Time'};
str(3)={' '};
```

```
str(4)={' '};
str(5)={'                    T-6'};
str(6)={' '};
set(gcf,'currentaxes',h)
text(0.35,0.013,str,'FontSize',12)
hold off
%
% this is detailed plot of idopp variable
%
figure(7)
h=axes('Position',[0 0 1 1],'Visible','off');
axes('Position',[.2 .15 .7 .75])
plot(t(1:3000,:),idopp(1:3000,:))
zoom
ylabel('Doppler Frequency Offset(Hz) by PRN #')
xlabel('Time(minutes)')
title('Start Time 1430Z 17 Dec 98')
str(1)={' '};
str(2)={'Figure T.7. Doppler Frequency vs Time'};
str(3)={' '};
str(4)={' '};
str(5)={'                    T-7'};
str(6)={' '};
set(gcf,'currentaxes',h)
text(0.35,0.013,str,'FontSize',12)
hold off
%
% this is a detailed plot of idopp variable
%
figure(8)
h=axes('Position',[0 0 1 1],'Visible','off');
axes('Position',[.2 .15 .7 .75])
plot(t(3000:6000,:),idopp(3000:6000,:))
zoom
ylabel('Doppler Frequency Offset(Hz) by PRN #')
xlabel('Time(minutes)')
title('Start Time 1430Z 17 Dec 98')
str(1)={' '};
str(2)={'Figure T.8. Doppler Frequency vs Time'};
str(3)={' '};
str(4)={' '};
str(5)={'                    T-8'};
str(6)={' '};
set(gcf,'currentaxes',h)
```

```
text(0.35,0.013,str,'FontSize',12)
hold off
%
% this detailed plot of idopp variable
%
figure(9)
h=axes('Position',[0 0 1 1],'Visible','off');
axes('Position',[.2 .15 .7 .75])
plot(t(6000:9300,:),idopp(6000:9300,:))
zoom
ylabel('Doppler Frequency Offset(Hz) by PRN #')
xlabel('Time(minutes)')
title('Start Time 1430Z 17 Dec 98')
str(1)={' '};
str(2)={'Figure T.9. Doppler Frequency vs Time'};
str(3)={' '};
str(4)={' '};
str(5)={'                    T-9'};
str(6)={' '};
set(gcf,'currentaxes',h)
text(0.35,0.013,str,'FontSize',12)
hold off
%
% plot for gpsfix variable vs time
% provides indication of receiver fix
% status, 2 means 3D FIX, 1 means 2D FIX
% and a zero means NO FIX
% this variable can be used with variable 'dfsoln'
% to show whether fix is based on a differentially
% determined solution or without differential
% this results if one of the channels used in the
% nav solution is not input from the base station
% this plot shows only whether it is 2D, 3D or NO FIX
%
figure(10)
h=axes('Position',[0 0 1 1],'Visible','off');
axes('Position',[.2 .15 .7 .75])
plot(t,gpsfix);axis([0 155 -.5 2.5])
zoom
ylabel('Receiver Fix Status')
xlabel('Time(minutes)')
title('Start Time 1430Z 17 Dec 98')
str(1)={' '};
str(2)={'Figure T.10. Receiver Fix Status vs Time'};
```

```
str(3)={' '};
str(4)={' '};
str(5)={'                    T-10'};
str(6)={' '};
set(gcf,'currentaxes',h)
text(0.35,0.013,str,'FontSize',12)
hold off
%
% plot for x,y,z in ECEF coords miss distance
% in meters and norm of x,y,z in meters
%
figure(11)
subplot(4,1,1)
plot(t,miss2b(:,1))
title('Start Time 1430Z 17 Dec 98')
ylabel('X axis Miss(m)')
subplot(4,1,2)
plot(t,miss2b(:,2))
ylabel('Y axis Miss(m)')
subplot(4,1,3)
plot(t,miss2b(:,3))
ylabel('Z axis Miss(m)')
xlabel('Time(minutes)')
subplot(4,1,4)
plot(t,miss3b)
ylabel('3D Miss(m)')
xlabel('Time(minutes)')
h=axes('Position',[0 0 1 1],'Visible','off');
axes(h)
str(1)={' '};
str(2)={'Figure T.11. X,Y,Z and 3D Error(m) vs Time'};
str(3)={' '};
str(4)={' '};
str(5)={'                    T-11'};
str(6)={' '};
set(gcf,'currentaxes',h)
text(0.30,0.002,str,'FontSize',12)
hold off
%
% detailed plot for x,y,z in ECEF coords
% miss distance in meters and norm of x,y,z in meters
%
figure(12)
subplot(4,1,1)
```

```
plot(t(1:8040,:),miss2b(1:8040,1))
title('Start Time 1430Z 17 Dec 98')
ylabel('X axis Miss(m)')
subplot(4,1,2)
plot(t(1:8040,:),miss2b(1:8040,2))
ylabel('Y axis Miss(m)')
subplot(4,1,3)
plot(t(1:8040,:),miss2b(1:8040,3))
ylabel('Z axis Miss(m)')
xlabel('Time(minutes)')
subplot(4,1,4)
plot(t(1:8040,:),miss3b(1:8040,:))
ylabel('3D Miss(m)')
xlabel('Time(minutes)')
h=axes('Position',[0 0 1 1],'Visible','off');
axes(h)
str(1)={' '};
str(2)={'Figure T.12. X,Y,Z and 3D Error(m) vs Time'};
str(3)={' '};
str(4)={' '};
str(5)={'                    T-12'};
str(6)={' '};
set(gcf,'currentaxes',h)
text(0.30,0.002,str,'FontSize',12)
hold off
%
% detailed plot for x,y,z in ECEF coords
% miss distance in meters and norm of x,y,z in meters
%
figure(13)
subplot(4,1,1)
plot(t(8040:8340,:),miss2b(8040:8340,1))
title('Start Time 1430Z 17 Dec 98')
ylabel('X axis Miss(m)')
subplot(4,1,2)
plot(t(8040:8340,:),miss2b(8040:8340,2))
ylabel('Y axis Miss(m)')
subplot(4,1,3)
plot(t(8040:8340,:),miss2b(8040:8340,3))
ylabel('Z axis Miss(m)')
xlabel('Time(minutes)')
subplot(4,1,4)
plot(t(8040:8340,:),miss3b(8040:8340,:))
ylabel('3D Miss(m)')
```

```
xlabel('Time(minutes)')
h=axes('Position',[0 0 1 1],'Visible','off');
axes(h)
str(1)={' '};
str(2)={'Figure T.12. X,Y,Z and 3D Error(m) vs Time'};
str(3)={' '};
str(4)={' '};
str(5)={'                    T-13'};
str(6)={' '};
set(gcf,'currentaxes',h)
text(0.30,0.002,str,'FontSize',12)
hold off
%
% detailed plot for x,y,z in ECEF coords
% miss distance in meters and norm of x,y,z in meters
%
figure(14)
subplot(4,1,1)
plot(t(8340:9300,:),miss2b(8340:9300,1))
title('Start Time 1430Z 17 Dec 98')
ylabel('X axis Miss(m)')
subplot(4,1,2)
plot(t(8340:9300,:),miss2b(8340:9300,2))
ylabel('Y axis Miss(m)')
subplot(4,1,3)
plot(t(8340:9300,:),miss2b(8340:9300,3))
ylabel('Z axis Miss(m)')
xlabel('Time(minutes)')
subplot(4,1,4)
plot(t(8340:9300,:),miss3b(8340:9300,:))
ylabel('3D Miss(m)')
xlabel('Time(minutes)')
h=axes('Position',[0 0 1 1],'Visible','off');
axes(h)
str(1)={' '};
str(2)={'Figure T.14. X,Y,Z and 3D Error(m) vs Time'};
str(3)={' '};
str(4)={' '};
str(5)={'                    T-14'};
str(6)={' '};
set(gcf,'currentaxes',h)
text(0.30,0.002,str,'FontSize',12)
hold off
%
```

```
% this is a plot of Receiver Clock
% Bias and Receiver Clock Drift
%
figure(15)
subplot(2,1,1)
plot(t,npclkb)
ylabel('Receiver Clock Bias (seconds)')
xlabel('Time(minutes)')
title('Start Time 1430Z 17 Dec 98')
subplot(2,1,2)
plot(t,npclkd)
ylabel('Receiver Clock Drift (seconds/second)')
xlabel('Time(minutes)')
h=axes('Position',[0 0 1 1],'Visible','off');
axes(h)
str(1)={' '};
str(2)={'Figure T.15. Receiver Clock Bias and Drift vs Time'};
str(3)={' '};
str(4)={' '};
str(5)={'                    T-15'};
str(6)={''};
set(gcf,'currentaxes',h)
text(0.26,0.002,str,'FontSize',12)
hold off
%
% this is a plot of C/No vs time
% for two channels per page
% plot of receiver channel 1 and 2
%
figure(16)
subplot(2,1,1)
plot(t,icno(:,1));axis([0 160 0 60])
ylabel('C/No (dB-Hz) Channel 1')
xlabel('Time(minutes)')
title('Start Time 1430Z 17 Dec 98')
subplot(2,1,2)
plot(t,icno(:,2));axis([0 160 0 60])
ylabel('C/No (dB-Hz) Channel 2')
xlabel('Time(minutes)')
h=axes('Position',[0 0 1 1],'Visible','off');
axes(h)
str(1)={' '};
str(2)={' '};
str(3)={'Figure T.16. C/No vs Time'};
```

```
str(4)={' '};
str(5)={' '};
str(6)={'                T-16'};
str(7)={''};
set(gcf,'currentaxes',h)
text(0.38,0.013,str,'FontSize',12)
hold off
%
% plot of C/No for receiver channel 3 and 4
%
figure(17)
subplot(2,1,1)
plot(t,icno(:,3));axis([0 160 0 60])
ylabel('C/No (dB-Hz) Channel 3')
xlabel('Time(minutes)')
title('Start Time 1430Z 17 Dec 98')
subplot(2,1,2)
plot(t,icno(:,4));axis([0 160 0 60])
ylabel('C/No (dB-Hz) Channel 4')
xlabel('Time(minutes)')
h=axes('Position',[0 0 1 1],'Visible','off');
axes(h)
str(1)={' '};
str(2)={' '};
str(3)={'Figure T.17. C/No vs Time'};
str(4)={' '};
str(5)={' '};
str(6)={'                T-17'};
str(7)={''};
set(gcf,'currentaxes',h)
text(0.38,0.013,str,'FontSize',12)
hold off
%
% plot of C/No for receiver channel 5 and 6
figure(18)
subplot(2,1,1)
plot(t,icno(:,5));axis([0 160 0 60])
ylabel('C/No (dB-Hz) Channel 5')
xlabel('Time(minutes)')
title('Start Time 1430Z 17 Dec 98')
subplot(2,1,2)
plot(t,icno(:,6));axis([0 160 0 60])
ylabel('C/No (dB-Hz) Channel 6')
xlabel('Time(minutes)')
```

```
h=axes('Position',[0 0 1 1],'Visible','off');
axes(h)
str(1)={' '};
str(2)={' '};
str(3)={'Figure T.18. C/No vs Time'};
str(4)={' '};
str(5)={' '};
str(6)={'                T-18'};
str(7)={''};
set(gcf,'currentaxes',h)
text(0.38,0.013,str,'FontSize',12)
hold off
%
% plot of C/No for receiver channel 7 and 8
figure(19)
subplot(2,1,1)
plot(t,icno(:,7));axis([0 160 0 60])
ylabel('C/No (dB-Hz) Channel 7')
xlabel('Time(minutes)')
title('Start Time 1430Z 17 Dec 98')
subplot(2,1,2)
plot(t,icno(:,8));axis([0 160 0 60])
ylabel('C/No (dB-Hz) Channel 8')
xlabel('Time(minutes)')
h=axes('Position',[0 0 1 1],'Visible','off');
axes(h)
str(1)={' '};
str(2)={' '};
str(3)={'Figure T.19. C/No vs Time'};
str(4)={' '};
str(5)={' '};
str(6)={'                T-19'};
str(7)={''};
set(gcf,'currentaxes',h)
text(0.38,0.013,str,'FontSize',12)
hold off
%
% plot of C/No for receiver channel 9 and 10
figure(20)
subplot(2,1,1)
plot(t,icno(:,9));axis([0 160 0 60])
ylabel('C/No (dB-Hz) Channel 9')
xlabel('Time(minutes)')
title('Start Time 1430Z 17 Dec 98')
```

```
subplot(2,1,2)
plot(t,icno(:,10));axis([0 160 0 60])
ylabel('C/No (dB-Hz) Channel 10')
xlabel('Time(minutes)')
h=axes('Position',[0 0 1 1],'Visible','off');
axes(h)
str(1)={' '};
str(2)={' '};
str(3)={'Figure T.20. C/No vs Time'};
str(4)={' '};
str(5)={' '};
str(6)={'                T-20'};
str(7)={''};
set(gcf,'currentaxes',h)
text(0.38,0.013,str,'FontSize',12)
hold off
%
% plot of C/No for receiver channel 11 and 12
figure(21)
subplot(2,1,1)
plot(t,icno(:,11));axis([0 160 0 60])
ylabel('C/No (dB-Hz) Channel 11')
xlabel('Time(minutes)')
title('Start Time 1430Z 17 Dec 98')
subplot(2,1,2)
plot(t,icno(:,12));axis([0 160 0 60])
ylabel('C/No (dB-Hz) Channel 12')
xlabel('Time(minutes)')
h=axes('Position',[0 0 1 1],'Visible','off');
axes(h)
str(1)={' '};
str(2)={' '};
str(3)={'Figure T.21. C/No vs Time'};
str(4)={' '};
str(5)={' '};
str(6)={'                T-21'};
str(7)={''};
set(gcf,'currentaxes',h)
text(0.38,0.013,str,'FontSize',12)
hold off
%
% this is plot of J/S vs time using "stairs" function
%
figure(22)
```

```
t1=[    0     5     15    20    30    35    45    50    60    65
    75    80    90    95    105   110   120   125   135   140   150
    155];
y=[0    35.7  0     35.7  0     35.7  0     35.7  0     35.7  0
    35.7  0     35.7  0     35.7  0     35.7  0     35.7  0     0];
h=axes('Position',[0 0 1 1],'Visible','off');
axes('Position',[.2 .15 .7 .75])
stairs(t1,y);axis([0 155 0 40])
ylabel('J/S')
xlabel('Time(minutes)')
title('Start Time 1430Z 17 Dec 98')
str(1)={' '};
str(2)={'Figure T.22. Jamming Level J/S vs Time'};
str(3)={' '};
str(4)={' '};
str(5)={'                    T-22'};
str(6)={' '};
set(gcf,'currentaxes',h)
text(0.33,0.013,str,'FontSize',12)
hold off
% End of File
%%%%%%%%%%%%%%%%%%%%%%%%%%%%%%%%%%%%%%%%%%%
```

The MATLAB® file "ll2ecef.m" was used to convert geodetic latitude, longitude and height to ECEF coordinates using equations from page 27 of [KAP96]. The file was specifically written to use the coordinates for the Doppler Station 32058 in WGS 84 provided in Appendix A as follows:

Latitude	N 39 46 55.424
Longitude	W 084 04 57.918
Ellipsoid Height	271.77 meters

A detailed comparison of the results of using MATLAB® and Kaplan's equations are discussed further in Appendix B. The software code is as follows:

```
% File name is "ll2ecef.m"
% This file was generated to compare lat/lon/ht conversion to ECEF
% using transformation from Kaplan page 27
% for a set of lat/lon/ht and ECEF coordinates given by 1988 survey for
% AFIT Building 640 rooftop
%
% Convert geodetic lat long ht to ECEF for Doppler Antenna location
%
b=6356752.3142;
a=6378137;
asq=a^2;
bsq=b^2;
e=sqrt(1-(bsq/asq));
latd=39*pi/180;
latm=(46/60)*pi/180;
lats=(55.424/3600)*pi/180;
lat=latd+latm+lats
lond=84*pi/180;
lonm=(04/60)*pi/180;
lons=(57.918/3600)*pi/180;
lon=-(lond+lonm+lons)
h=271.77
x1=(a*cos(lon));
x2=1+(1-e^2)*((tan(lat))^2);
x3=sqrt(x2);
x=(x1/x3)+(h*((cos(lon))*cos(lat)));
y1=(a*sin(lon));
y2=1+(1-e^2)*((tan(lat))^2);
y3=sqrt(y2);
y=(y1/y3)+(h*((sin(lon))*cos(lat)));
z1=a*(1-e^2)*sin(lat);
z2=sqrt(1-(e^2)*(sin(lat))^2);
```

```
z=(z1/z2)+(h*sin(lat));
u=[x y z]'
%
% ECEF values WGS 84 from survey sheet 1988 for Doppler station 32058
%
u1=[506020.04 -4882282.48 4059593.06]'
%
% Difference between Matlab/Kaplan equations and DMA calculated position
delta=u-u1
%
% Difference between XR5 calculated and 1988 Surveyed location for Doppler
% station
%
xr5=[506020.1624427695 -4882283.308111367 4059593.728202703]';
delta2=u1-xr5
% End of File
%%%%%%%%%%%%%%%%%%%%%%%%%%%%%%%%%%%%%%%%%%%%%%
```

APPENDIX G - SOURCES OF INTERFERENCE TO GPS RECEIVERS AND MITIGATION TECHNIQUES

SOURCES OF INTERFERENCE

A summary of the various forms of interference to the GPS signals is provided below. For more detailed information the reader is referred to reference [PAR96].

TROPOSPHERIC/IONOSPHERIC

Tropospheric/Ionospheric interference can cause several effects on the reception of GPS signals especially at low elevation angles. The main sources of ionospheric errors are: 1) group delay of the signal modulation, 2) carrier phase advance, 3) Doppler shift, 4) Faraday rotation on linearly polarized signals, 5) refraction of the radio waves, 6) distortion of pulse waveforms, 7) signal amplitude fading or amplitude scintillation; and 8) phase scintillations. Tropospheric effects can result in attenuation, scintillation, and signal delay [PAR96].

MULTIPATH

Multipath results when a signal arrives at a receiver via multiple paths due to reflection and diffraction of the signal. Differential techniques are normally used to eliminate or minimize errors that are common between two receivers; unfortunately, multipath effects can be very different between a Base Station and a Mobile receiver. For C/A code the maximum multipath error is approximately 15 meters [PAR96].

HARMONICS OR INTER-MODULATION PRODUCTS

Radio Frequency Interference (RFI) can have a narrow bandwidth of about 25 kHz. One usually expects harmonic signals to be weak and filtered; however, it is possible that harmonics or products from airborne and ground based transmitters may fall within the L1 frequency band. As an example transmitters at 787.71 MHz, 525.14 MHz, 315.084 MHz, 225.06 MHz, 105.028 MHz, have harmonics at L1 (the 2^{nd}, 3^{rd}, 5^{th}, 7^{th}, and 15^{th} respectively). The 13^{th} harmonic of lower VHF frequencies of 121.150, 121.175, 121.200 MHz and the 12^{th} harmonic of 131.200, 131.250, and 131.300 MHz also appear within the GPS bandwidth [PAR96].

PULSED INTERFERENCE

Inadequately filtered signals in nearby frequency bands may generate pulsed interference, such as from radar systems. In the case of intentional interference, a pulsed jammer's power is cycled on and off and the pulse repetition frequency and pulse duration modified to improve jamming effects [PAR96].

IN-BAND INTERFERENCE

As highlighted with the incident at the Air Force Research Lab [GWM98], in-band interference can be caused by accidentally transmitting in the GPS band. Anyone intentionally attempting to jam the reception of GPS signals would choose to operate within the bandwidth of GPS receivers. A wide band jammer would need to cover a sufficiently wide portion of the spectrum between the first nulls which is typically at least ± 1.023 MHz for C/A code receivers at L1 and ± 10.23 MHz for P(Y) code receivers at L1 and L2 [PAR96].

OUT-OF-BAND INTERFERENCE

Out of band interference is normally caused from nearby transmitters and poor RF filtering in the GPS receiver, although satellite communication links that bracket the GPS signals have potential to cause interference problems. As the demand for valuable frequency spectrum allocation continues to grow there will be increased efforts by other organizations to encroach into the allocated GPS frequency spectrum.

SPOOFING

Intelligent spoofing attempts to fool a GPS receiver by creating a false satellite signal that is locked on to by the GPS receiver as though it were a valid satellite signal. The information in the false signal is slowly made erroneous and the GPS receiver calculations grow in error. Although one would normally associate the generation of PRN codes with spoofing, this thesis demonstrated that simple CW signals can be used to spoof a receiver to more than 12 kilometers (see Section 4.8.1).

MITIGATION TECHNIQUES

INTRODUCTION

The two general forms of interference suppression may be categorized as spatial and signal processing. Since GPS signals are transmitted at L1 and L2 frequencies, the signals are masked by obstacles and do not diffract around them in the same manner as lower frequency signals. If the interfering source is ground based or at low elevation angles it must have line-of-sight with the intended victim. Signal processing techniques are used to filter out interfering sources while spatial techniques use direction of arrival of the jamming signals to reduce the jamming effectiveness while enhancing the direction of arrival of the satellite signals.

RF AND IF FILTERING

Out-of-band interference can cause non-linear or saturation effects in the low noise amplifier as well as inter-modulation effects in down-converter mixers. High peak power pulses can damage the sensitive RF front end. The application of filtering at RF and IF reduces these effects. A C/A code receiver may have a RF/IF filter bandwidth as wide as 20 MHz. This bandwidth may be narrowed to 1-2 MHz in order to gain greater selectivity against out-of-band interference [PAR96]. In the case of the XR5-M receiver the first IF stage is at 295 MHz and has a bandwidth of 20 MHz, the second stage IF is at 24.58 MHz and has a bandwidth of 8 MHz [BUT99]. Rejection of narrow band interference at IF may be achieved by using adaptive frequency nulling filters.

ADAPTIVE INTERFERENCE CANCELLER (AIC) 2100

Mayflower Communications Company, Inc. is now marketing a unit titled the "AIC 2100 Adaptive Interference Canceller Module." The unit is designed to operate at RF and plug directly in between the GPS antenna and receiver. It is reported to provide an improvement of up to 50 dB of suppression to narrowband interference for C/A and P(Y) code receivers [UPT98]. It should be mentioned that the device is not designed to reduce wideband noise jamming.

ANTENNA AND ADAPTIVE ARRAYS

Several techniques are used in a GPS receiver to take advantage of the fact that the interfering sources are usually earth based. A simple antenna system may have a typical gain of 0 dB to + 6 dB for the upper hemispherical portion but may drop off near the horizon (less than 5 degrees elevation) to approximately -5dB. For an elevation angle less than 5 degrees other error sources such as ionospheric, atmospheric, multipath and physical obstructions may be more predominant than RF interference (except for the case where the RF interference is intentional i.e. jamming).

Spatial interference suppression is achieved by using a multi-element antenna array. Such an antenna increases the gain in the direction of the various satellite positions; the satellite position is available from the almanac or ephemeris data.

Adaptive weighting of antenna elements can be used to null out sources of interference; the limiting factor is the number of elements in the array as well as how close in azimuth the satellite is to the actual interfering source. The Controlled Reception Pattern Antenna (CRPA) is an example of such a system.

At the US Navy test range at China Lake, modeling has demonstrated that a 16 kW GPS jammer can be used in a directional antenna beam to reduce interference with other civilian aircraft at locations outside the main beam of the jamming signal [BOG97]. Directional jamming may be used in the future as civilians become more concerned about the jamming of GPS signals. In a hostile environment the operational benefits of jamming certain corridors would allow friendly forces to continue to operate in a GPS jamming environment.

INTERFERENCE SUPPRESSION UNIT (ISU)

Electro-Radiation Inc. manufactures the ISU that has been tested at Holloman, AFB with four ground based jammers and one airborne jammer [BRASNY98]. The unit uses a uniquely designed antenna along with the ISU to provide an additional margin of 20 dB for broadband noise and 35 dB for narrowband noise. Future testing of this device in the AFIT lab environment may be challenging given the company's use of polarization as a means of reducing interference.

AIDING OF THE RECEIVER TRACKING LOOPS

Once interference is detected it may be possible to reduce the effects of the interference by narrowing the bandwidth of the code tracking loop or the carrier tracking loop. One means is to use inputs from an inertial reference unit to aid the tracking loops. The use of integrated GPS and Inertial Reference Systems is likely to increase in future operations due to the complimentary capabilities of both systems.

ANTI-SPOOFING (A/S)

Spoofing of satellite signals is considered to be challenging given that the spoofer normally needs to know the receivers position and velocity in order to create the false signal that will have the correct Doppler shift and transmission delay of the codes. The encryption of the P code into Y code is designed to eliminate this threat. The C/A code receiver is more susceptible to spoofing given the lack of anti-spoofing capability; in the future as ground navigation aids may be replaced by a global air traffic control system using GPS, this could become of greater concern with terrorist activity. This thesis has demonstrated that even CW interference can spoof a DGPS C/A code receiver to a relatively large error. As a result, improvements in commercial receiver design to reduce CW interference will serve as a technique to reduce the impact of this simple form of spoofing.

MULTIPATH

One method of reducing multipath interference is the use of RF absorbing materials around the receiver antenna. Additionally since the P(Y) code is modulated at ten times the rate of C/A code the P(Y) code chips are one tenth the length and the multipath errors are also one tenth that of C/A code. Since multipath normally arrives from angles near the horizon the effects can be minimized by using an antenna with low gain at the horizon. A choke ring antenna is commonly used to reduce multipath effects.

APPENDIX H - SUMMARY OF LESSONS LEARNED

OVERVIEW

A summary is provided in Chapter 4 of the results of Tests 1 to 12. The purpose of this Appendix was to capture lessons learned during the course of thesis research for use by students interested in follow-on research. The Appendix is divided into two main areas of interest; equipment related and MATLAB® comments.

EQUIPMENT RELATED

The following comments are provided with respect to the equipment used during the course of thesis research:

a. The XR5-M receiver is an excellent tool for education purposes. Access to a wide range of variables allows a user to tailor data capture for post processing analysis;

b. The XR5-M data monitor program requires a master symbol file <m1237.sy> to be loaded prior to writing or loading customized symbol variable files. Customized symbol variable files are written into unique XR5-M code and the files are not easily modified once saved. If the user wishes to add a new variable to the symbol file after it has been saved it is necessary to re-write the entire set of desired variables to file;

c. An upgrade of the XR5-M receiver firmware to version 4.9 would provide the capability to transmit/receive RTCM messages Type 20 and 21. These messages provide for the real-time broadcast of differential carrier phase corrections. Mobile position measurements could be reduced to sub-meter accuracy with this upgrade;

d. Mr. Simon Butcher who is the field service and technical support manager from Navstar Systems Ltd in England, the original manufacturer of the XR5-M receiver, was very responsive to technical questions and provided answers promptly and to the level of detail requested. Mr Butcher may be contacted at sbutcher@telecom.com or toll free from the USA at 1-800-456-0910;

e. The maximum data rate of communication between the two receivers via the RTCM port was 4800 Baud. The maximum rate of data transfer via the Control Display Unit (CDU) was 9600 Baud. The CDU 9600 Baud rate limits the amount of data which can be captured from the XR5-M receiver each second. Adjusting the sample rate to slower periods did not alleviate the problem. This requires judicious selection of symbol variables for data capture if post processing of a large number of variables is desired;

f. The XR5-M and the HP signal generator and spectrum analyzer should be warmed up for at least thirty minutes prior to use for detailed measurements;

g. "Hotwiring" the two XR5-M receivers together to provide differential corrections worked well; and,

h. The HP spectrum analyzer has a maximum DC input of 0 volts. The XR5-M receiver antenna has a DC powered pre-amplifier that is powered from the XR5-M receiver through the antenna cable. There was potential for the DC output from the XR5-M receiver to feed back through the jamming cables and damage the spectrum analyzer. The HP variable attenuator was verified that it blocked DC signals to the spectrum analyzer; however, a separate DC block is recommended at the spectrum analyzer as an additional precaution to prevent equipment damage.

MATLAB® COMMENTS

On both PC and Mactintosh® platforms it is necessary to set the file path to the desired "m" files. Copying of MATLAB® figures into Microsoft™ Word® or Powerpoint® resulted in degraded quality of the figures. Efforts to edit the figure once converted to MS Word® also caused undesired changes to the MATLAB® figure. Saving of MATLAB® figures into encapsulated post-script files resulted in the loss of some of the text strings which had been added to the MATLAB® figures. The best quality was achieved by doing all plots in MATLAB®. Editing and annotating specific figures was completed using the "gtext" MATLAB® command and saving the particular figure as a separate "m" file. By saving the figure as an "m" file it could be modified by opening the actual "m" file and editing the text code. A copy of all MATLAB® files (version 5.2) on compact disk (CD) accompanies the AFIT copy of the thesis should the reader desire to review specific test results in detail. The MATLAB® files on CD are compatible with both PC and Macintosh version 5.2 of MATLAB®. For further details the reader should refer to the <readme.doc> file included with the CD.

As a rookie MATLAB® user at the beginning of my thesis research I found the following MATLAB® software commands to be useful:

- *sptool* is a graphical user interface tool found in the Signal Processing Toolbox that was used extensively in conducting analysis of data. Variables may be imported from the MATLAB® workspace and saved into a MATLAB® "spt" file format;
- *fid(fopen) fscanf* was used for loading the data text file. An example of using these commands is provided in Appendix F;
- *legend* was used with a -1 at end of the string to place the legend off of the figure plot;
- *view* was used for switching and rotating a polar plot of satellite azimuth and elevation to a compass rose with west on left, and north up;
- *zoom* was used with the mouse to expand a portion of a figure. This was beneficial for deciding what detailed areas to plot;
- *stairs* was used to plot J/S levels; and,
- *gtext* was useful for annotating text to specific locations in figures using mouse/roller ball input device. This tool was used to label the various channels, PRN numbers and frequencies on the Appendix I to T figures.

MATLAB® "m" files did not execute if the file name began with a number. MATLAB® Signal Processing Toolbox "spt" files opened with "sptool" if the file name commenced with a number.

Finally running MATLAB® version 5.2 on a 200 MHz Pentium® II PC would often lock up the PC after printing several pages of figures. This would require rebooting Windows 95® when using "m" files with large matrices (9000 rows x 145 columns). This problem was less frequent when a 400 MHz Pentium II PC was used. No detailed troubleshooting of this problem was conducted; however, it was believed to be associated with either a MATLAB® memory allocation or a computer/printer network problem.

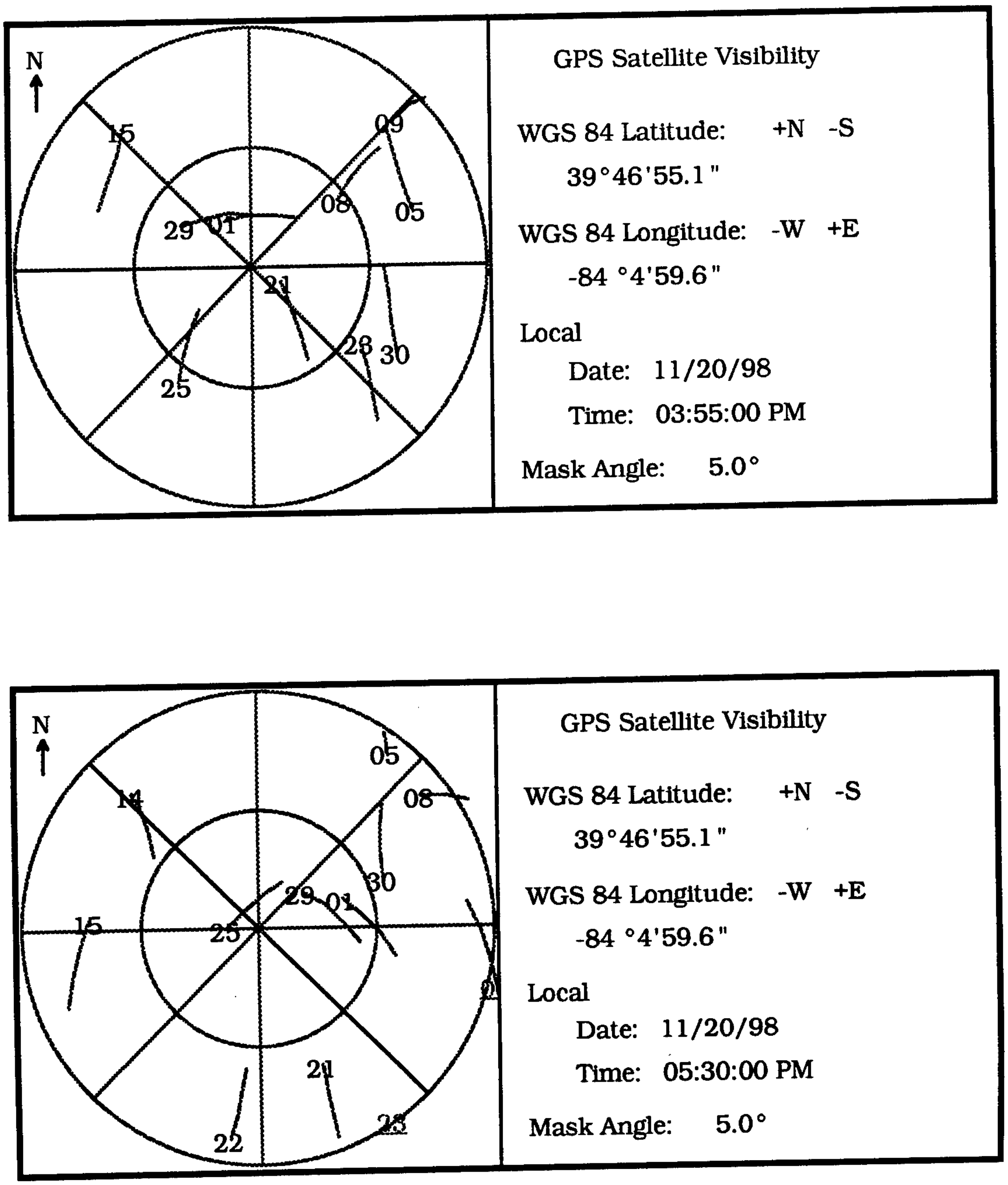

Figure I.1. GPS Satellites In View 20 Nov 98

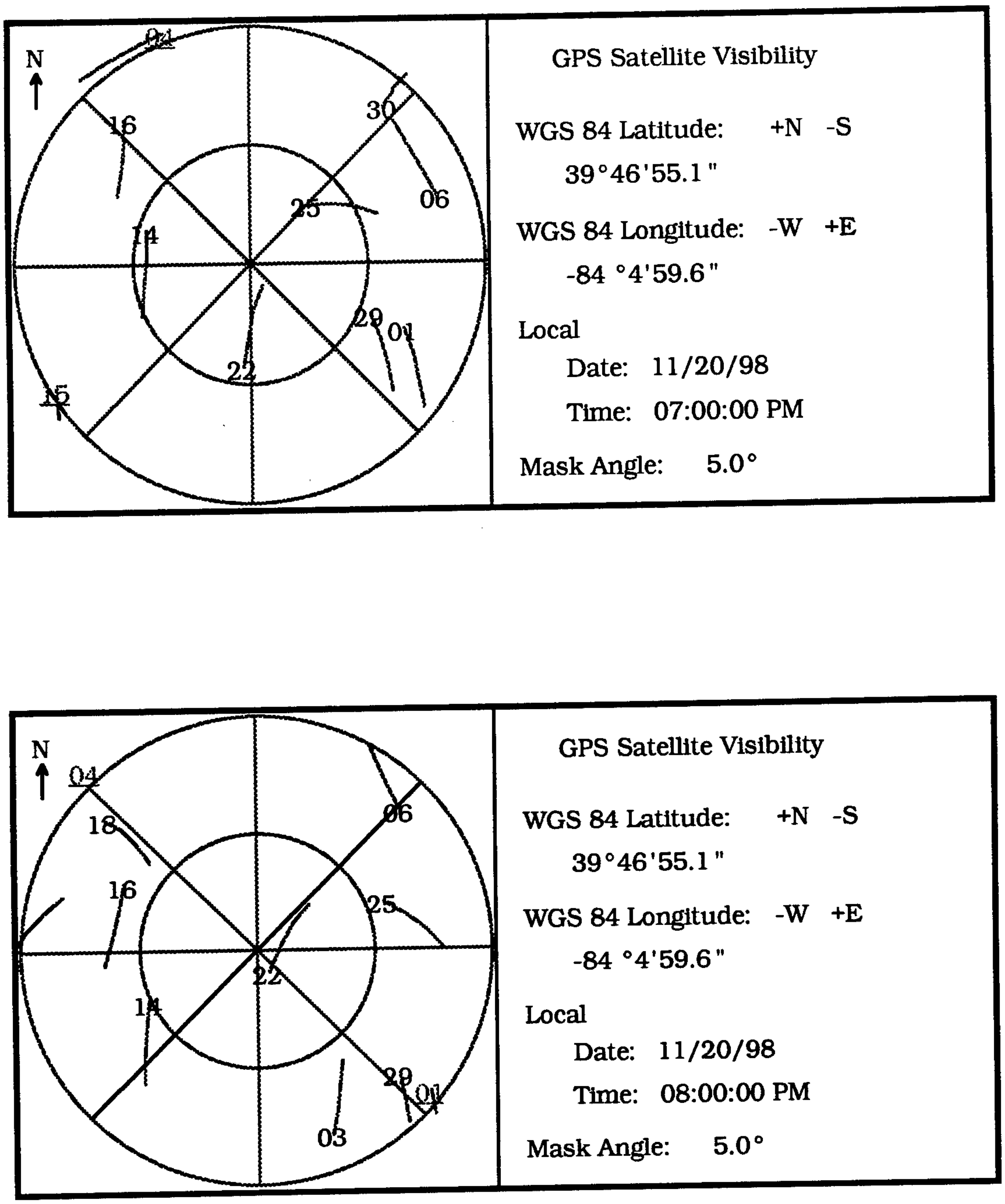

Figure I.2. GPS Satellites In View 20 Nov 98

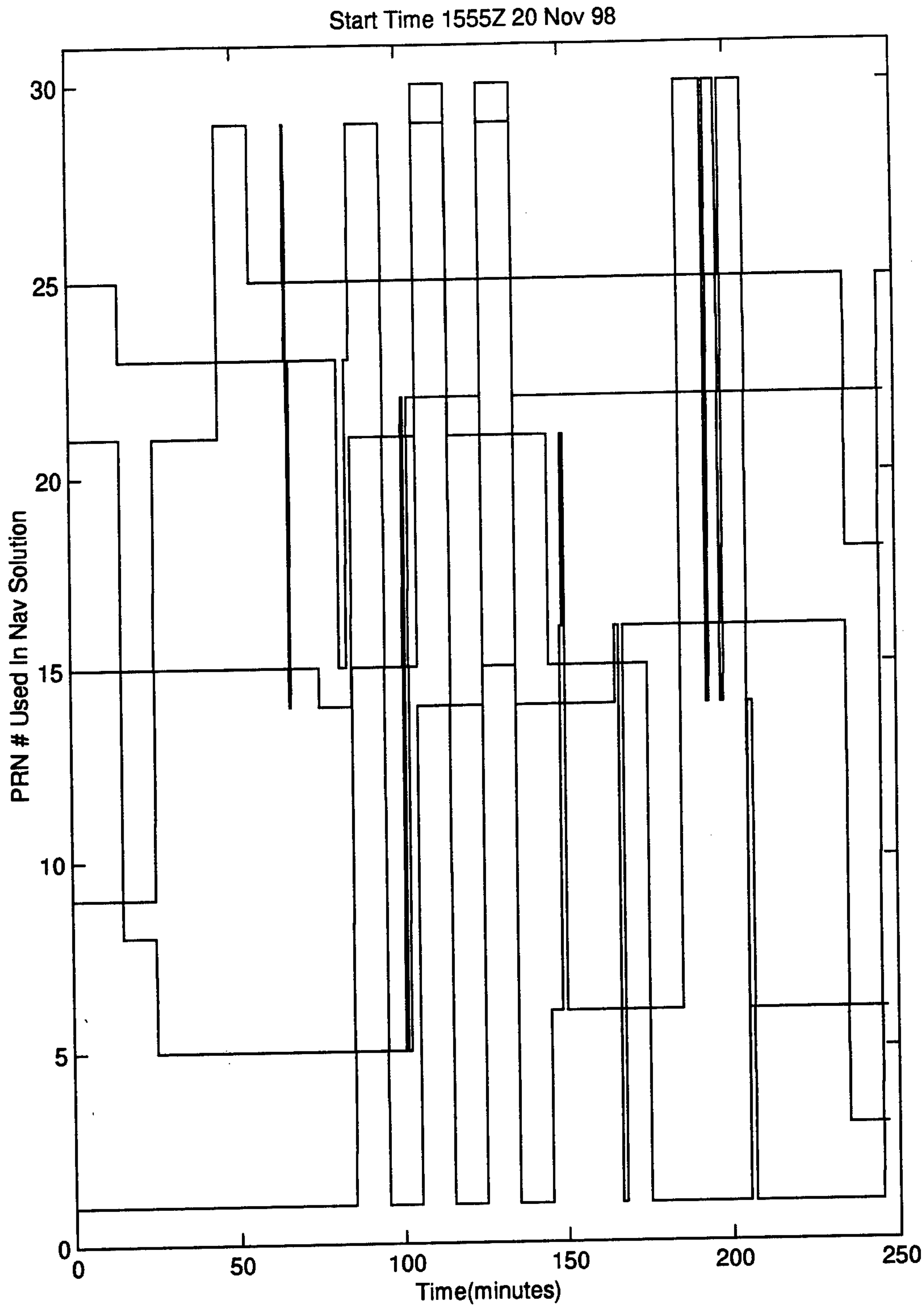

Figure I.3. PRN # Used In Nav Solution vs Time

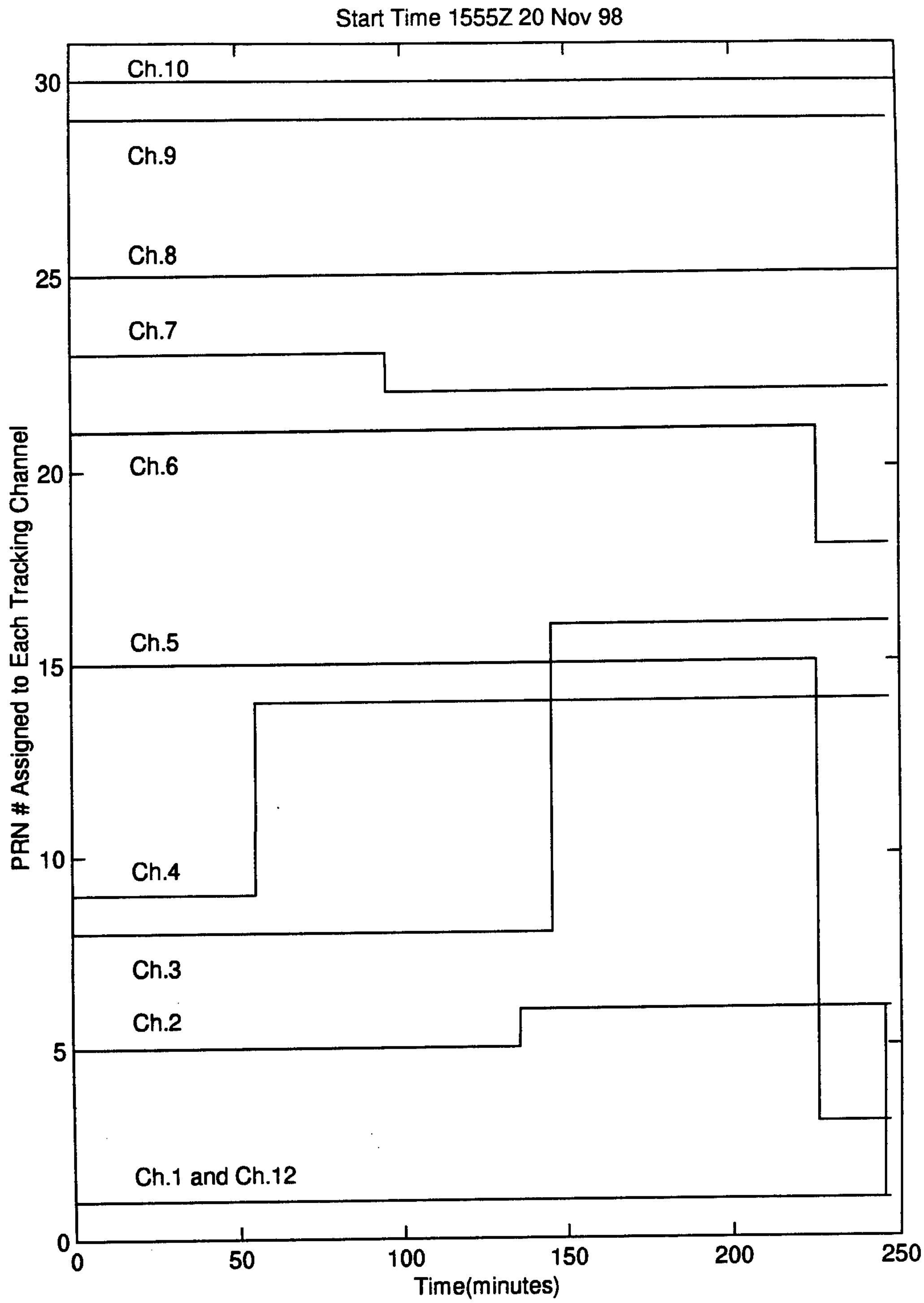

Figure I.4. PRN # Assigned to Each Tracking Channel vs Time

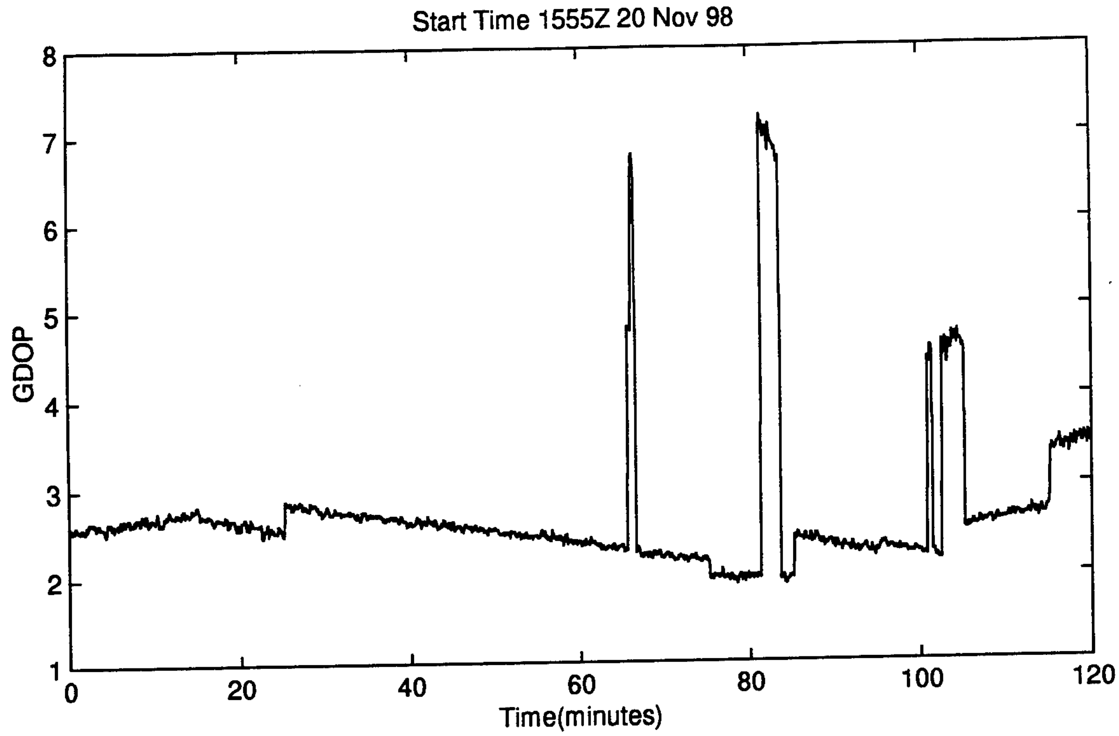

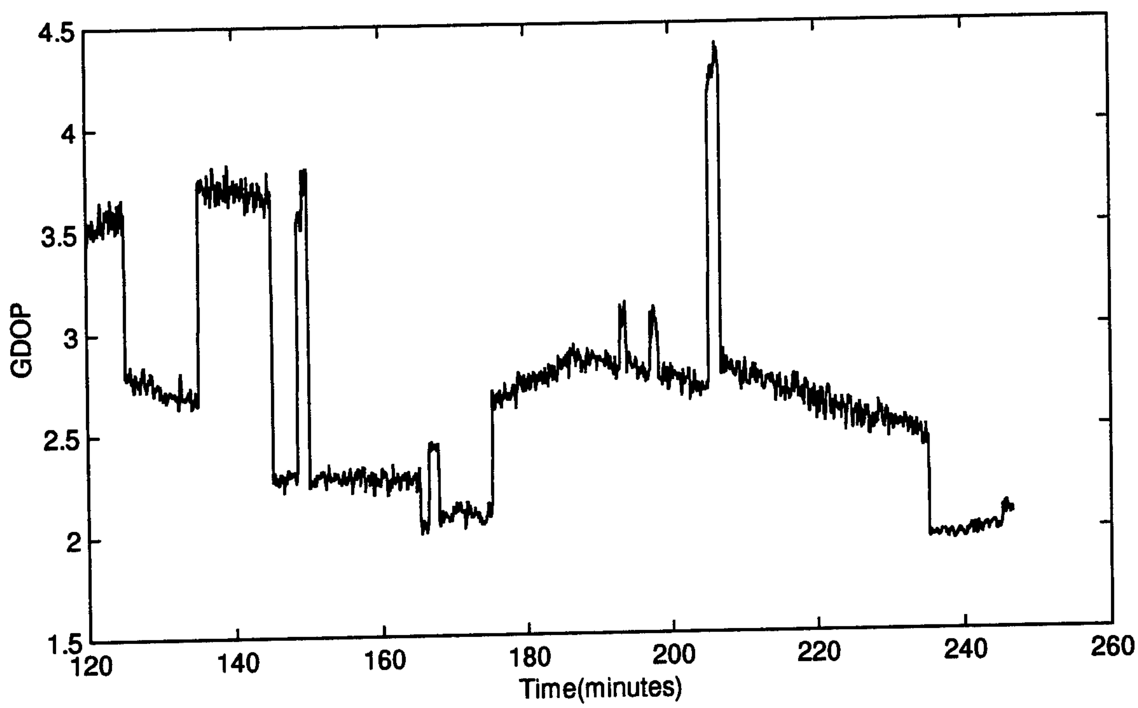

Figure I.5. GDOP vs Time

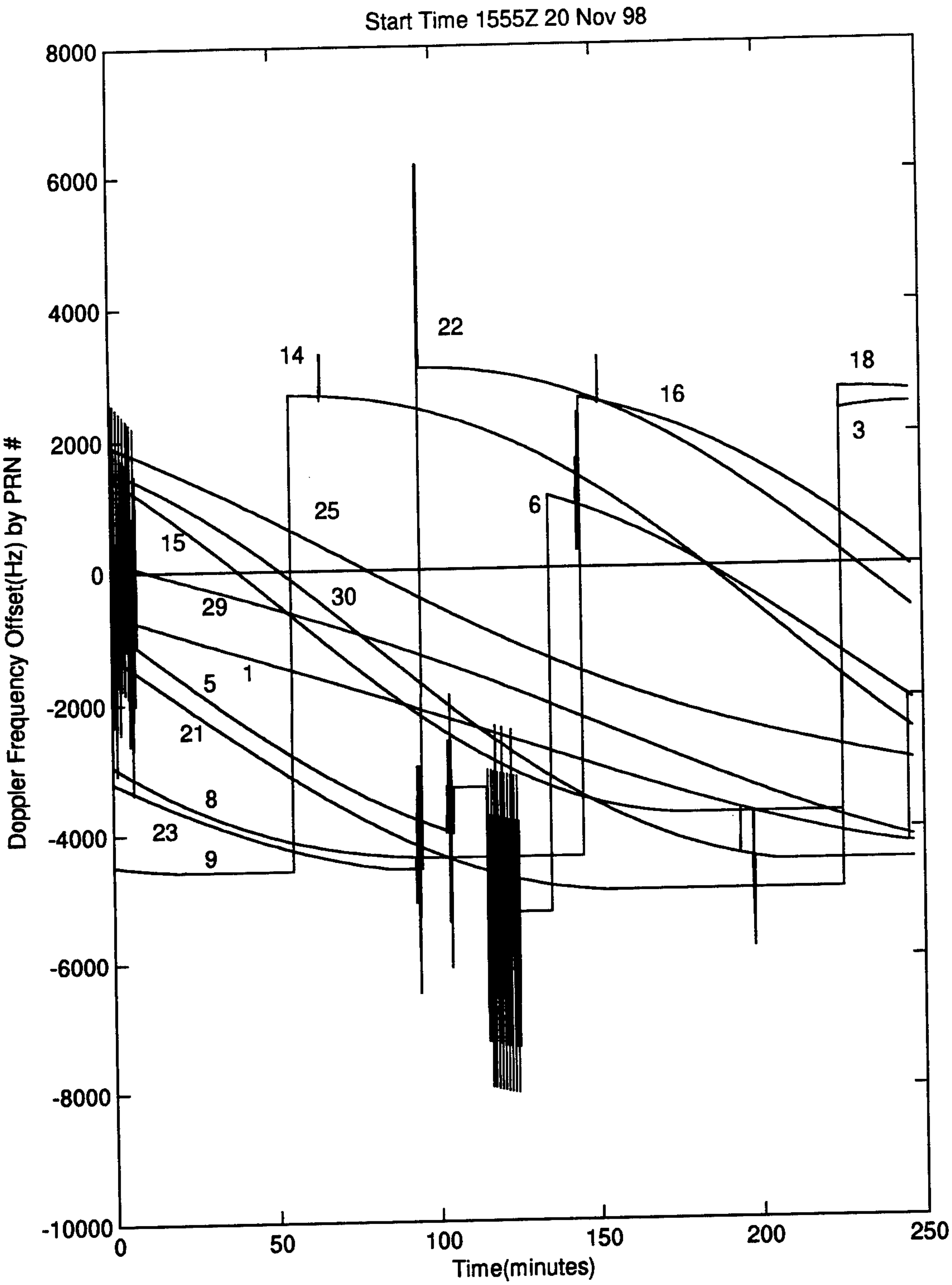

Figure I.6. Doppler Frequency vs Time

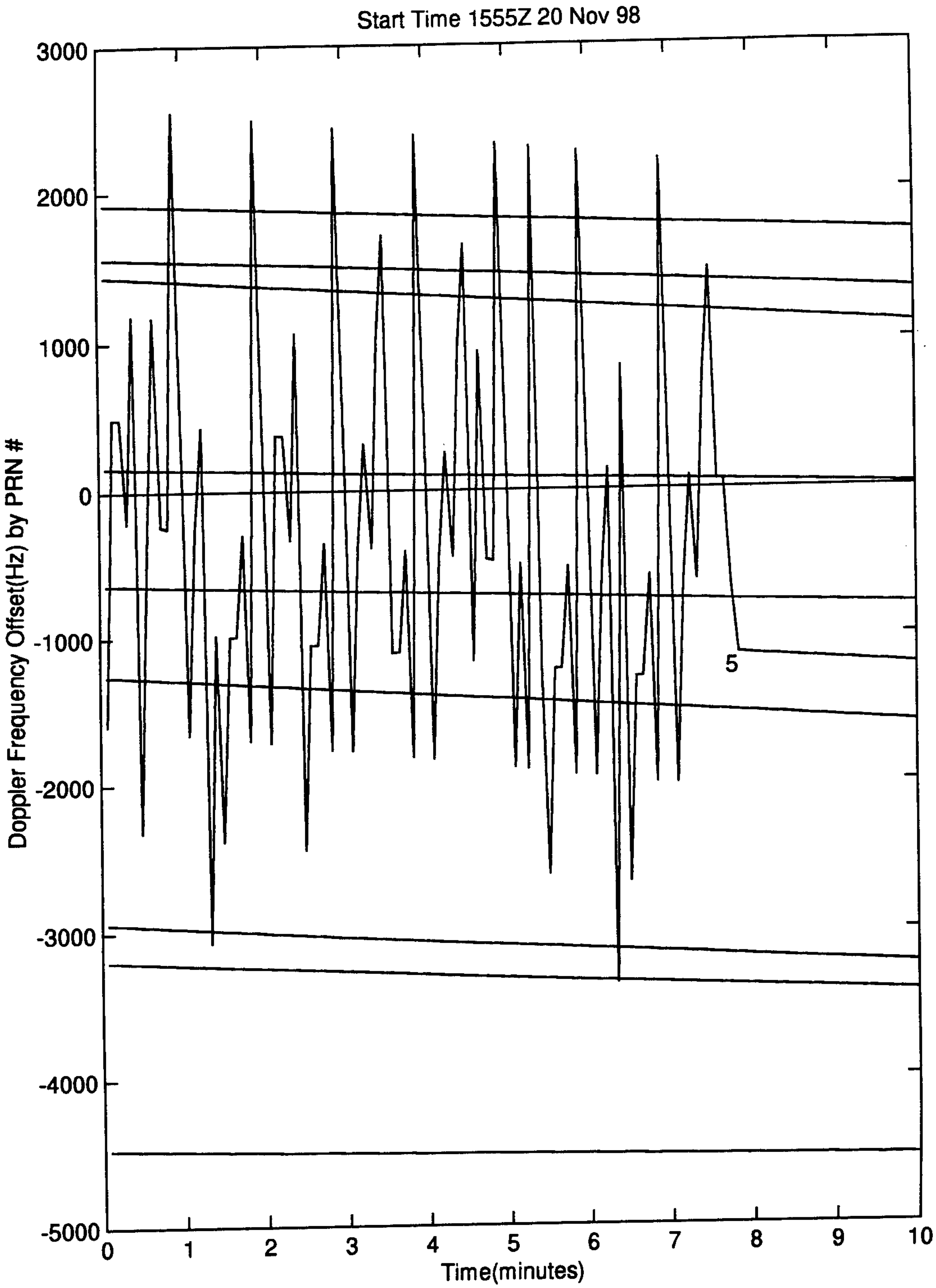

Figure I.7. Doppler Frequency vs Time

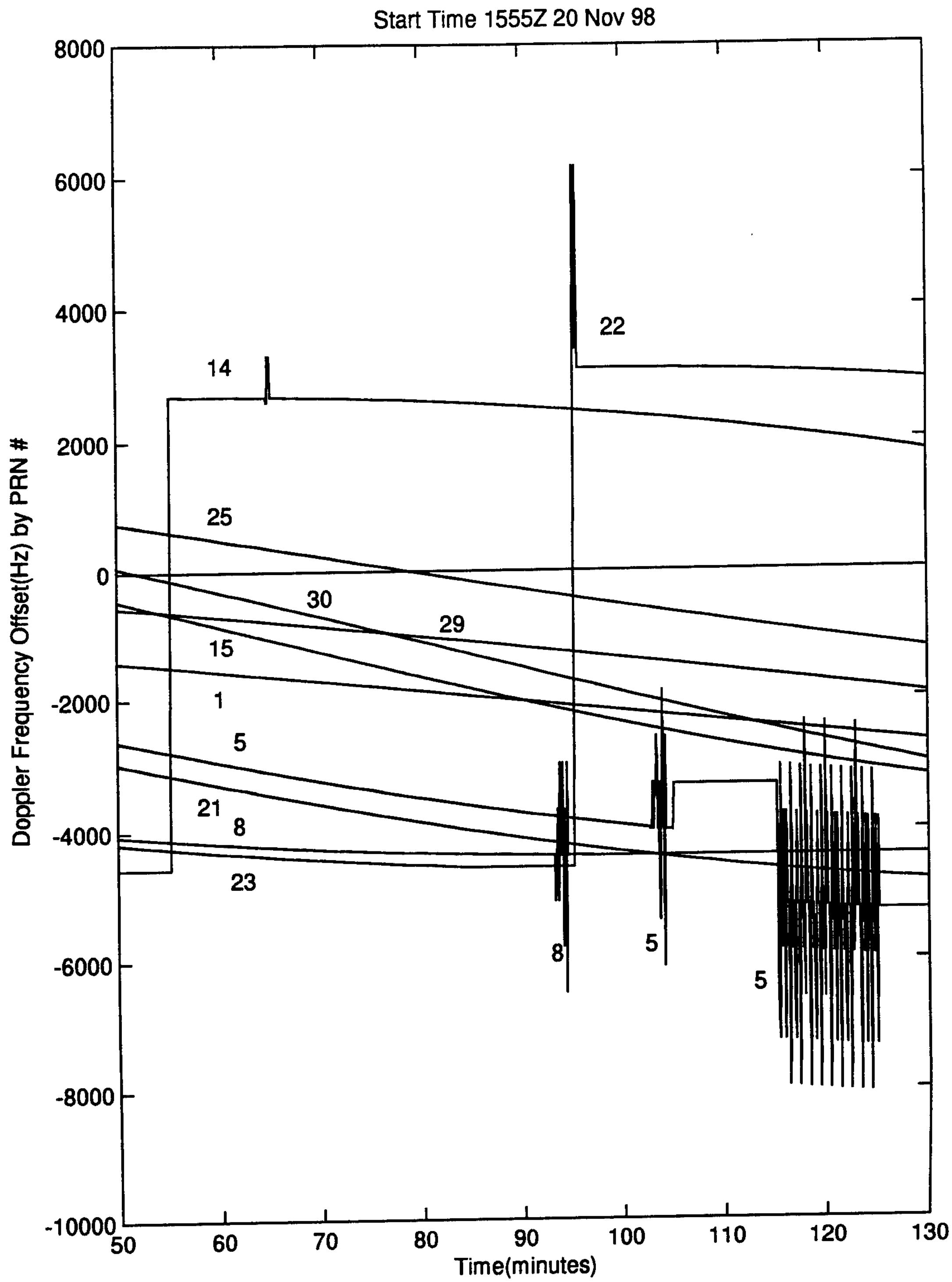

Figure I.8. Doppler Frequency vs Time

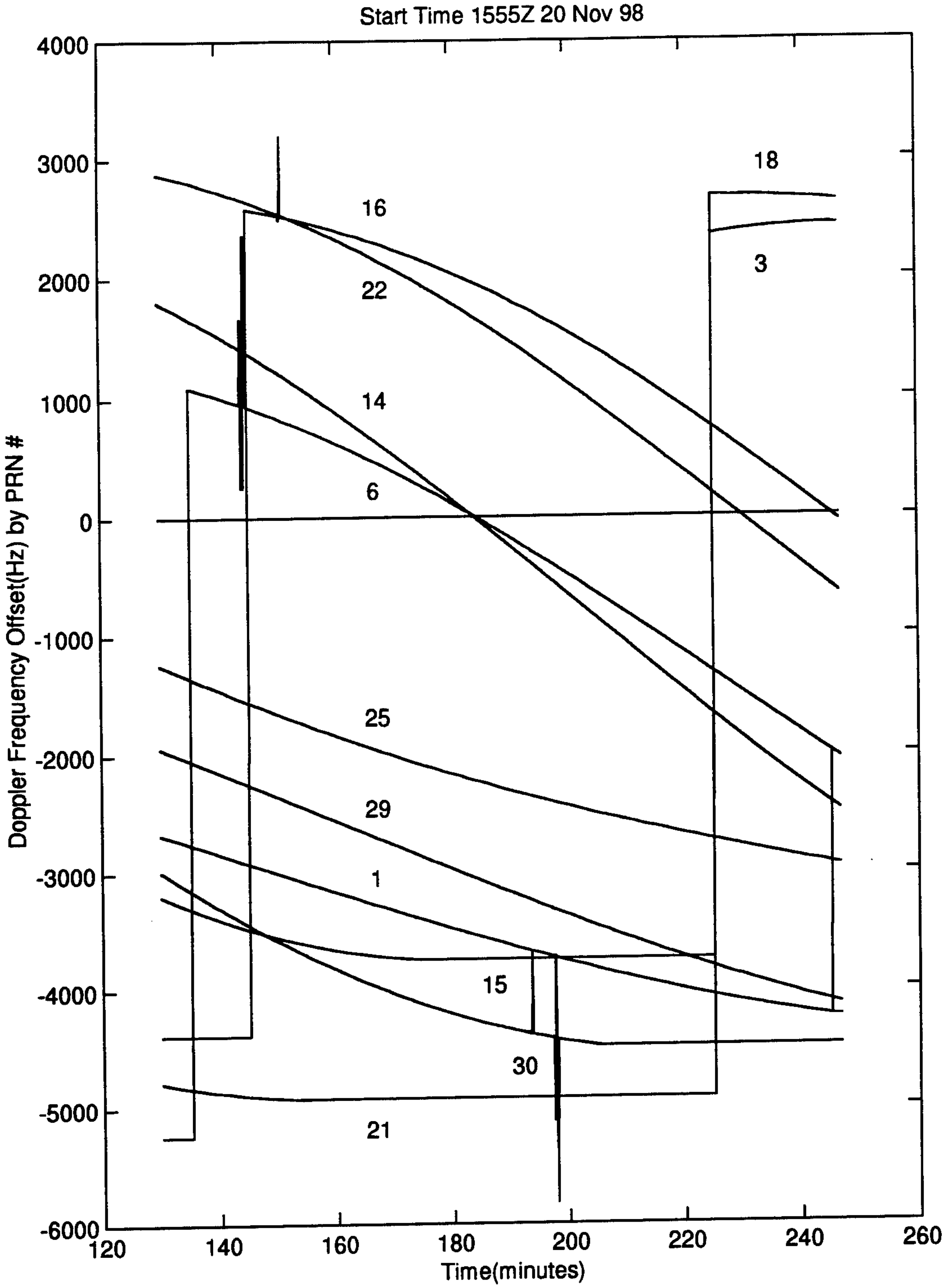

Figure I.9. Doppler Frequency vs Time

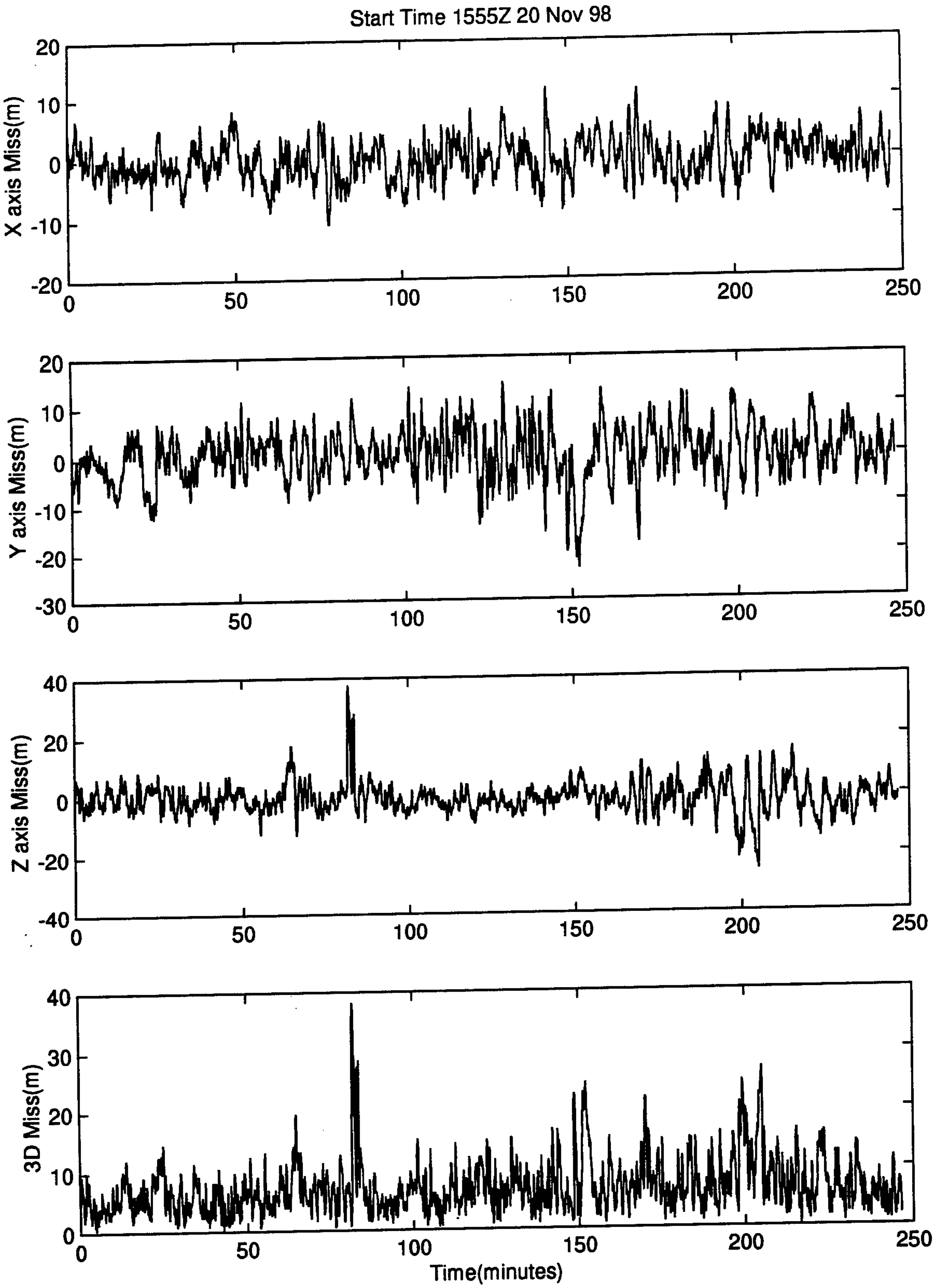

Figure I.10. X,Y,Z and 3D Error(m) vs Time

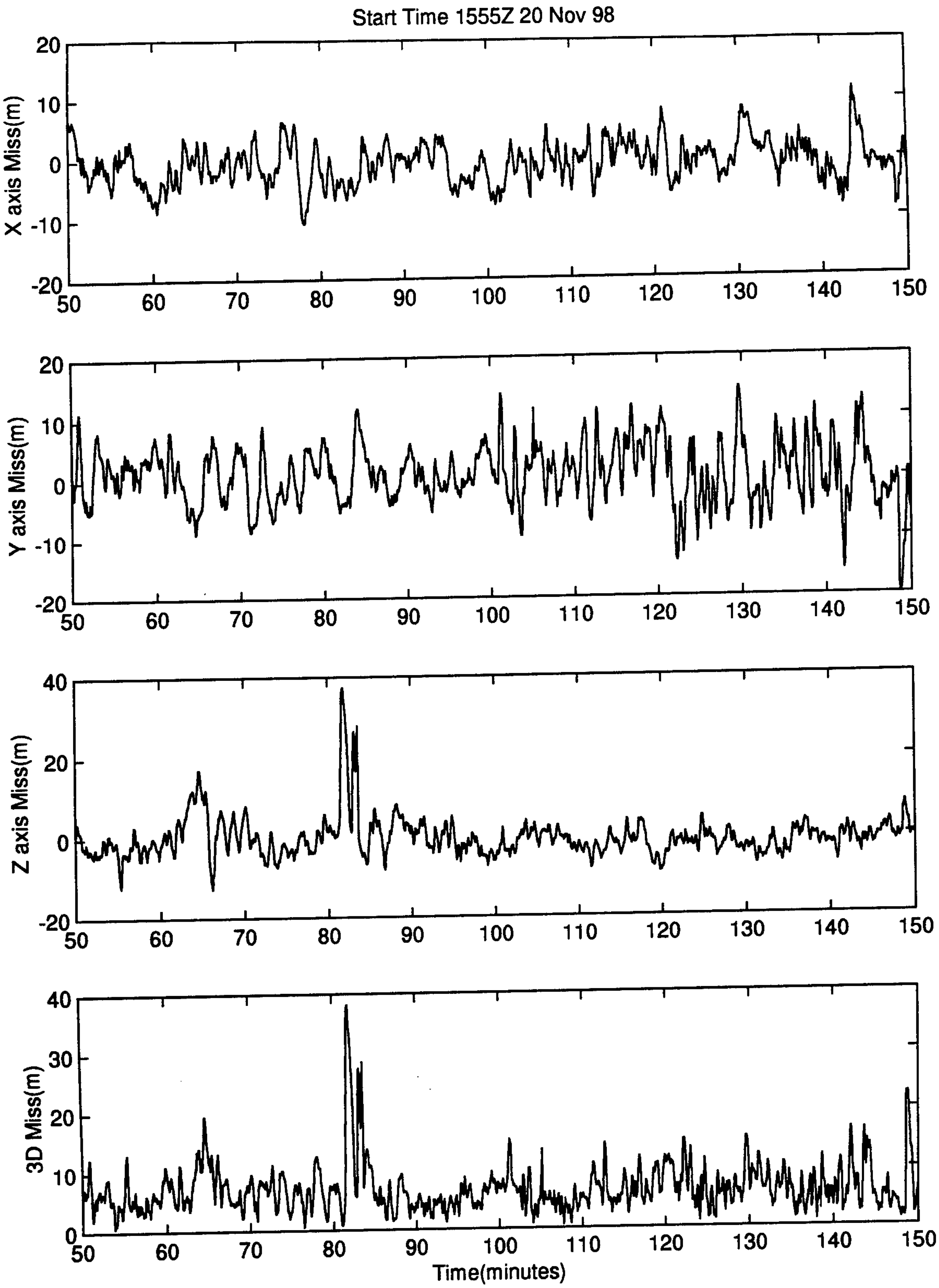

Figure I.11. X,Y,Z and 3D Error(m) vs Time

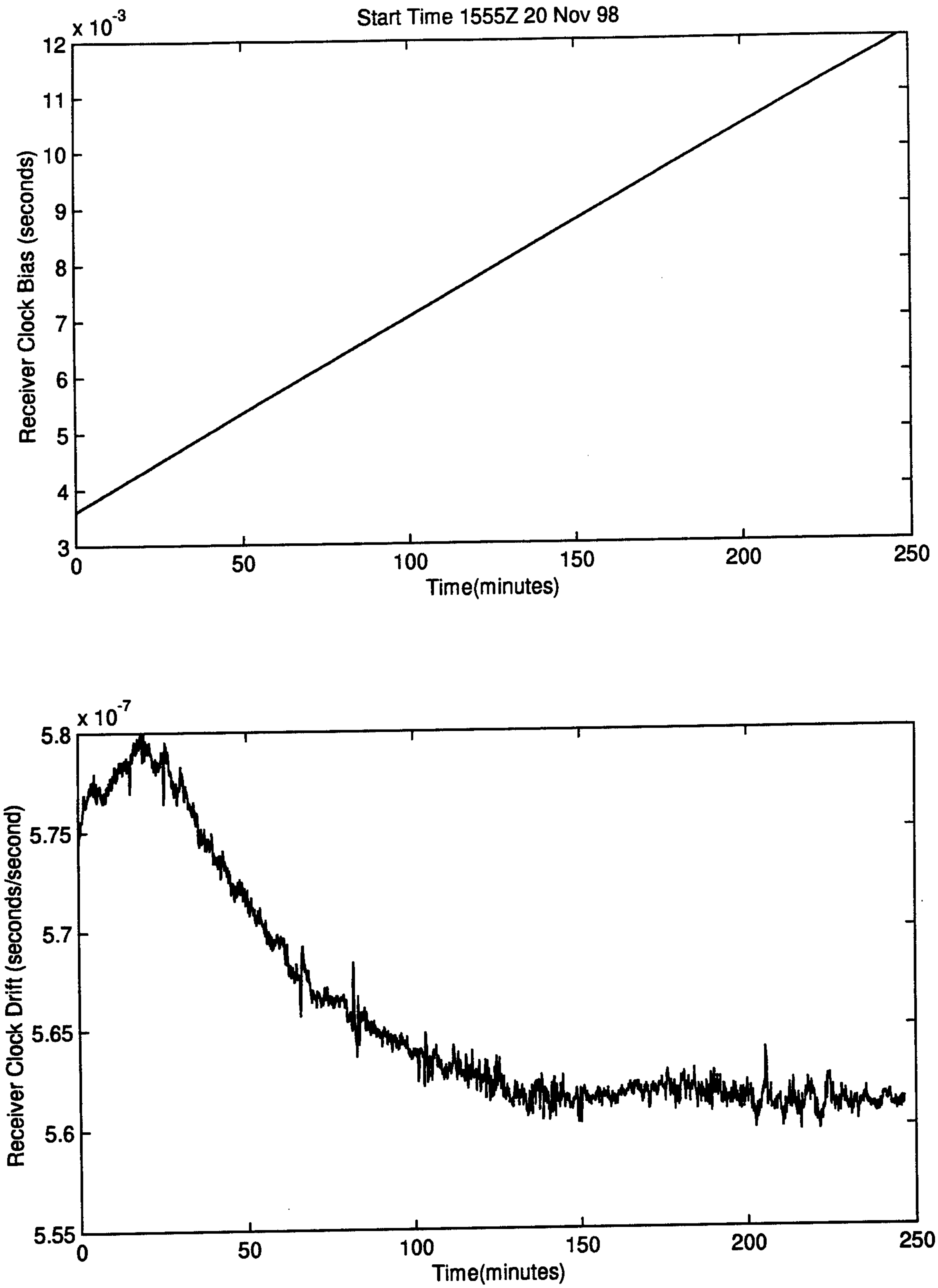

Figure I.12. Receiver Clock Bias and Drift vs Time

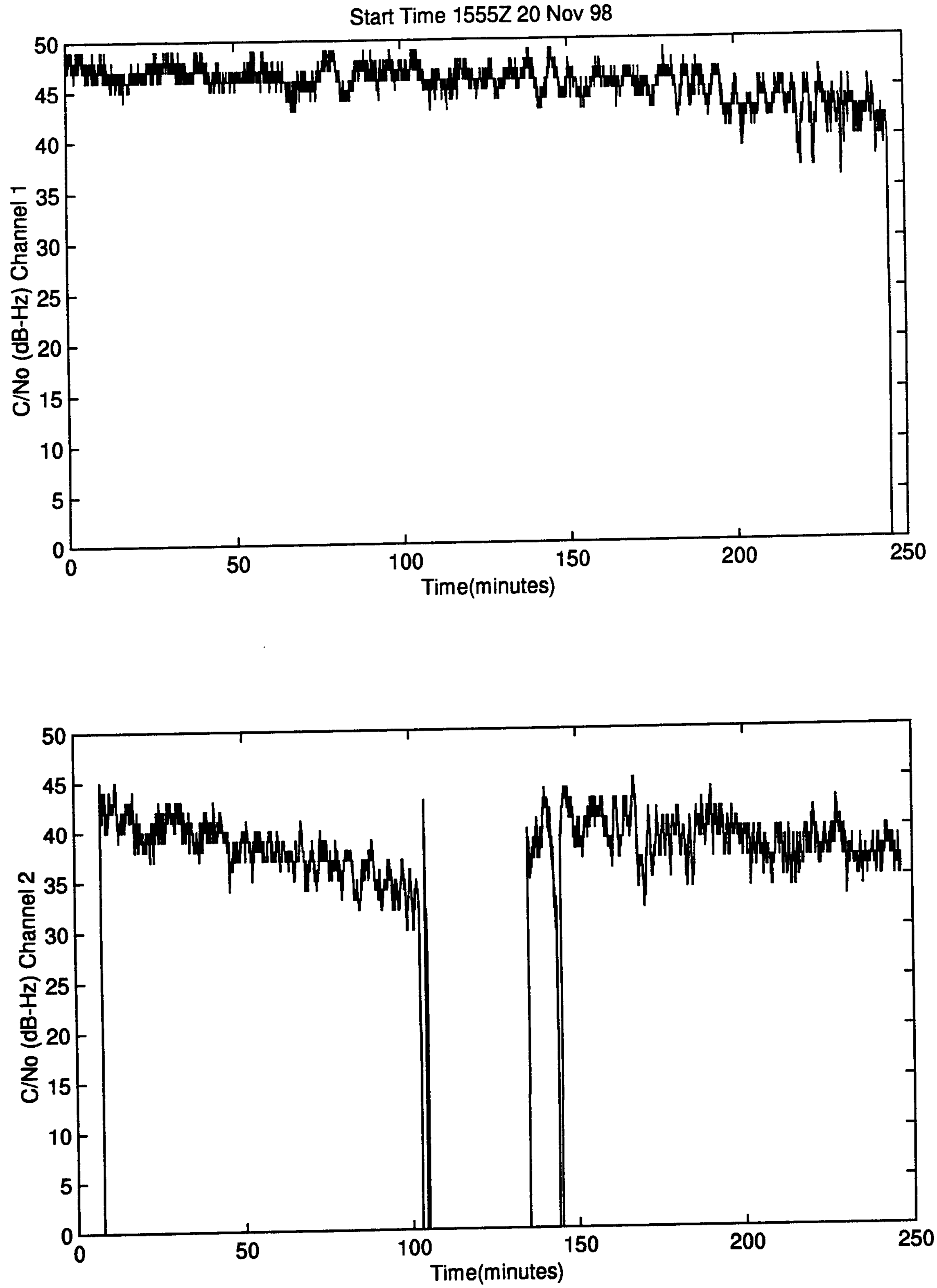

Figure I.13. C/No vs Time

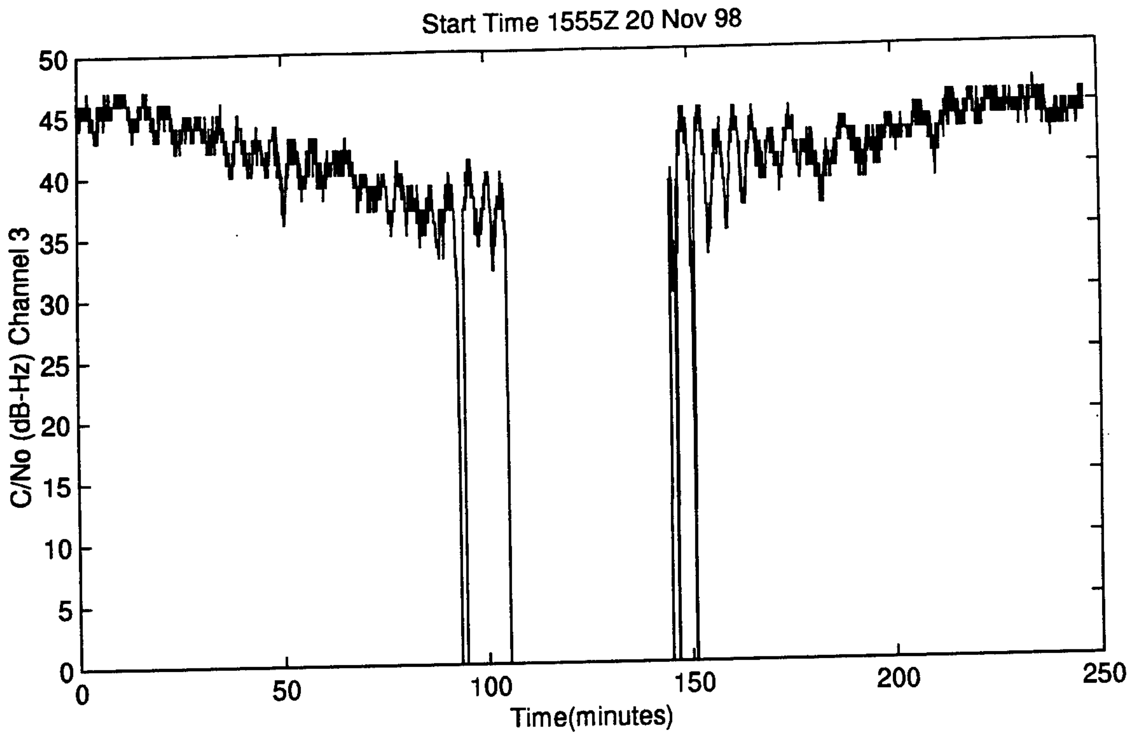

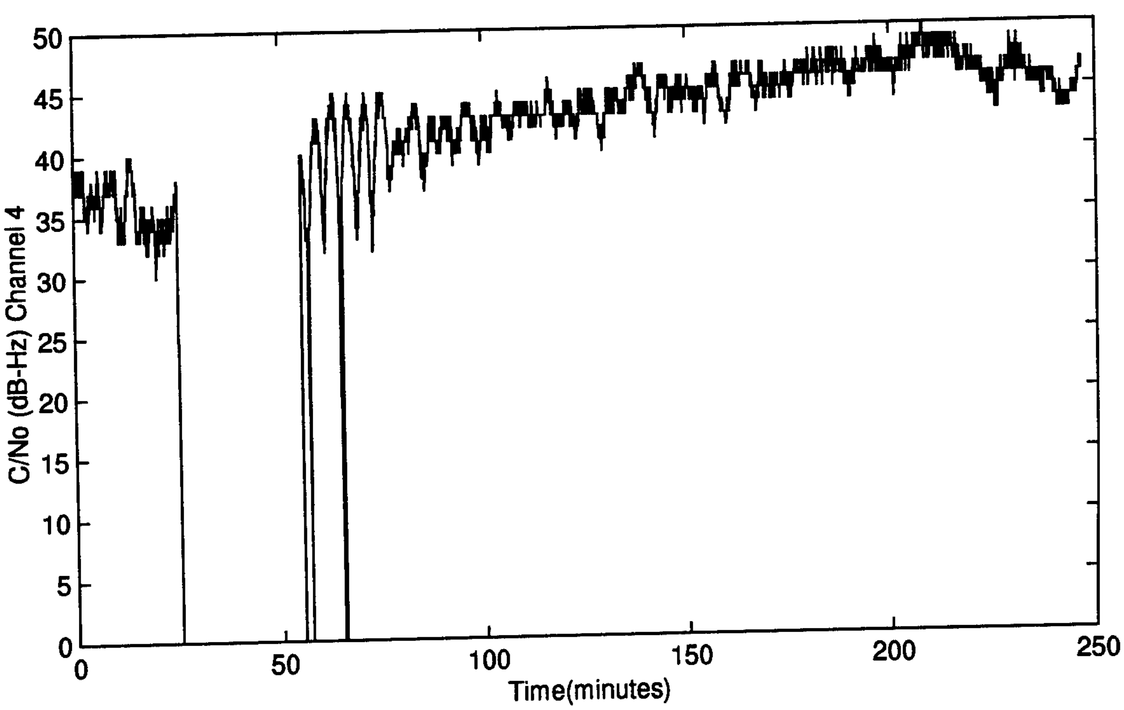

Figure I.14. C/No vs Time

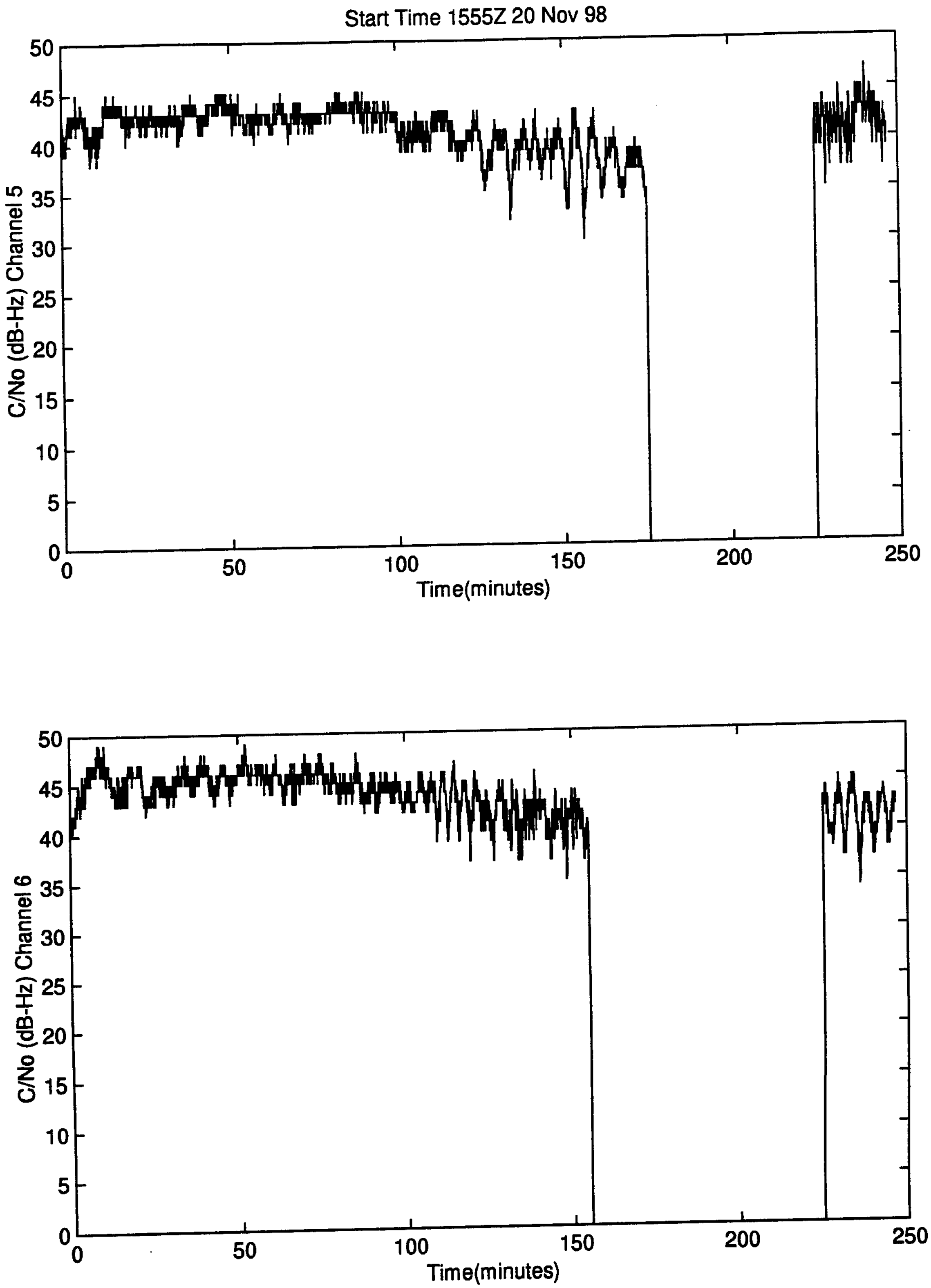

Figure I.15. C/No vs Time

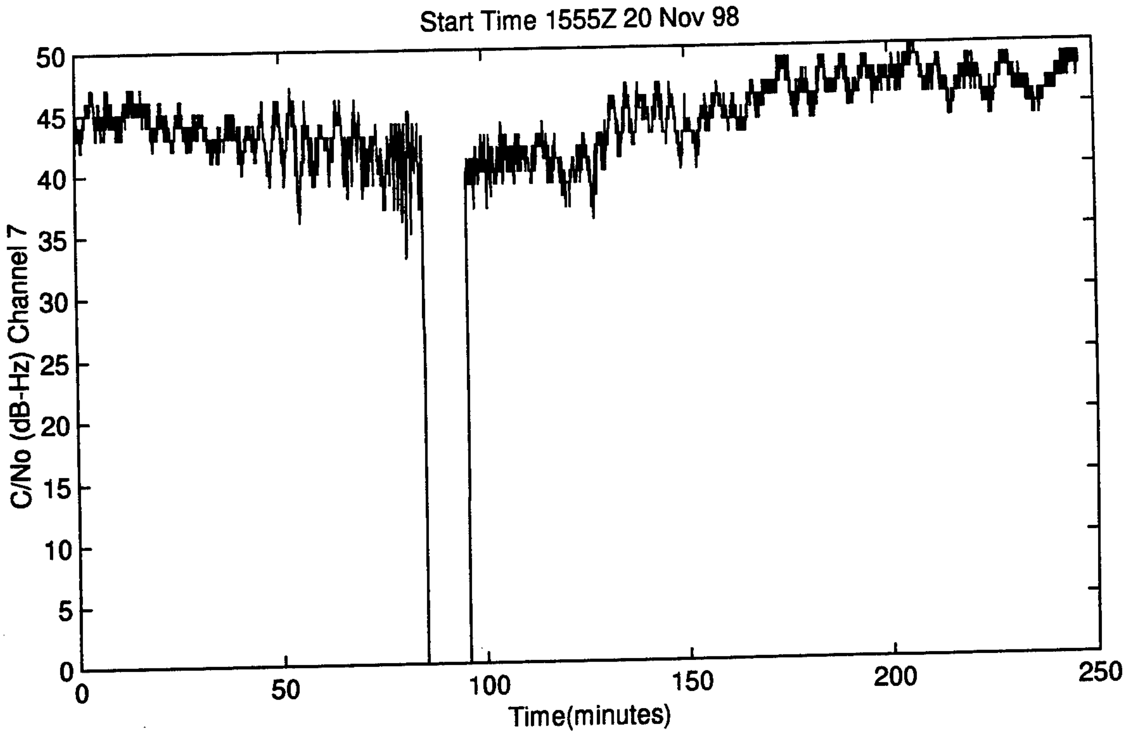

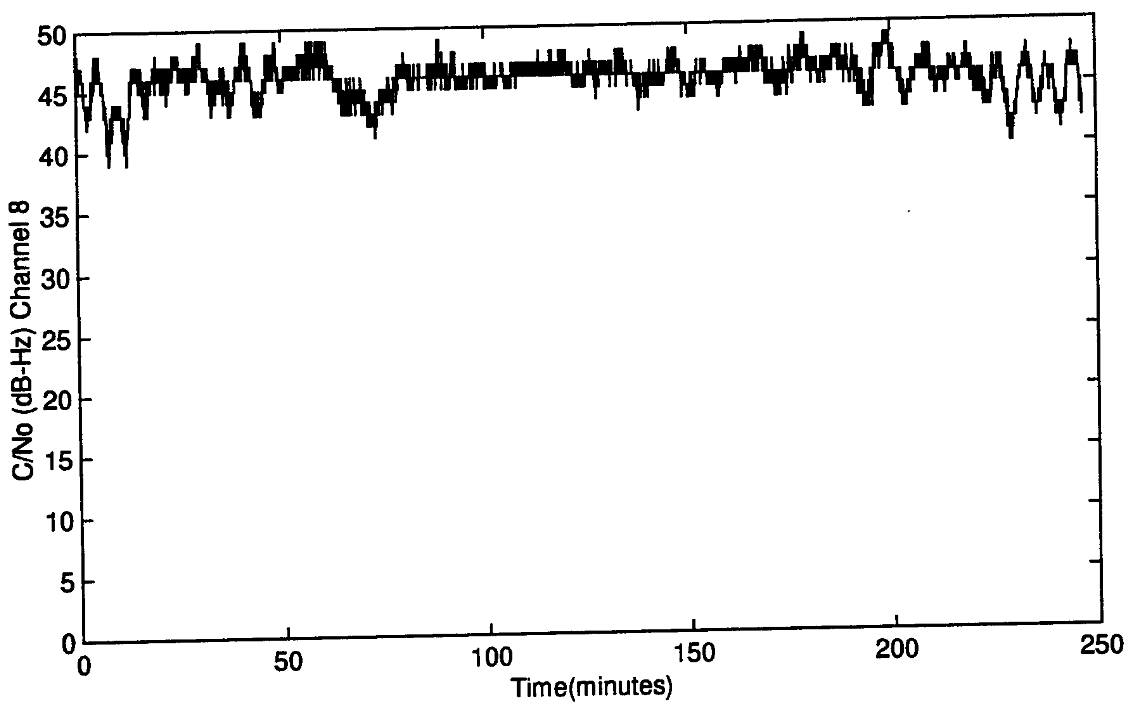

Figure I.16. C/No vs Time

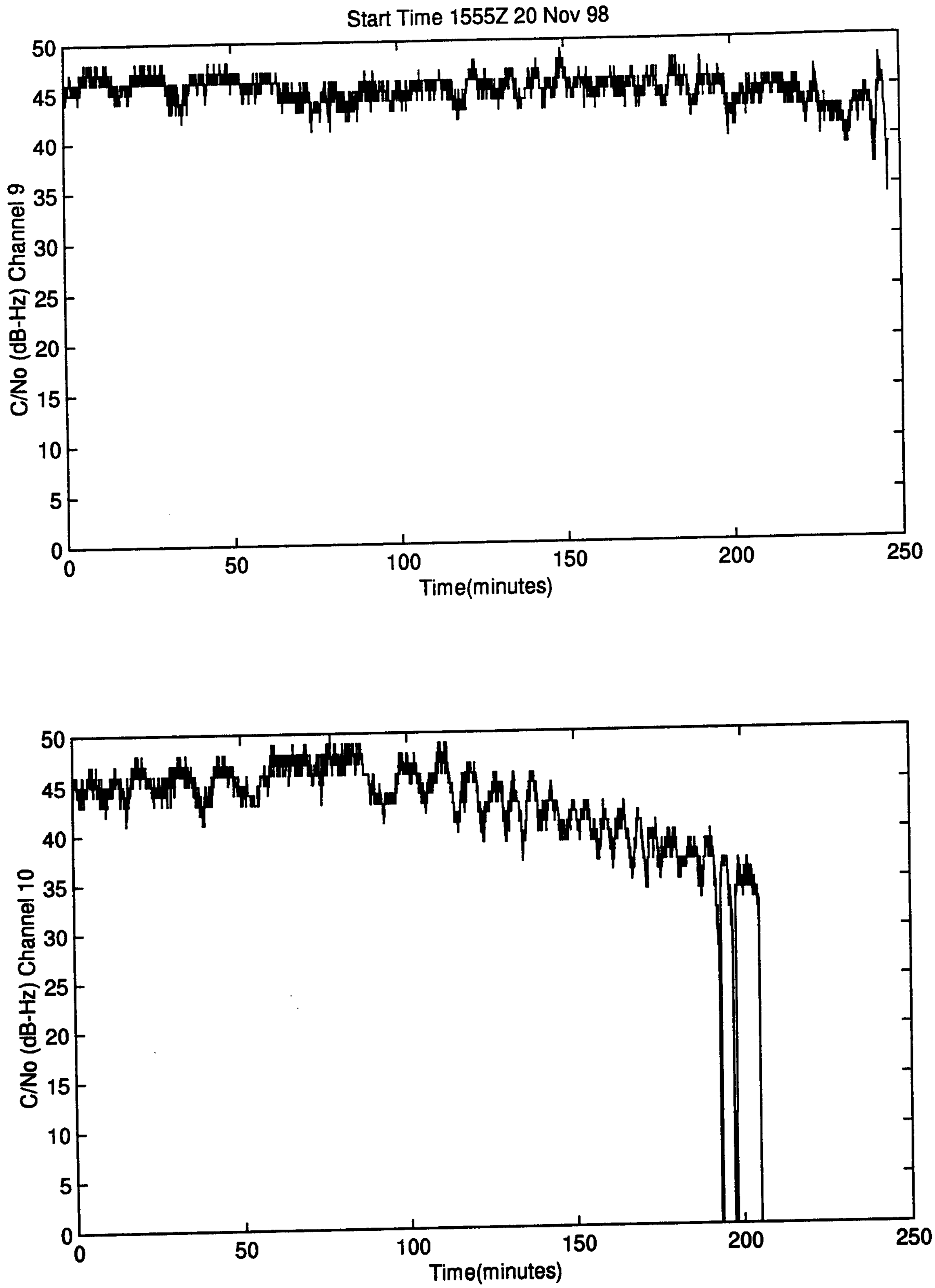

Figure I.17. C/No vs Time

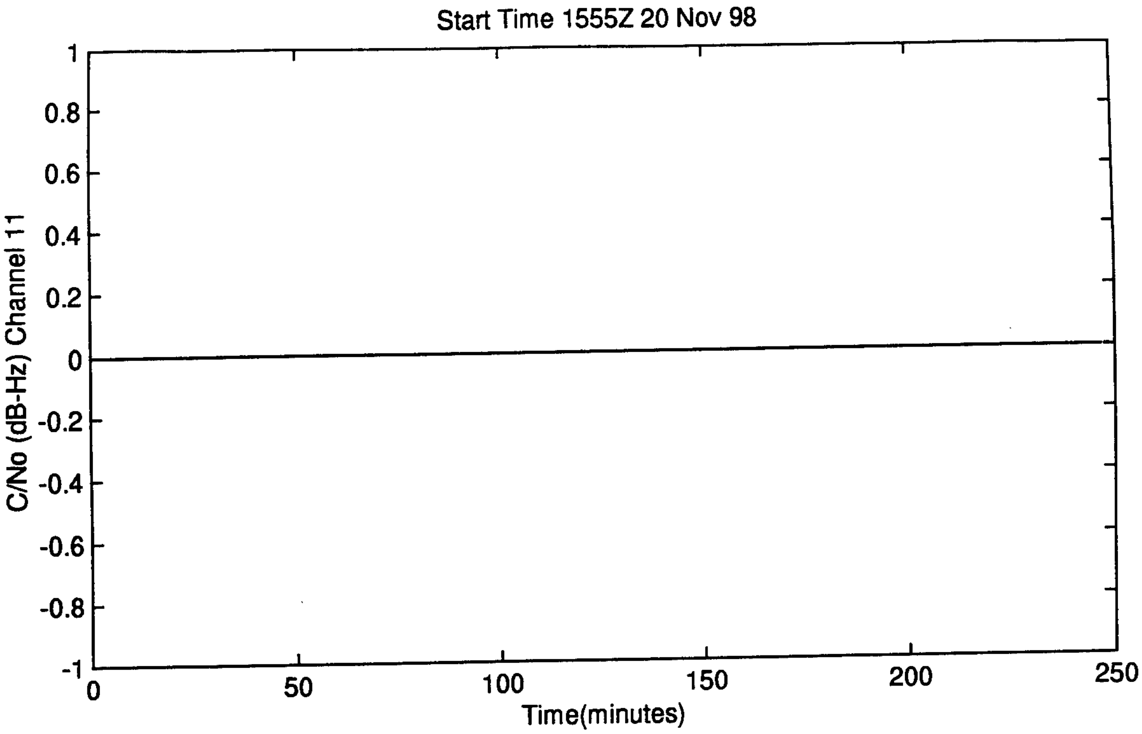

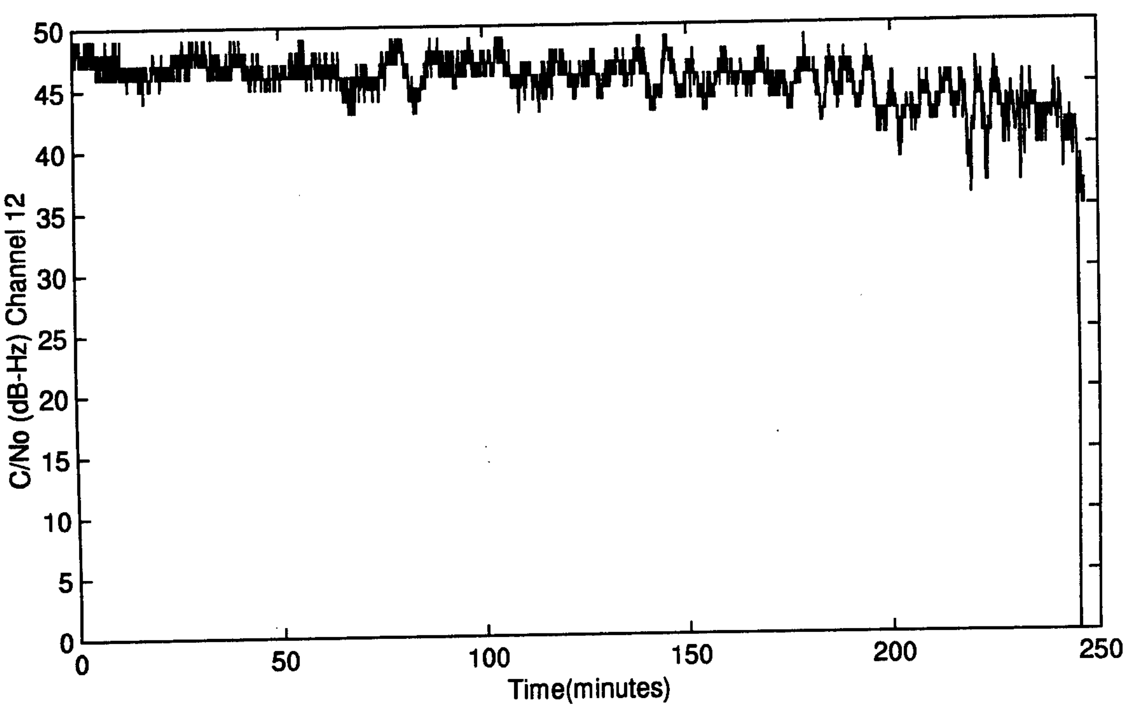

Figure I.18. C/No vs Time

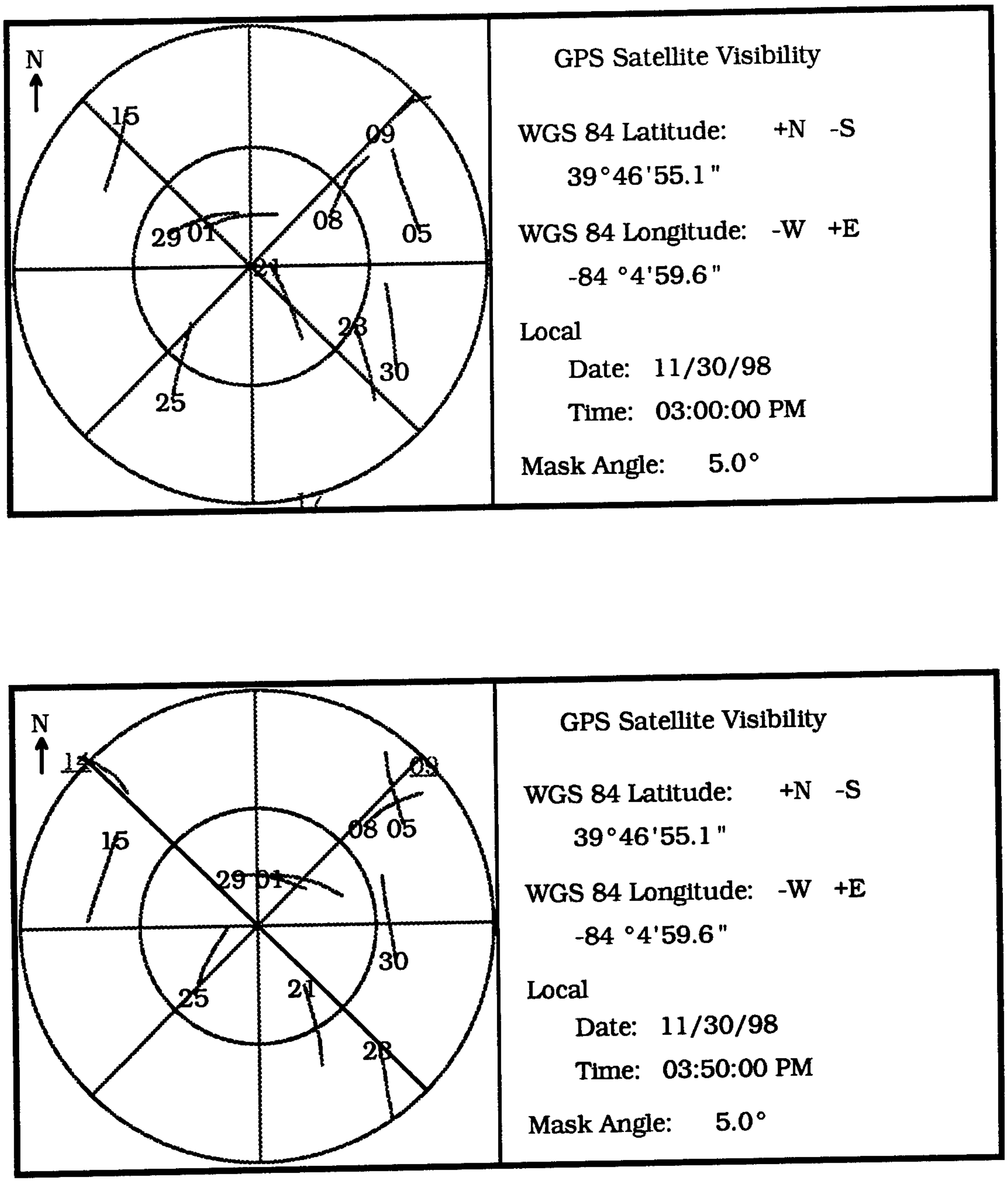

Figure J.1. GPS Satellites In View 30 Nov 98

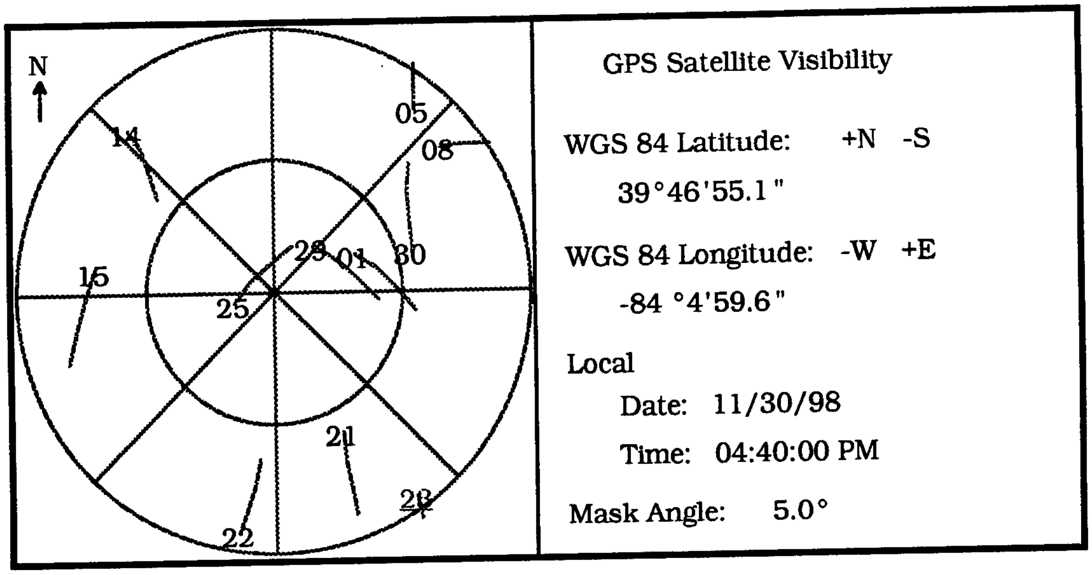

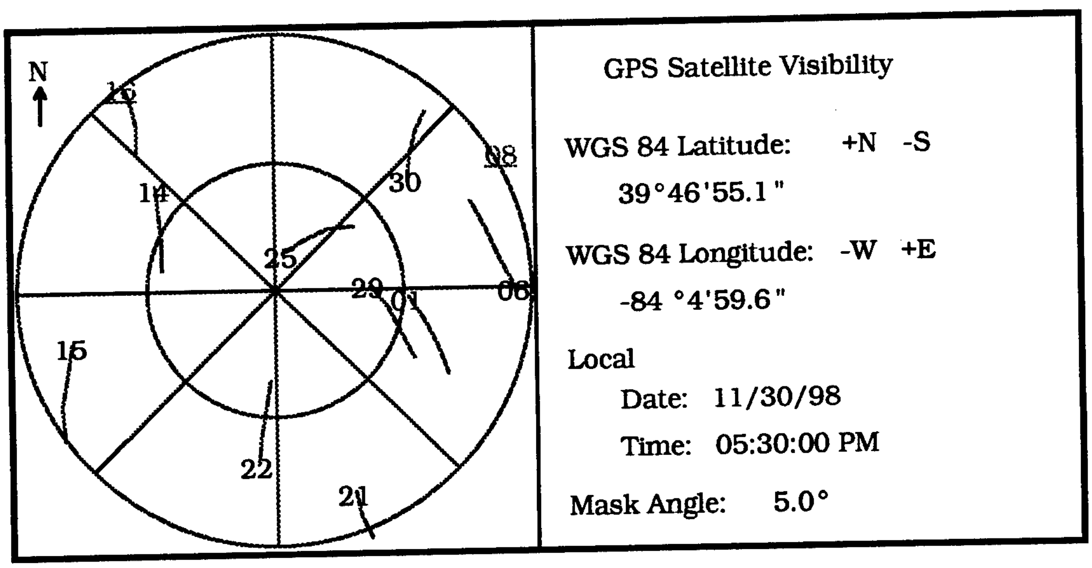

Figure J.2. GPS Satellites In View 30 Nov 98

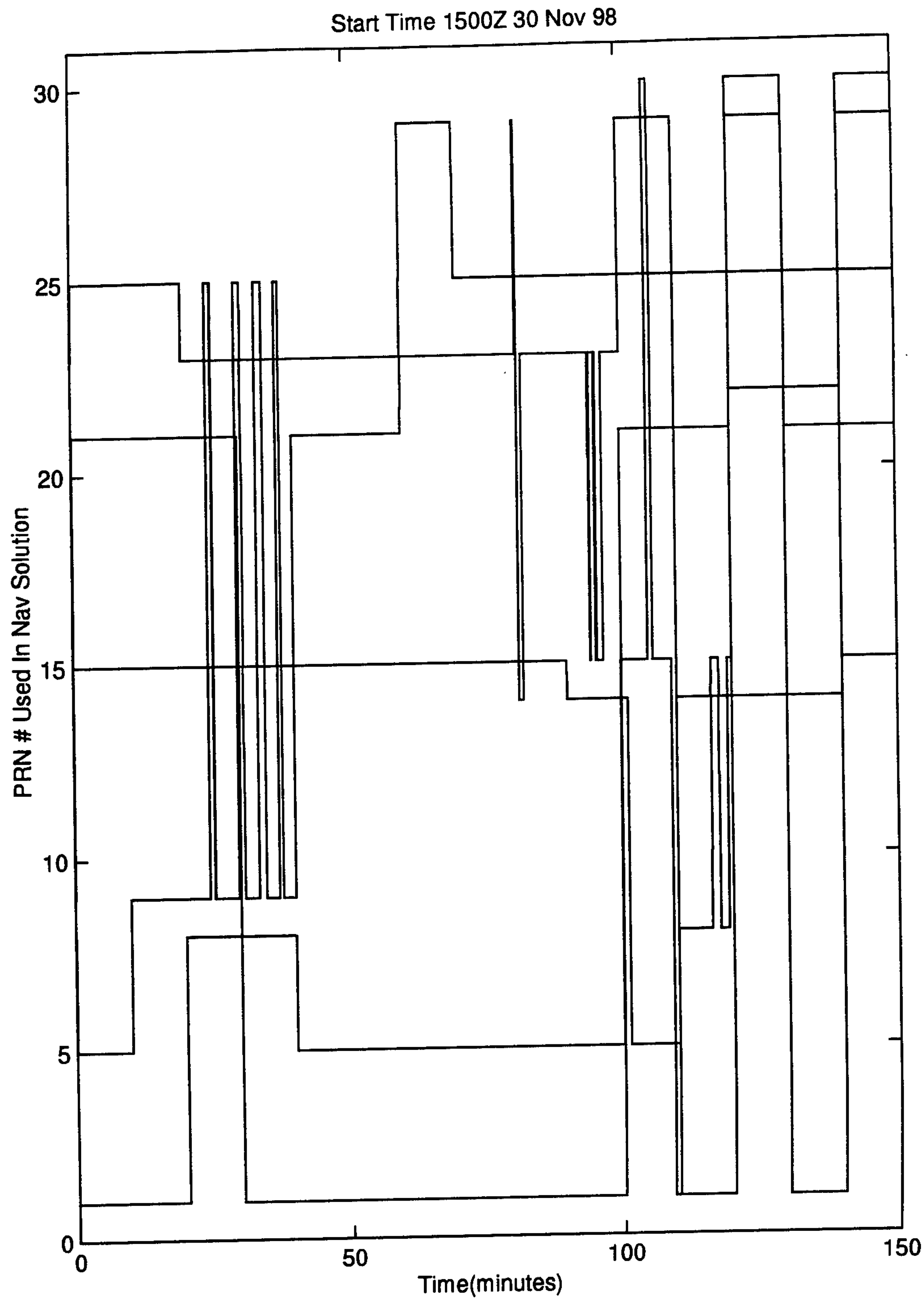

Figure J.3. PRN # Used In Nav Solution vs Time

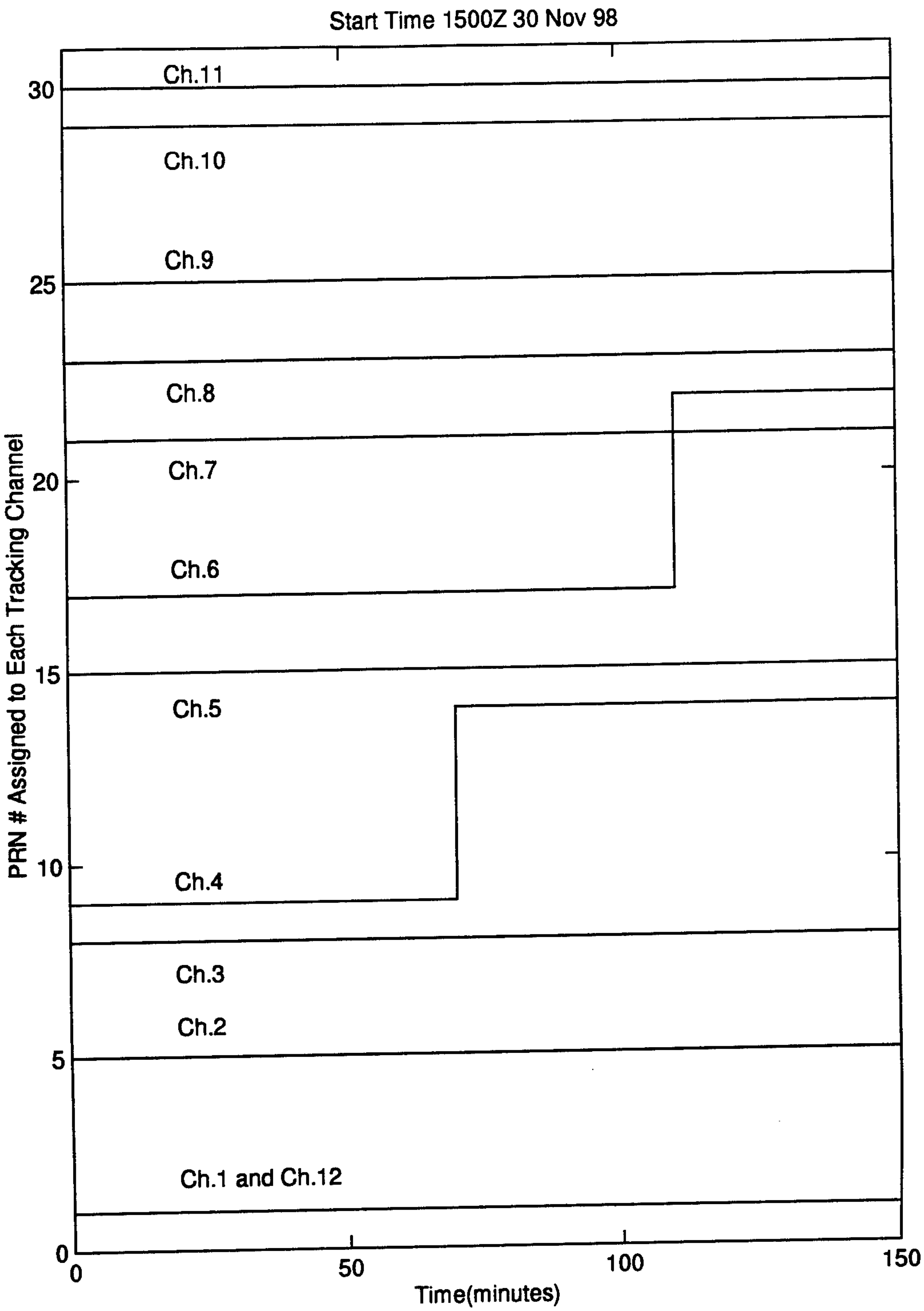

Figure J.4. PRN # Assigned to Each Tracking Channel vs Time

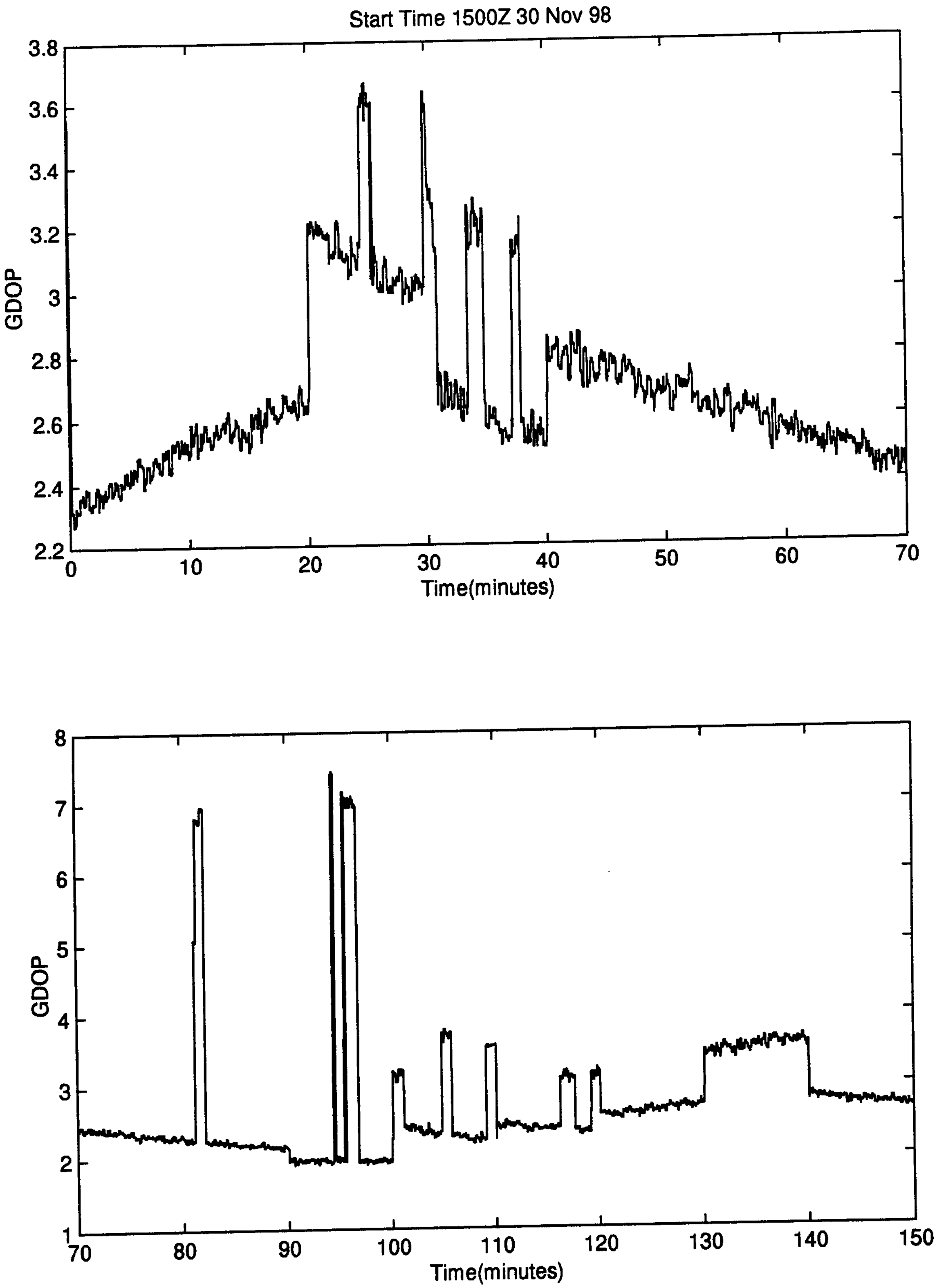

Figure J.5. GDOP vs Time

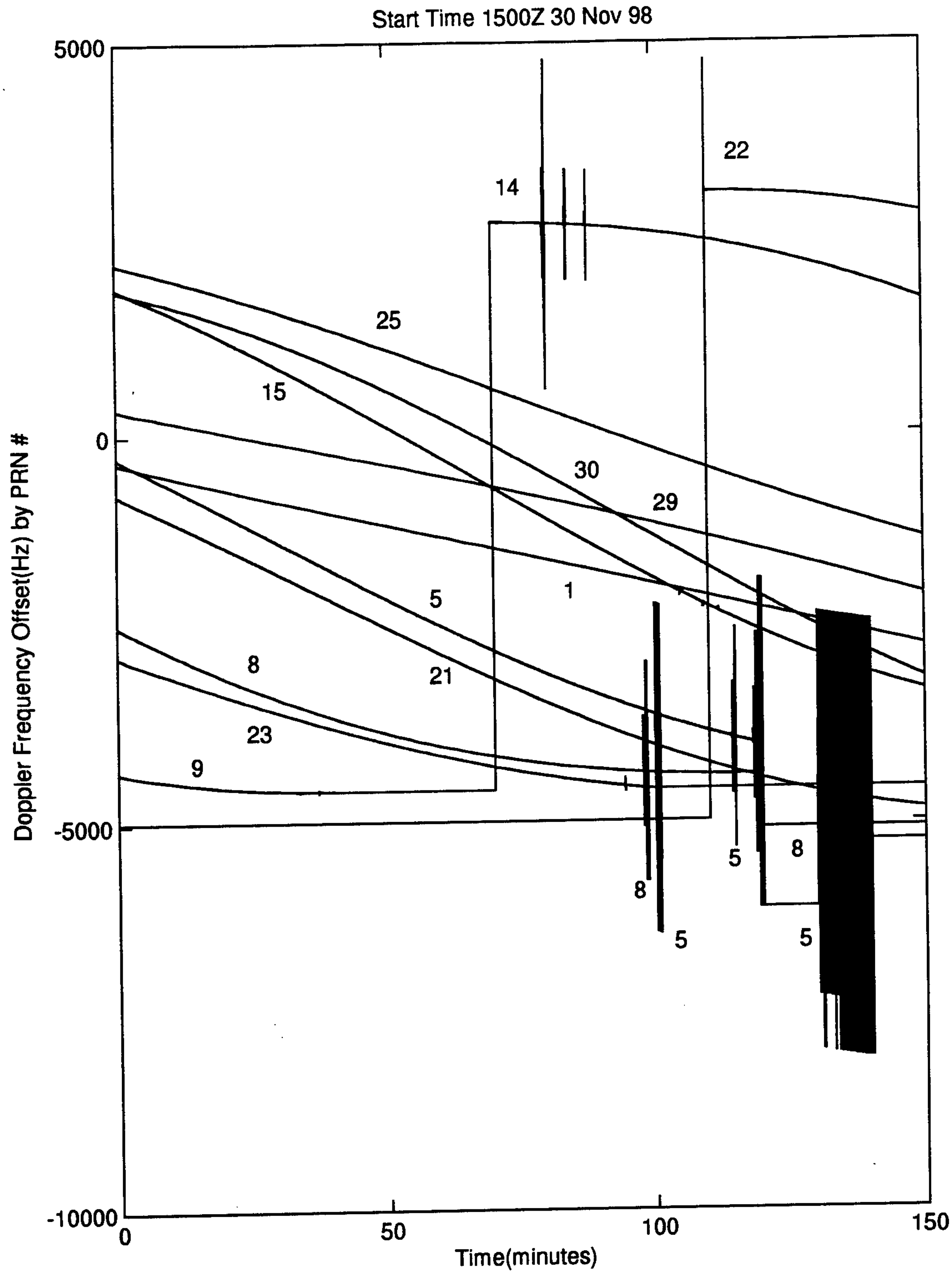

Figure J.6. Doppler Frequency vs Time

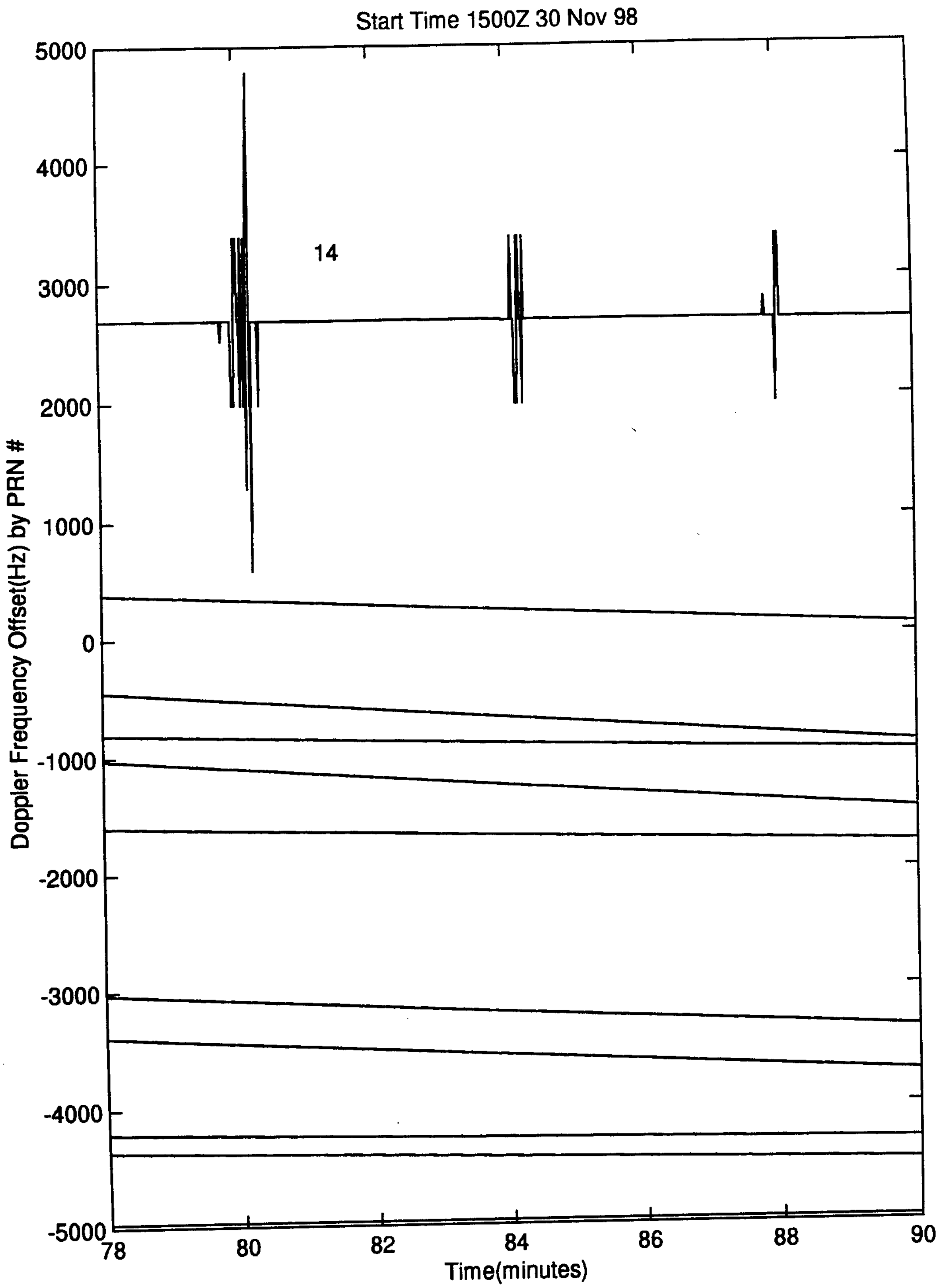

Figure J.7. Doppler Frequency vs Time

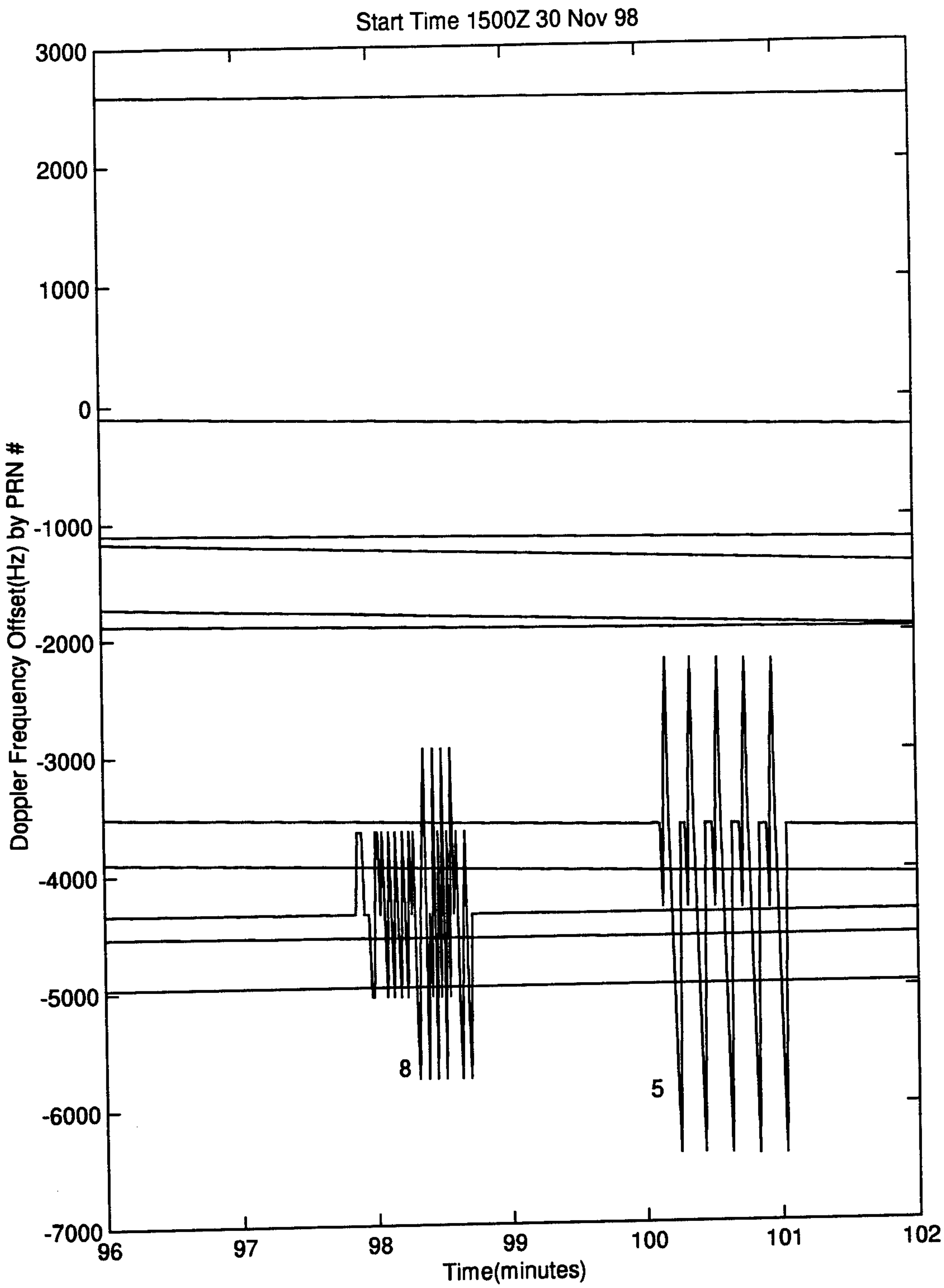

Figure J.8. Doppler Frequency vs Time

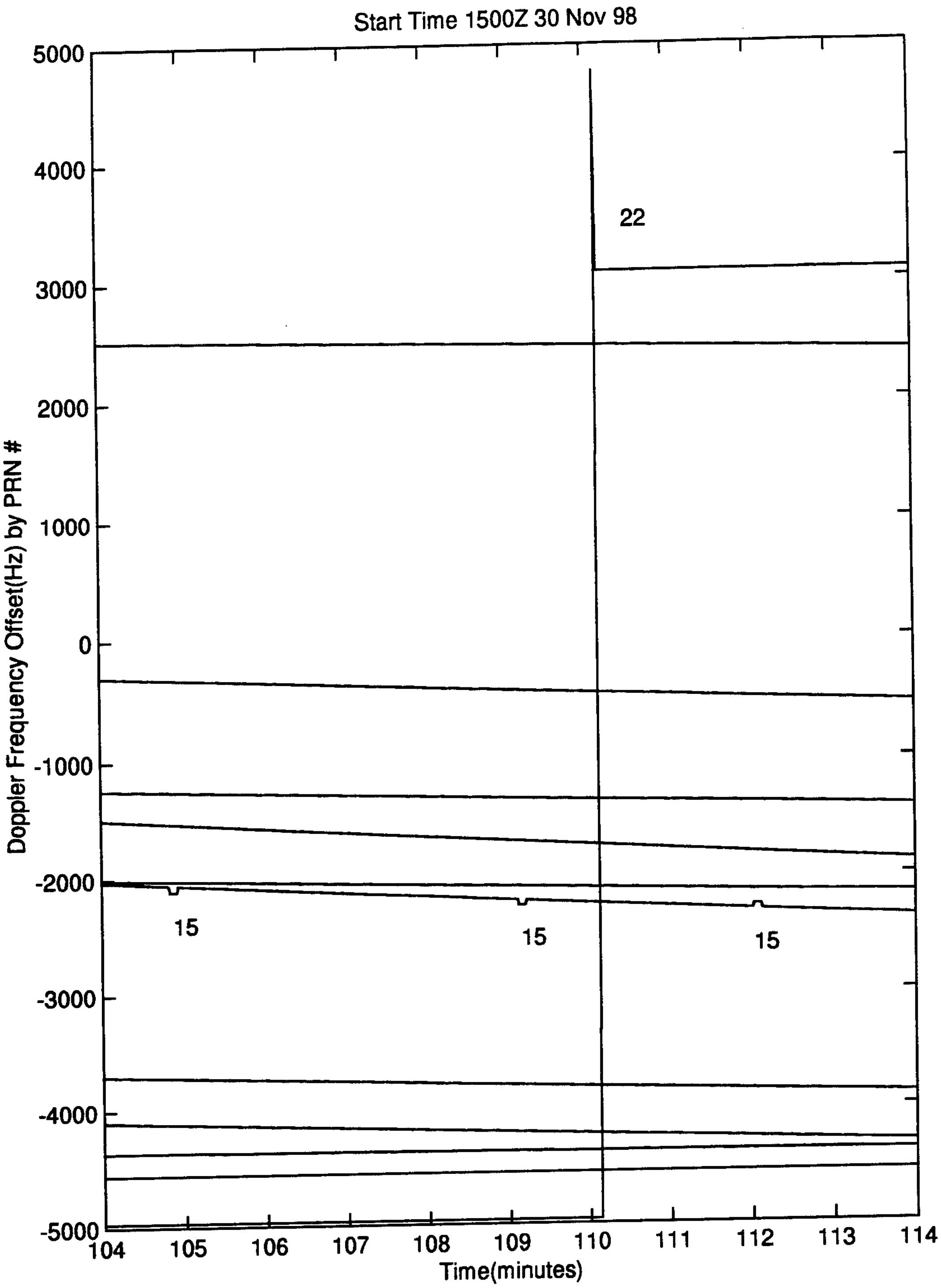

Figure J.9. Doppler Frequency vs Time

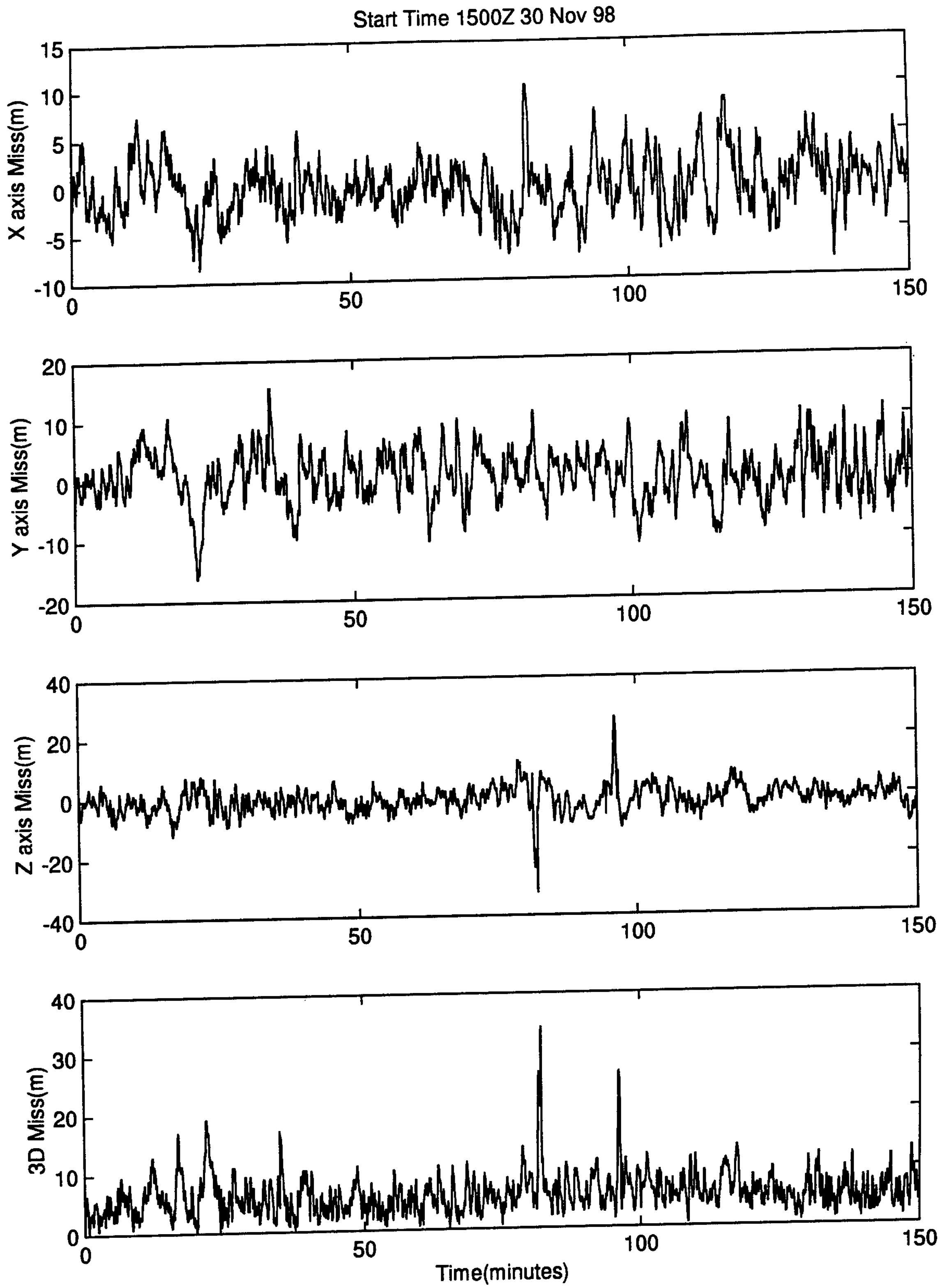

Figure J.10. X,Y,Z and 3D Error(m) vs Time

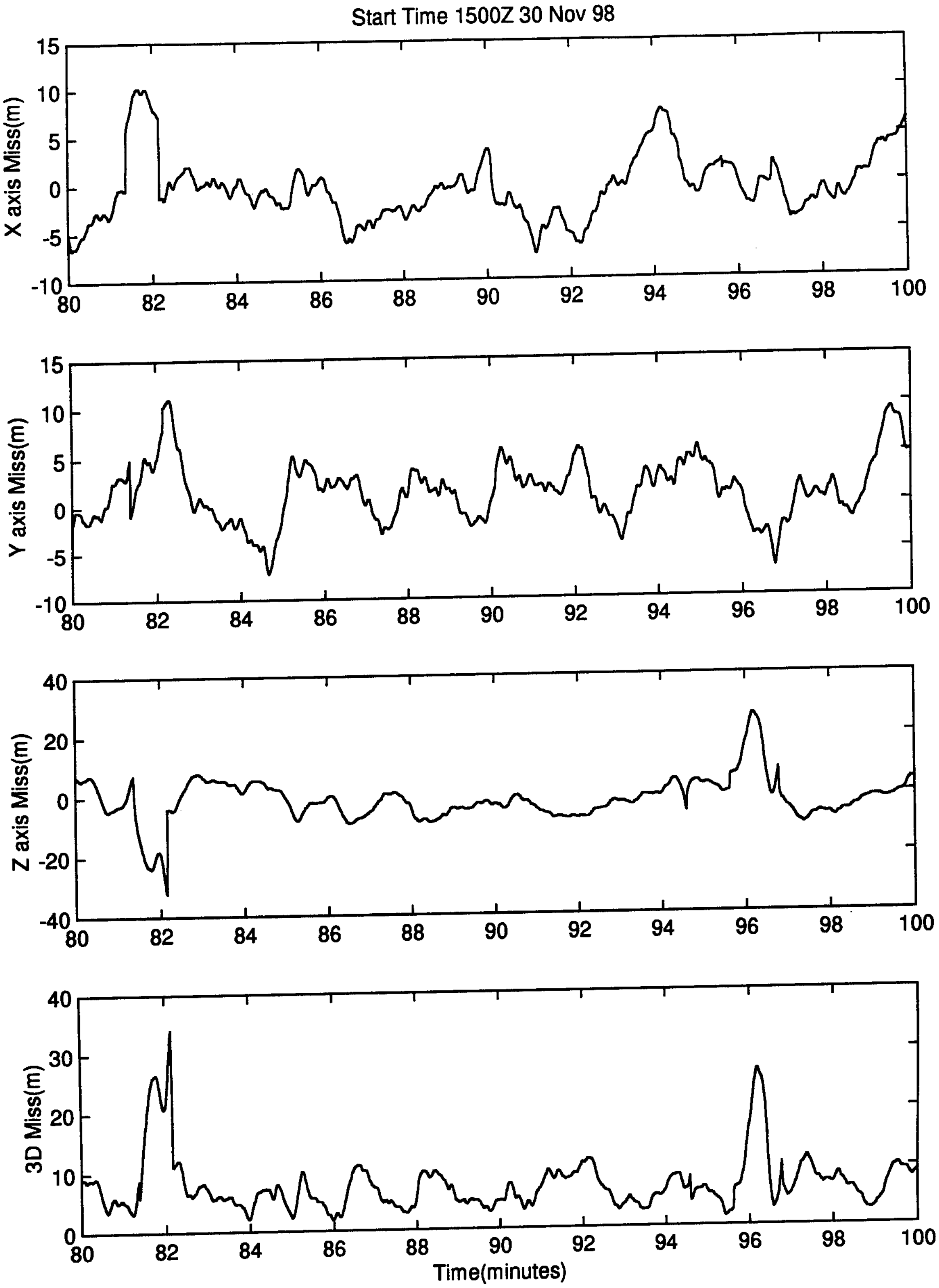

Figure J.11. X,Y,Z and 3D Error(m) vs Time

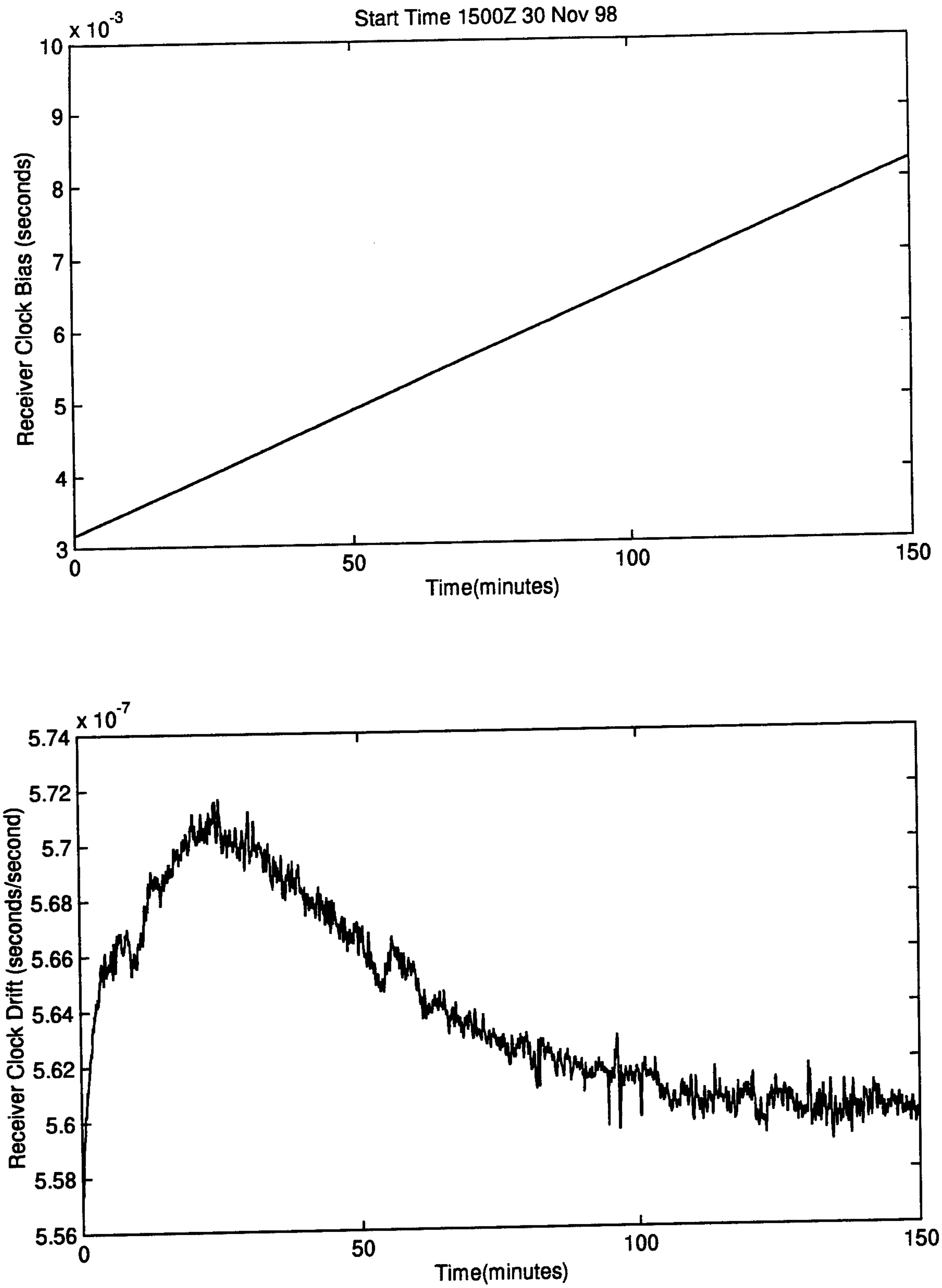

Figure J.12. Receiver Clock Bias and Drift vs Time

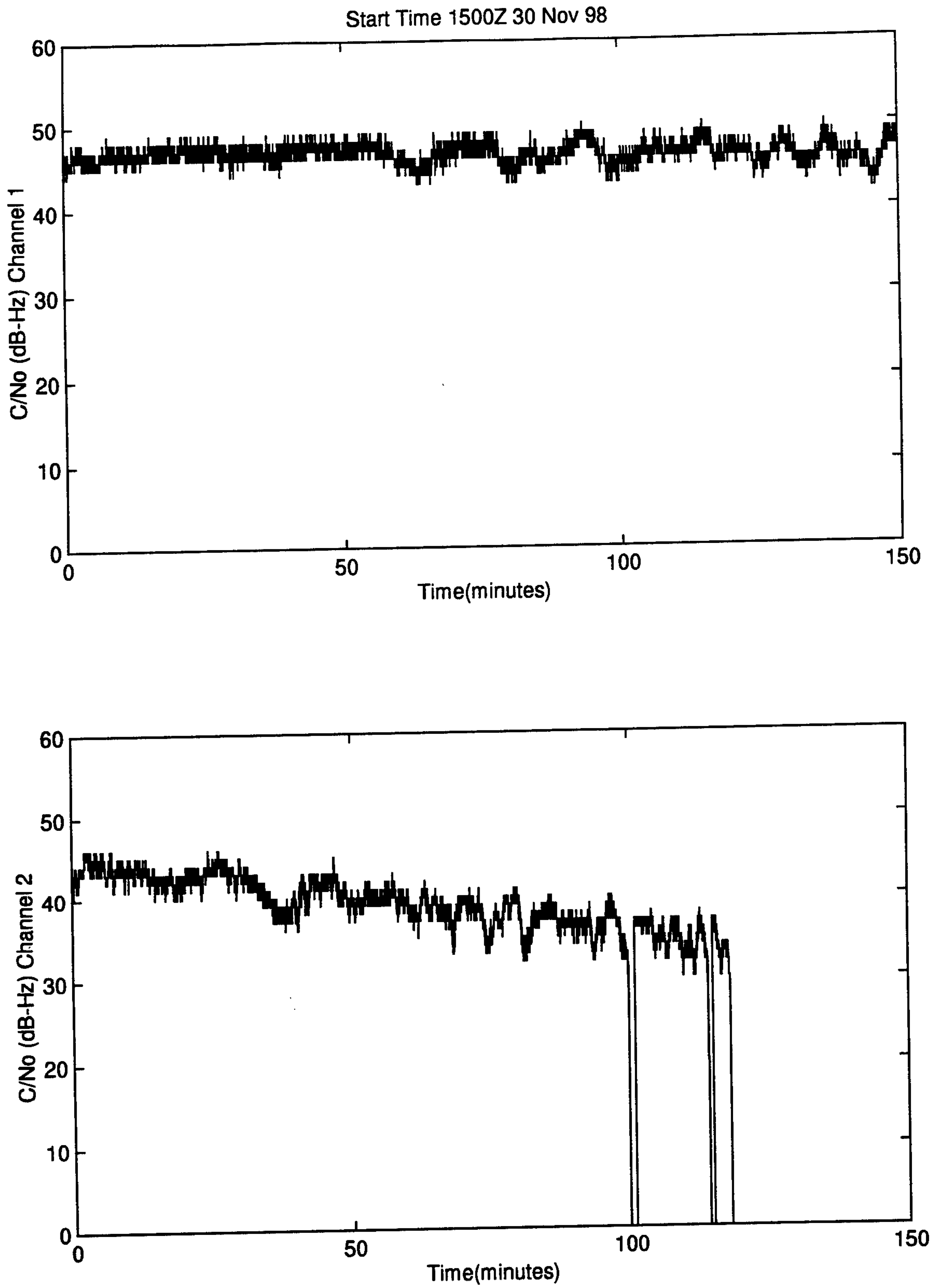

Figure J.13. C/No vs Time

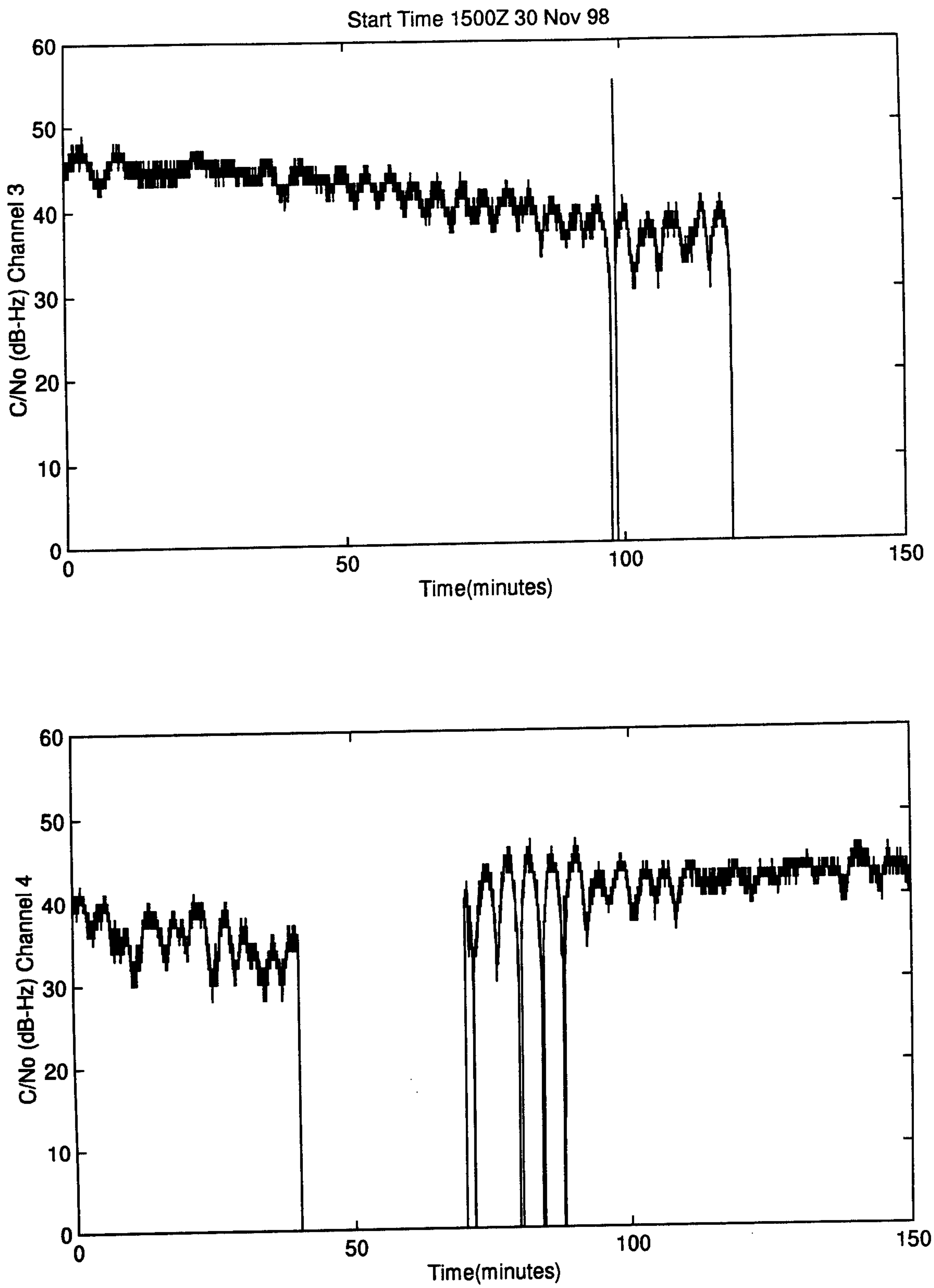

Figure J.14. C/No vs Time

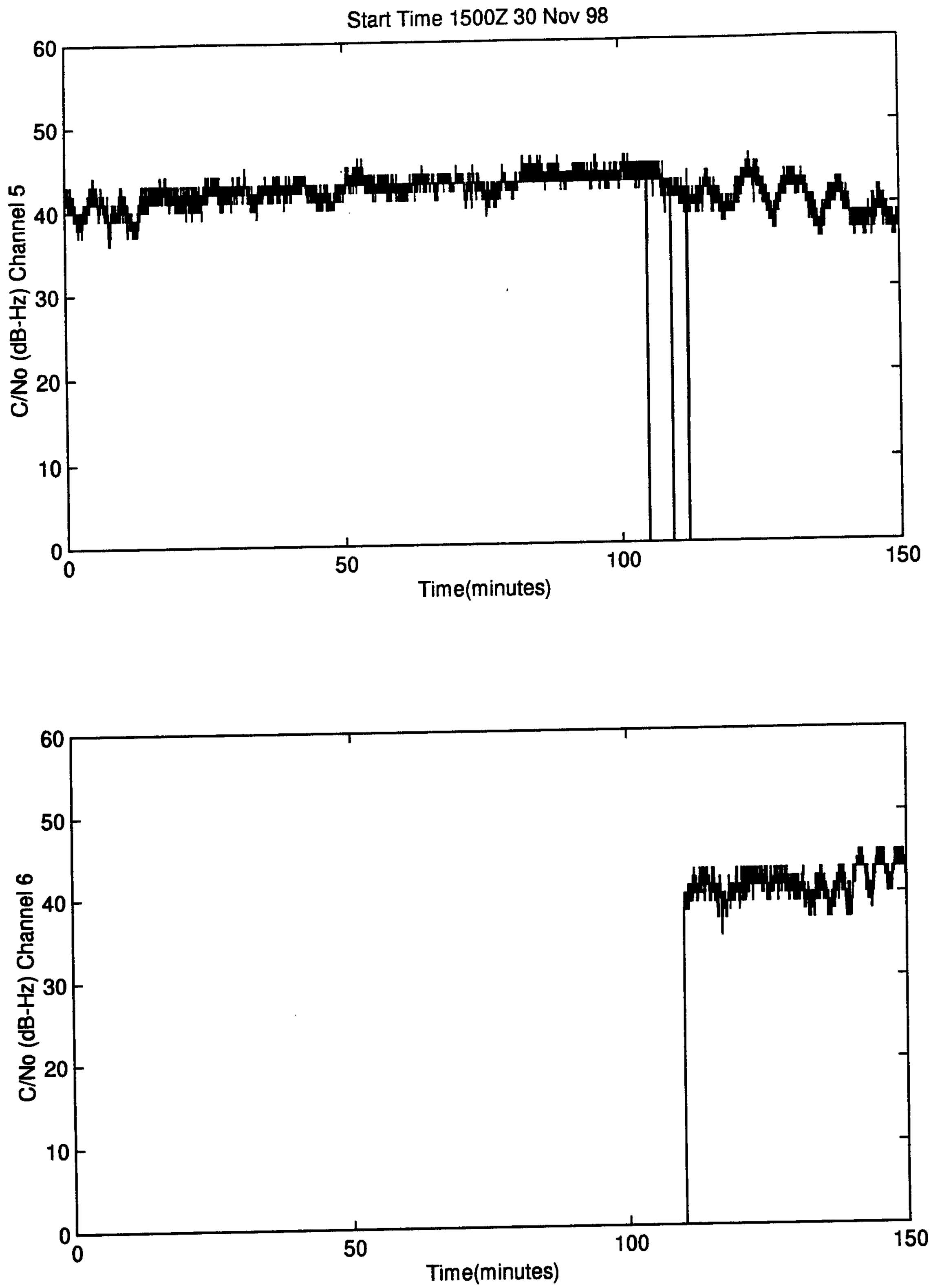

Figure J.15. C/No vs Time

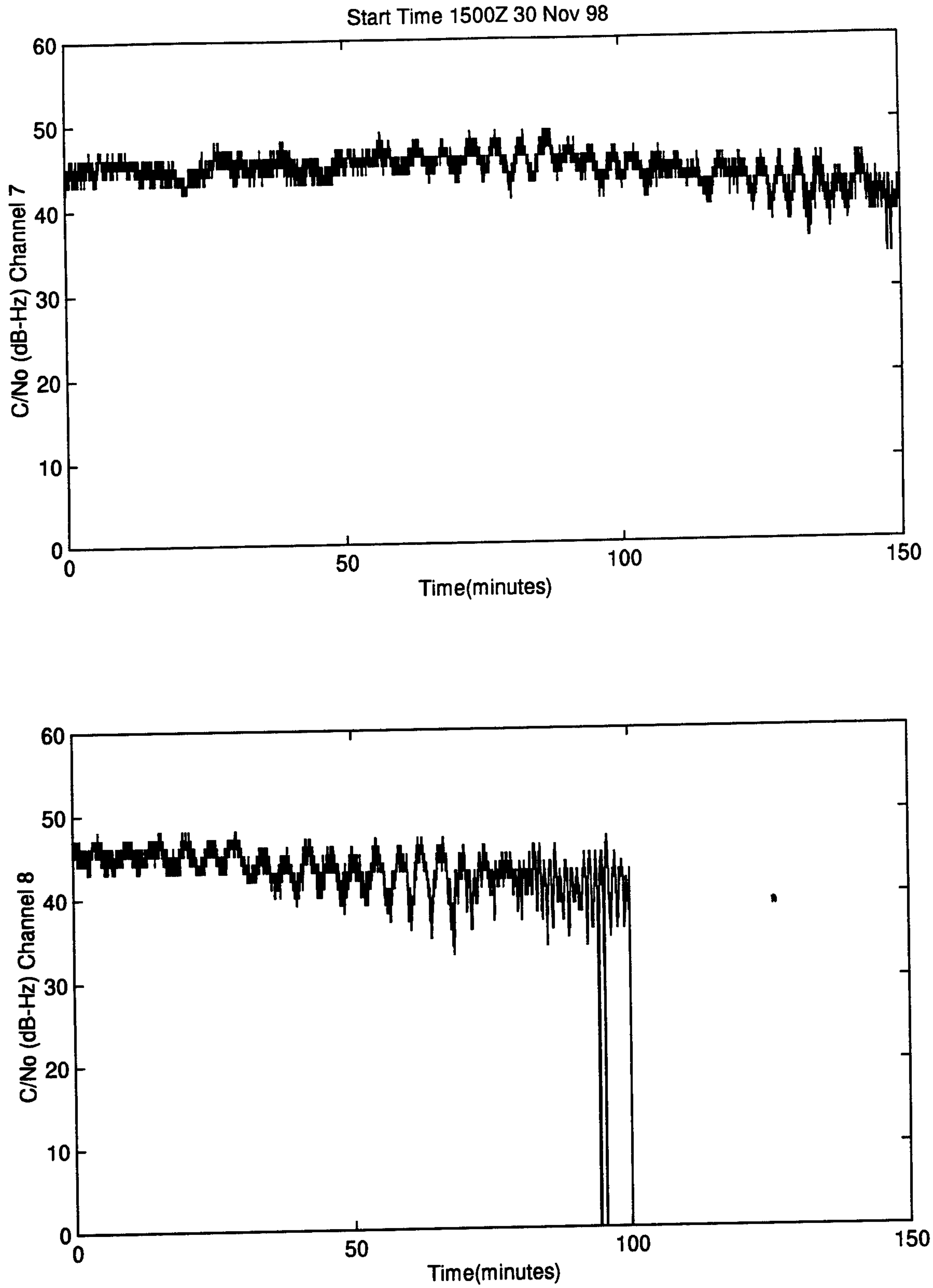

Figure J.16. C/No vs Time

Start Time 1500Z 30 Nov 98

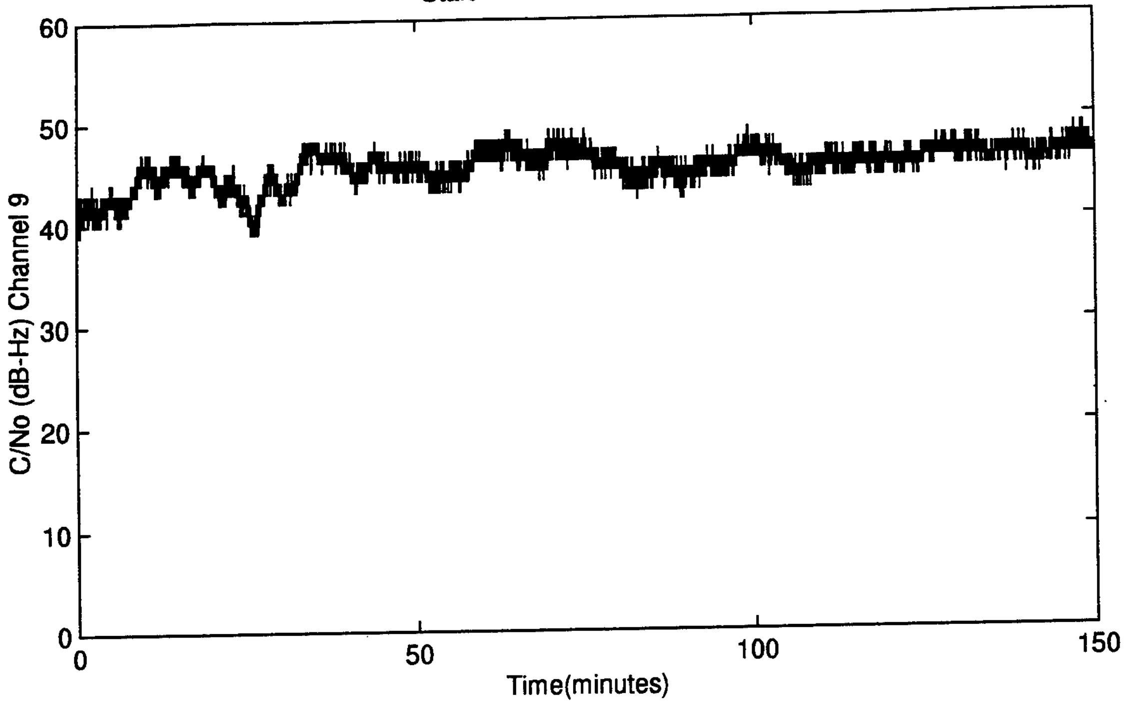

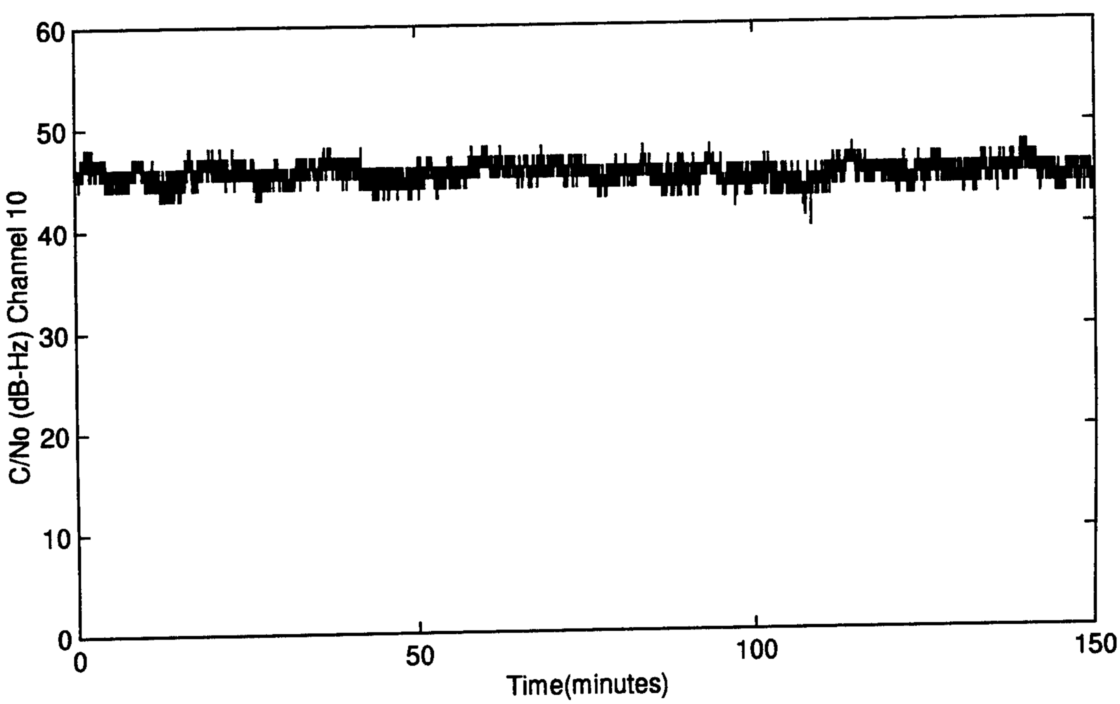

Figure J.17. C/No vs Time

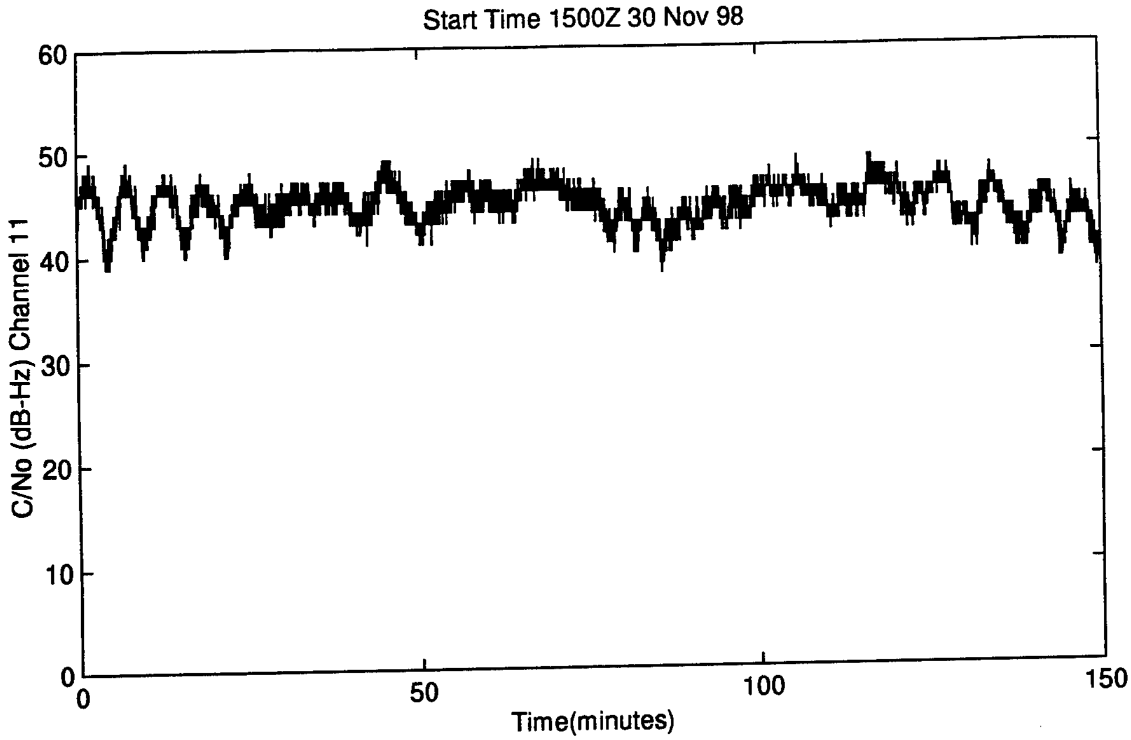

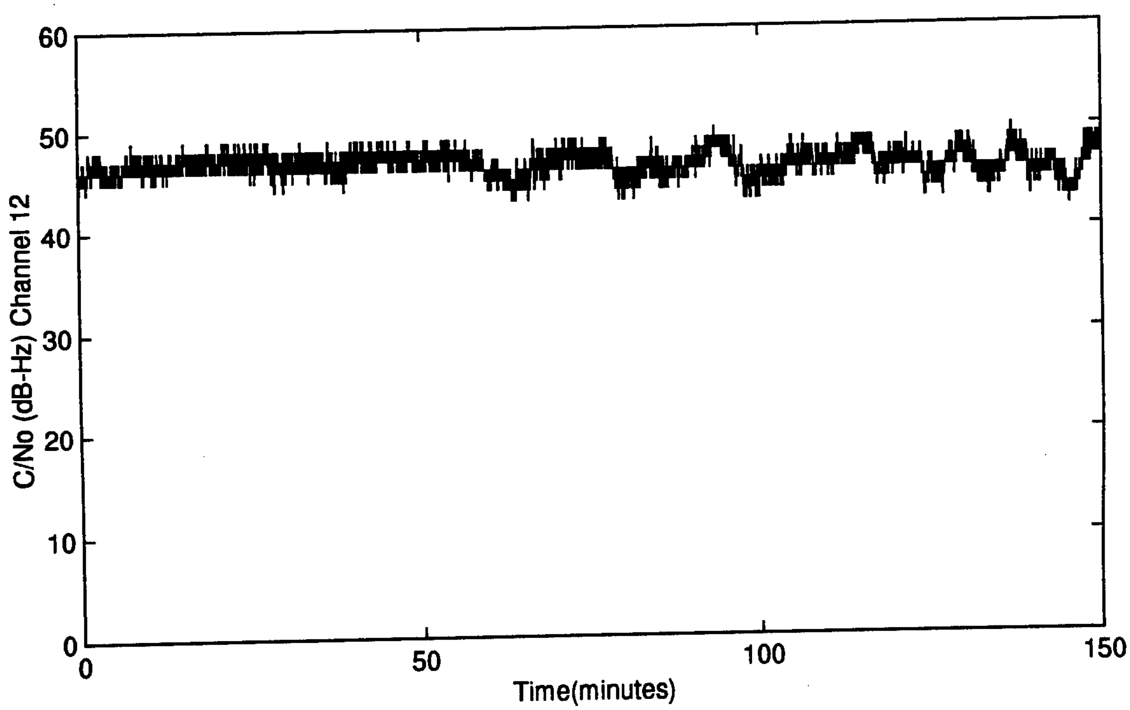

Figure J.18. C/No vs Time

APPENDIX K

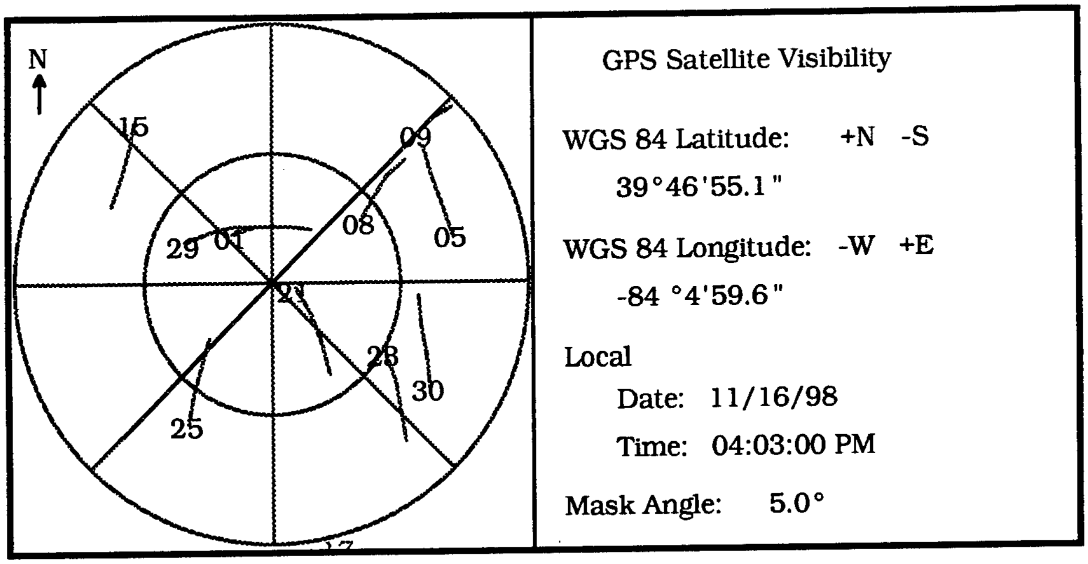

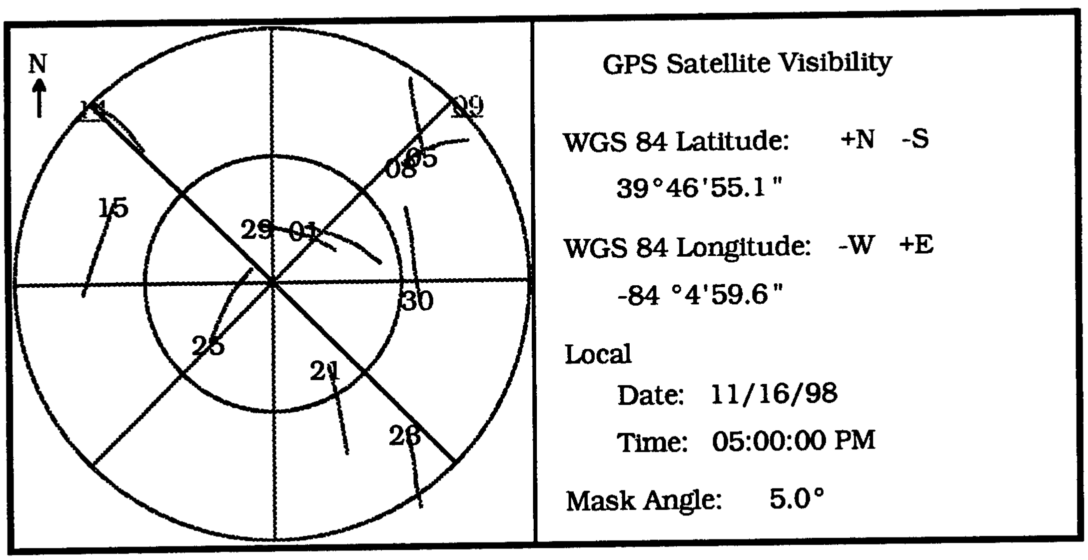

Figure K.1. GPS Satellites In View 16 Nov 98

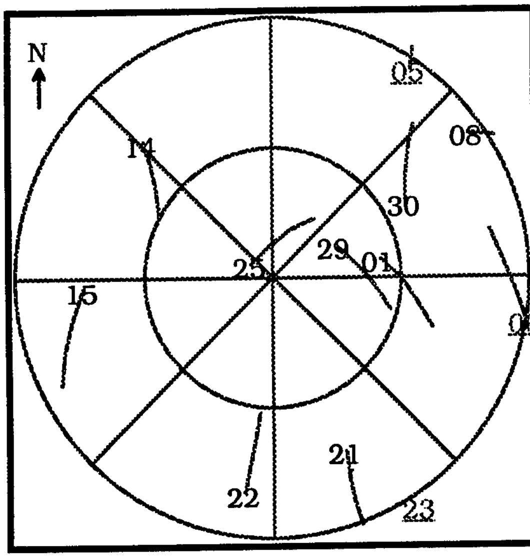

GPS Satellite Visibility

WGS 84 Latitude: +N -S
39°46'55.1"

WGS 84 Longitude: -W +E
-84 °4'59.6"

Local
Date: 11/16/98
Time: 06:00:00 PM

Mask Angle: 5.0°

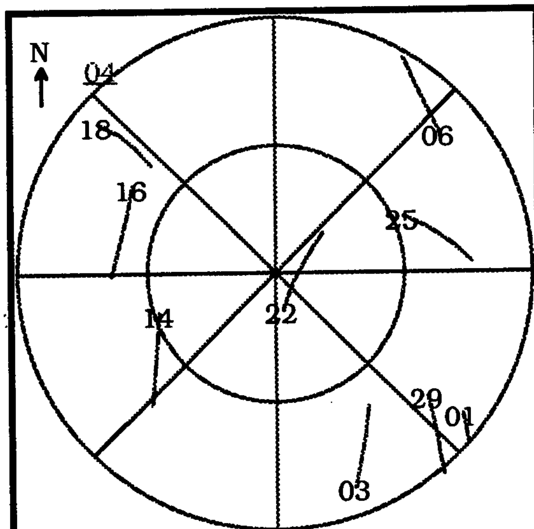

GPS Satellite Visibility

WGS 84 Latitude: +N -S
39°46'55.1"

WGS 84 Longitude: -W +E
-84 °4'59.6"

Local
Date: 11/16/98
Time: 8:07:00 PM

Mask Angle: 5.0°

Figure K.2. GPS Satellites In View 16 Nov 98

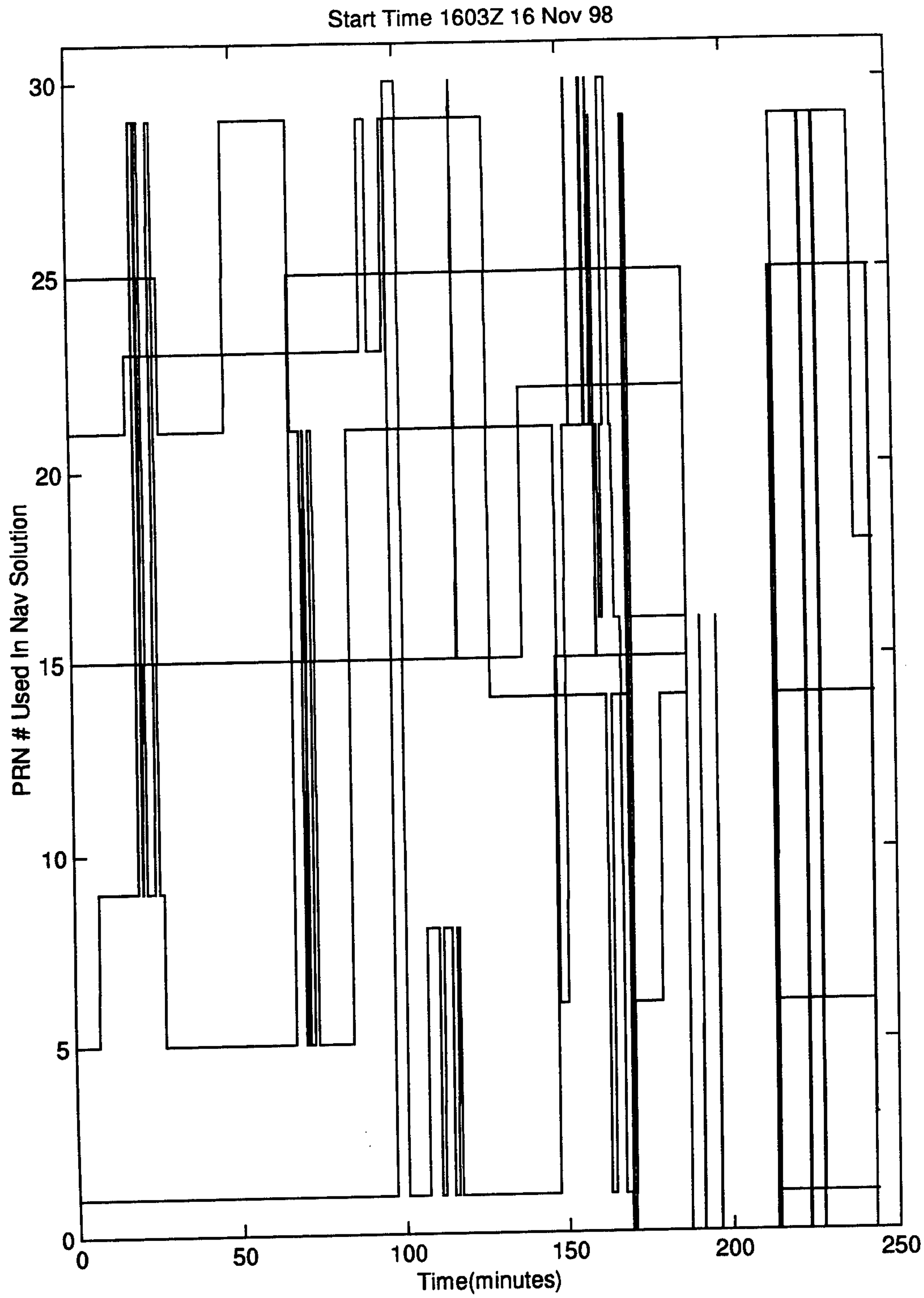

Figure K.3. PRN # Used In Nav Solution vs Time

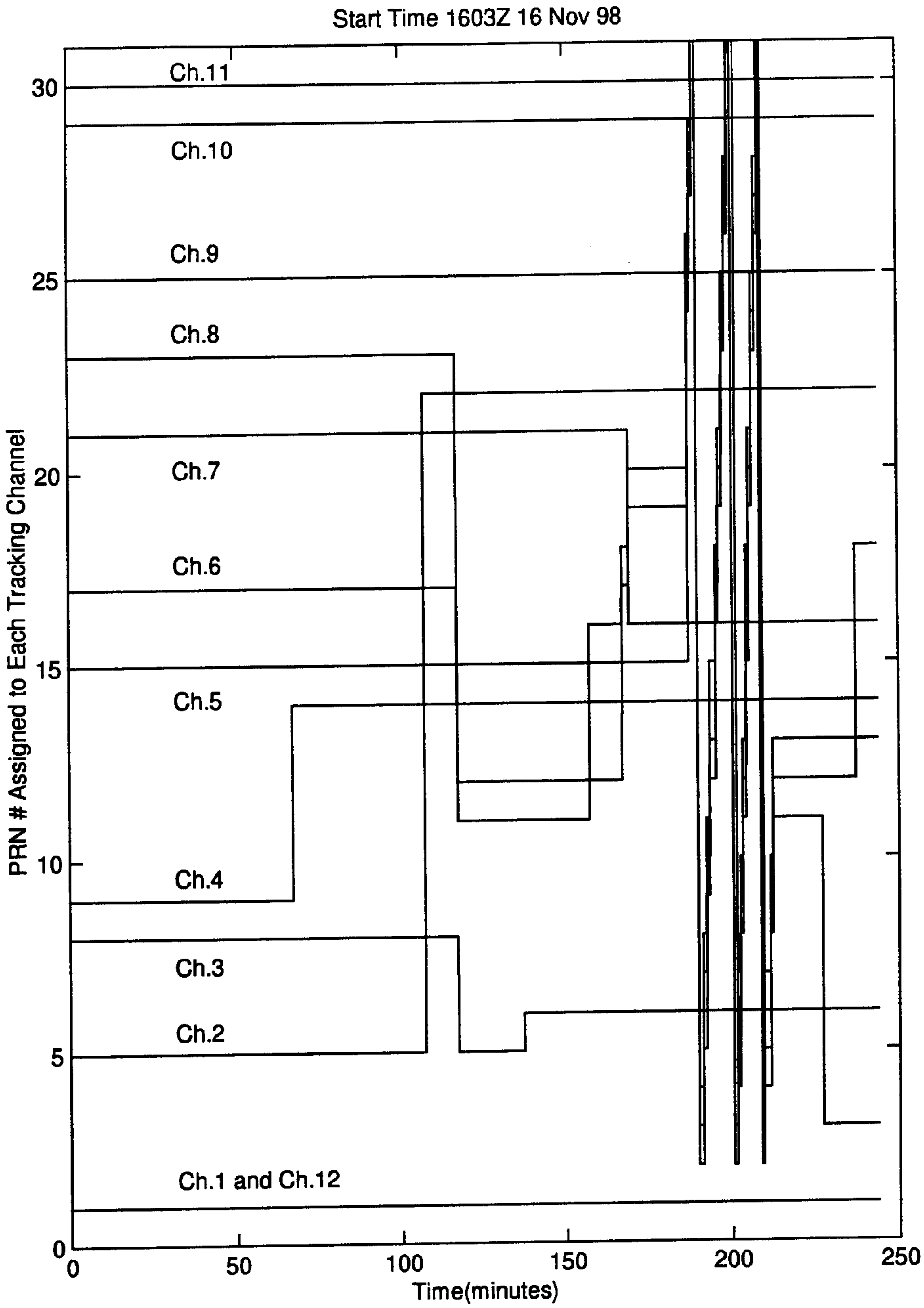

Figure K.4. PRN # Assigned to Each Tracking Channel vs Time

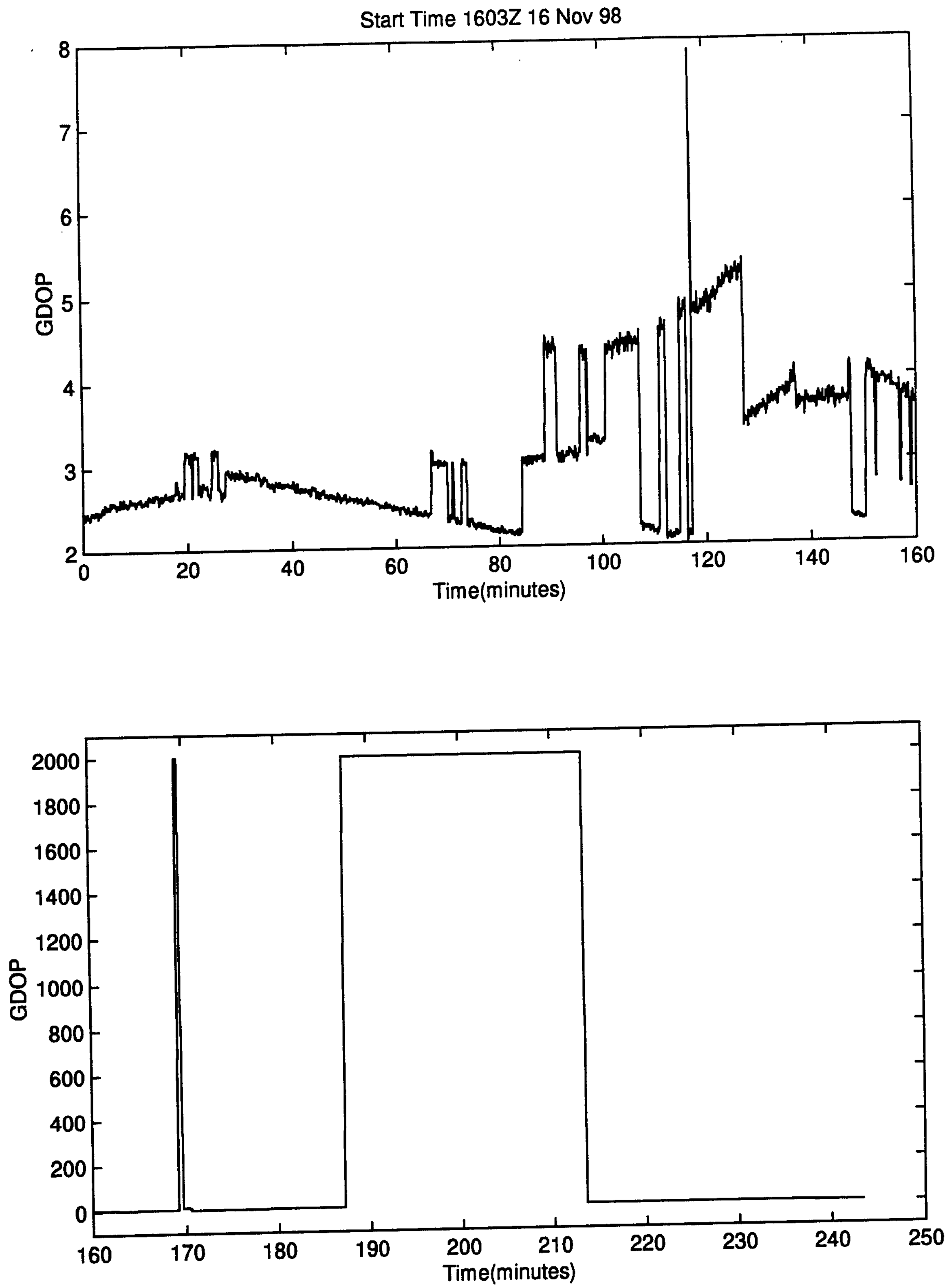

Figure K.5. GDOP vs Time

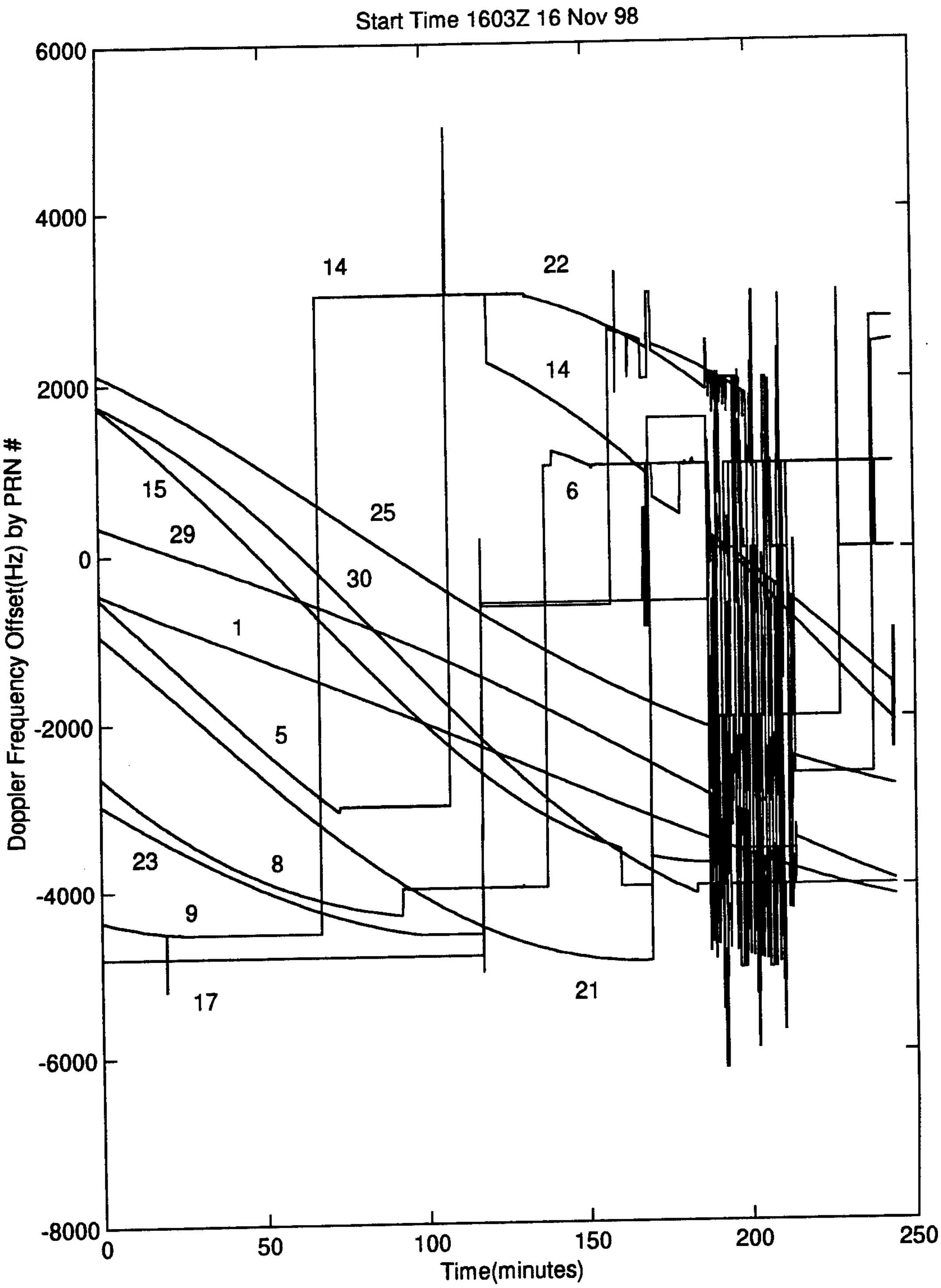

Figure K.6. Doppler Frequency vs Time

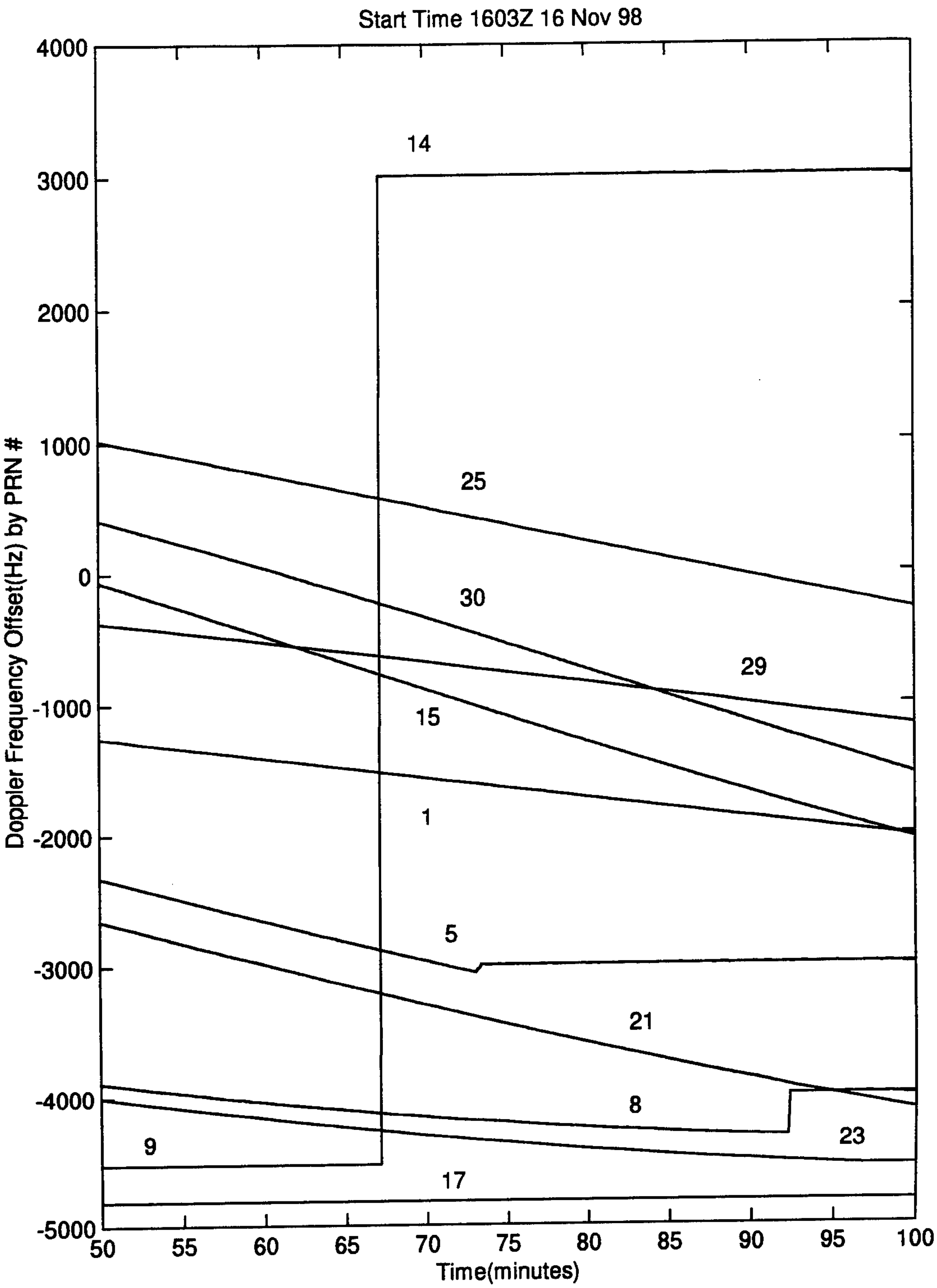

Figure K.7. Doppler Frequency vs Time

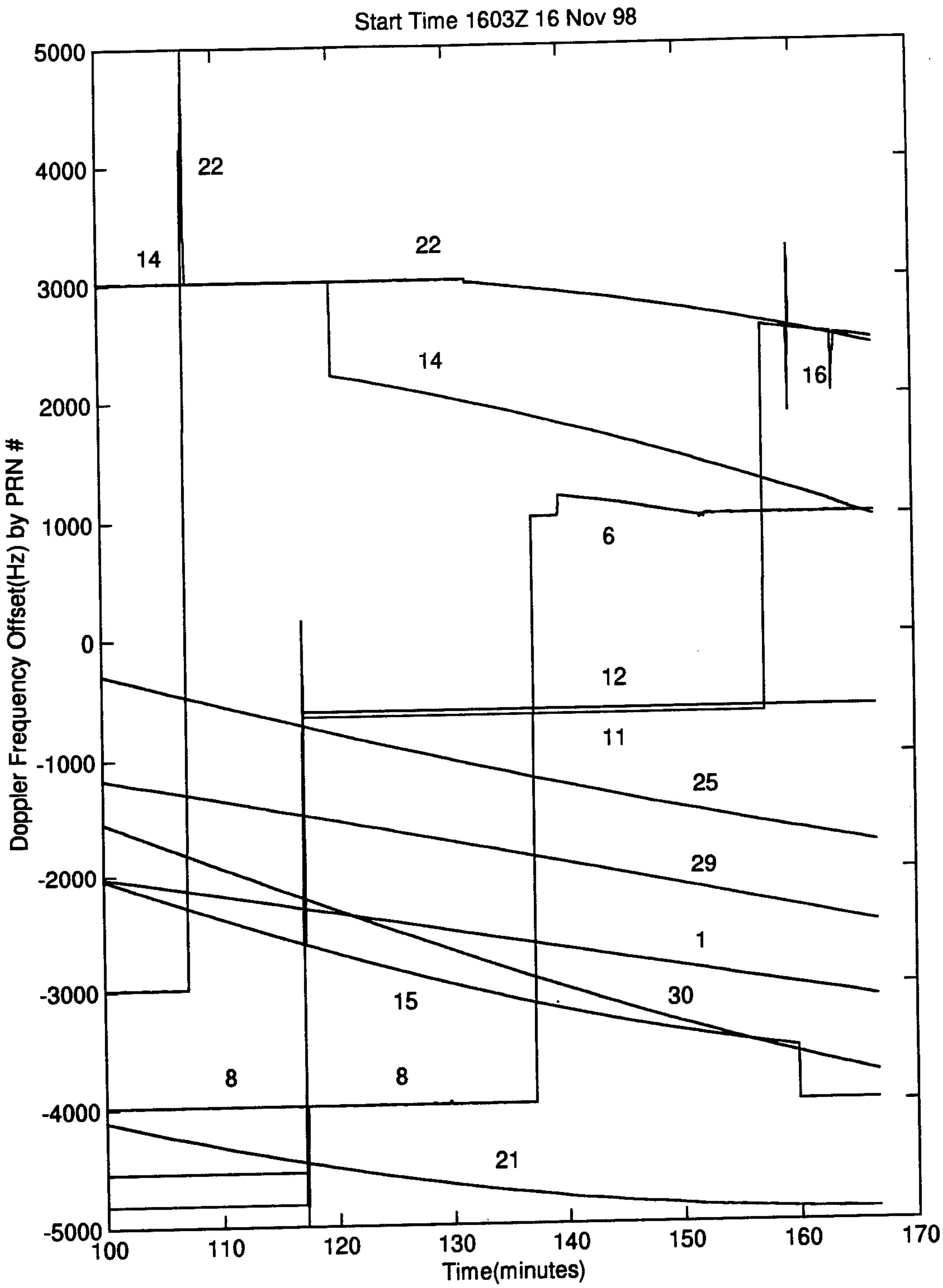

Figure K.8. Doppler Frequency vs Time

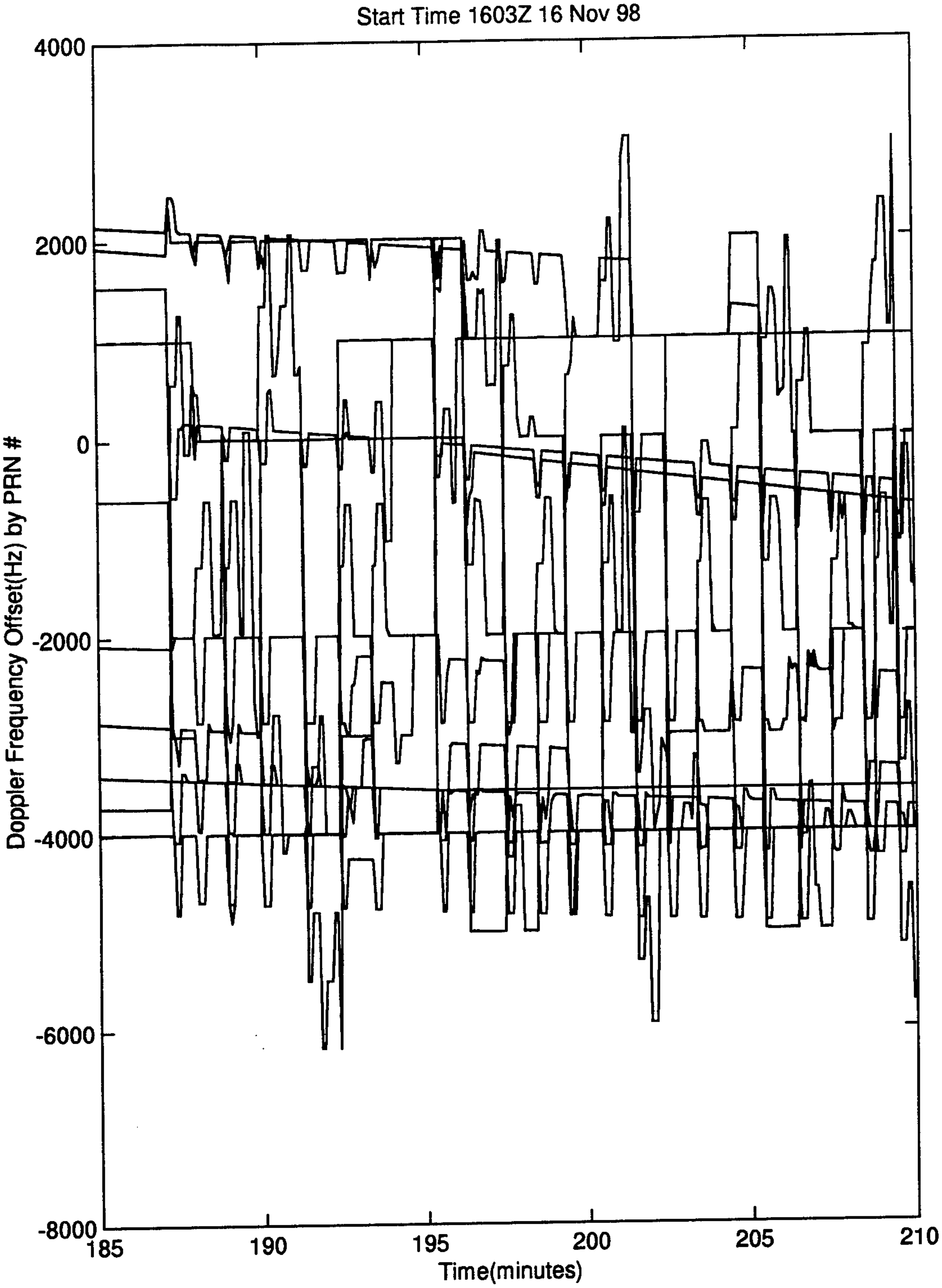

Figure K.9. Doppler Frequency vs Time

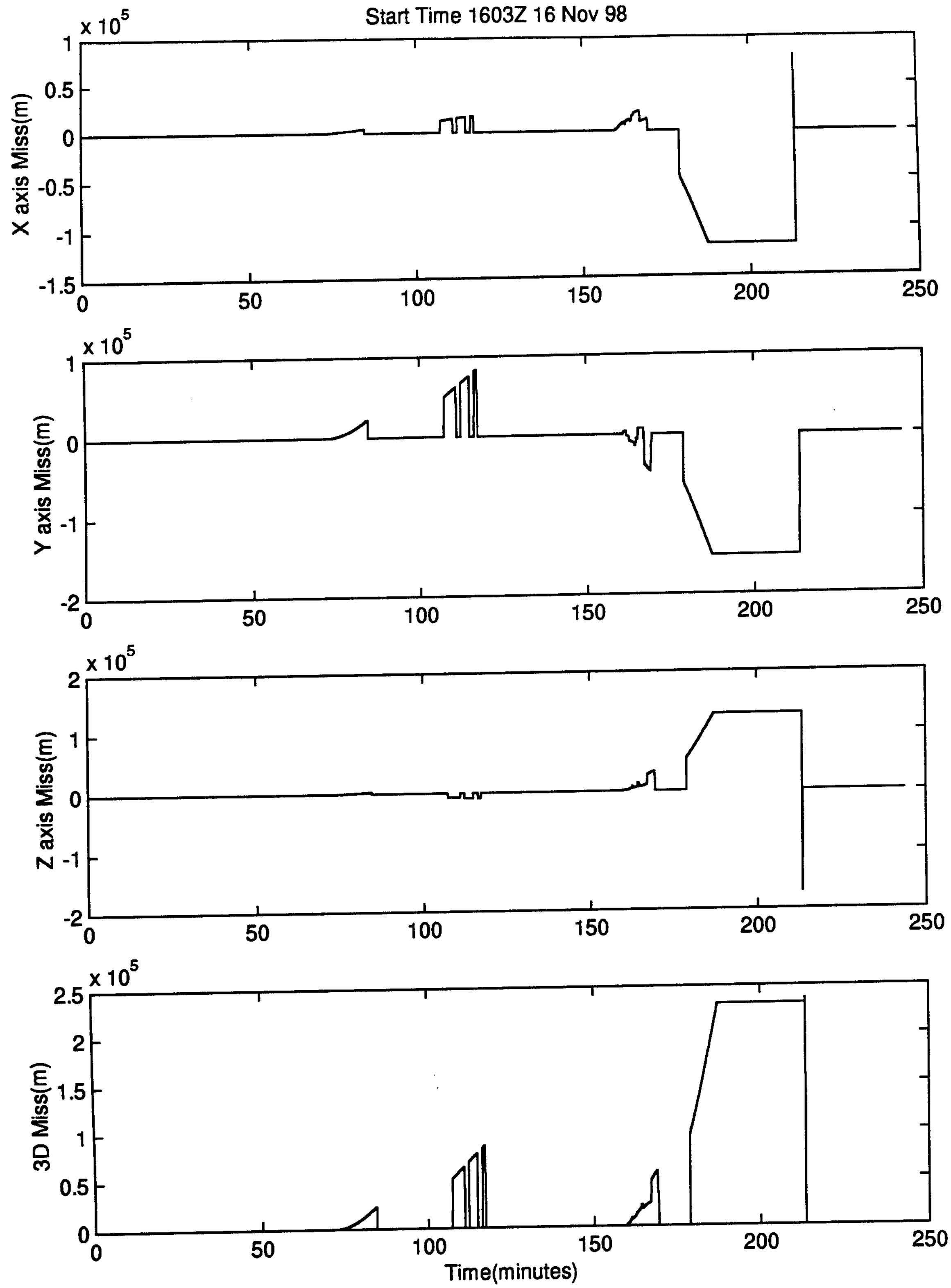

Figure K.10. X,Y,Z and 3D Error(m) vs Time

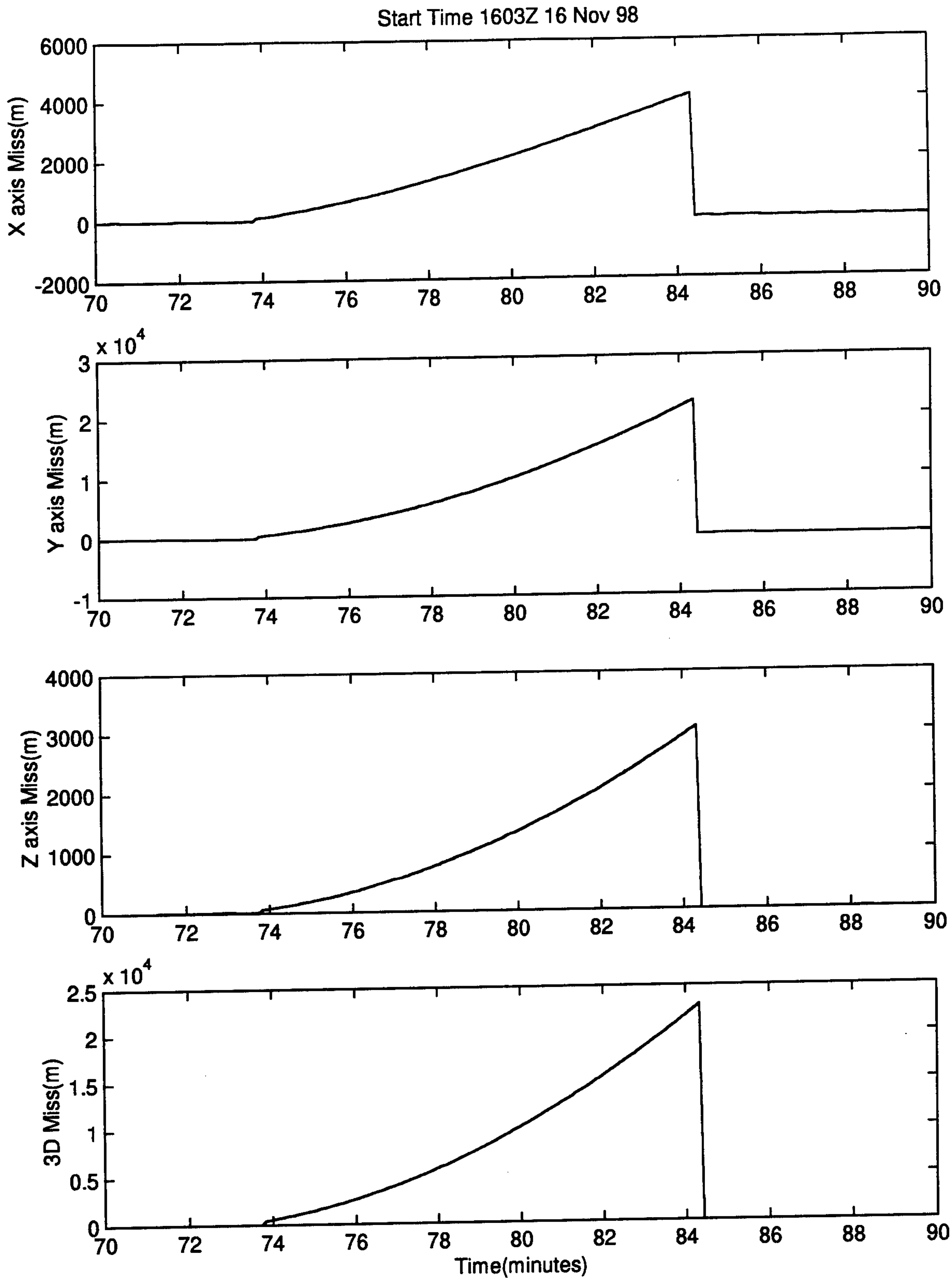

Figure K.11. X,Y,Z and 3D Error(m) vs Time

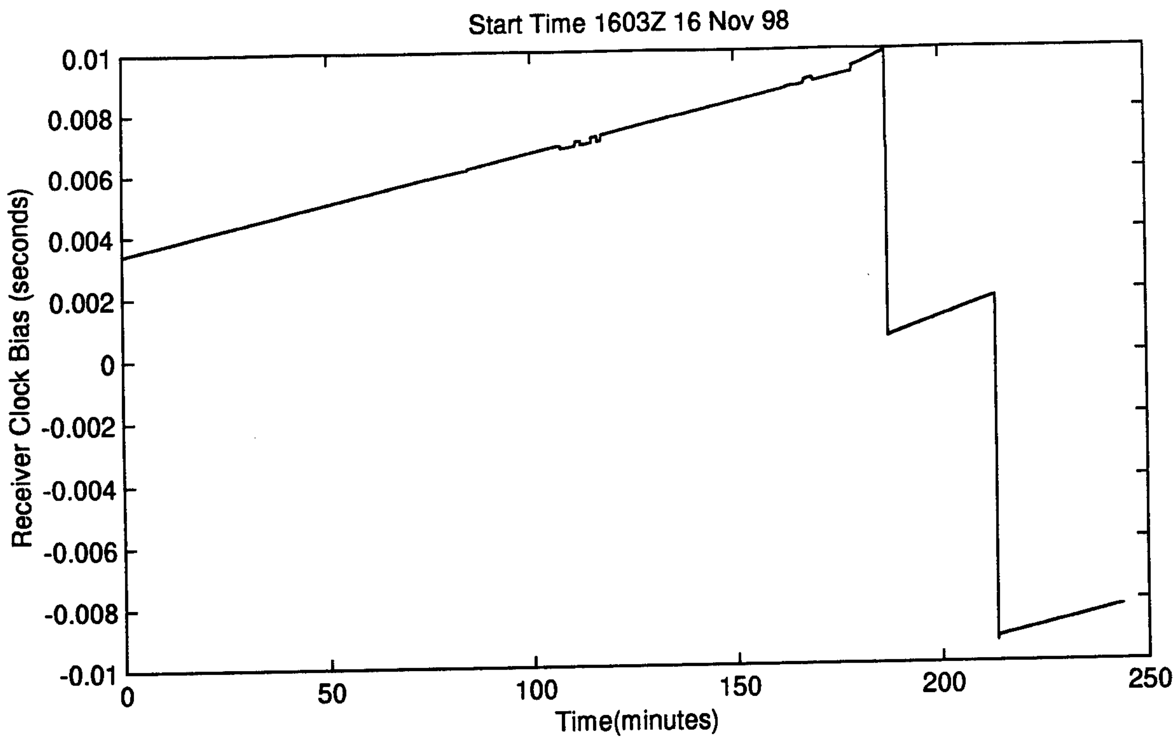

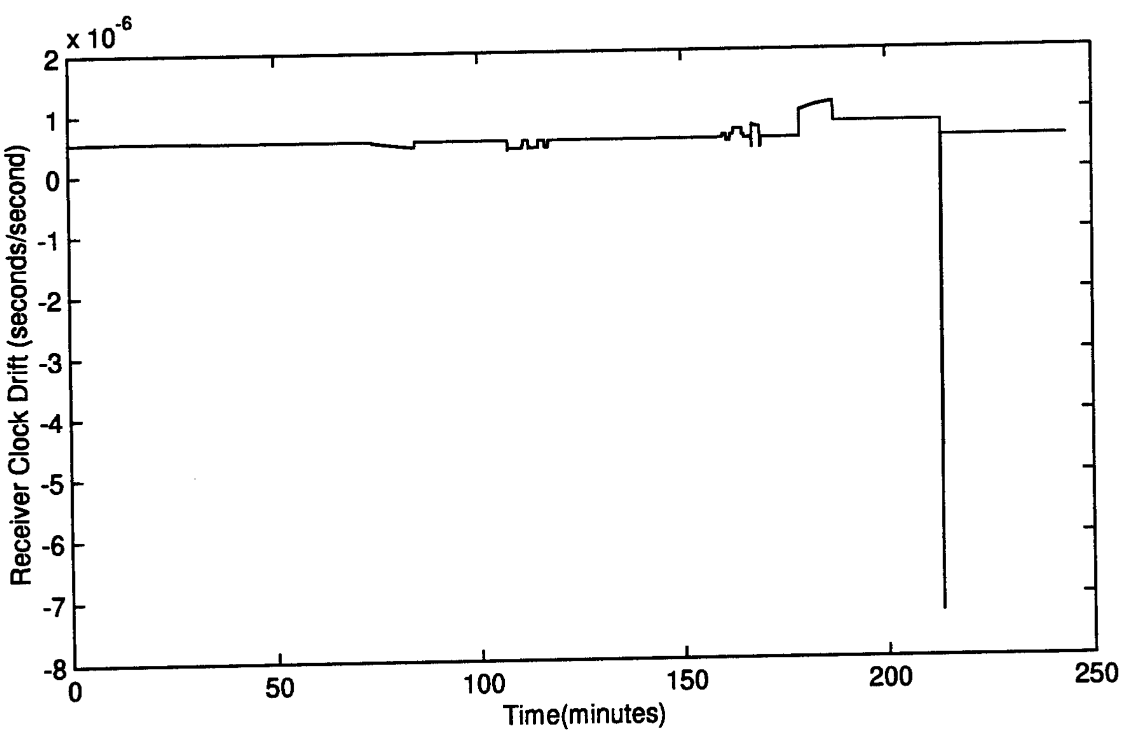

Figure K.12. Receiver Clock Bias and Drift vs Time

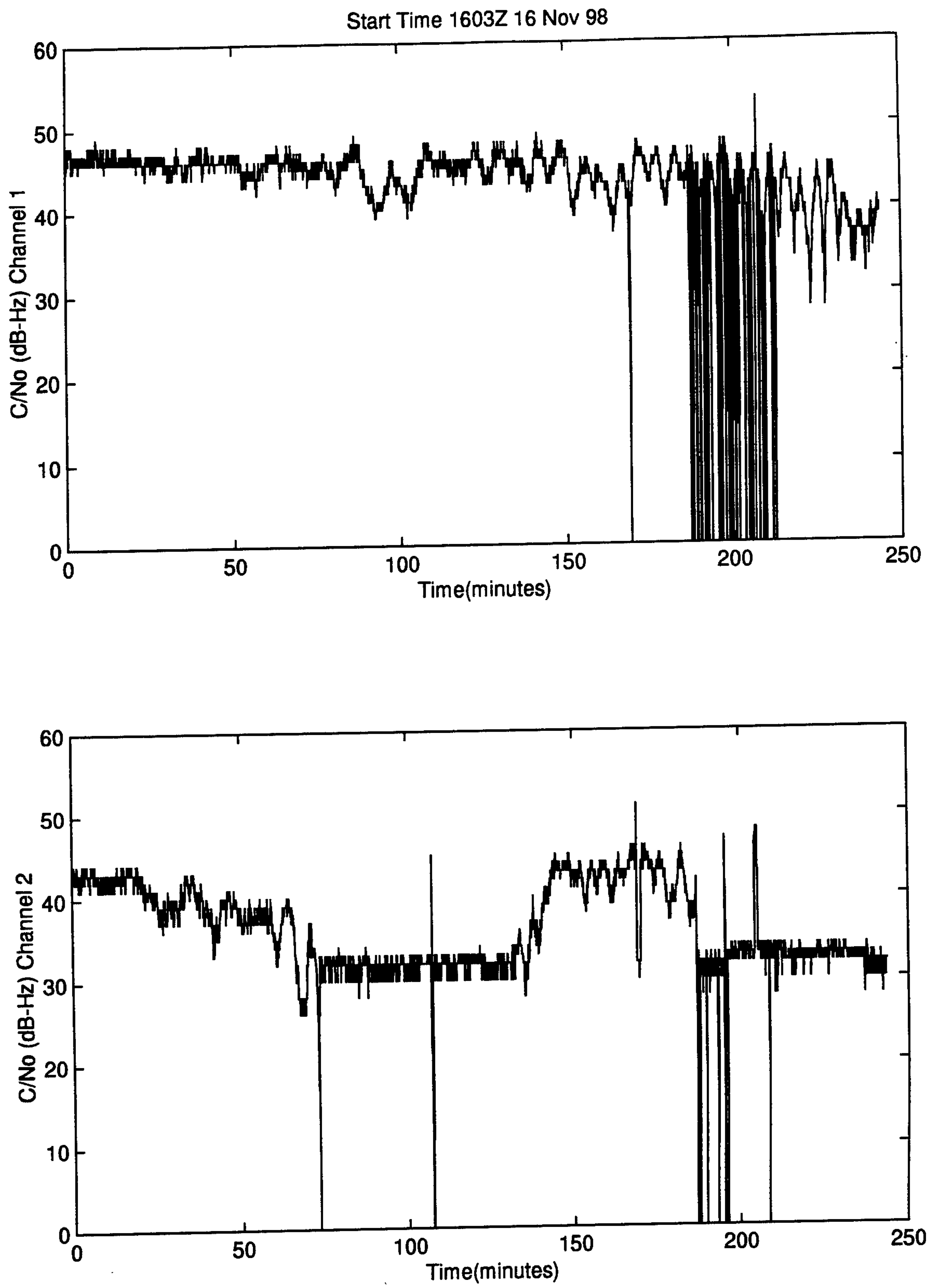

Figure K.13. C/No vs Time

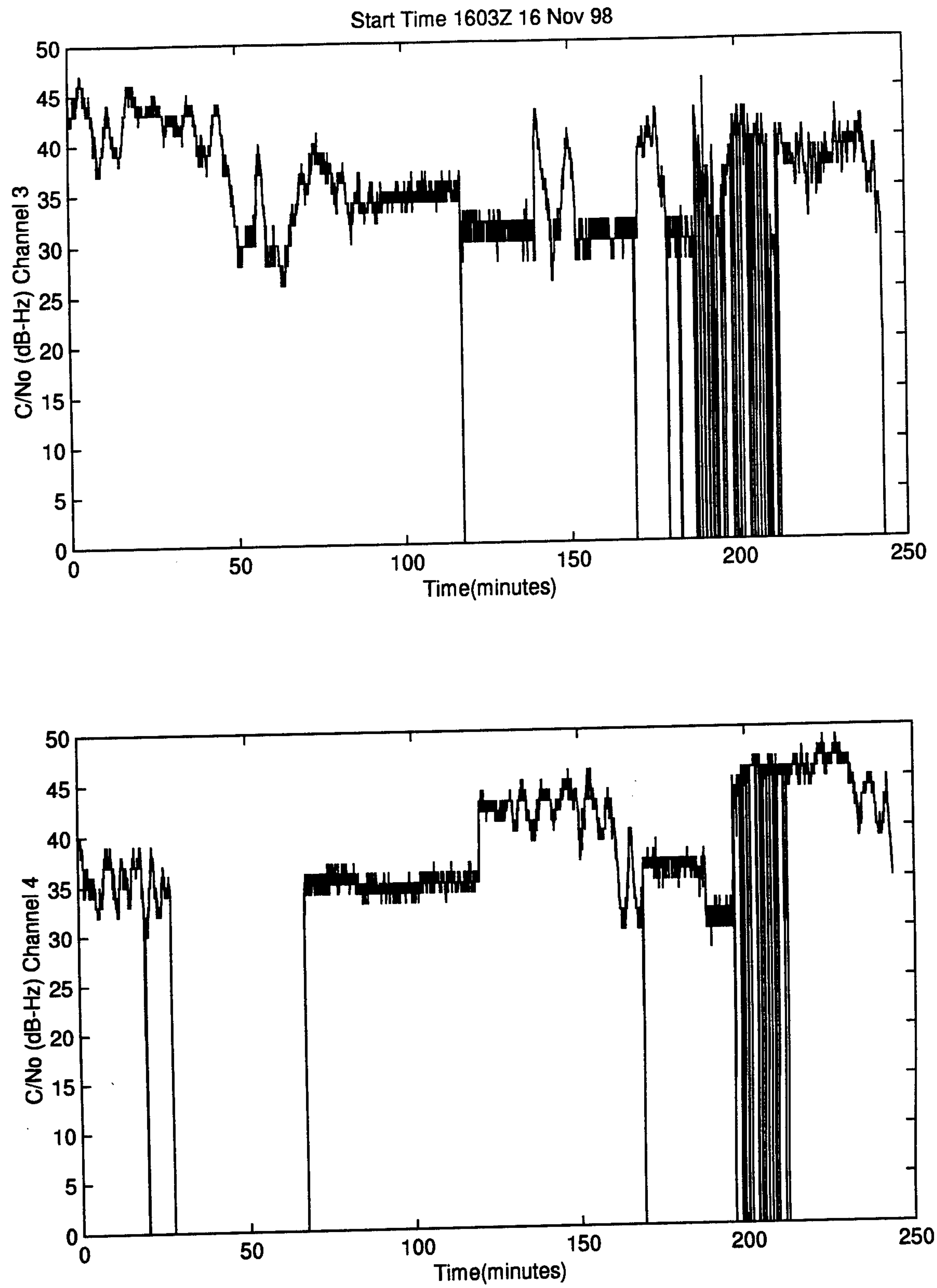

Figure K.14. C/No vs Time

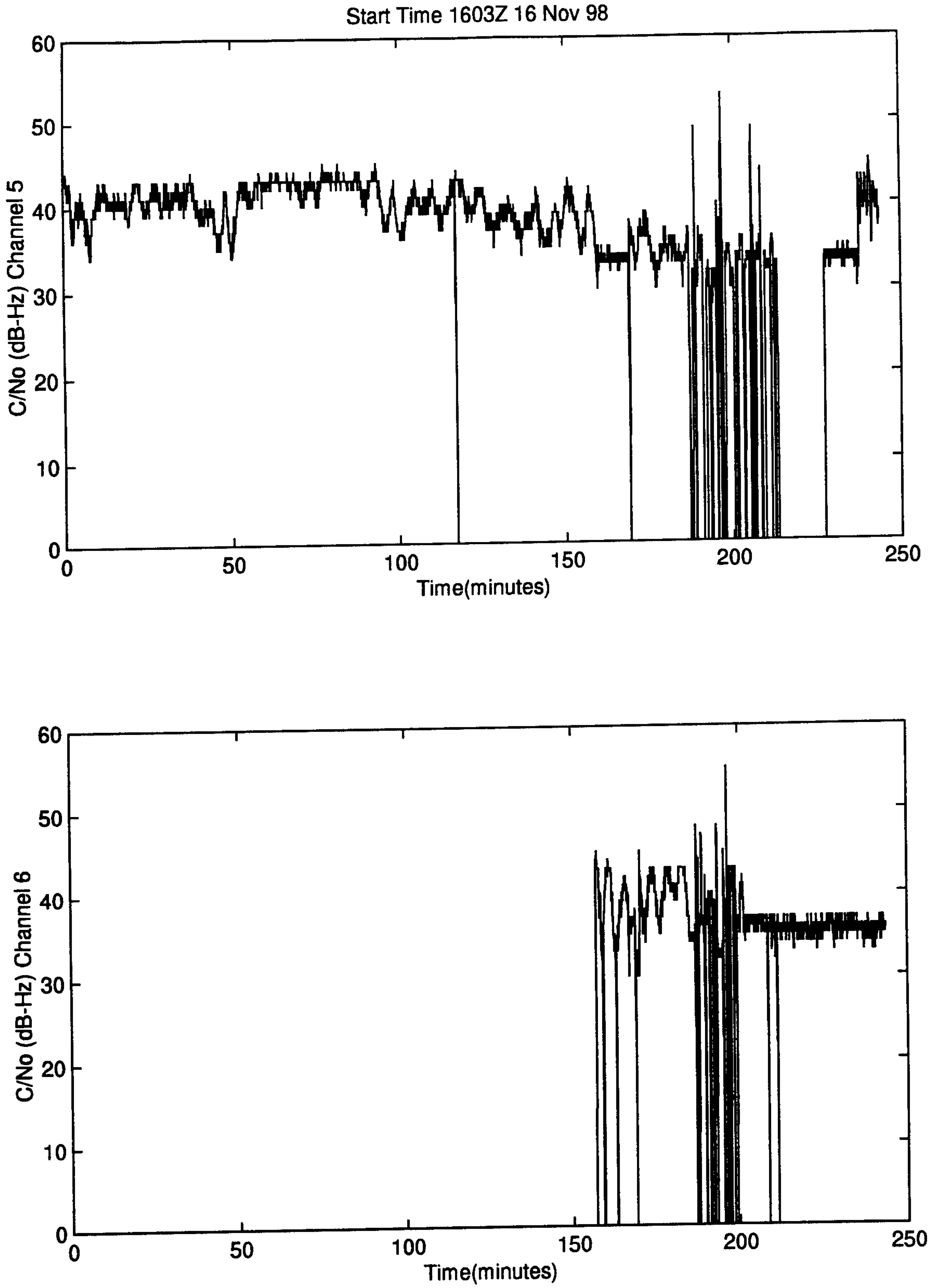

Figure K.15. C/No vs Time

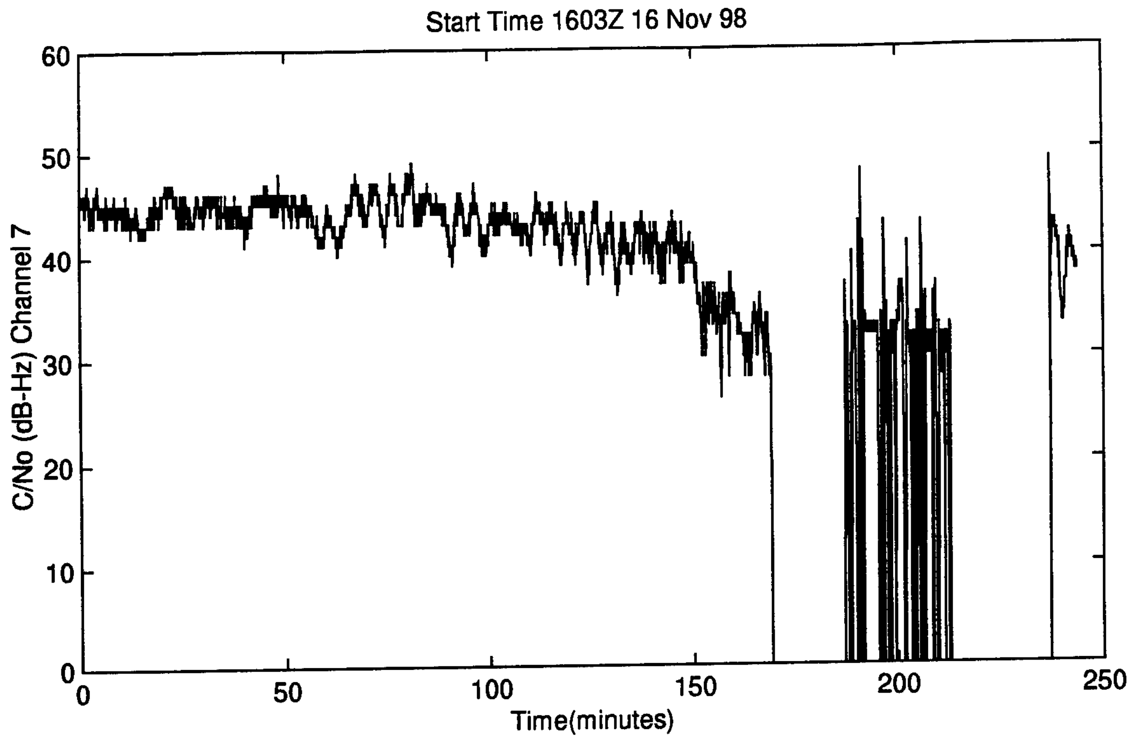

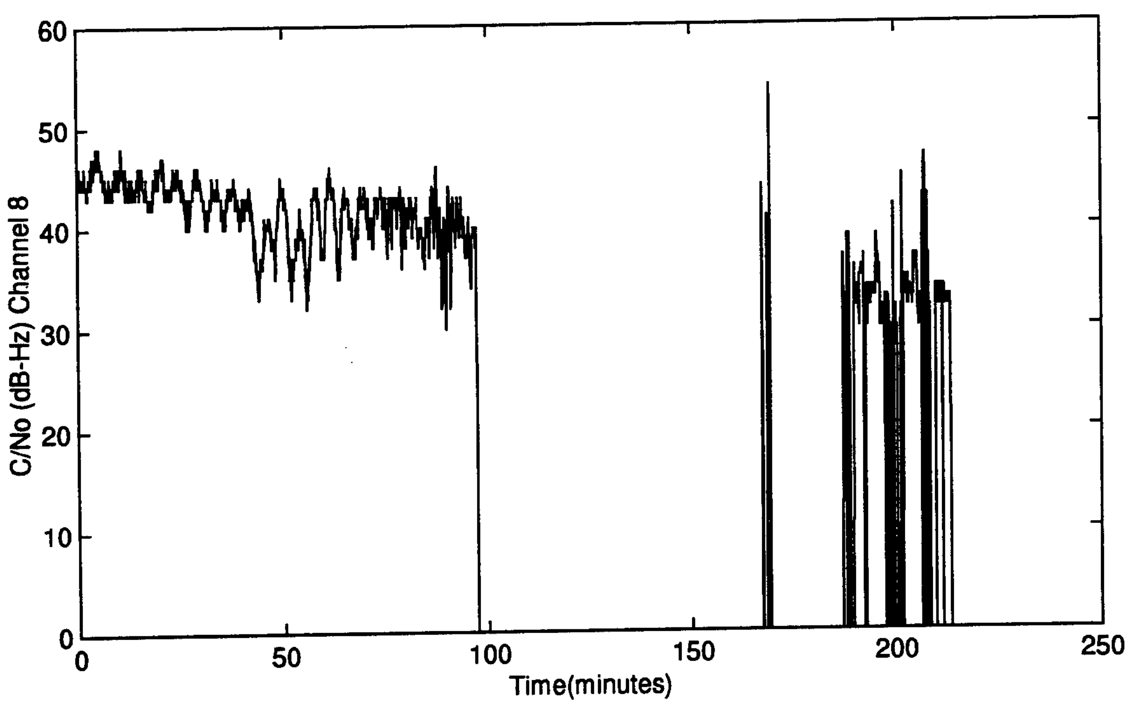

Figure K.16. C/No vs Time

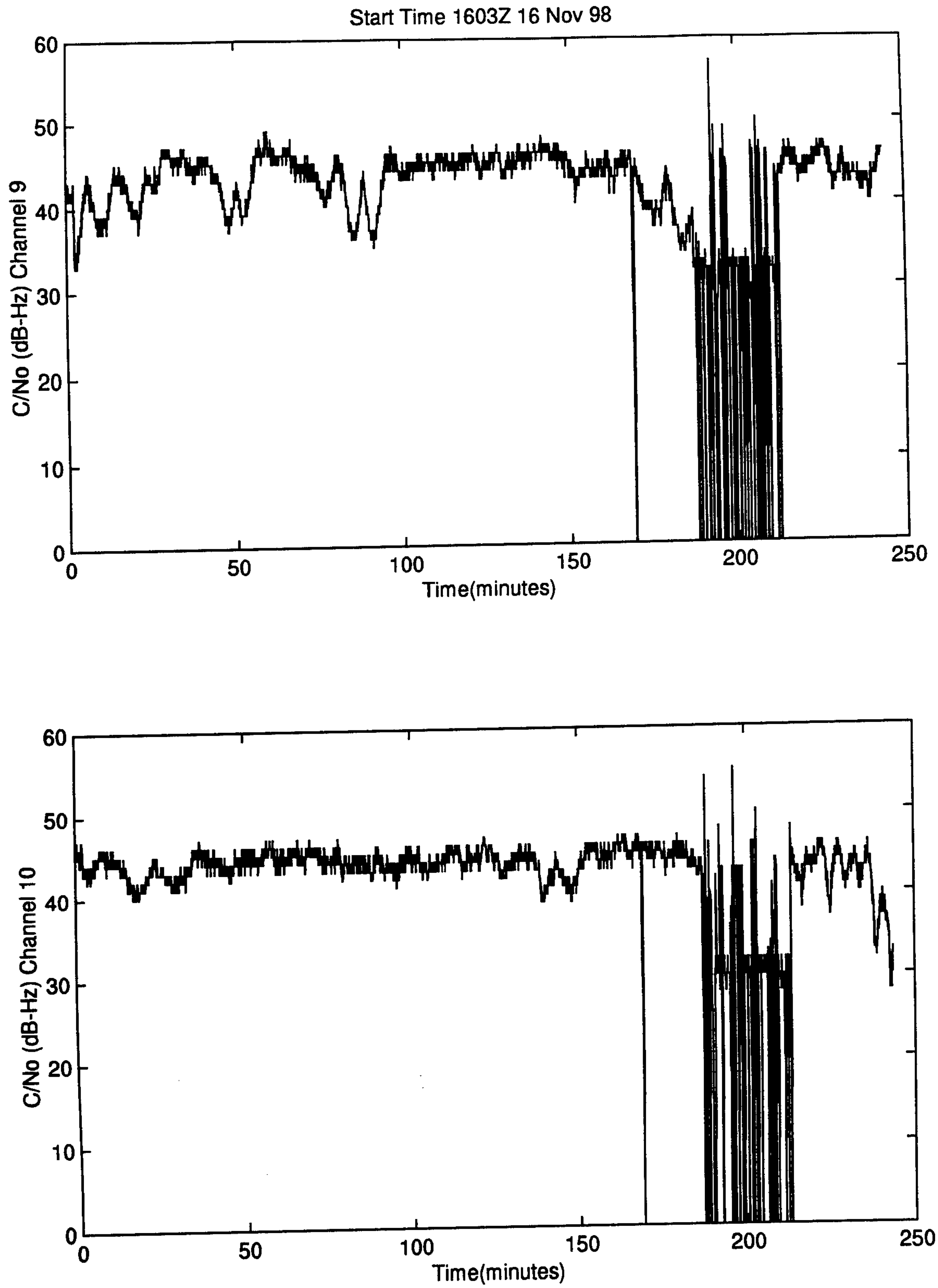

Figure K.17. C/No vs Time

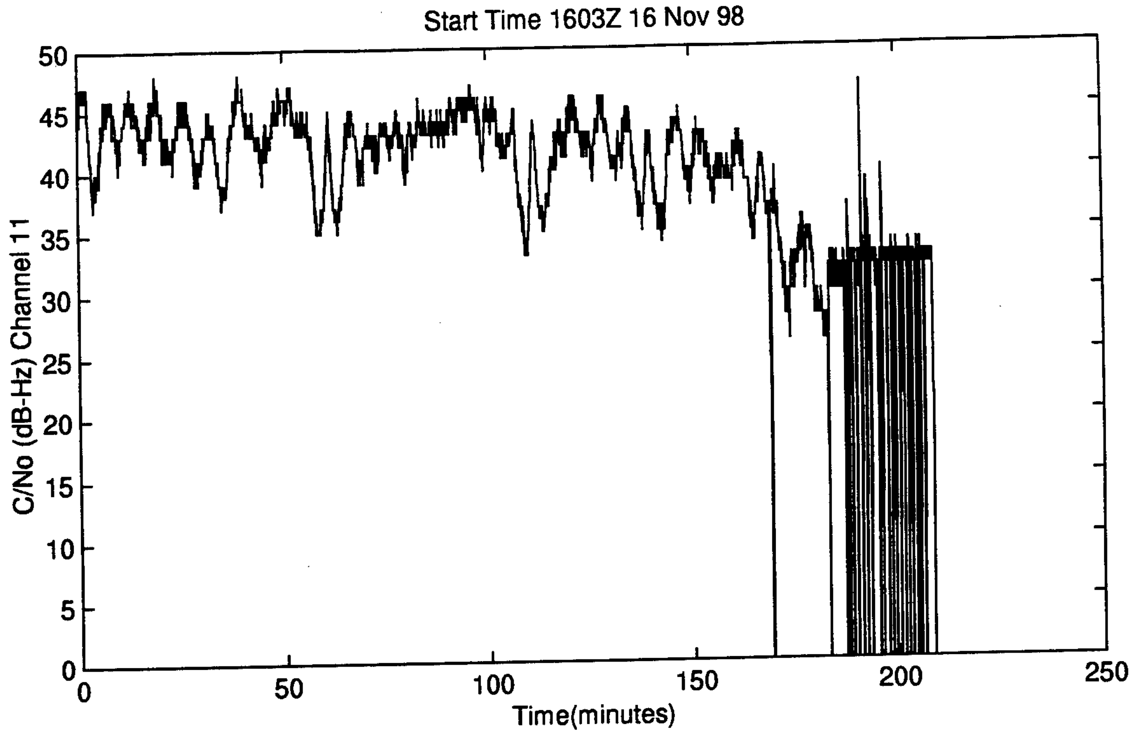

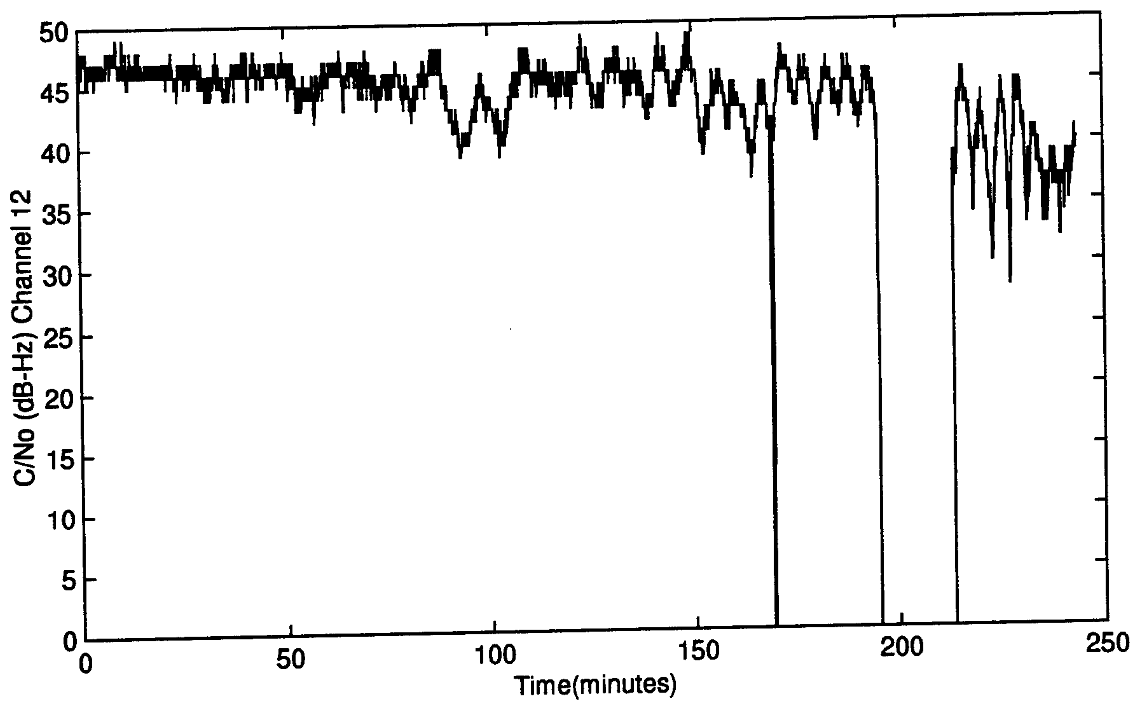

Figure K.18. C/No vs Time

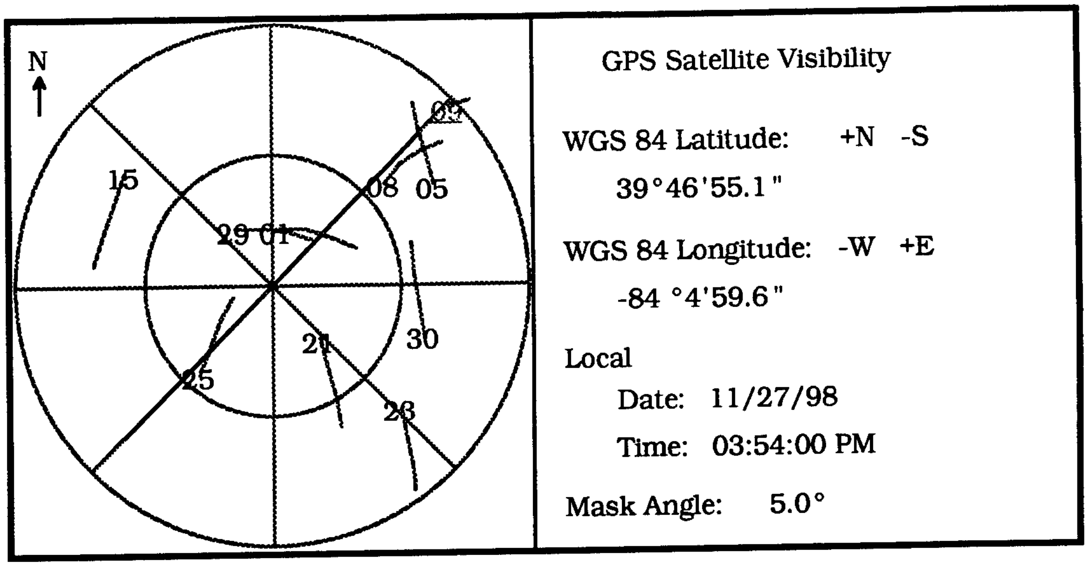

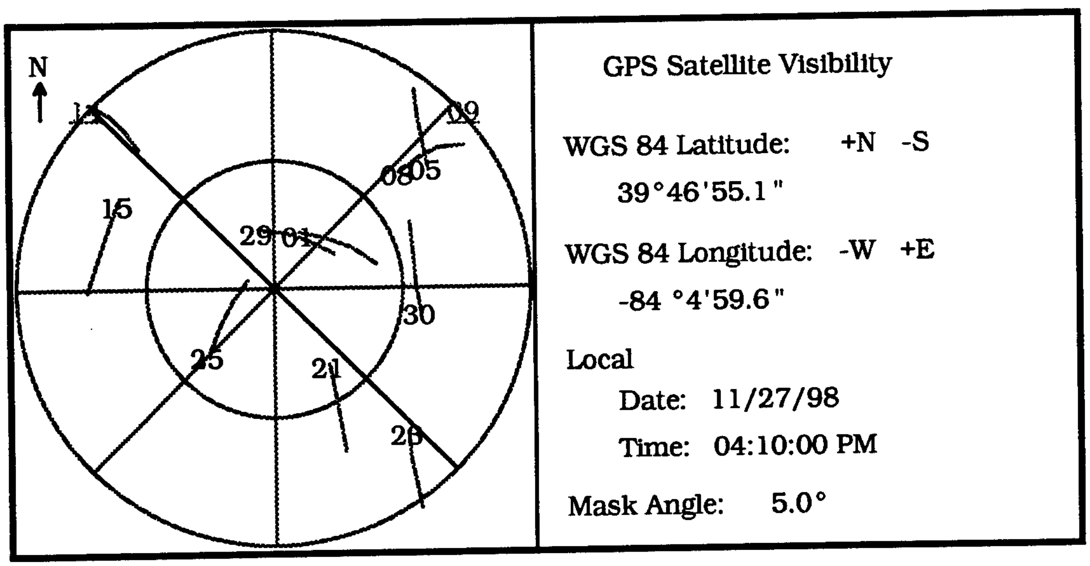

Figure L.1. GPS Satellites In View 27 Nov 98

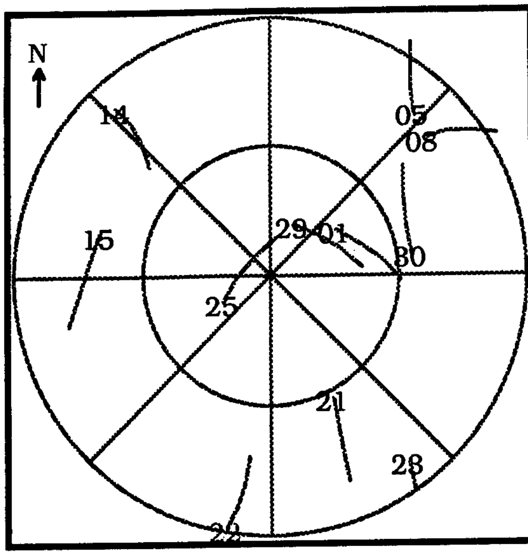

GPS Satellite Visibility

WGS 84 Latitude: +N -S
39°46'55.1"

WGS 84 Longitude: -W +E
-84 °4'59.6"

Local
Date: 11/27/98
Time: 04:40:00 PM

Mask Angle: 5.0°

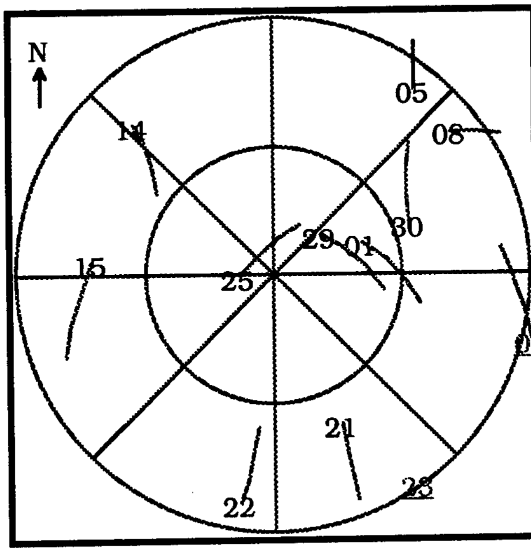

GPS Satellite Visibility

WGS 84 Latitude: +N -S
39°46'55.1"

WGS 84 Longitude: -W +E
-84 °4'59.6"

Local
Date: 11/27/98
Time: 05:00:00 PM

Mask Angle: 5.0°

Figure L.2. GPS Satellites In View 27 Nov 98

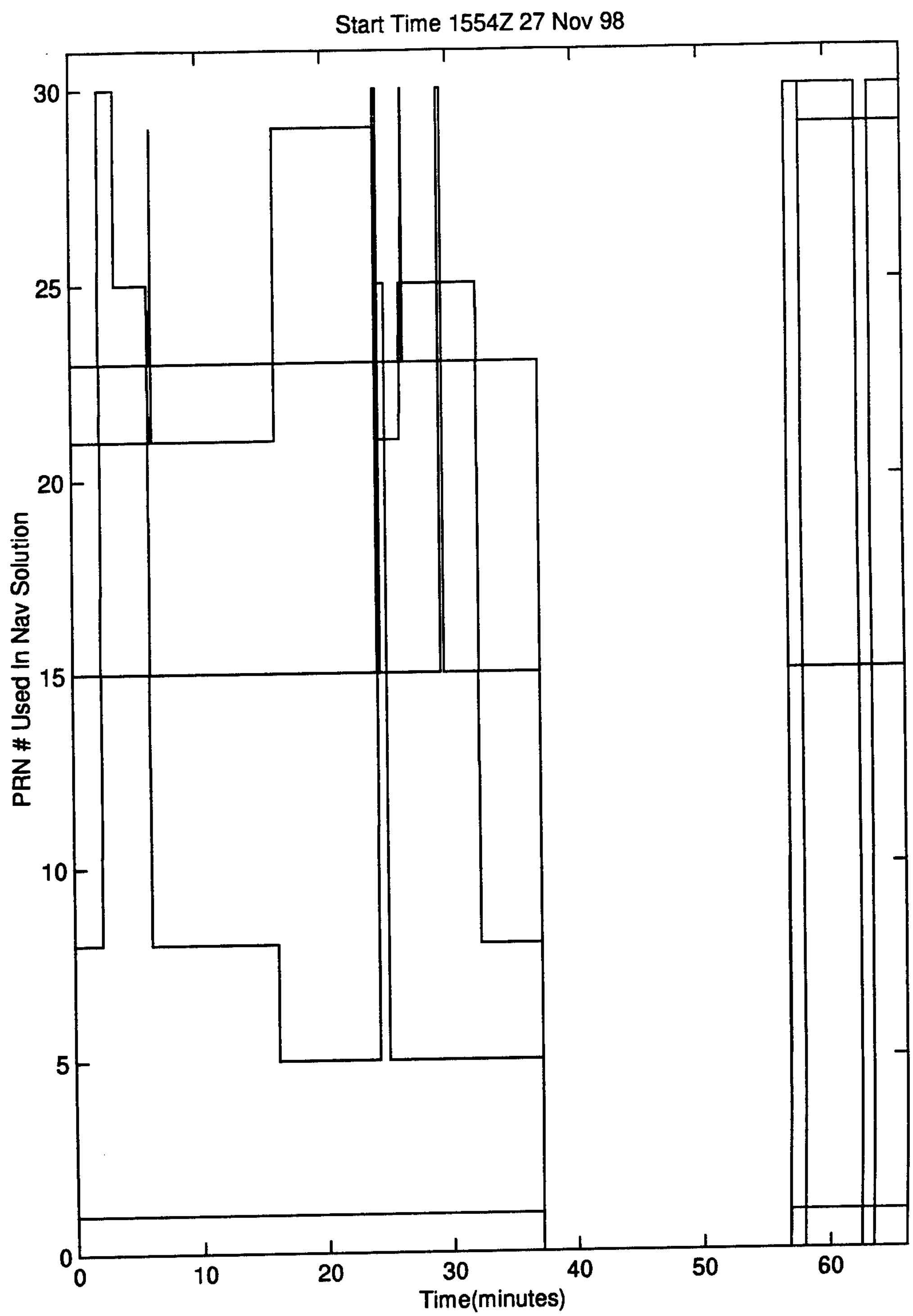

Figure L.3. PRN # Used In Nav Solution vs Time

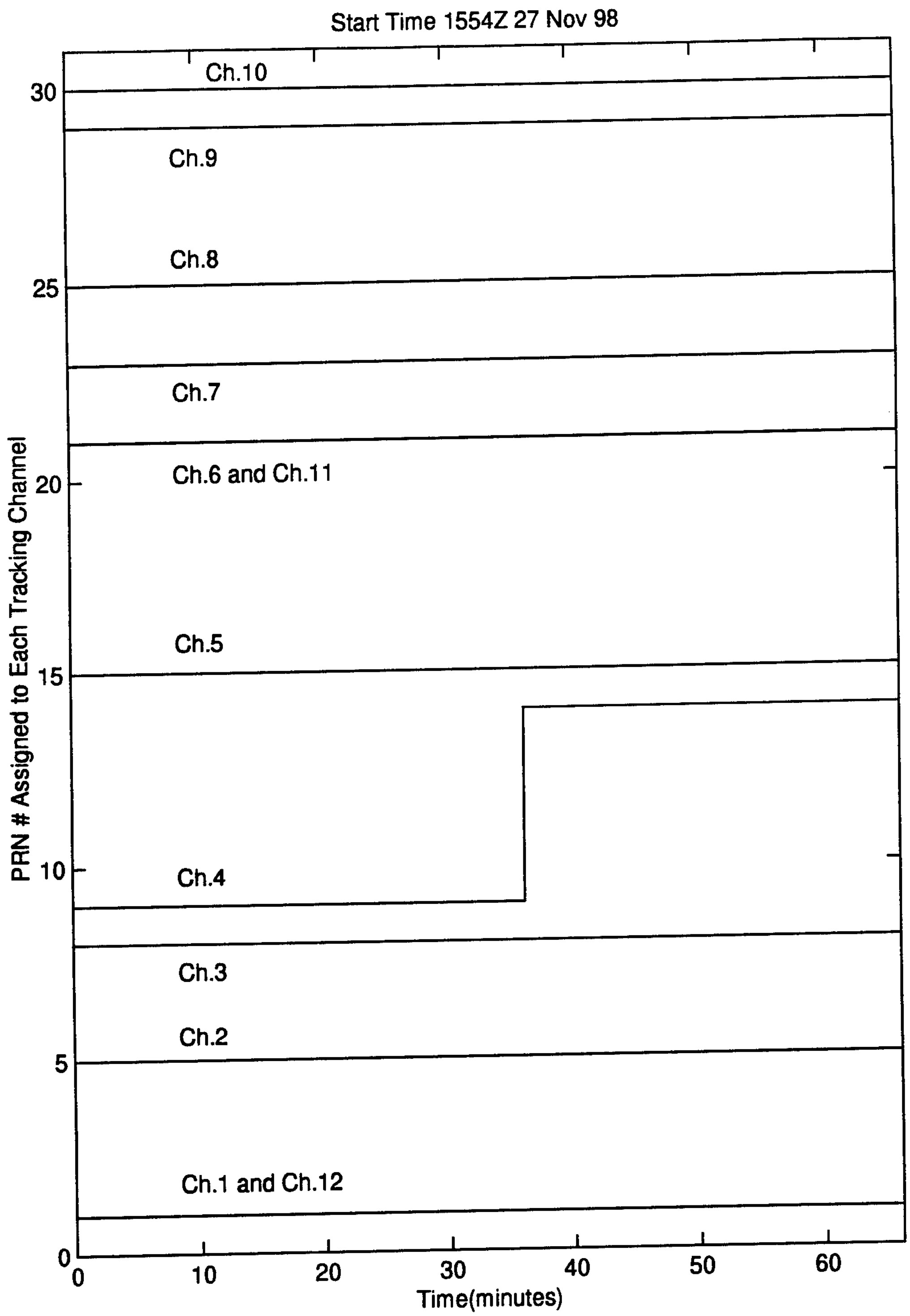

Figure L.4. PRN # Assigned to Each Tracking Channel vs Time

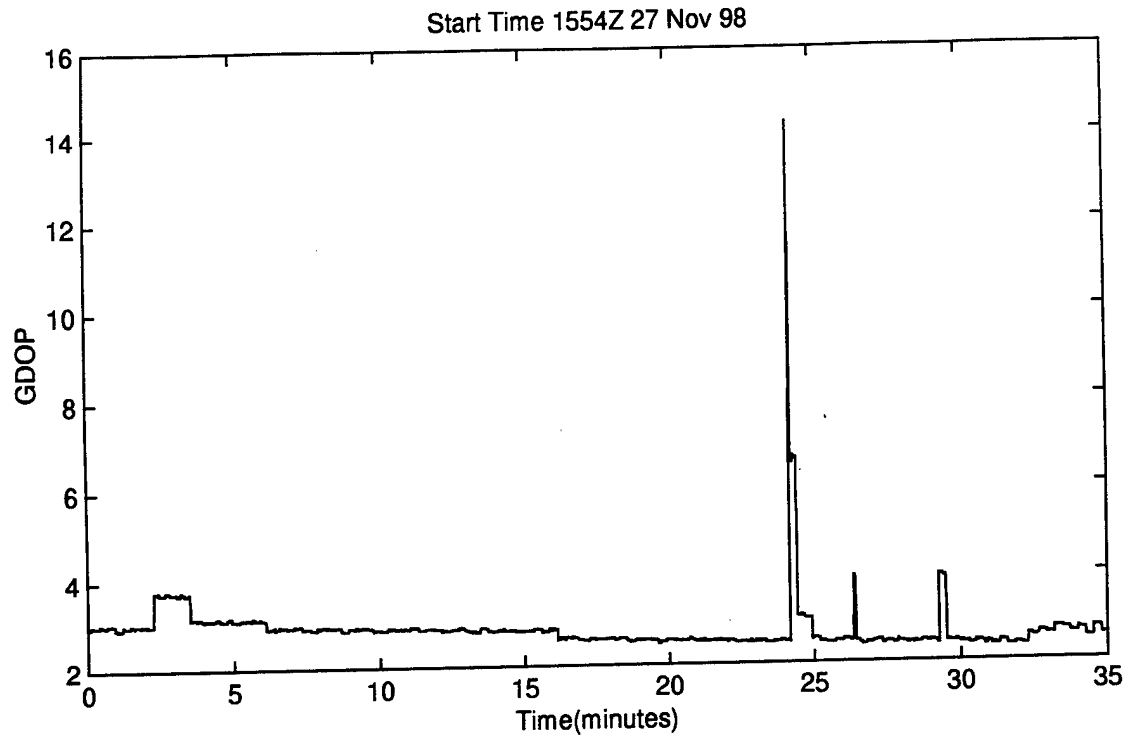

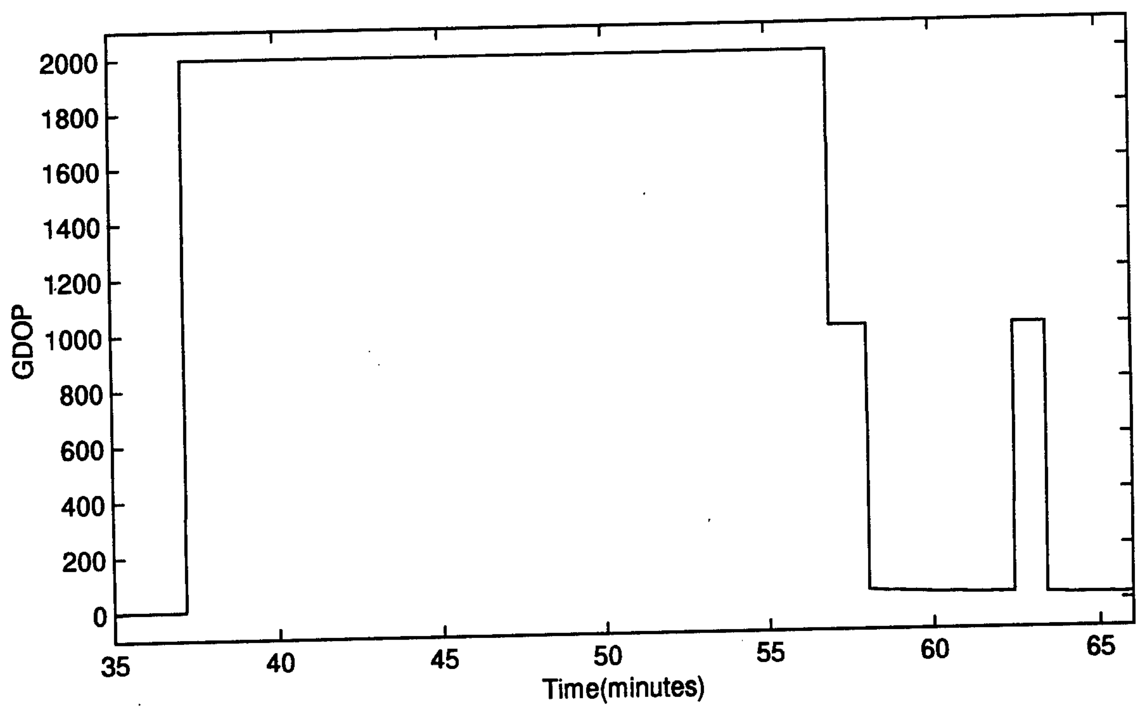

Figure L.5. GDOP vs Time

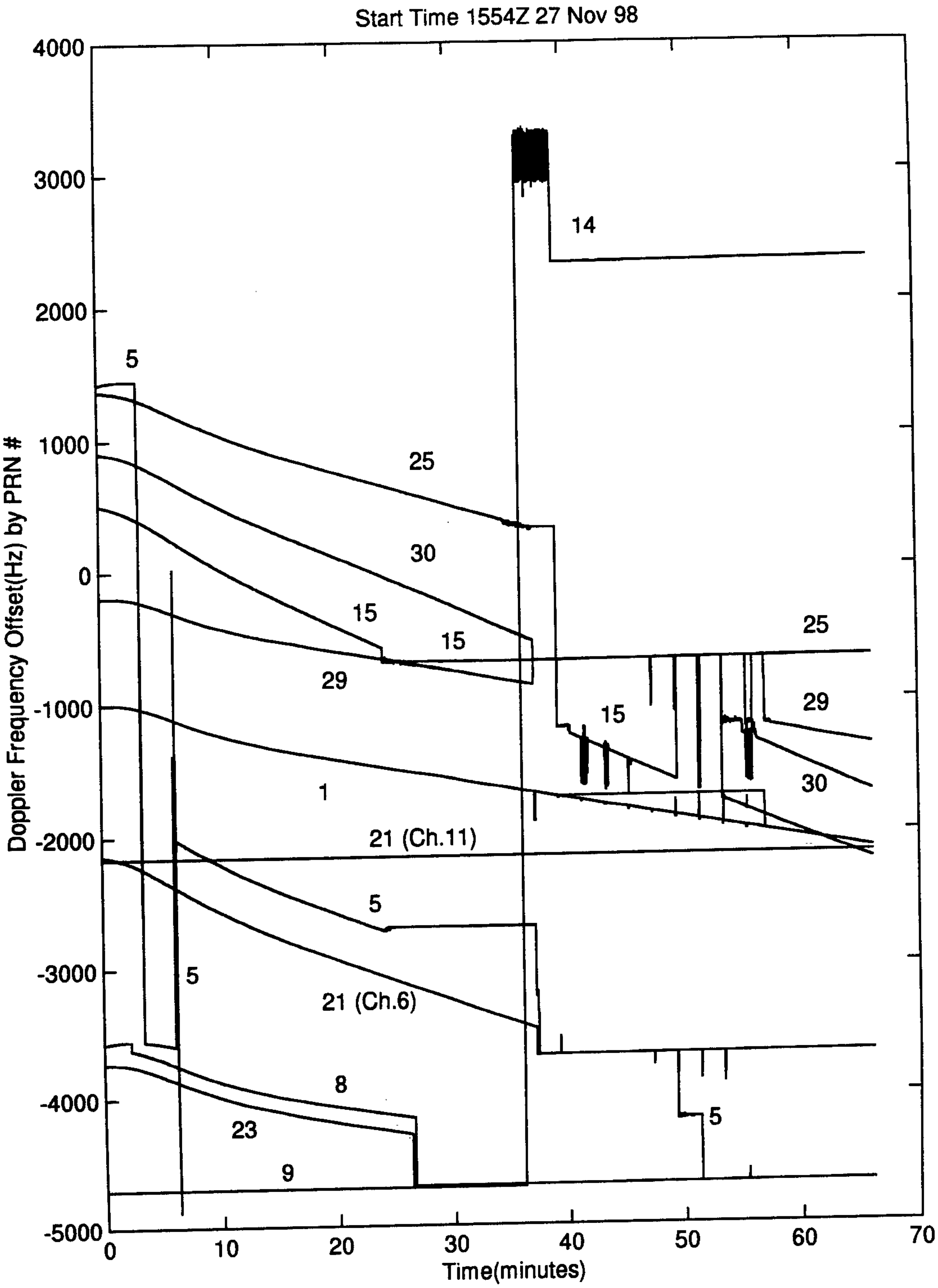

Figure L.6. Doppler Frequency vs Time

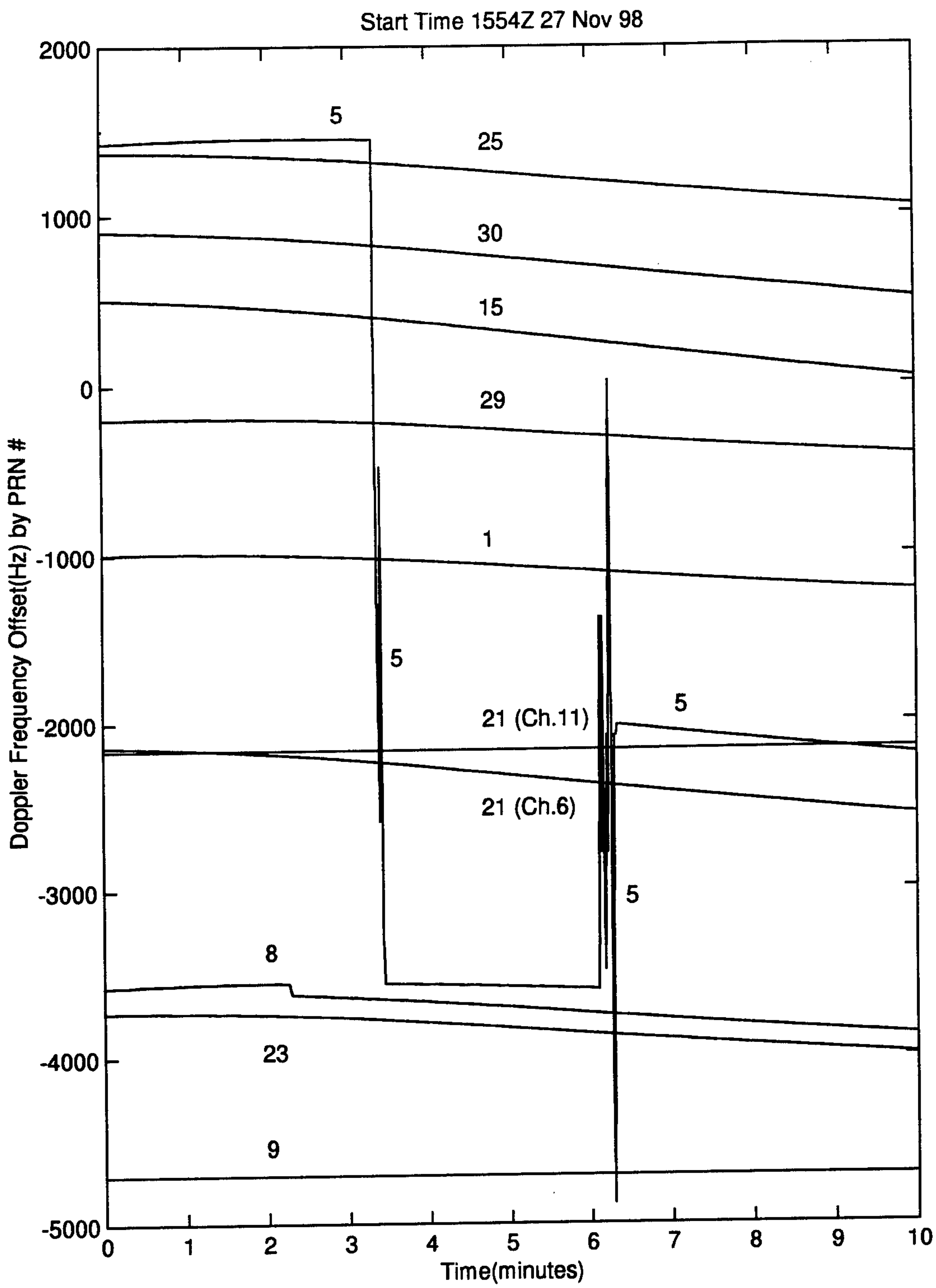

Figure L.7. Doppler Frequency vs Time

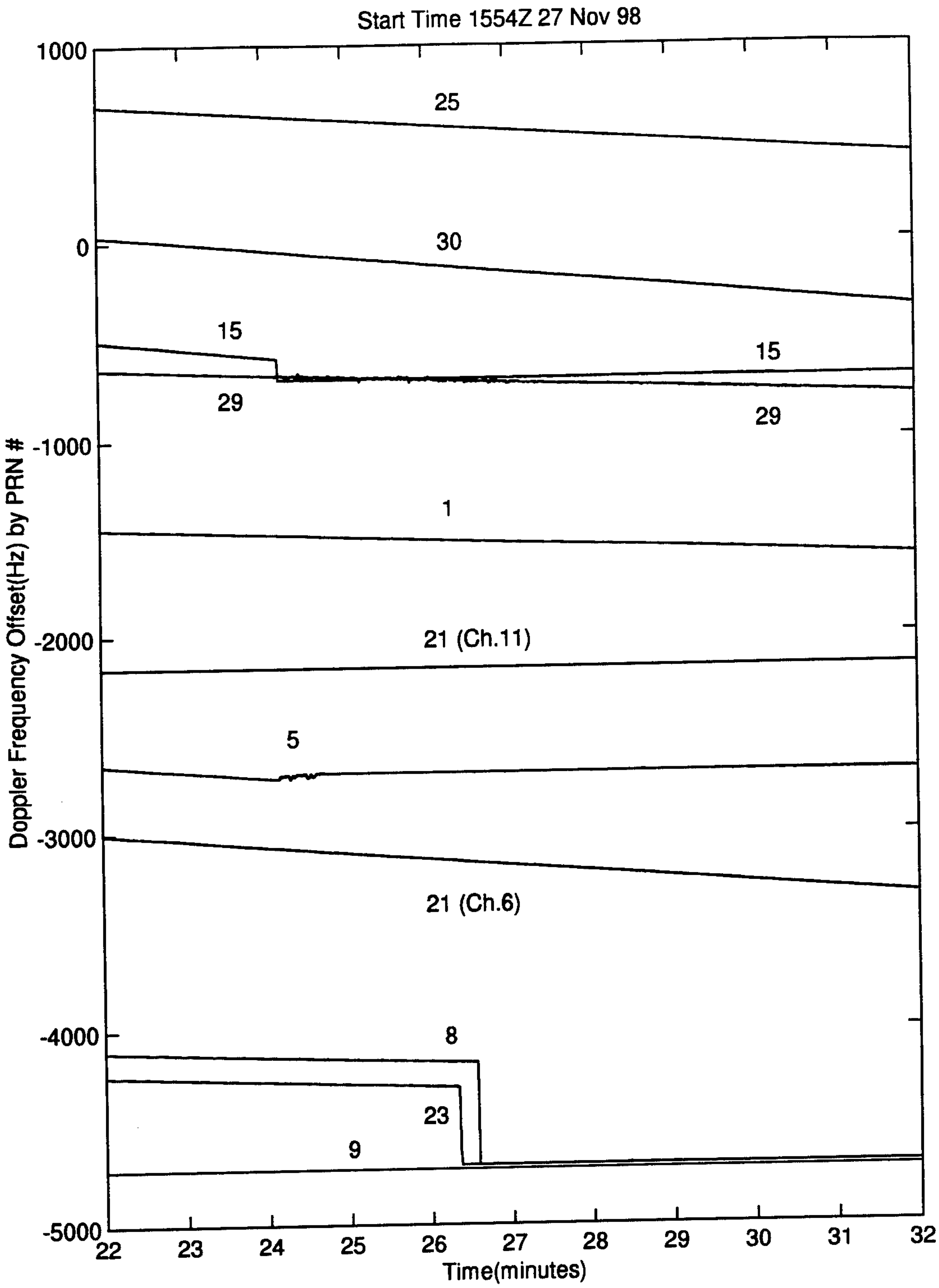

Figure L.8. Doppler Frequency vs Time

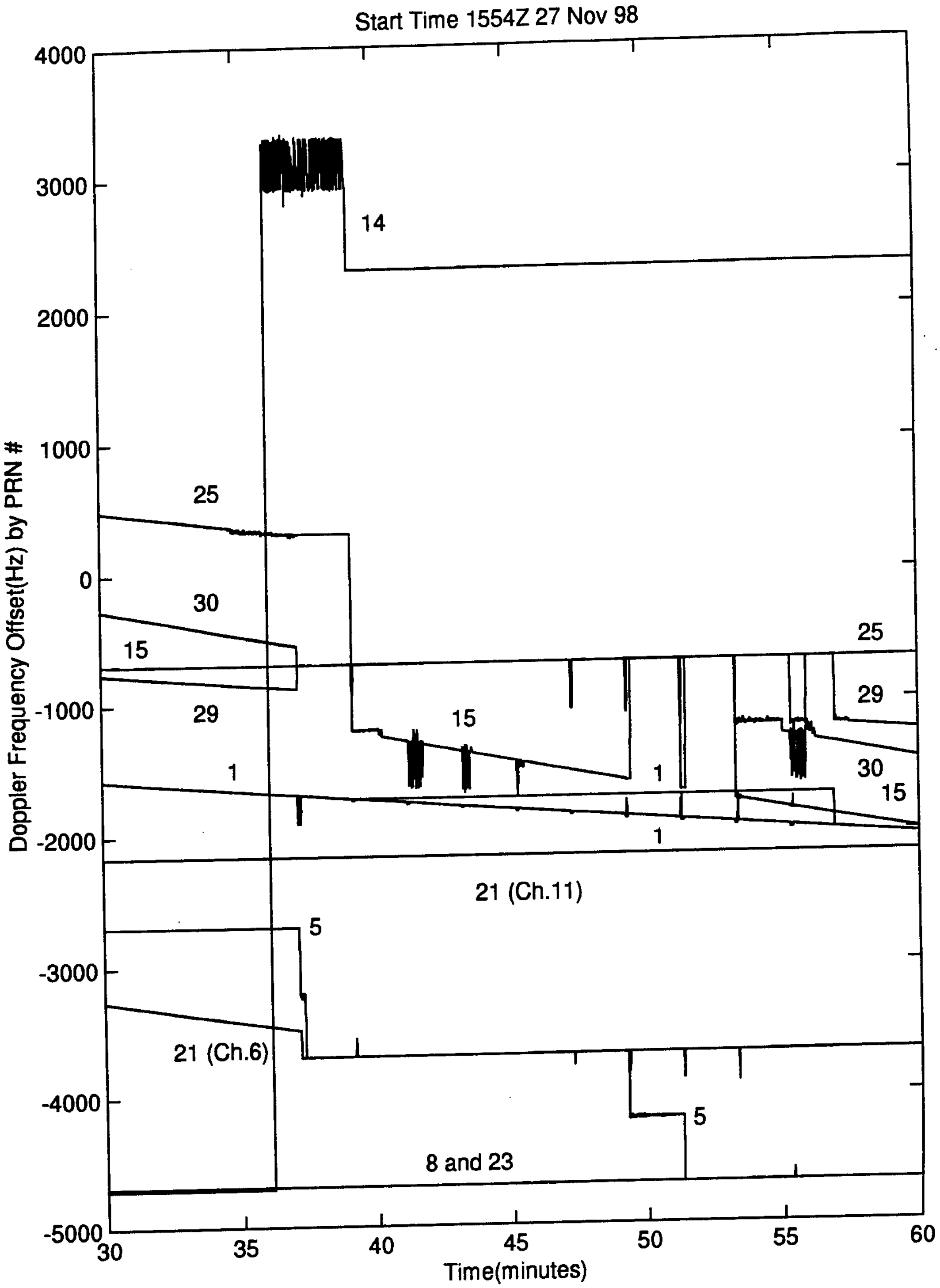

Figure L.9. Doppler Frequency vs Time

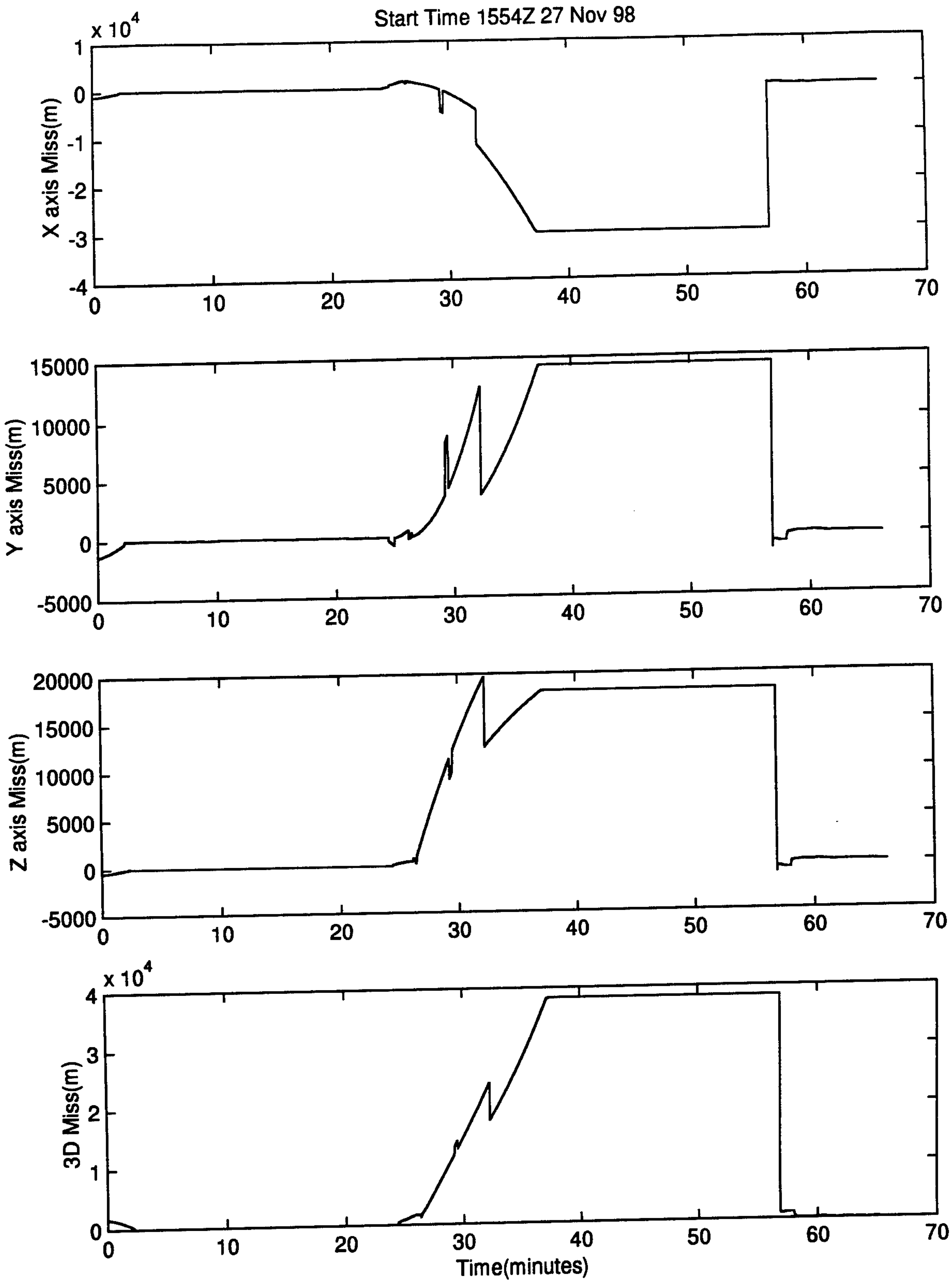

Figure L.10. X,Y,Z and 3D Error(m) vs Time

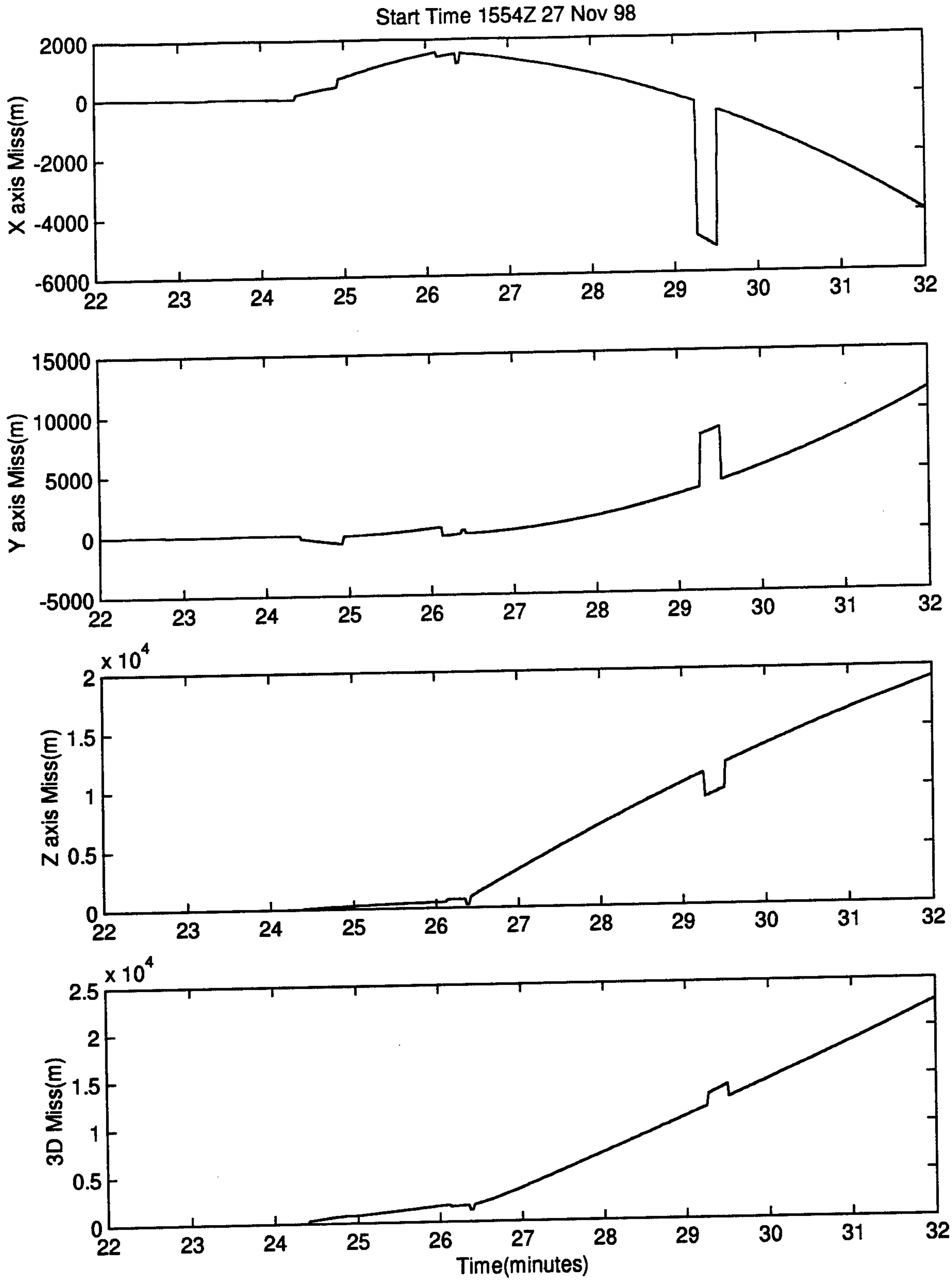

Figure L.11. X,Y,Z and 3D Error(m) vs Time

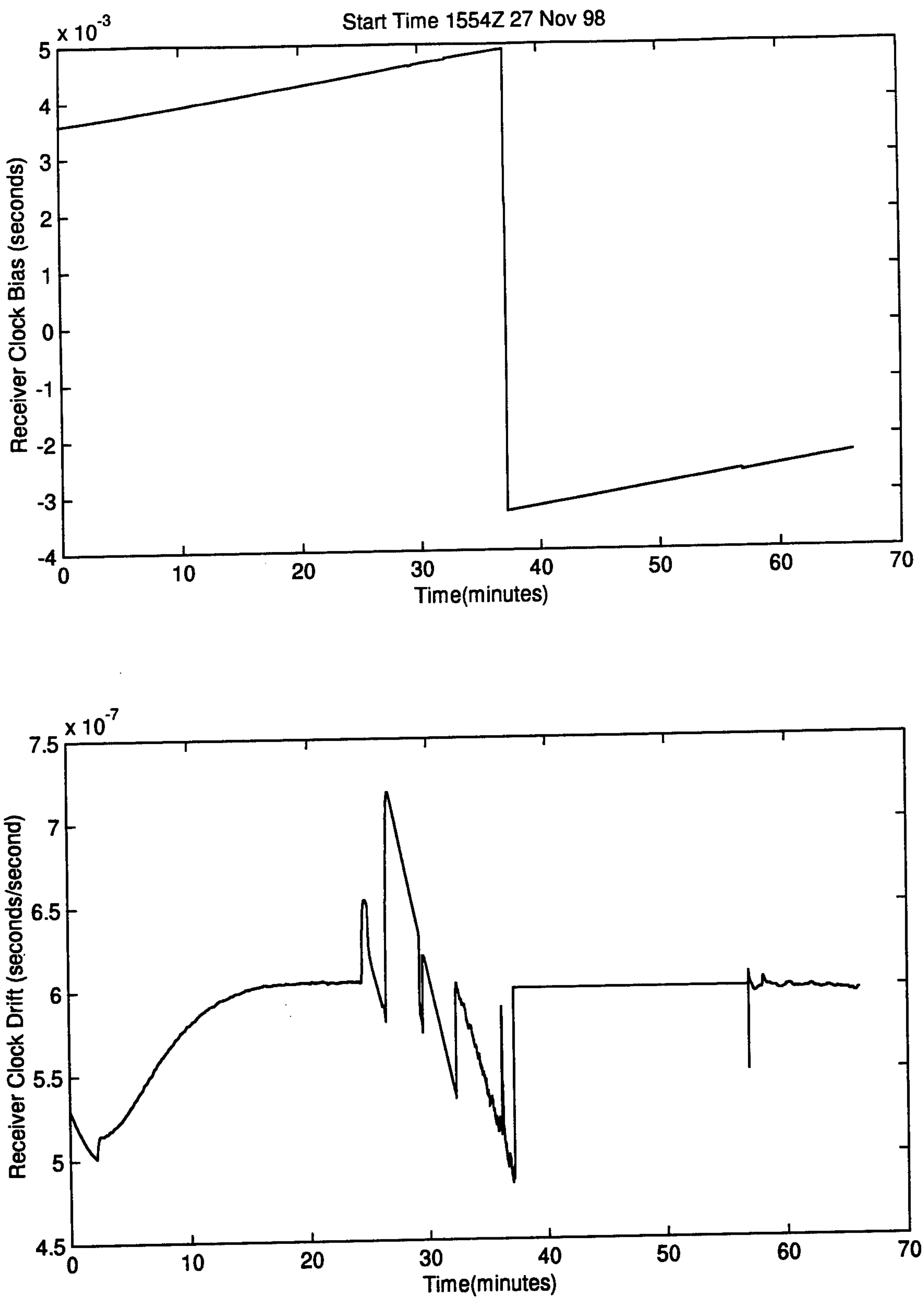

Figure L.12. Receiver Clock Bias and Drift vs Time

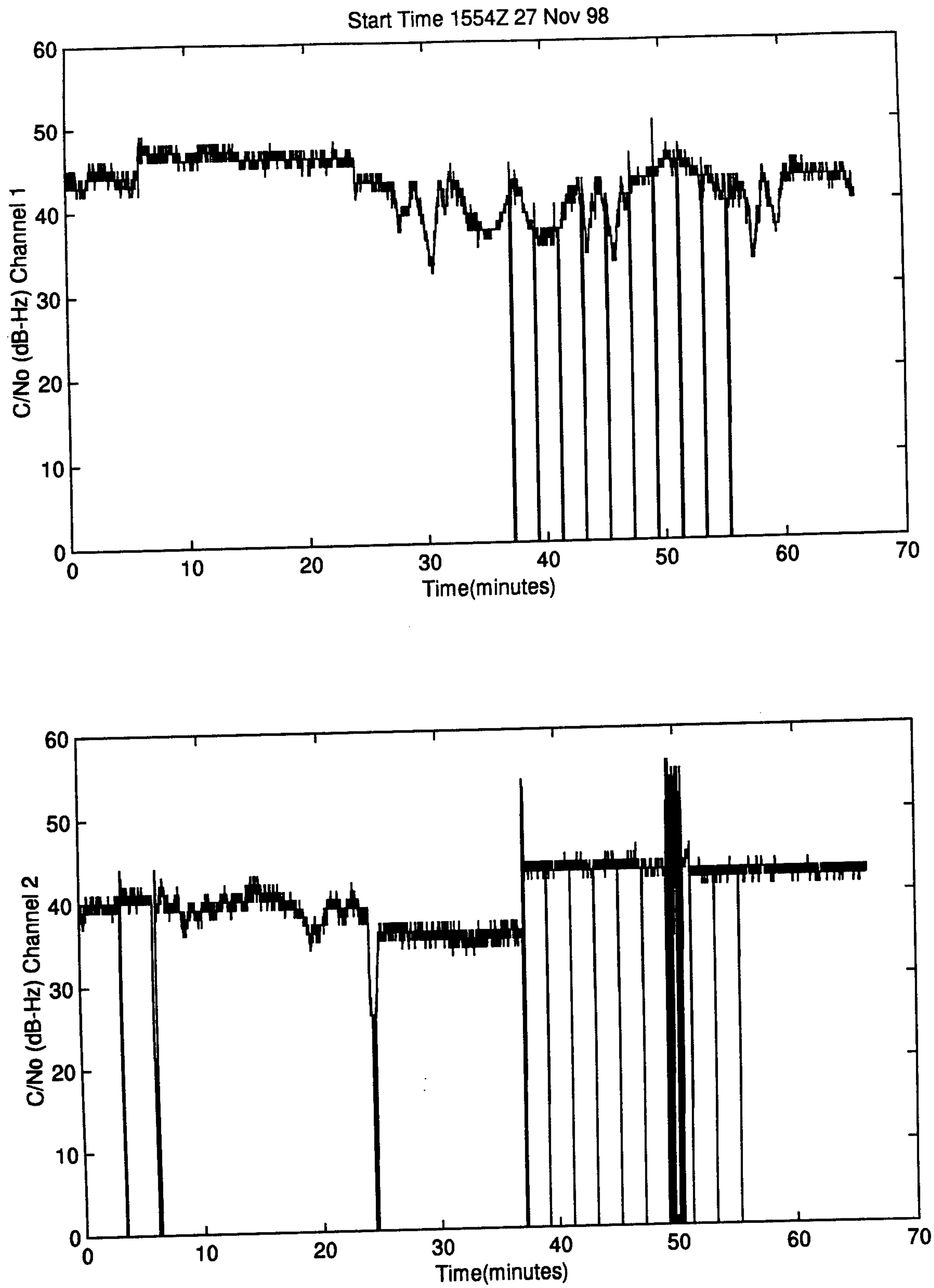

Figure L.13. C/No vs Time

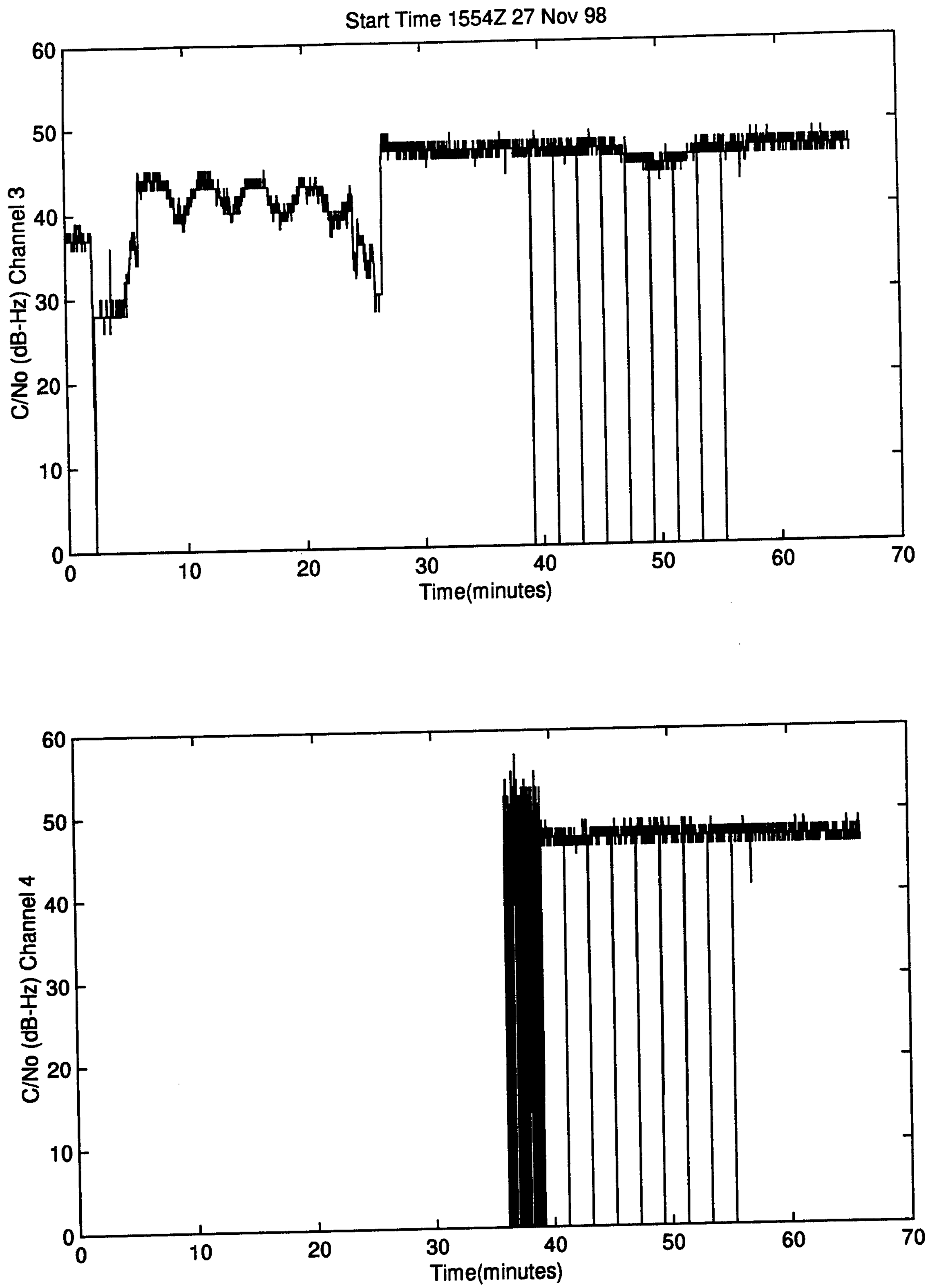

Figure L.14. C/No vs Time

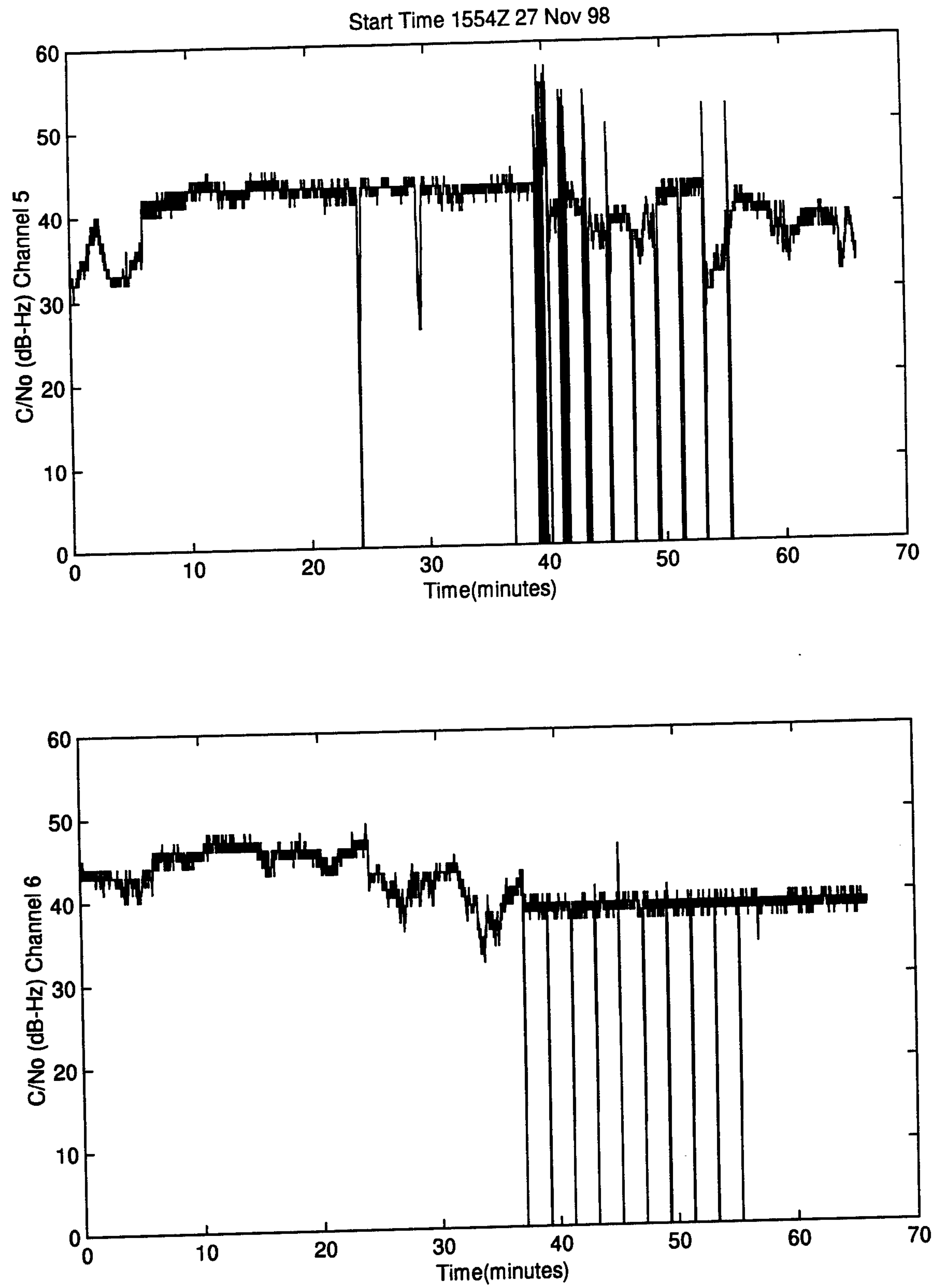

Figure L.15. C/No vs Time

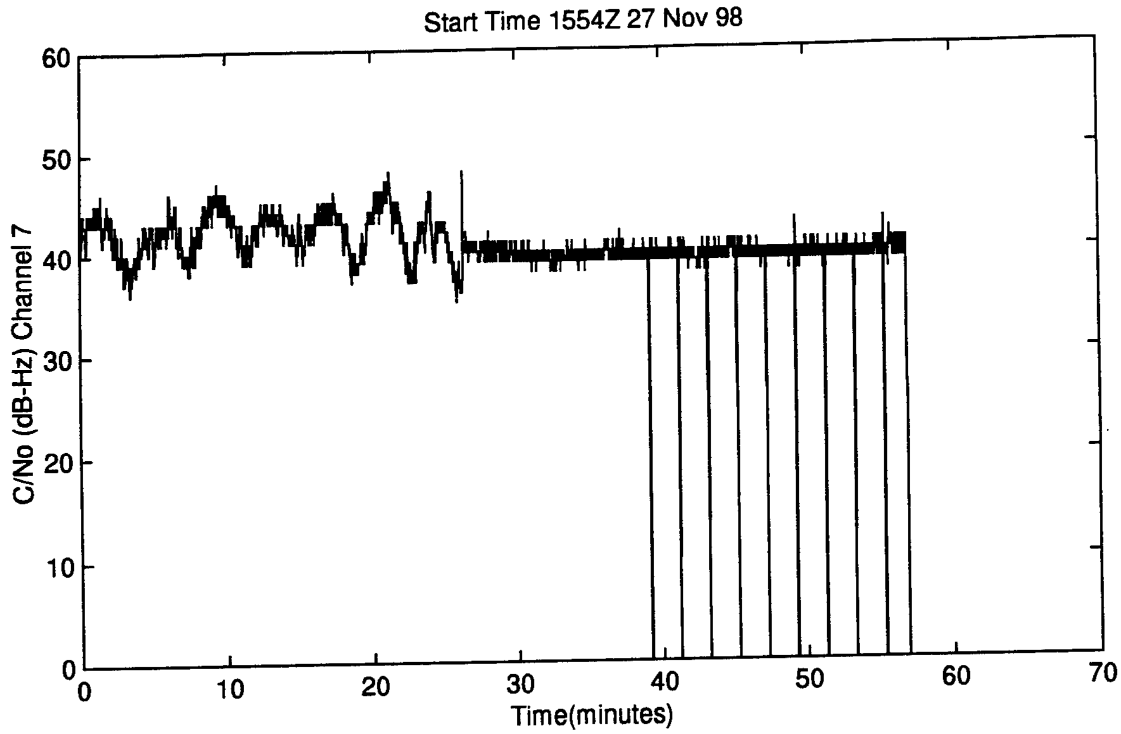

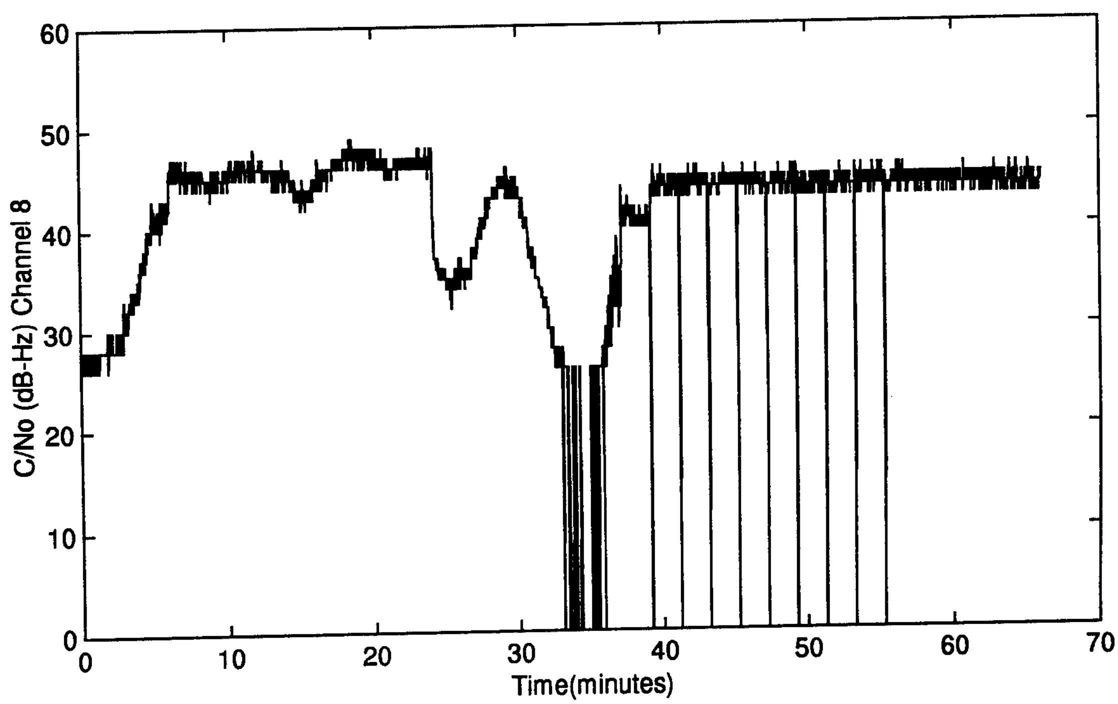

Figure L.16. C/No vs Time

Start Time 1554Z 27 Nov 98

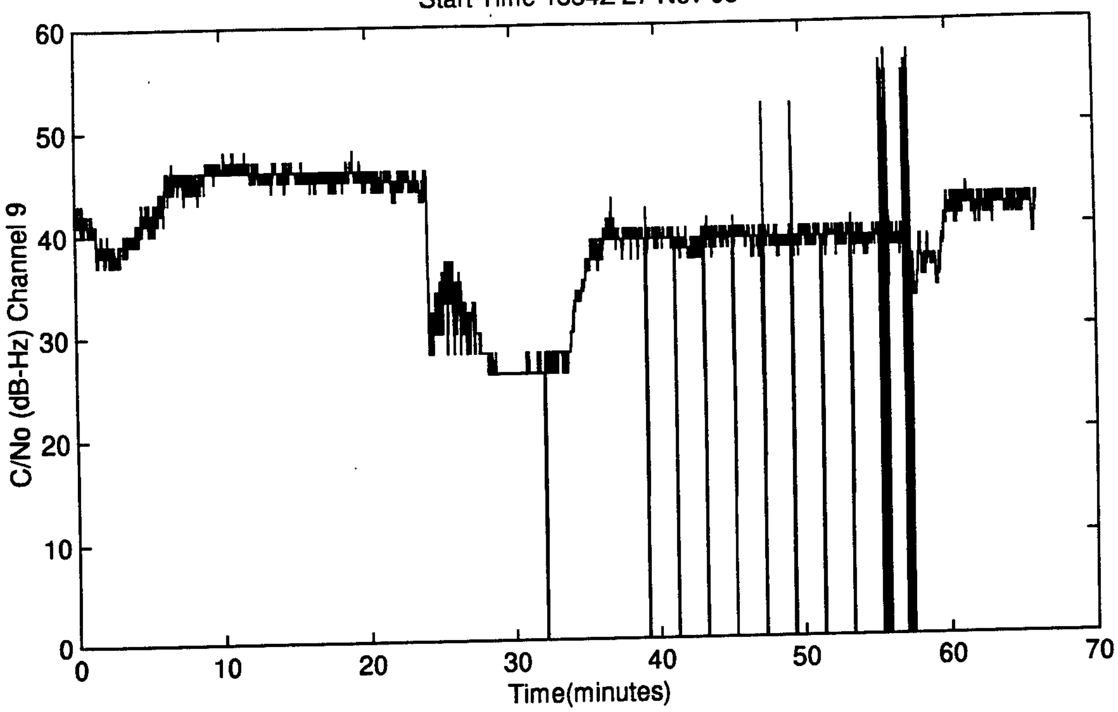

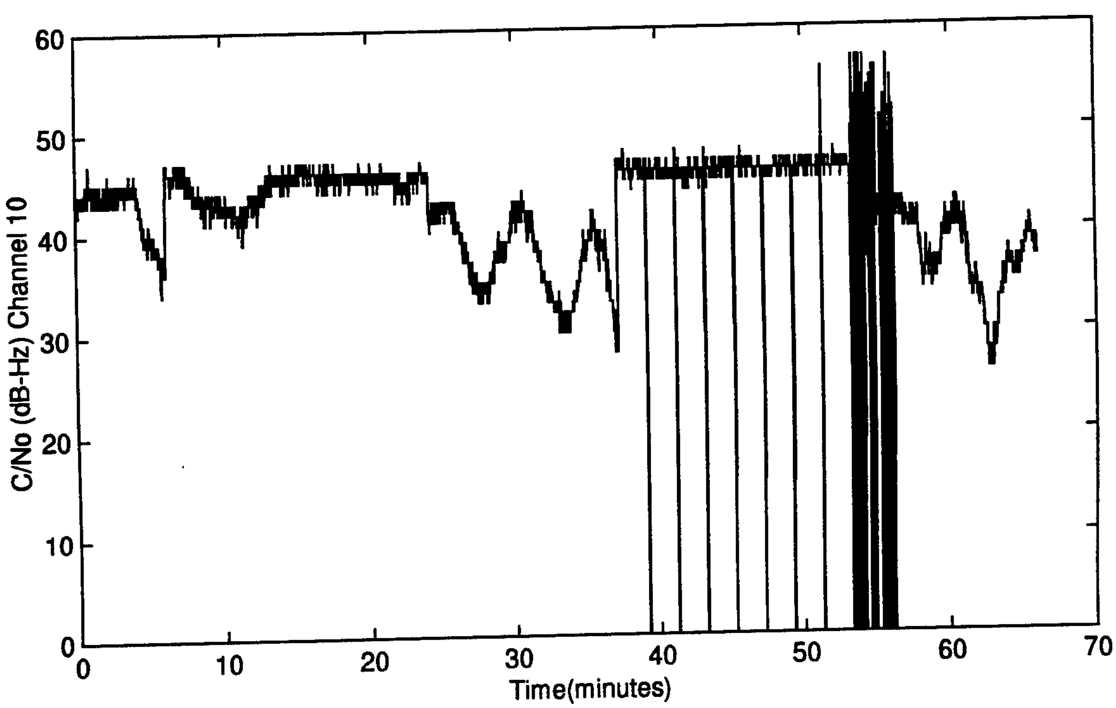

Figure L.17. C/No vs Time

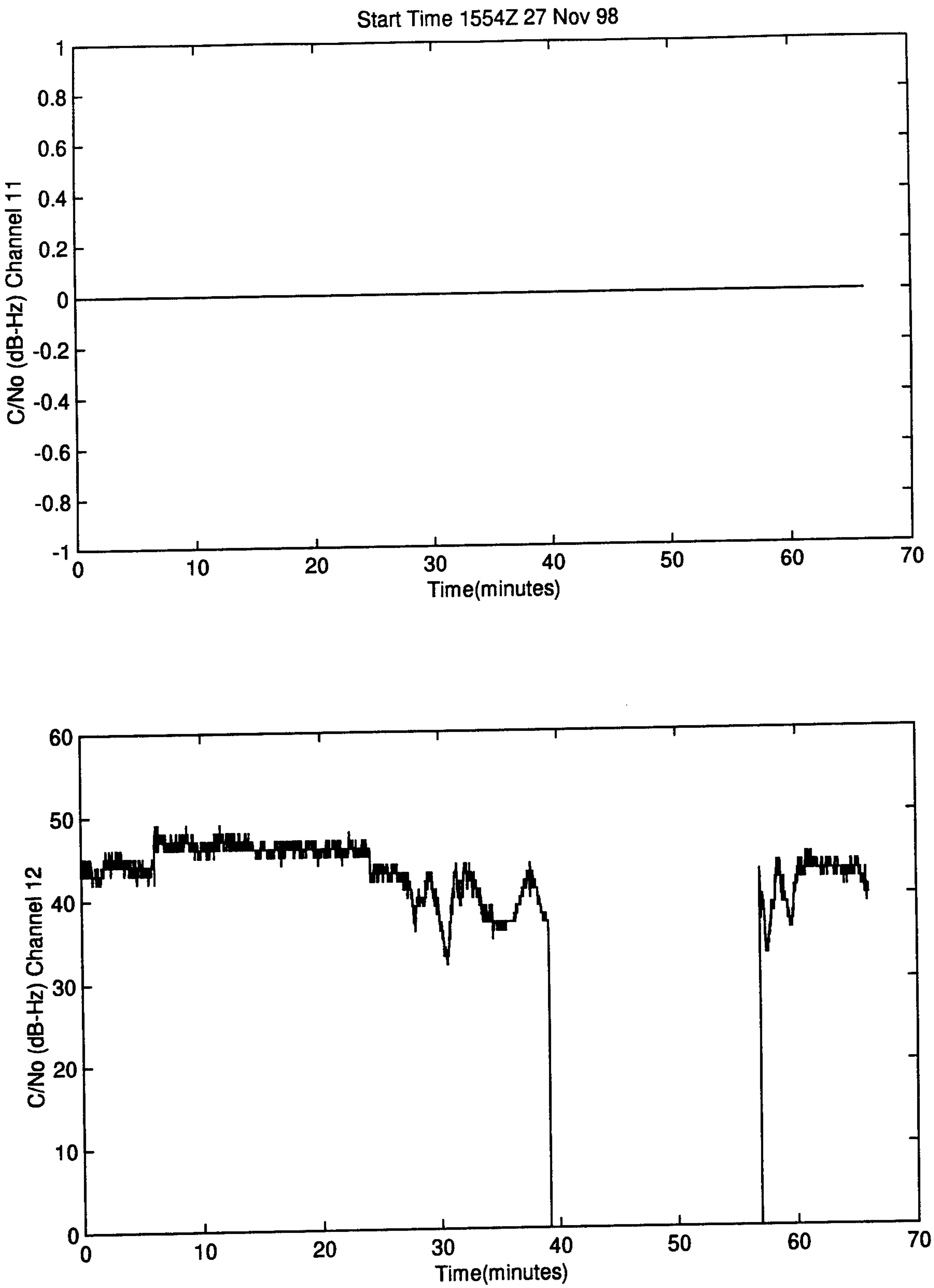

Figure L.18. C/No vs Time

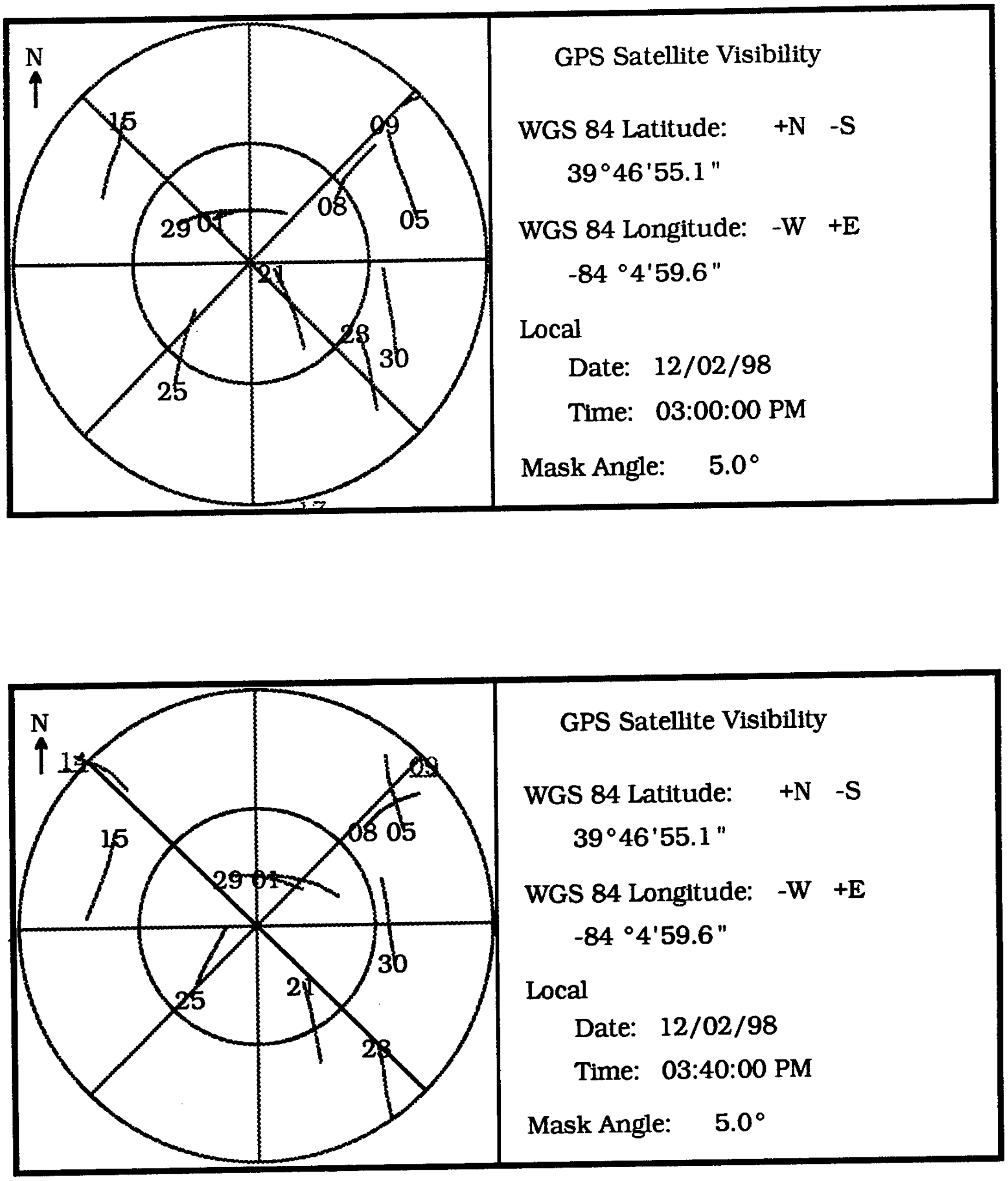

Figure M.1. GPS Satellites In View 02 Dec 98

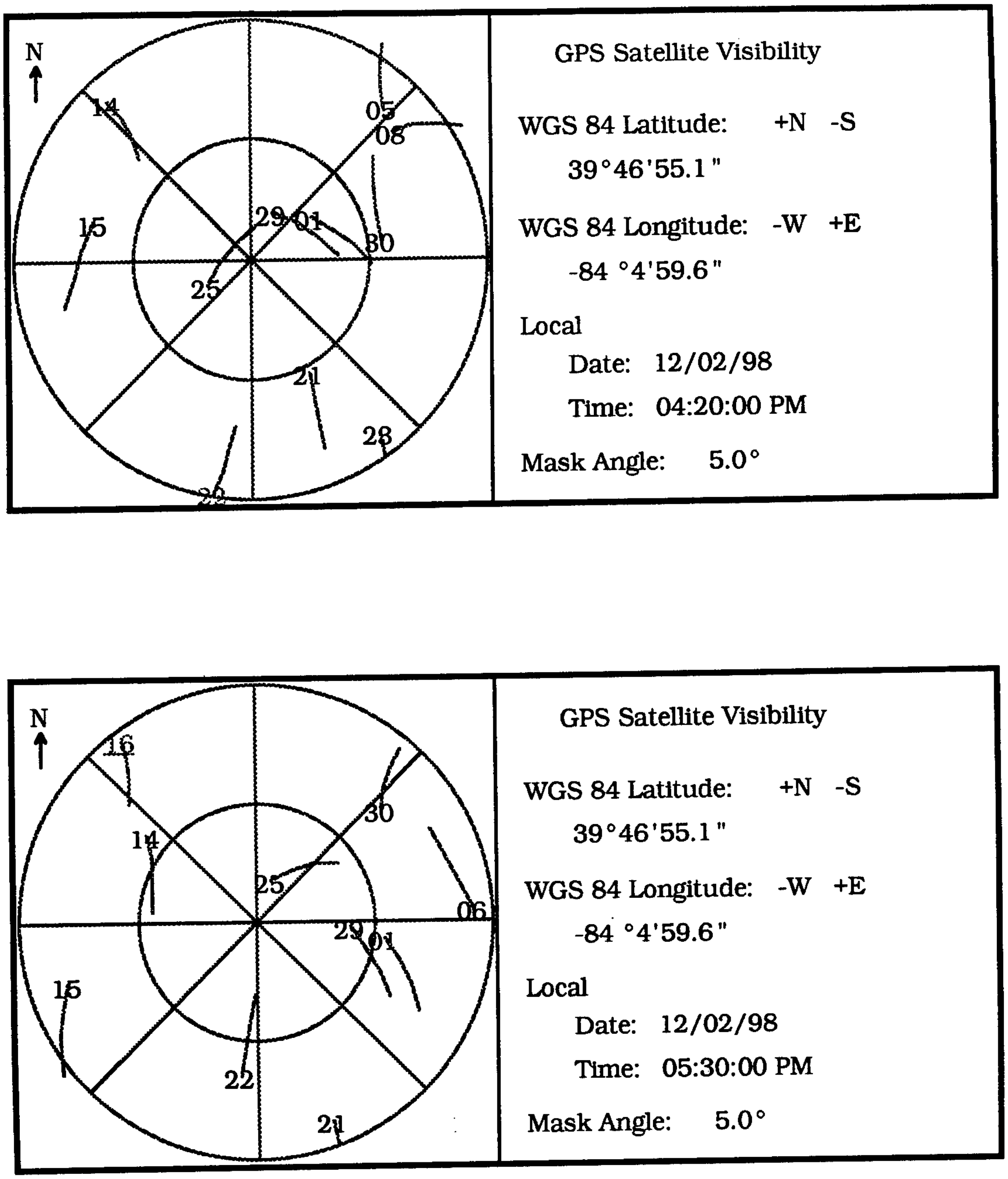

Figure M.2. GPS Satellites In View 02 Dec 98

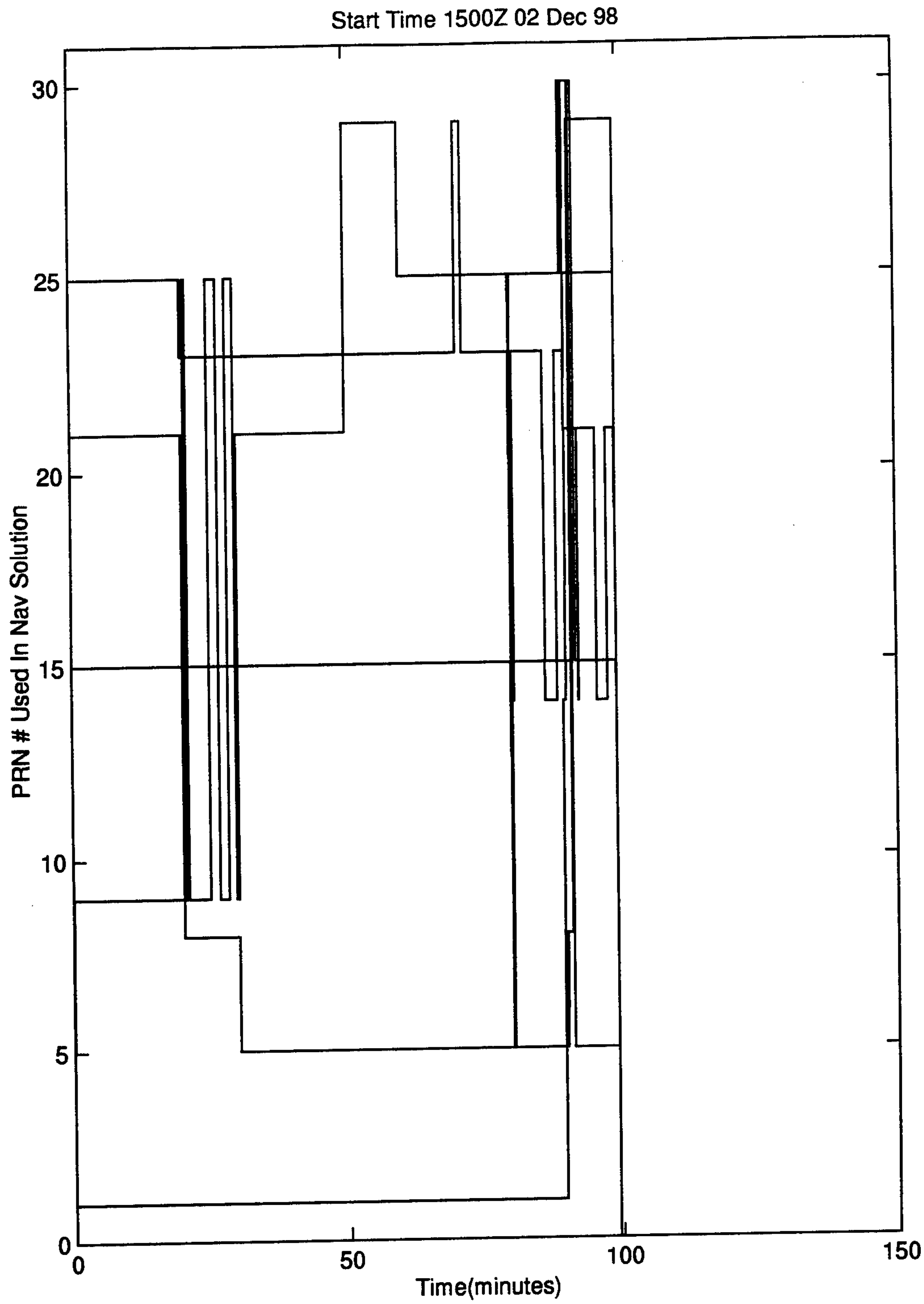

Figure M.3. PRN # Used In Nav Solution vs Time

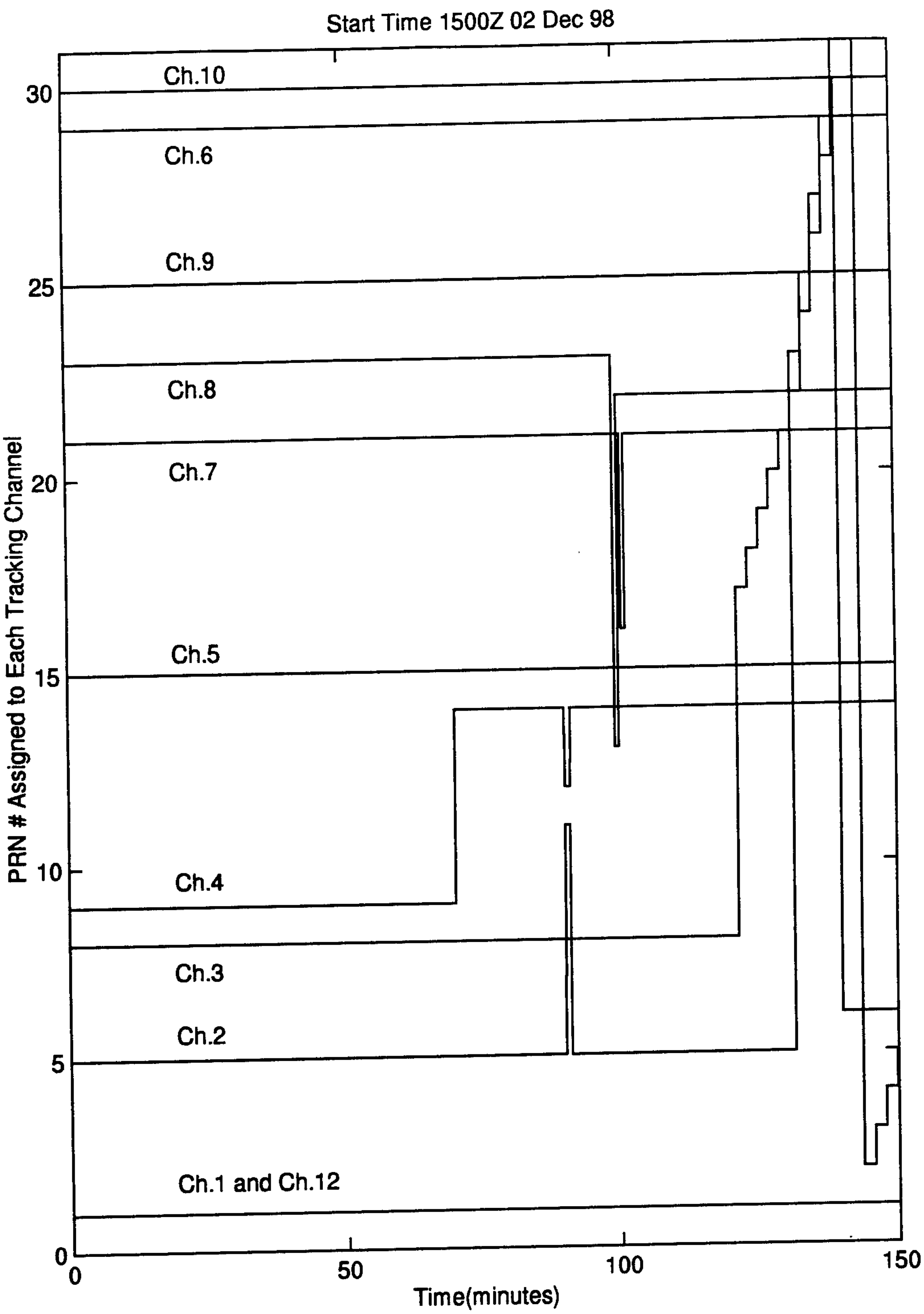

Figure M.4. PRN # Assigned to Each Tracking Channel vs Time

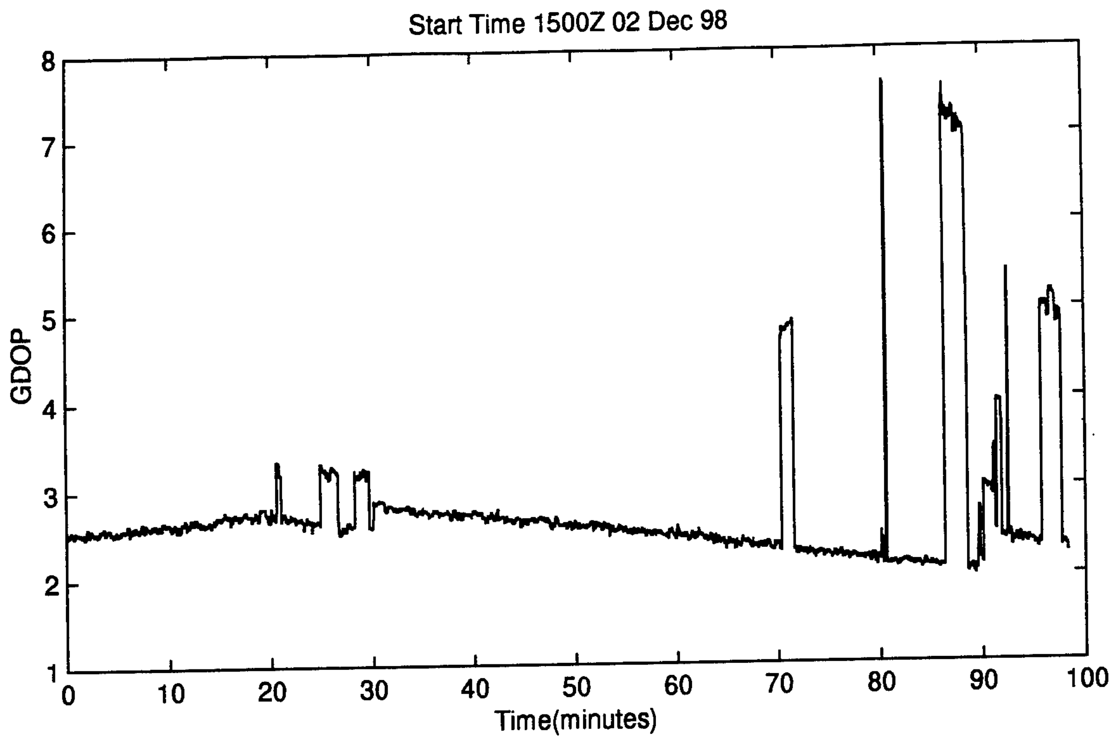

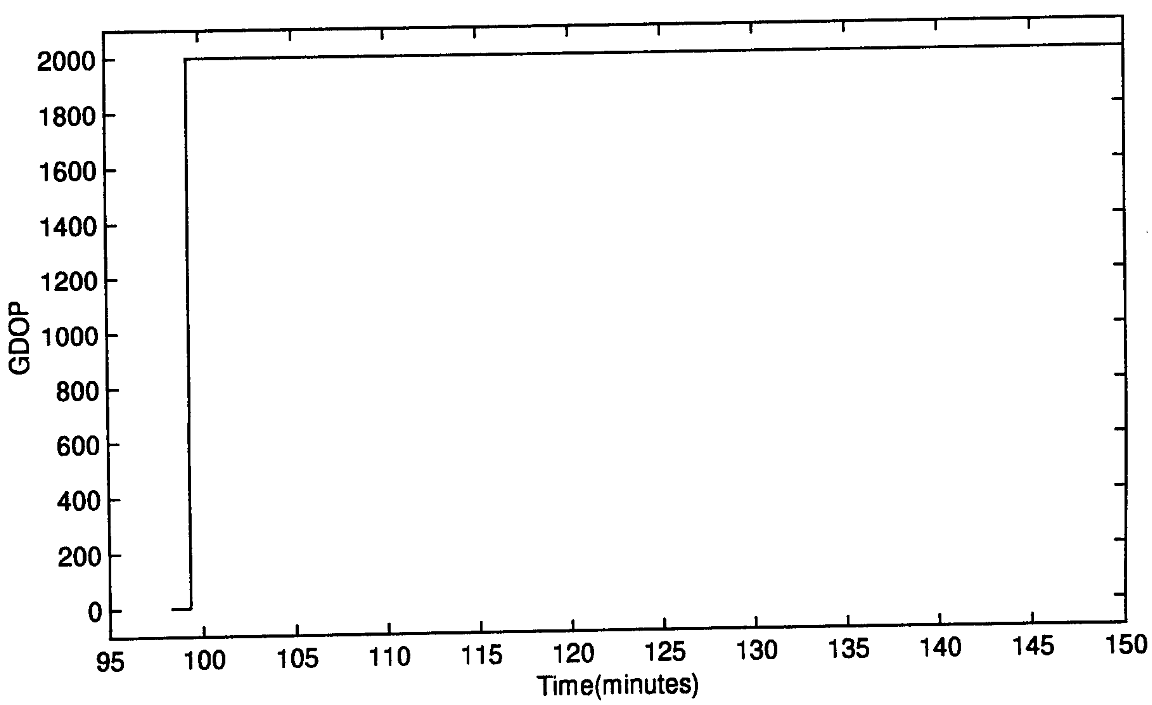

Figure M.5. GDOP vs Time

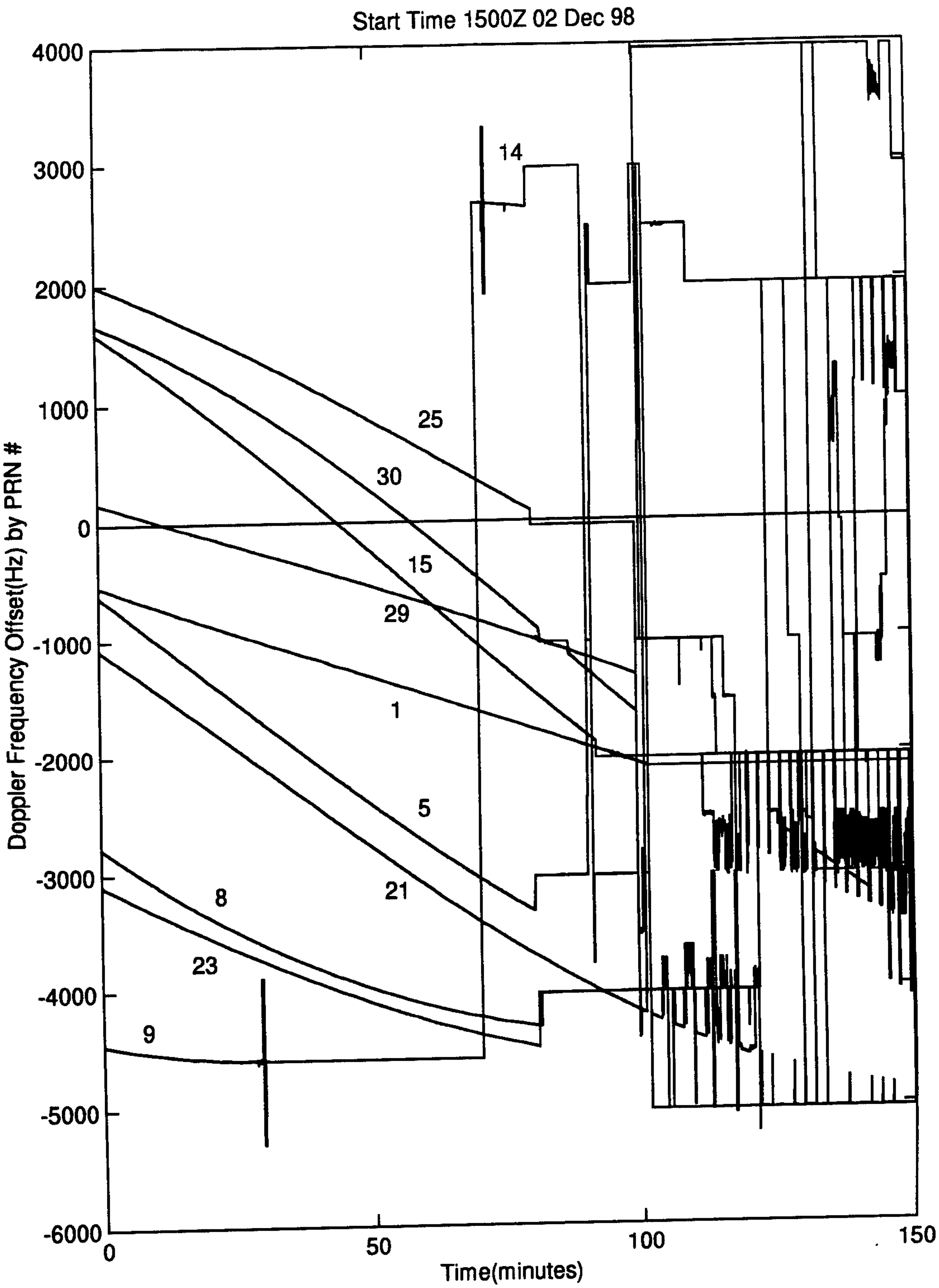

Figure M.6. Doppler Frequency vs Time

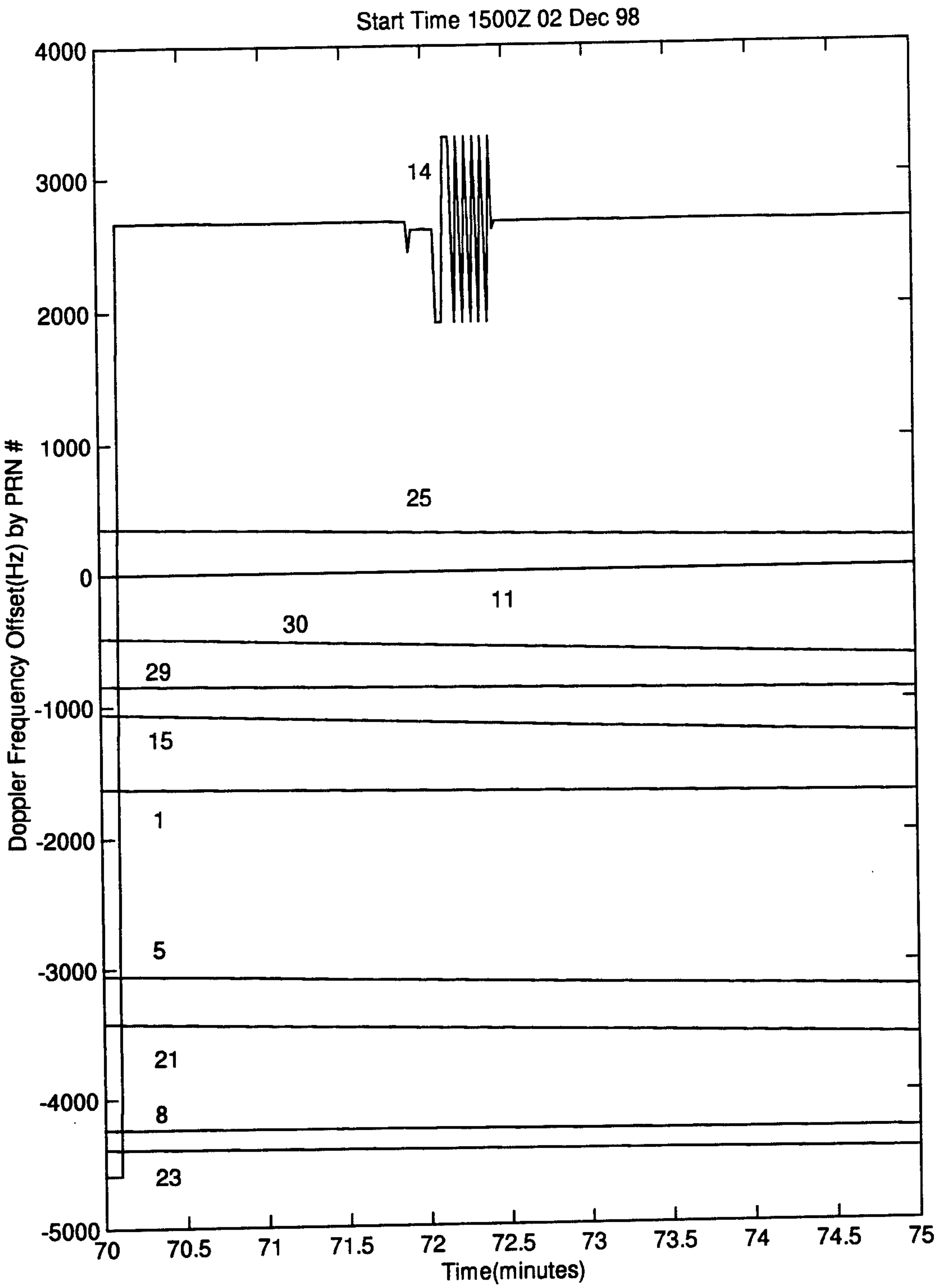

Figure M.7. Doppler Frequency vs Time

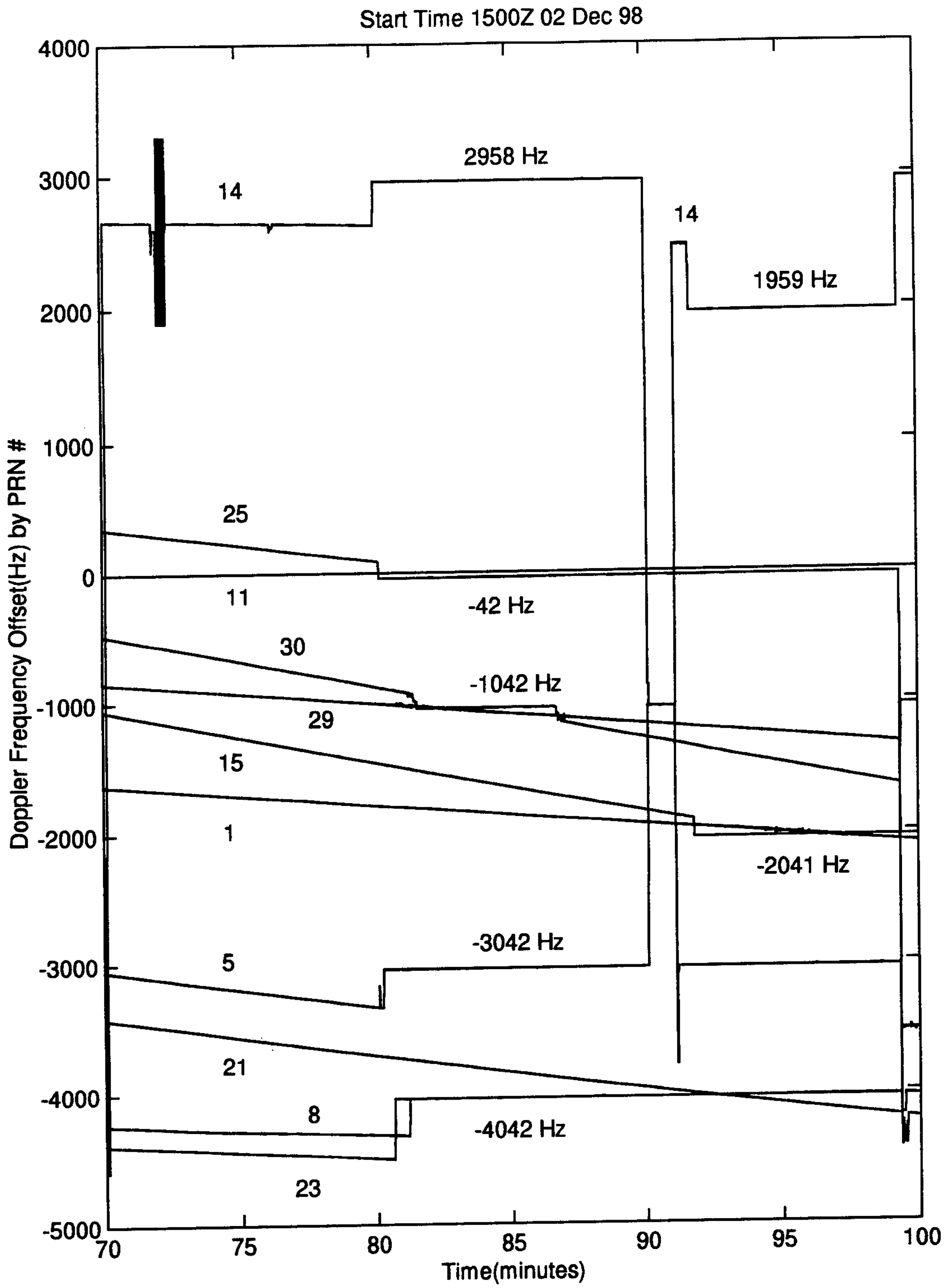

Figure M.8. Doppler Frequency vs Time

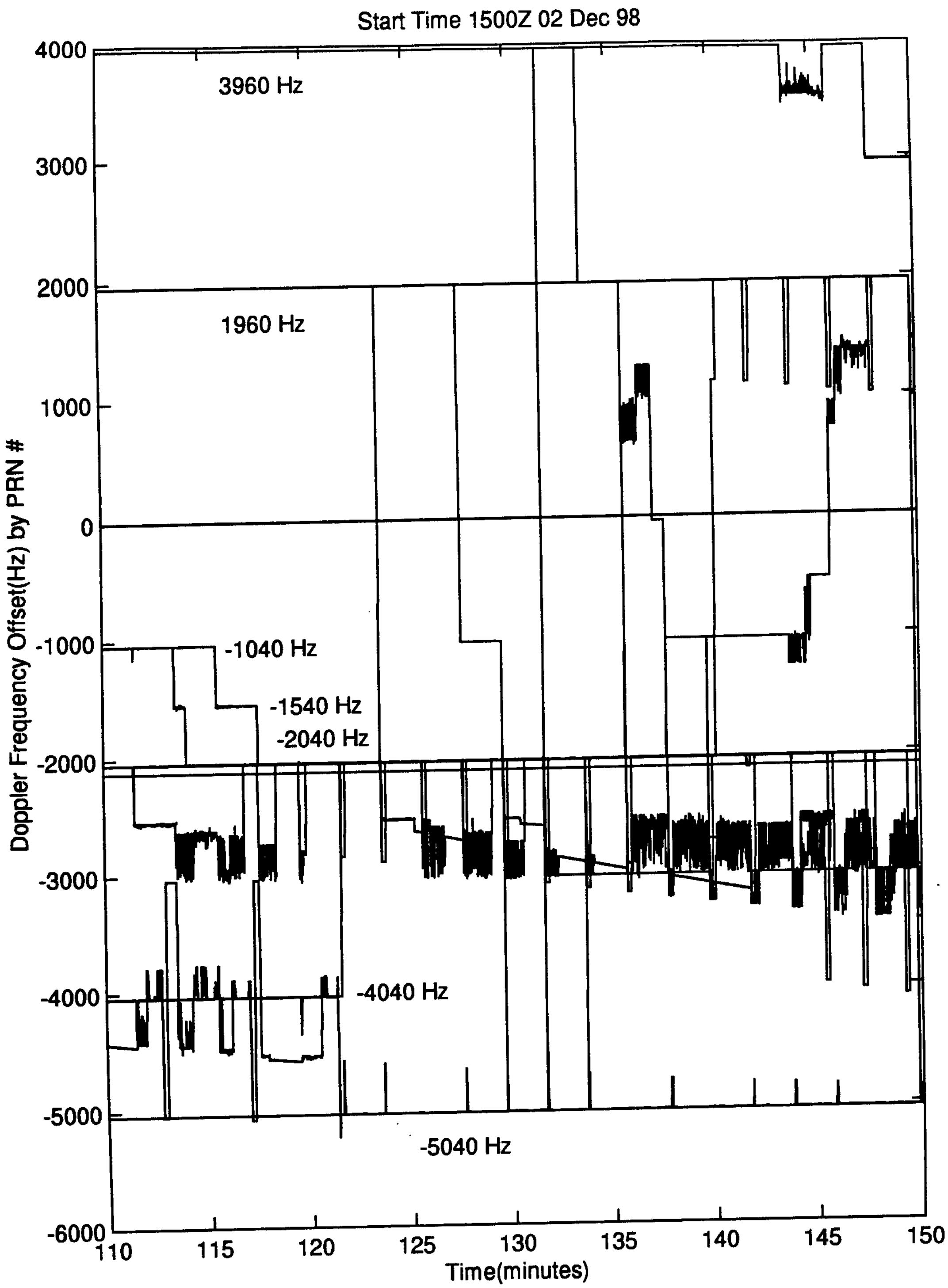

Figure M.9. Doppler Frequency vs Time

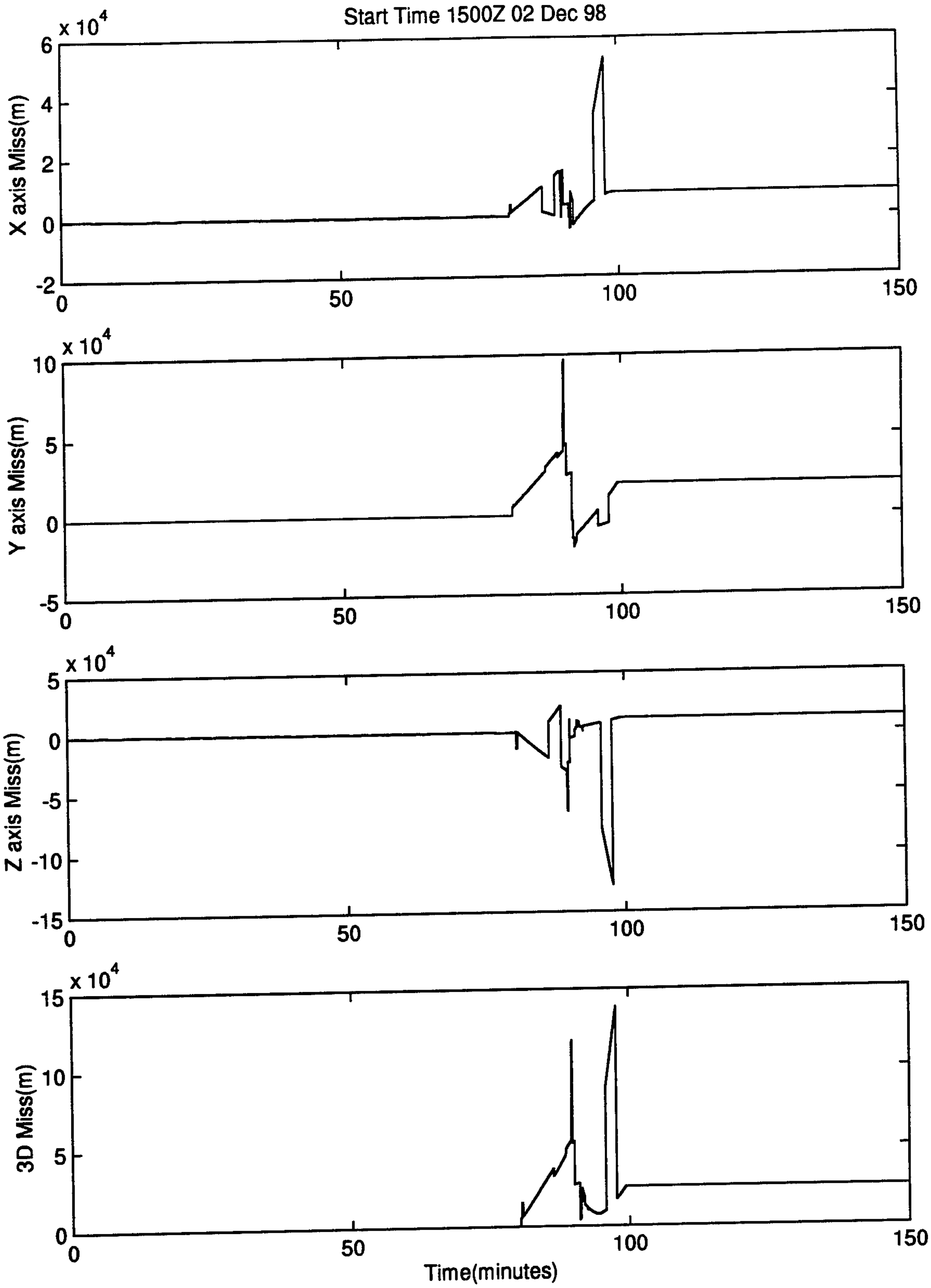

Figure M.10. X,Y,Z and 3D Error(m) vs Time

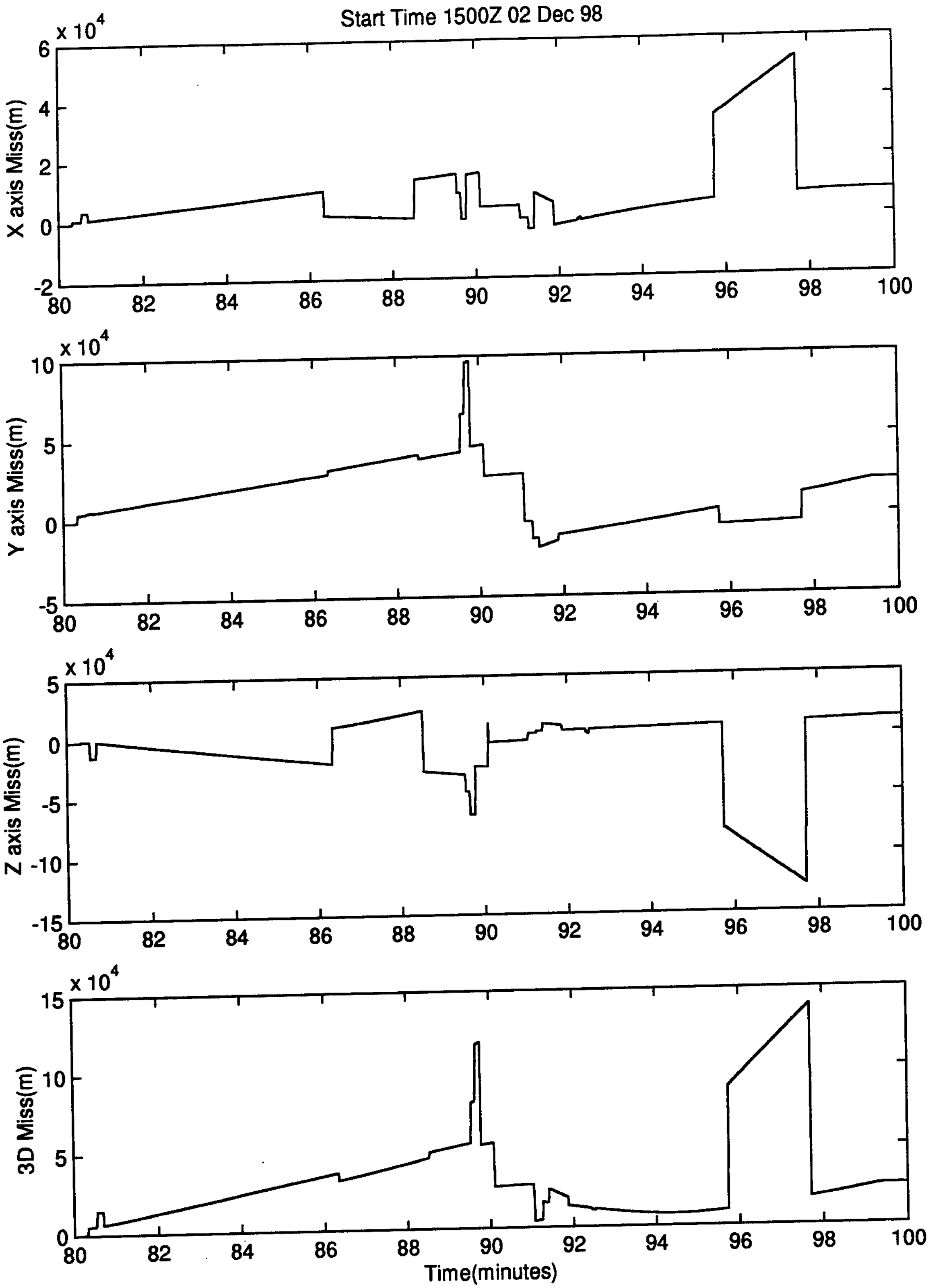

Figure M.11. X,Y,Z and 3D Error(m) vs Time

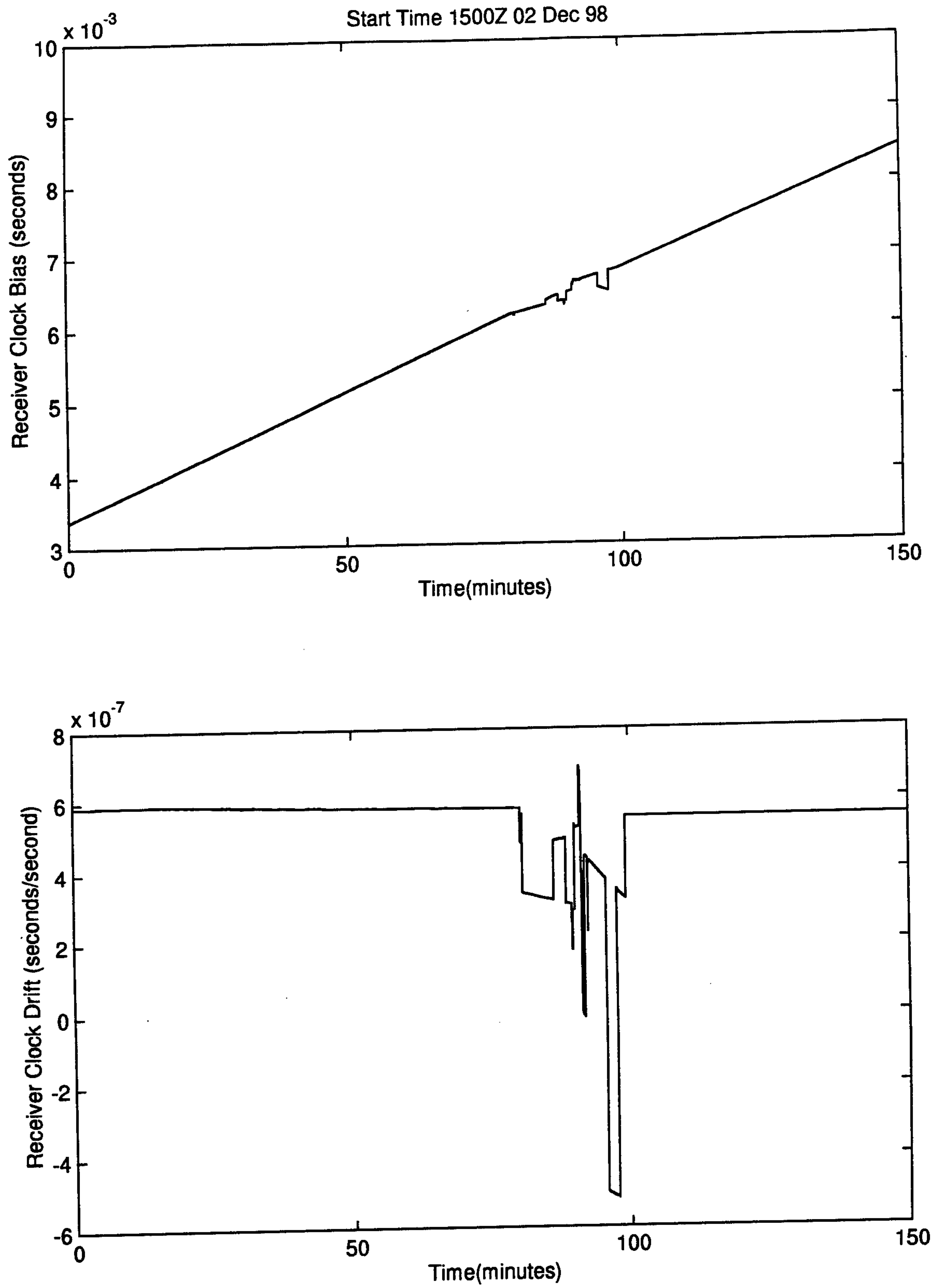

Figure M.12. Receiver Clock Bias and Drift vs Time

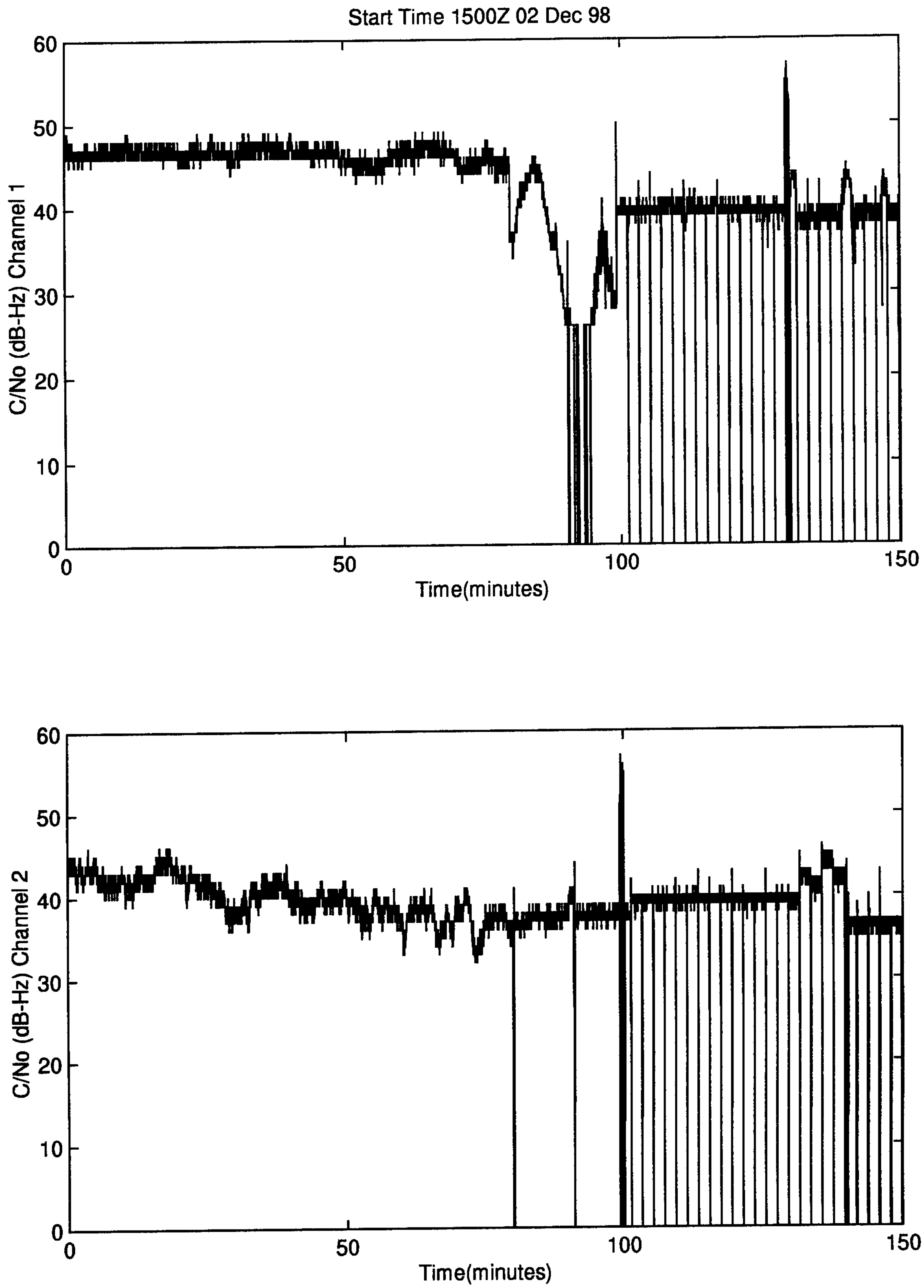

Figure M.13. C/No vs Time

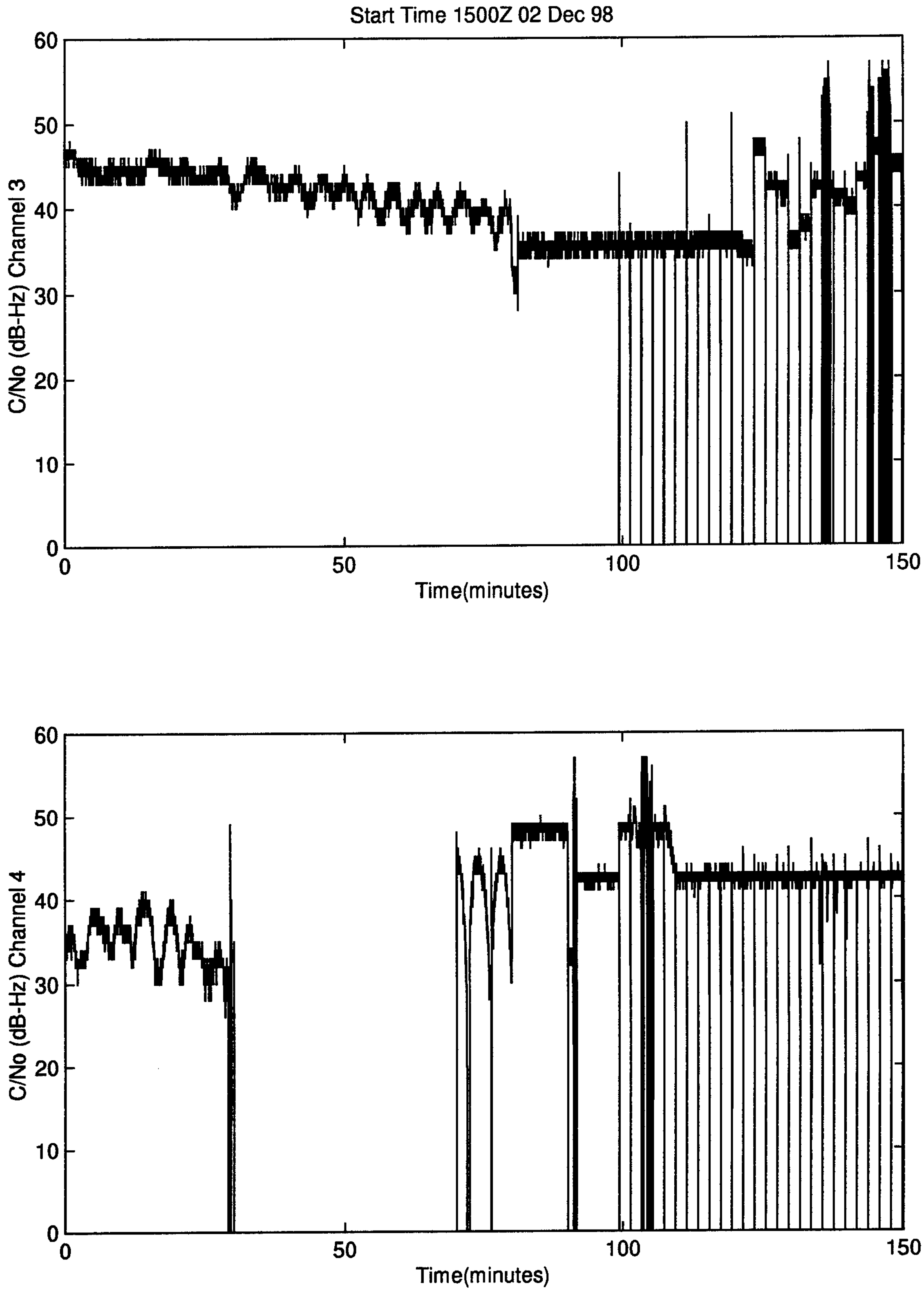

Figure M.14. C/No vs Time

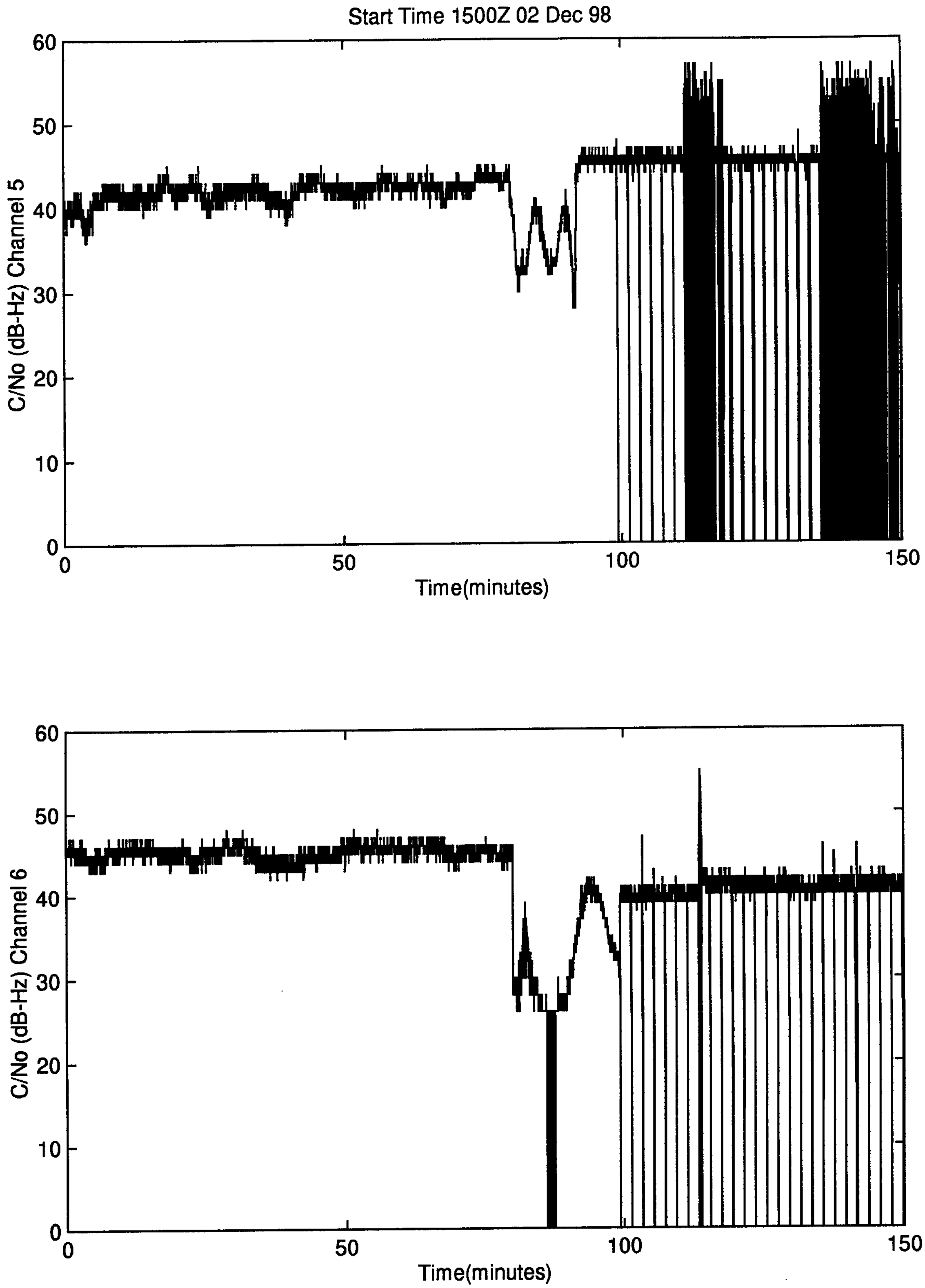

Figure M.15. C/No vs Time

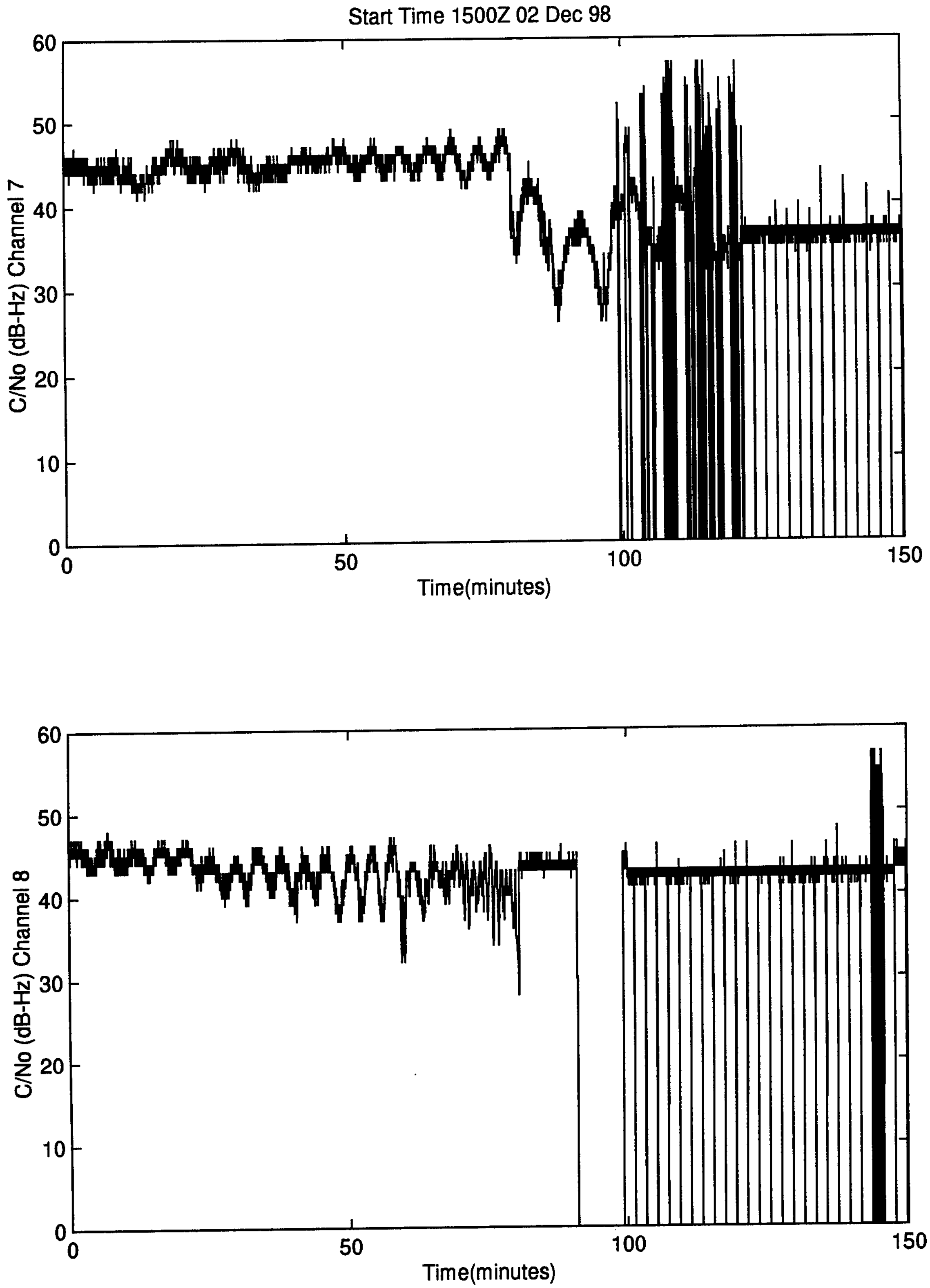

Figure M.16. C/No vs Time

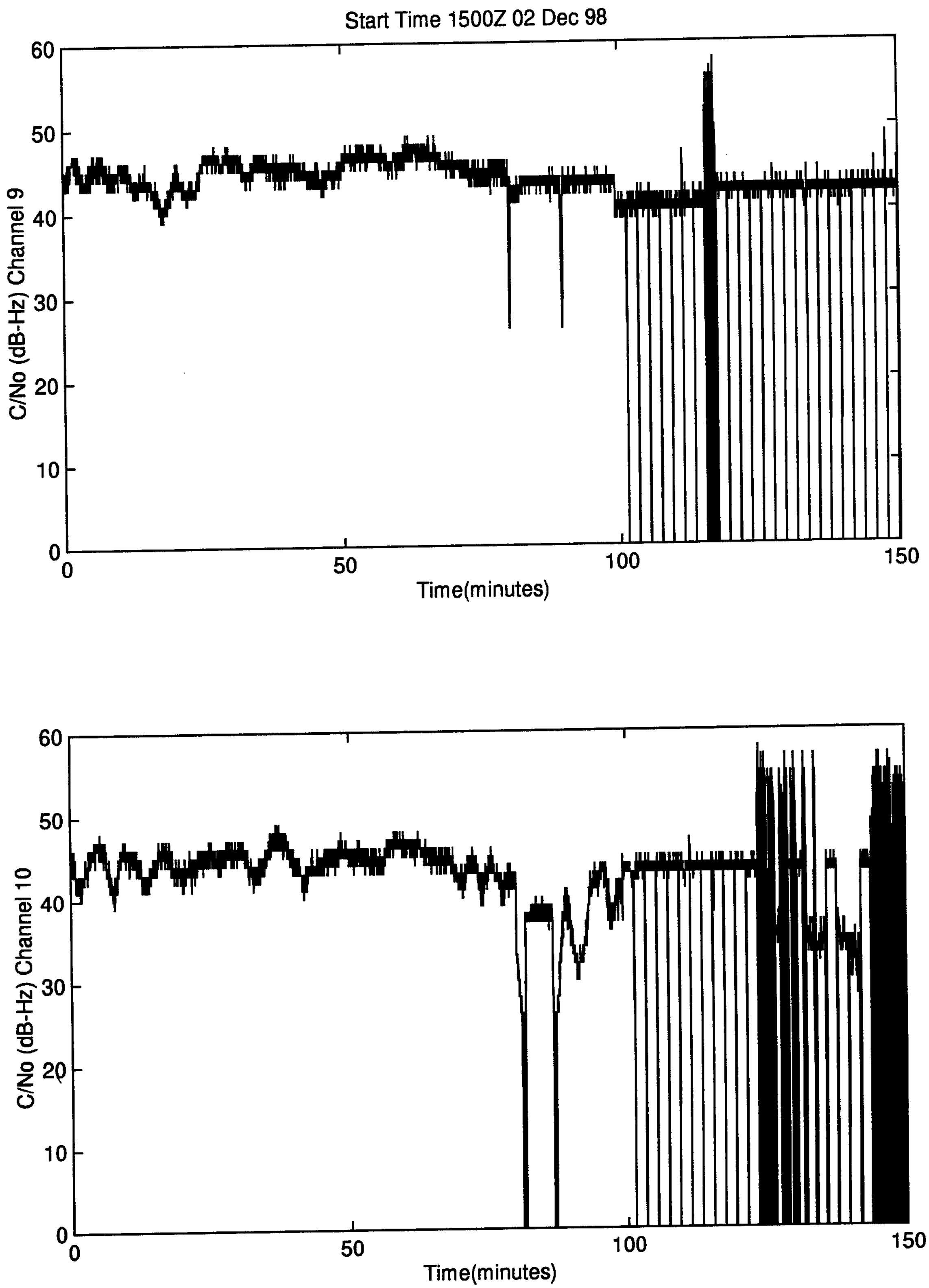

Figure M.17. C/No vs Time

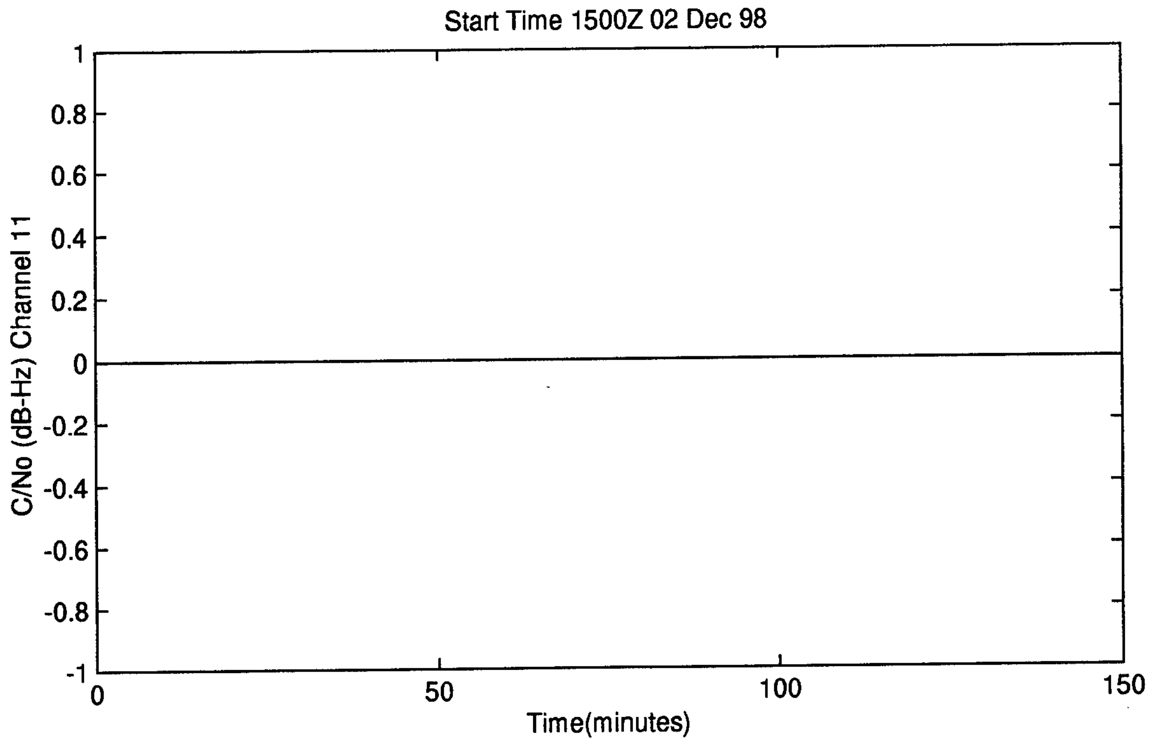

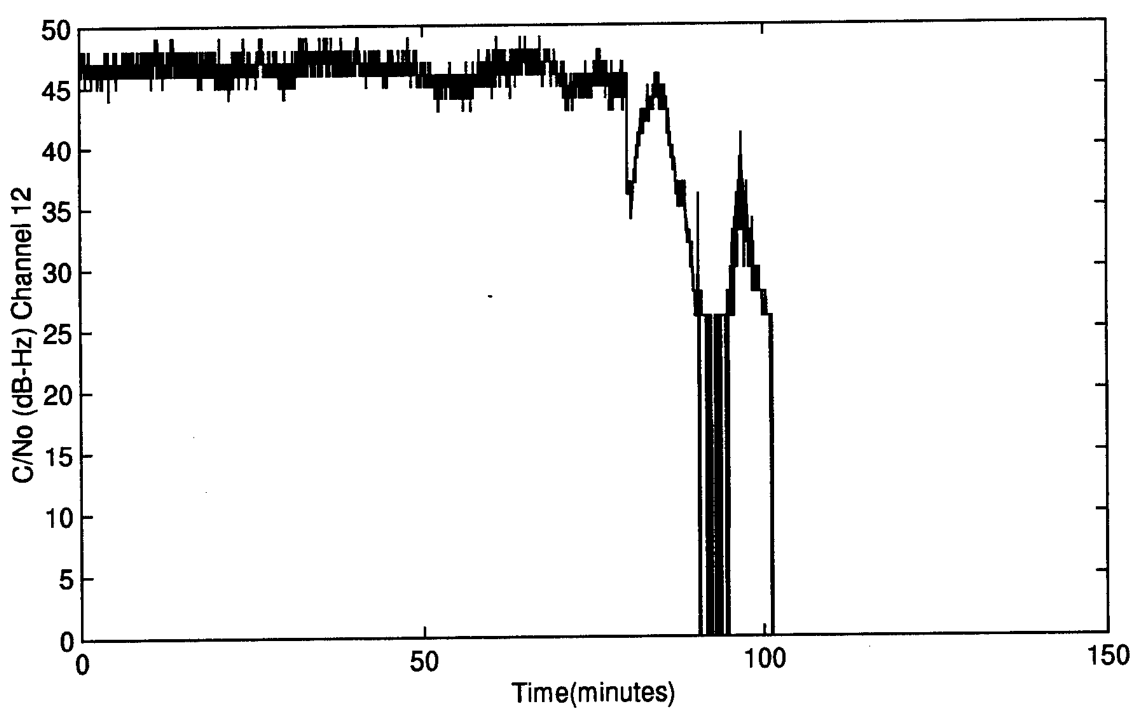

Figure M.18. C/No vs Time

APPENDIX N

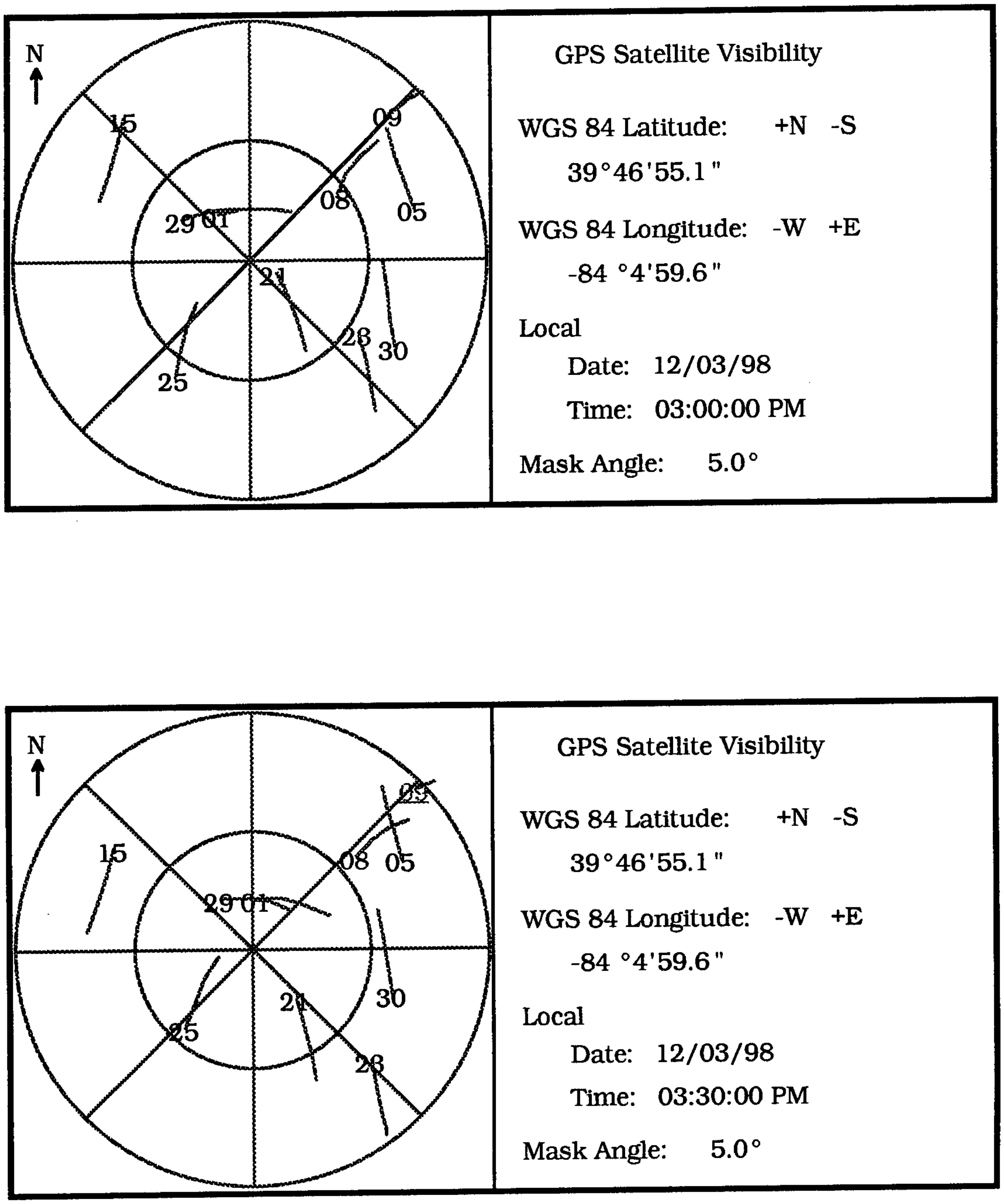

Figure N.1. GPS Satellites In View 03 Dec 98

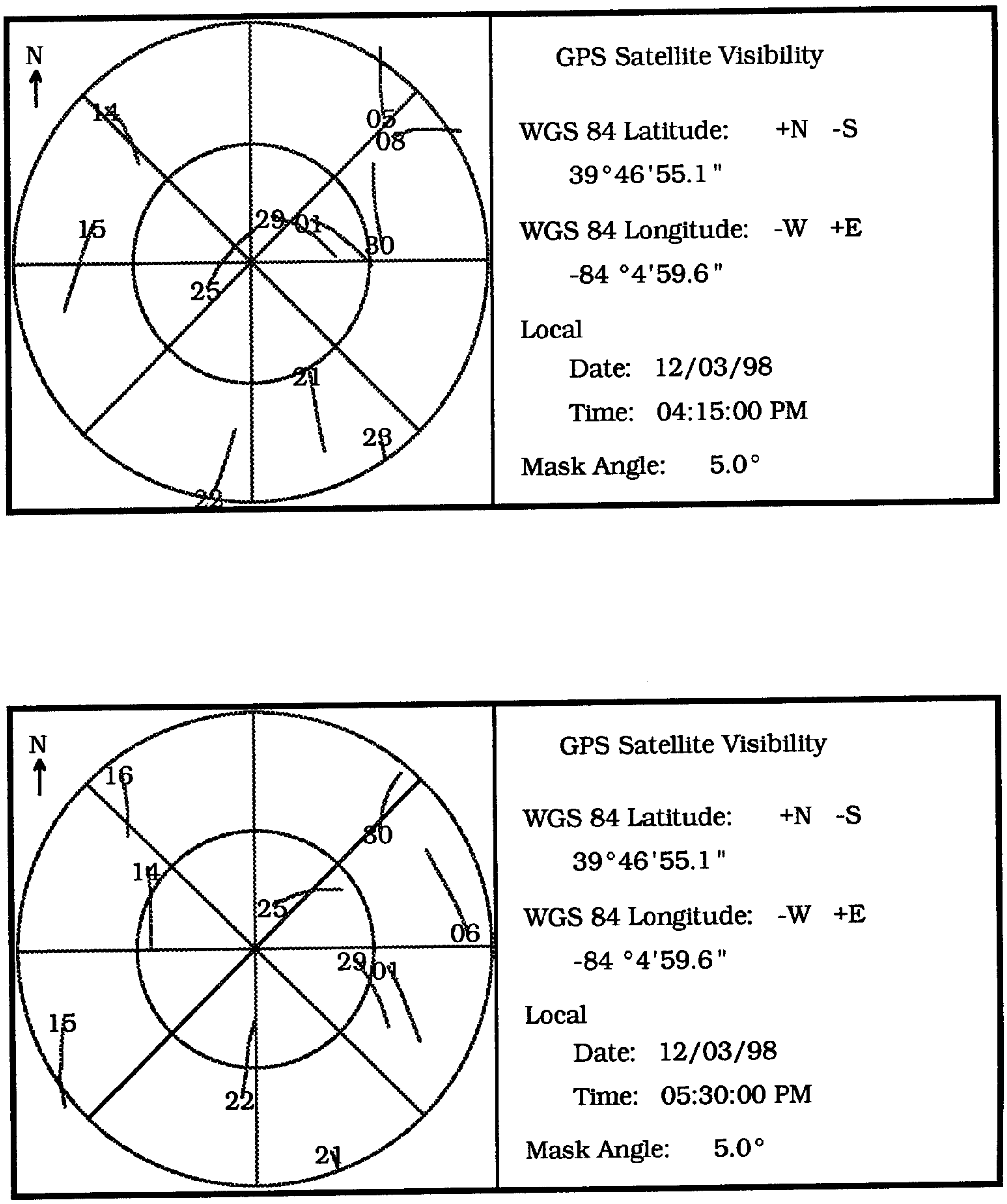

Figure N.2. GPS Satellites In View 03 Dec 98

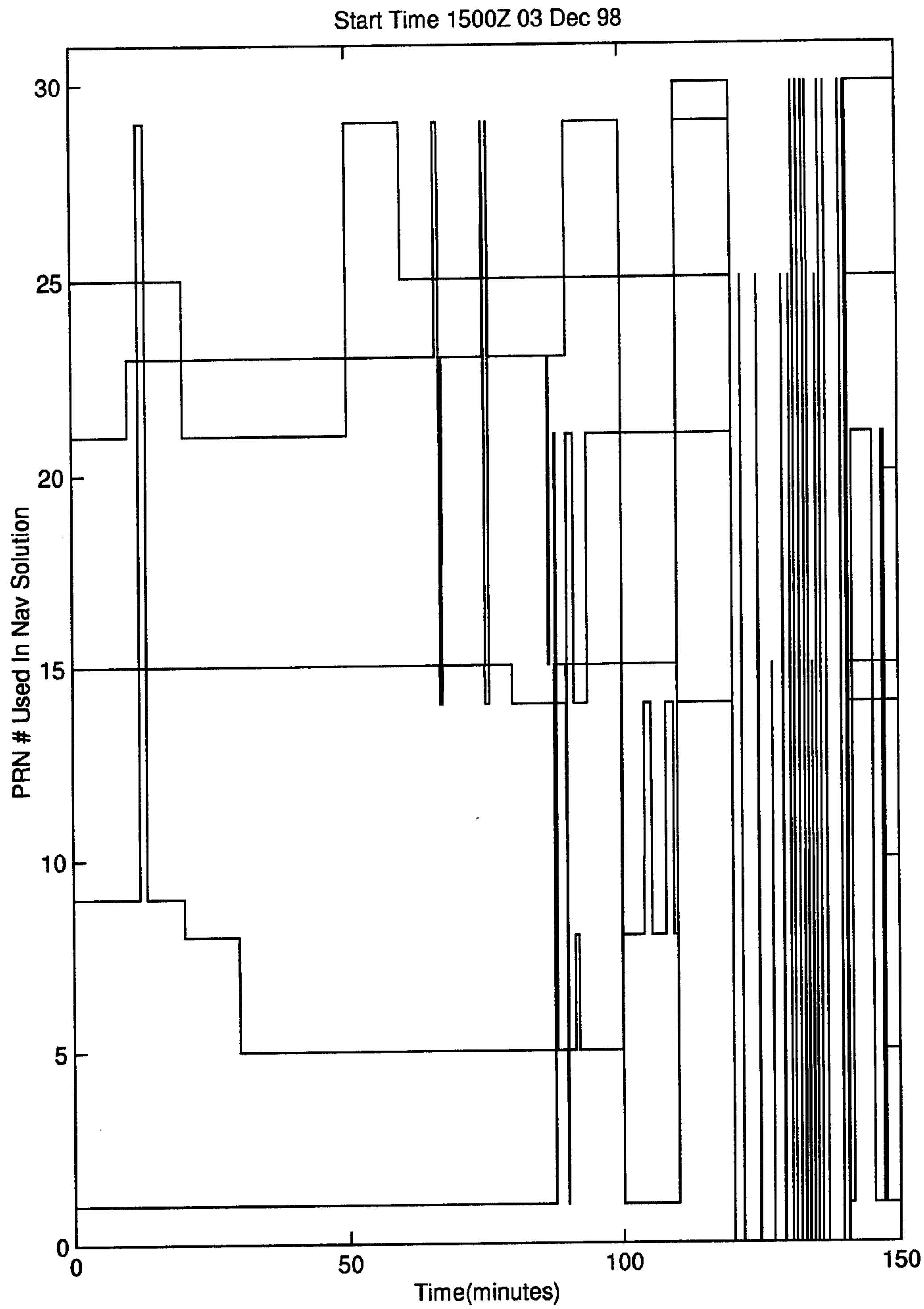

Figure N.3. PRN # Used In Nav Solution vs Time

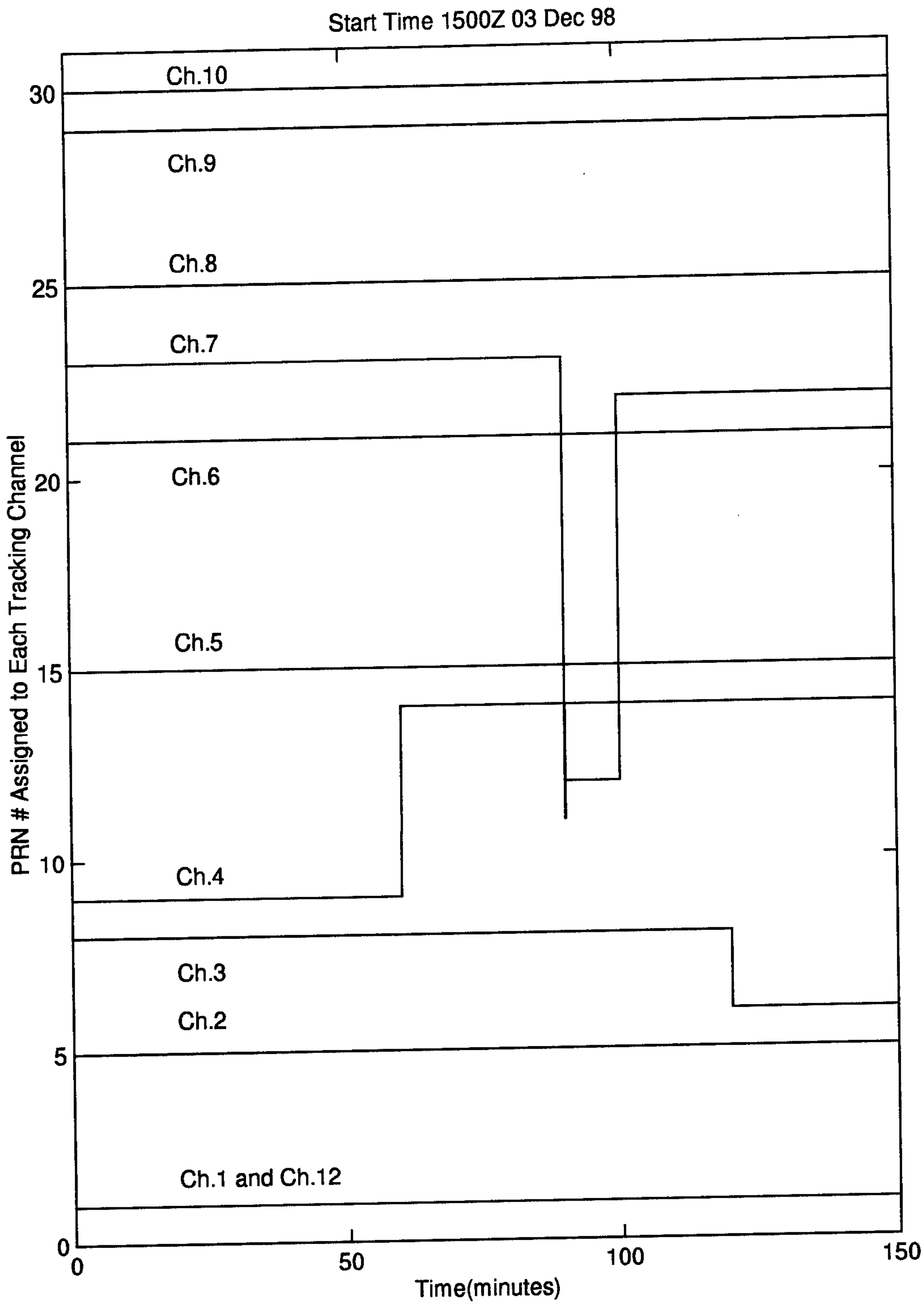

Figure N.4. PRN # Assigned to Each Tracking Channel vs Time

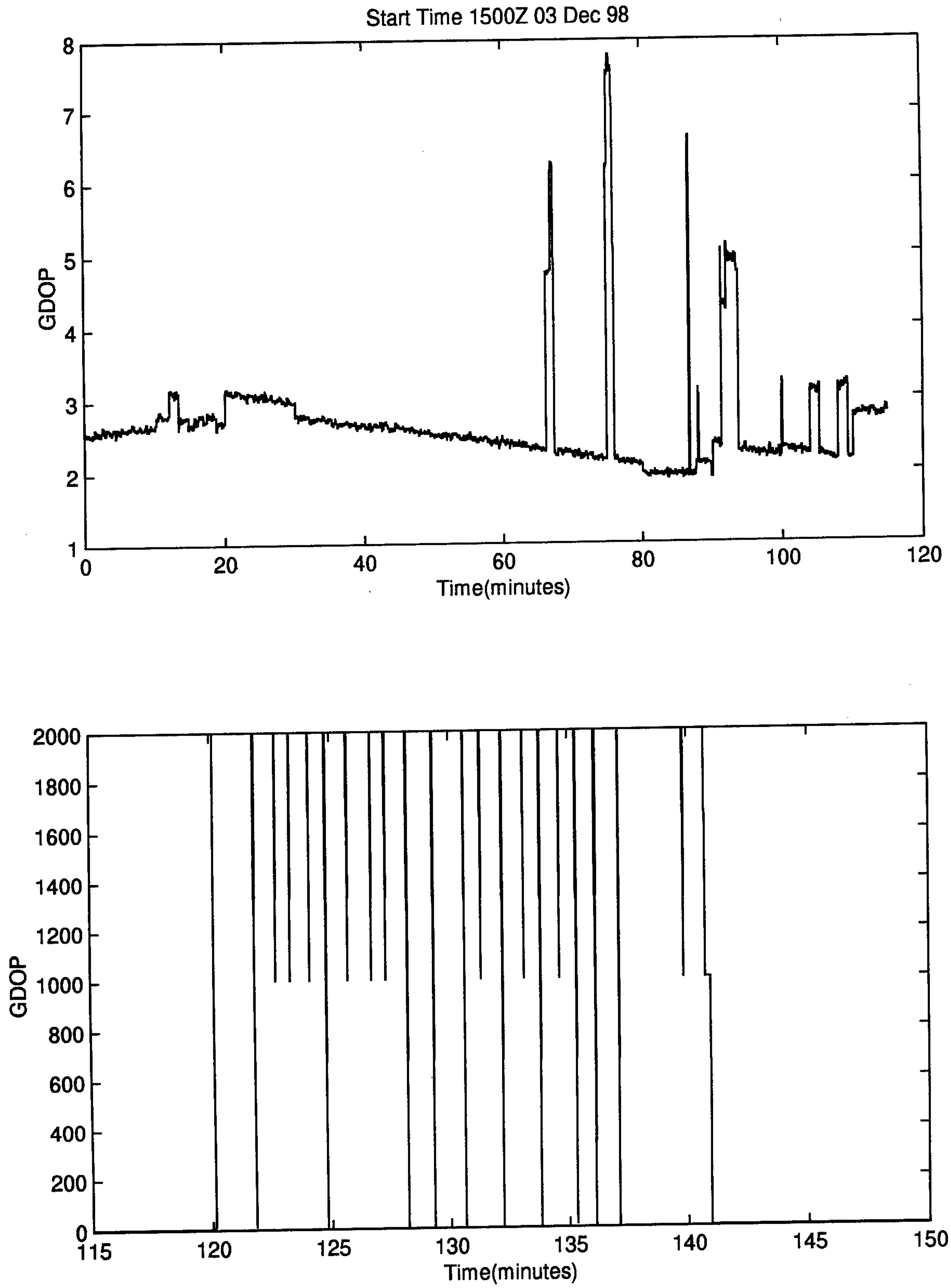

Figure N.5. GDOP vs Time

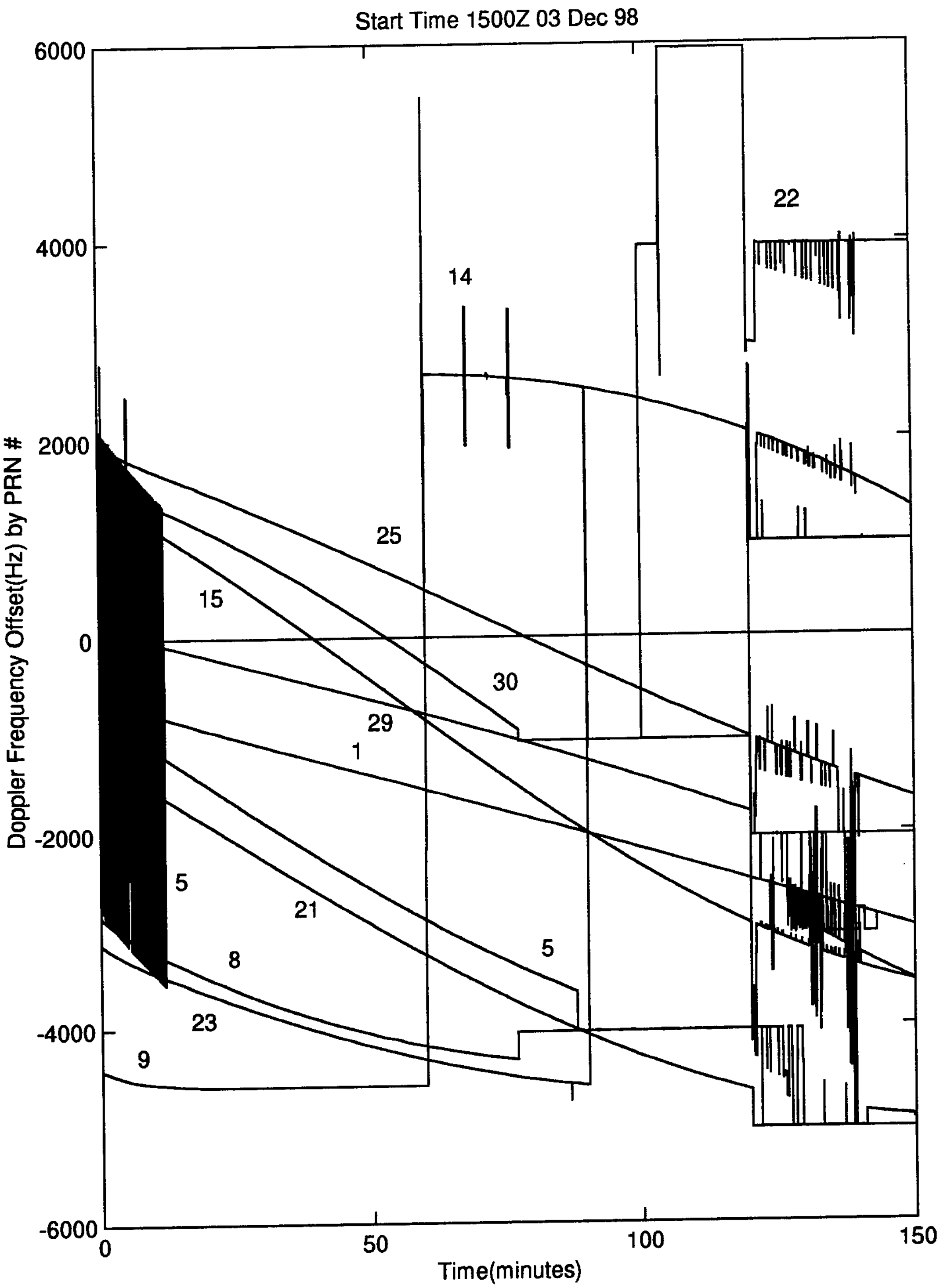

Figure N.6. Doppler Frequency vs Time

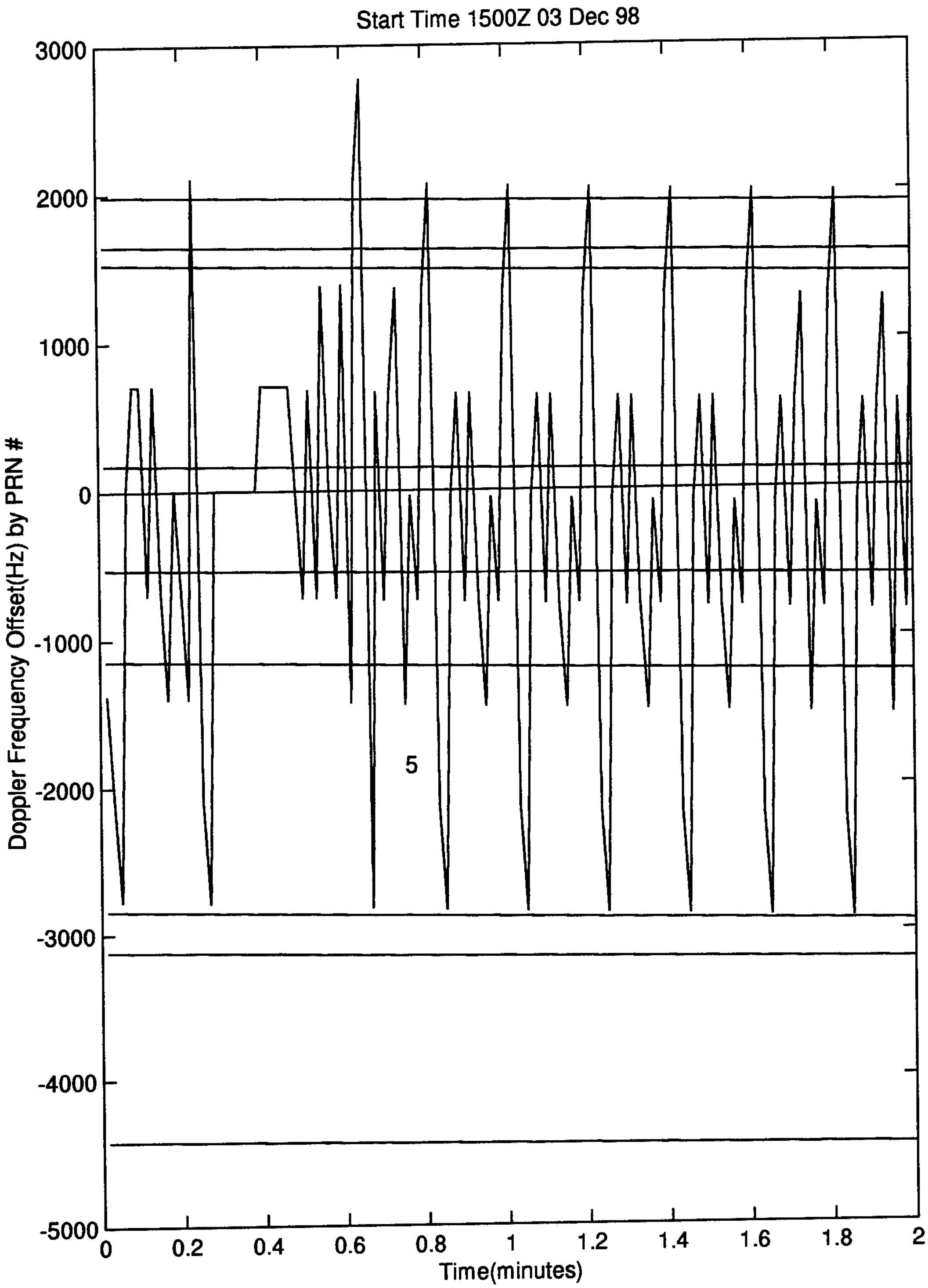

Figure N.7. Doppler Frequency vs Time

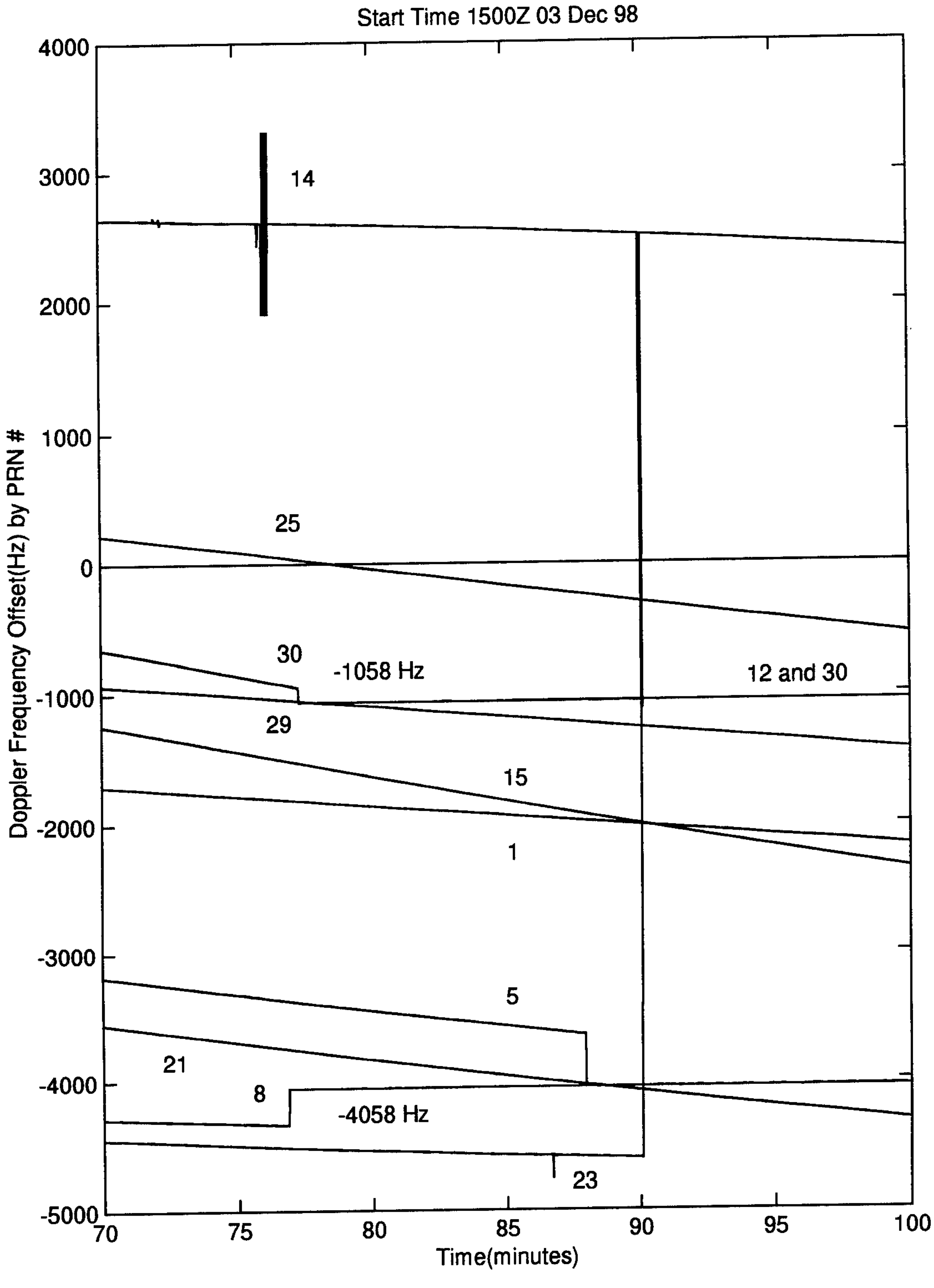

Figure N.8. Doppler Frequency vs Time

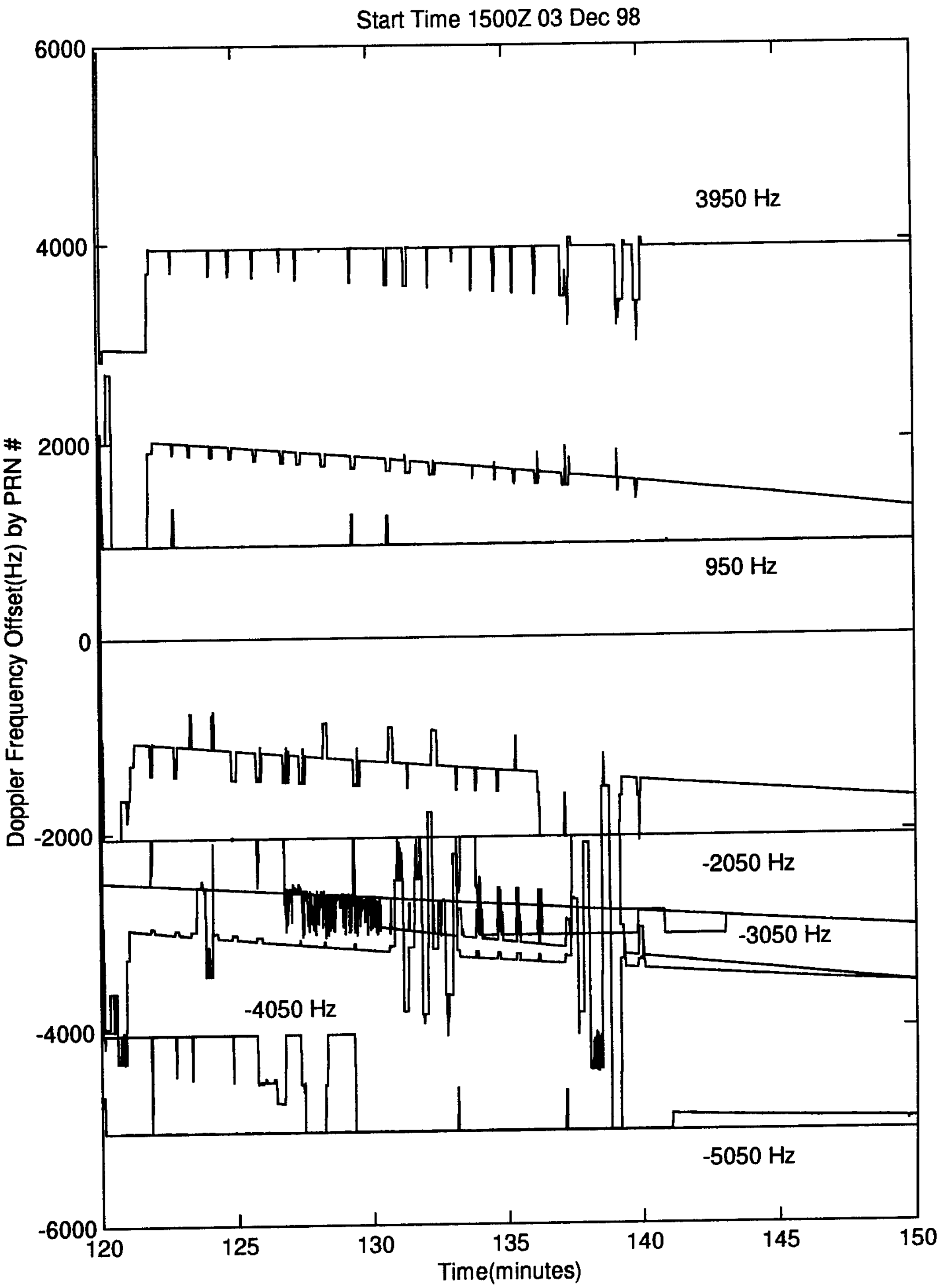

Figure N.9. Doppler Frequency vs Time

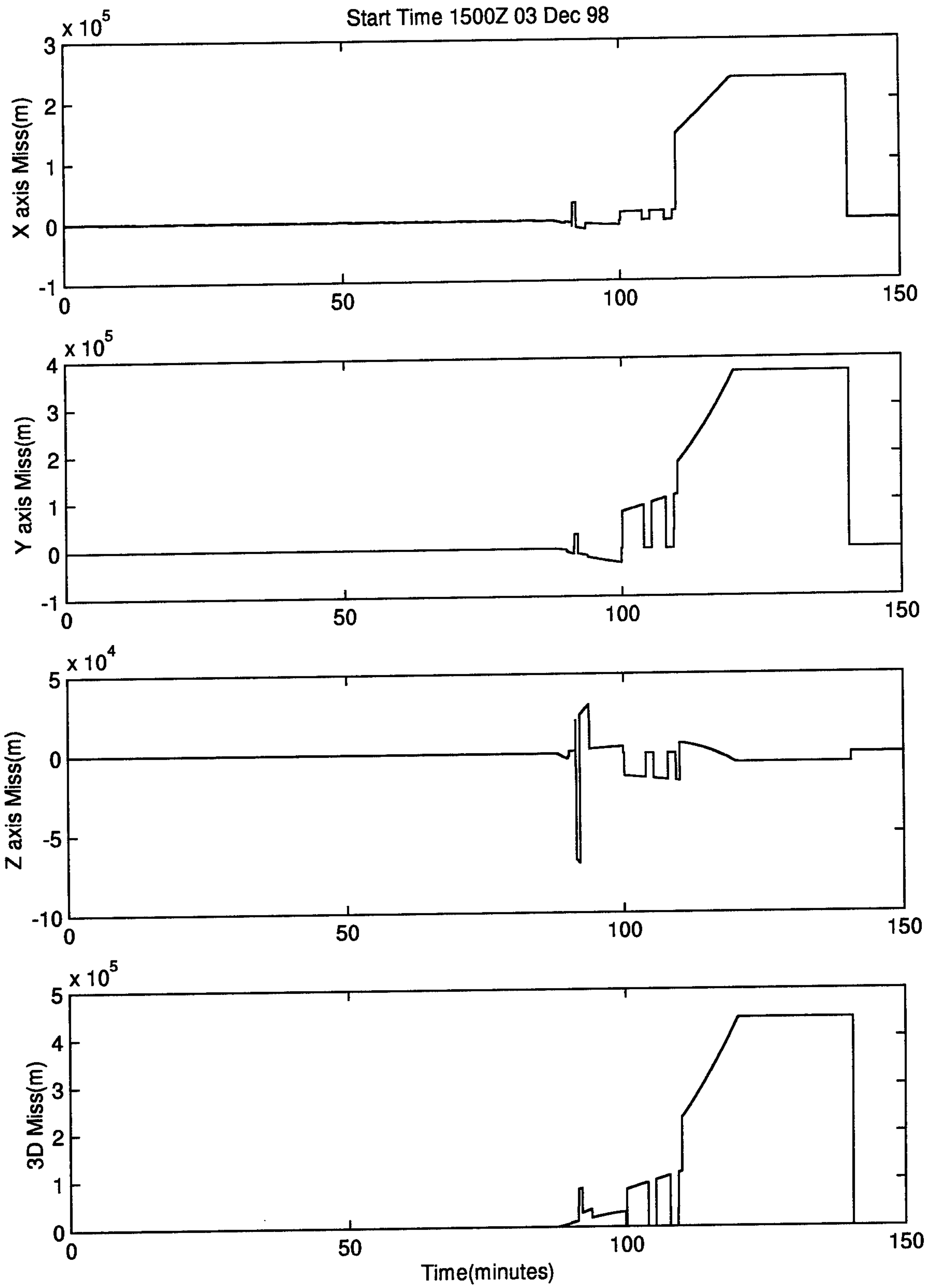

Figure N.10. X,Y,Z and 3D Error(m) vs Time

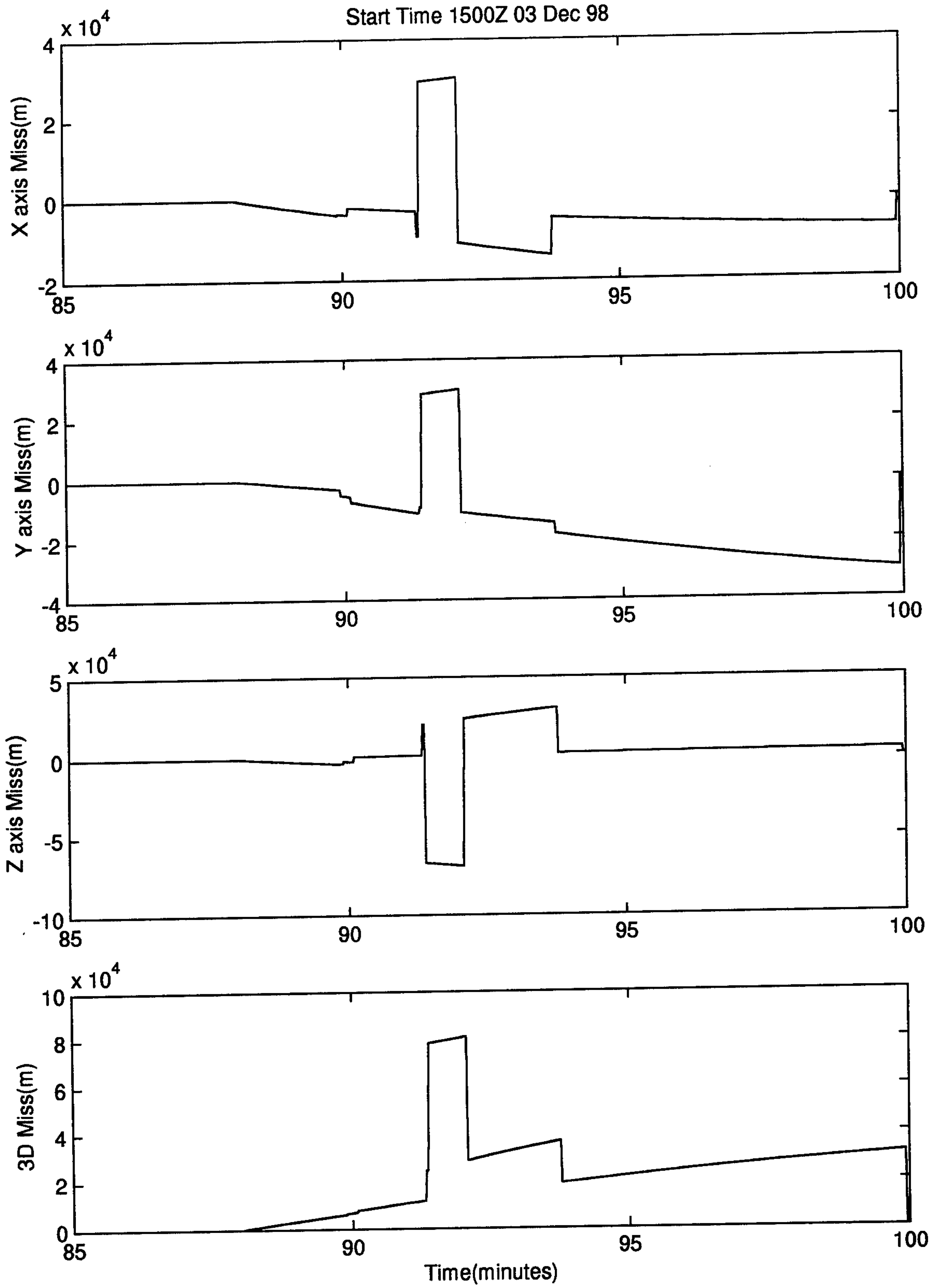

Figure N.11. X,Y,Z and 3D Error(m) vs Time

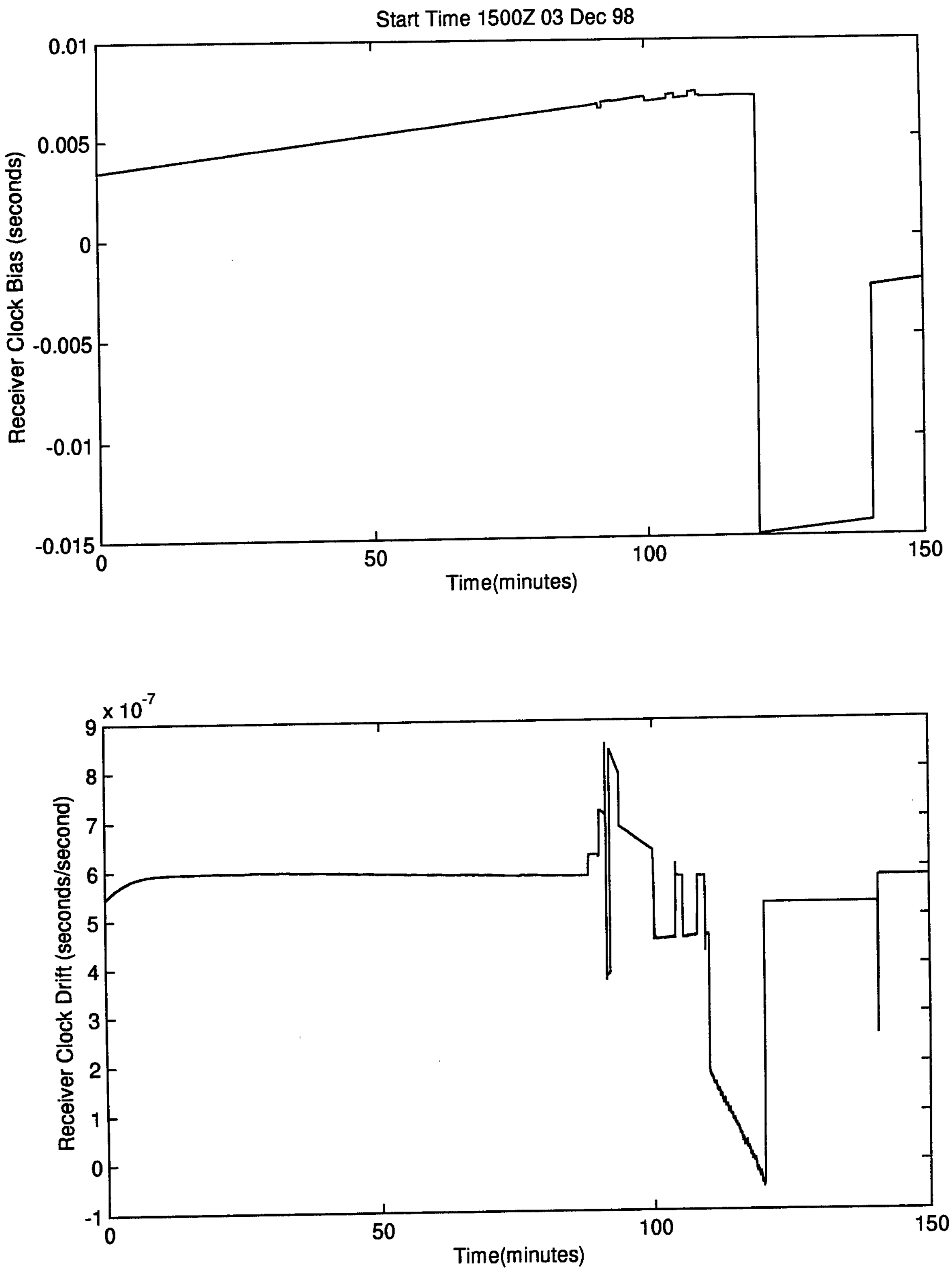

Figure N.12. Receiver Clock Bias and Drift vs Time

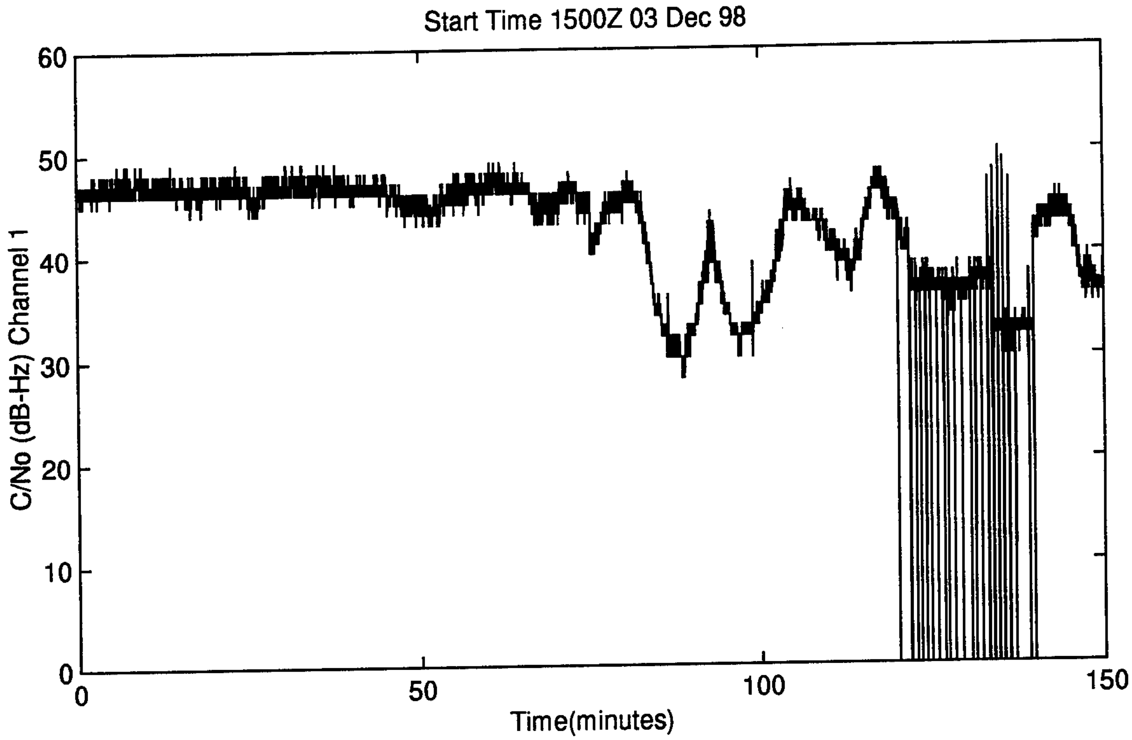

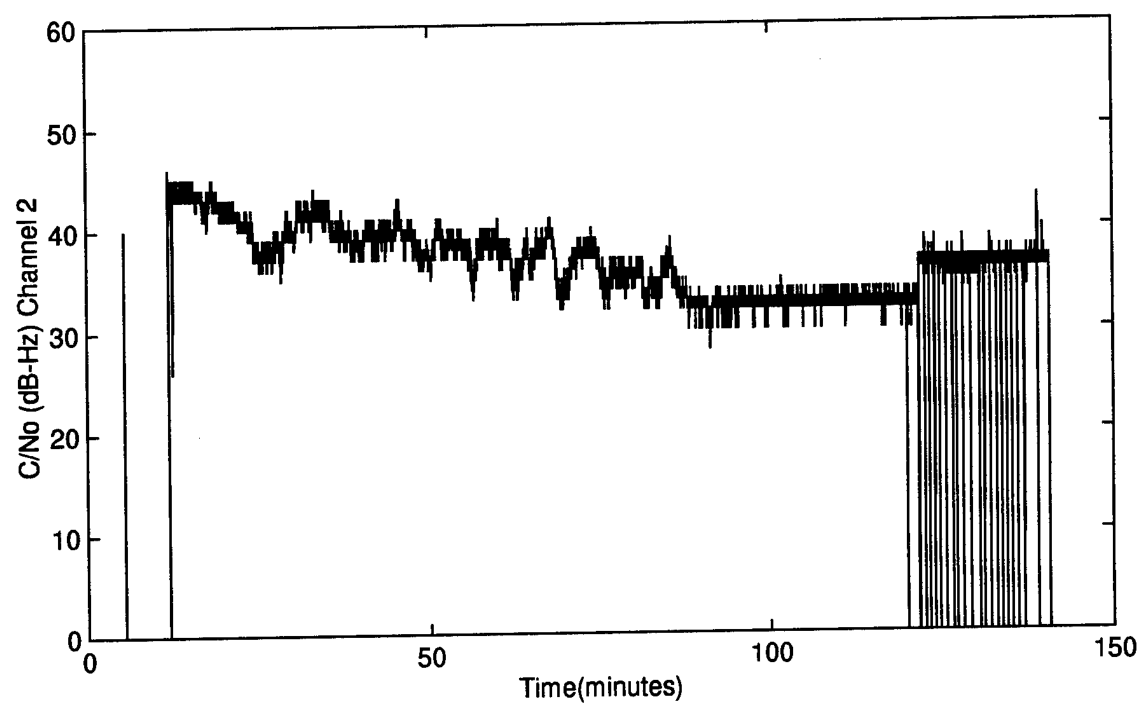

Figure N.13. C/No vs Time

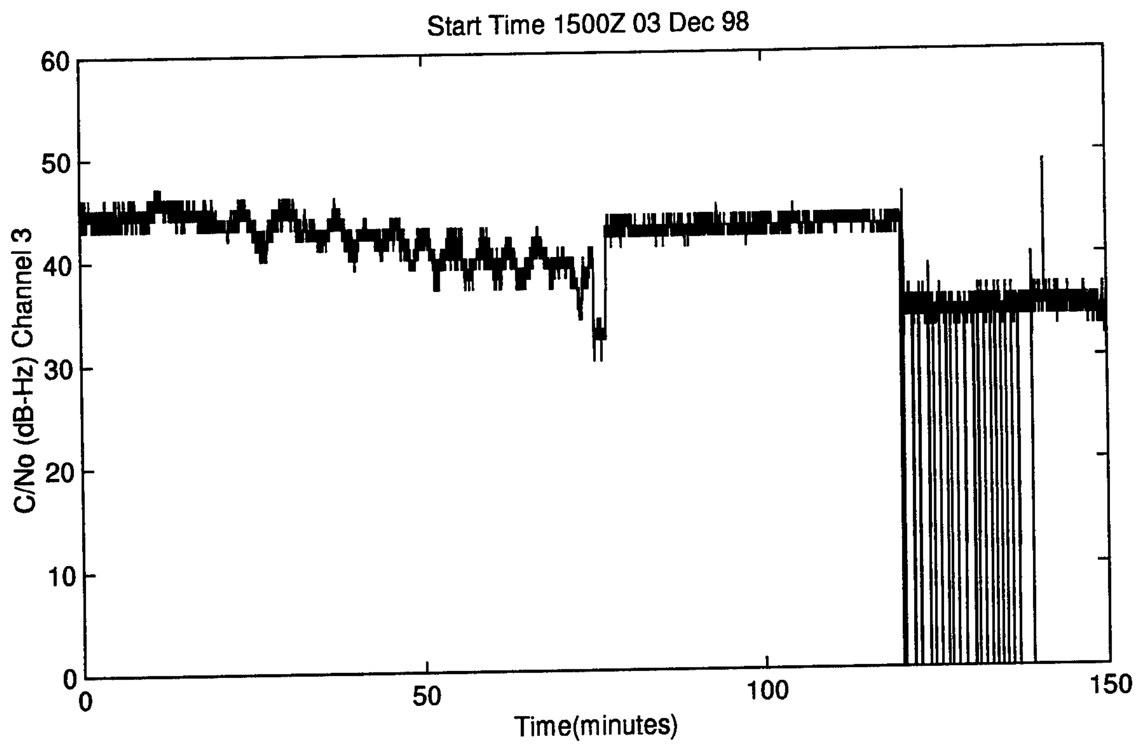

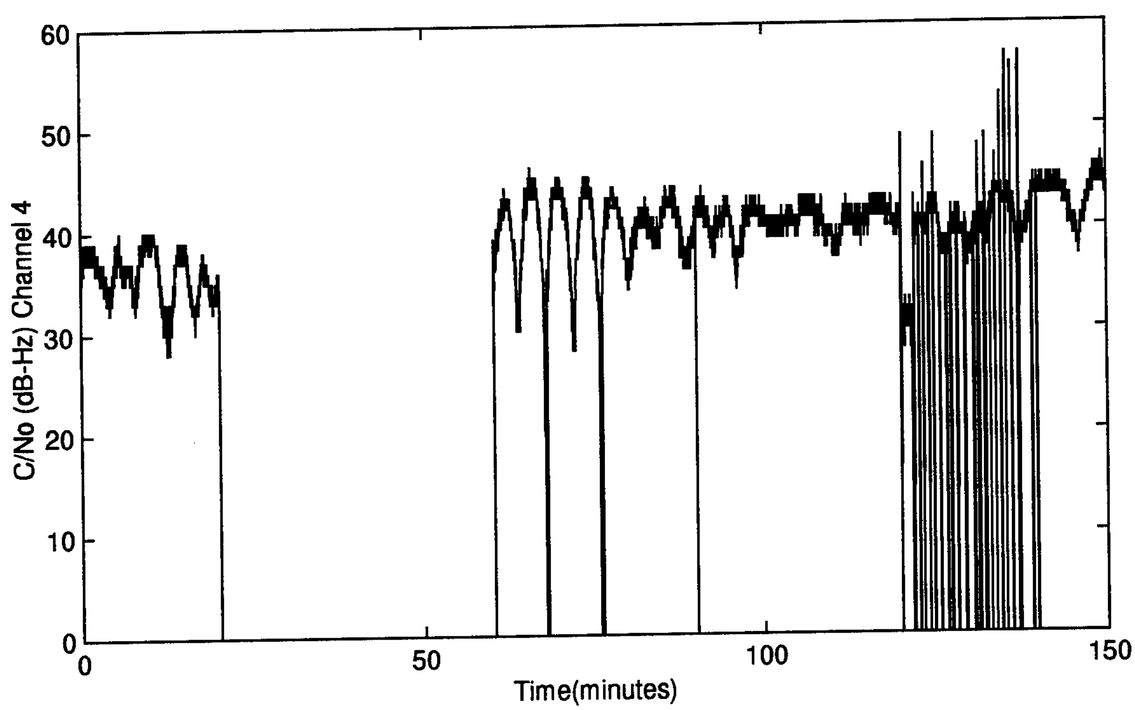

Figure N.14. C/No vs Time

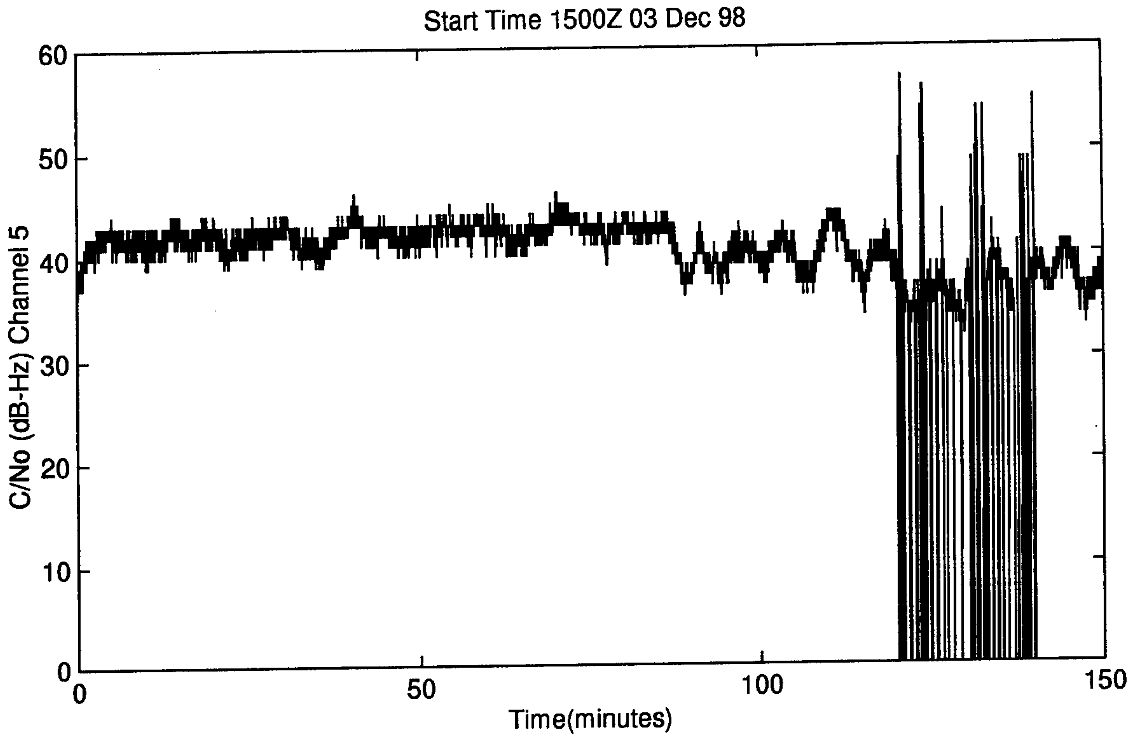

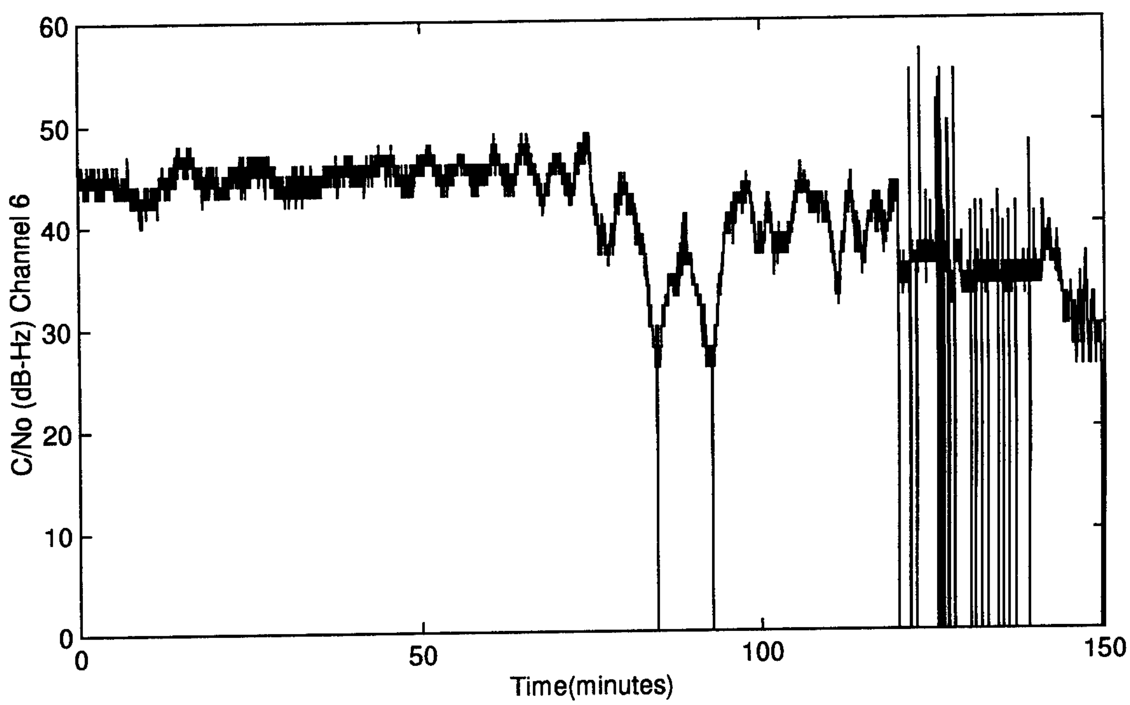

Figure N.15. C/No vs Time

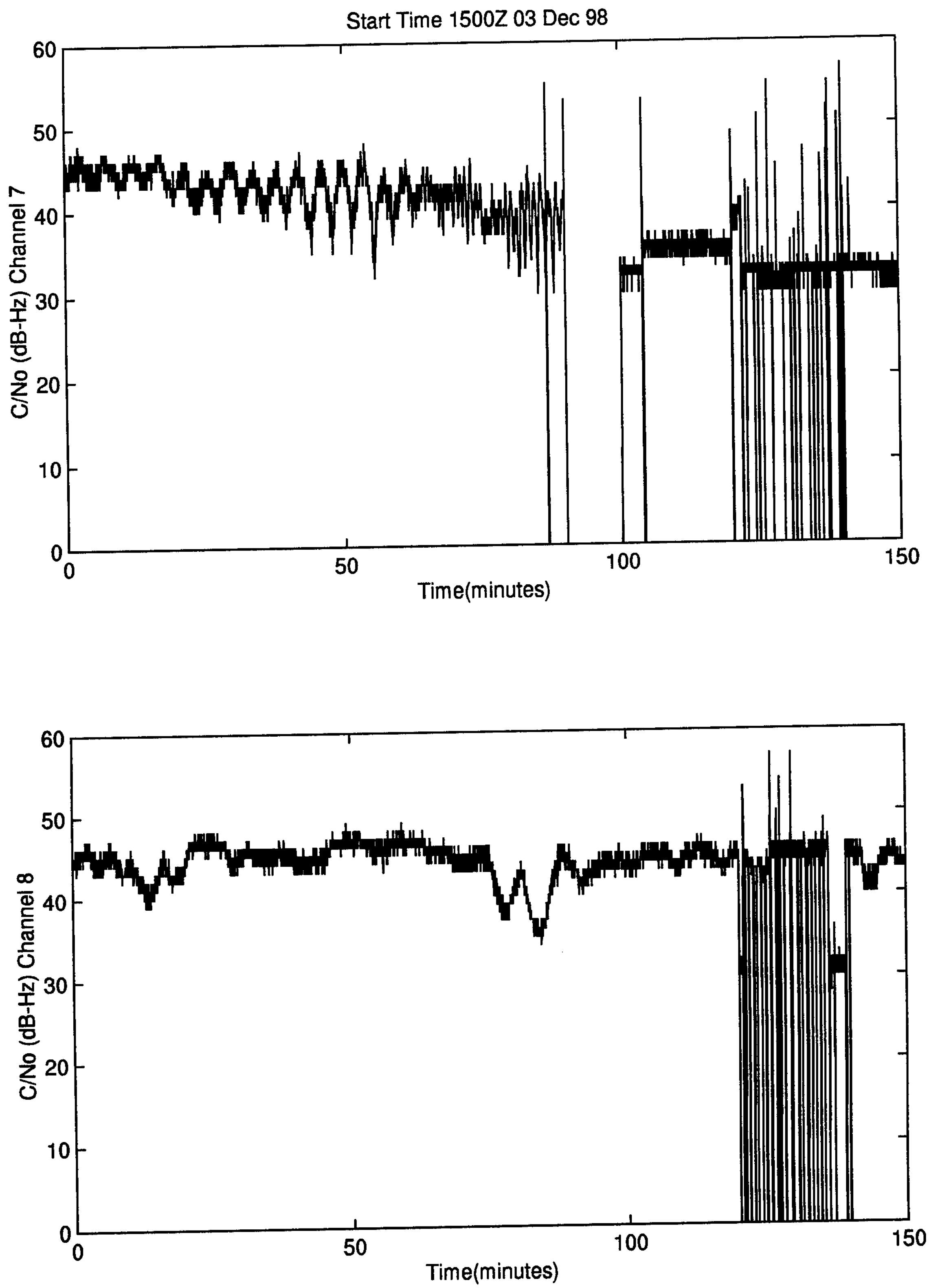

Figure N.16. C/No vs Time

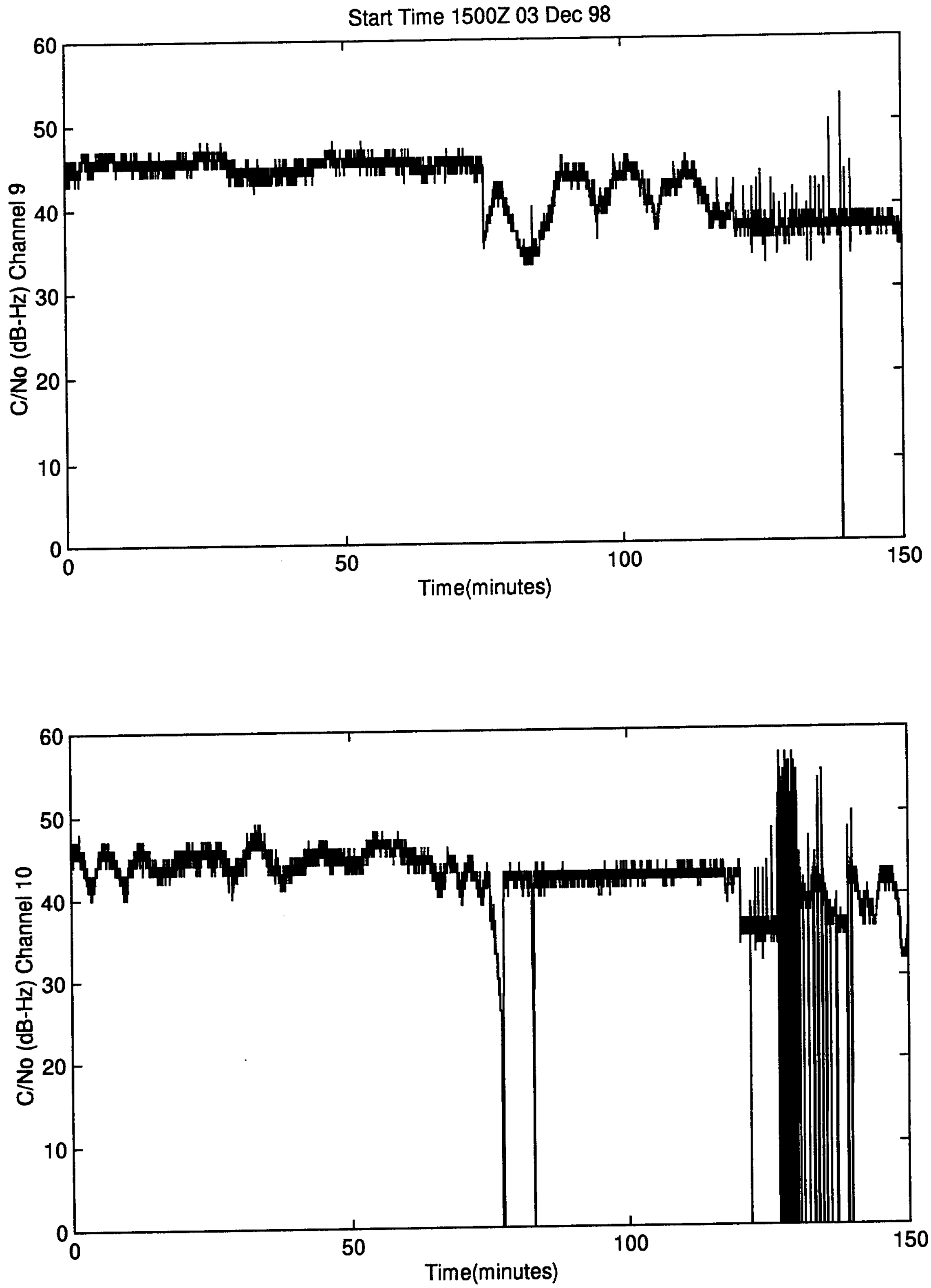

Figure N.17. C/No vs Time

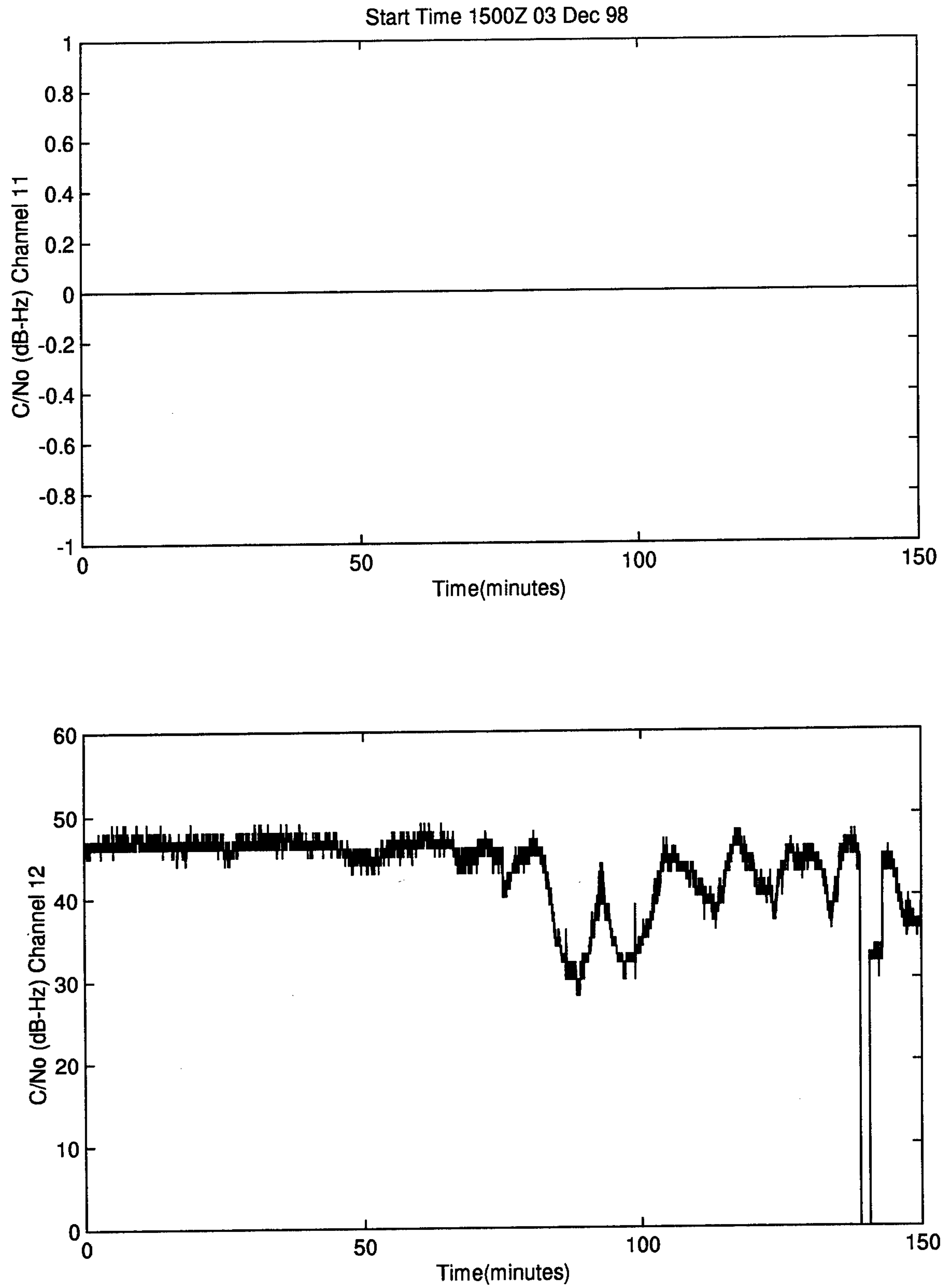

Figure N.18. C/No vs Time

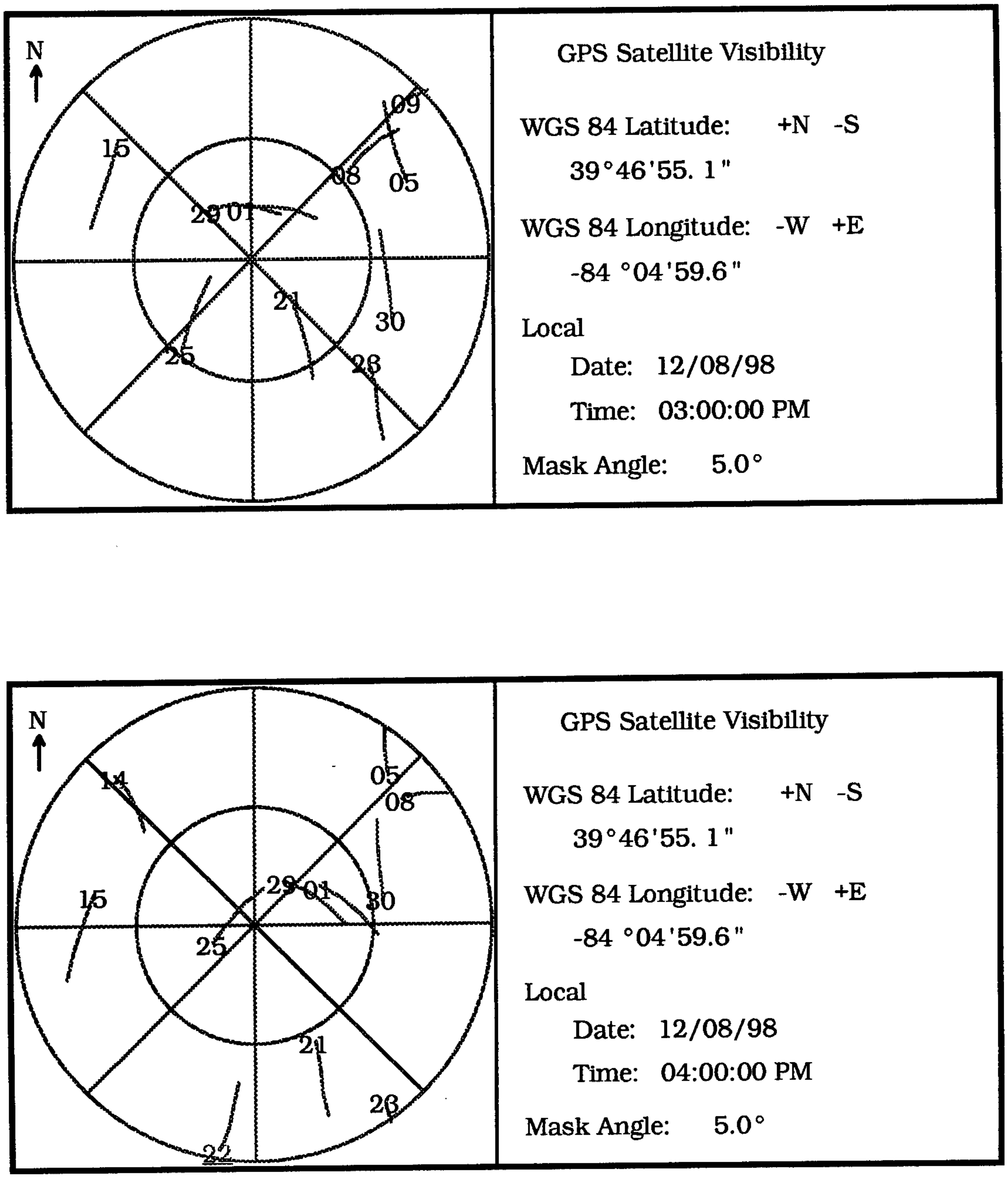

Figure O.1. GPS Satellites In View 08 Dec 98

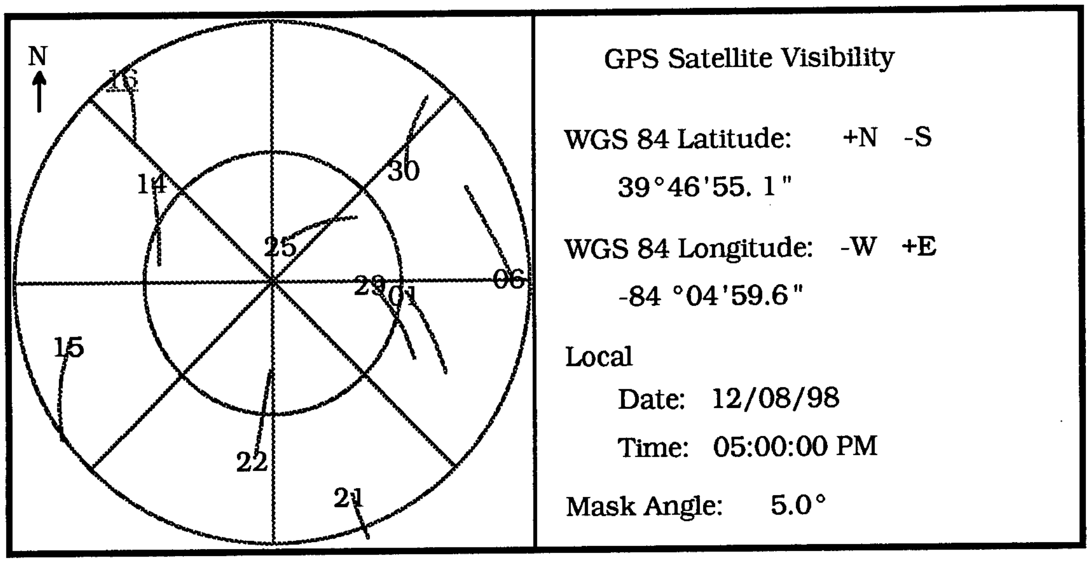

Figure O.2. GPS Satellites In View 08 Dec 98

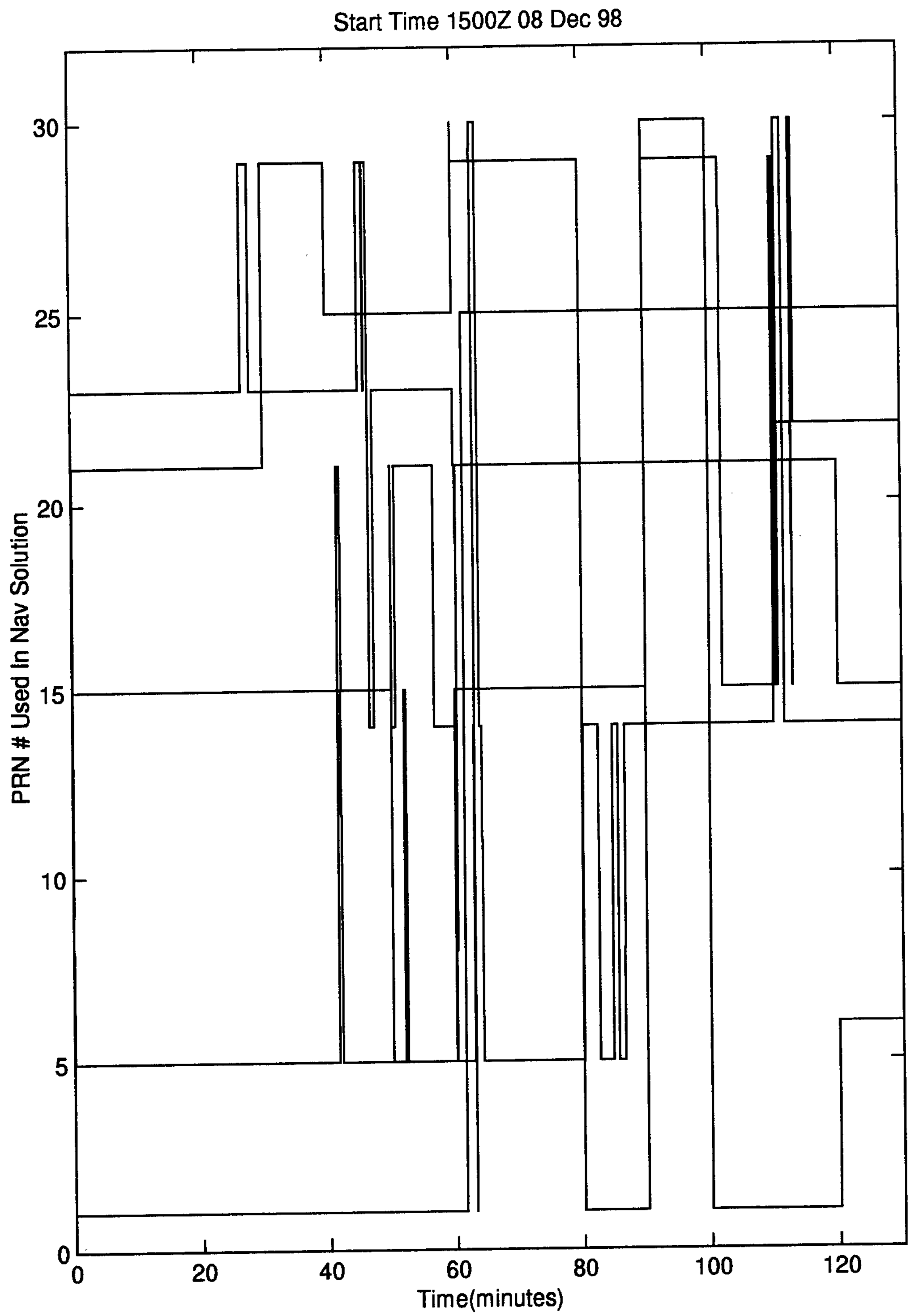

Figure O.3. PRN # Used In Nav Solution vs Time

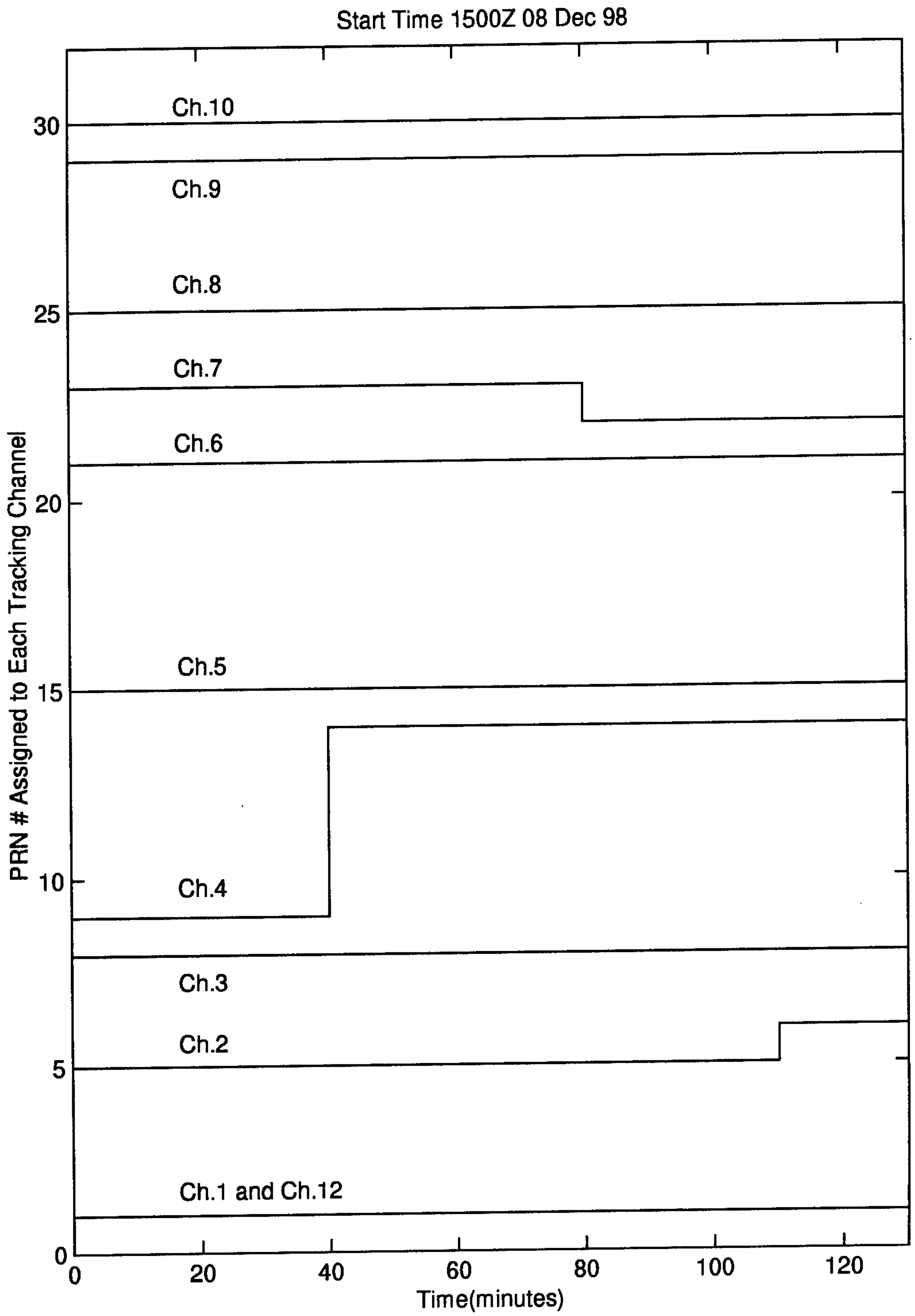

Figure O.4. PRN # Assigned to Each Tracking Channel vs Time

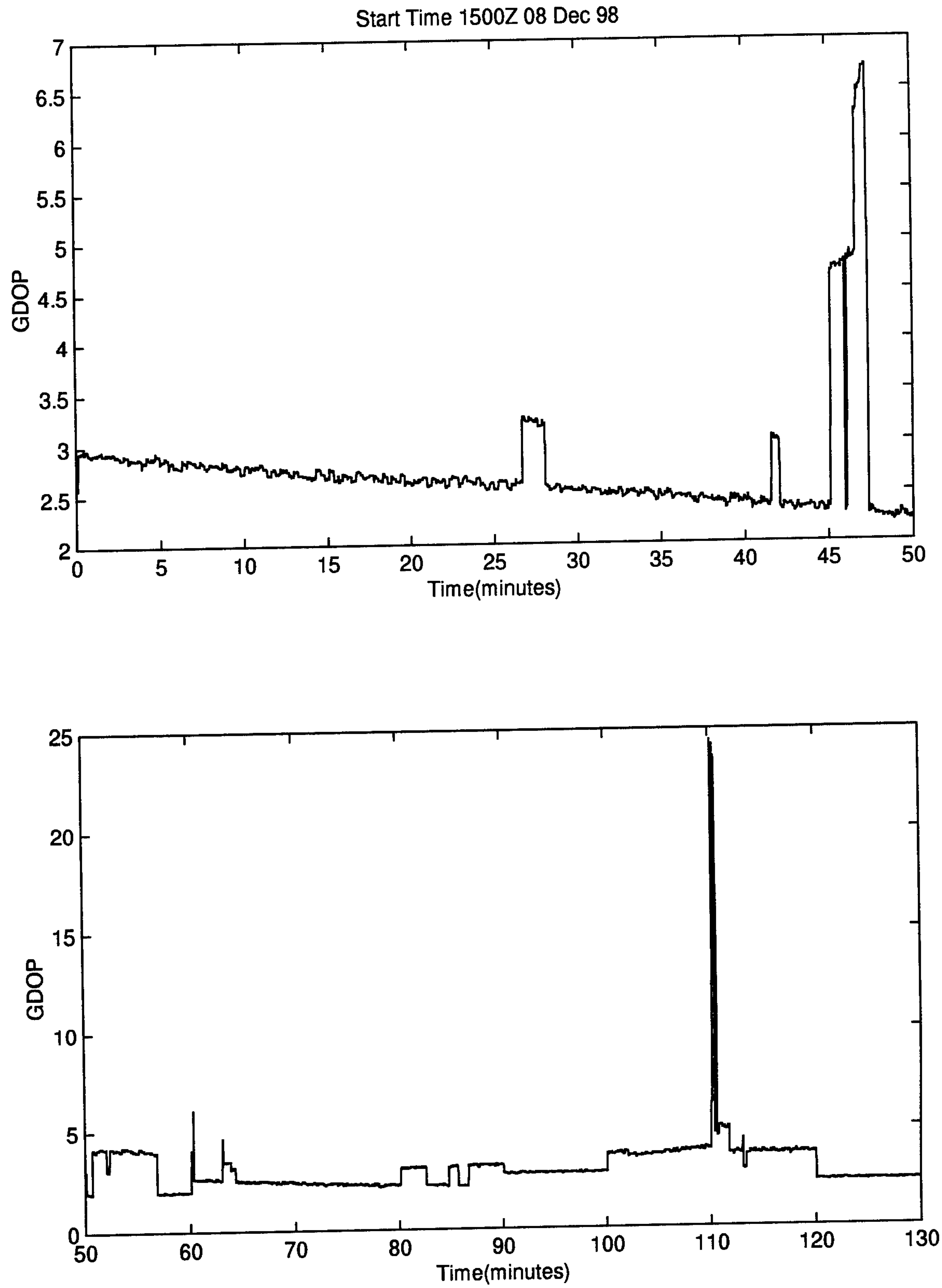

Figure O.5. GDOP vs Time

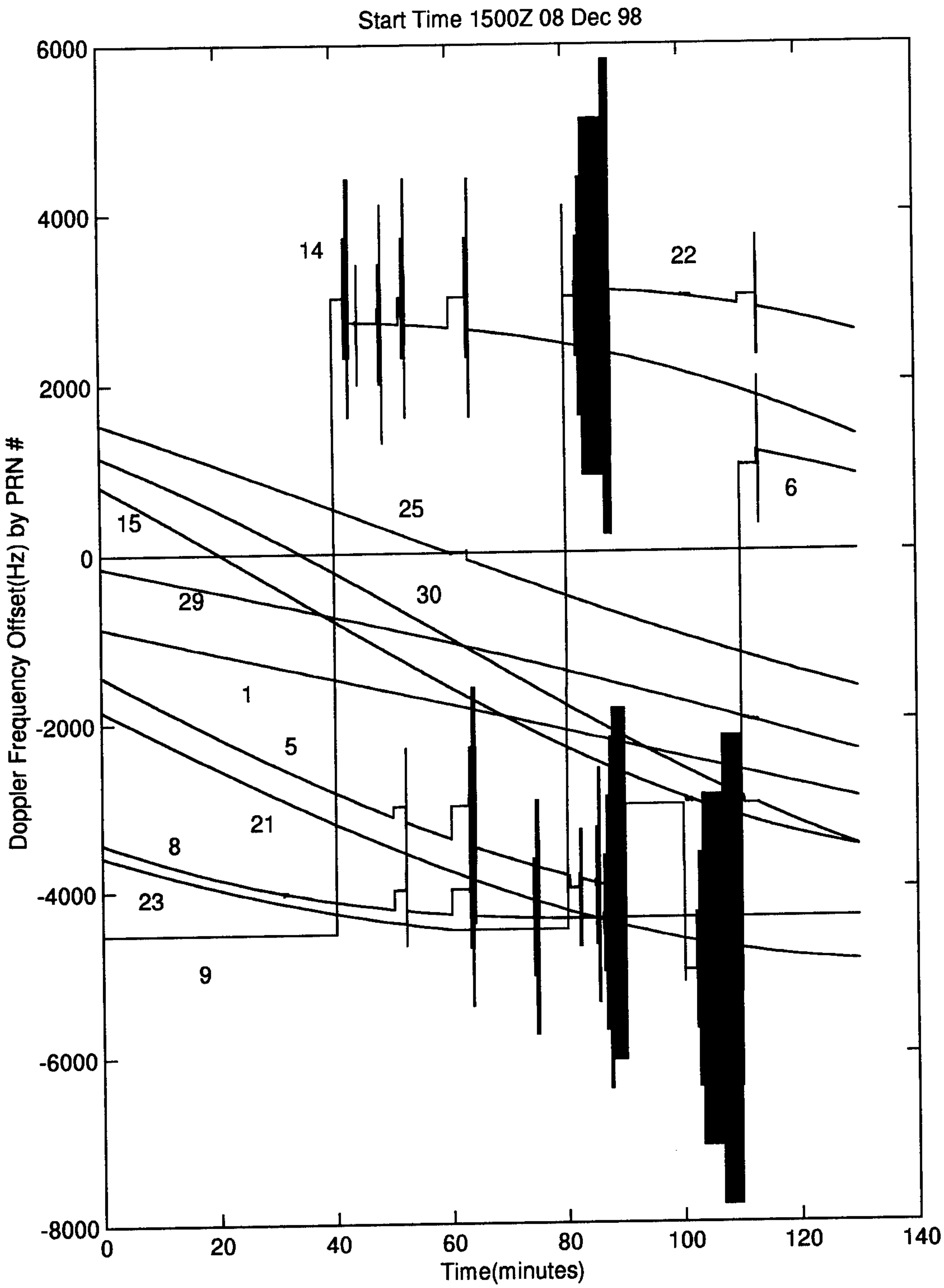

Figure O.6. Doppler Frequency vs Time

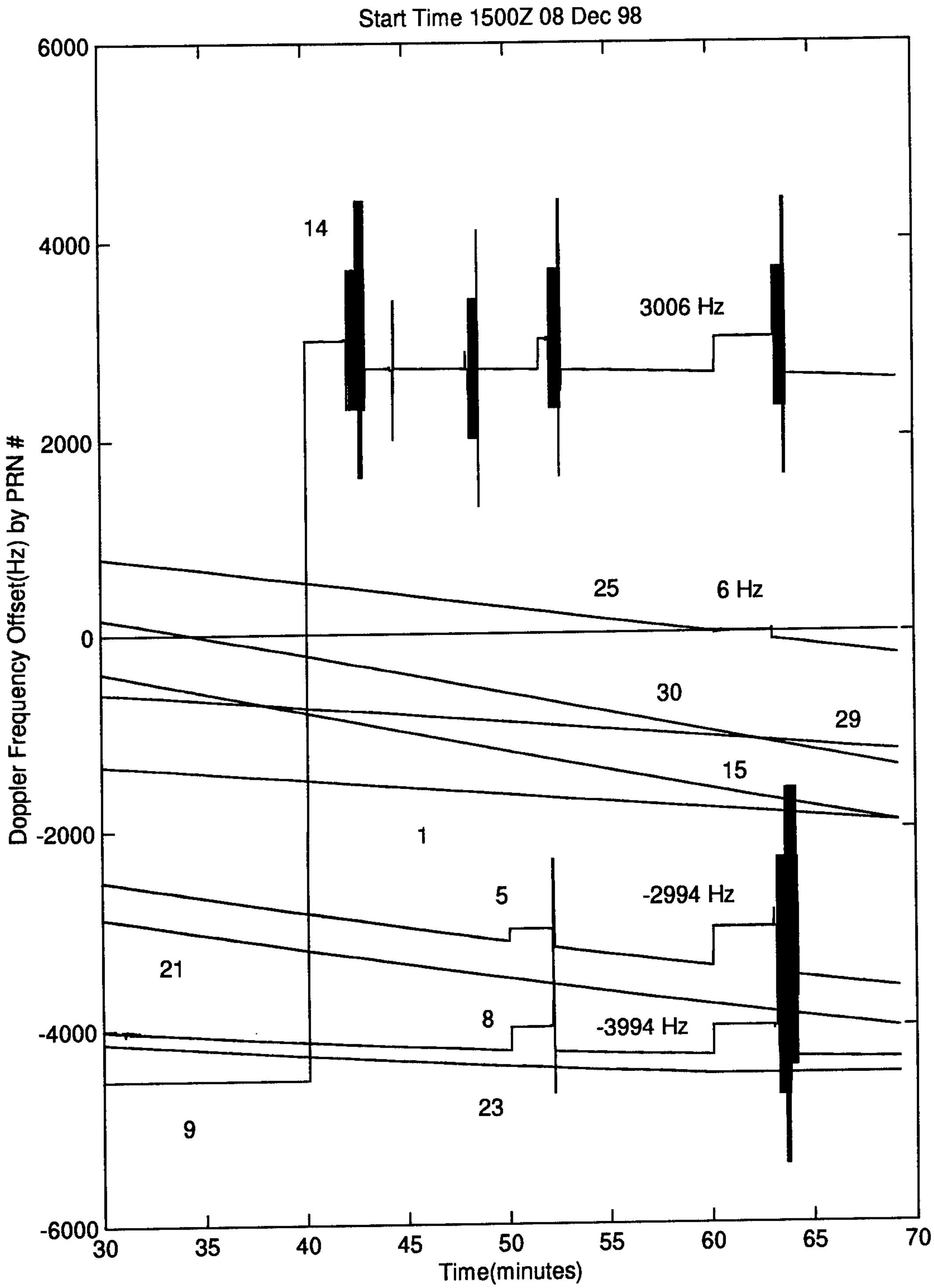

Figure O.7. Doppler Frequency vs Time

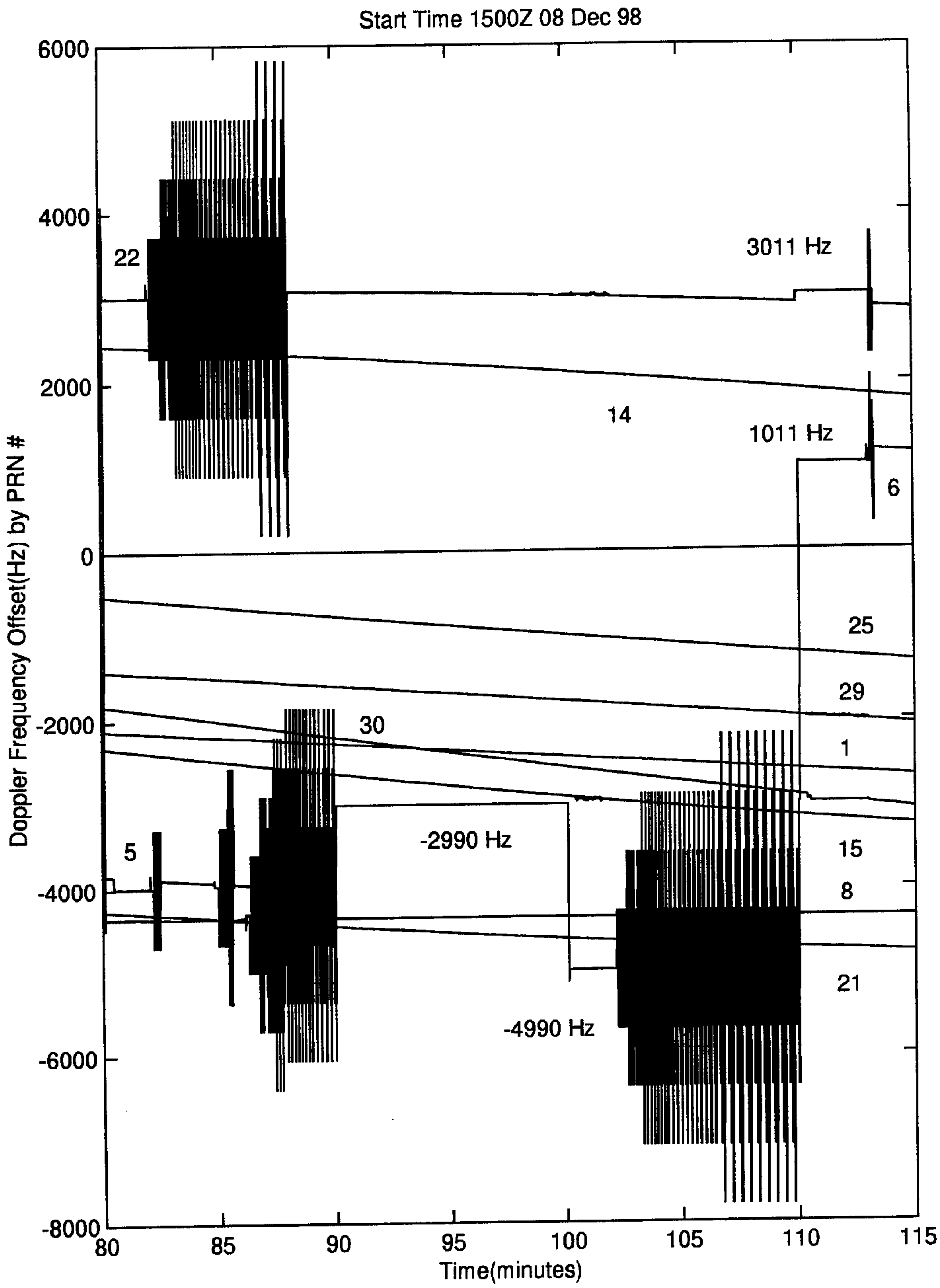

Figure O.8. Doppler Frequency vs Time

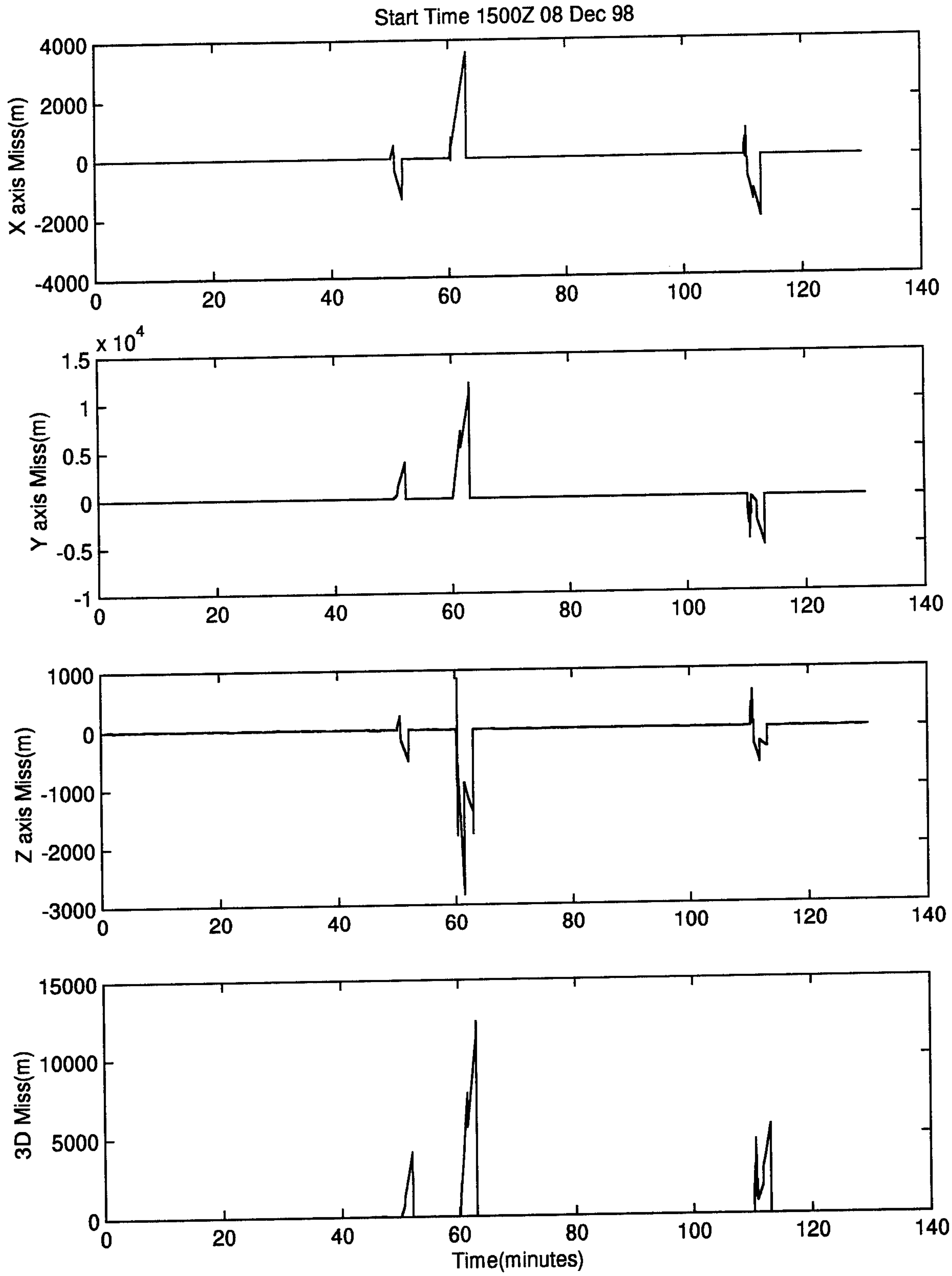

Figure O.9. X,Y,Z and 3D Error(m) vs Time

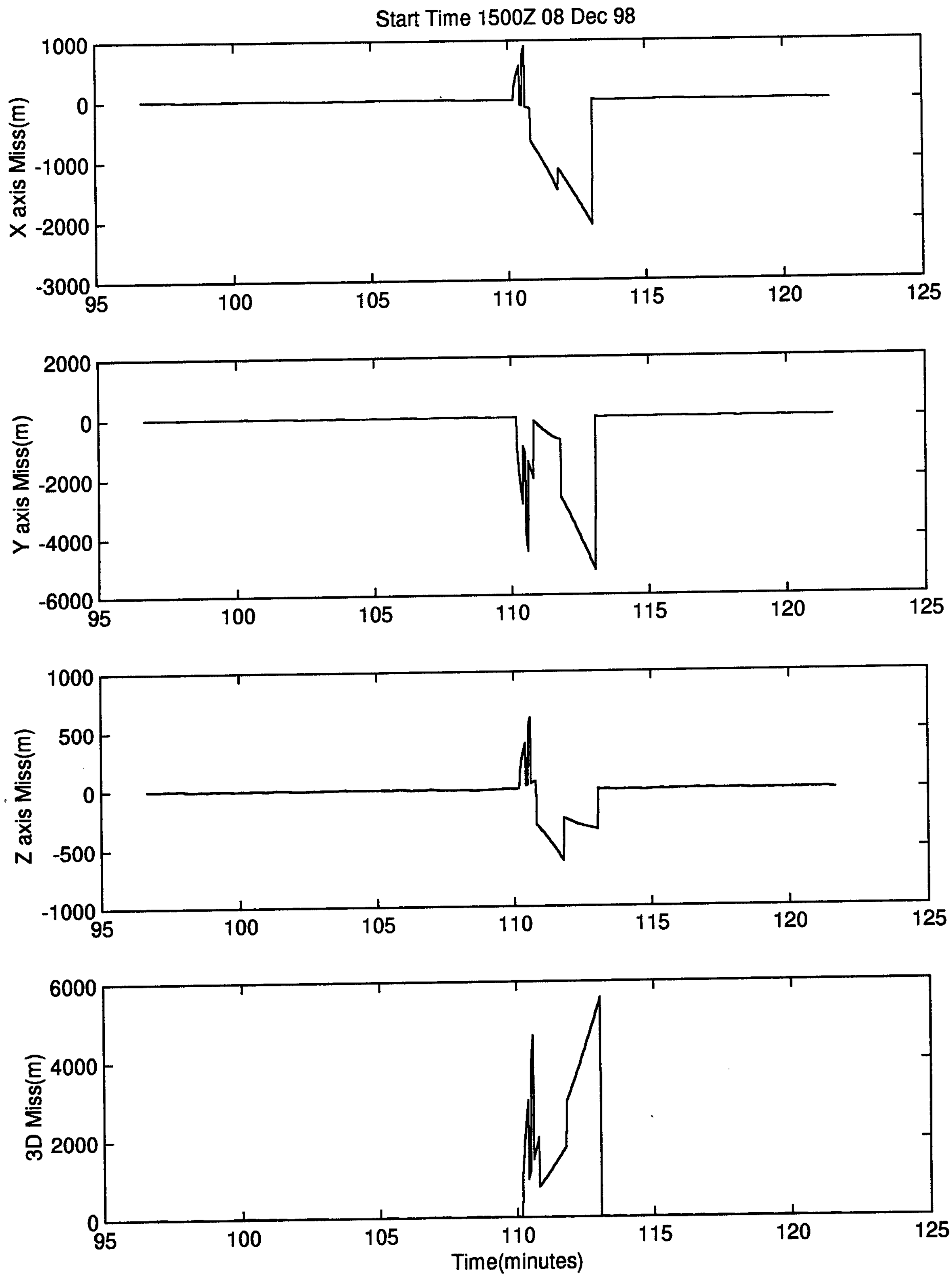

Figure O.10. X,Y,Z and 3D Error(m) vs Time

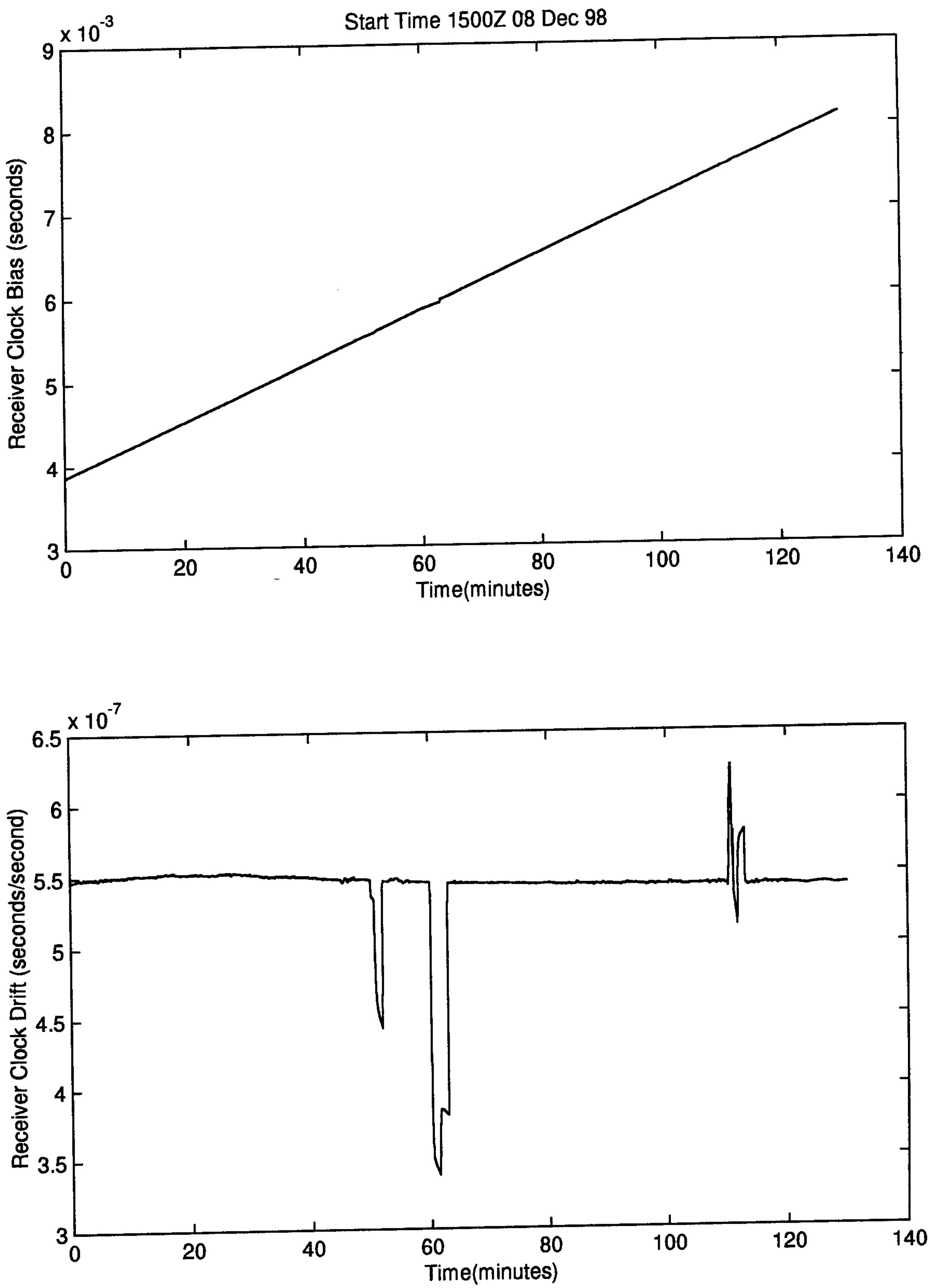

Figure O.11. Receiver Clock Bias and Drift vs Time

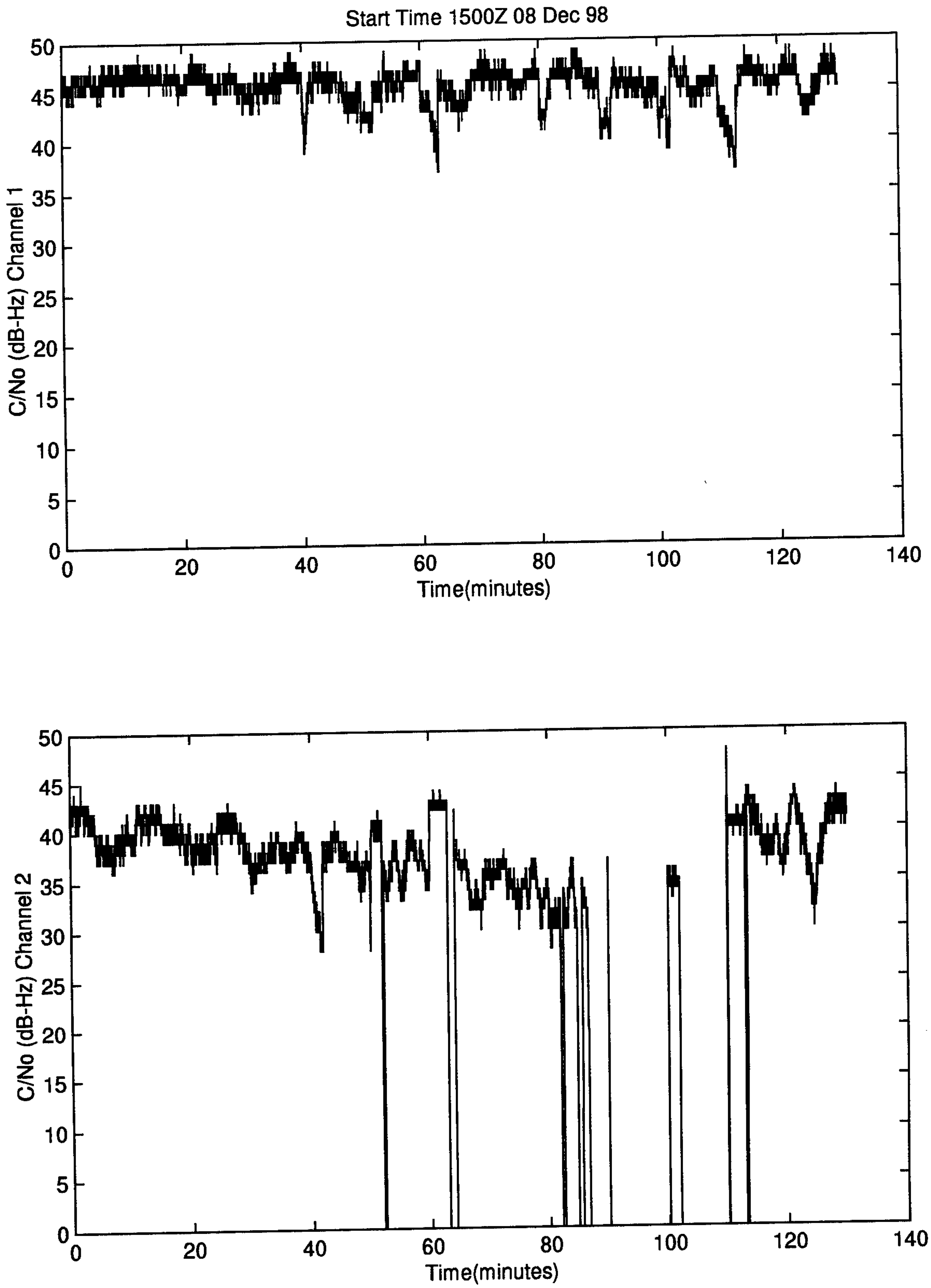

Figure O.12. C/No vs Time

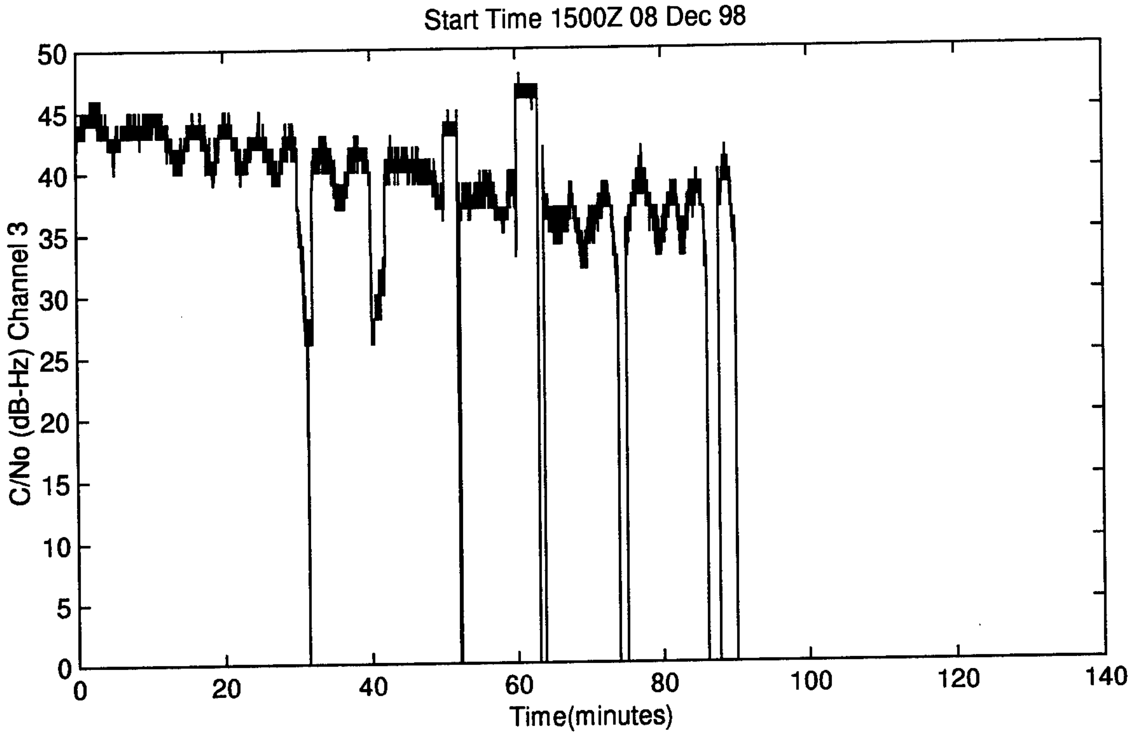

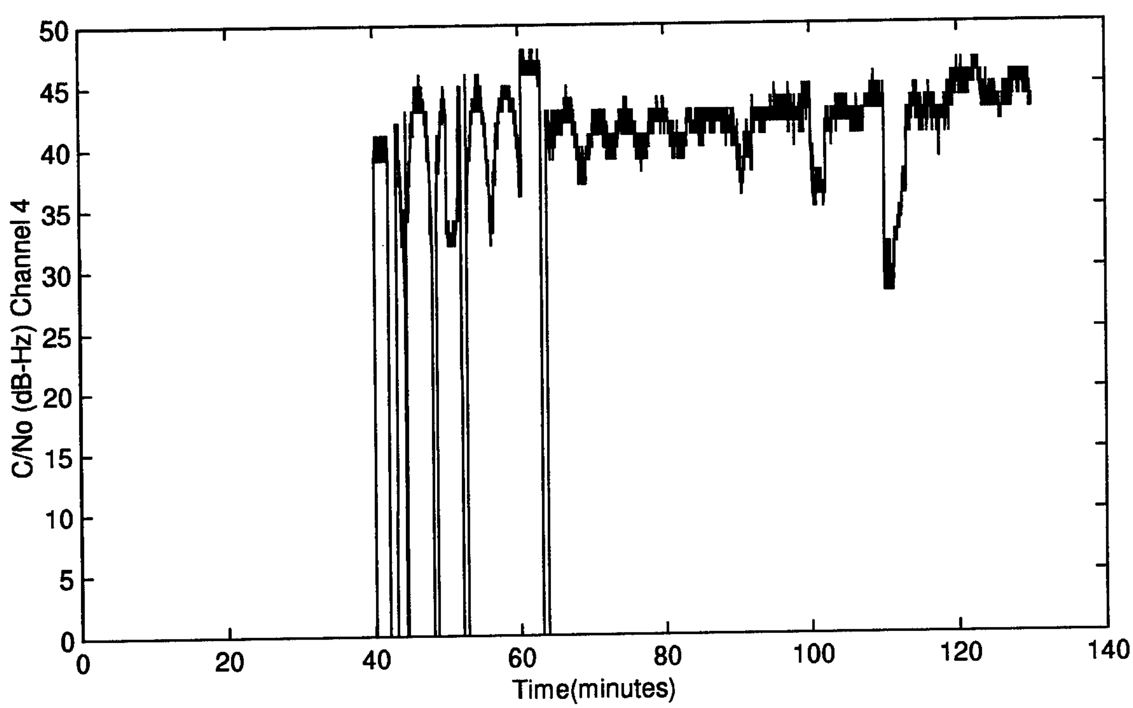

Figure O.13. C/No vs Time

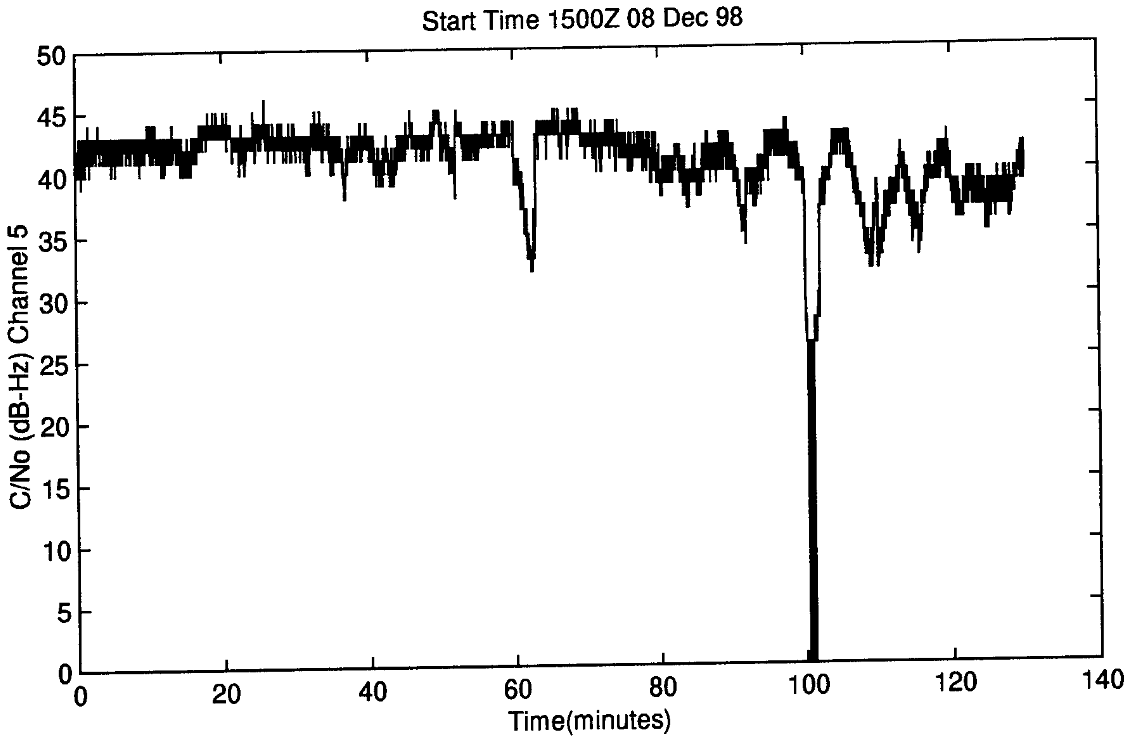

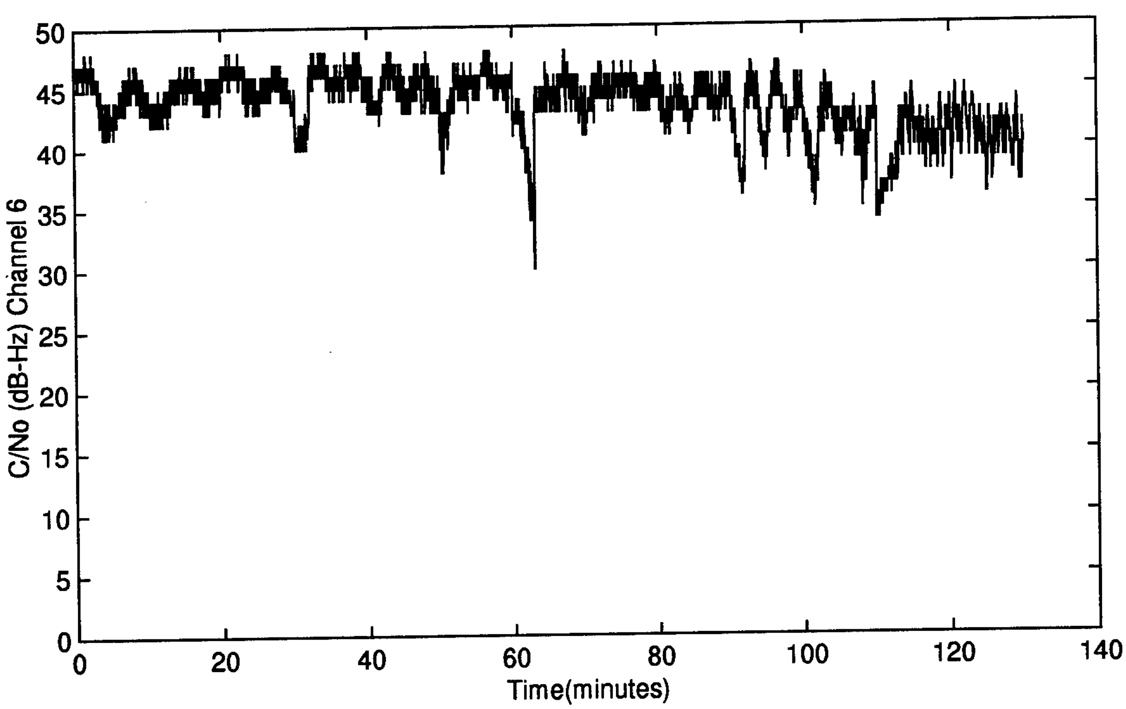

Figure O.14. C/No vs Time

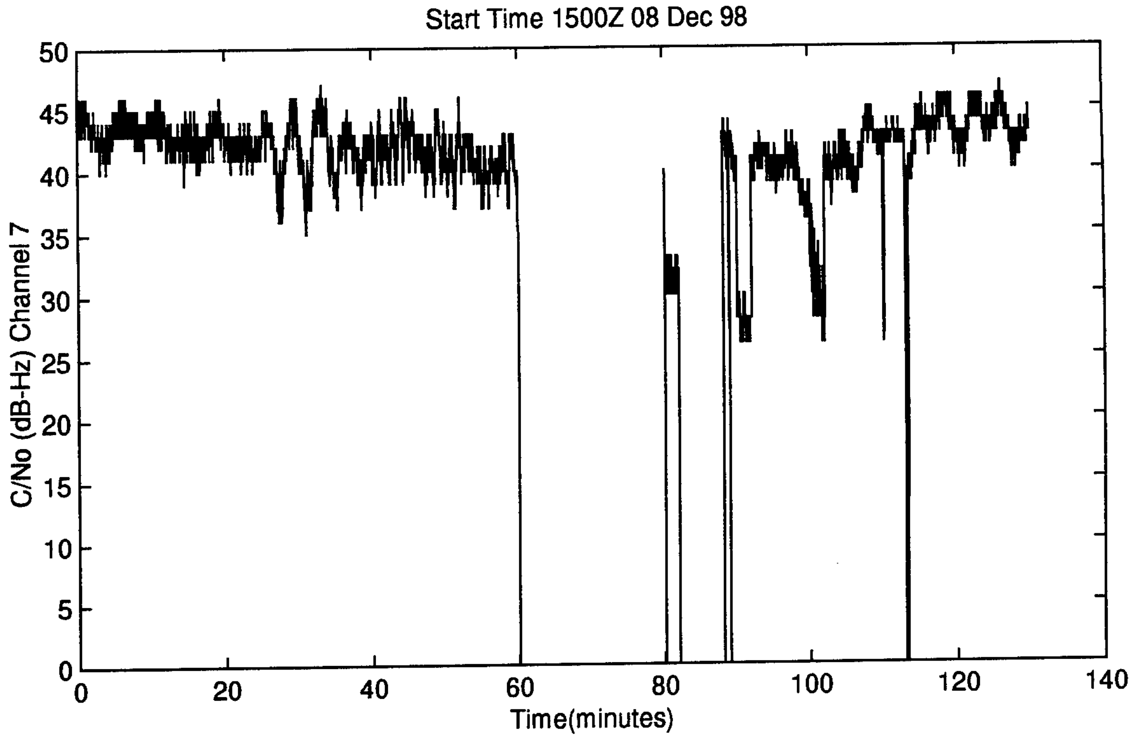

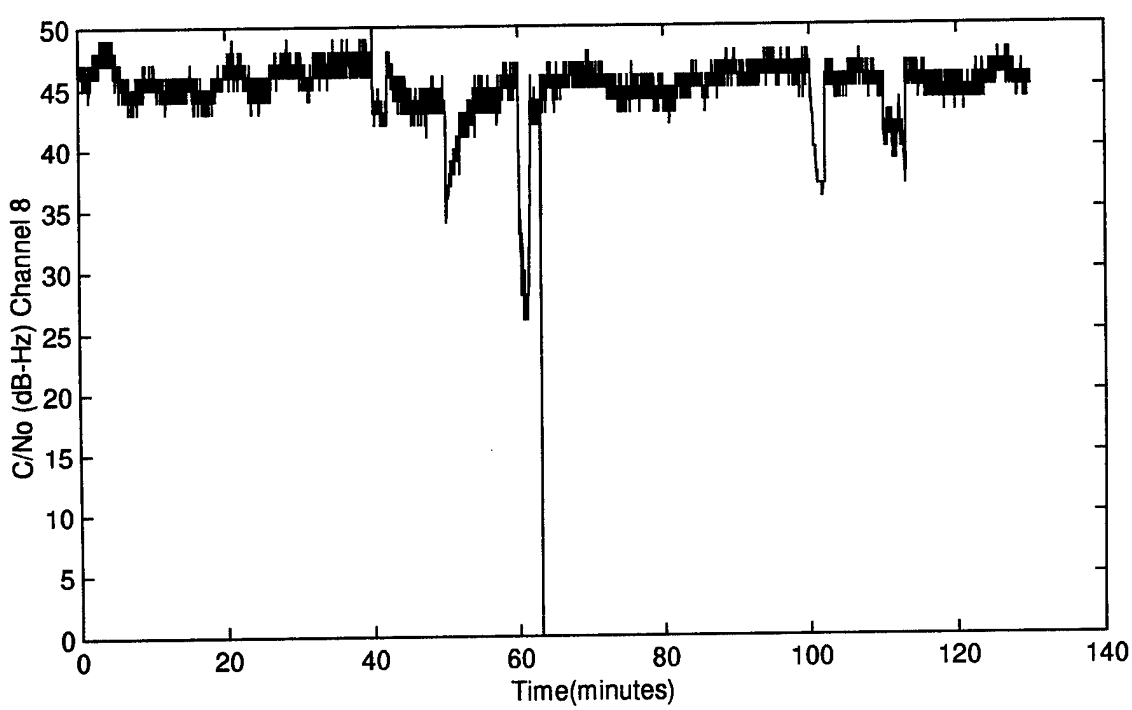

Figure O.15. C/No vs Time

Start Time 1500Z 08 Dec 98

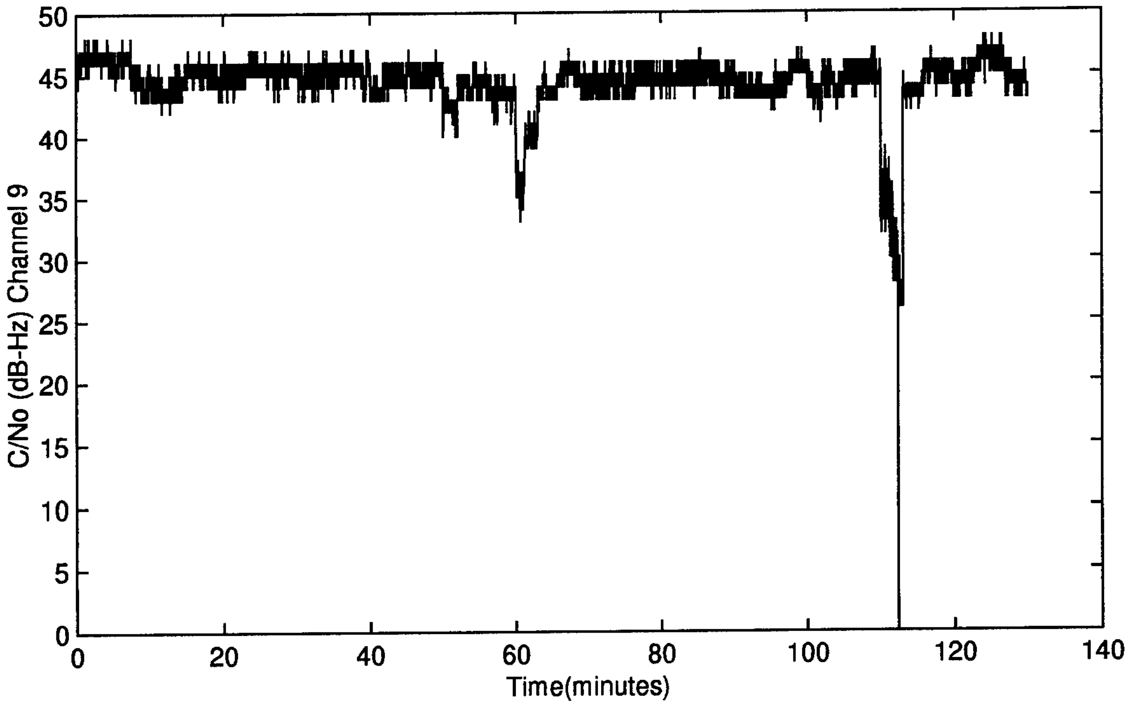

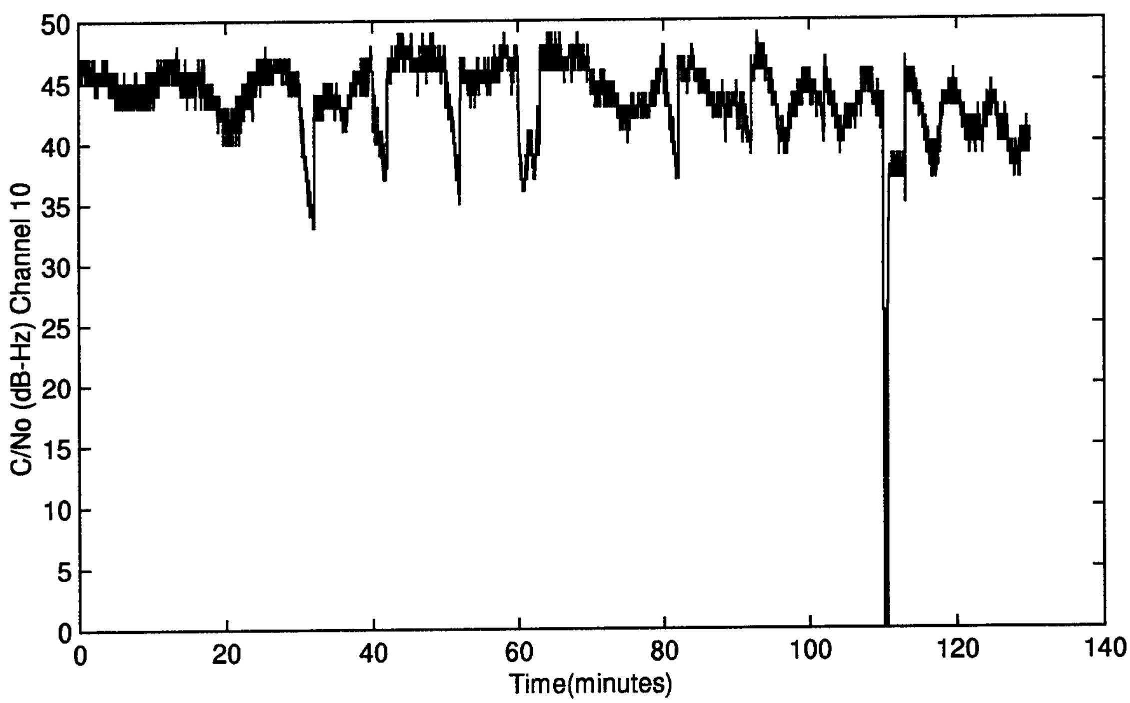

Figure O.16. C/No vs Time

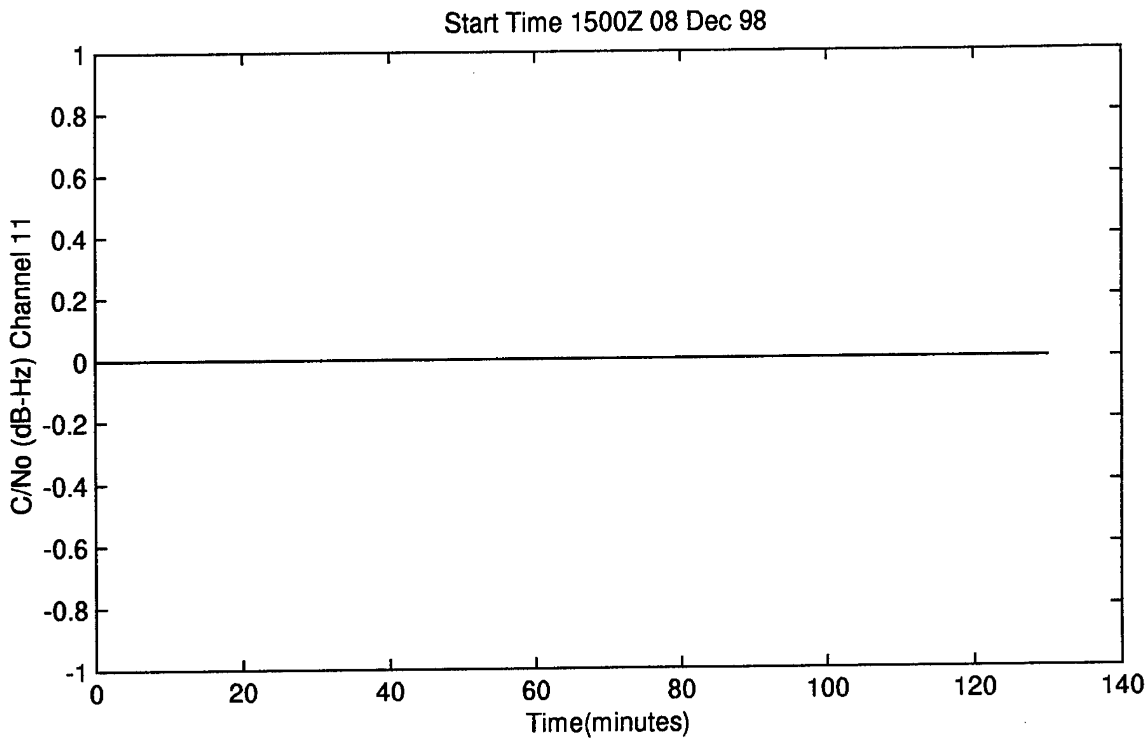

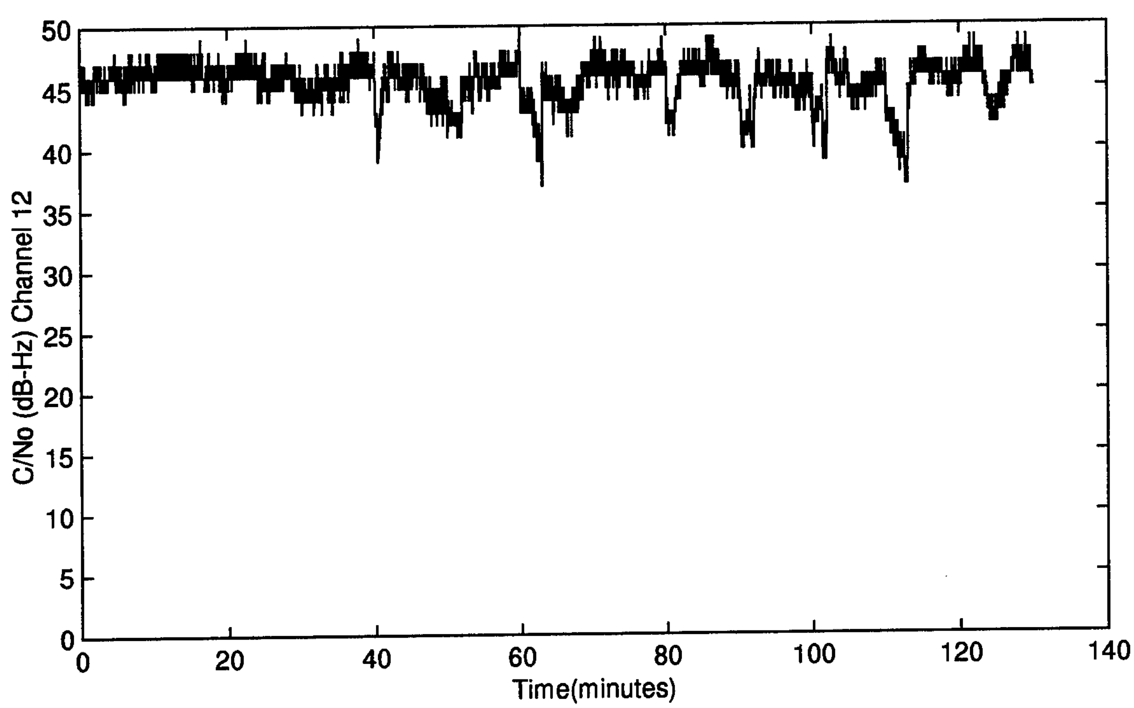

Figure O.17. C/No vs Time

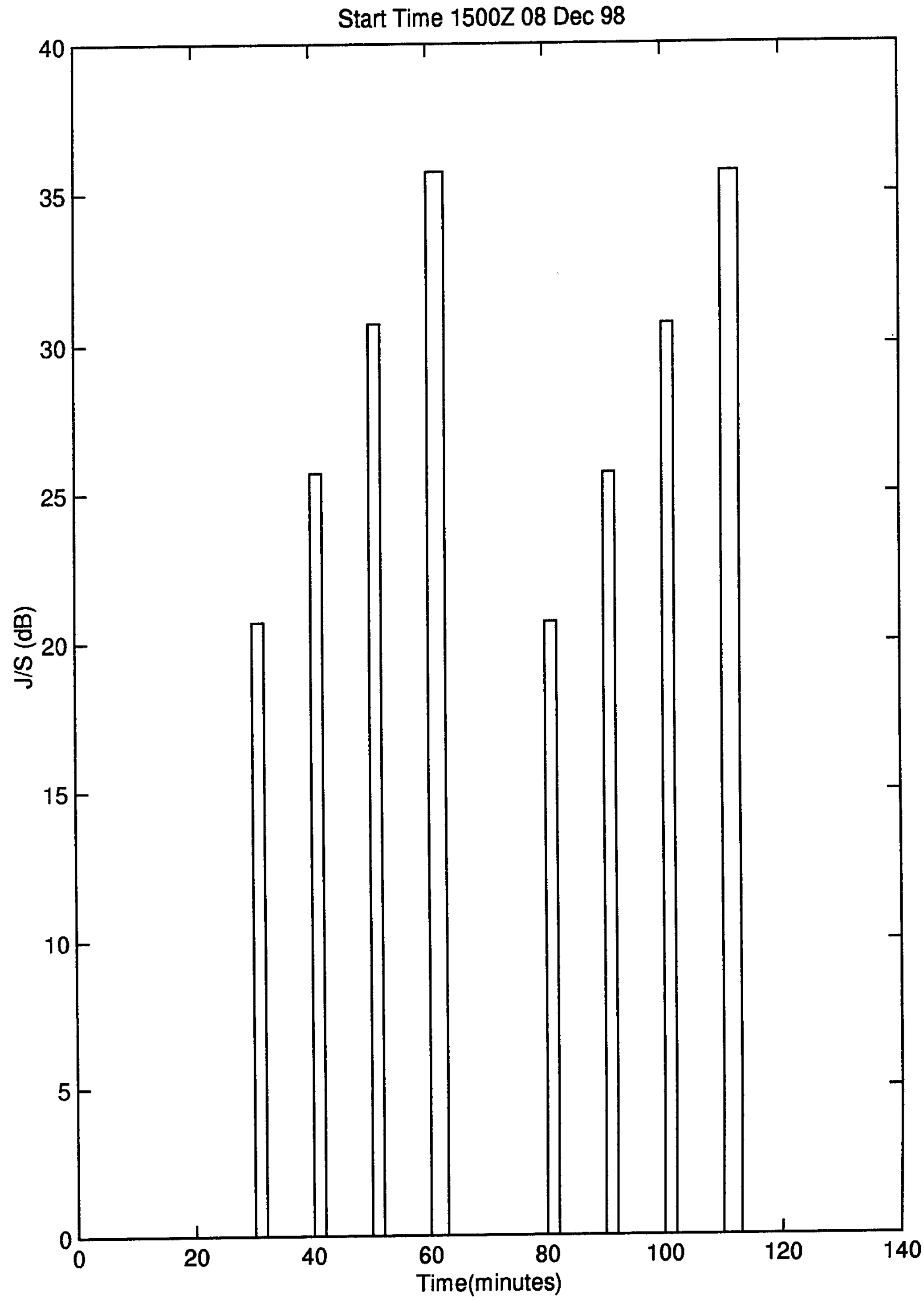

Figure O.18. Jamming Level J/S vs Time

APPENDIX P

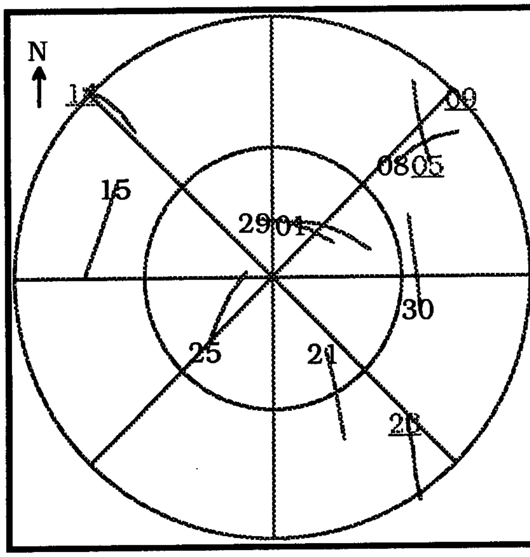

GPS Satellite Visibility

WGS 84 Latitude: +N -S
39°46'55.1"

WGS 84 Longitude: -W +E
-84 °4'59.6"

Local
Date: 12/11/98
Time: 03:10:00 PM

Mask Angle: 25.0°

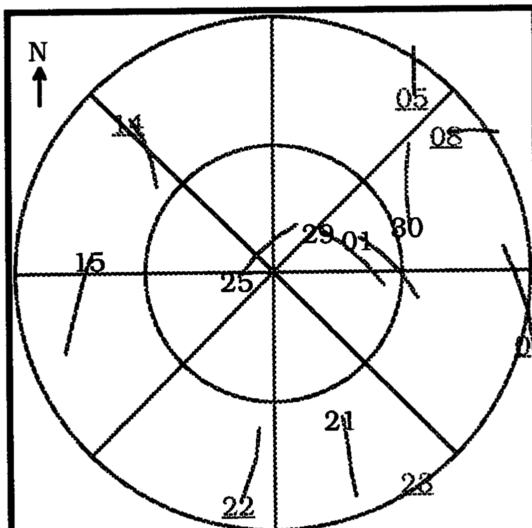

GPS Satellite Visibility

WGS 84 Latitude: +N -S
39°46'55.1"

WGS 84 Longitude: -W +E
-84 °4'59.6"

Local
Date: 12/11/98
Time: 04:00:00 PM

Mask Angle: 25.0°

Figure P.1 GPS Satellites In View 11 Dec 98

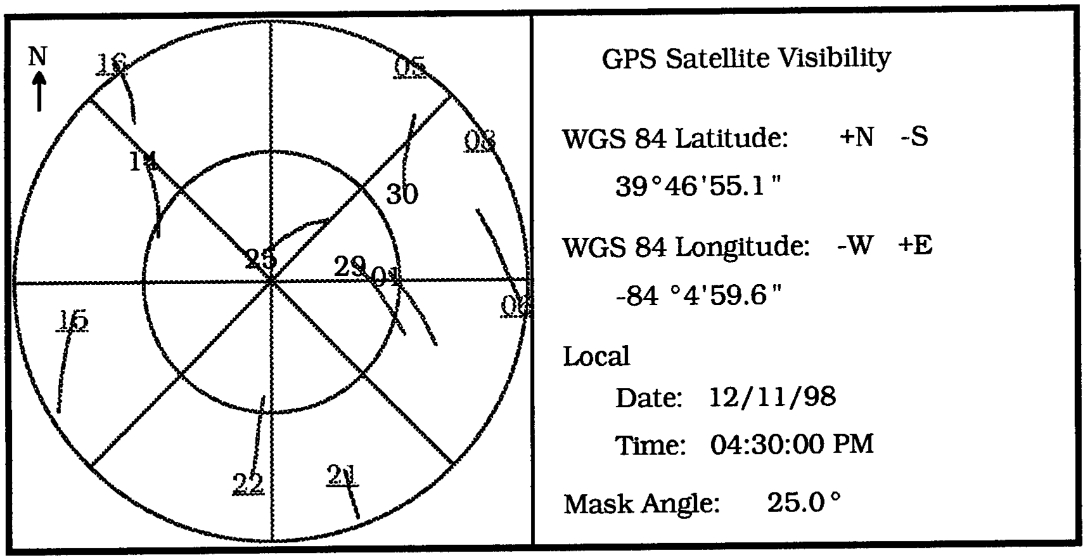

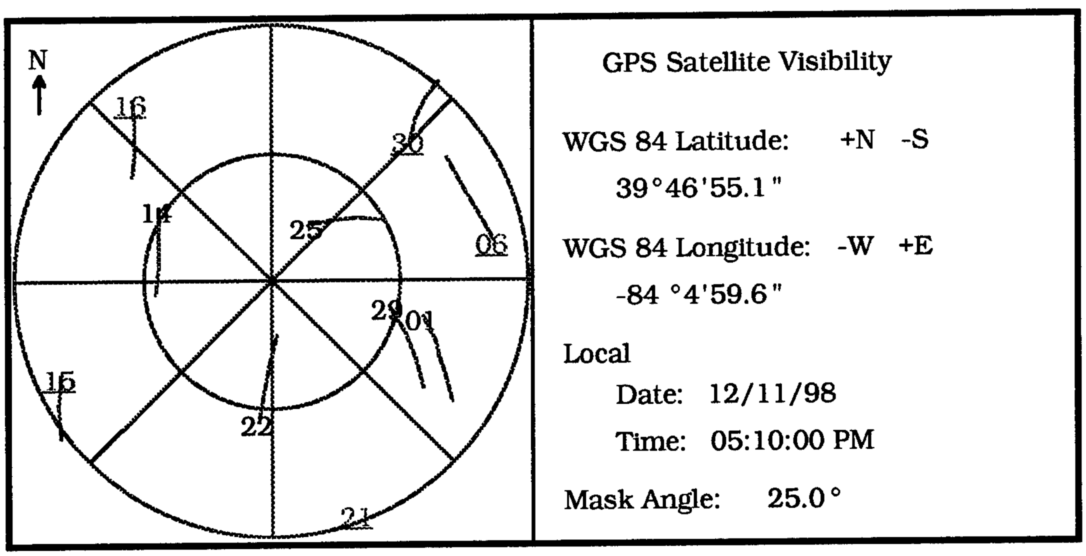

Figure P.2 GPS Satellites In View 11 Dec 98

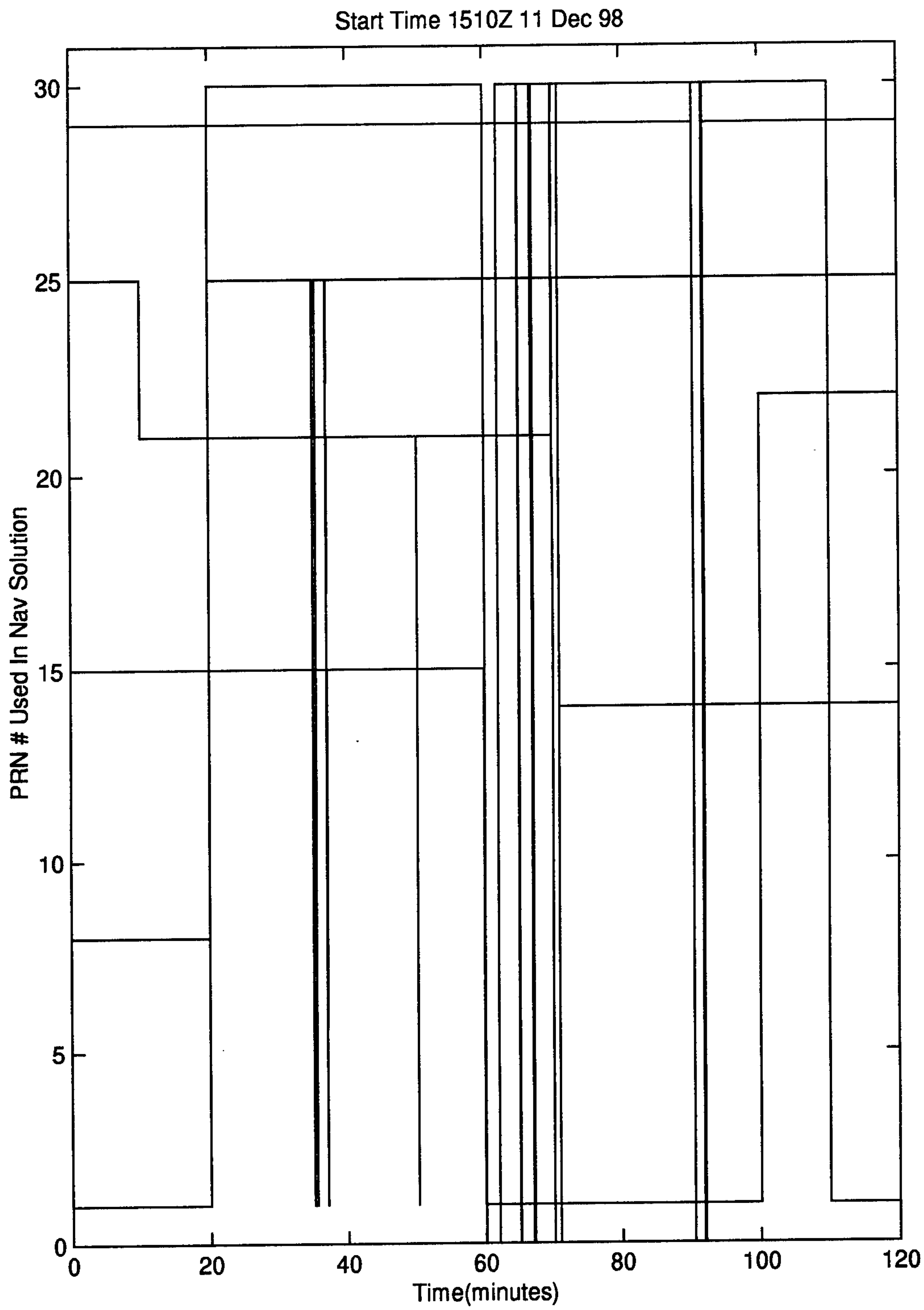

Figure P.3. PRN # Used In Nav Solution vs Time

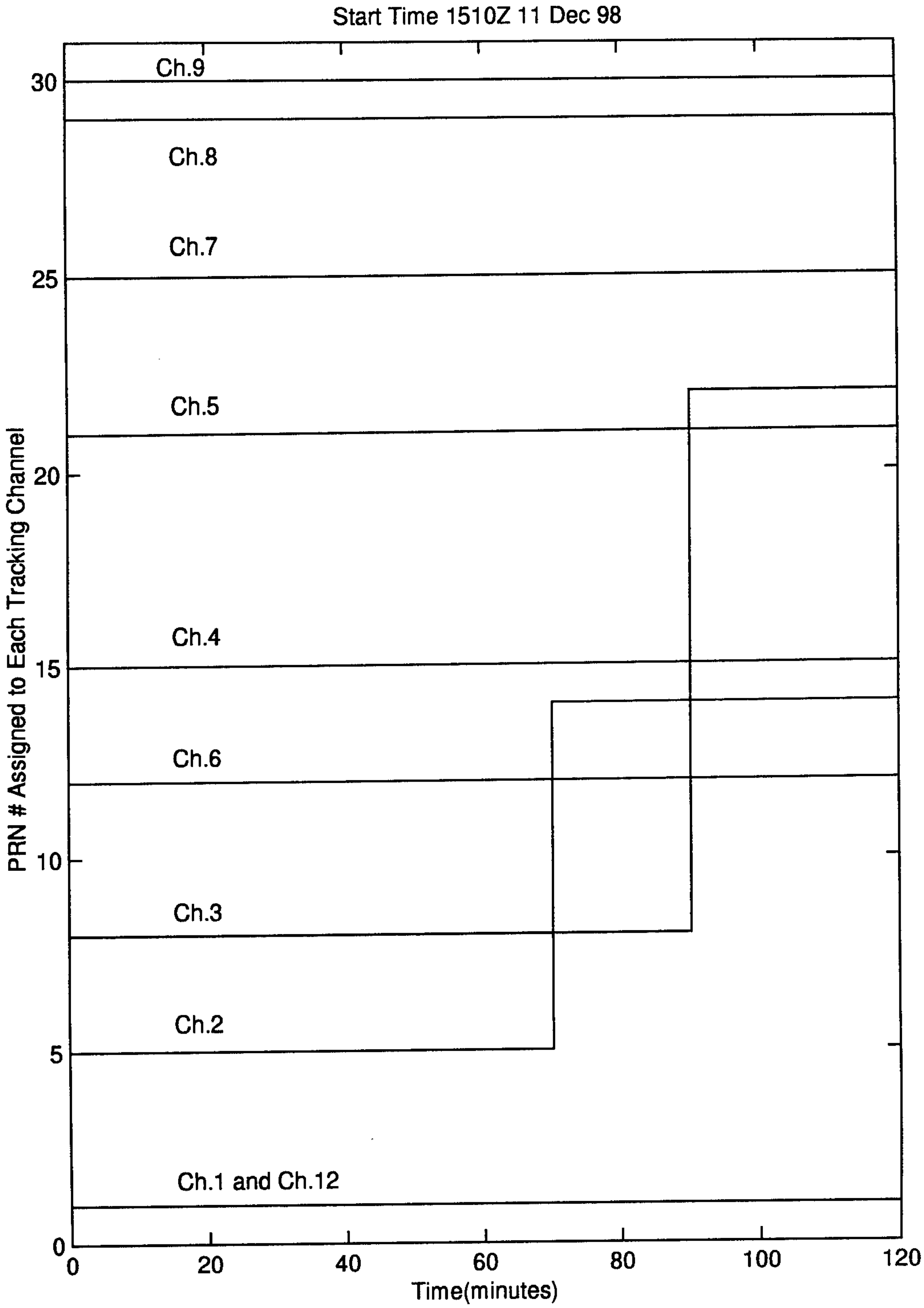

Figure P.4. PRN # Assigned to Each Tracking Channel vs Time

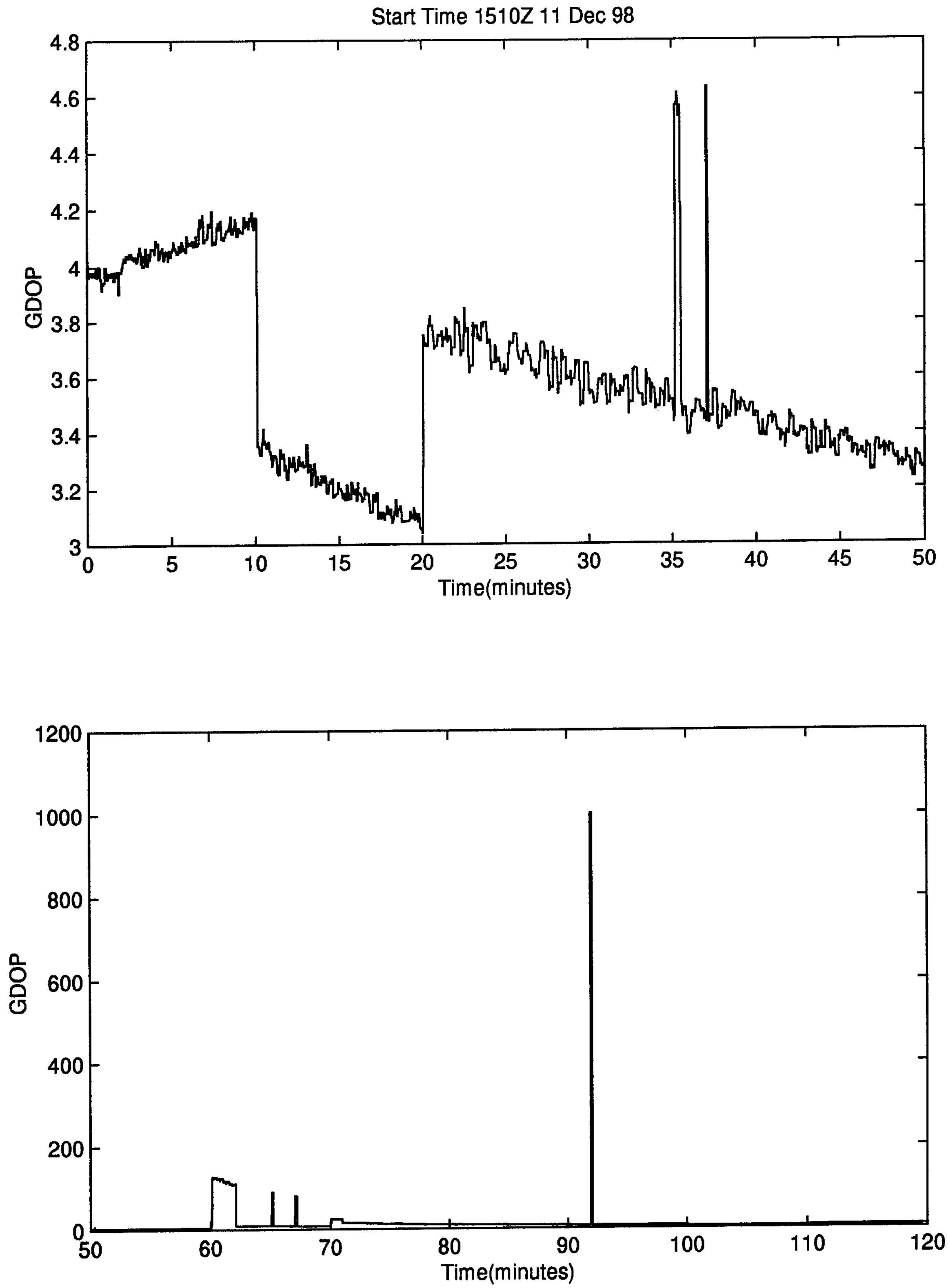

Figure P.5. GDOP vs Time

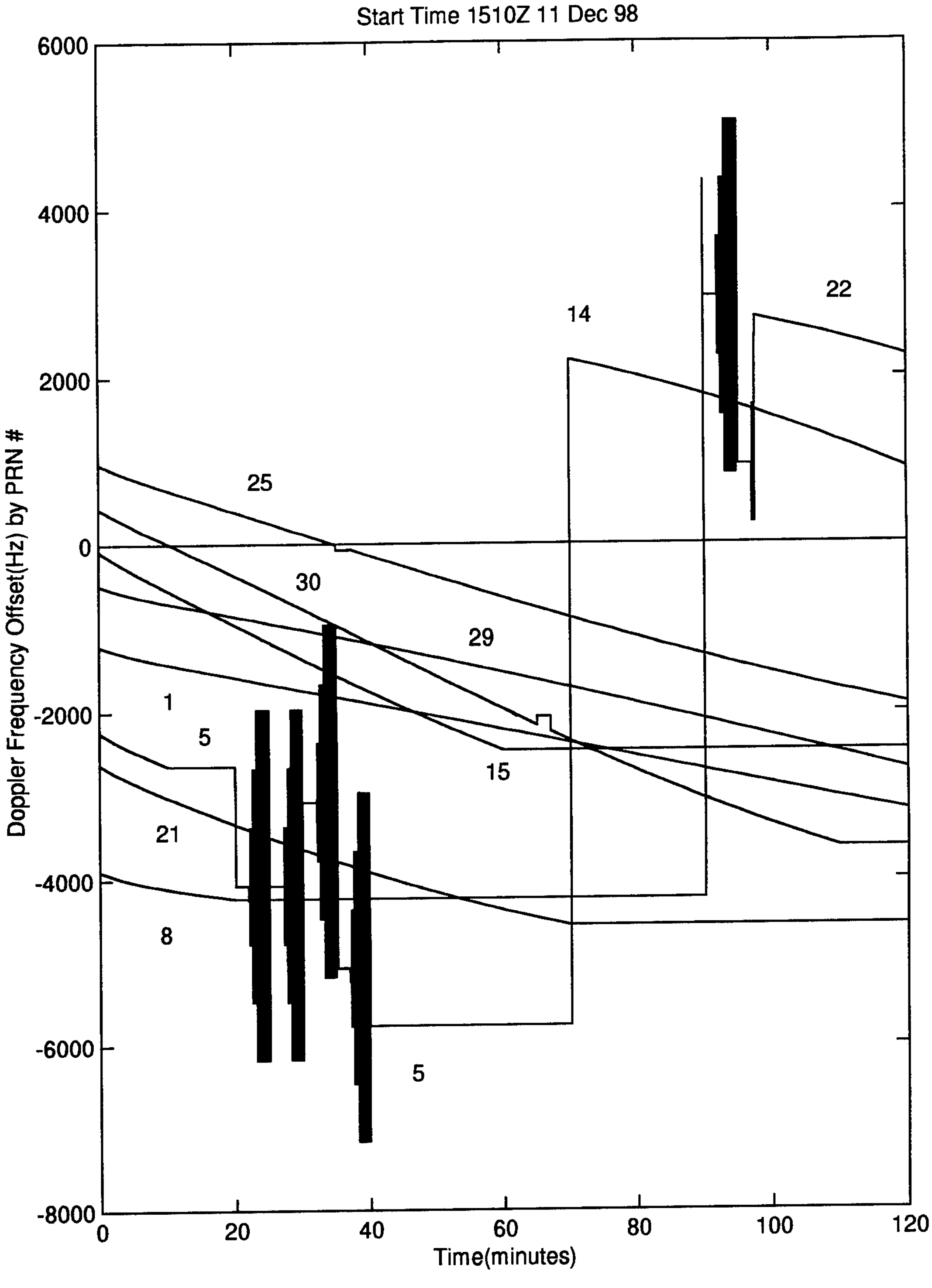

Figure P.6. Doppler Frequency vs Time

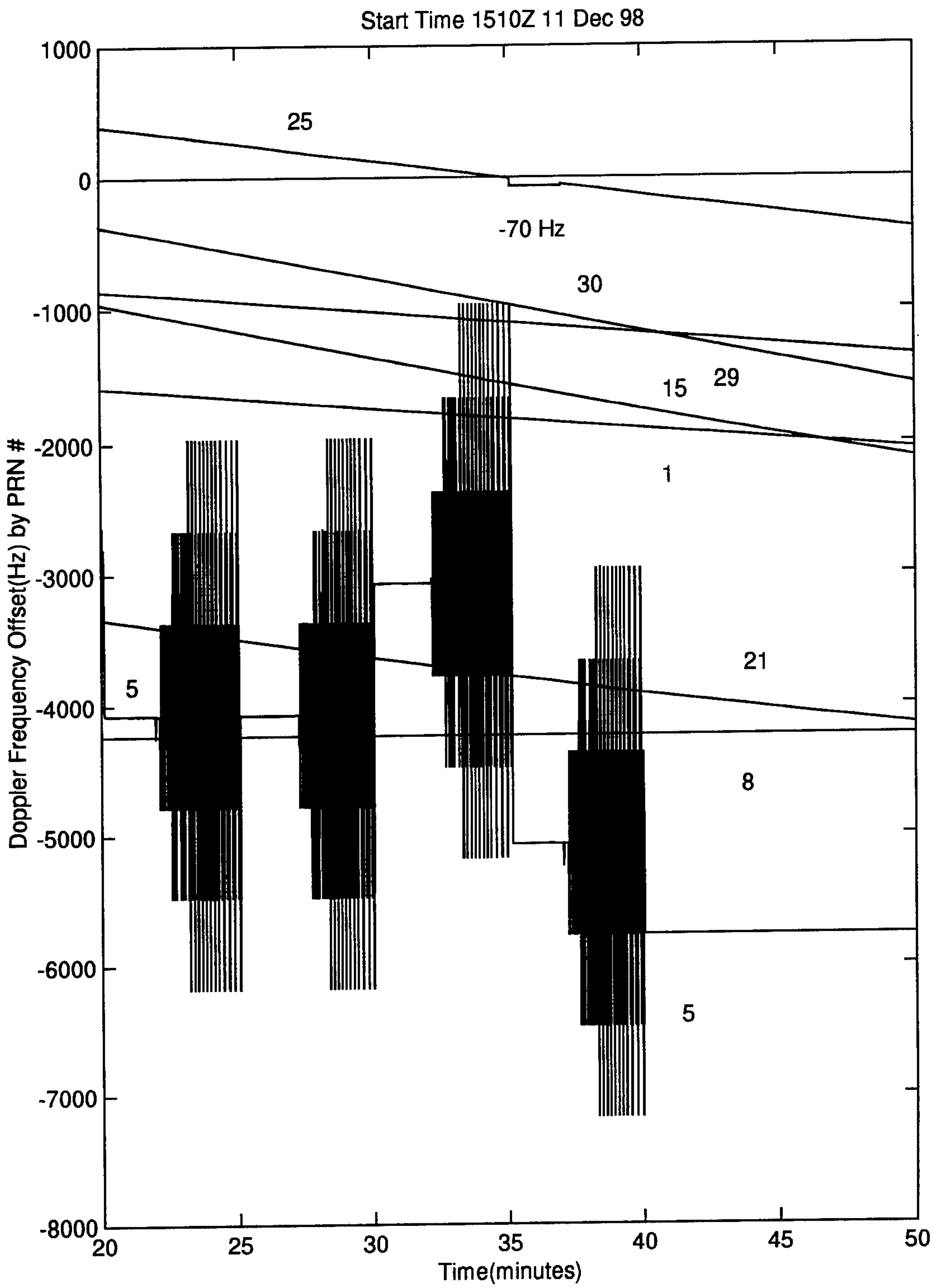

Figure P.7. Doppler Frequency vs Time

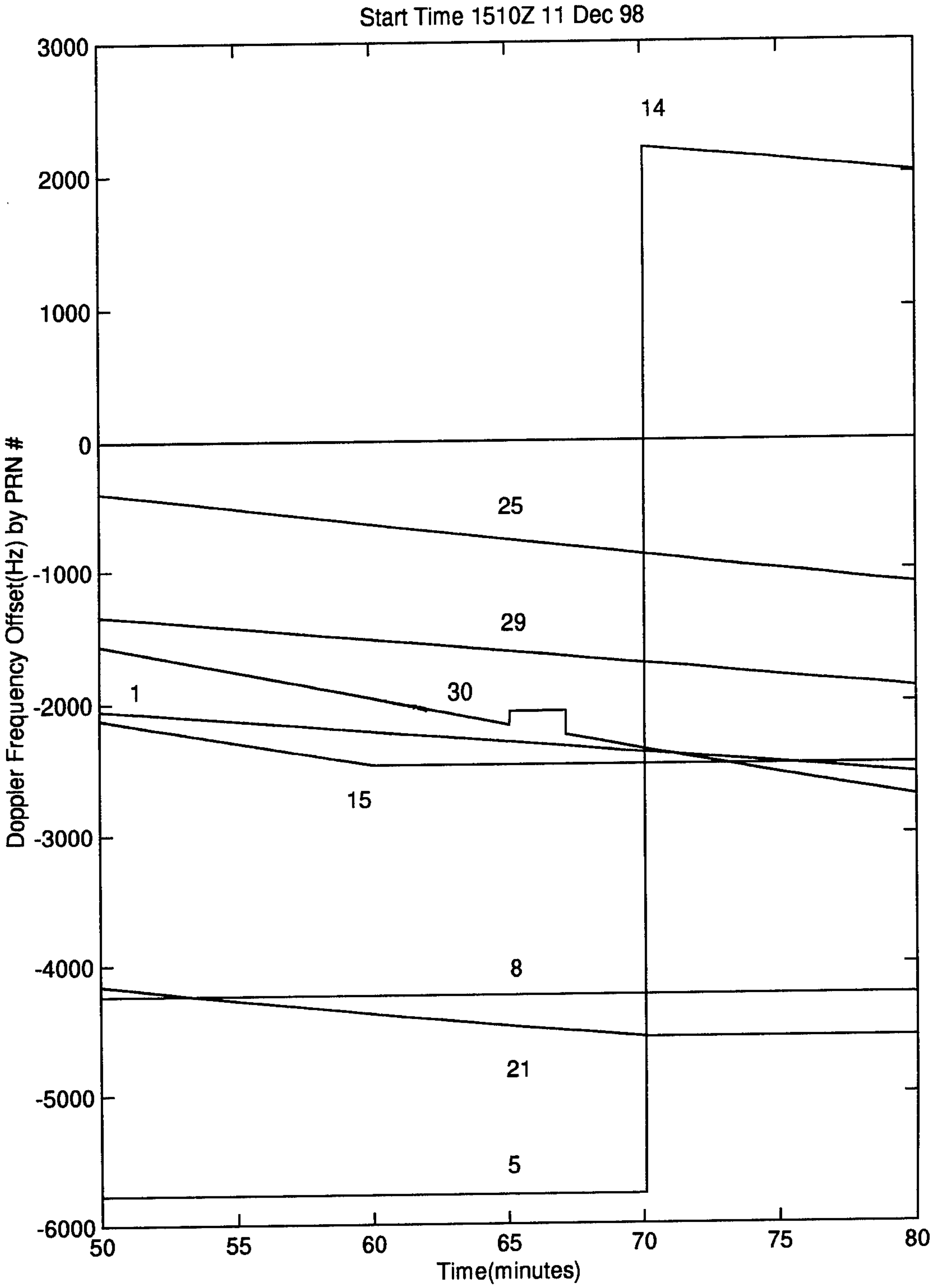

Figure P.8. Doppler Frequency vs Time

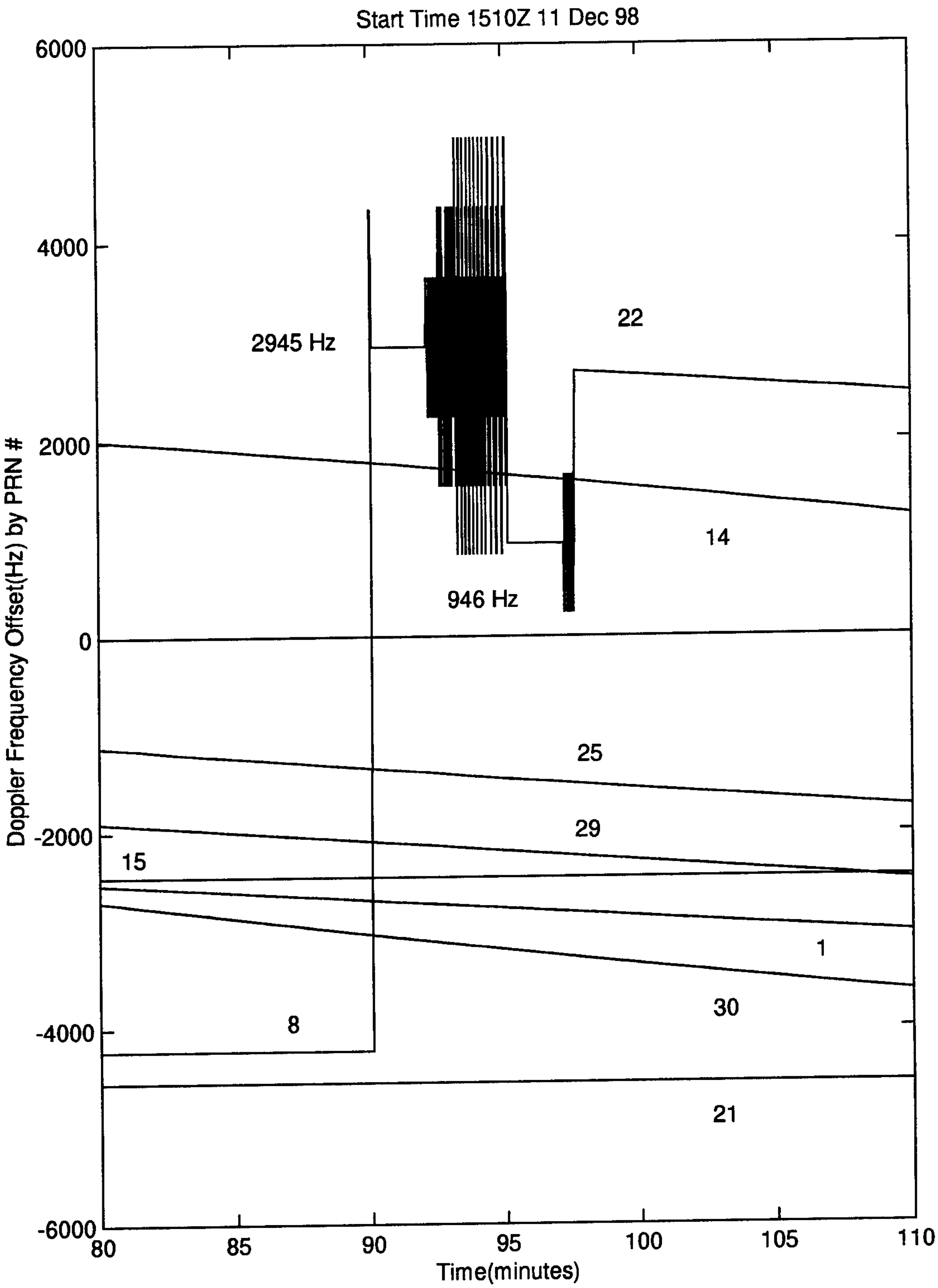

Figure P.9. Doppler Frequency vs Time

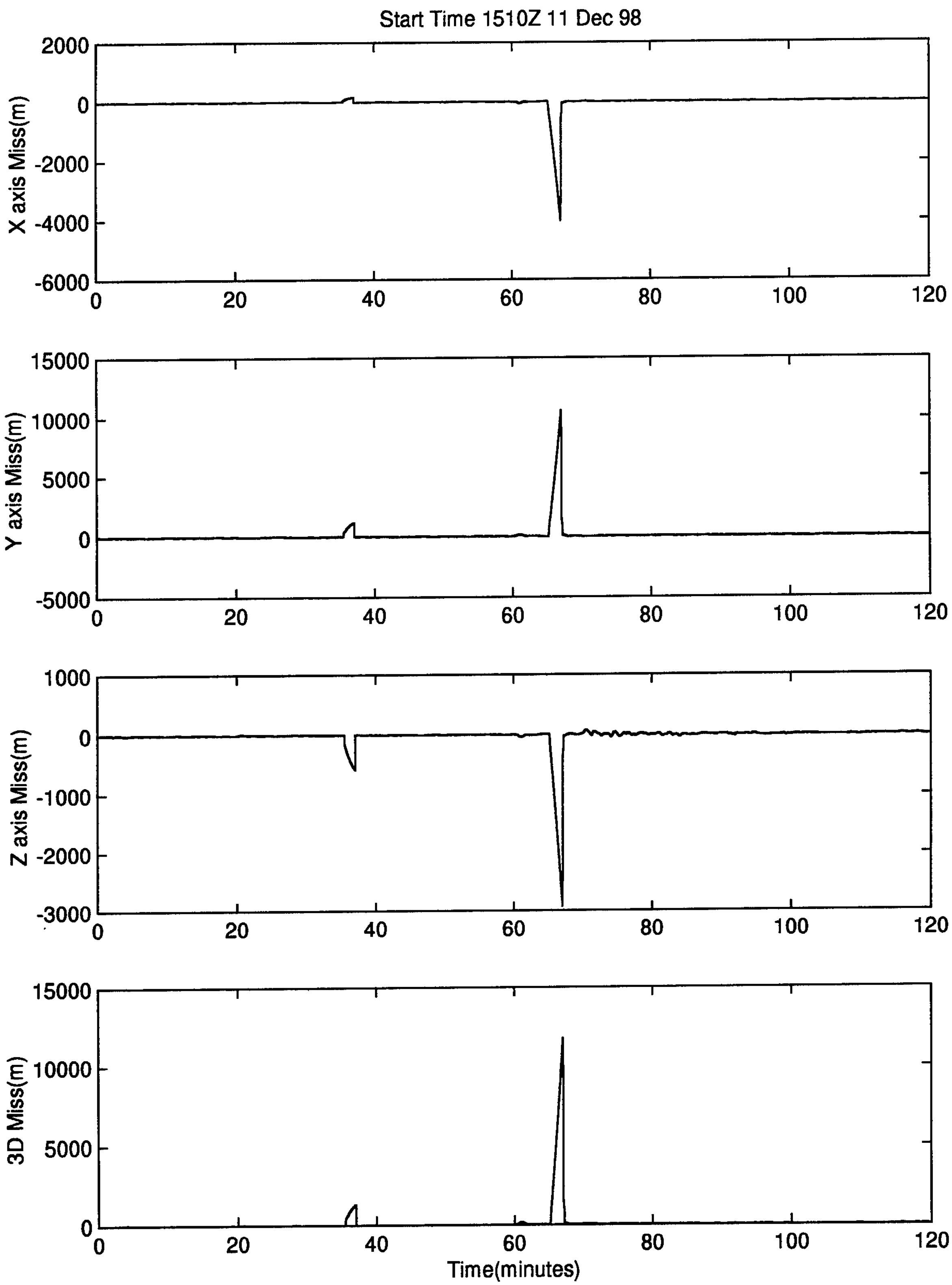

Figure P.10. X,Y,Z and 3D Error(m) vs Time

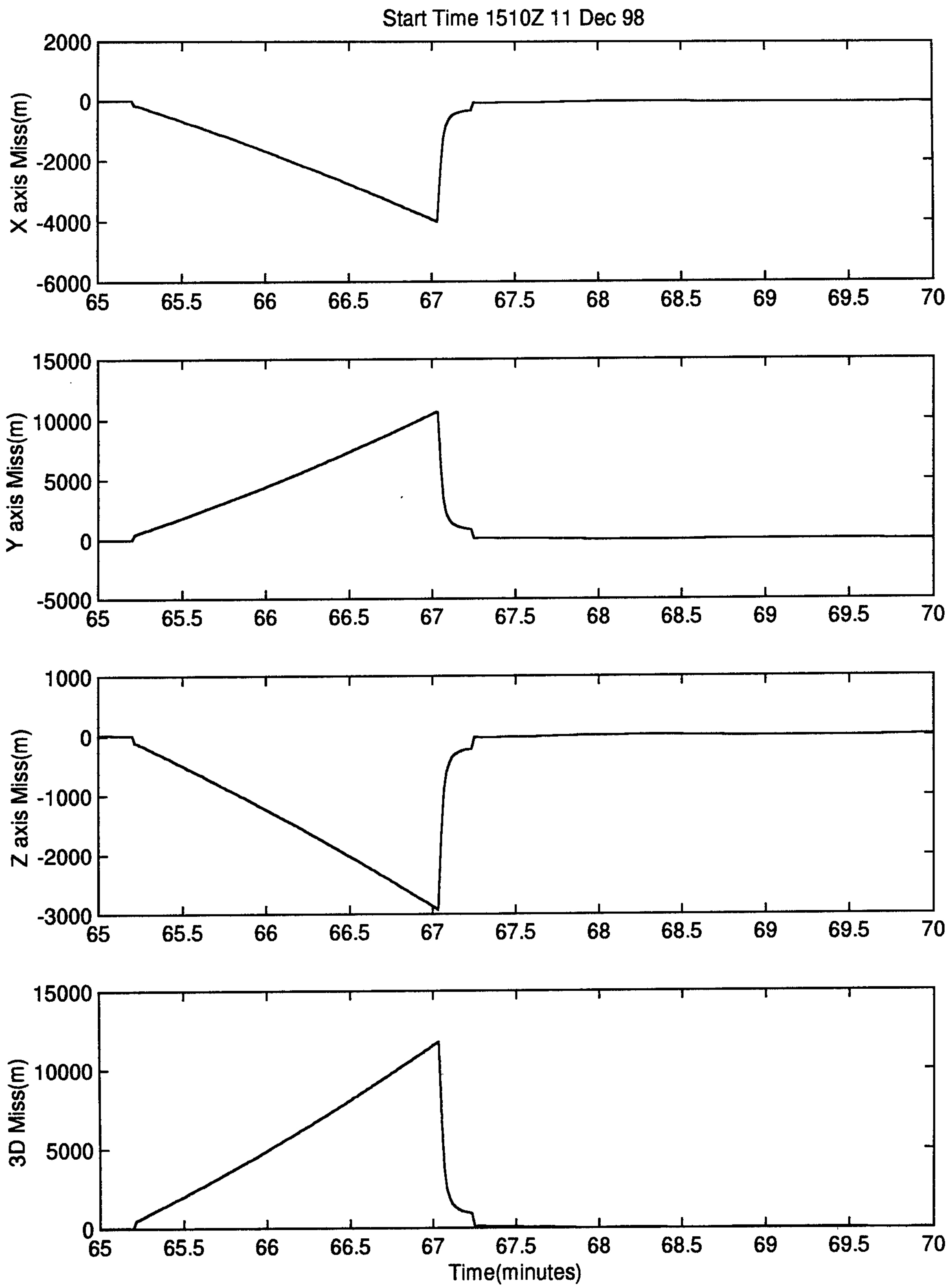

Figure P.11. X,Y,Z and 3D Error(m) vs Time

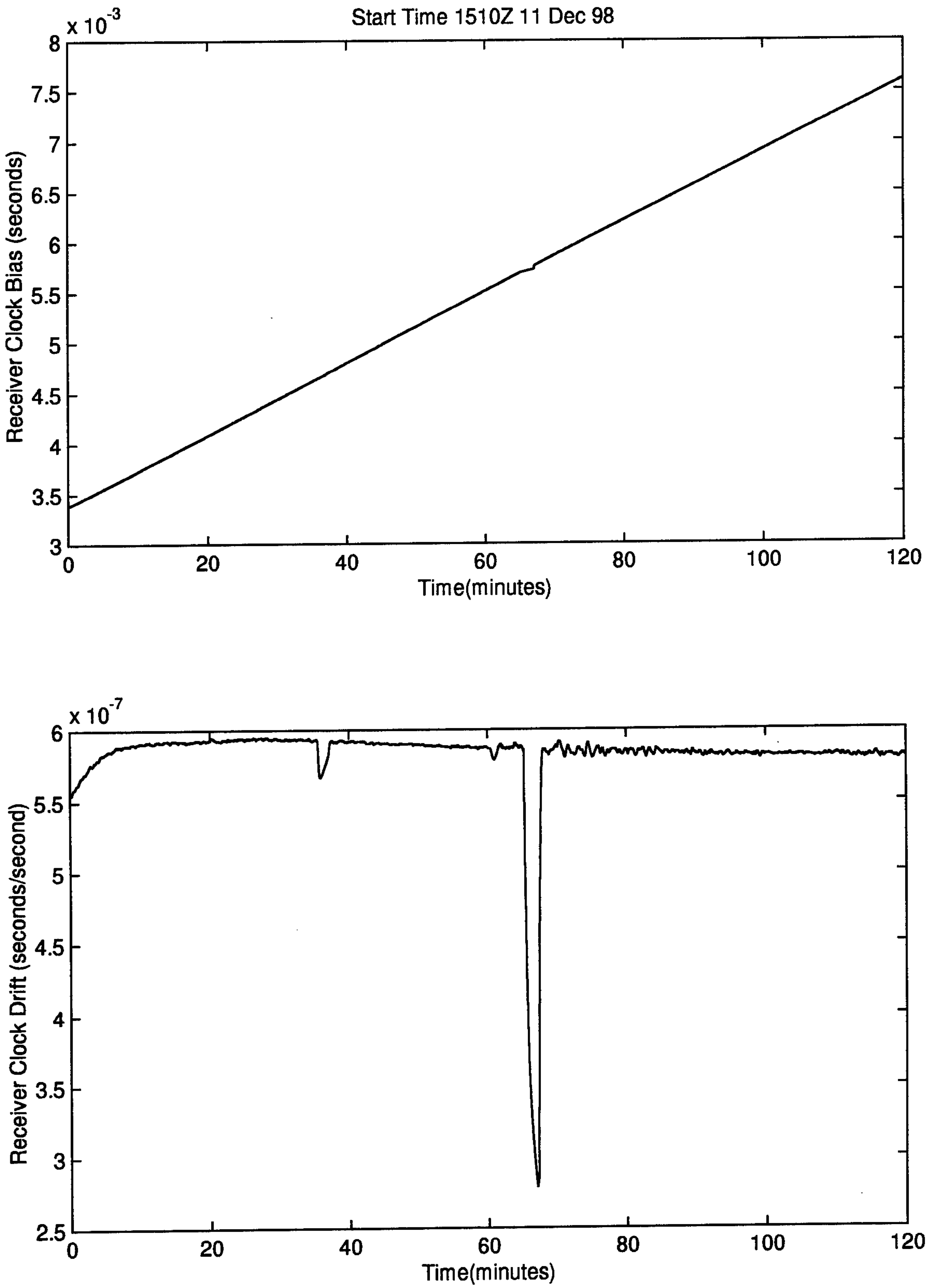

Figure P.12. Receiver Clock Bias and Drift vs Time

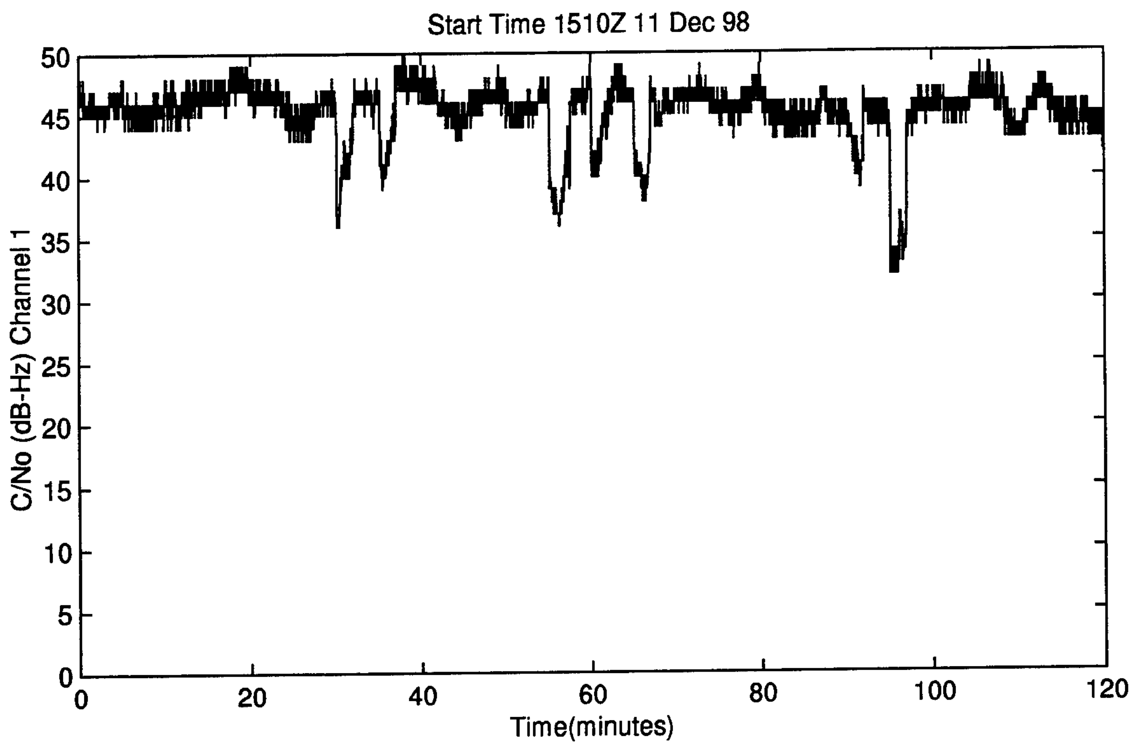

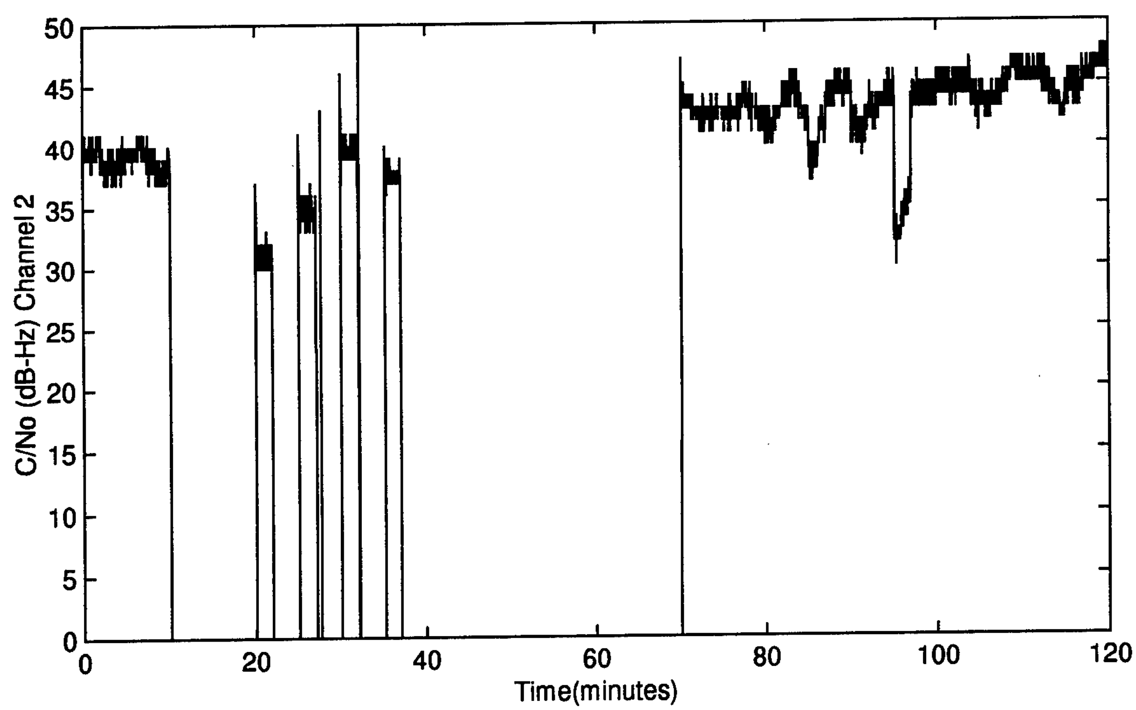

Figure P.13. C/No vs Time

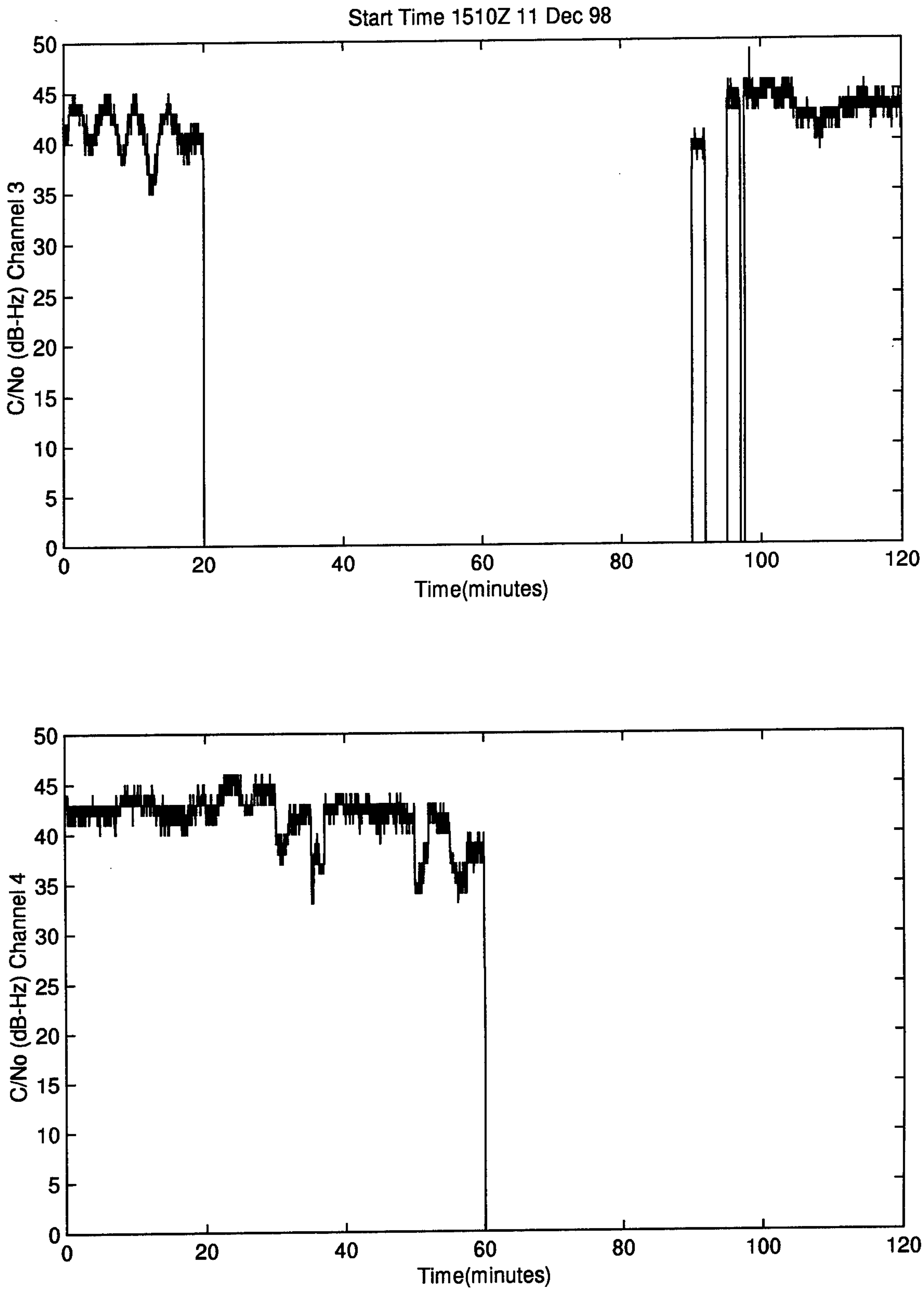

Figure P.14. C/No vs Time

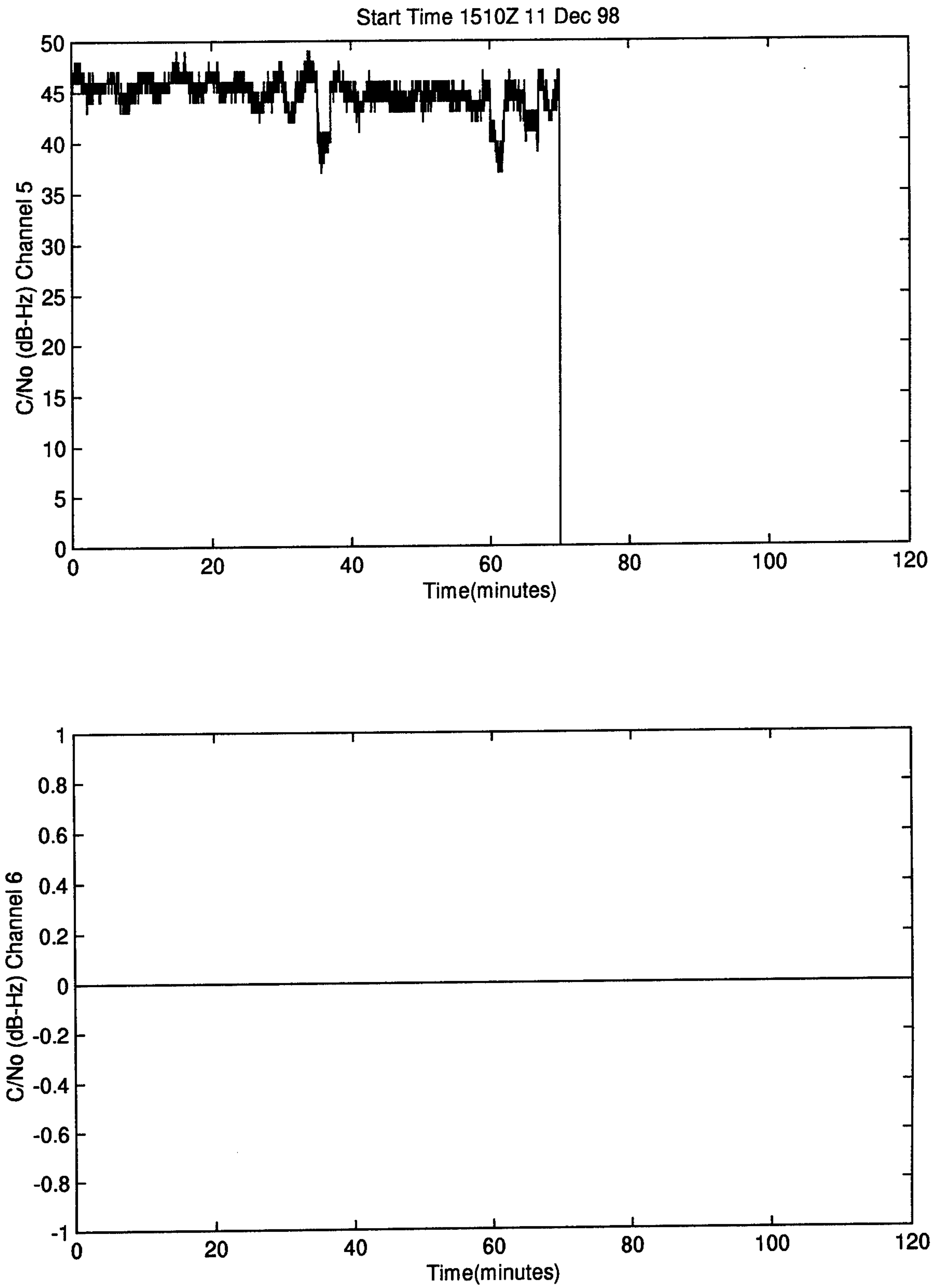

Figure P.15. C/No vs Time

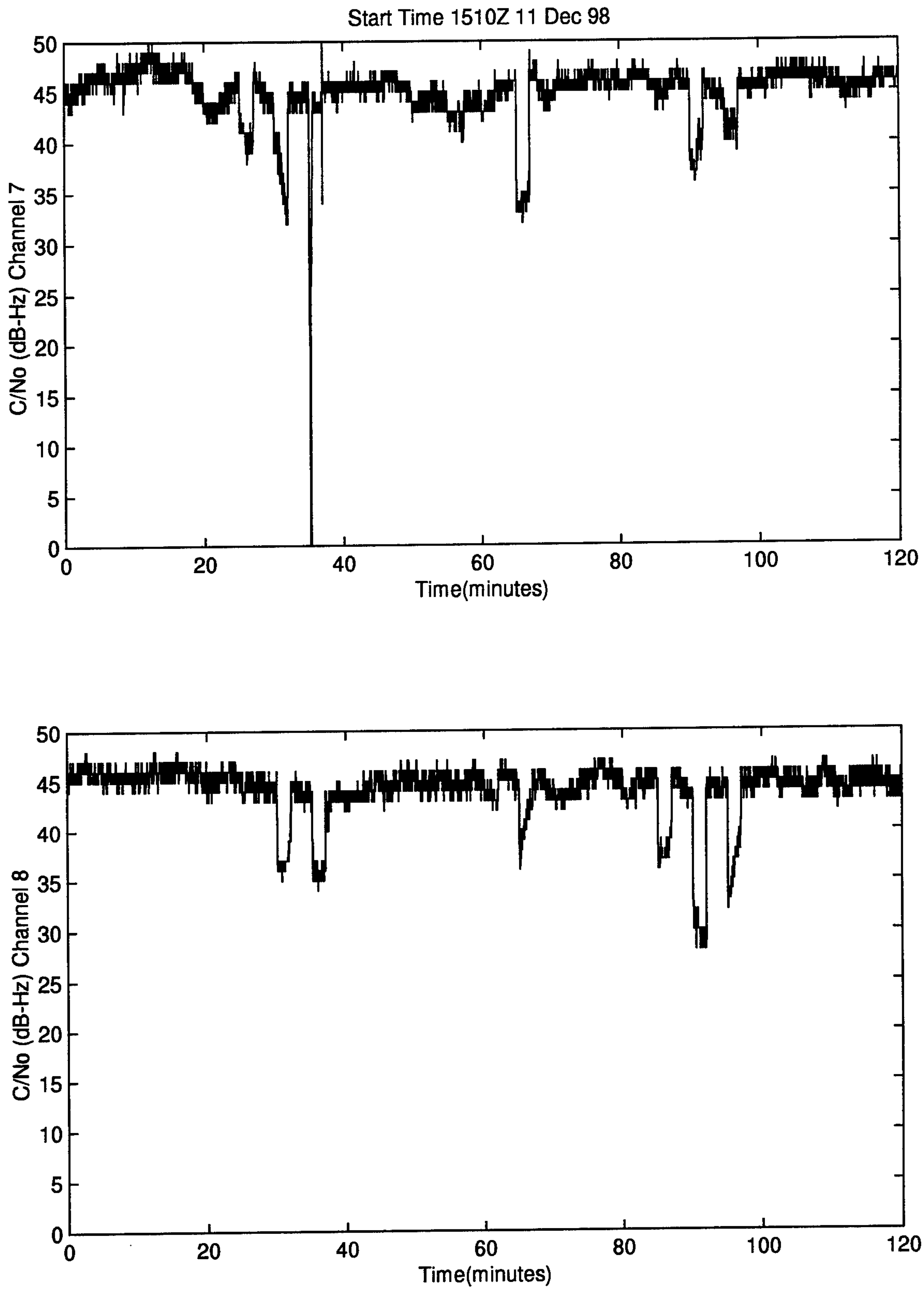

Figure P.16. C/No vs Time

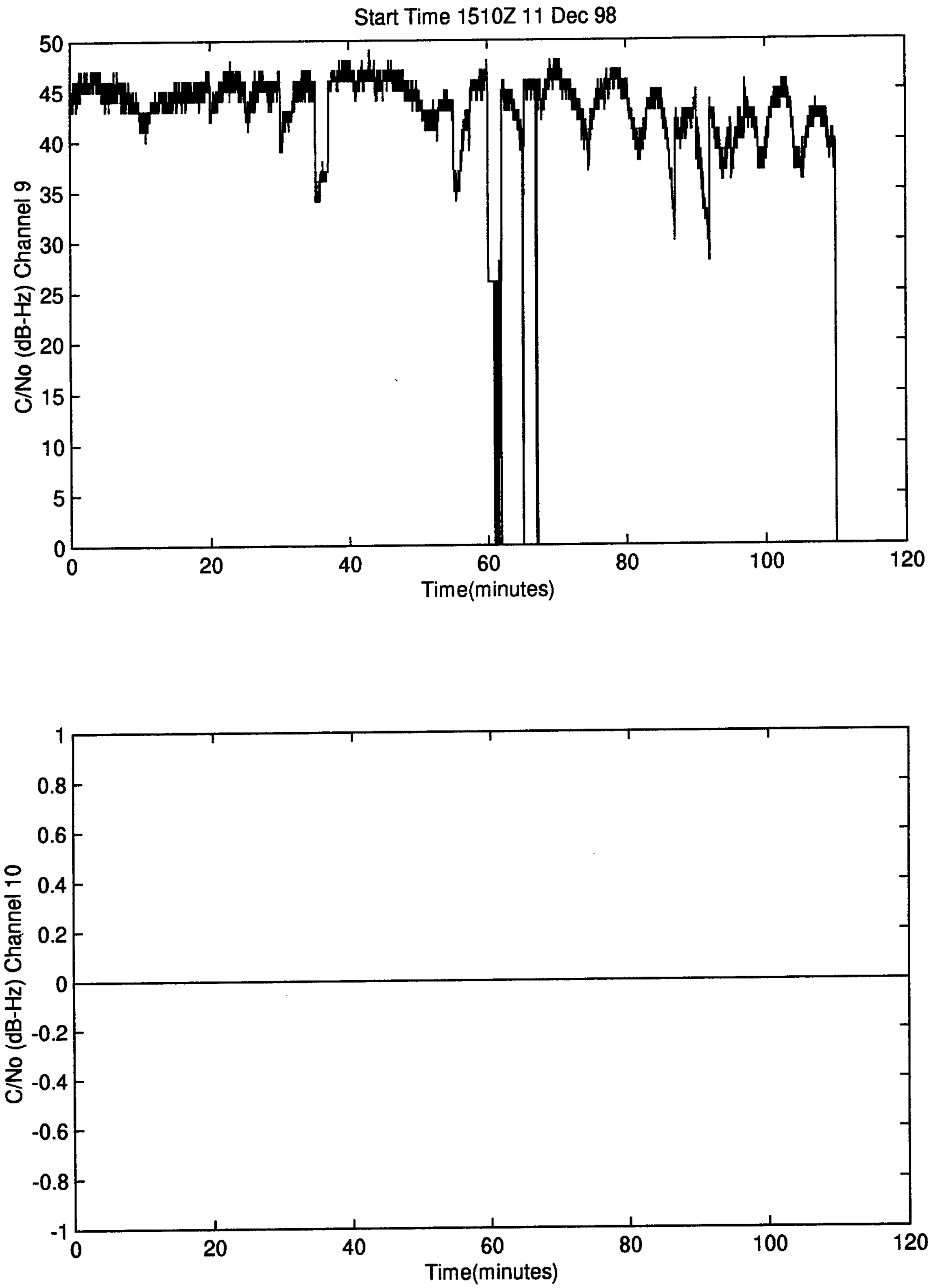

Figure P.17. C/No vs Time

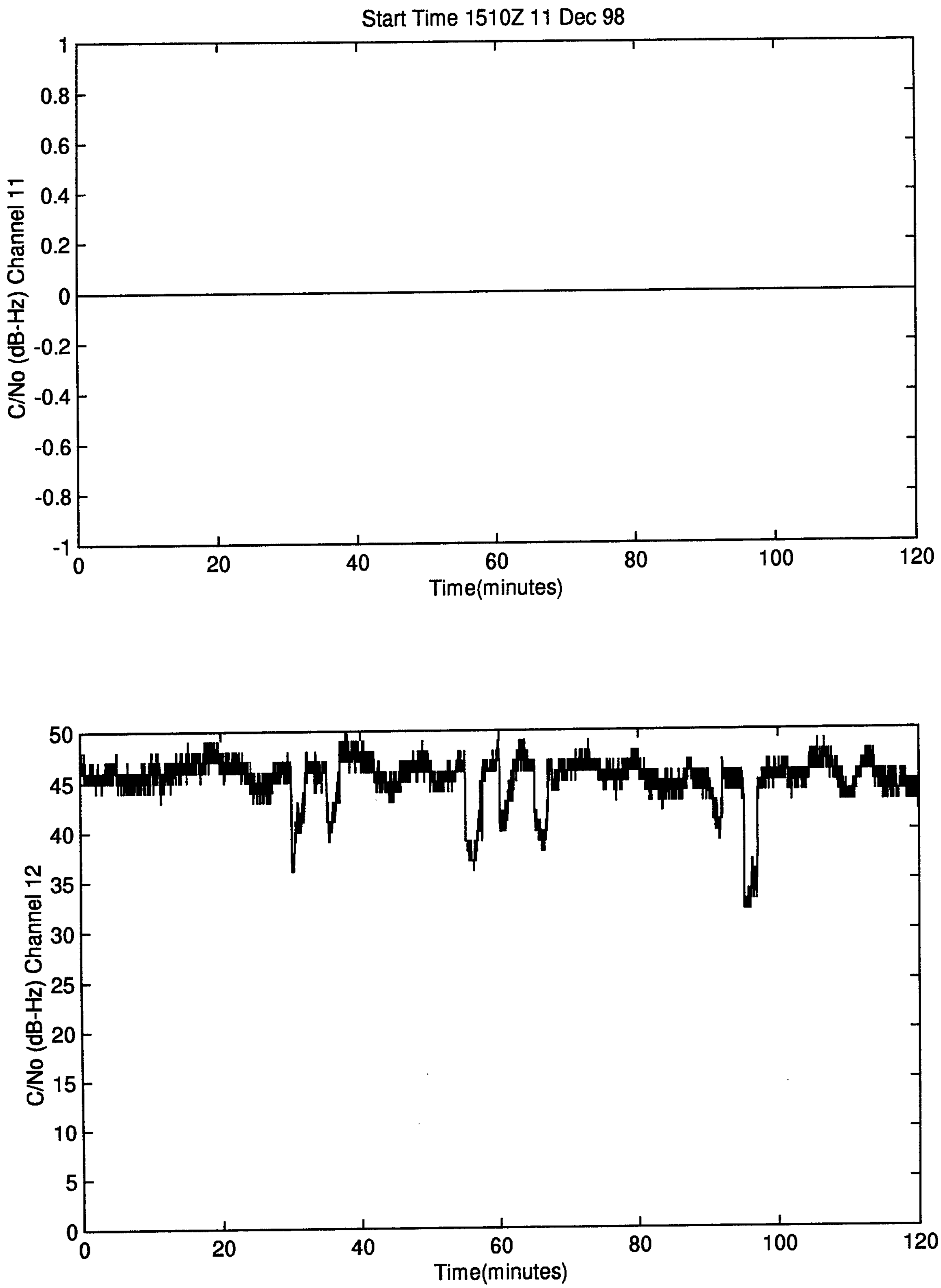

Figure P.18. C/No vs Time

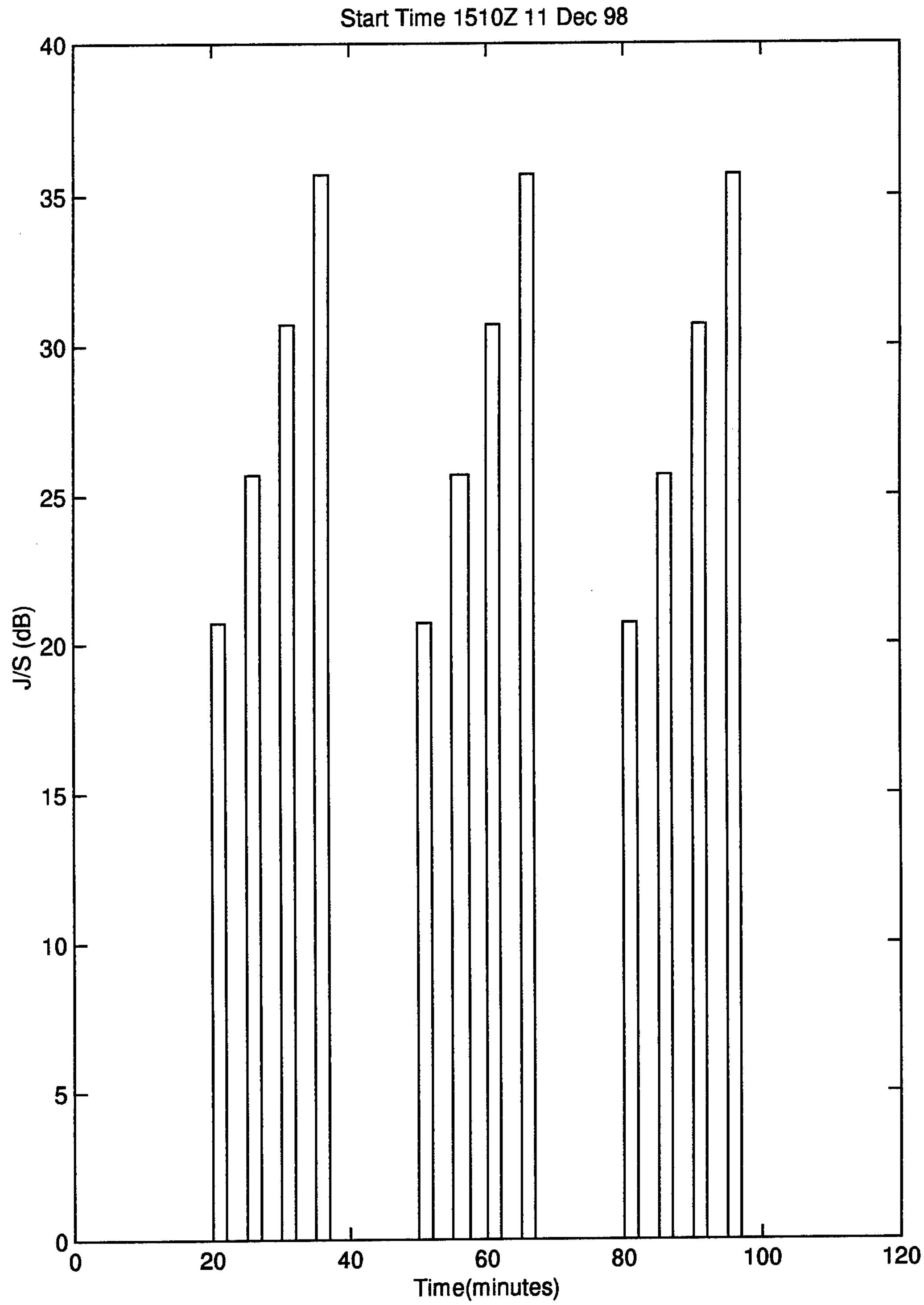

Figure P.19. Jamming Level J/S vs Time

APPENDIX Q

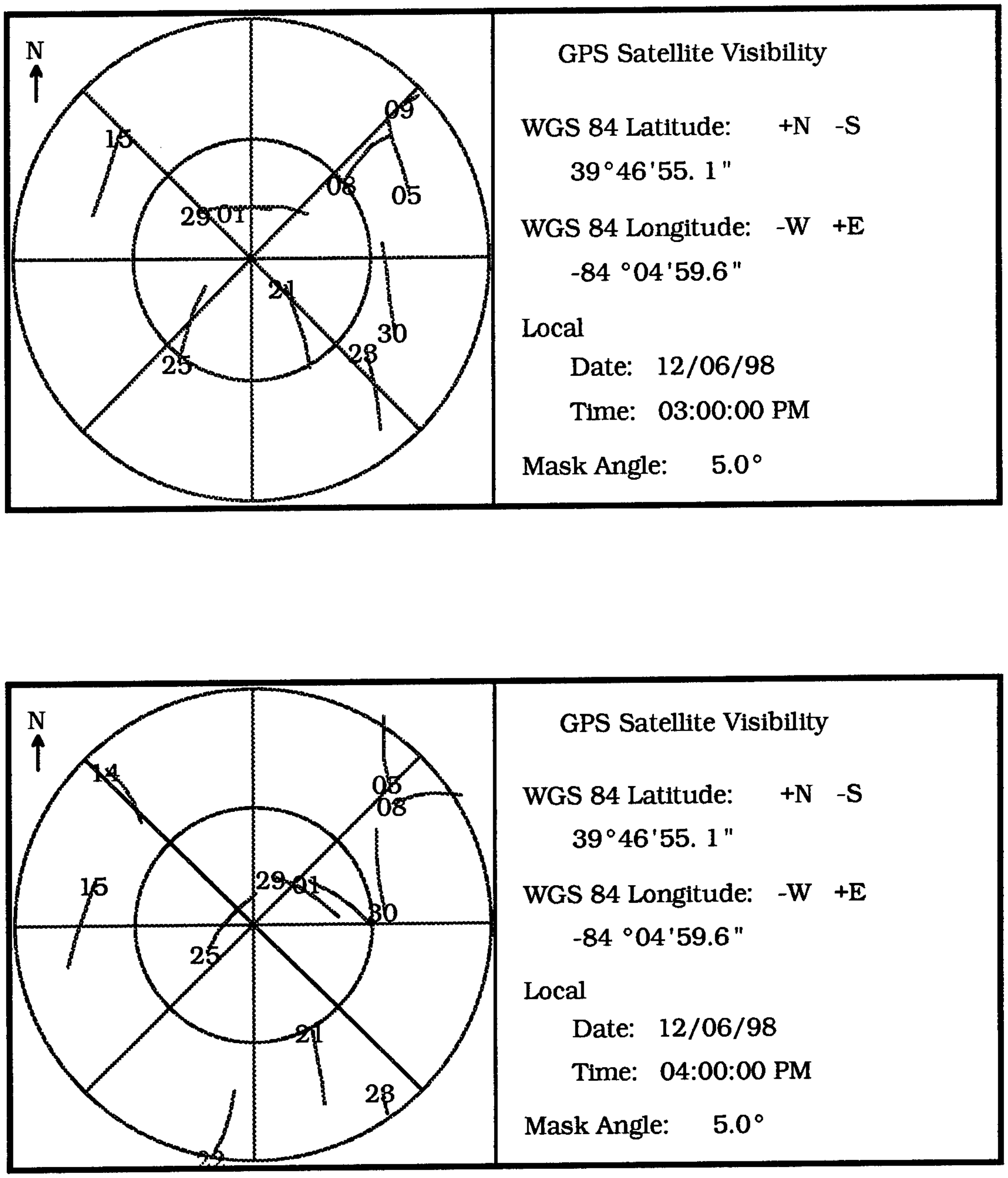

Figure Q.1. GPS Satellites In View 06 Dec 98

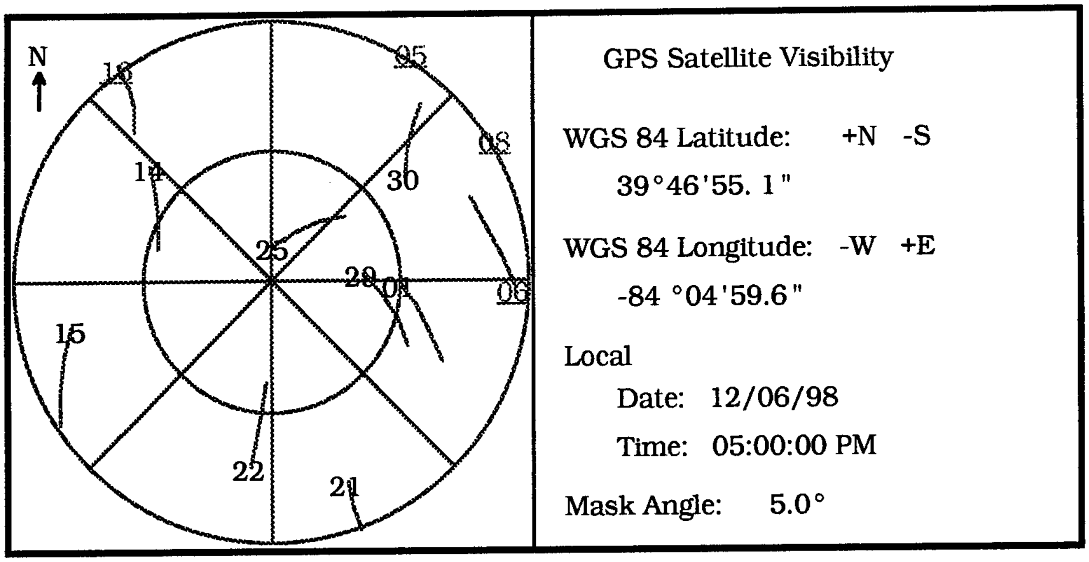

Figure Q.2. GPS Satellites In View 06 Dec 98

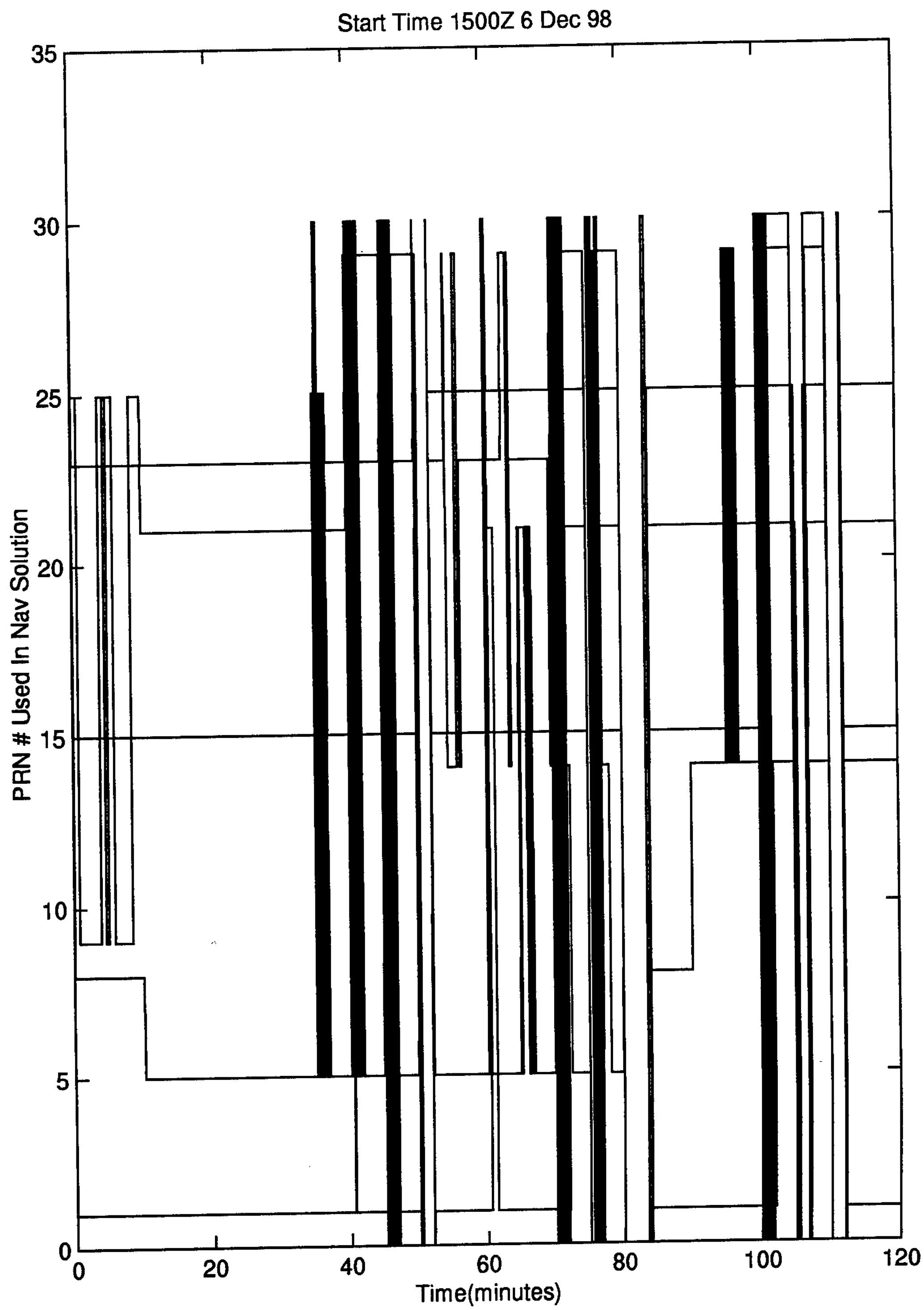

Figure Q.3. PRN # Used In Nav Solution vs Time

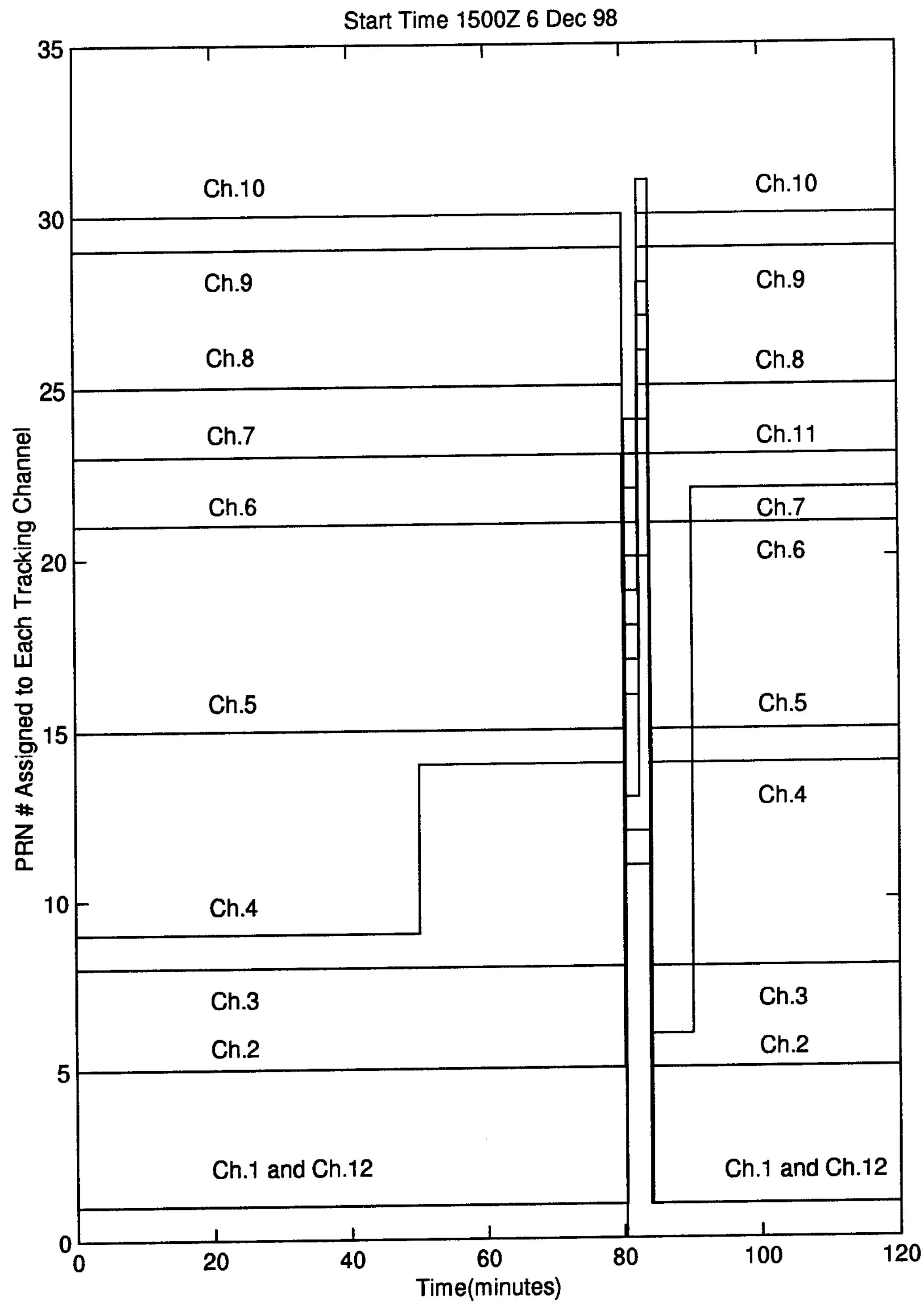

Figure Q.4. PRN # Assigned to Each Tracking Channel vs Time

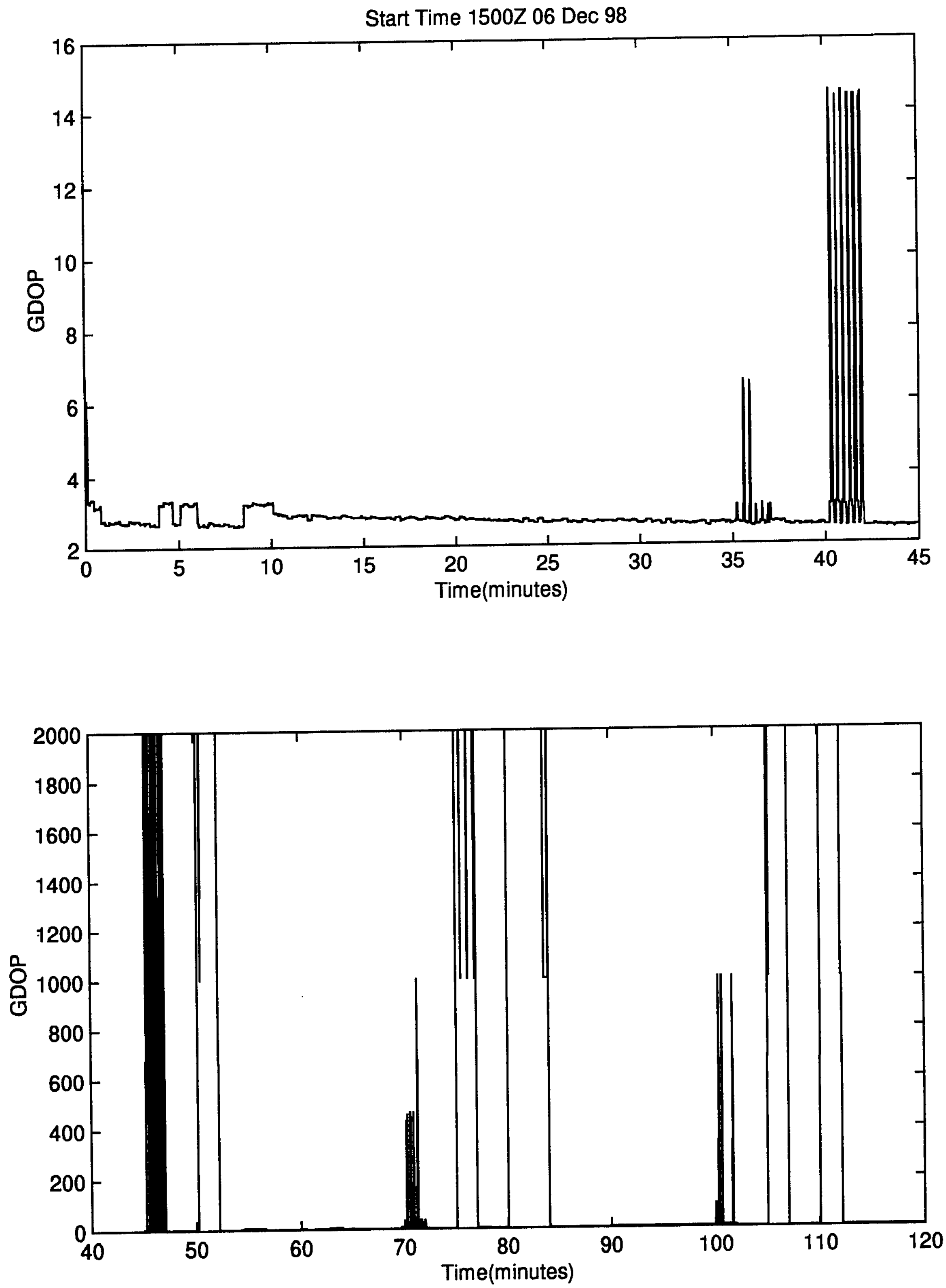

Figure Q.5. GDOP vs Time

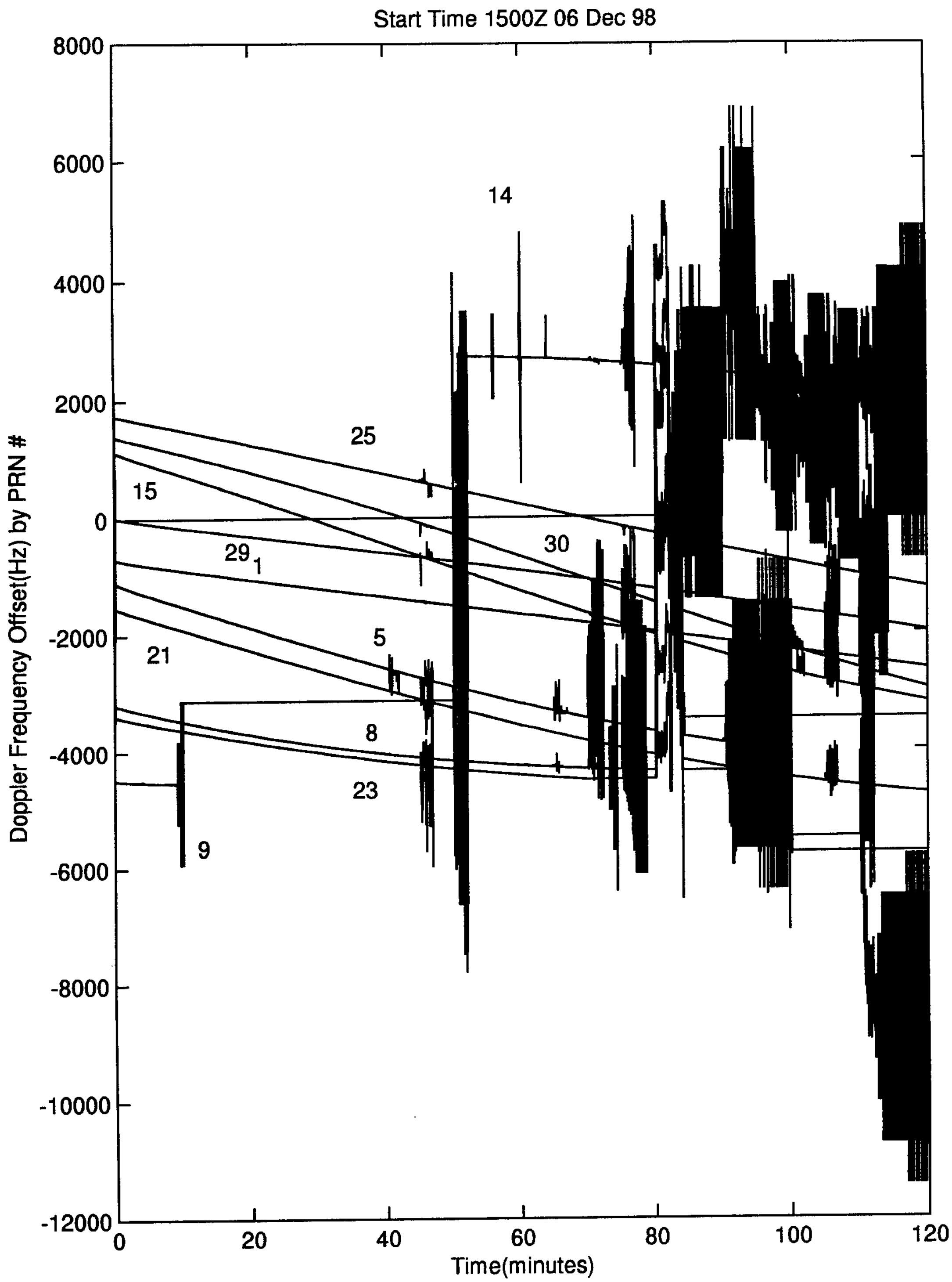

Figure Q.6. Doppler Frequency vs Time

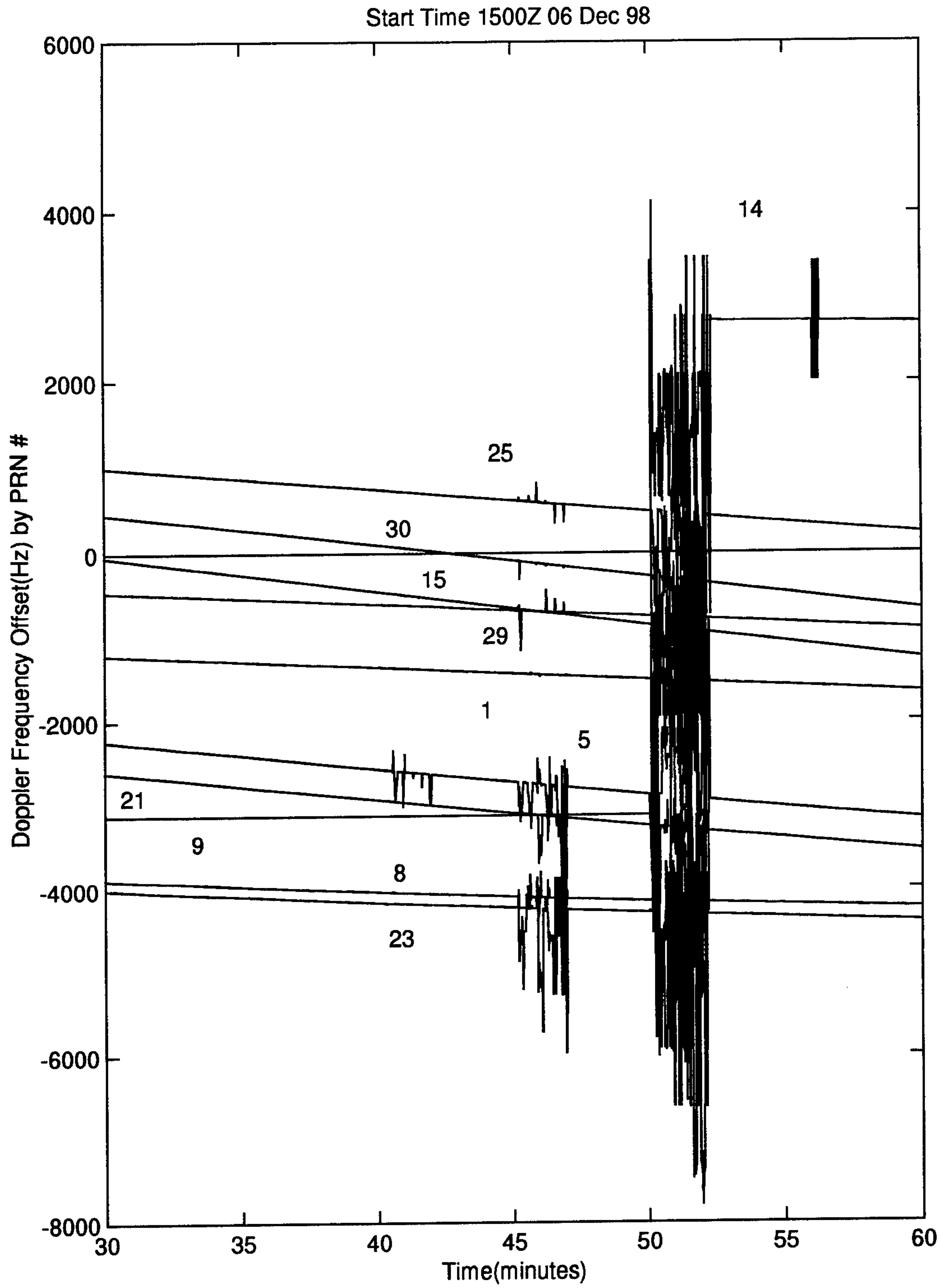

Figure Q.7. Doppler Frequency vs Time

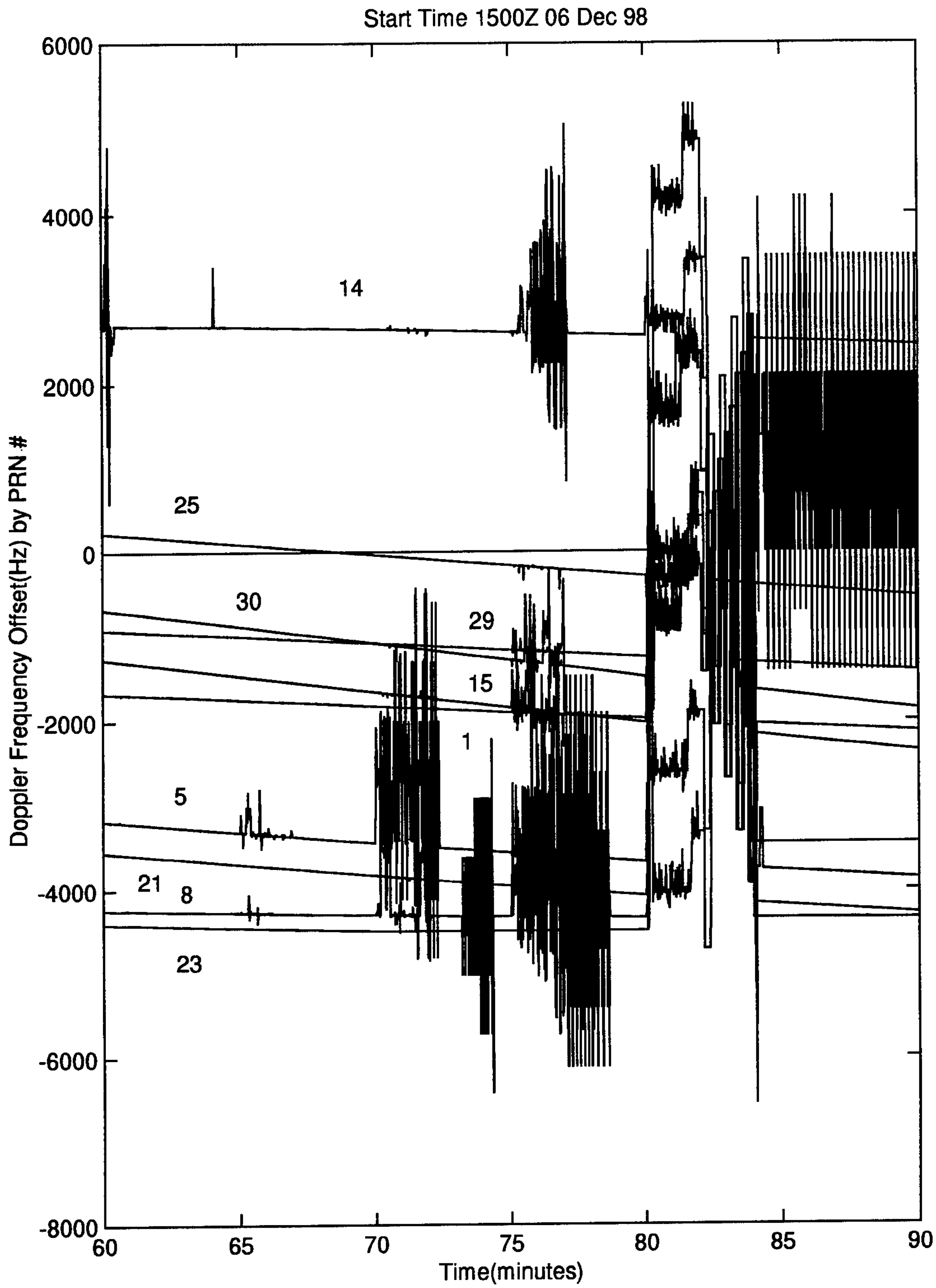

Figure Q.8. Doppler Frequency vs Time

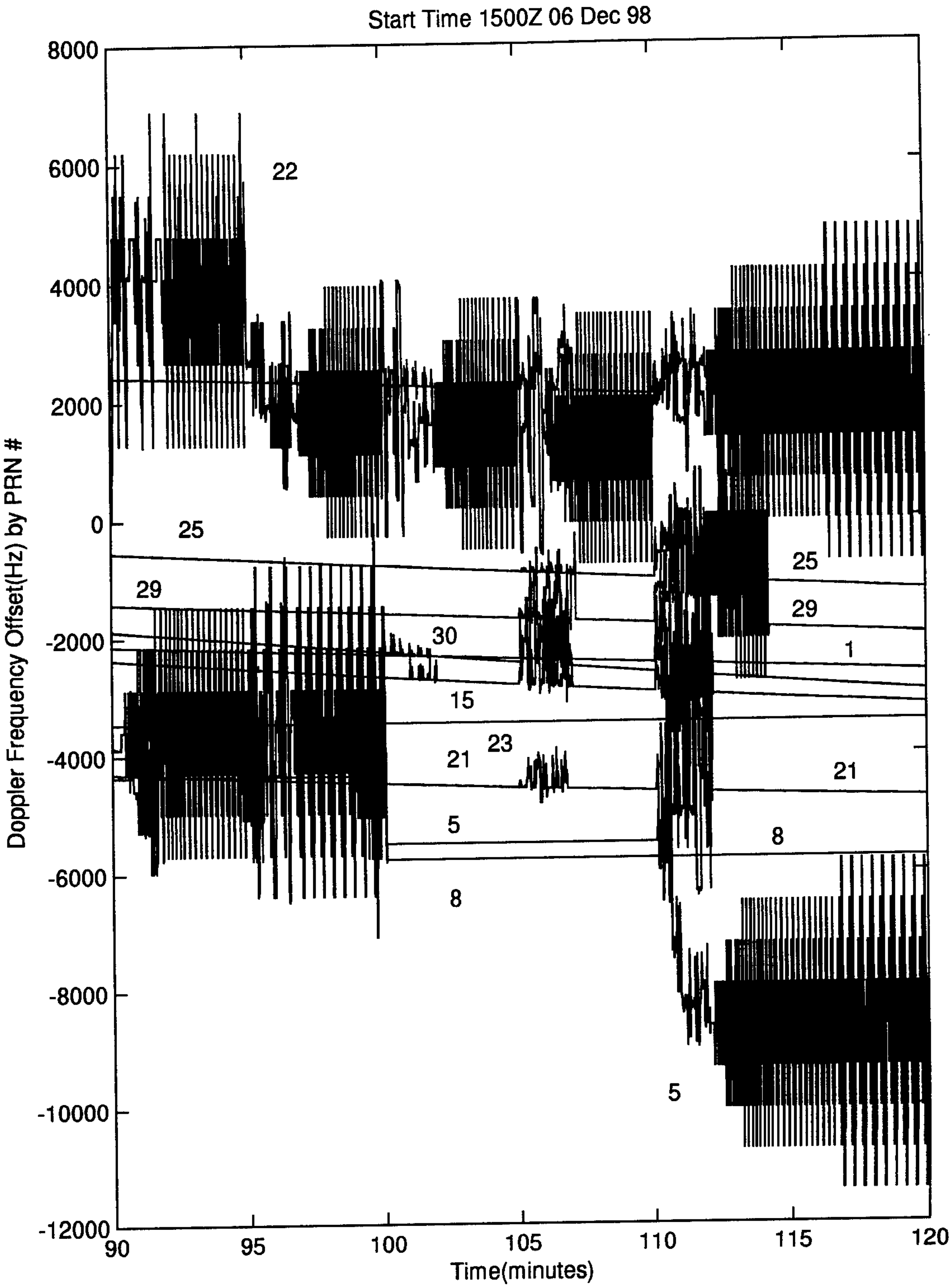

Figure Q.9. Doppler Frequency vs Time

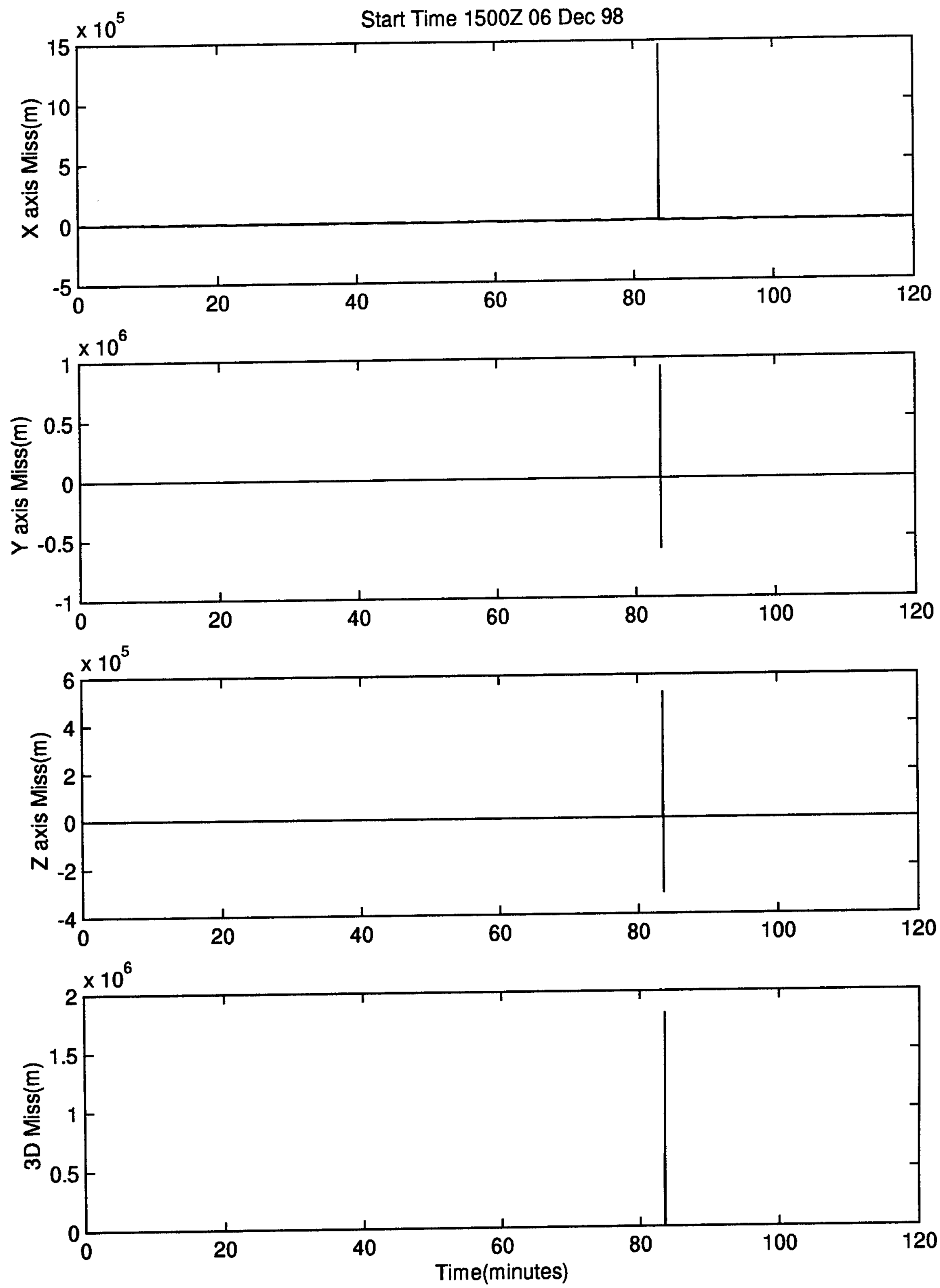

Figure Q.10. X,Y,Z and 3D Error(m) vs Time

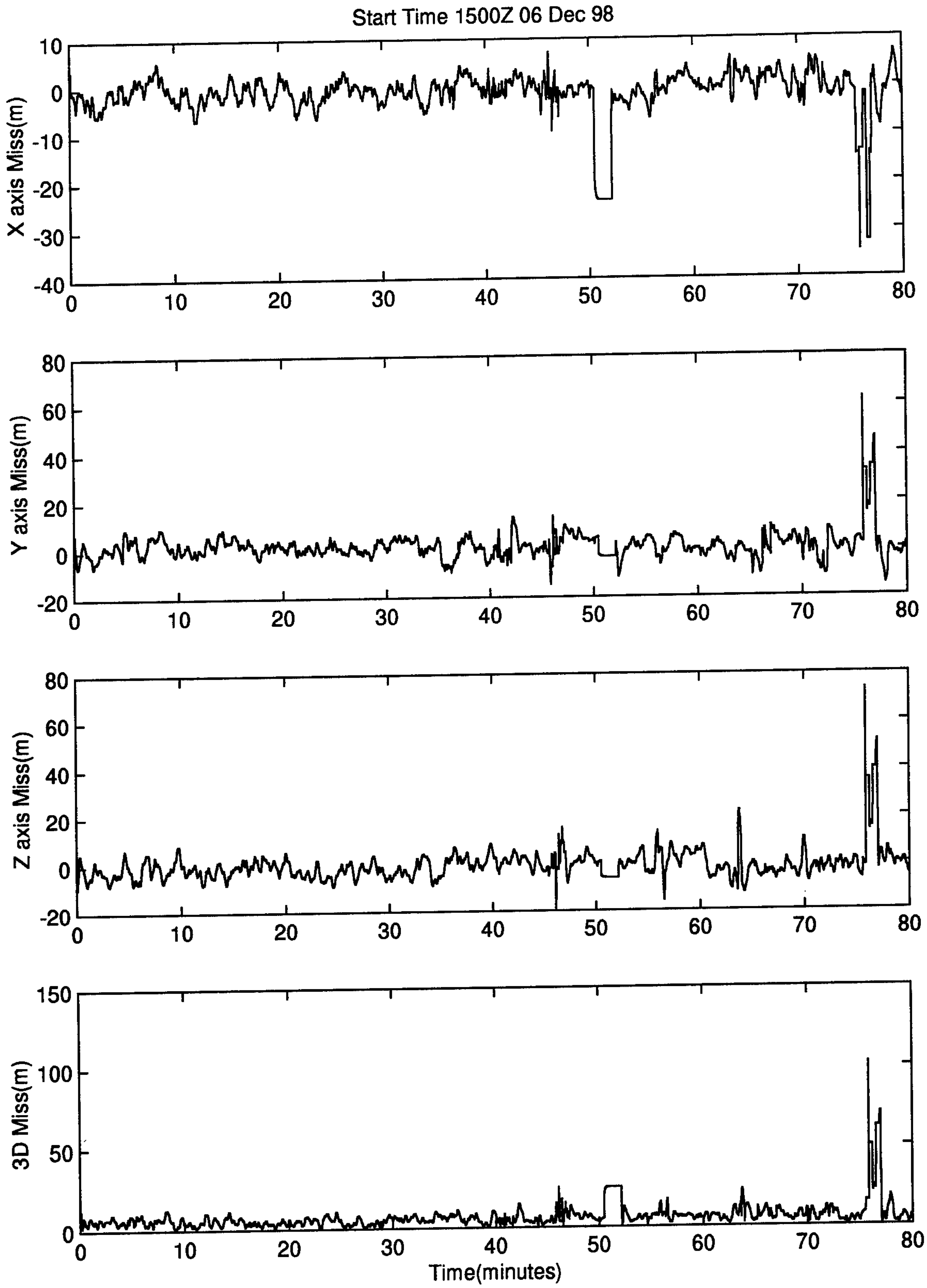

Figure Q.11. X,Y,Z and 3D Error(m) vs Time

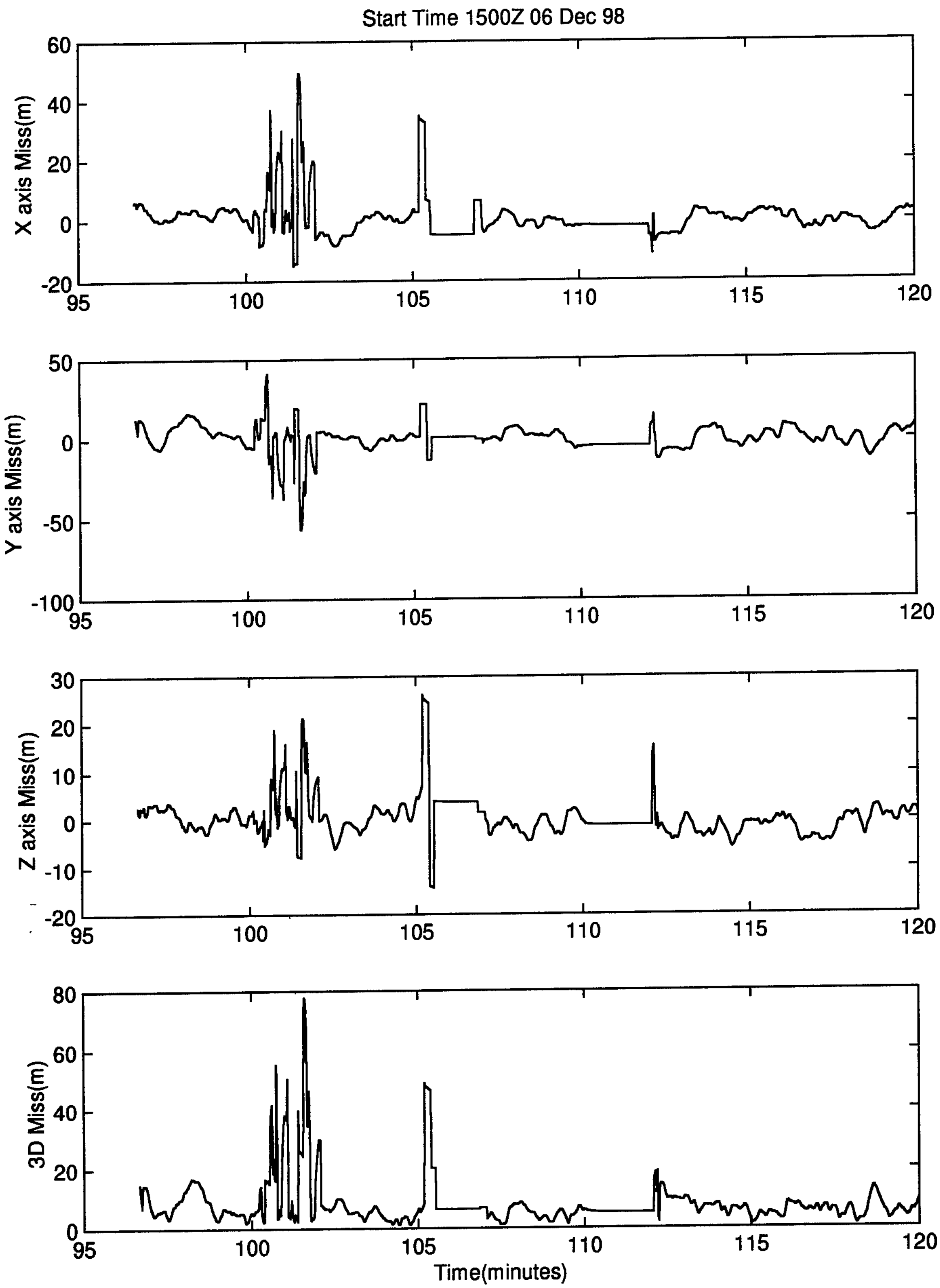

Figure Q.12. X,Y,Z and 3D Error(m) vs Time

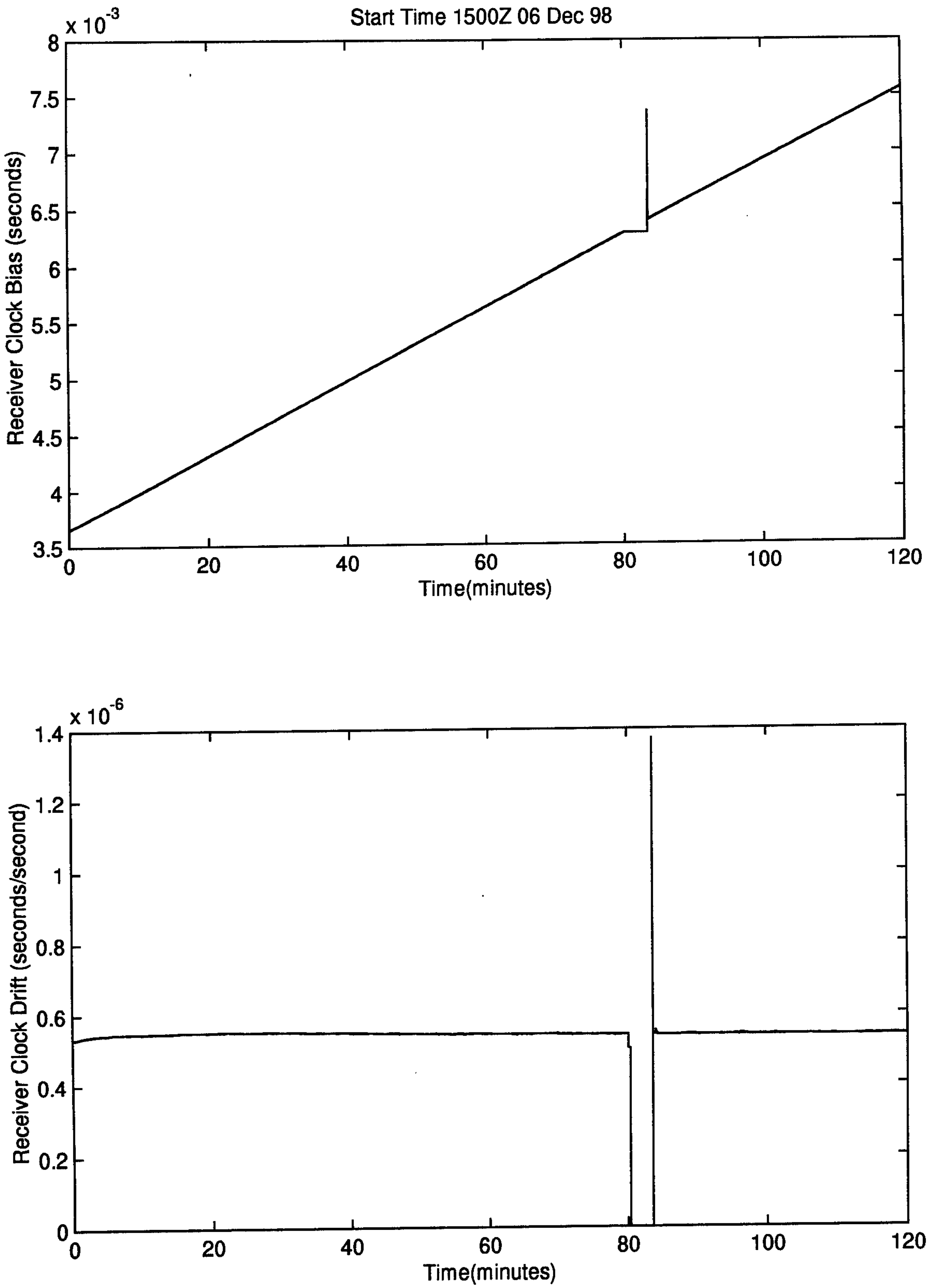

Figure Q.13. Receiver Clock Bias and Drift vs Time

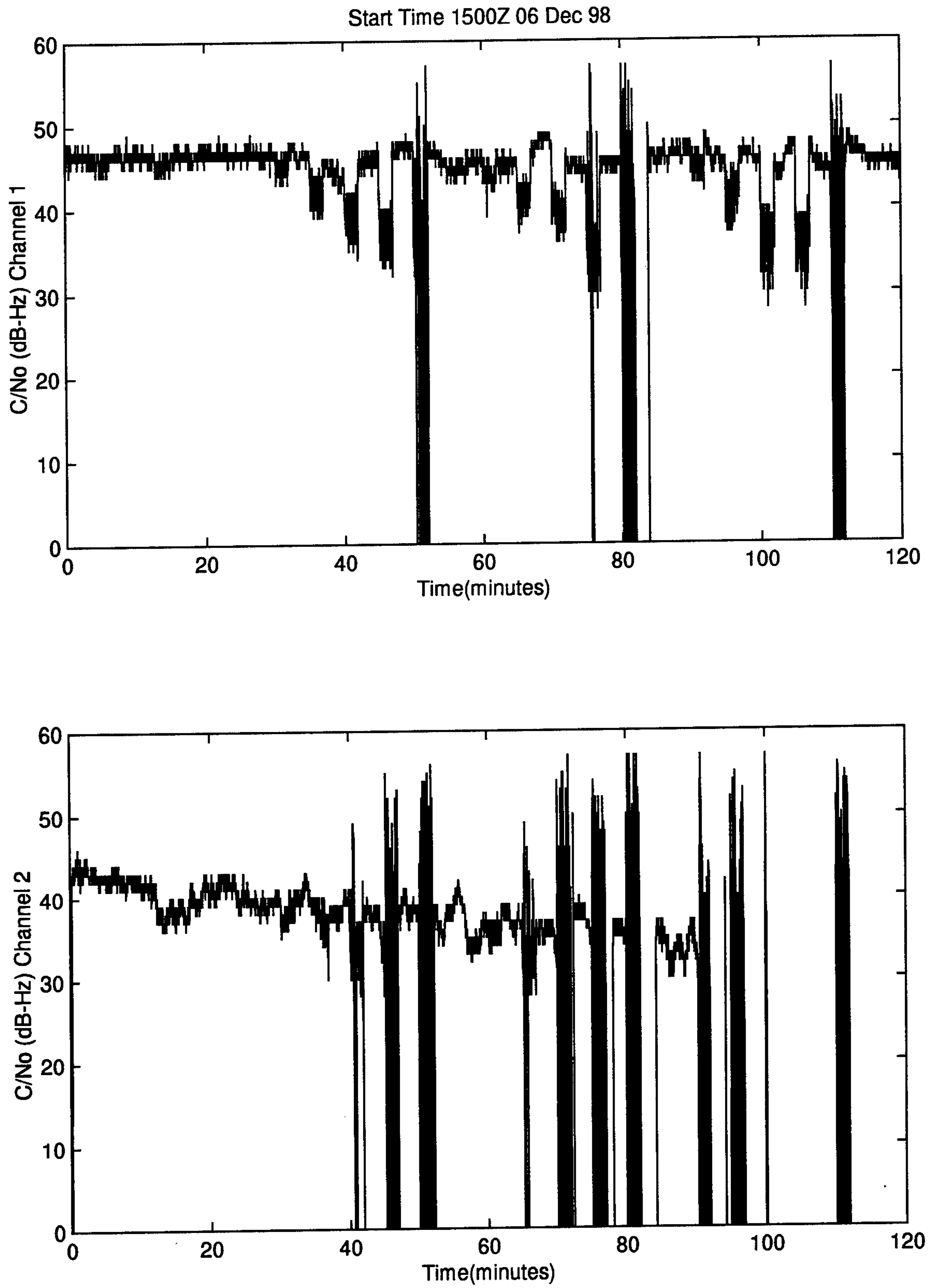

Figure Q.14. C/No vs Time

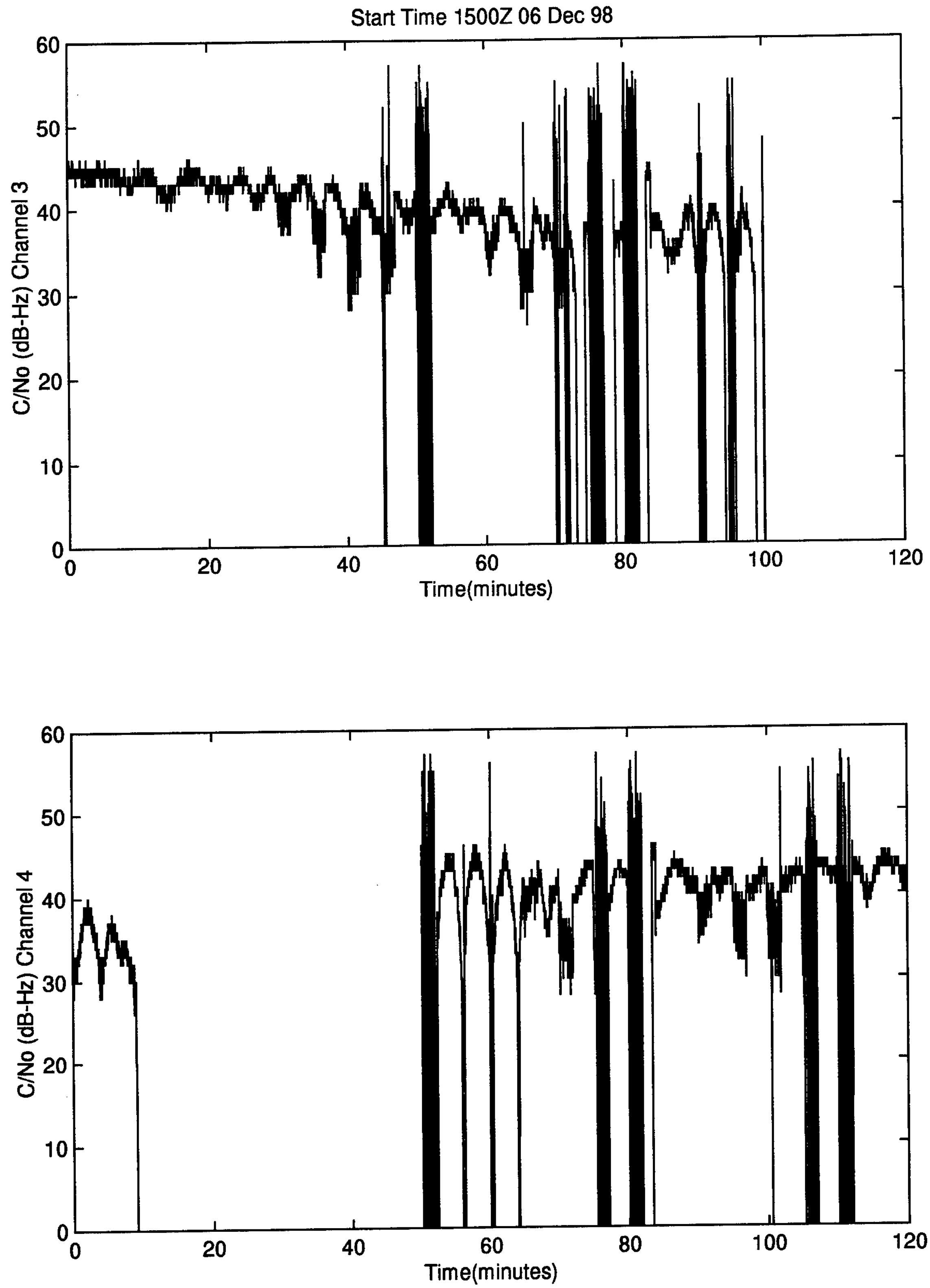

Figure Q.15. C/No vs Time

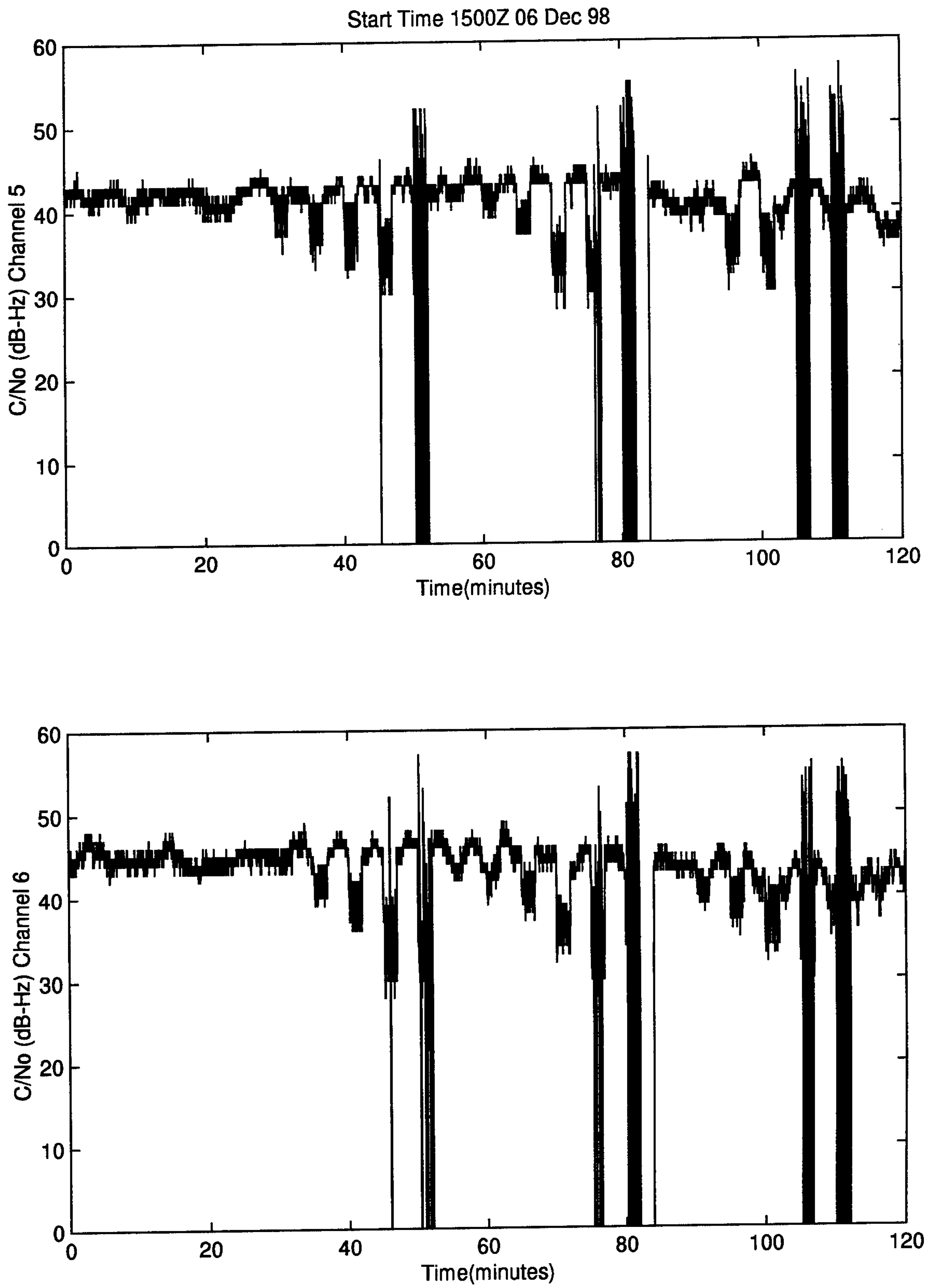

Figure Q.16. C/No vs Time

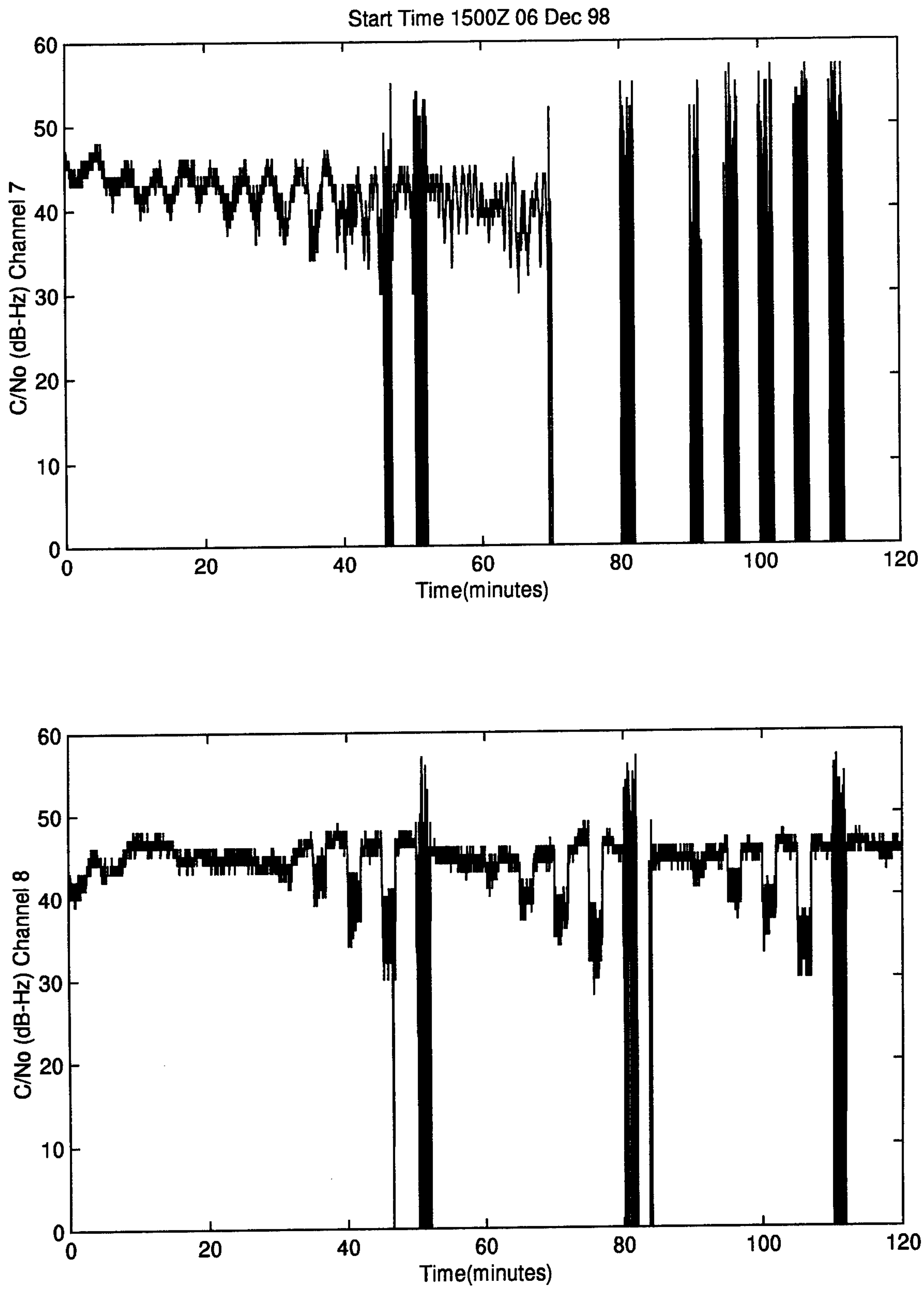

Figure Q.17. C/No vs Time

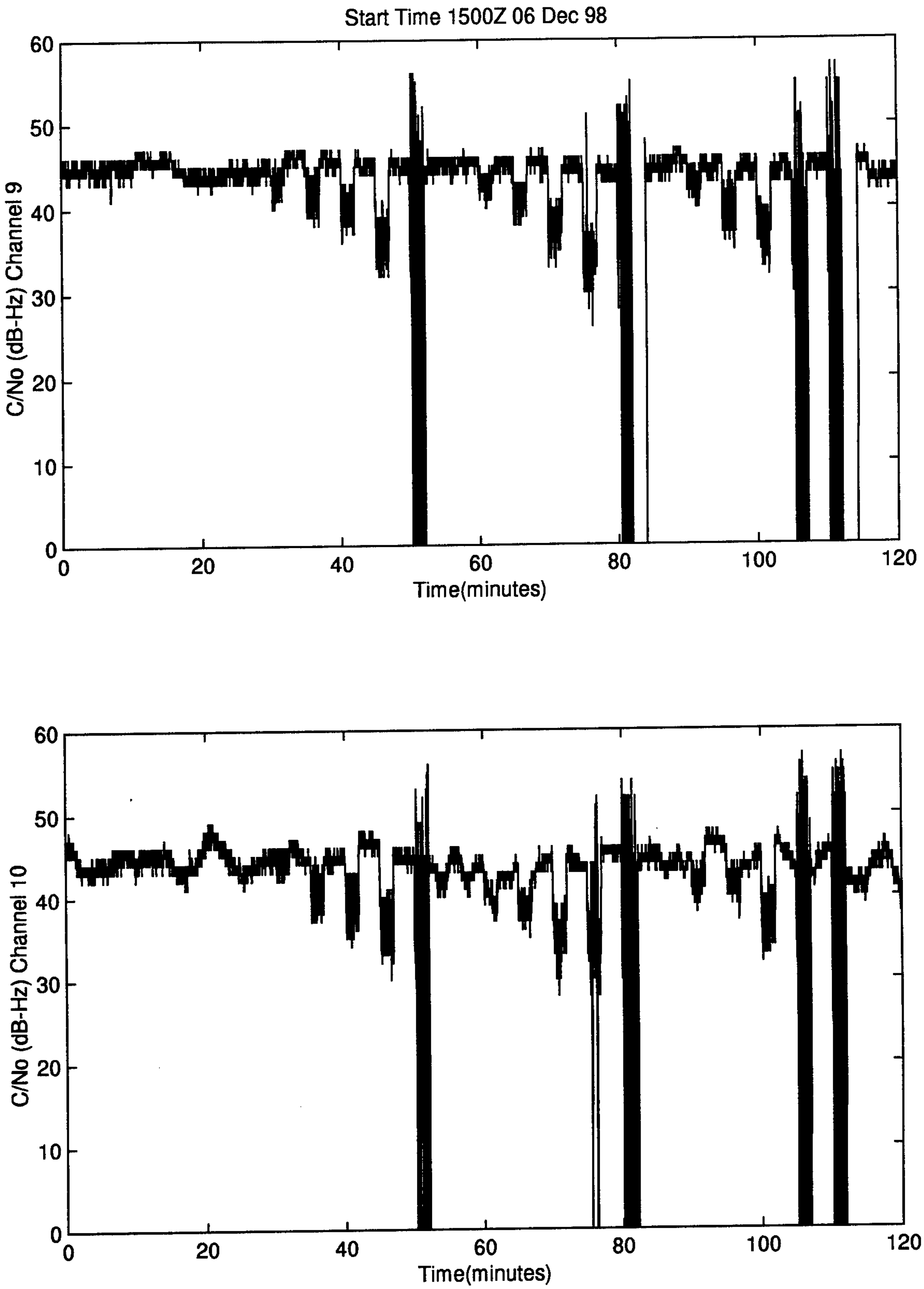

Figure Q.18. C/No vs Time

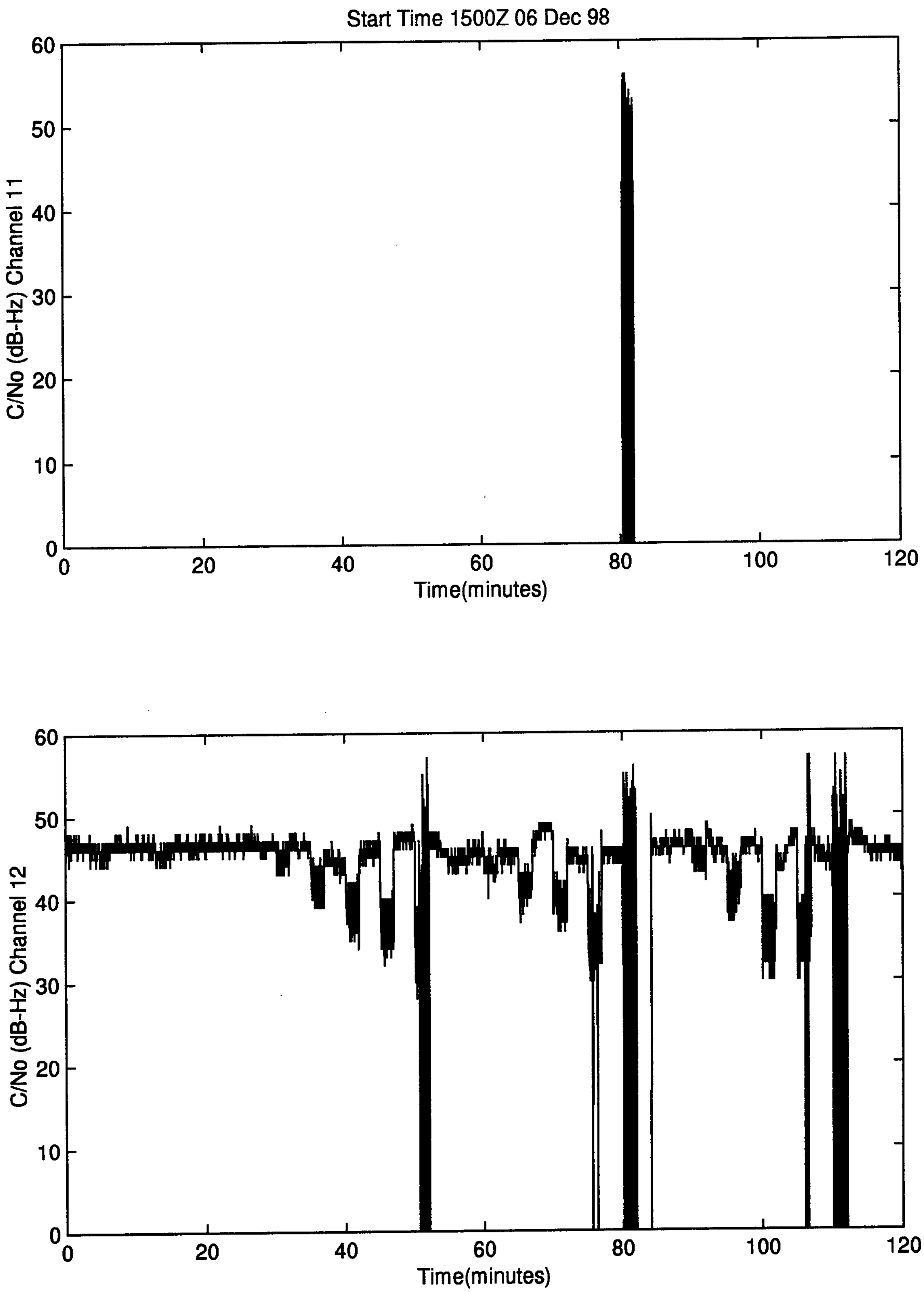

Figure Q.19. C/No vs Time

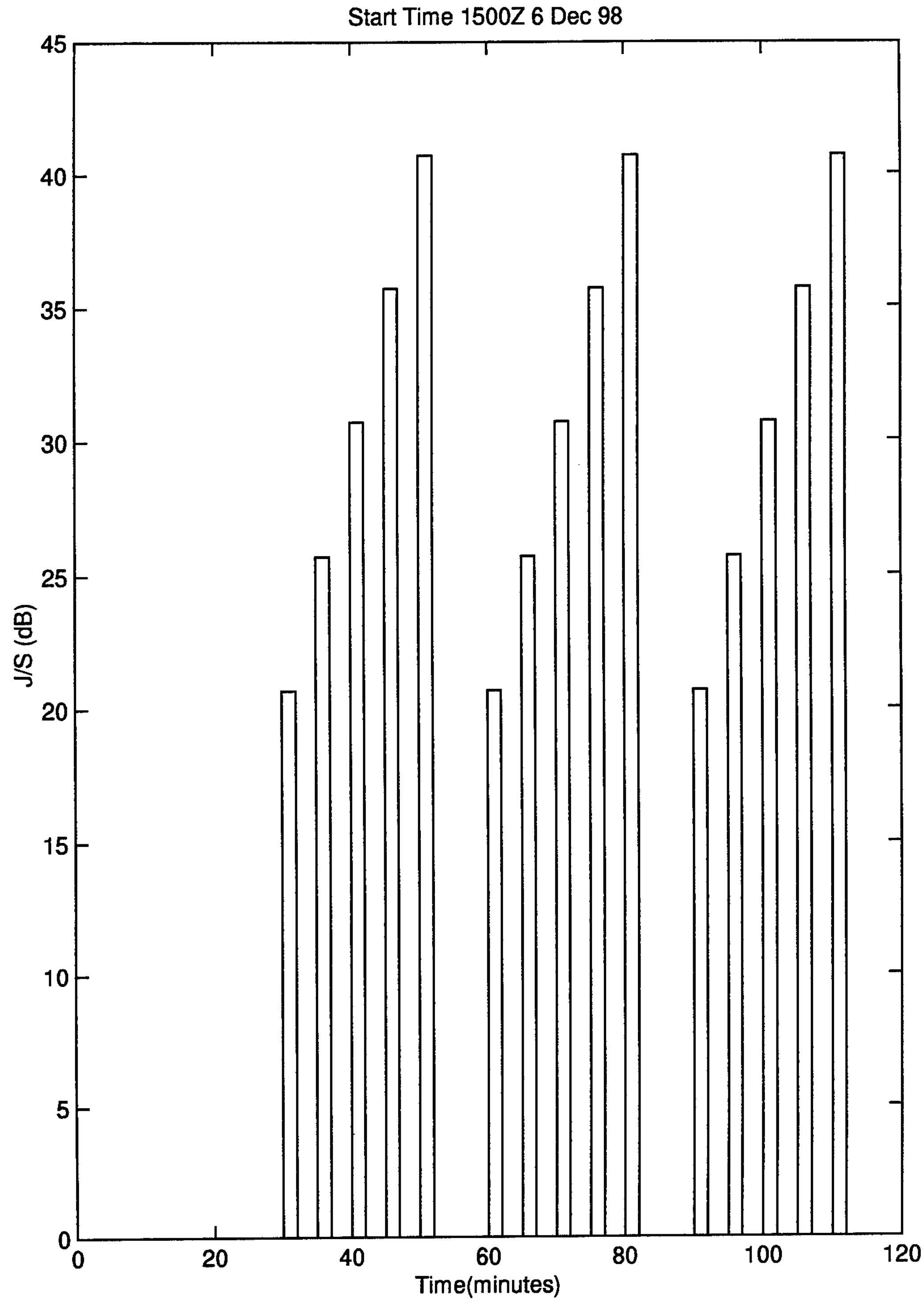

Figure Q.20. Jamming Level J/S vs Time

APPENDIX R

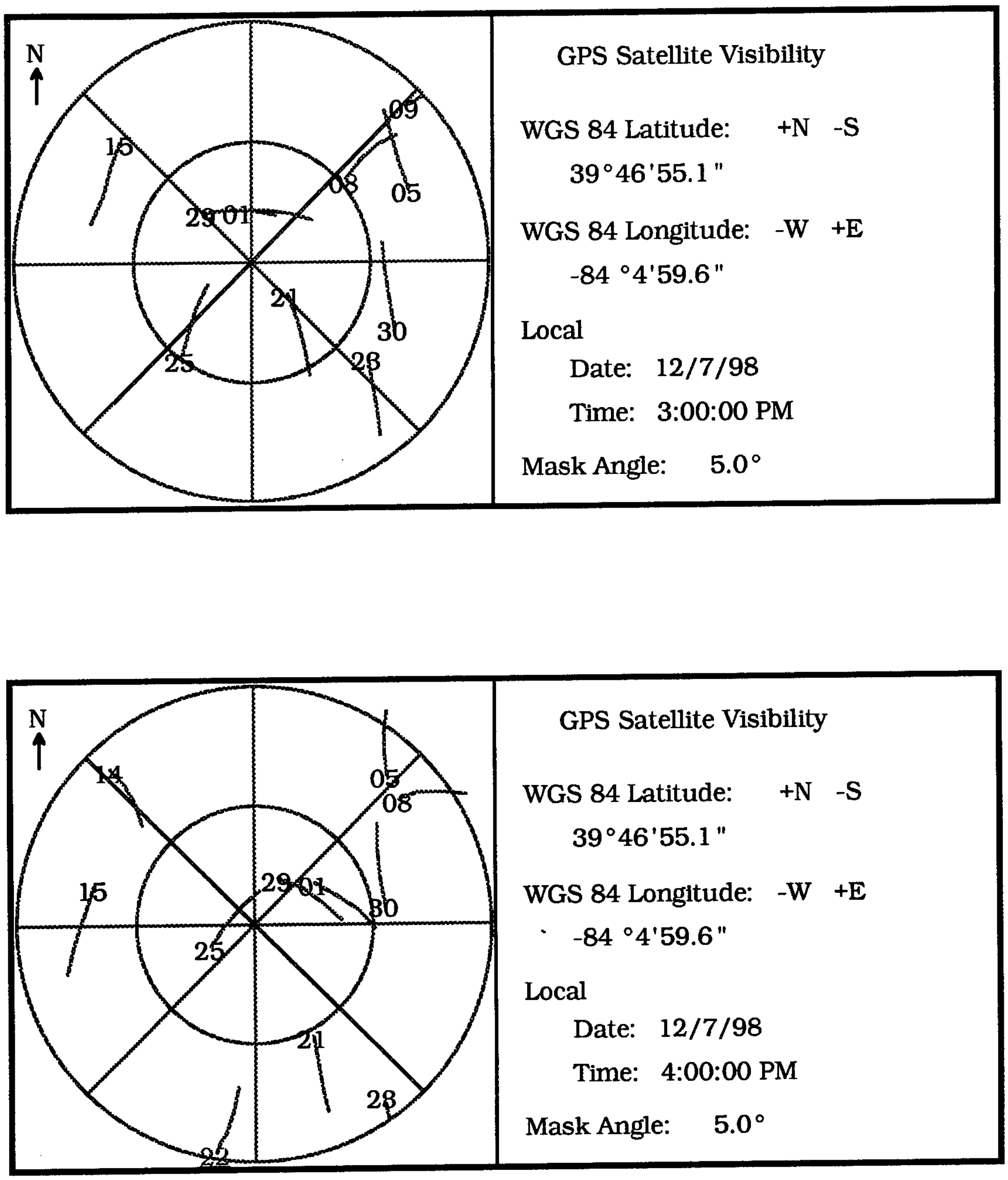

Figure R.1. GPS Satellites In View 7 Dec 98

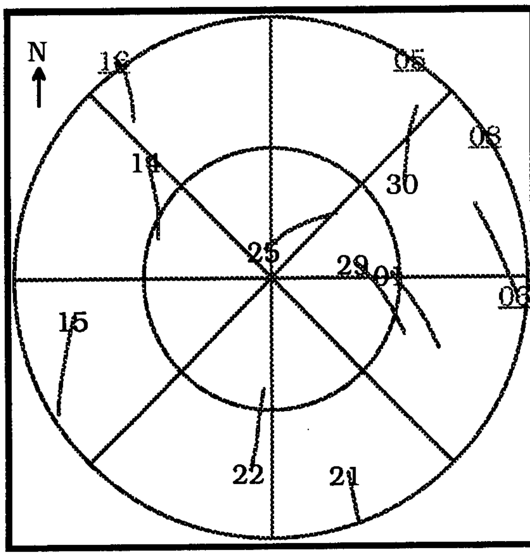

GPS Satellite Visibility

WGS 84 Latitude: +N -S

39°46'55.1"

WGS 84 Longitude: -W +E

-84 °4'59.6"

Local

Date: 12/7/98

Time: 4:50:00 PM

Mask Angle: 5.0°

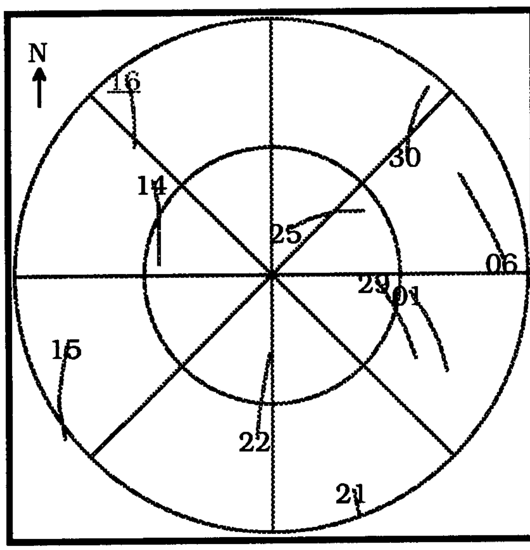

GPS Satellite Visibility

WGS 84 Latitude: +N -S

39°46'55.1"

WGS 84 Longitude: -W +E

-84 °4'59.6"

Local

Date: 12/7/98

Time: 5:10:00 PM

Mask Angle: 5.0°

Figure R.2. GPS Satellites In View 7 Dec 98

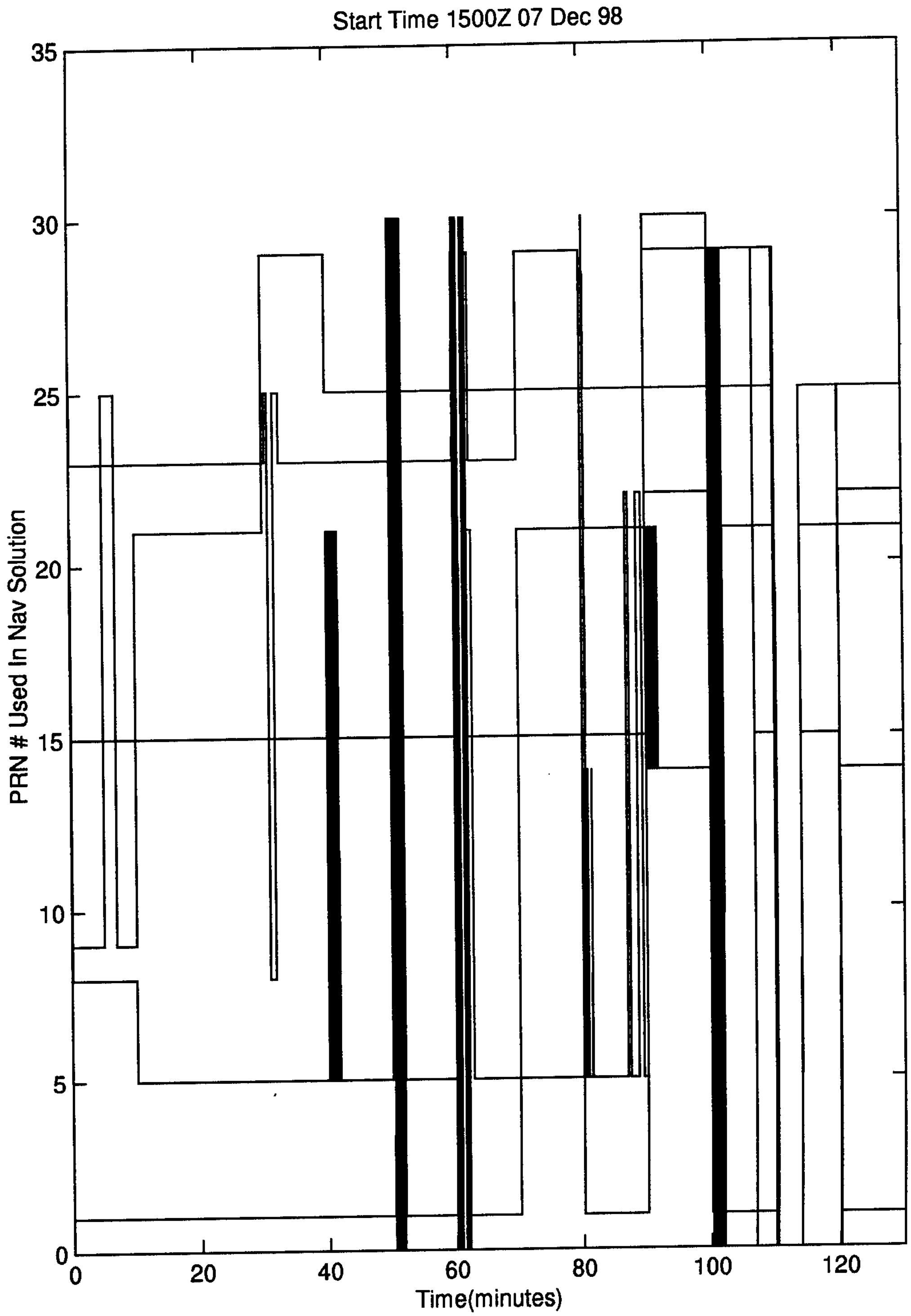

Figure R.3. PRN # Used In Nav Solution vs Time

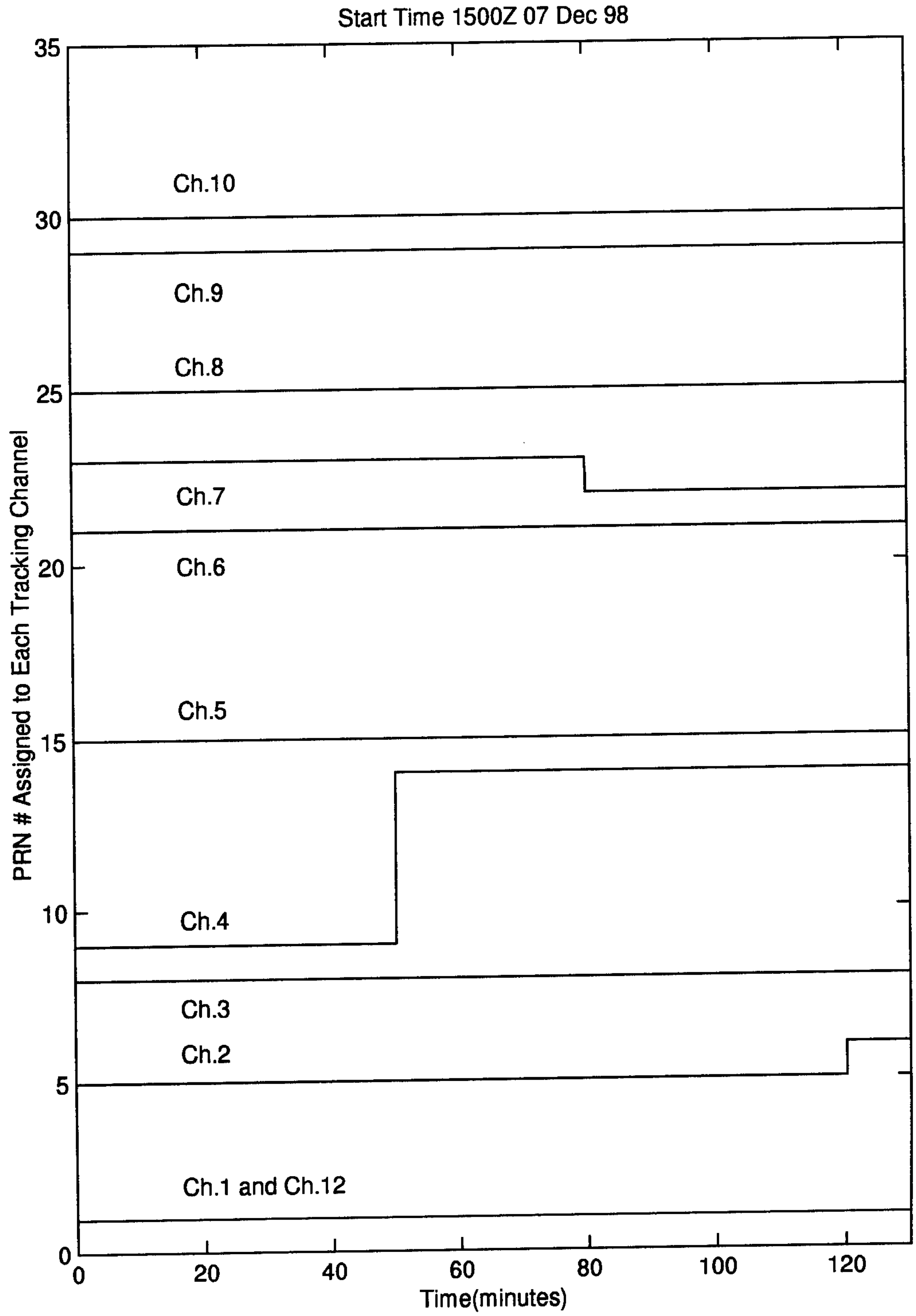

Figure R.4. PRN # Assigned to Each Tracking Channel vs Time

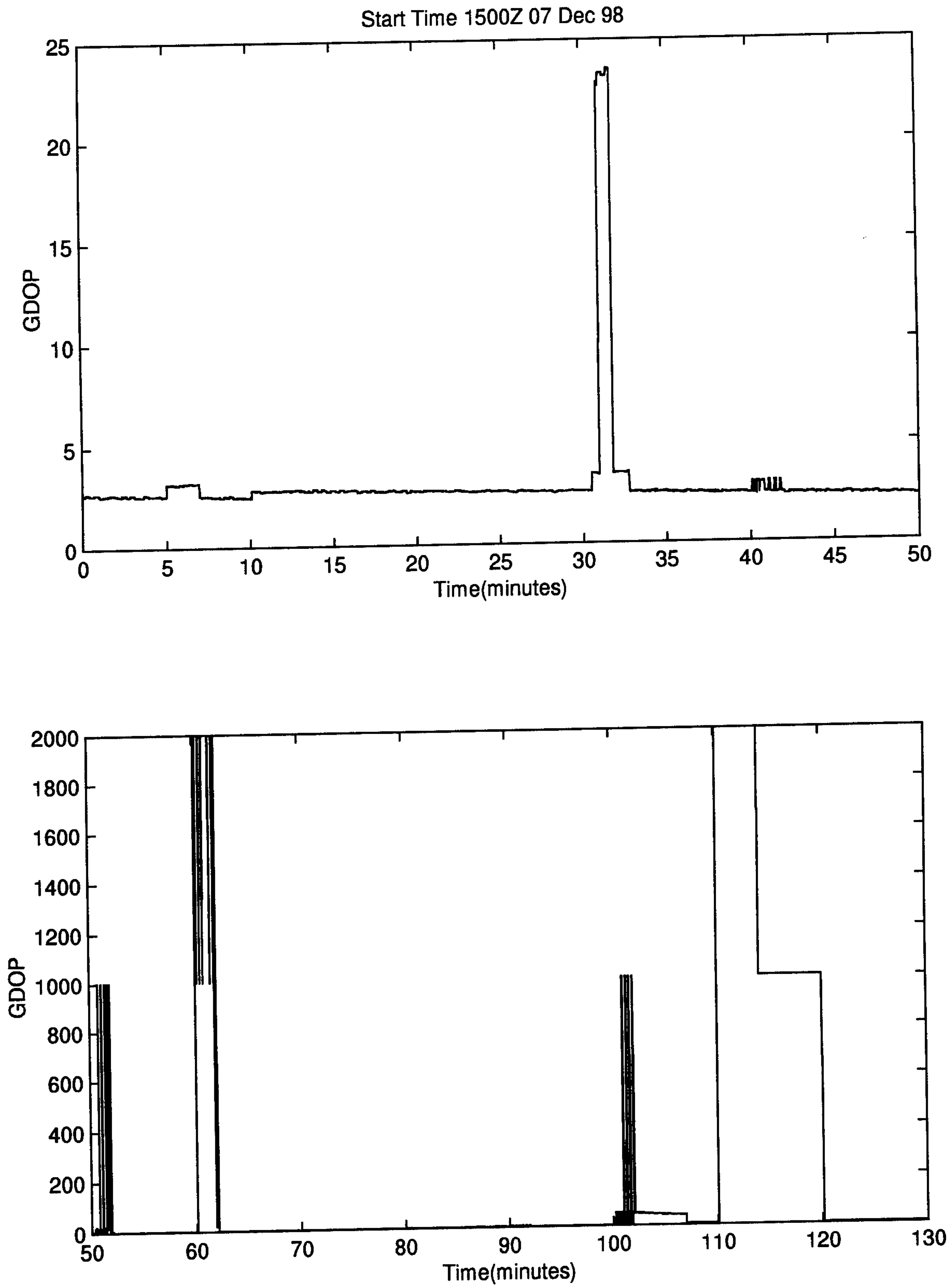

Figure R.5. GDOP vs Time

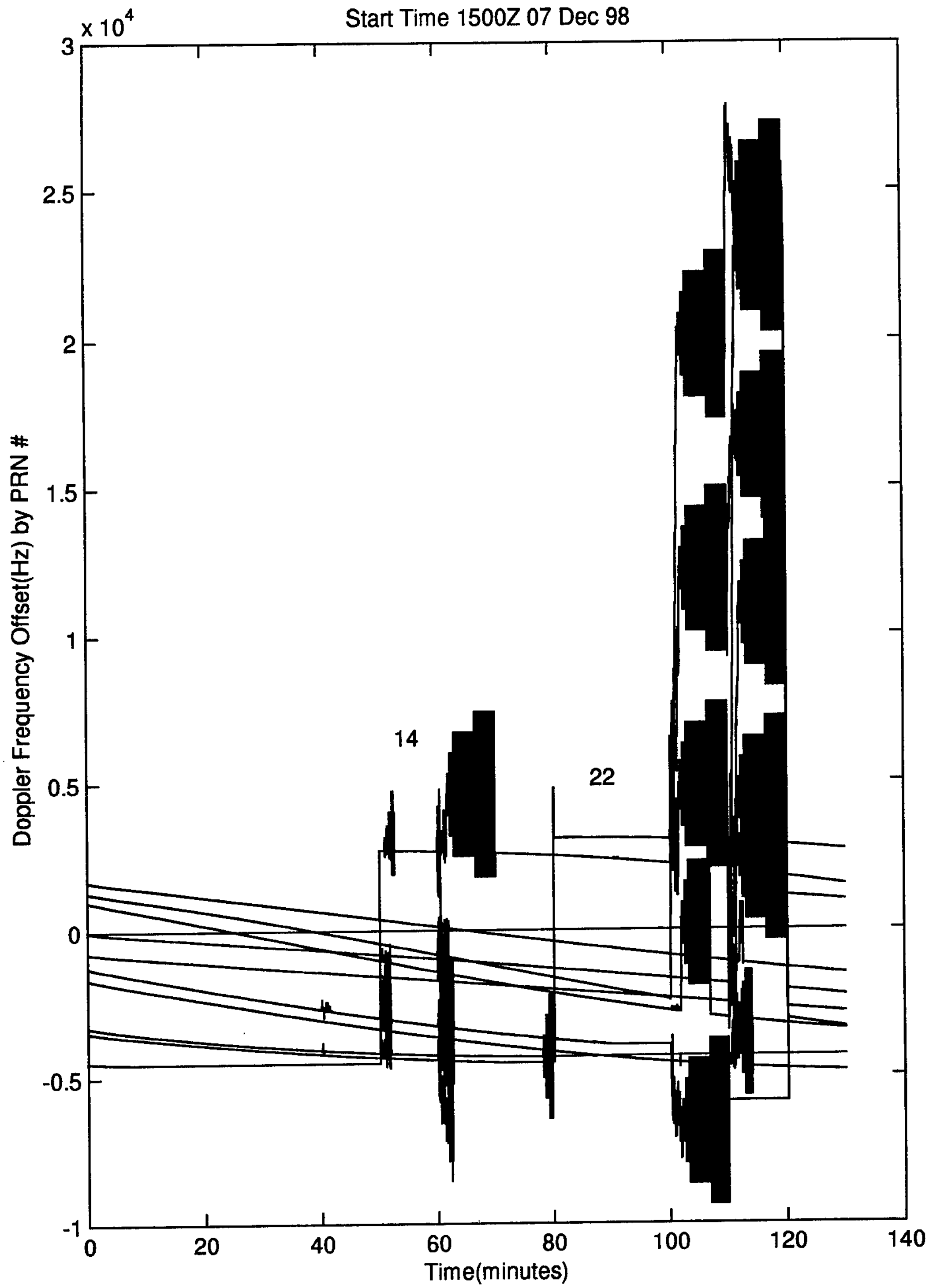

Figure R.6. Doppler Frequency vs Time

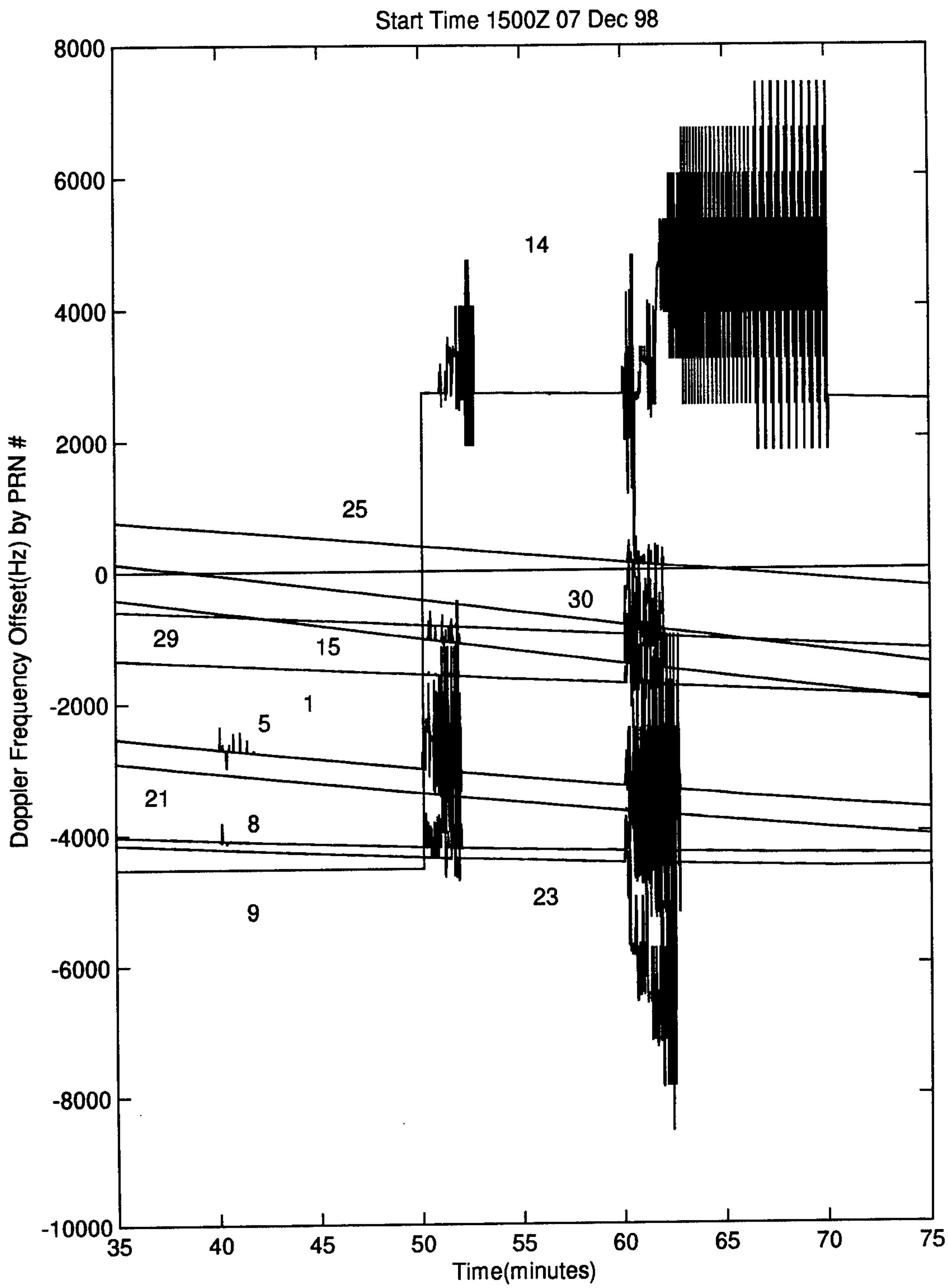

Figure R.7. Doppler Frequency vs Time

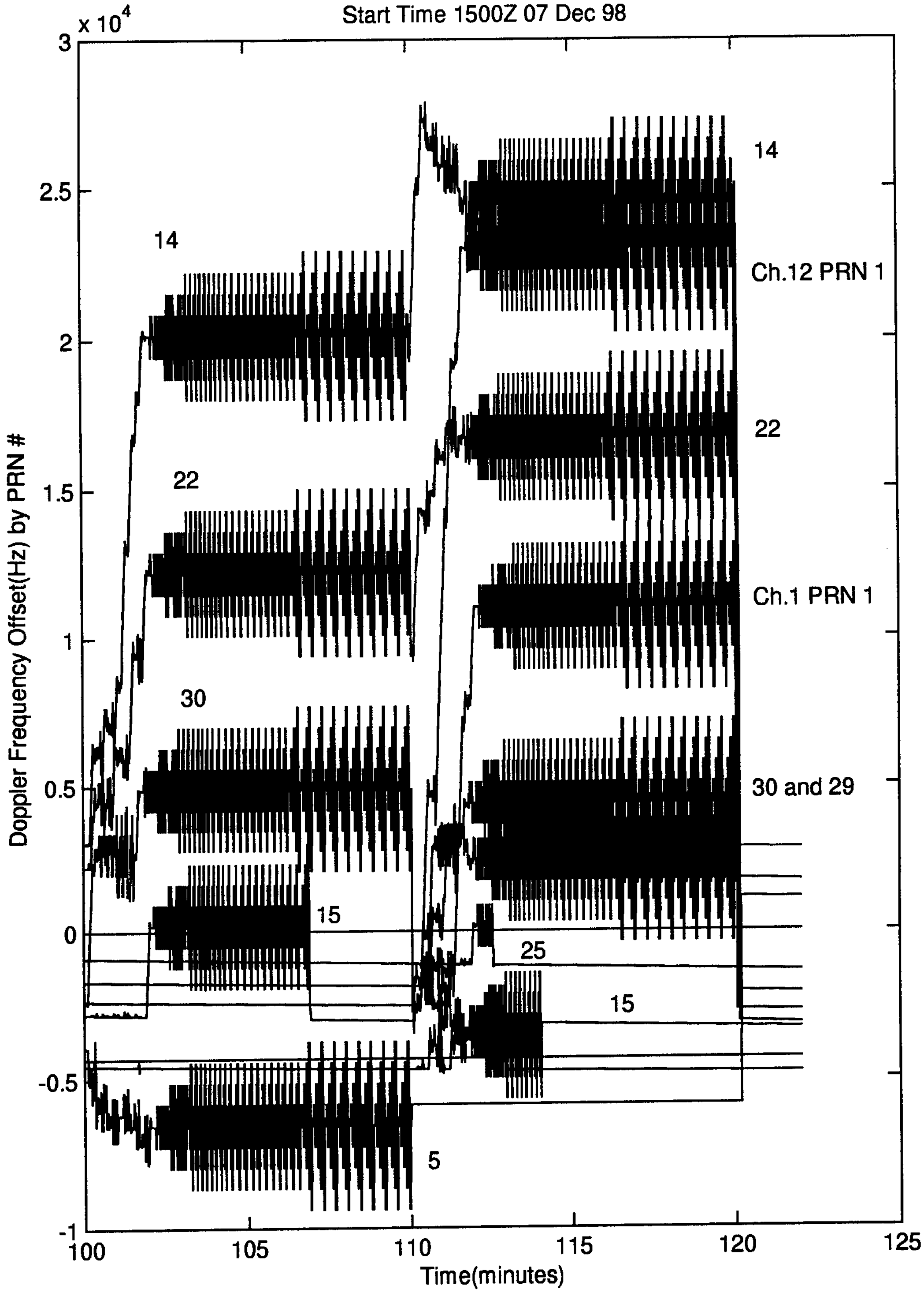

Figure R.8. Doppler Frequency vs Time

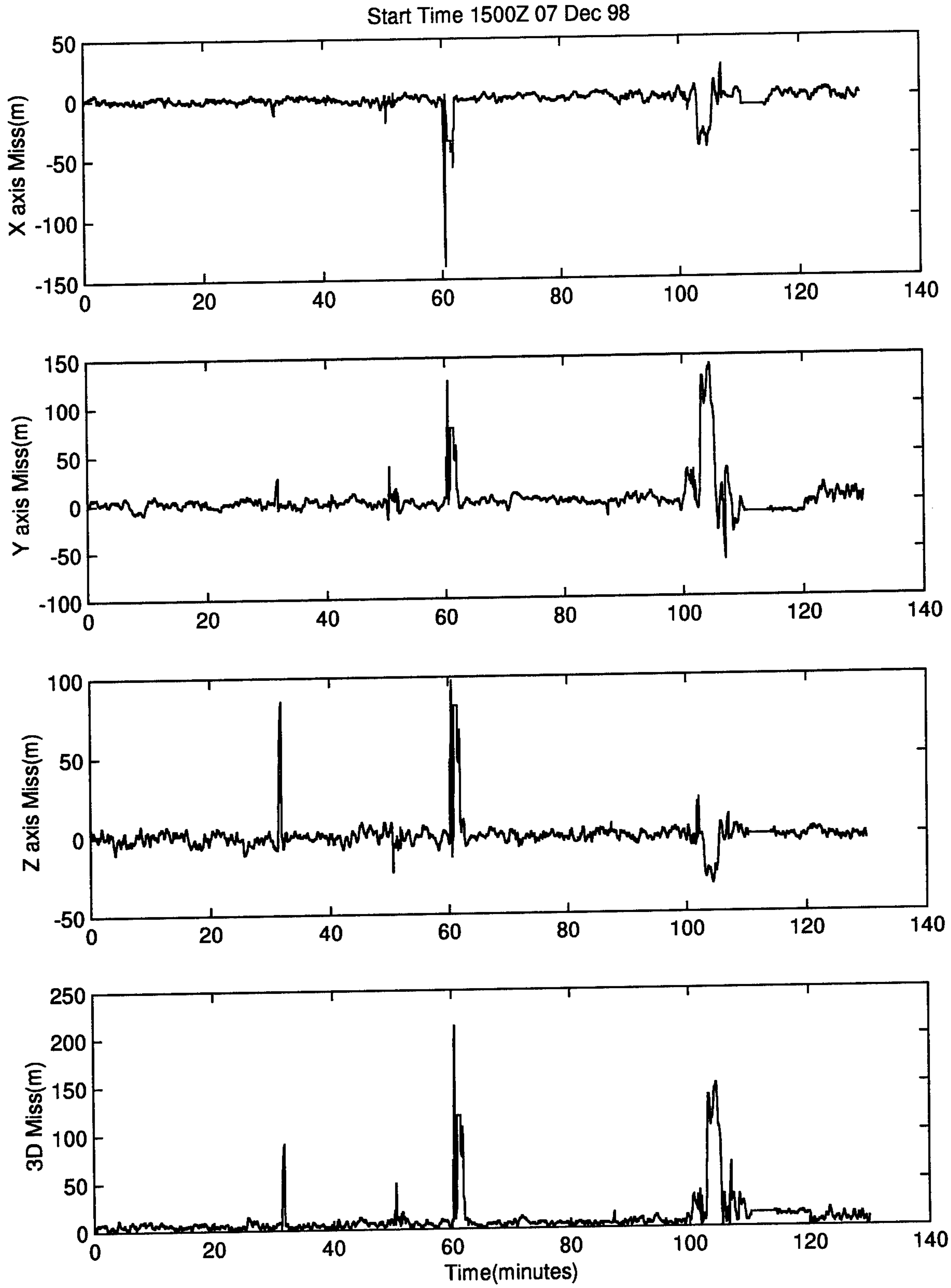

Figure R.9. X,Y,Z and 3D Error(m) vs Time

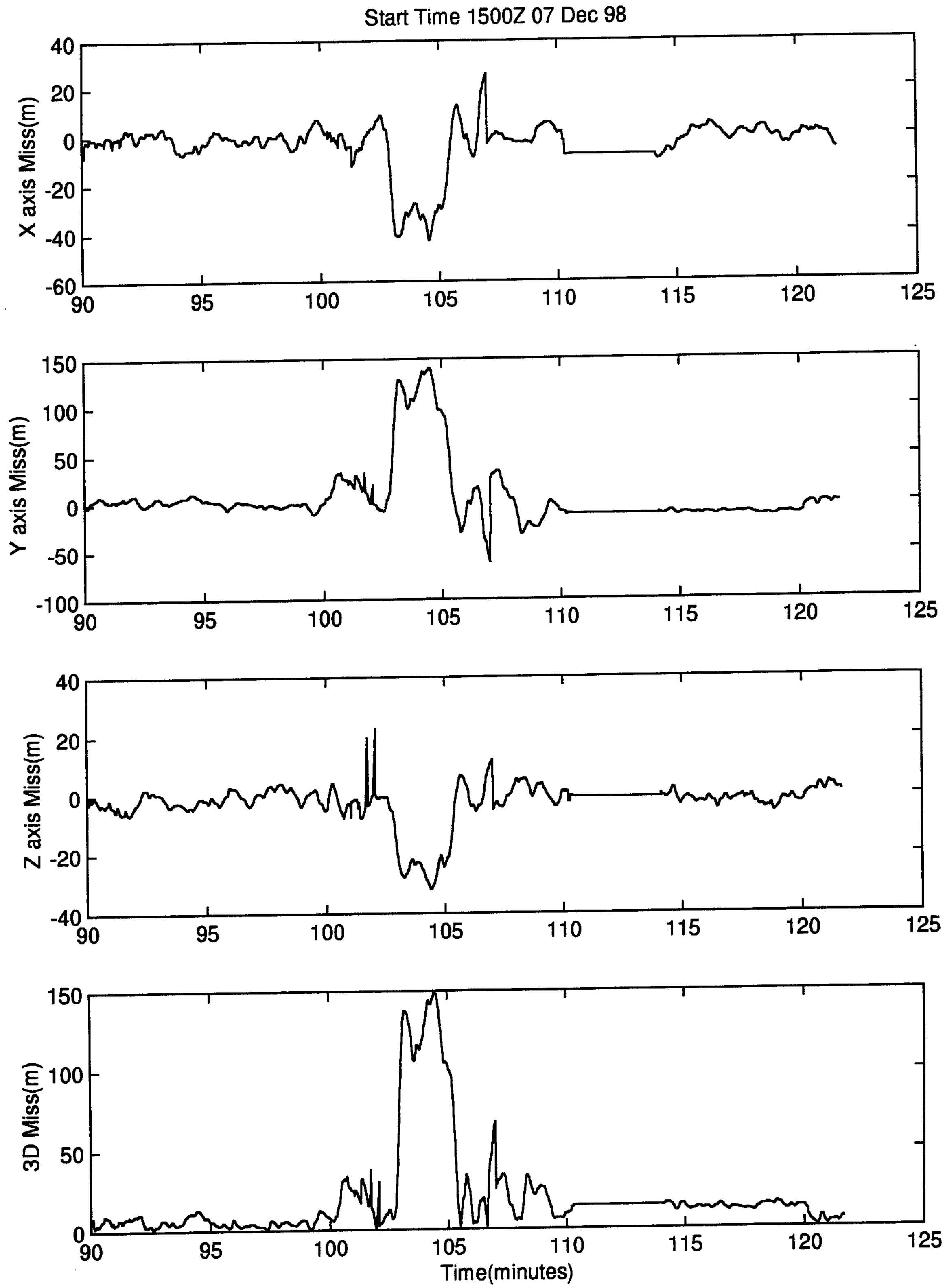

Figure R.10. X,Y,Z and 3D Error(m) vs Time

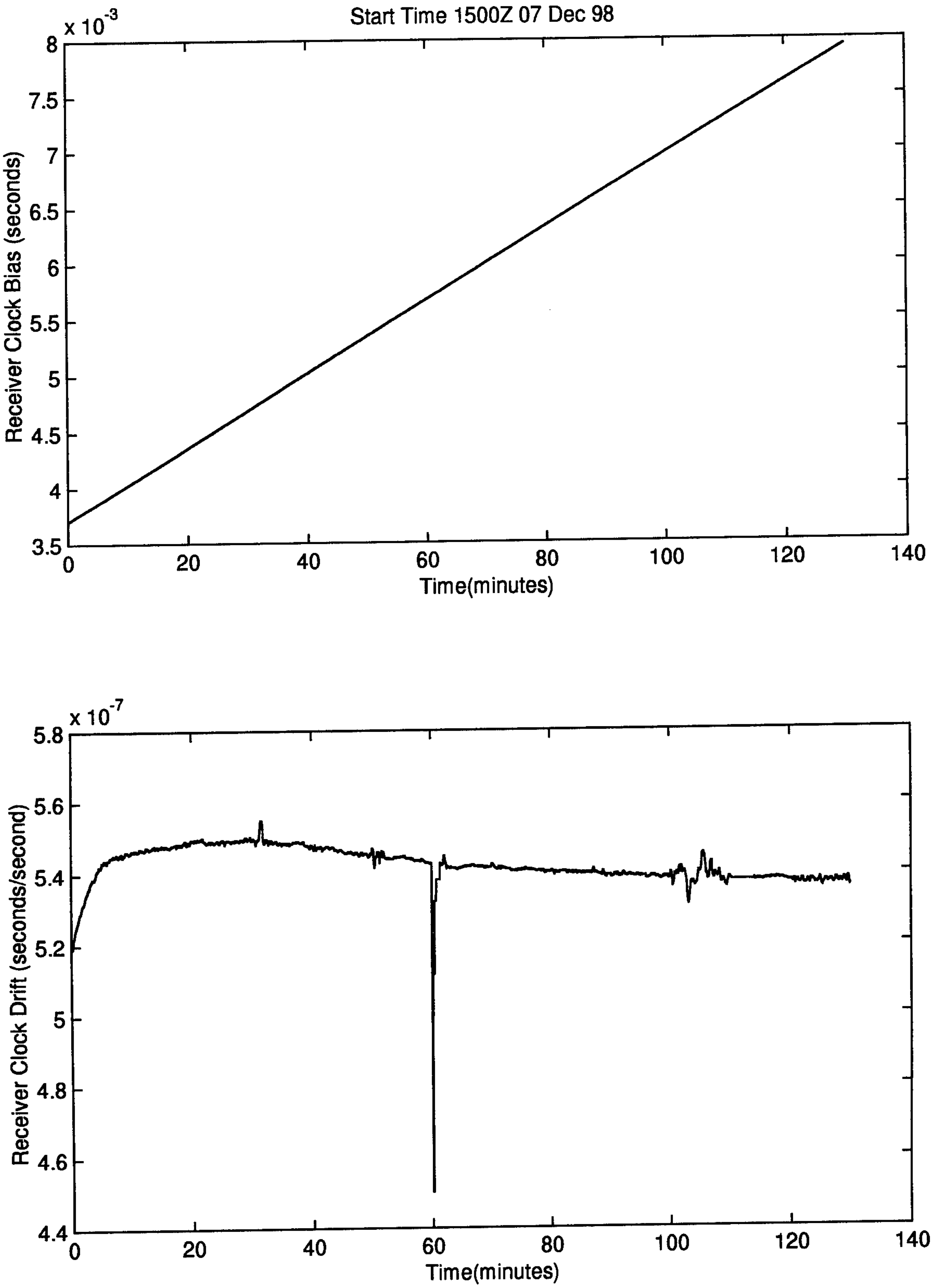

Figure R.11. Receiver Clock Bias and Drift vs Time

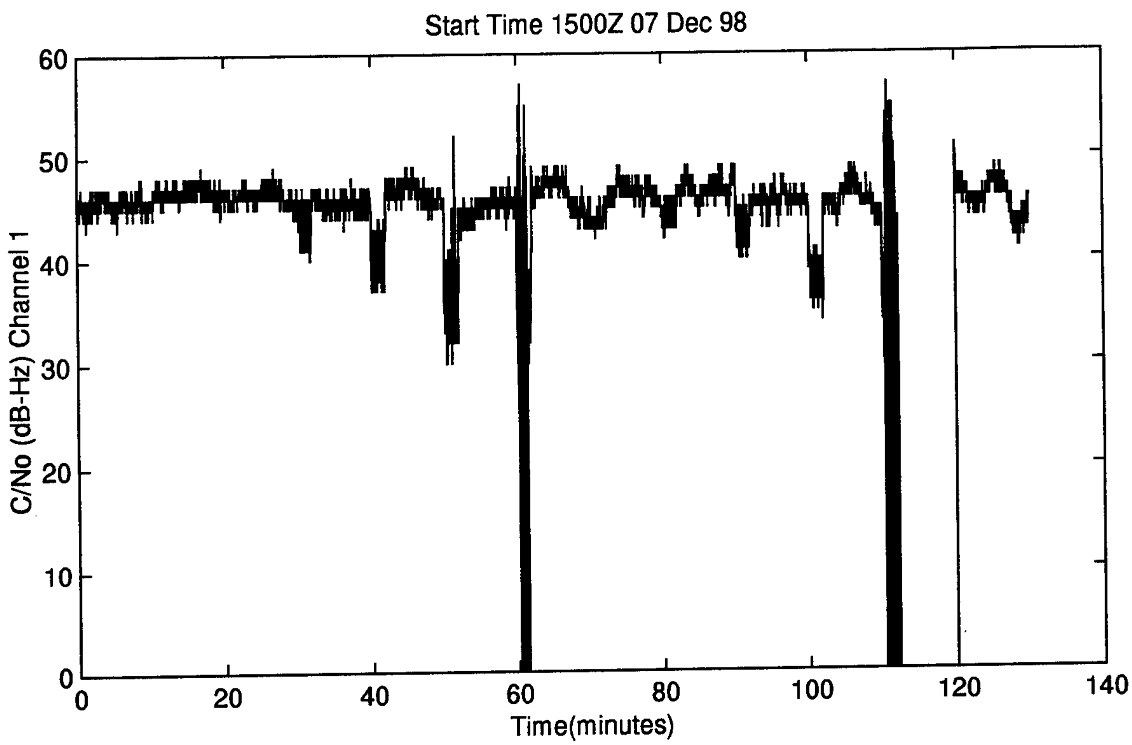

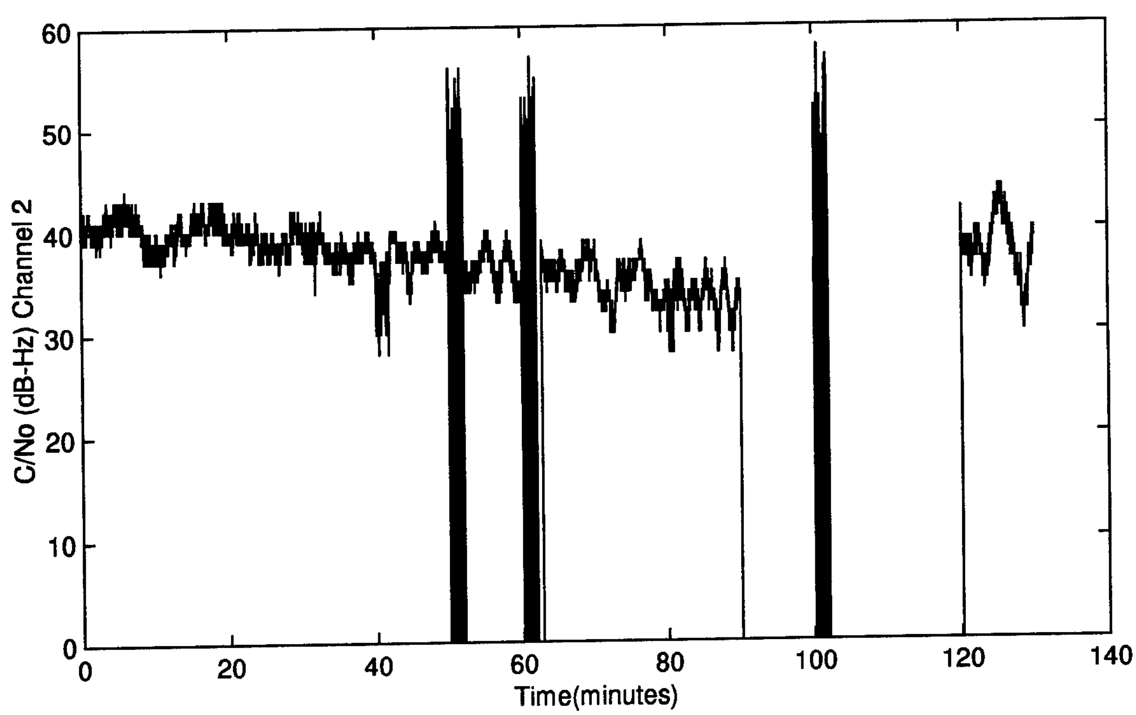

Figure R.12. C/No vs Time

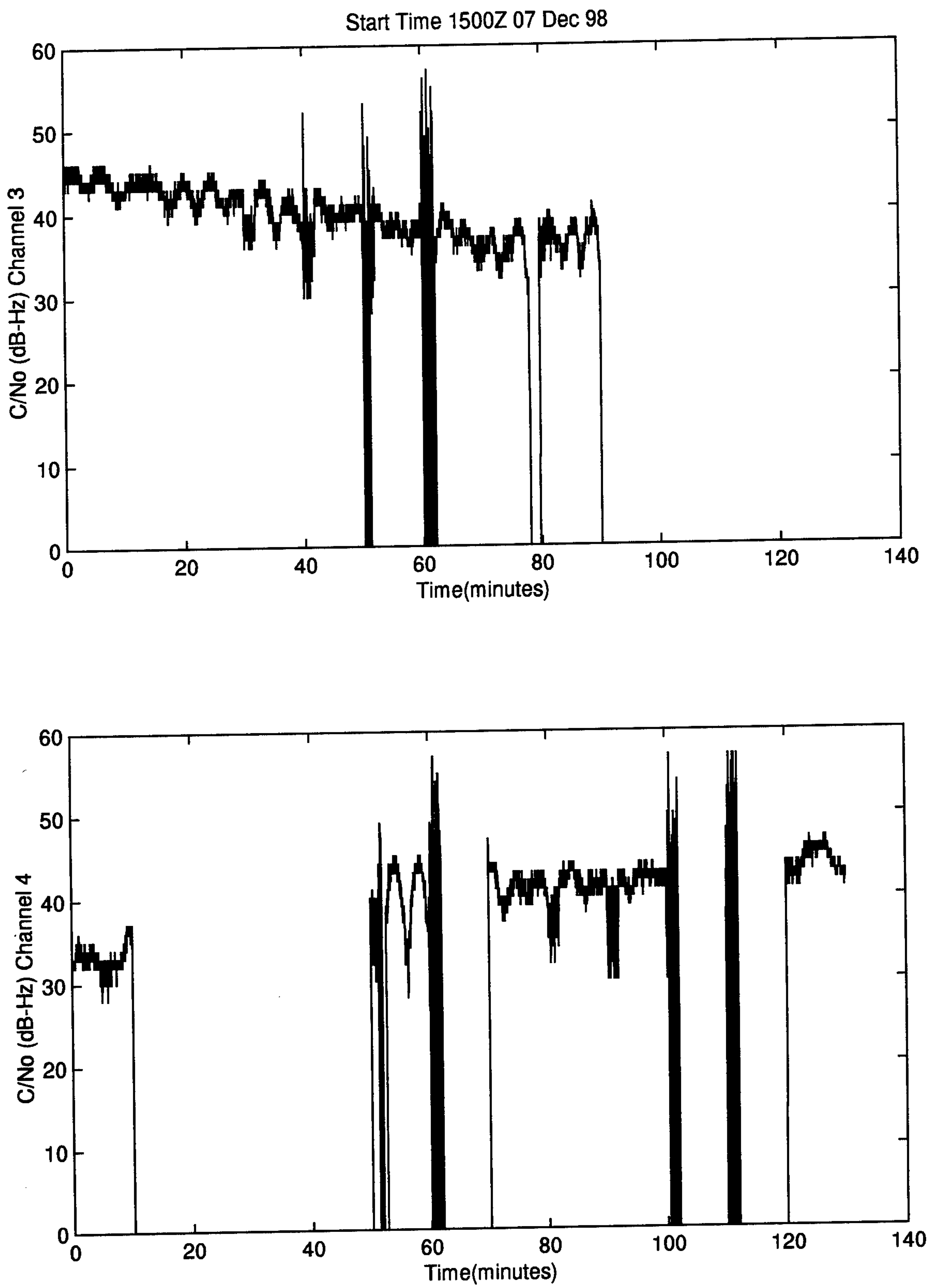

Figure R.13. C/No vs Time

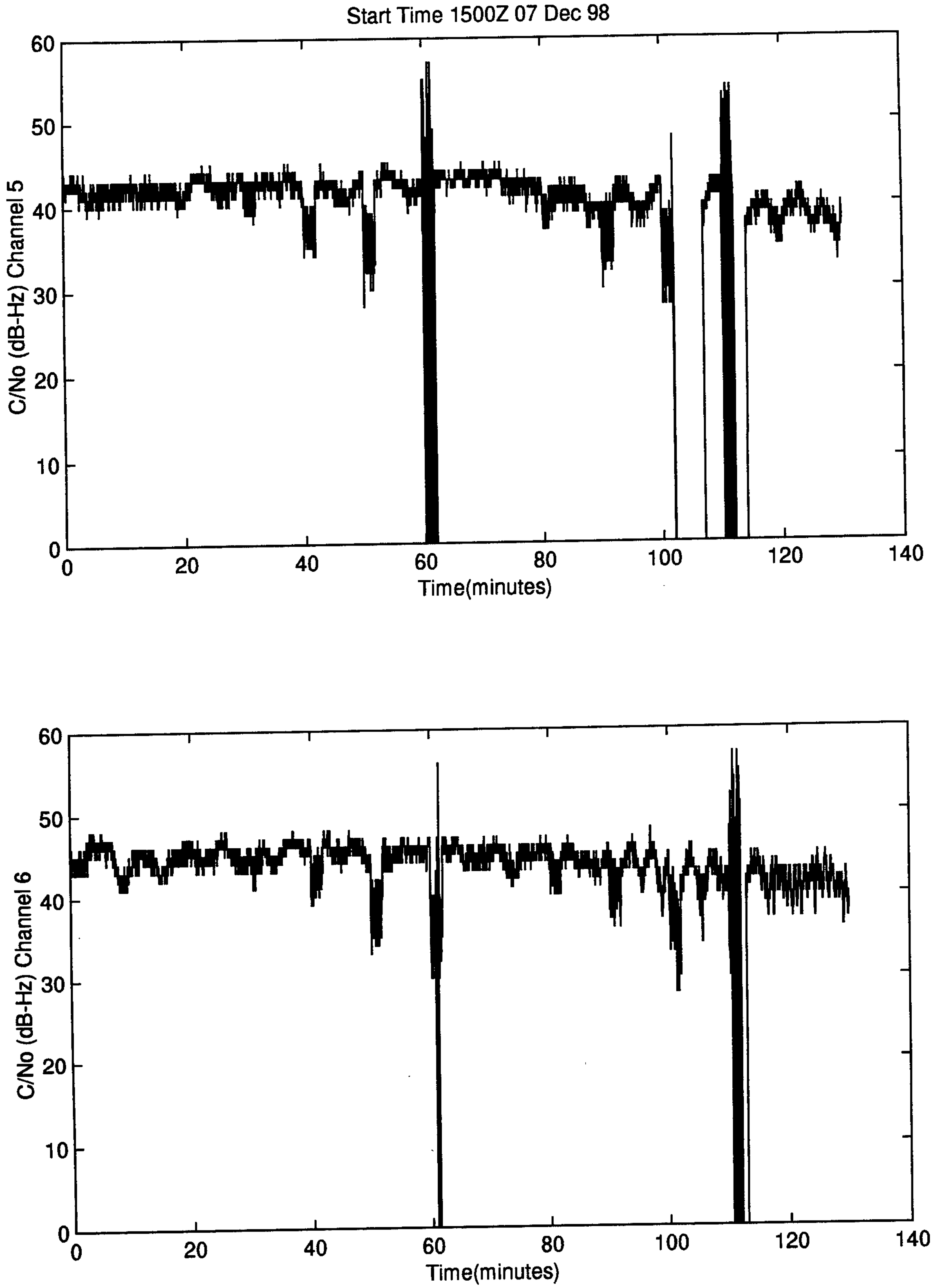

Figure R.14. C/No vs Time

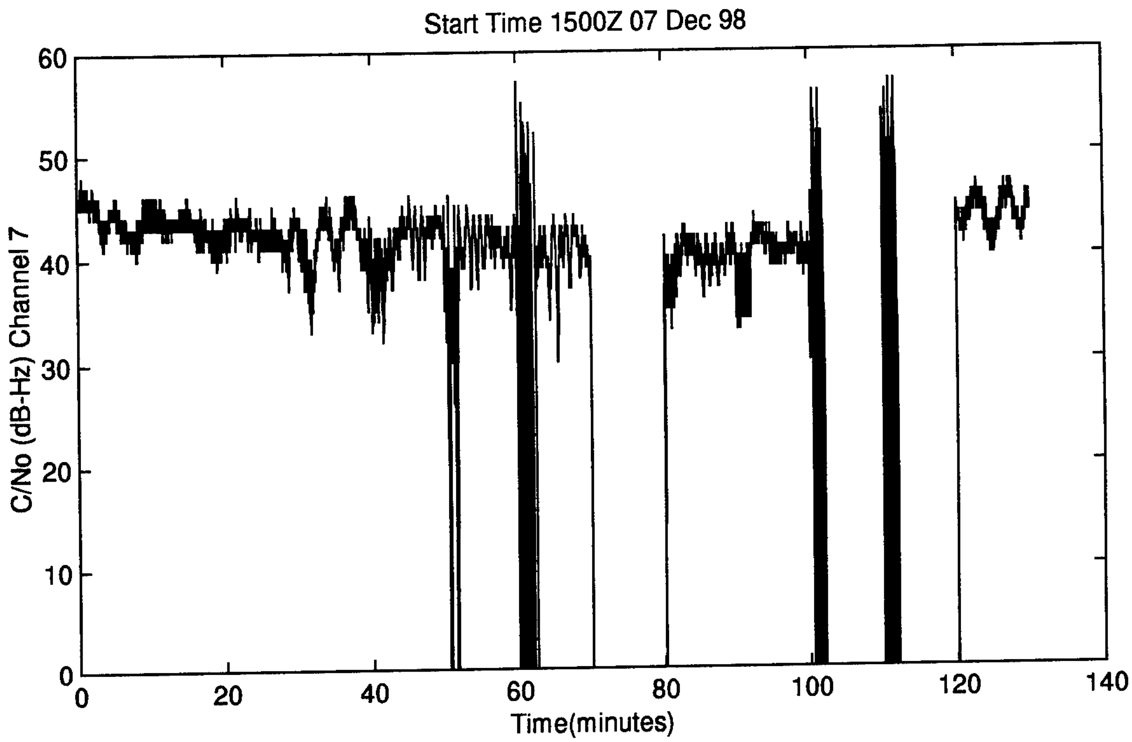

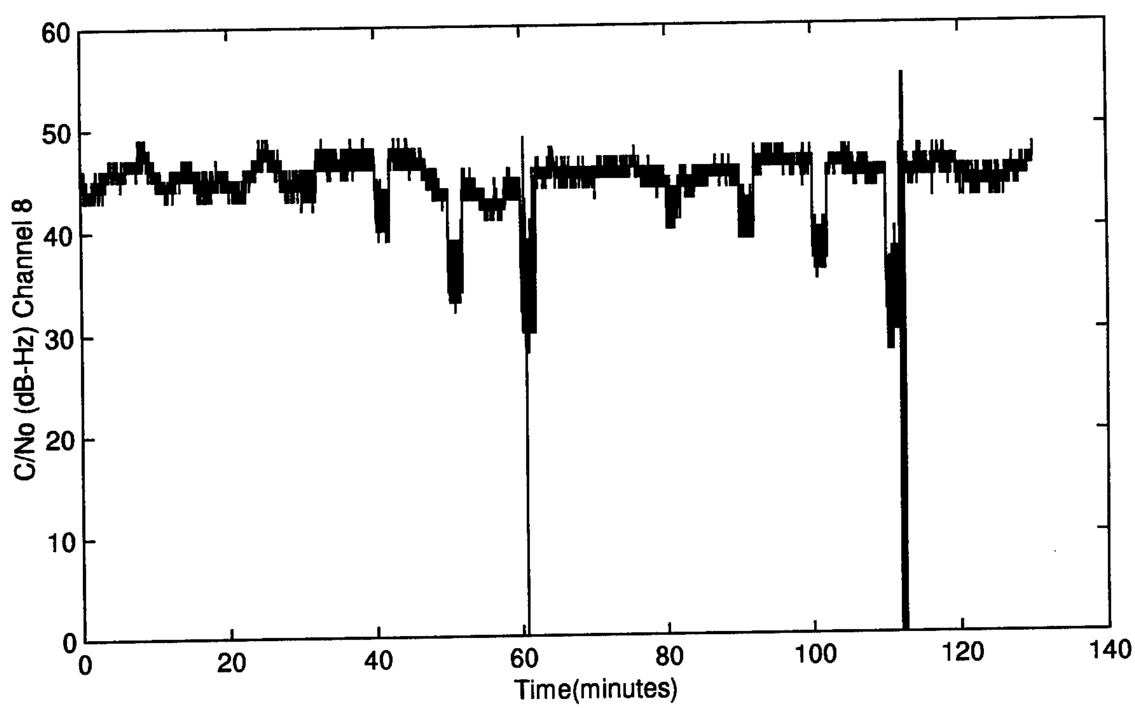

Figure R.15. C/No vs Time

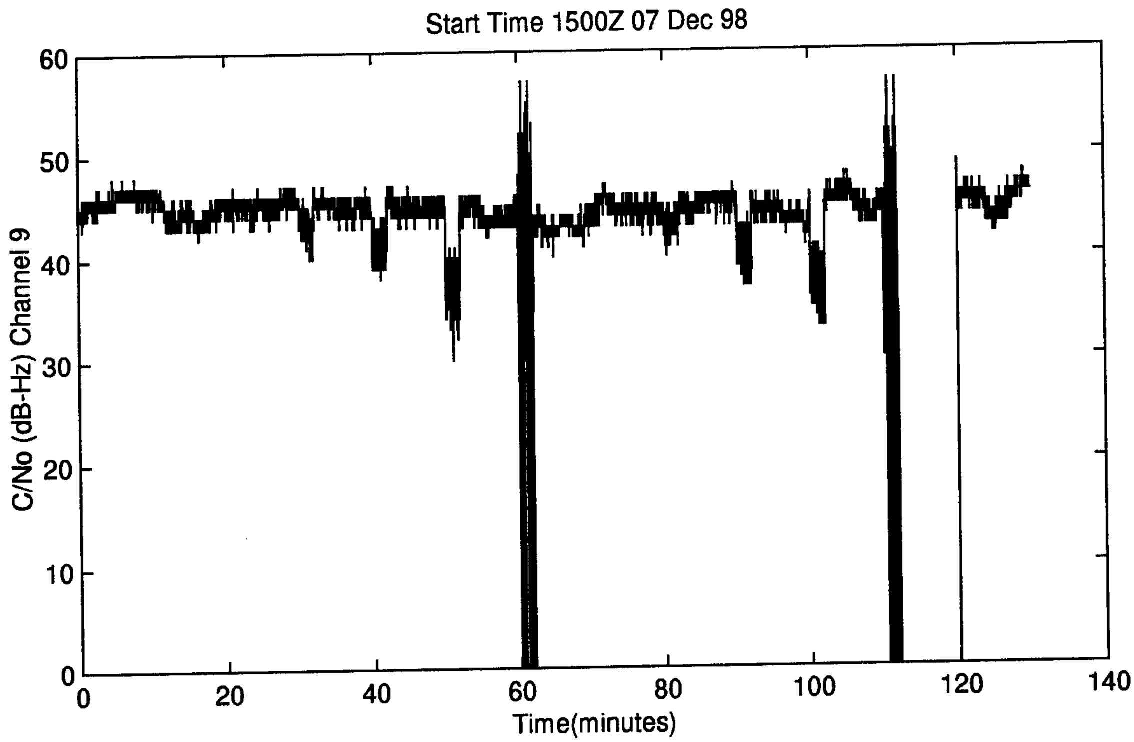

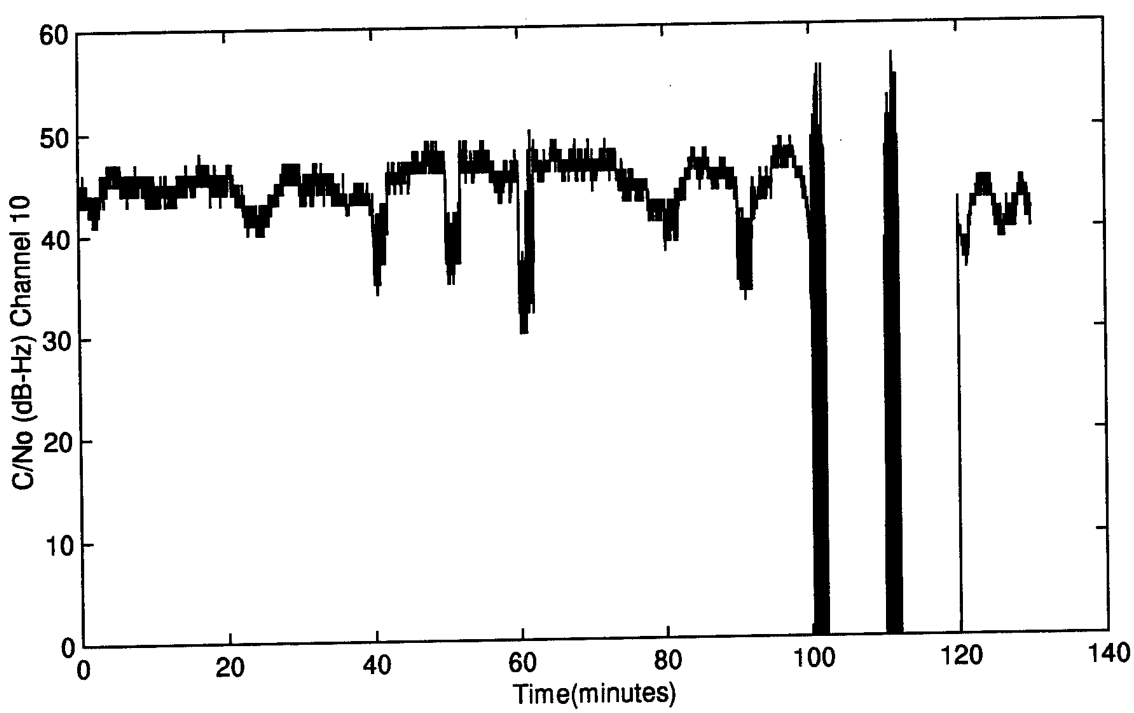

Figure R.16. C/No vs Time

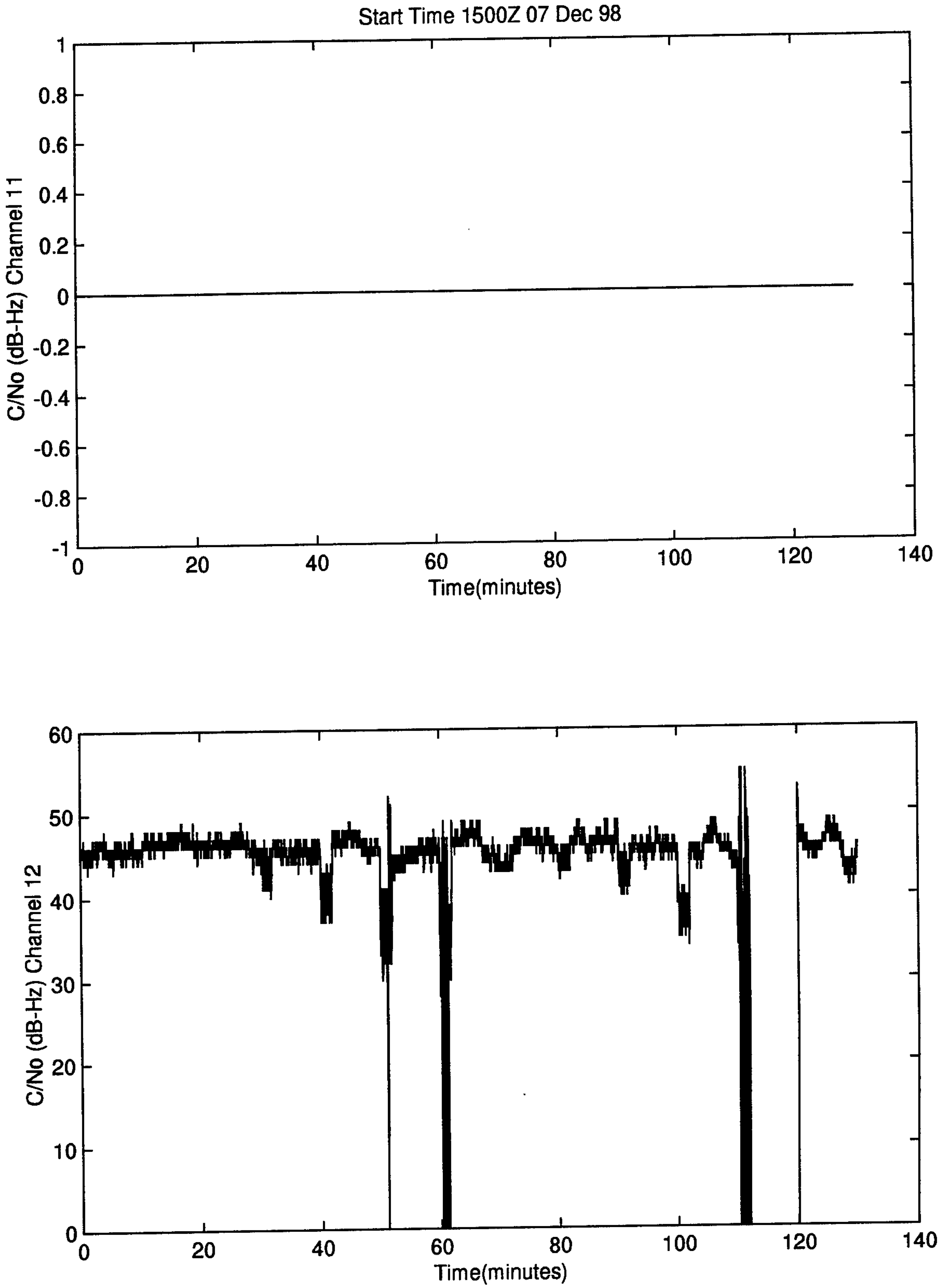

Figure R.17. C/No vs Time

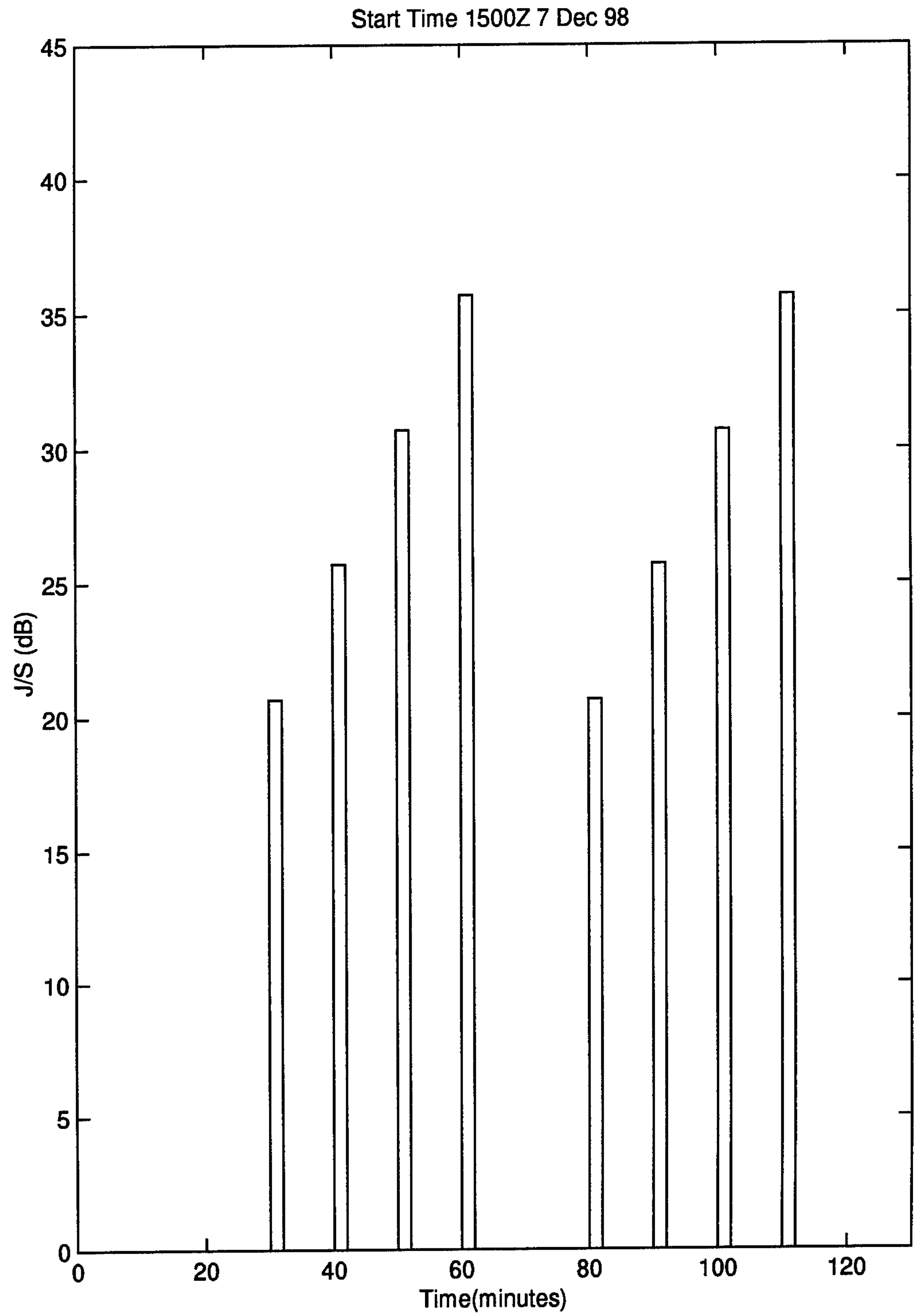

Figure R.18. Jamming Level J/S vs Time

APPENDIX S

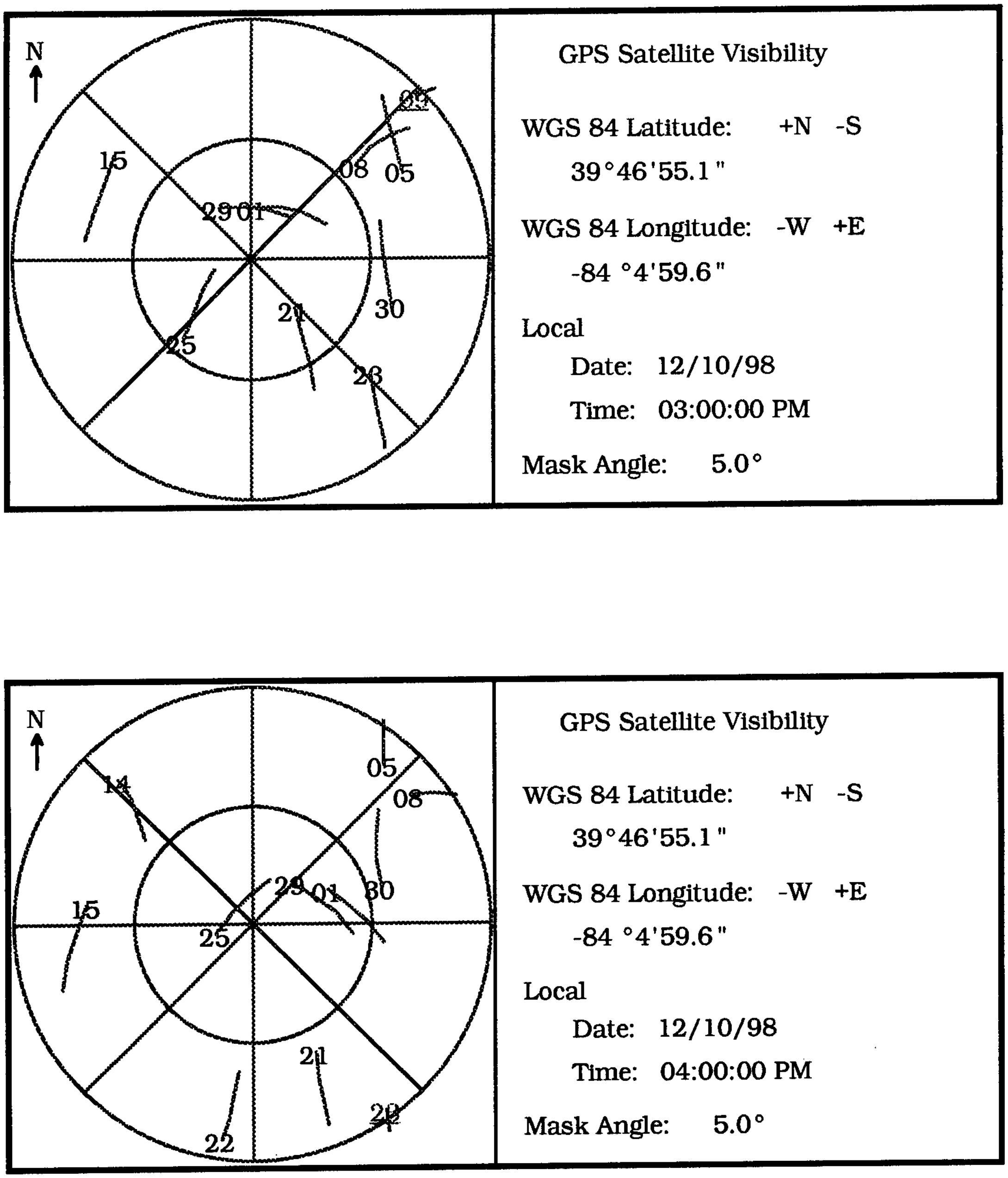

Figure S.1. GPS Satellites In View 10 Dec 98

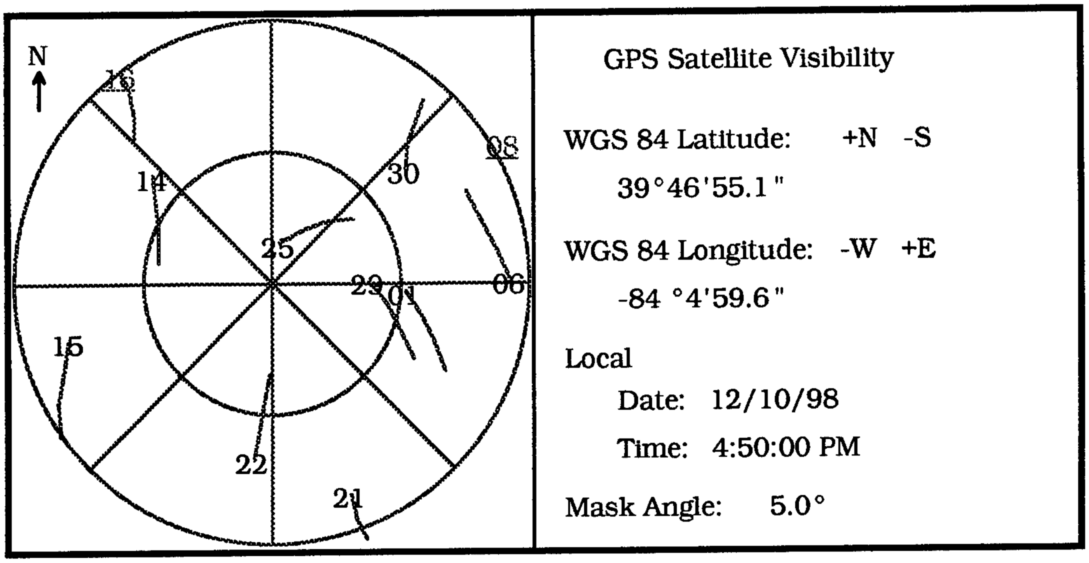

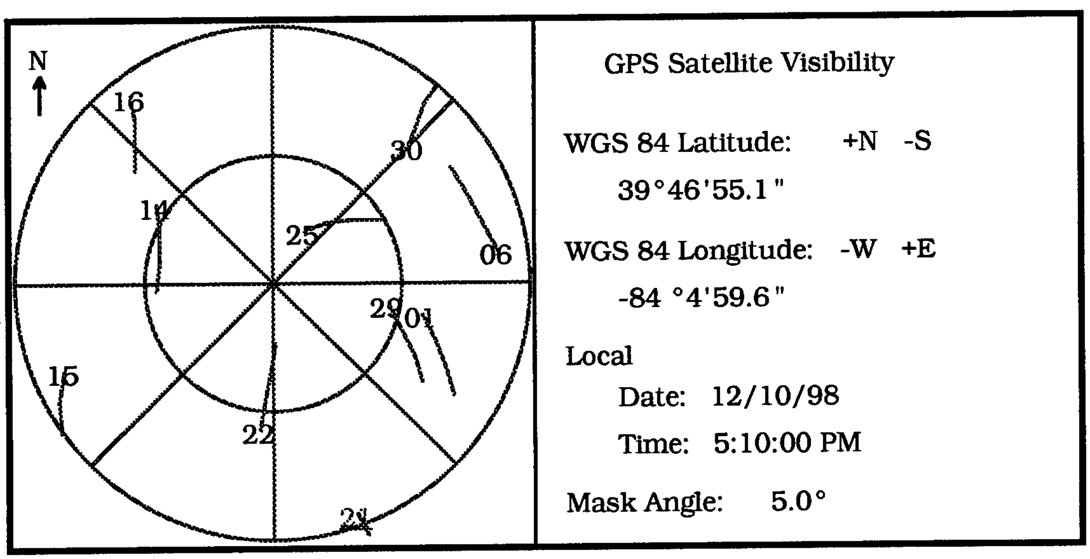

Figure S.2. GPS Satellites In View 10 Dec 98

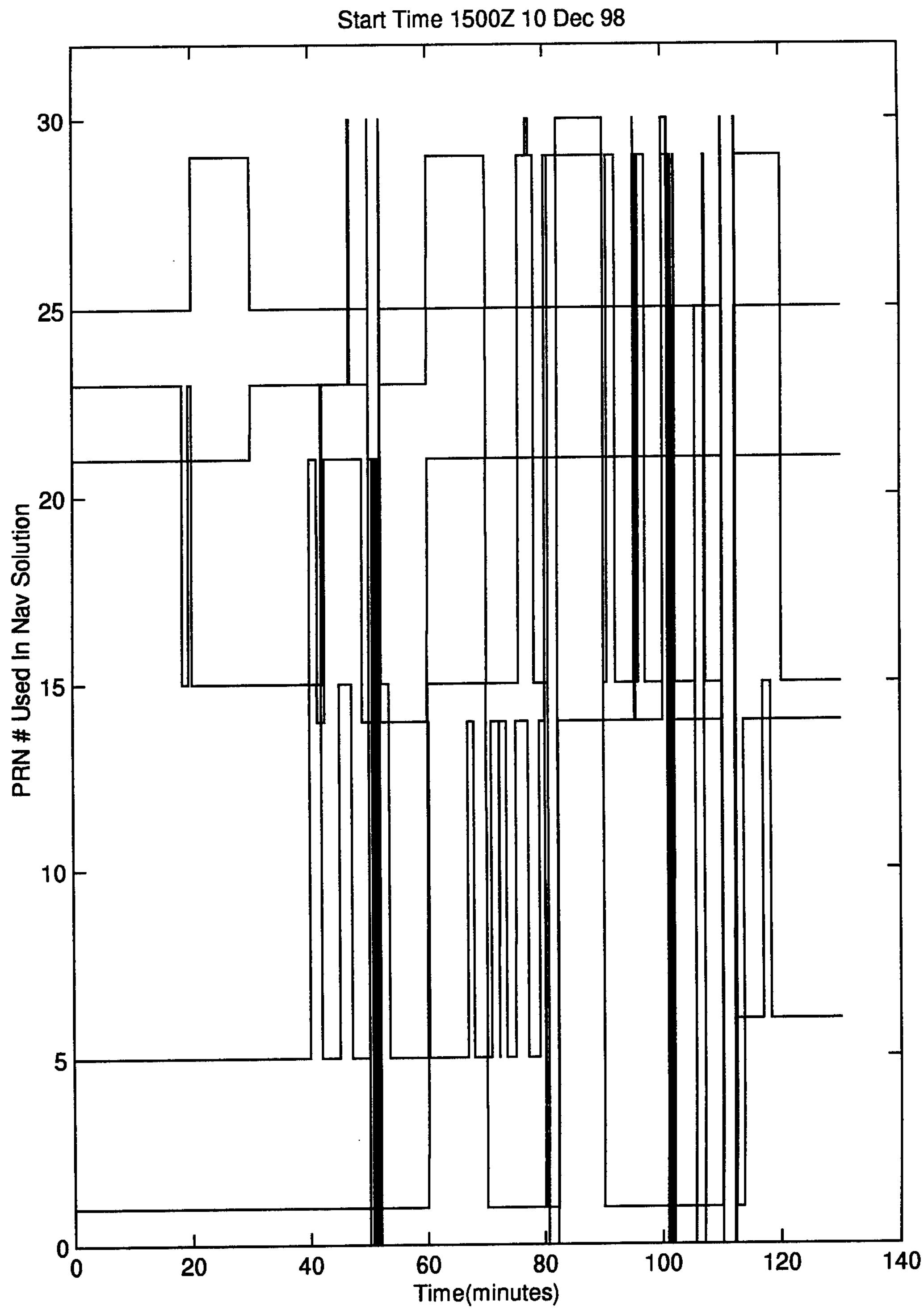

Figure S.3. PRN # Used In Nav Solution vs Time

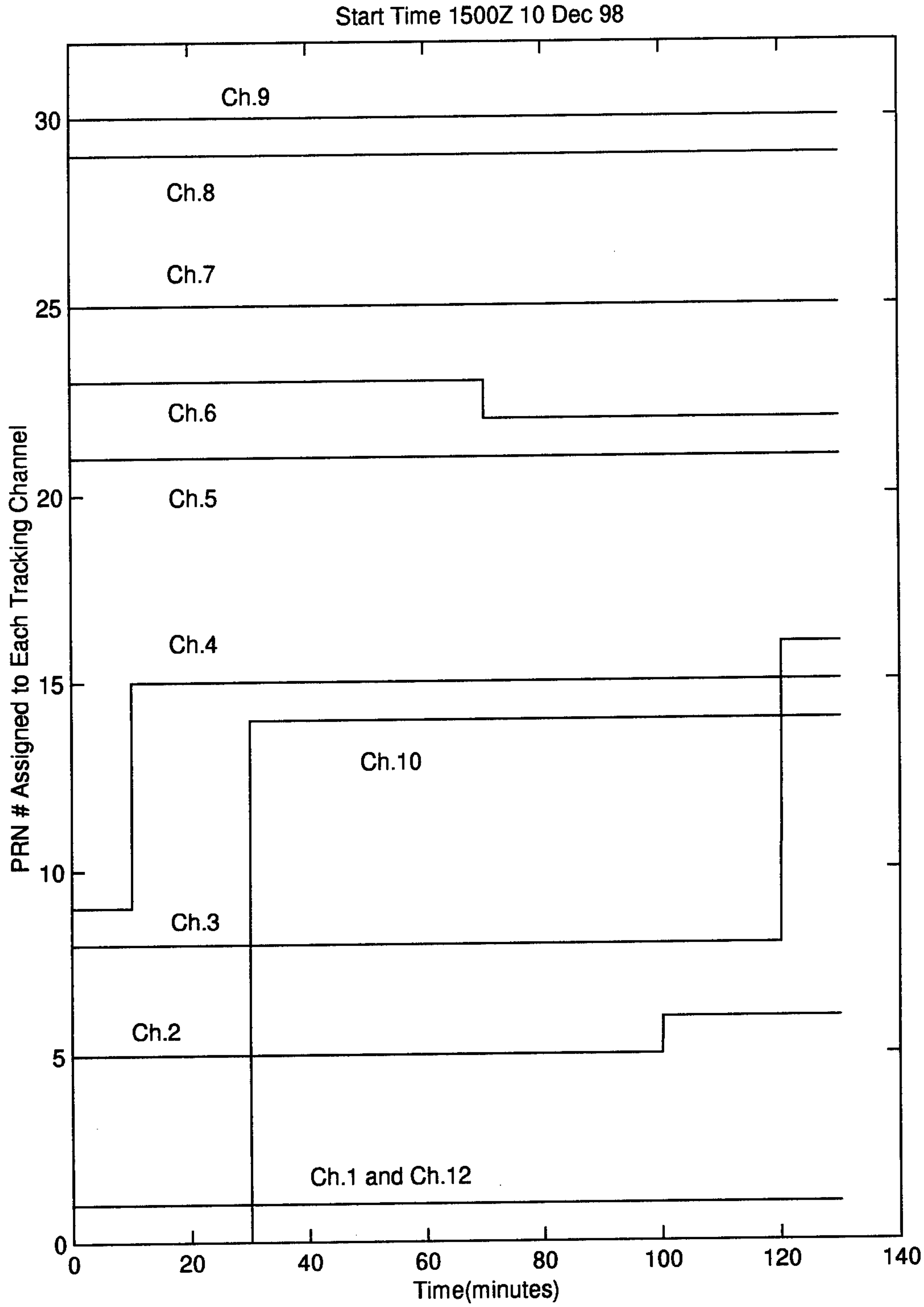

Figure S.4. PRN # Assigned to Each Tracking Channel vs Time

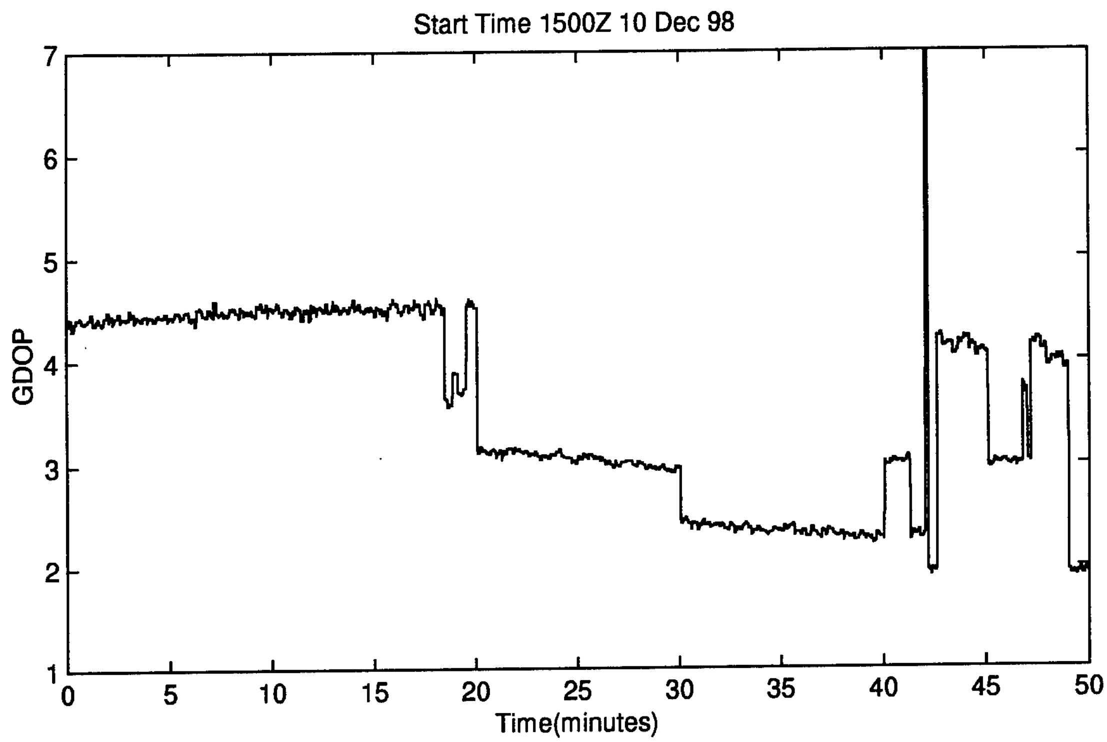

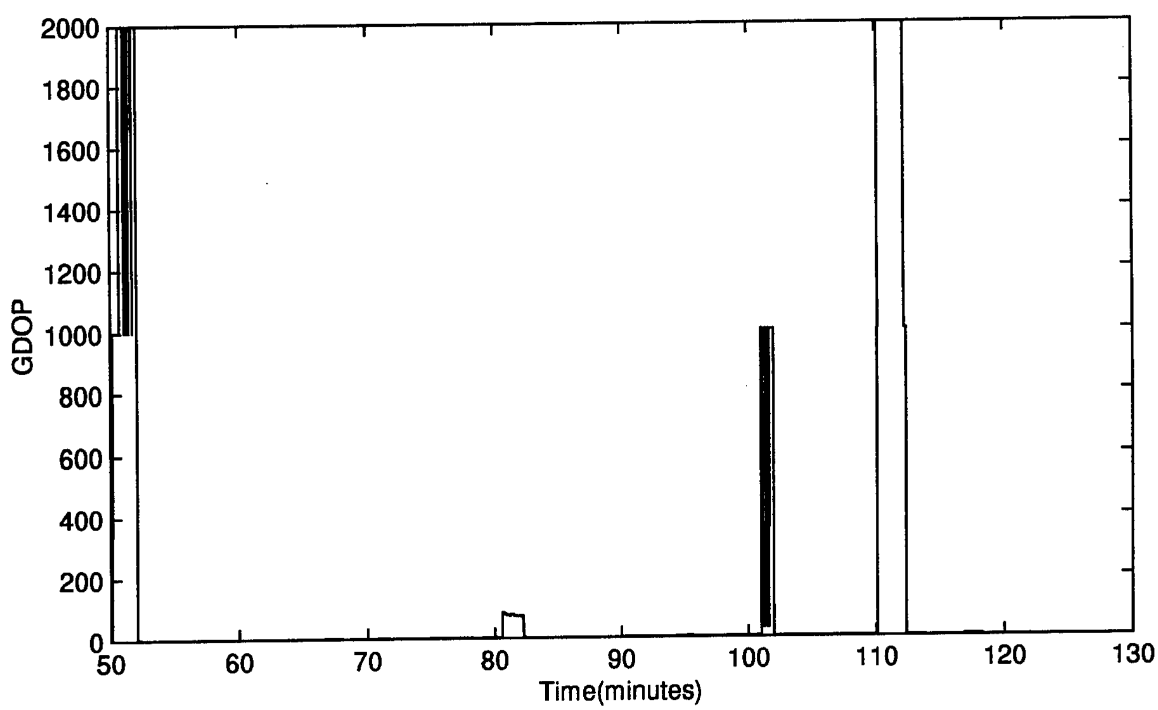

Figure S.5. GDOP vs Time

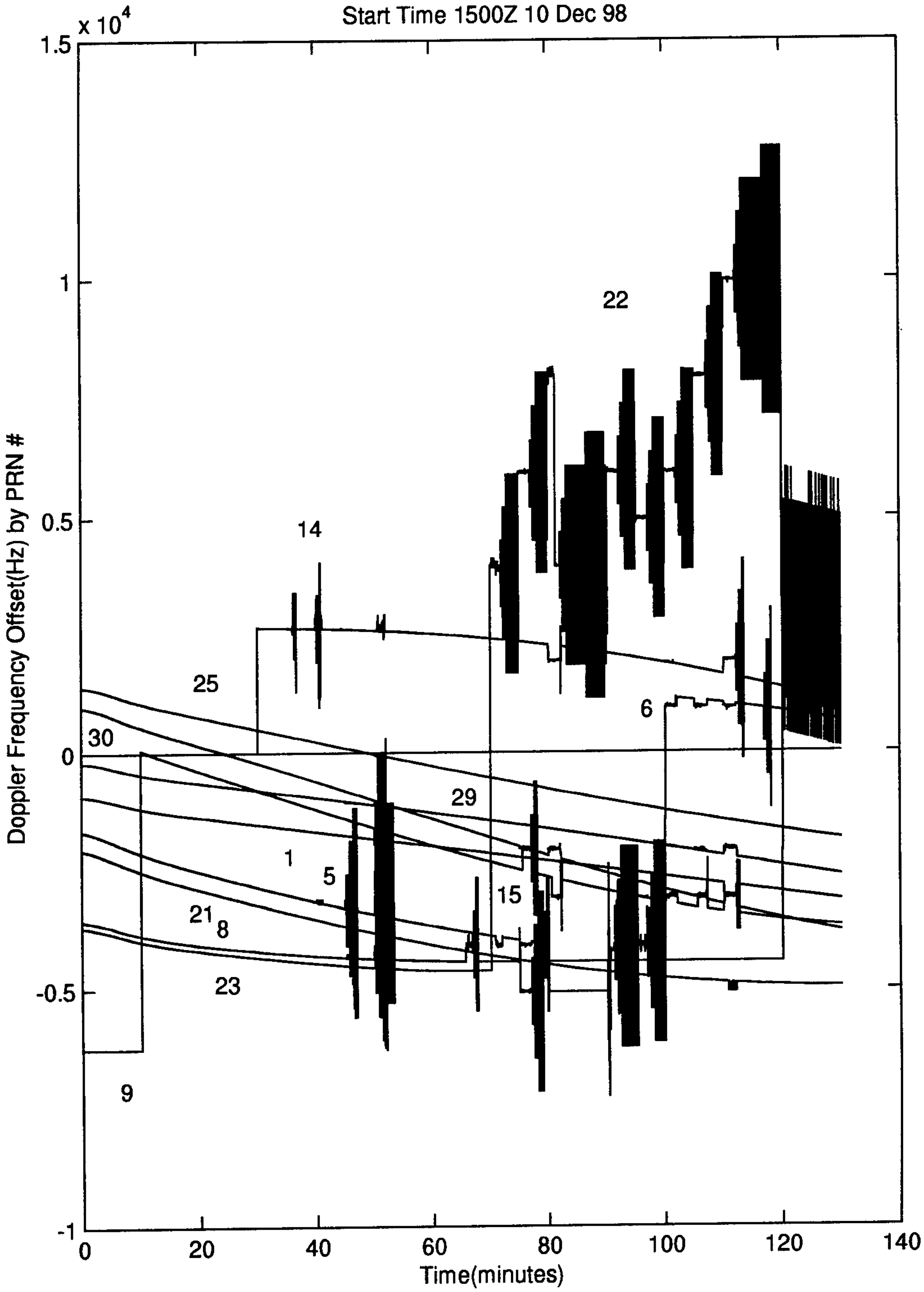

Figure S.6. Doppler Frequency vs Time

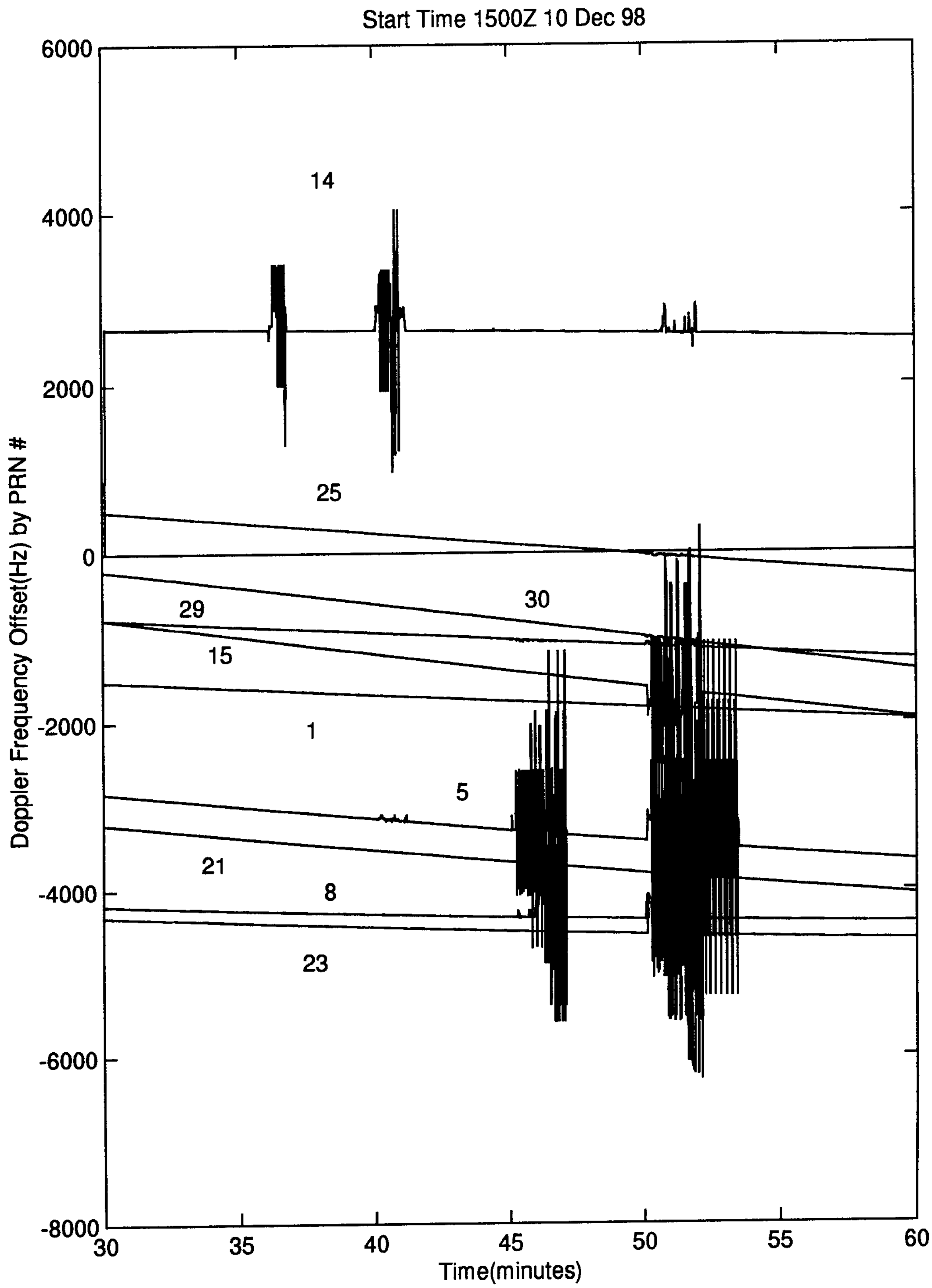

Figure S.7. Doppler Frequency vs Time

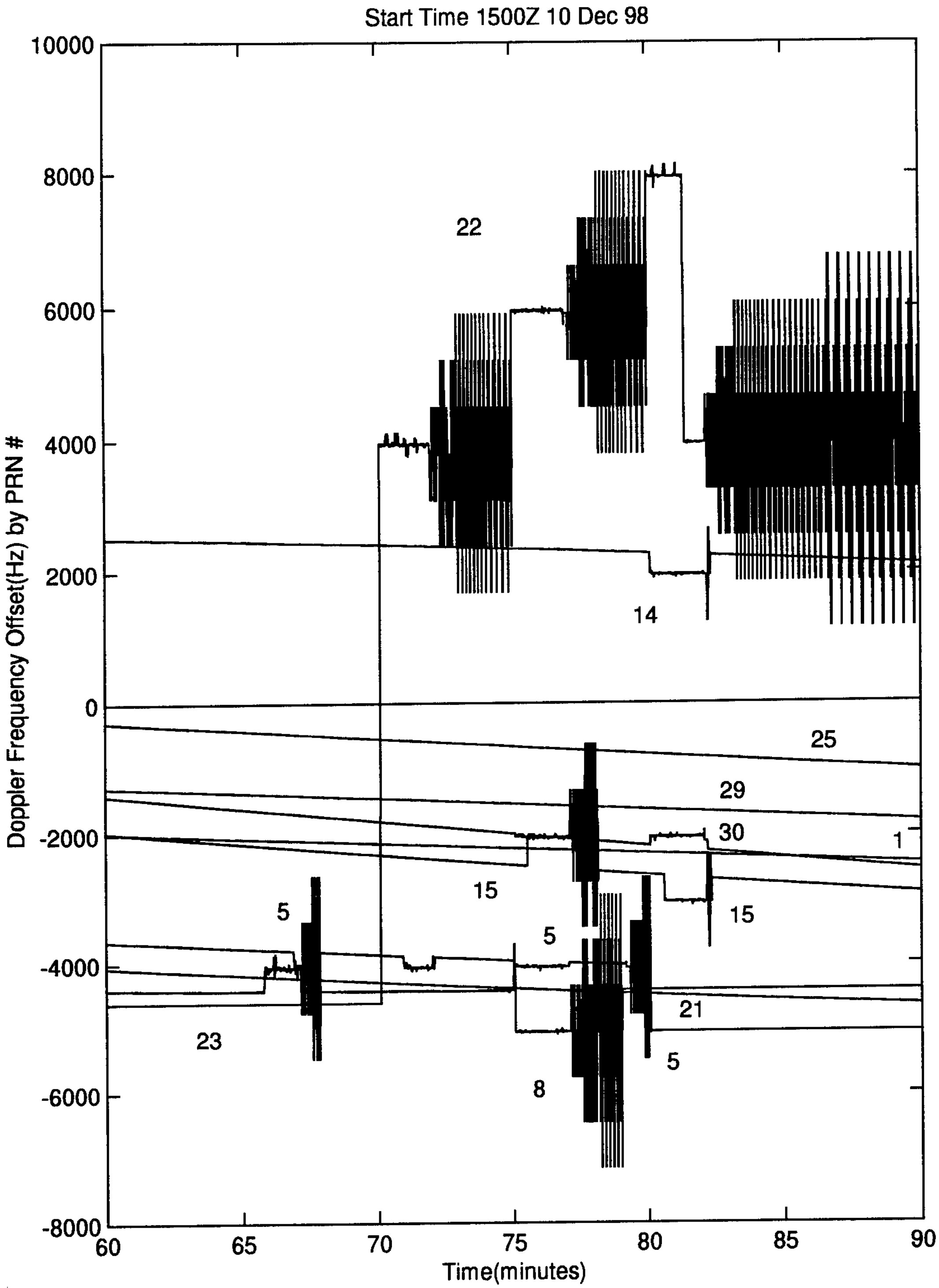

Figure S.8. Doppler Frequency vs Time

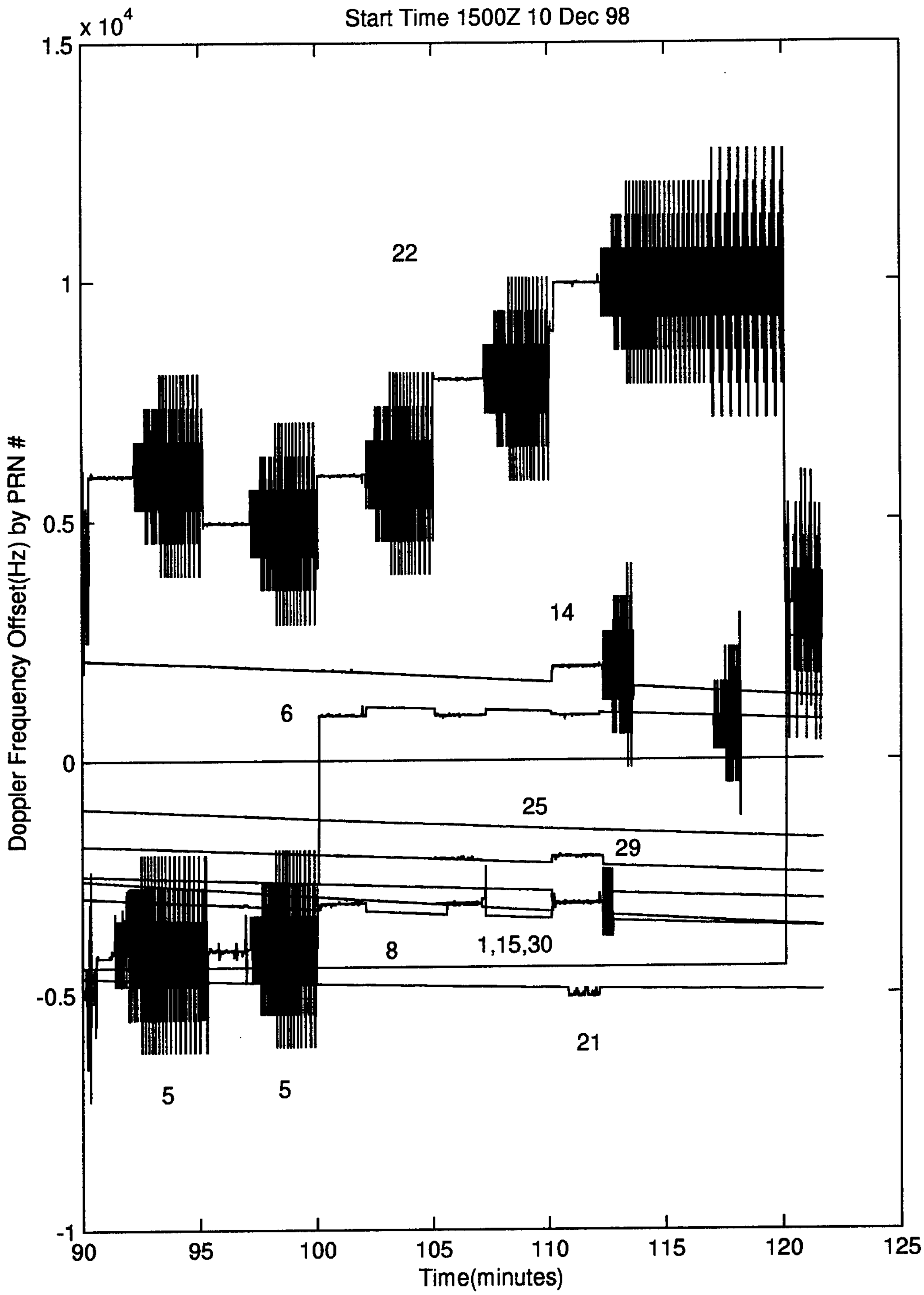

Figure S.9. Doppler Frequency vs Time

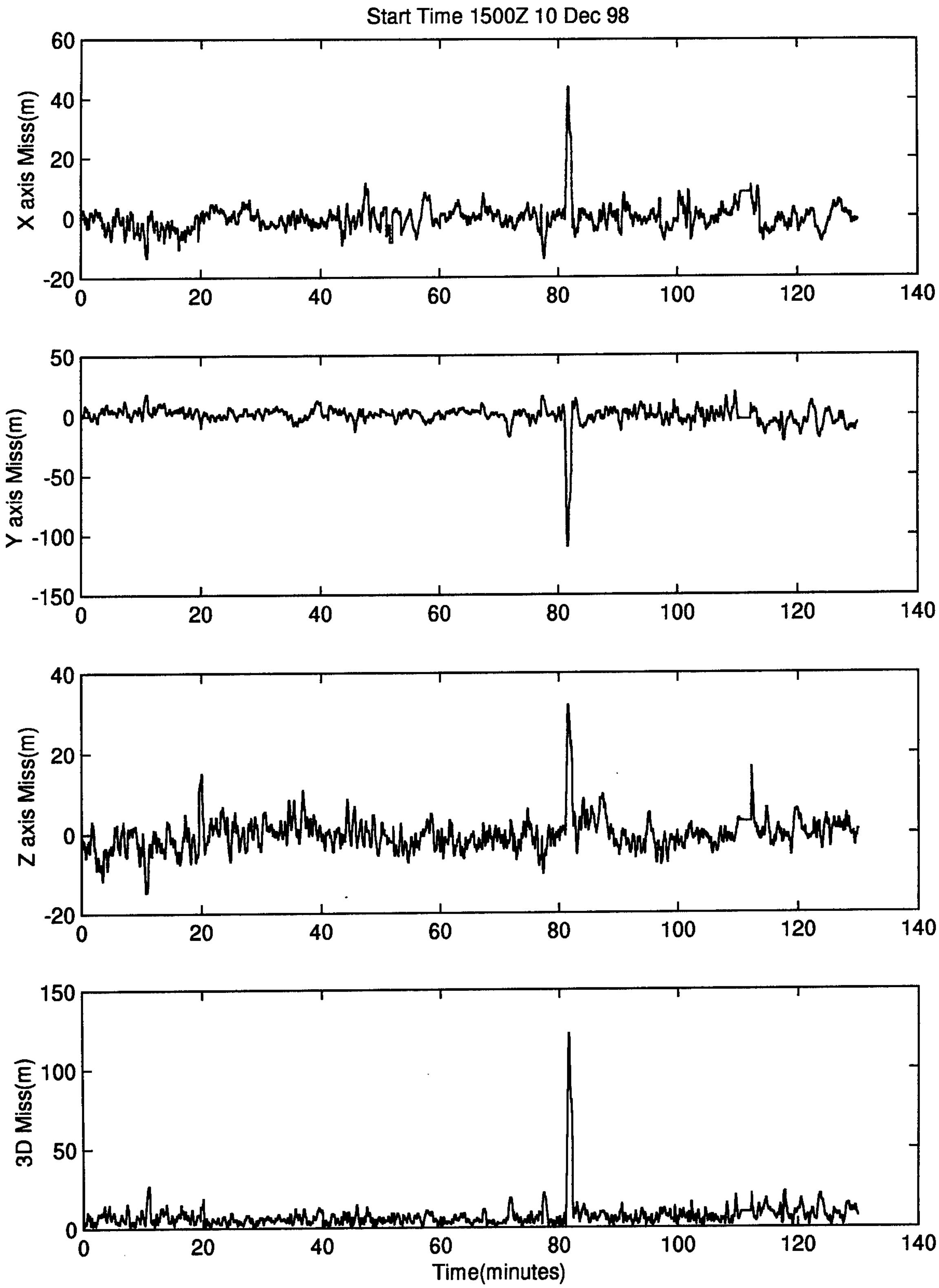

Figure S.10. X,Y,Z and 3D Error(m) vs Time

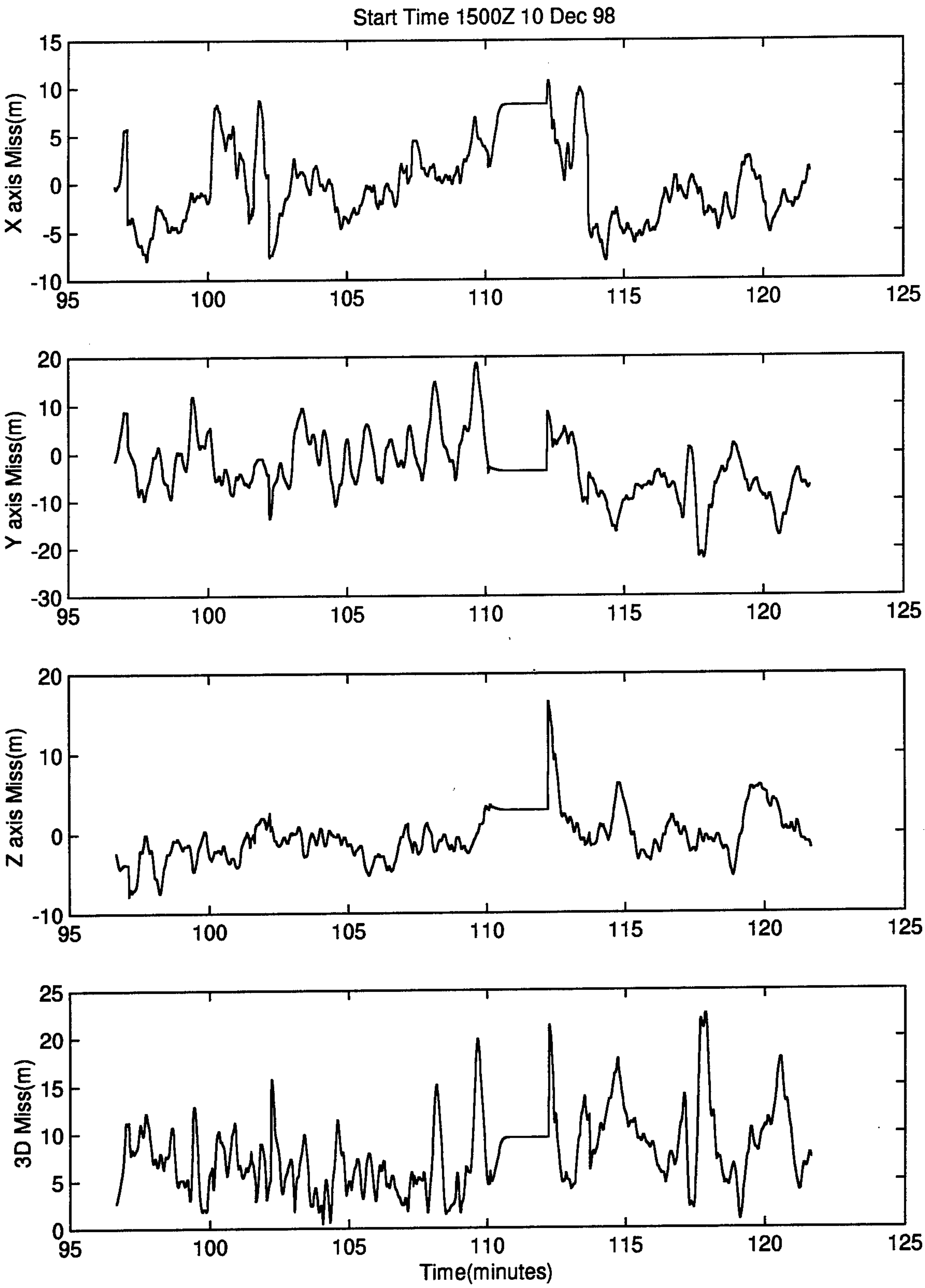

Figure S.11. X,Y,Z and 3D Error(m) vs Time

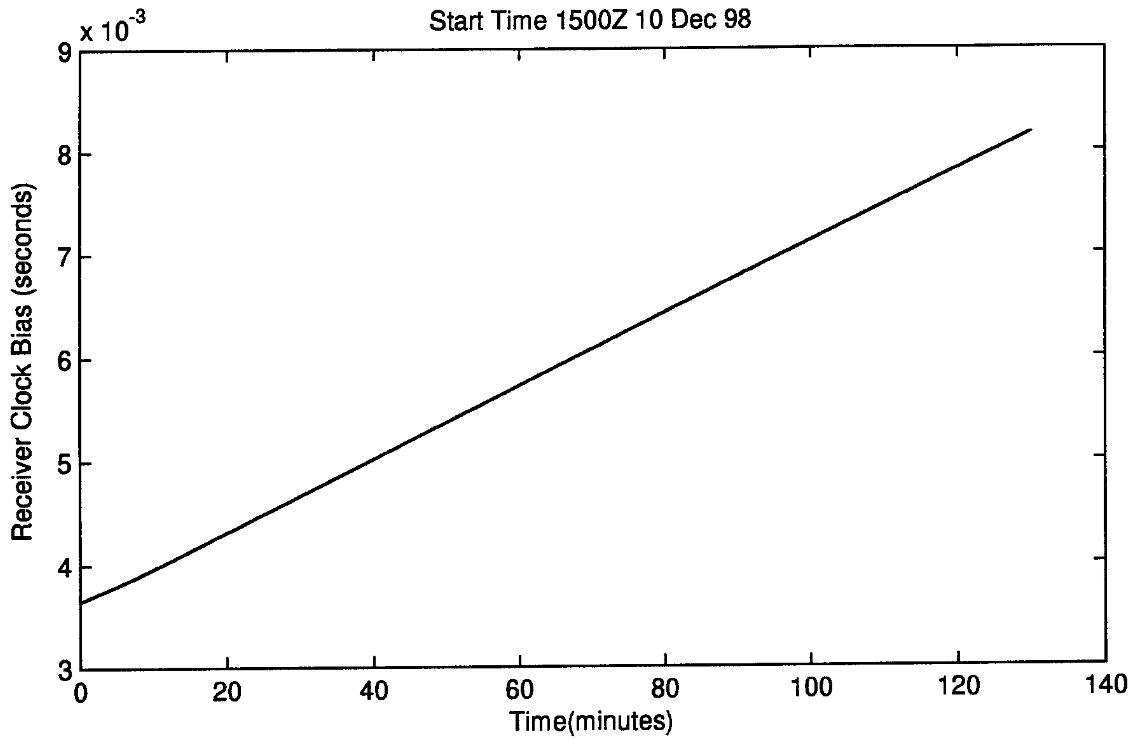

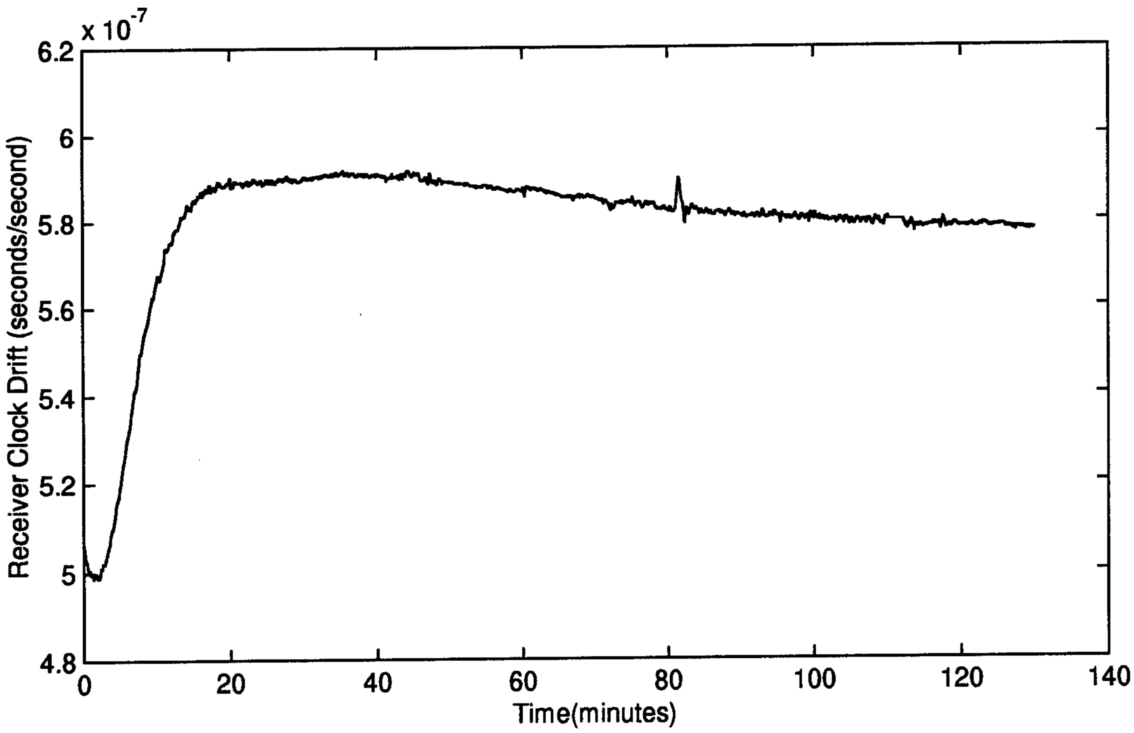

Figure S.12. Receiver Clock Bias and Drift vs Time

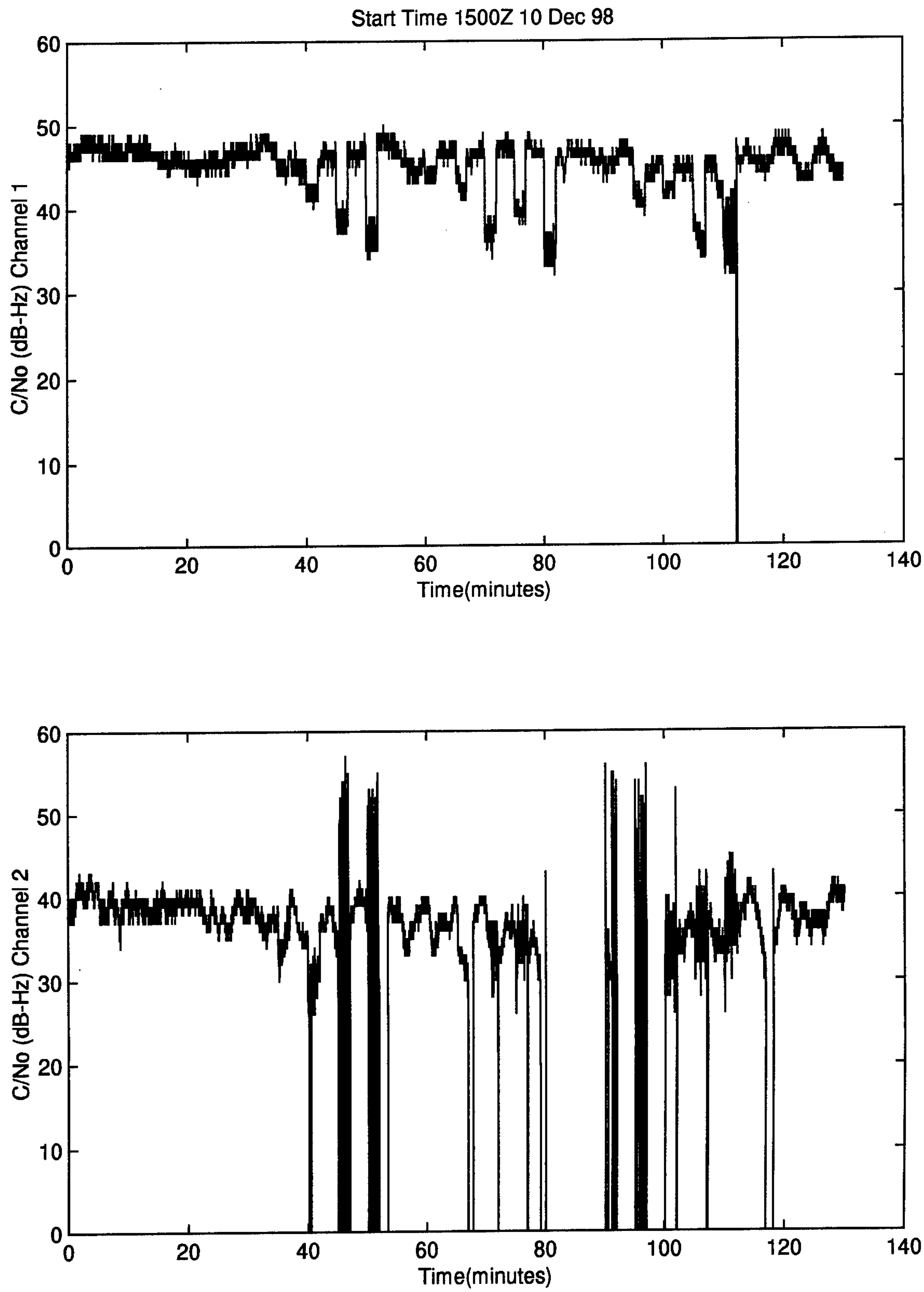

Figure S.13. C/No vs Time

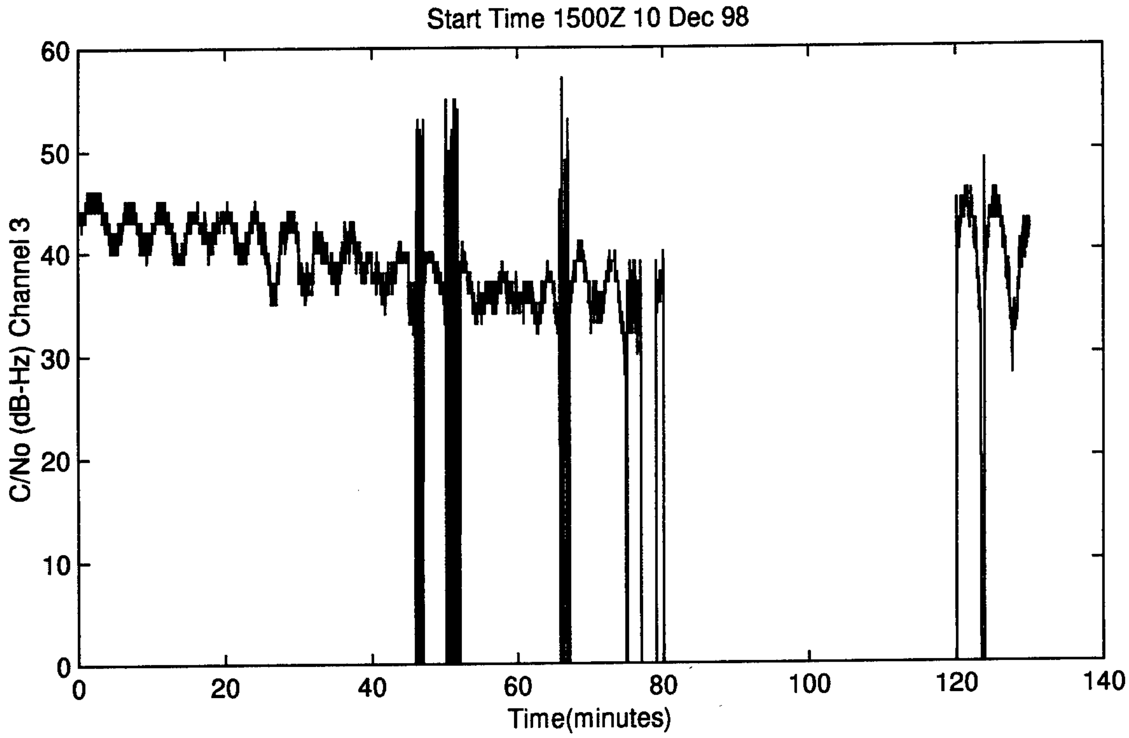

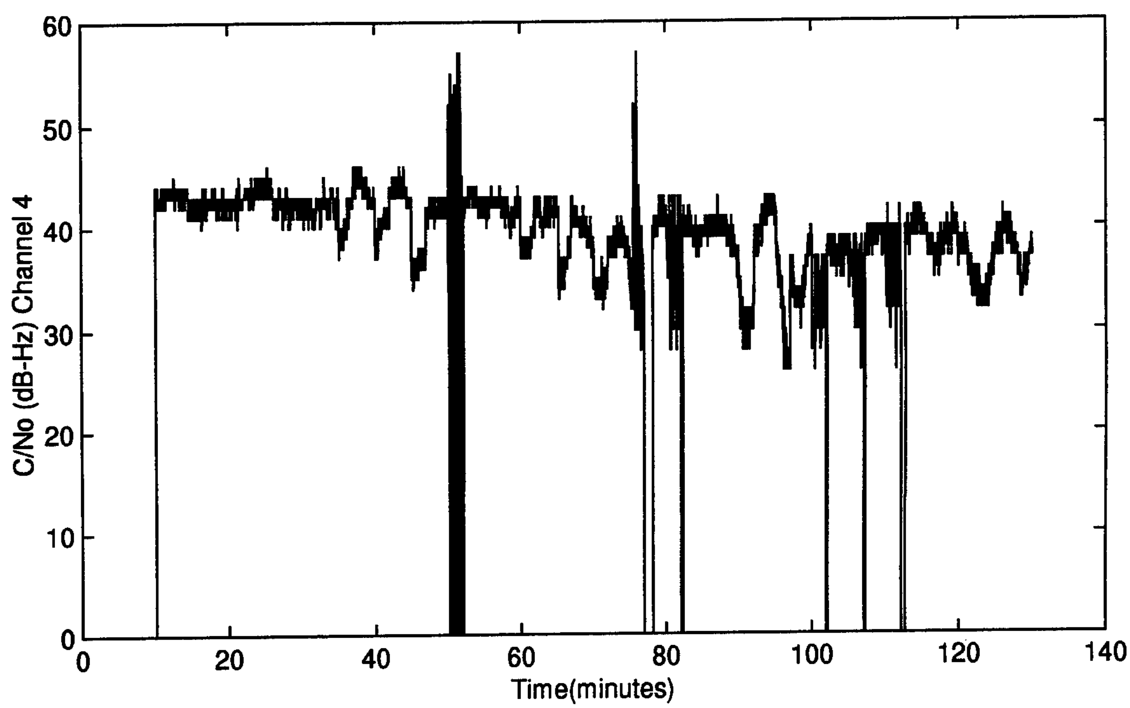

Figure S.14. C/No vs Time

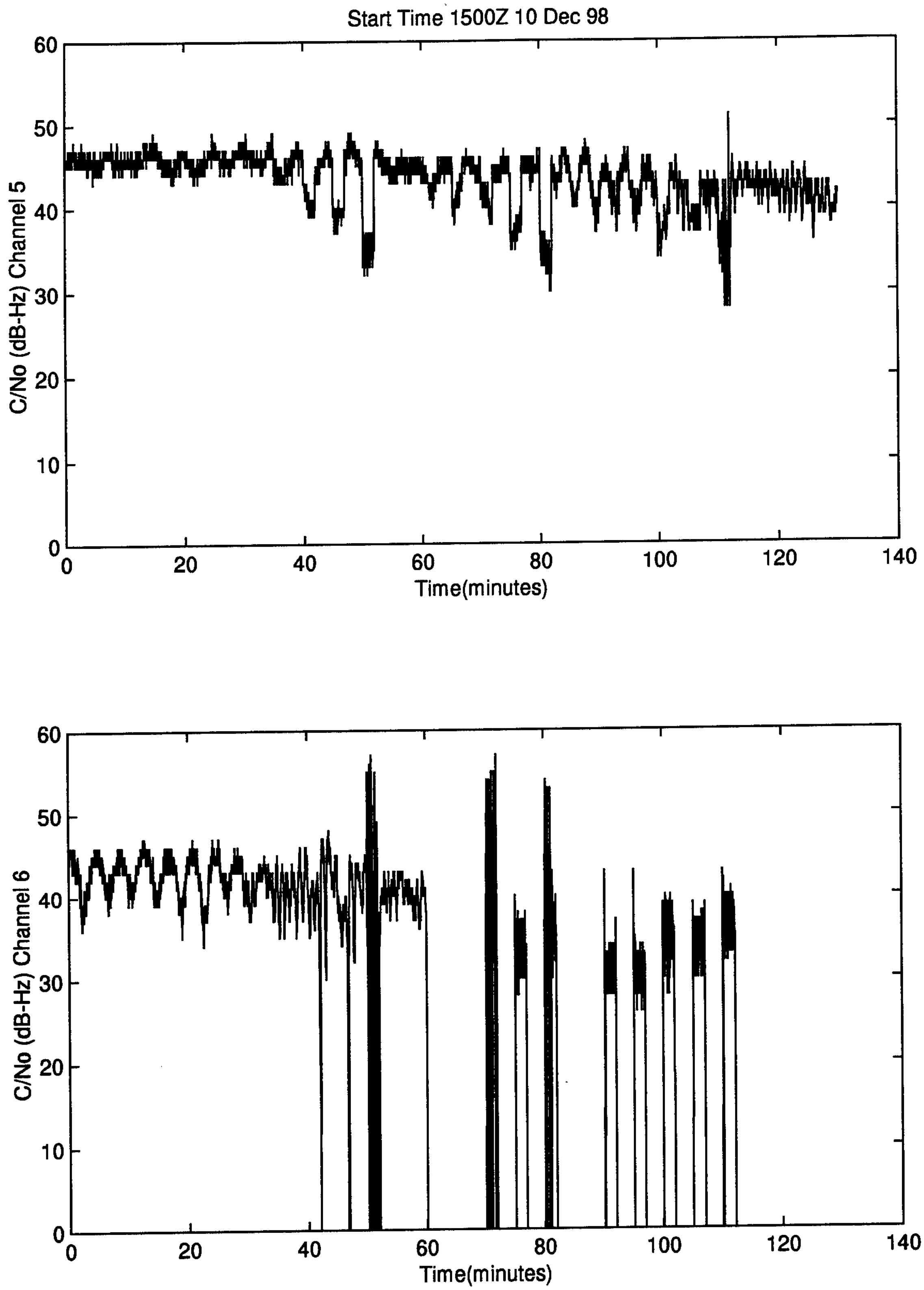

Figure S.15. C/No vs Time

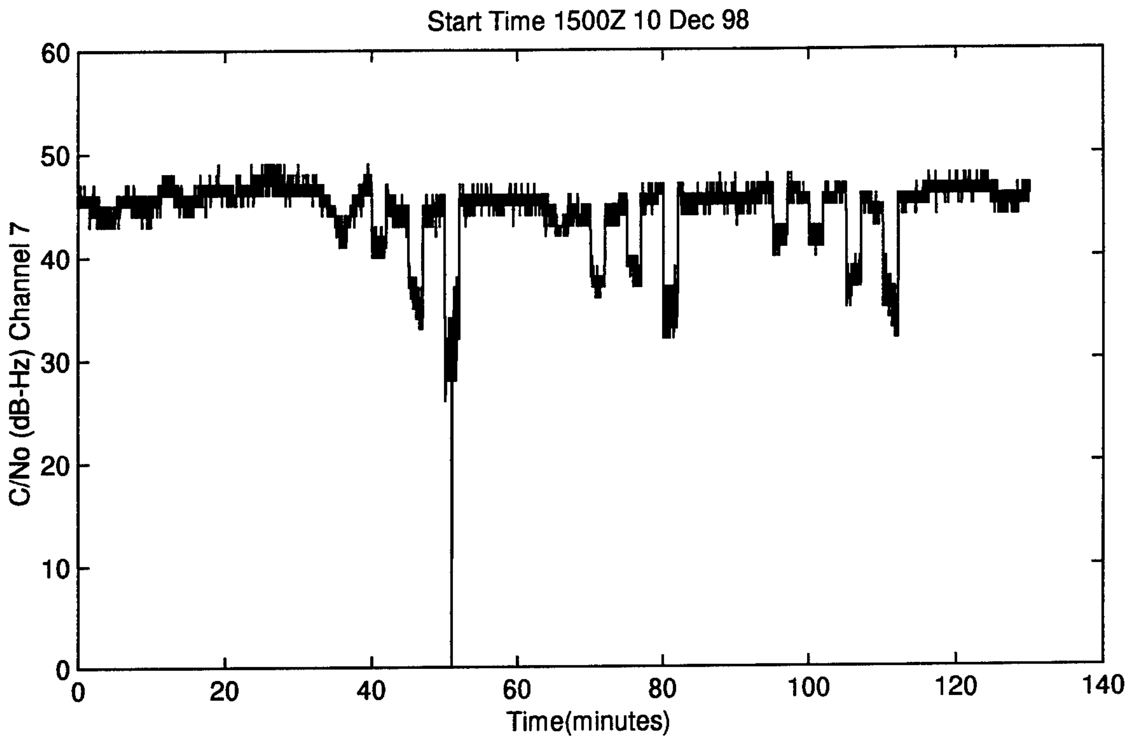

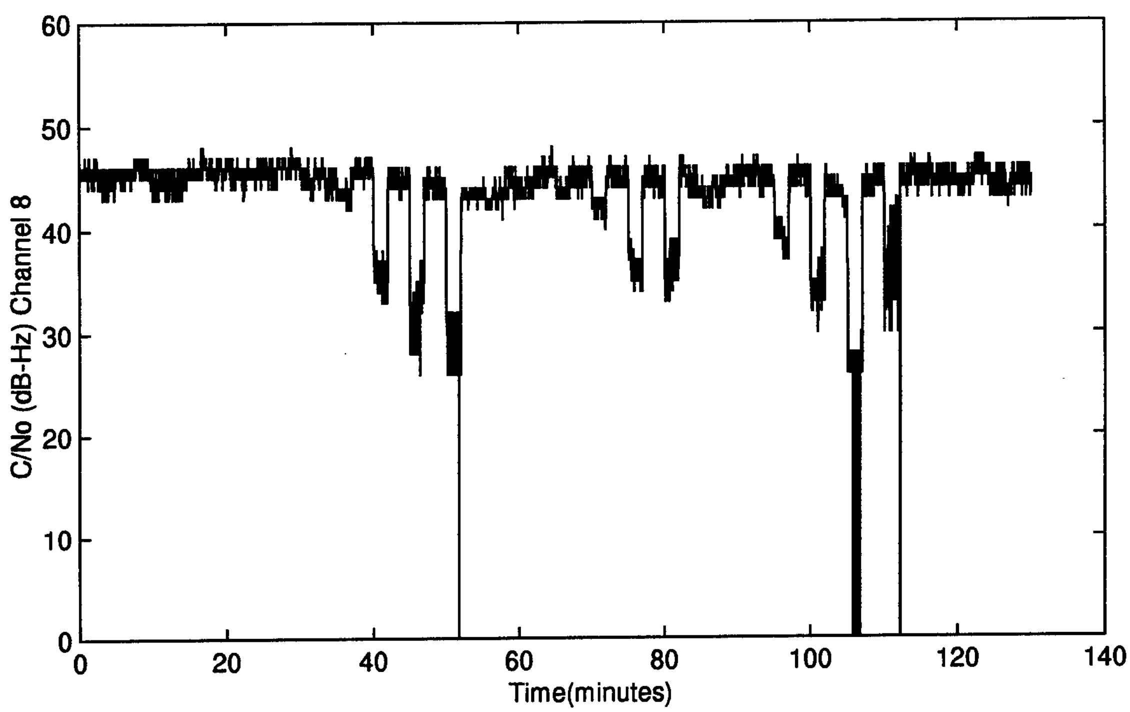

Figure S.16. C/No vs Time

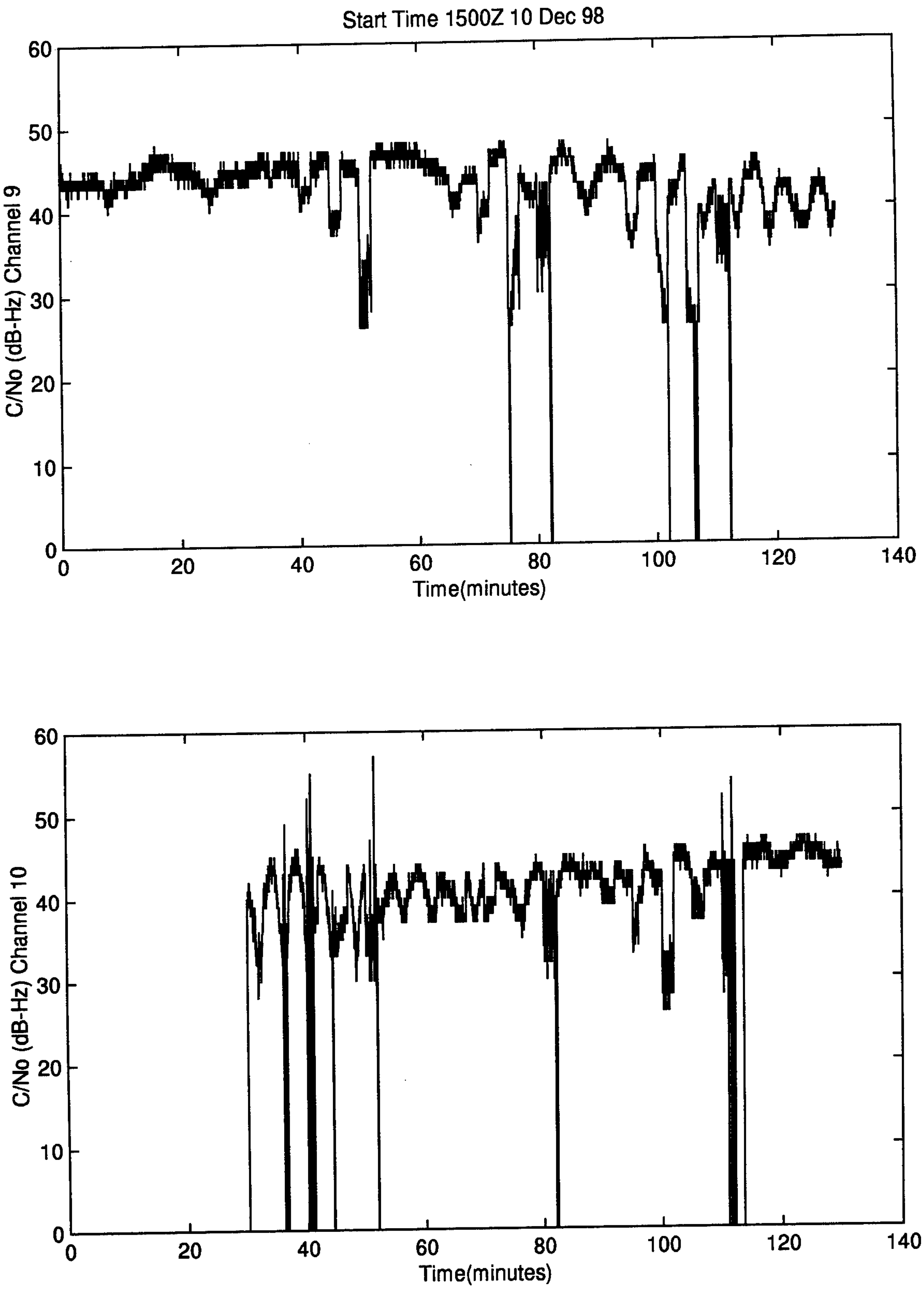

Figure S.17. C/No vs Time

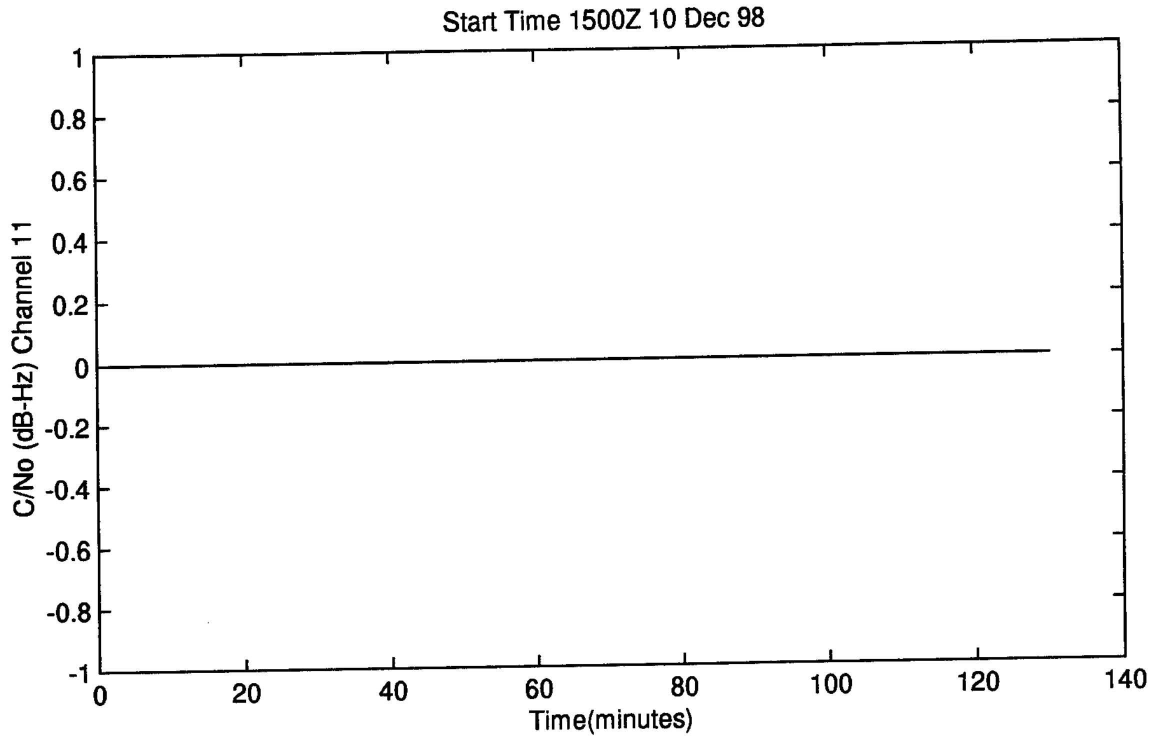

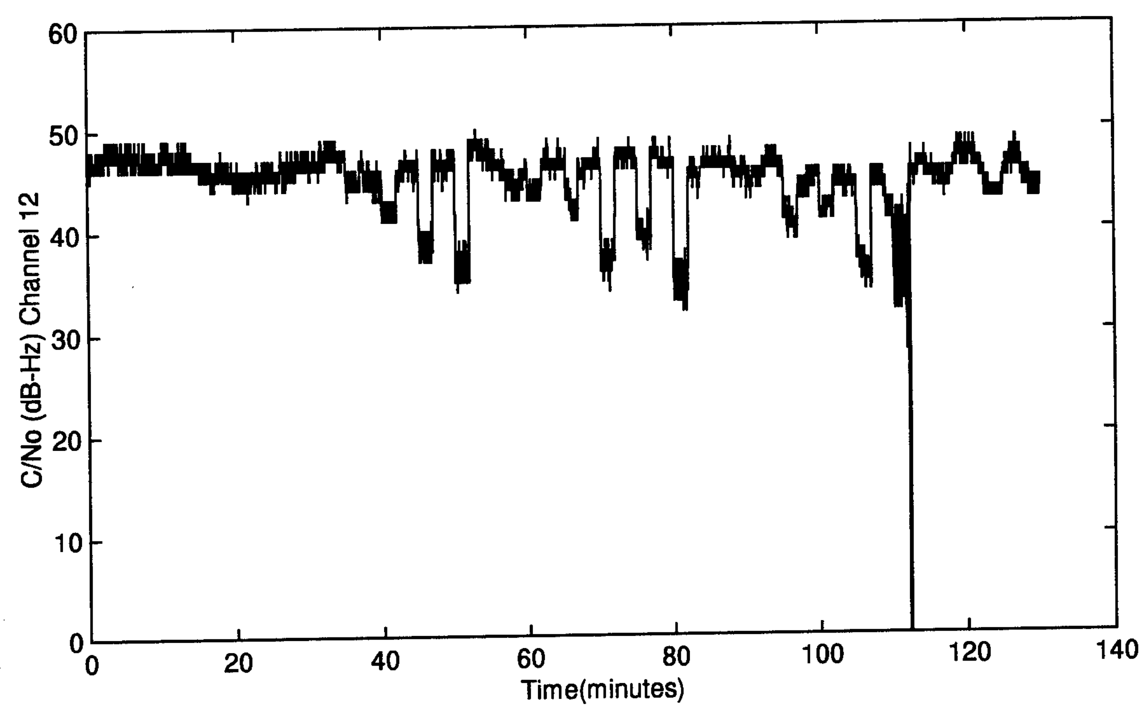

Figure S.18. C/No vs Time

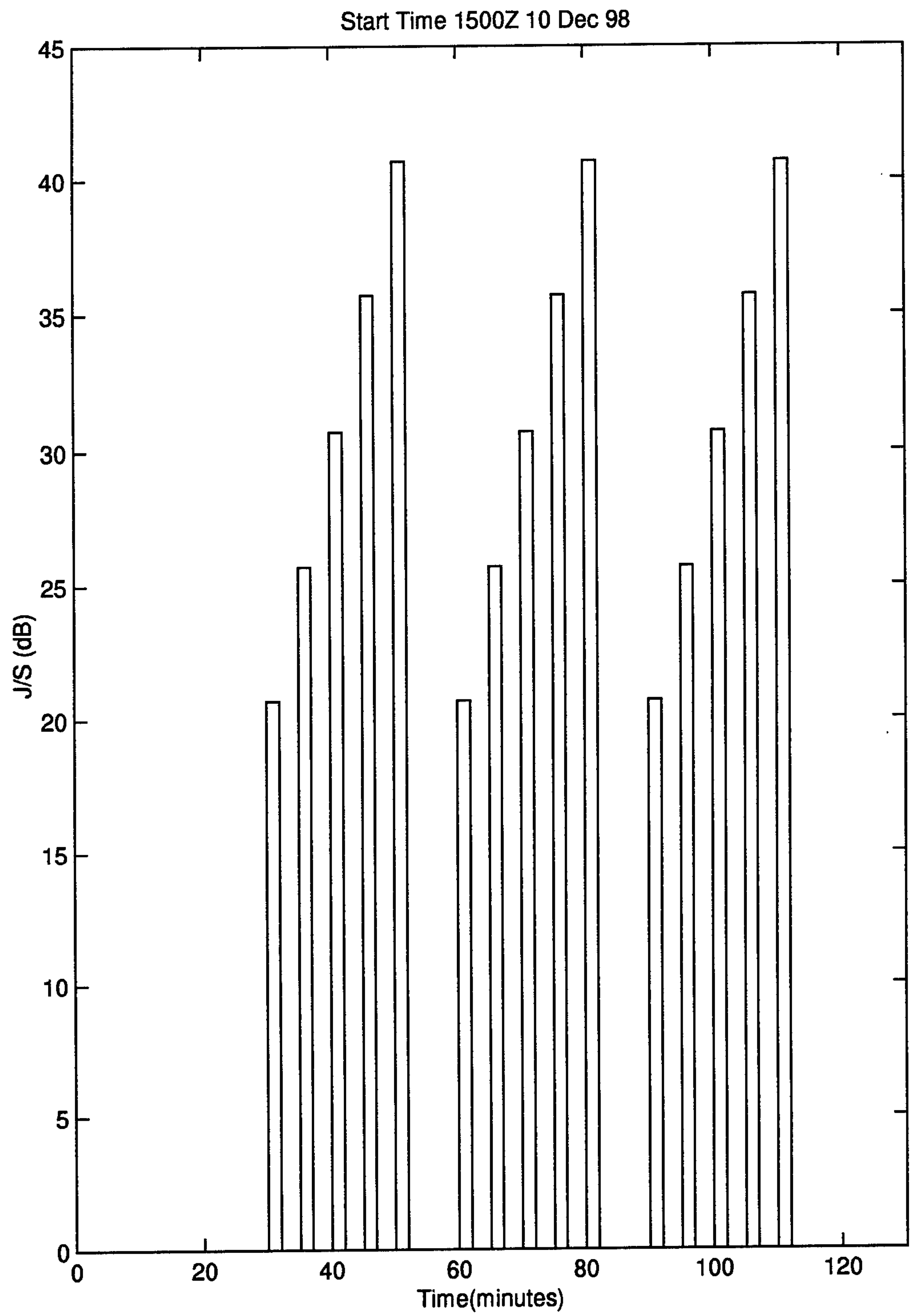

Figure S.19. Jamming Level J/S vs Time

APPENDIX T

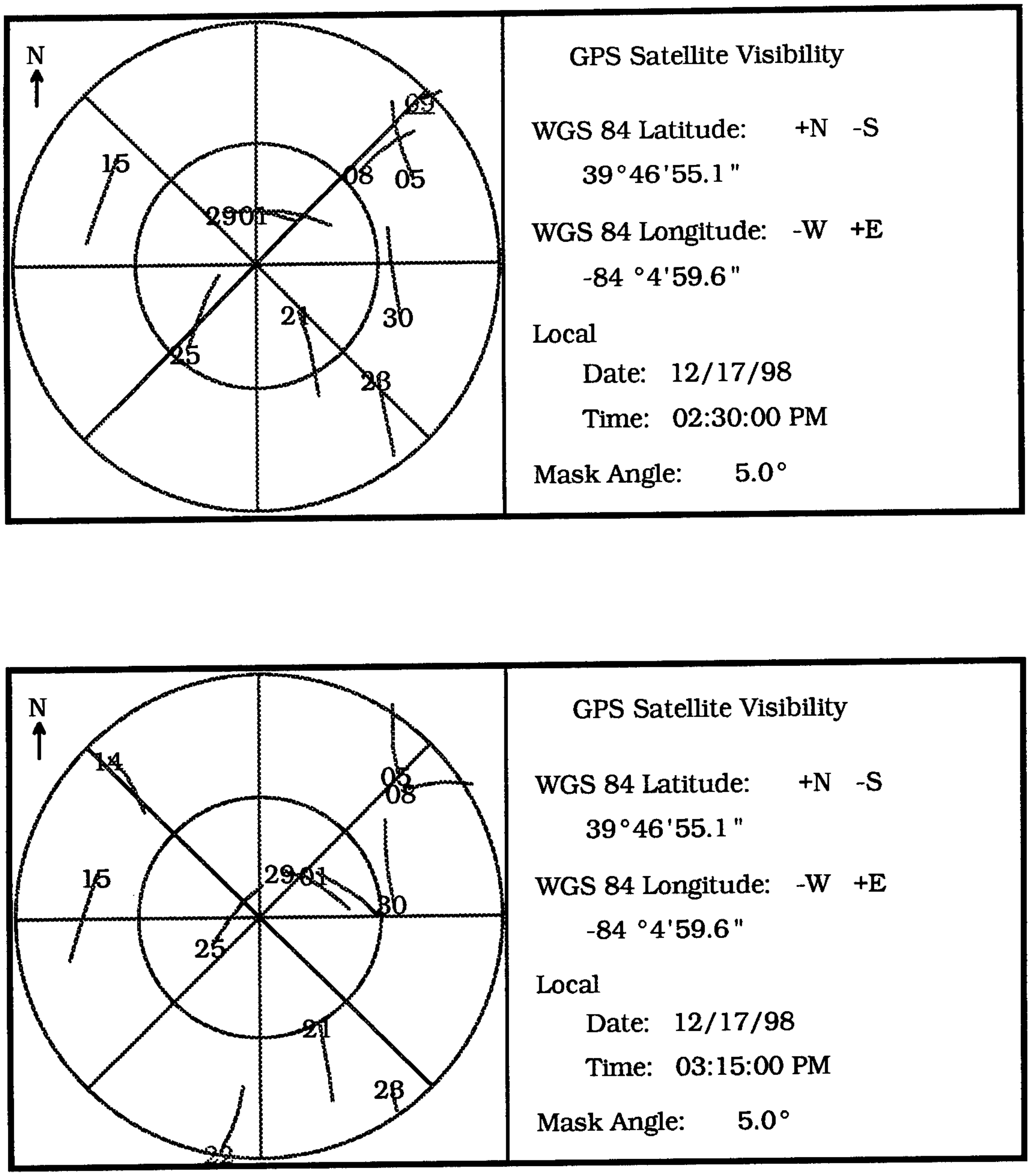

Figure T.1 GPS Satellites In View 17 Dec 98

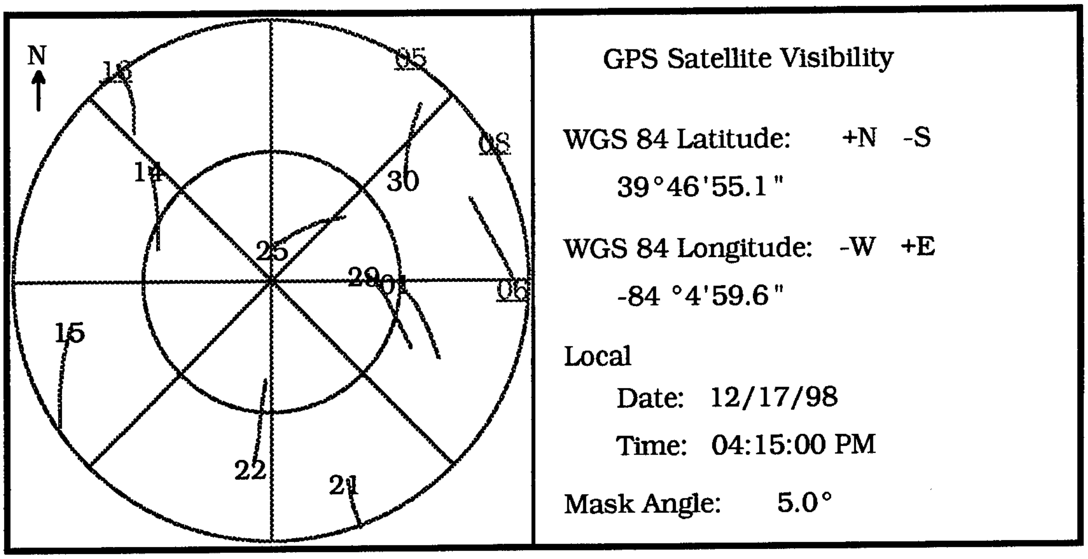

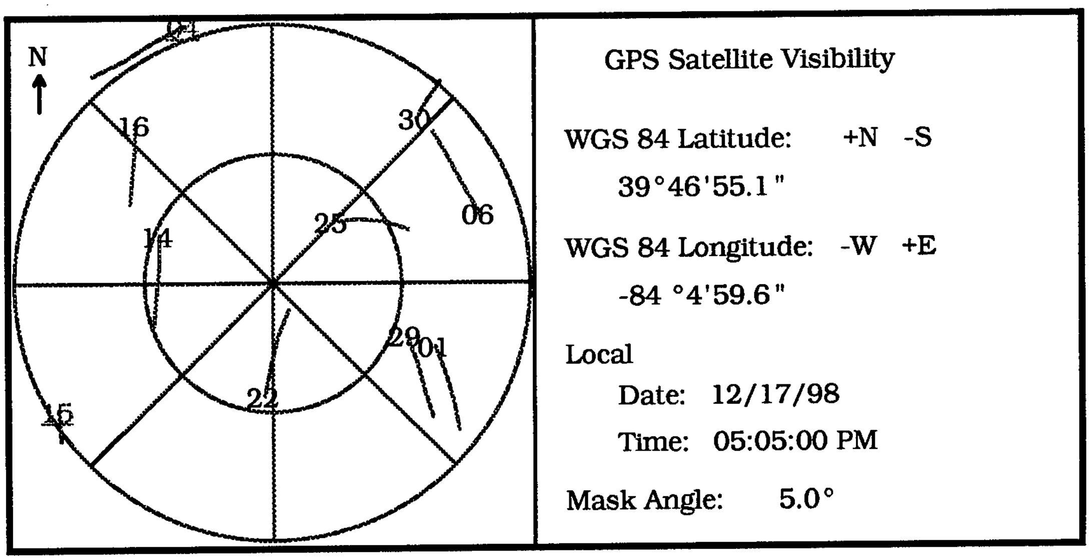

Figure T.2 GPS Satellites In View 17 Dec 98

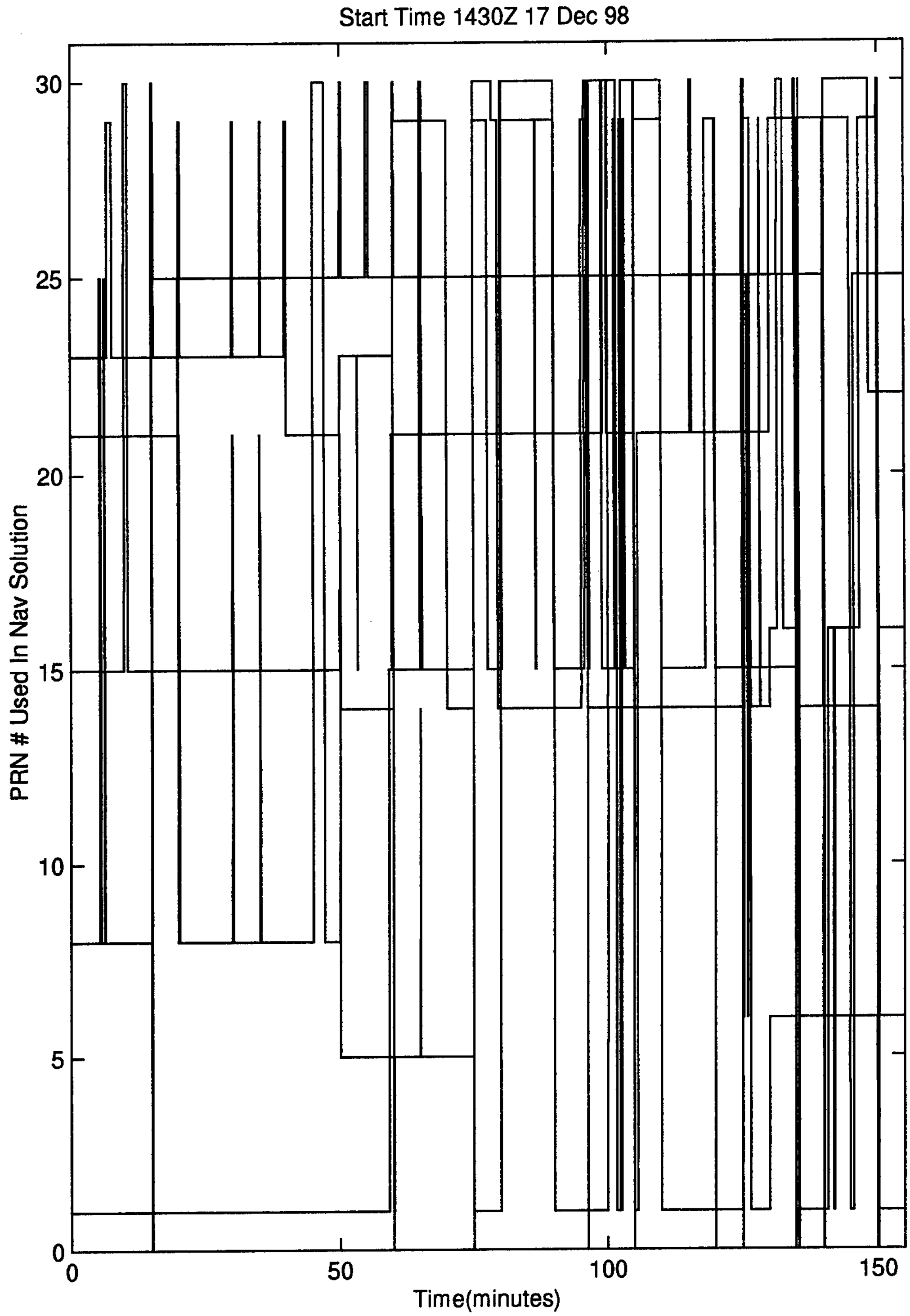

Figure T.3. PRN # Used In Nav Solution vs Time

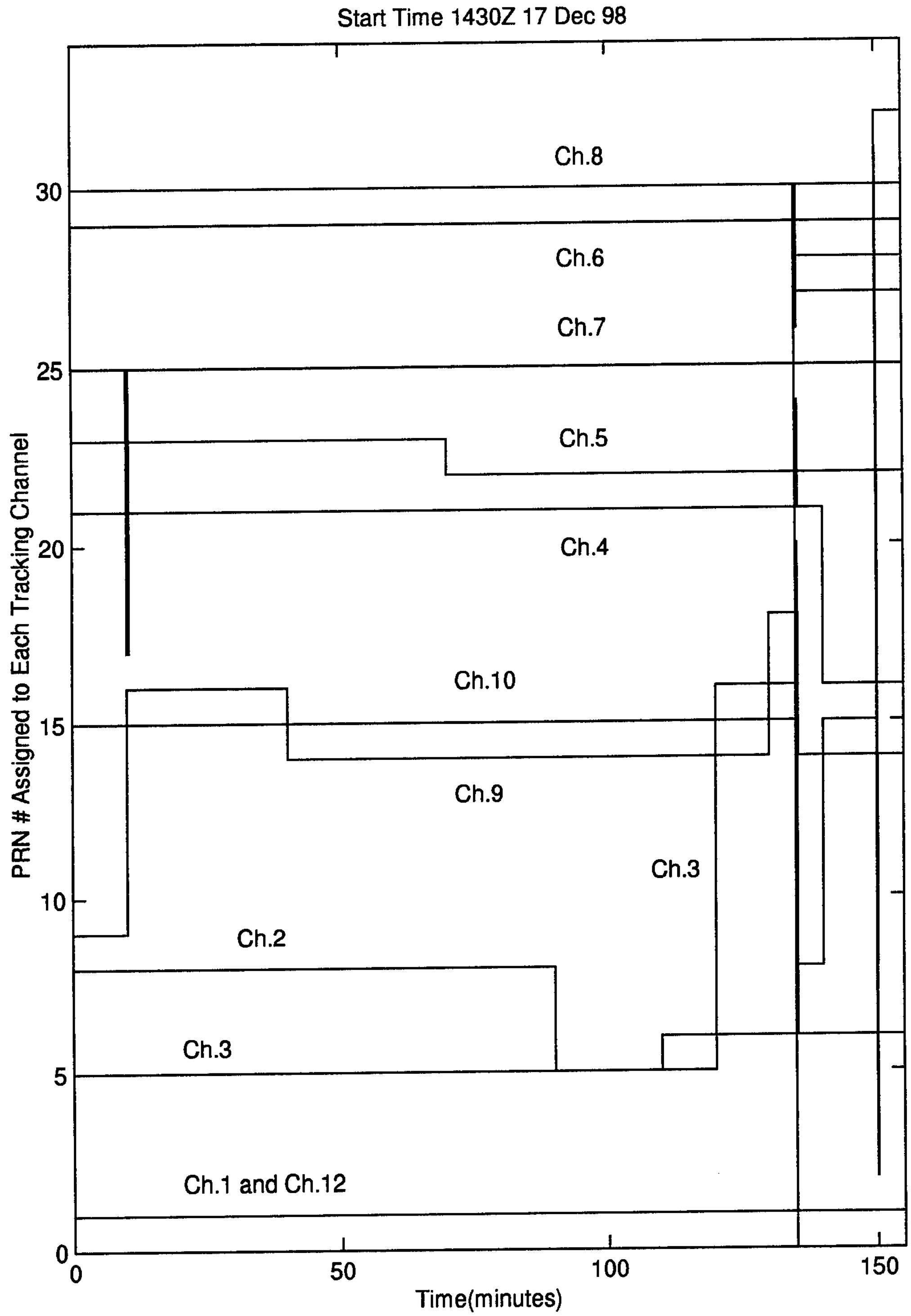

Figure T.4. PRN # Assigned to Each Tracking Channel vs Time

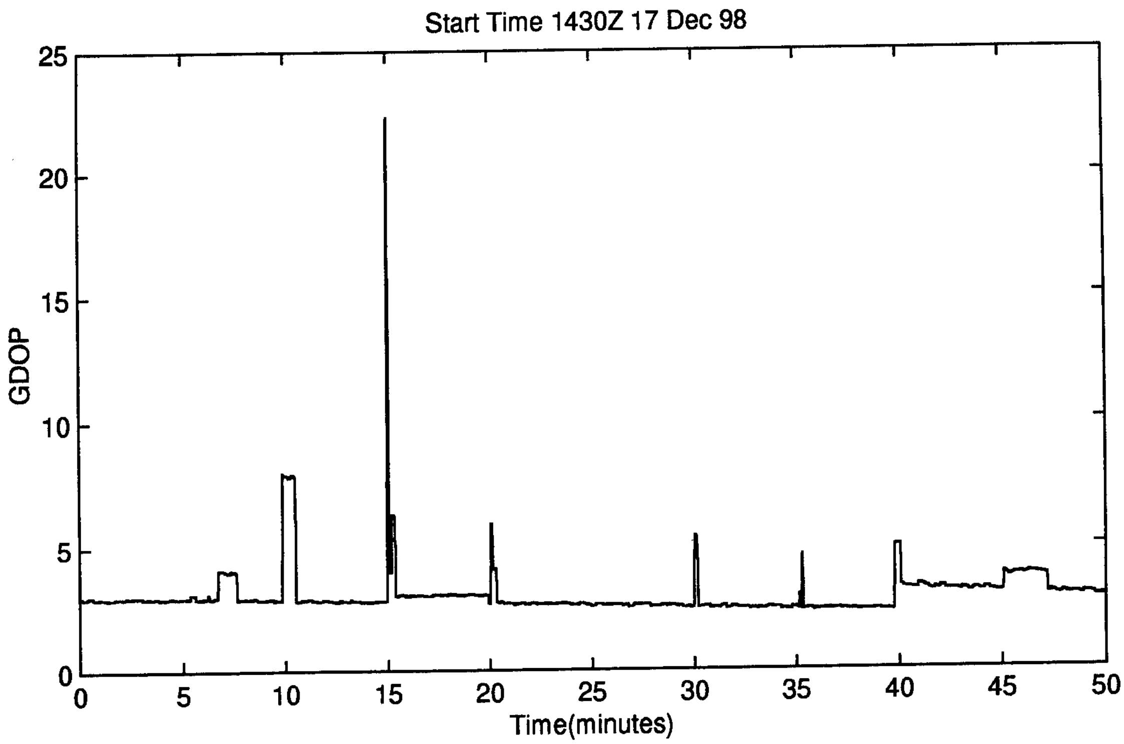

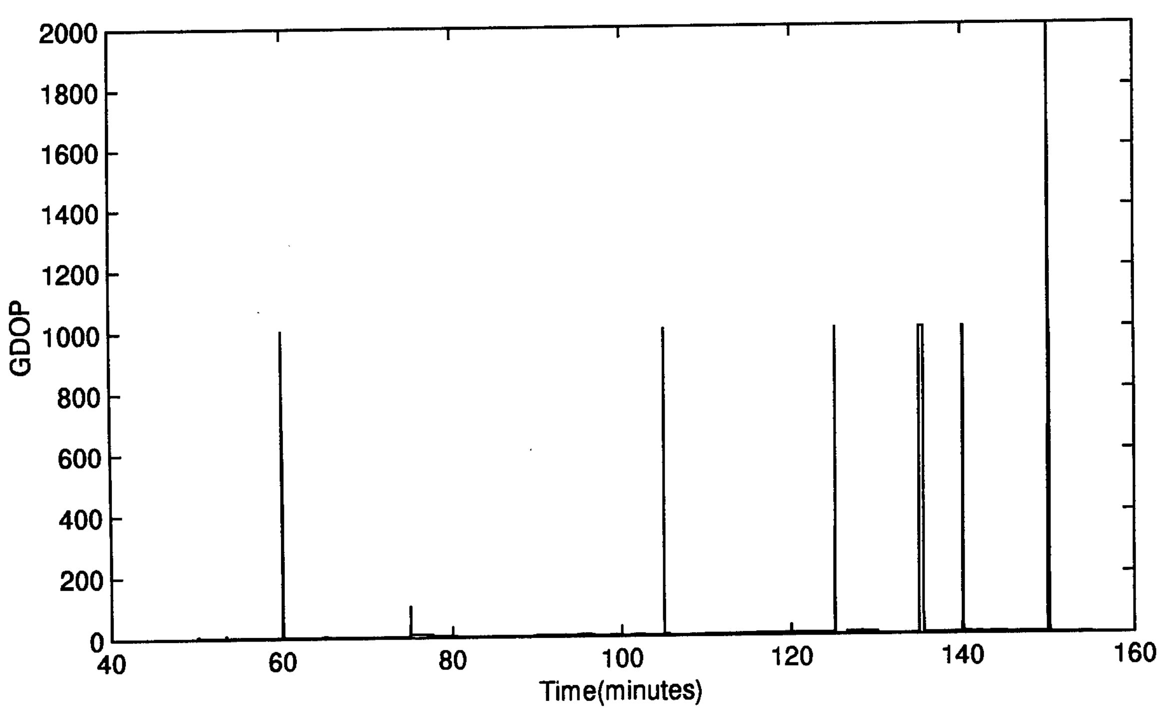

Figure T.5. GDOP vs Time

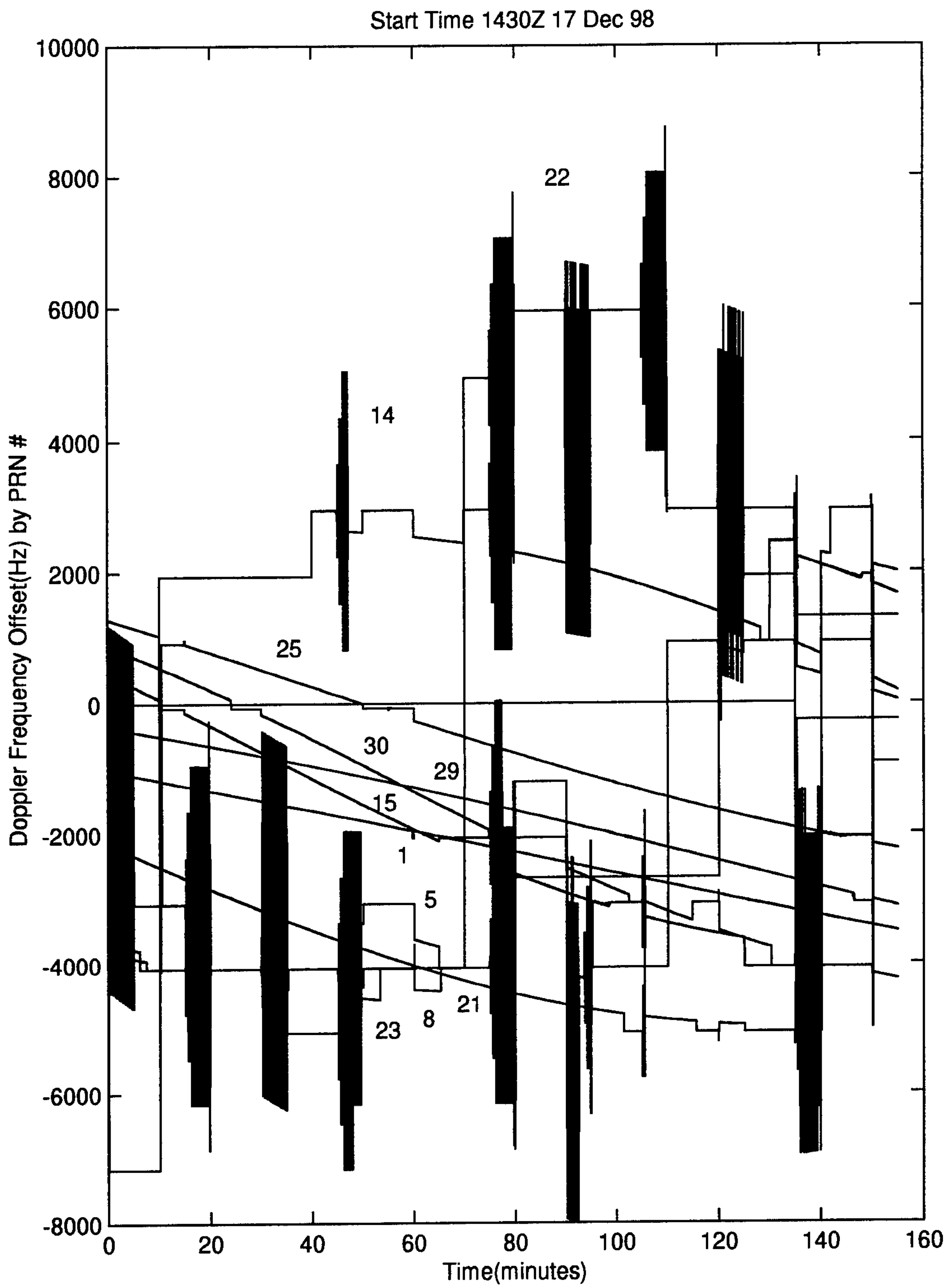

Figure T.6. Doppler Frequency vs Time

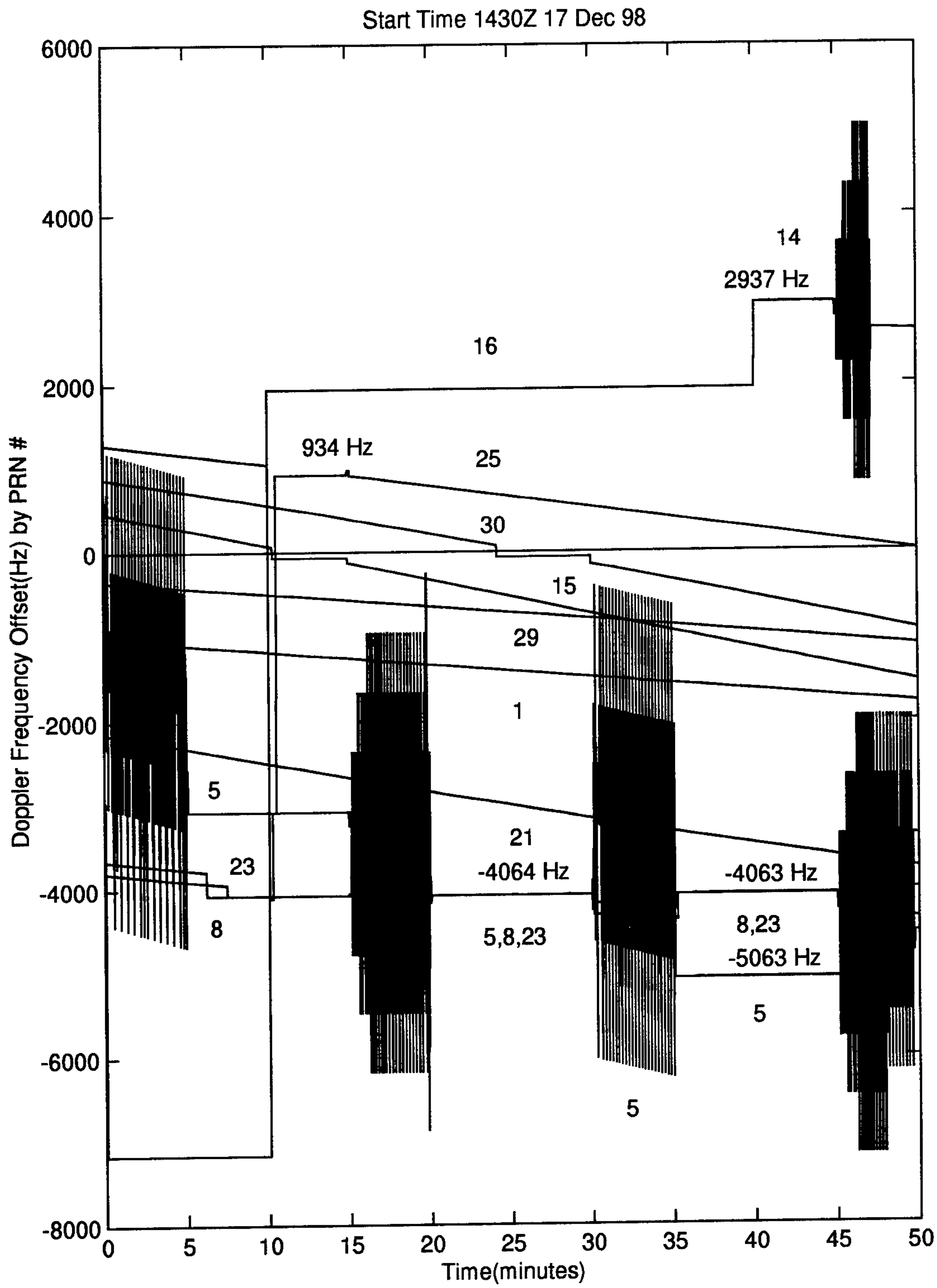

Figure T.7. Doppler Frequency vs Time

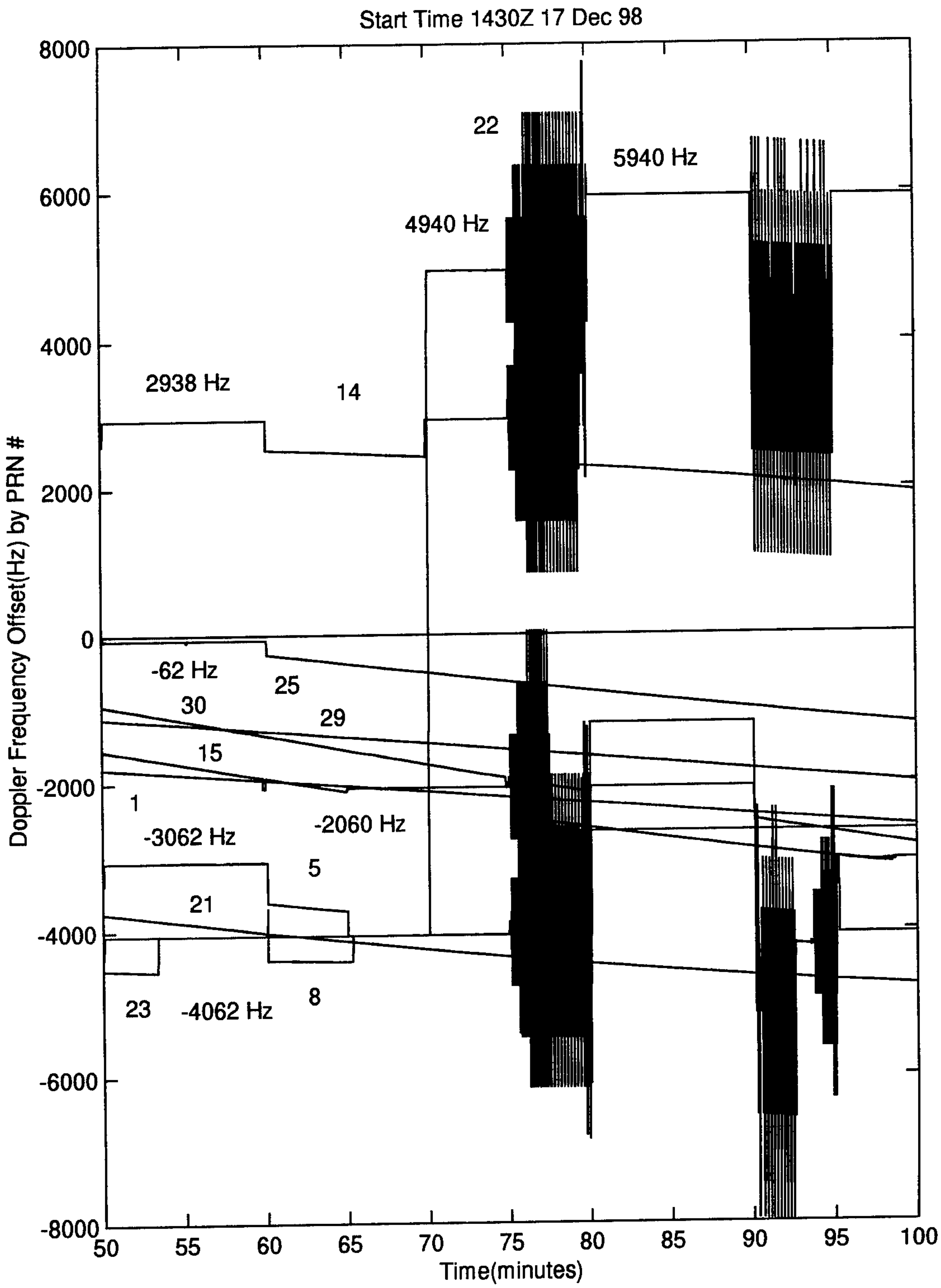

Figure T.8. Doppler Frequency vs Time

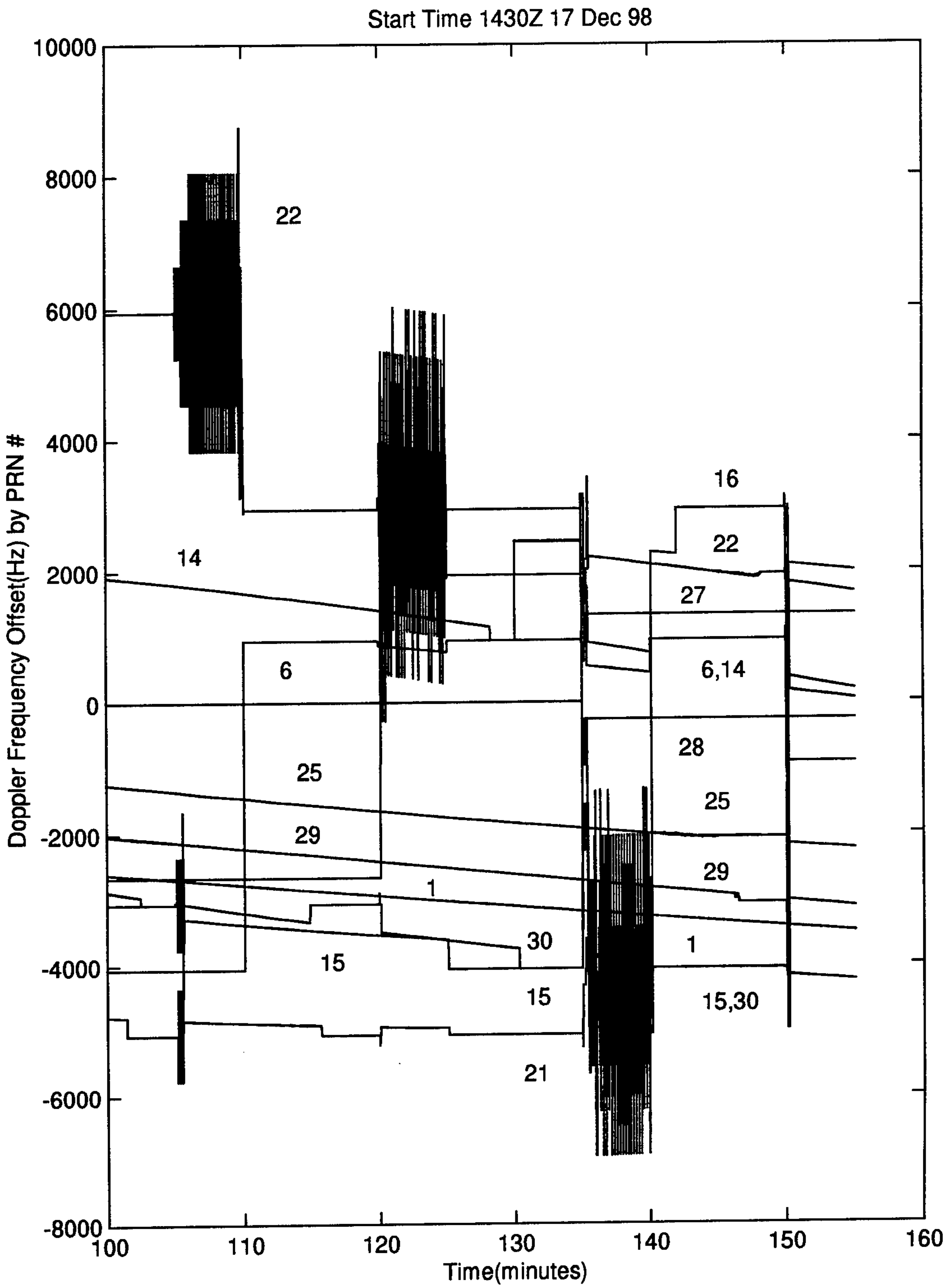

Figure T.9. Doppler Frequency vs Time

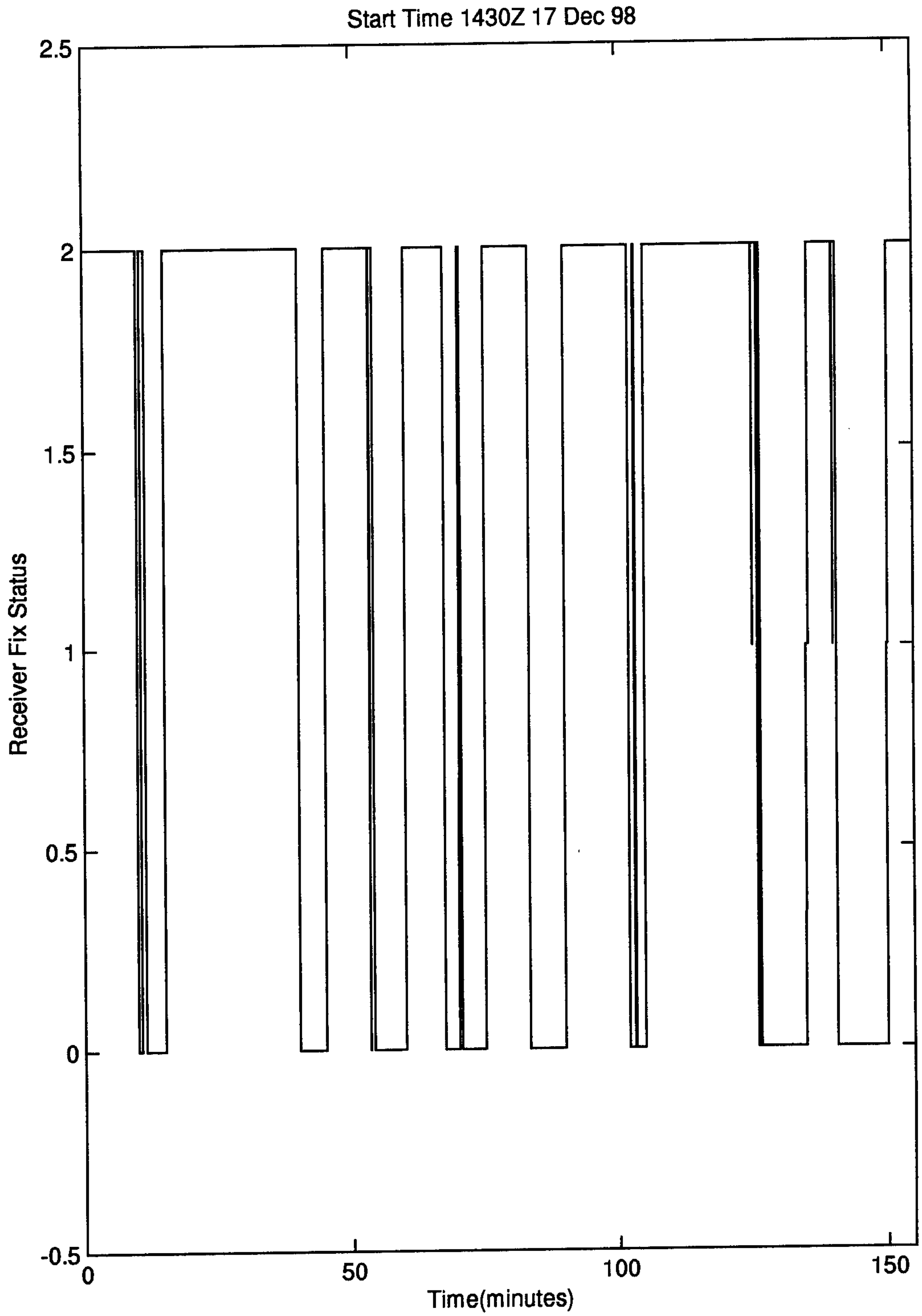

Figure T.10. Receiver Fix Status vs Time

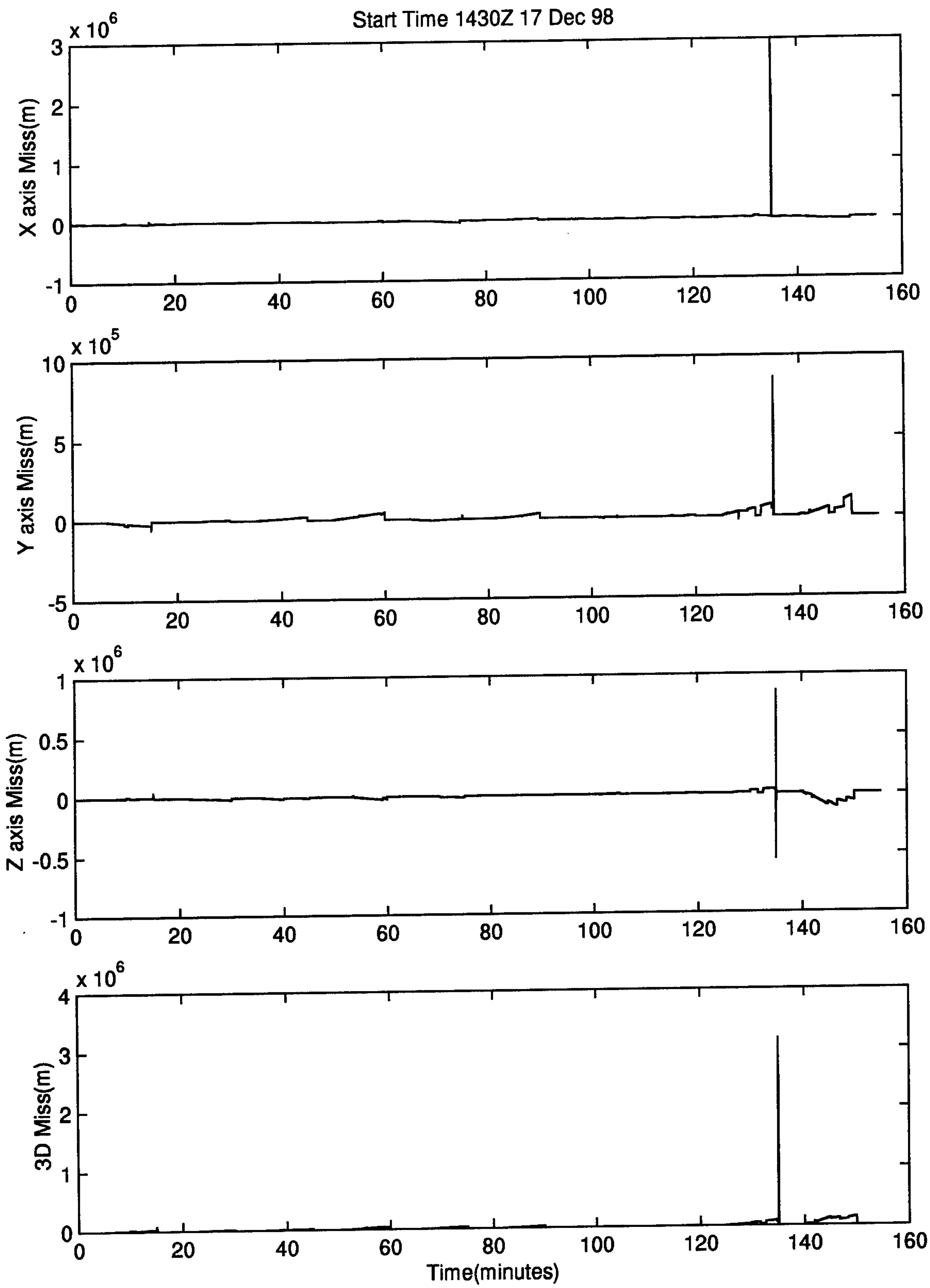

Figure T.11. X,Y,Z and 3D Error(m) vs Time

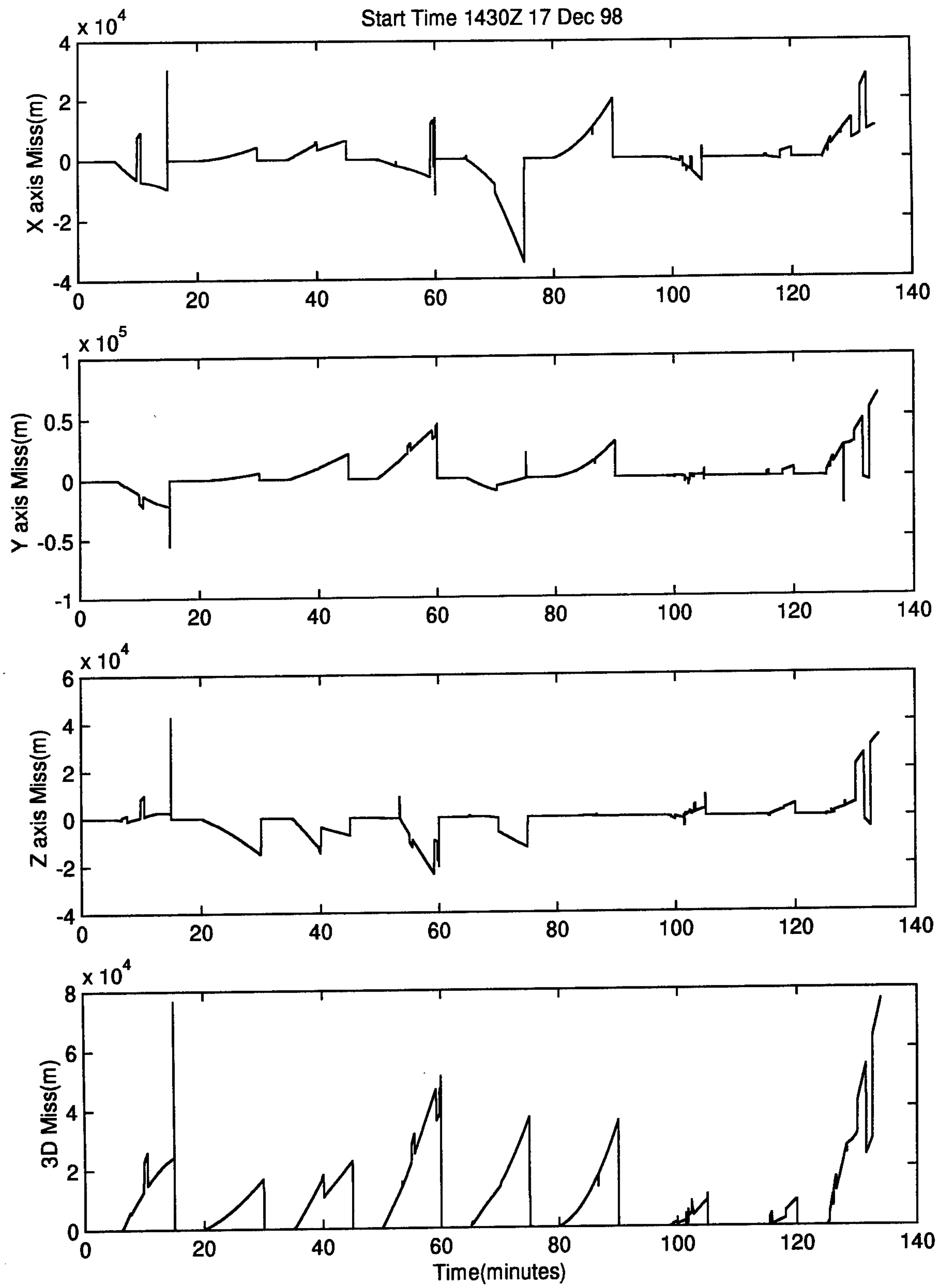

Figure T.12. X,Y,Z and 3D Error(m) vs Time

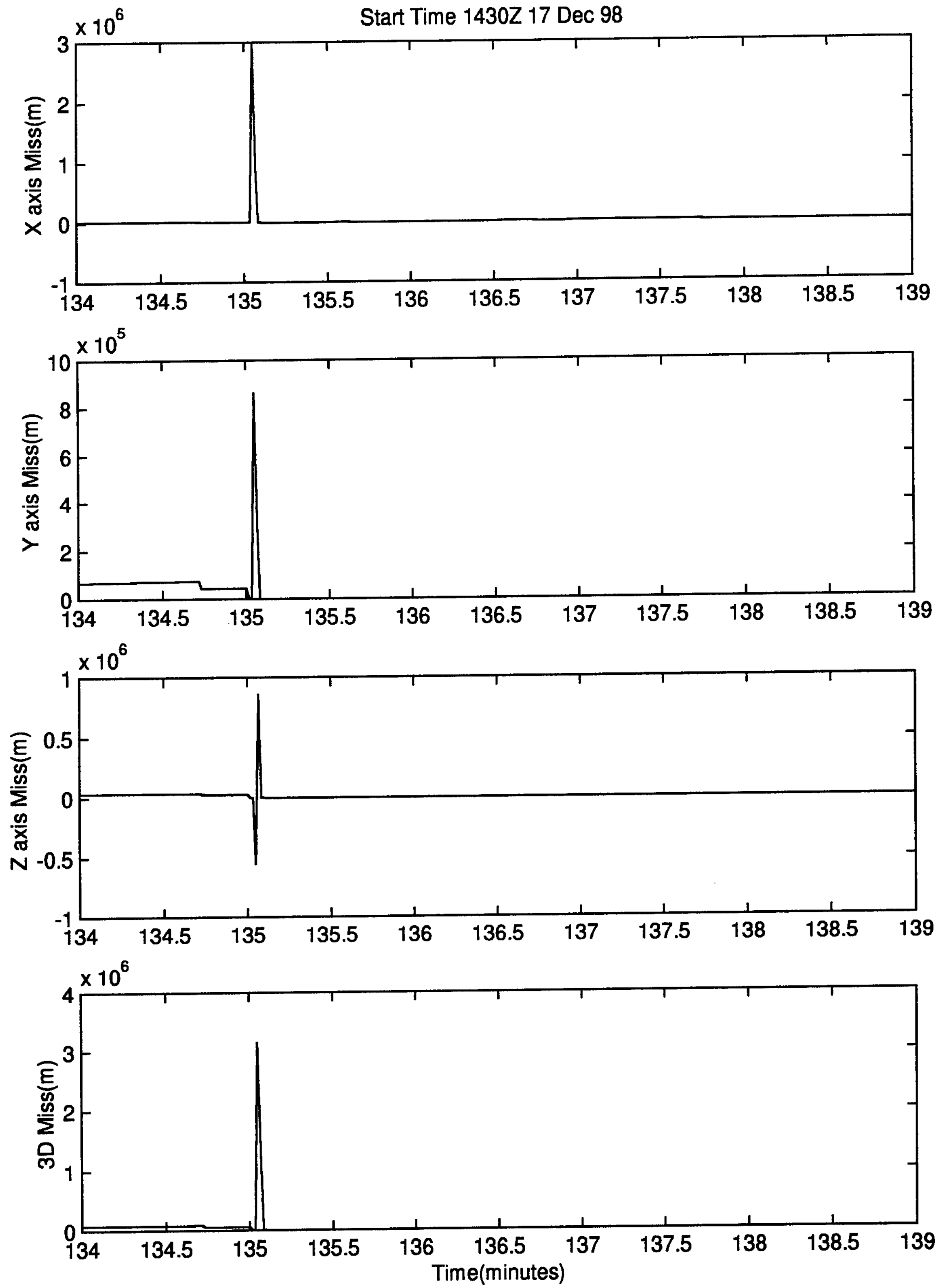

Figure T.12. X,Y,Z and 3D Error(m) vs Time

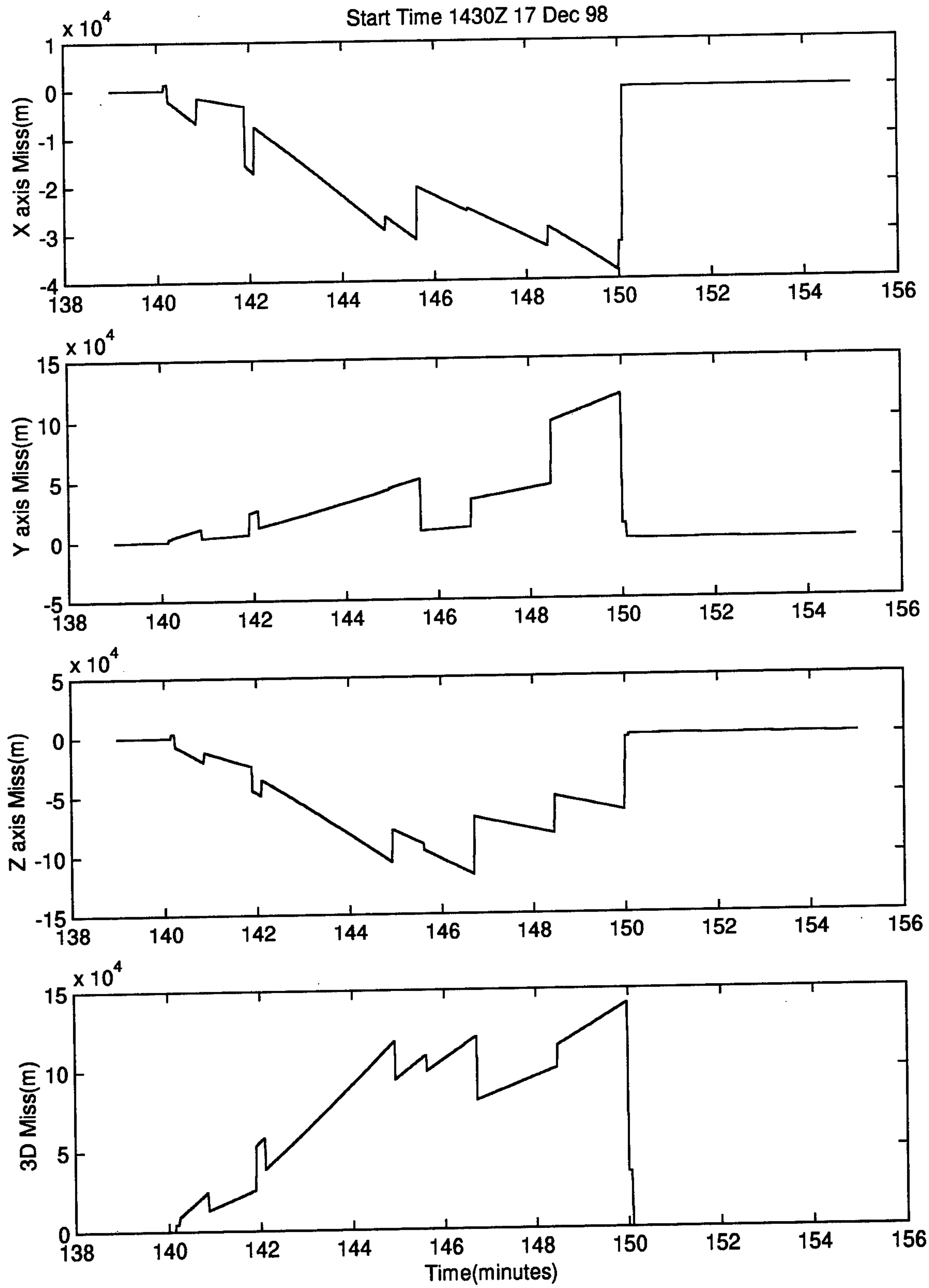

Figure T.14. X,Y,Z and 3D Error(m) vs Time

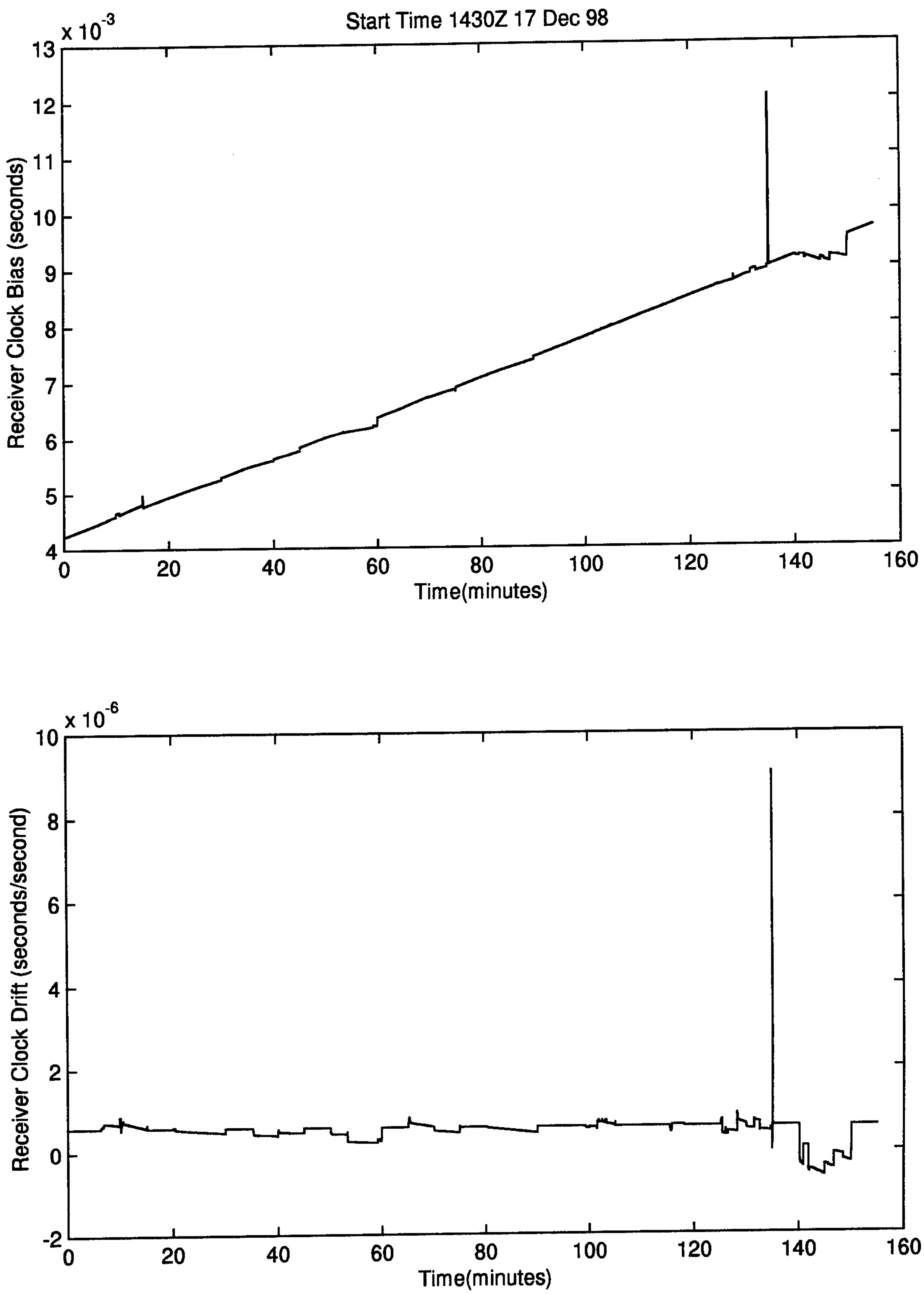

Figure T.15. Receiver Clock Bias and Drift vs Time

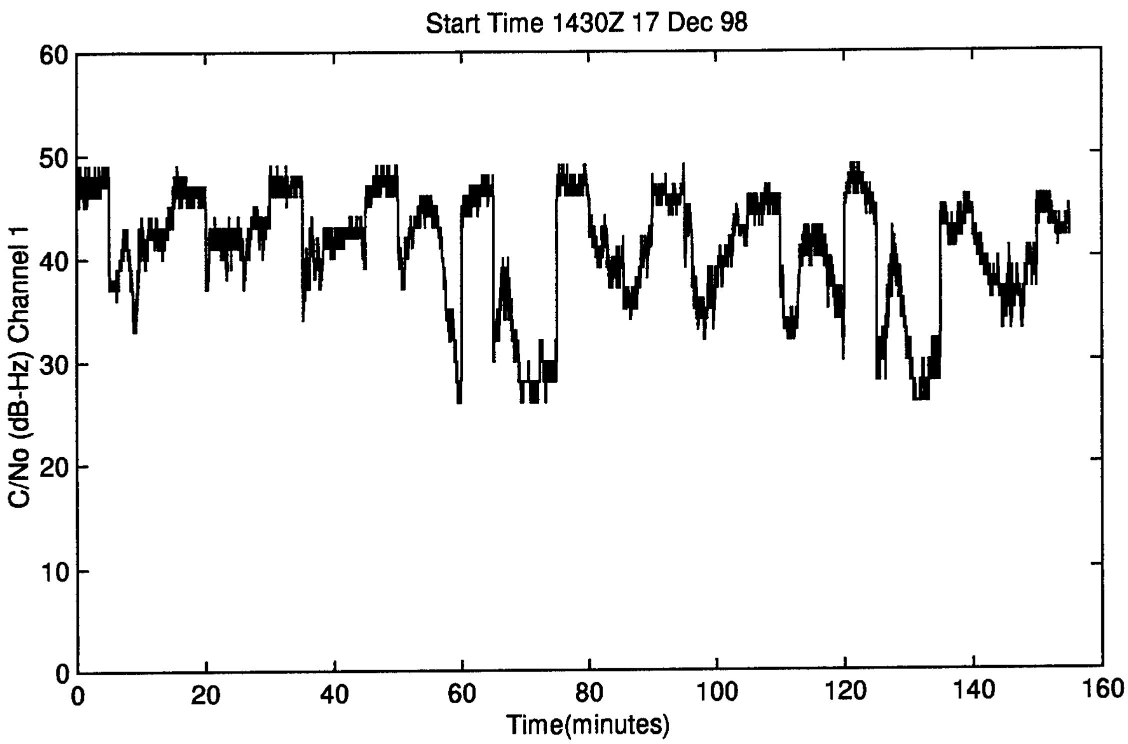

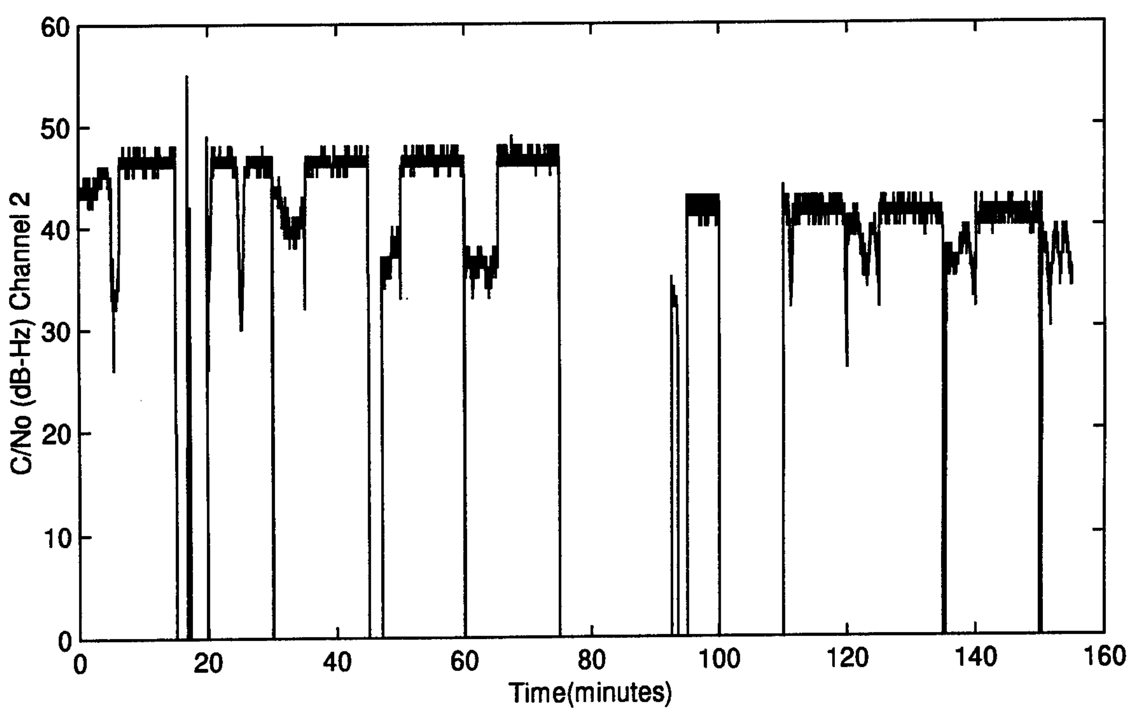

Figure T.16. C/No vs Time

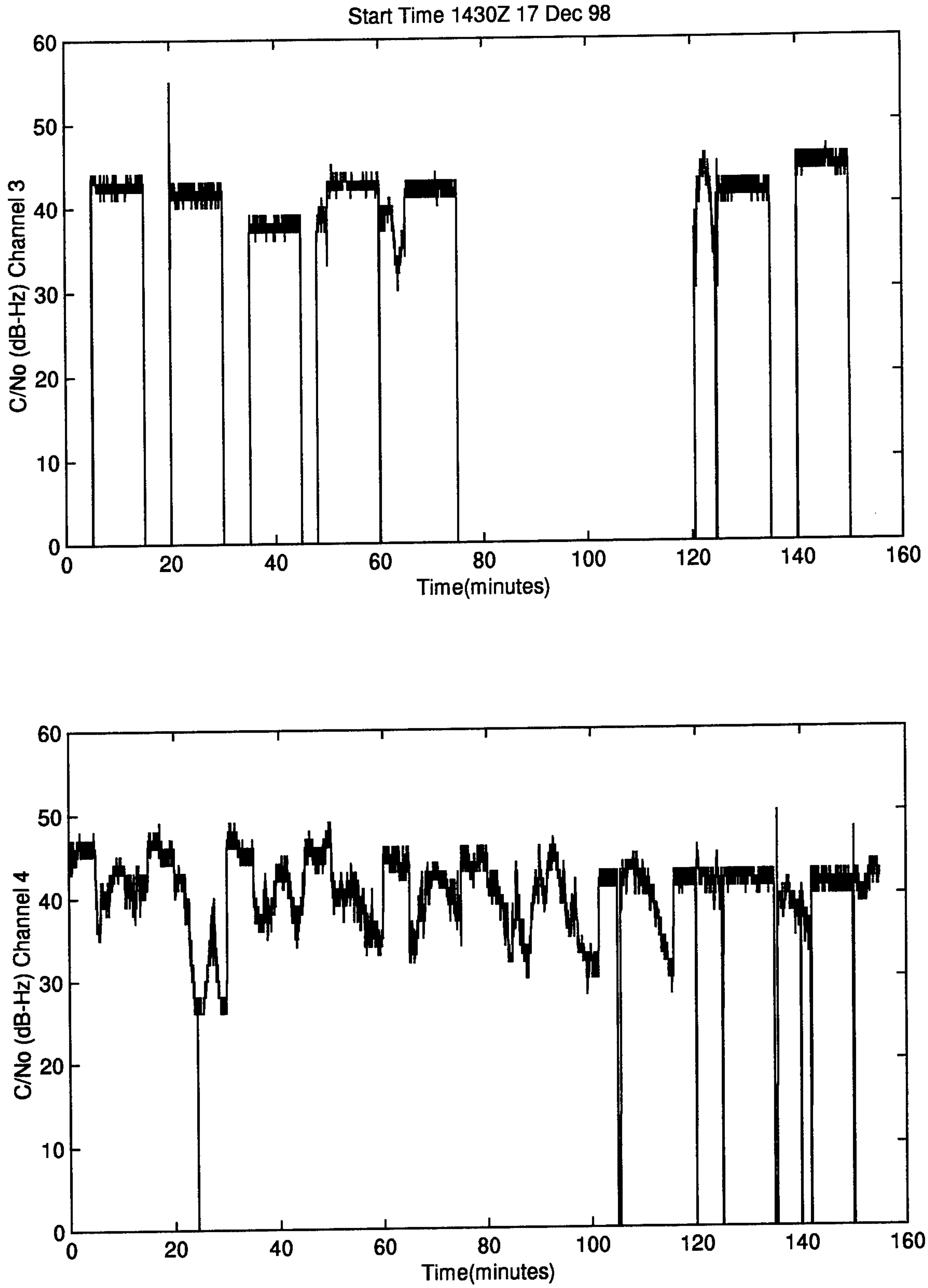

Figure T.17. C/No vs Time

Start Time 1430Z 17 Dec 98

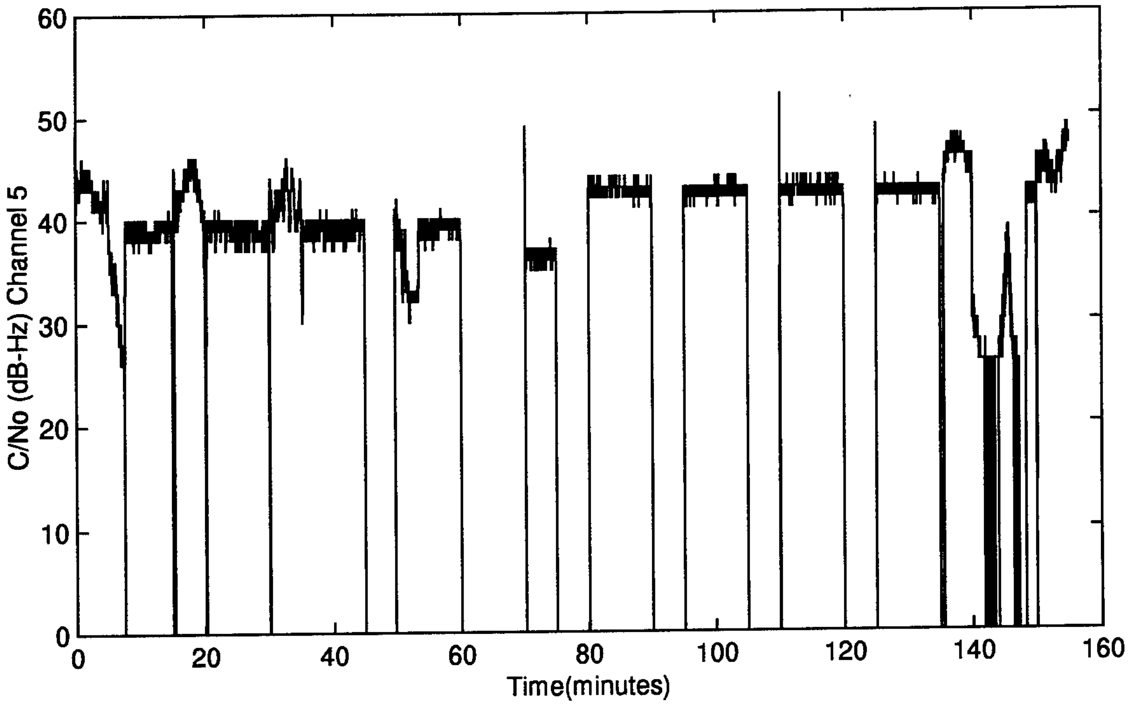

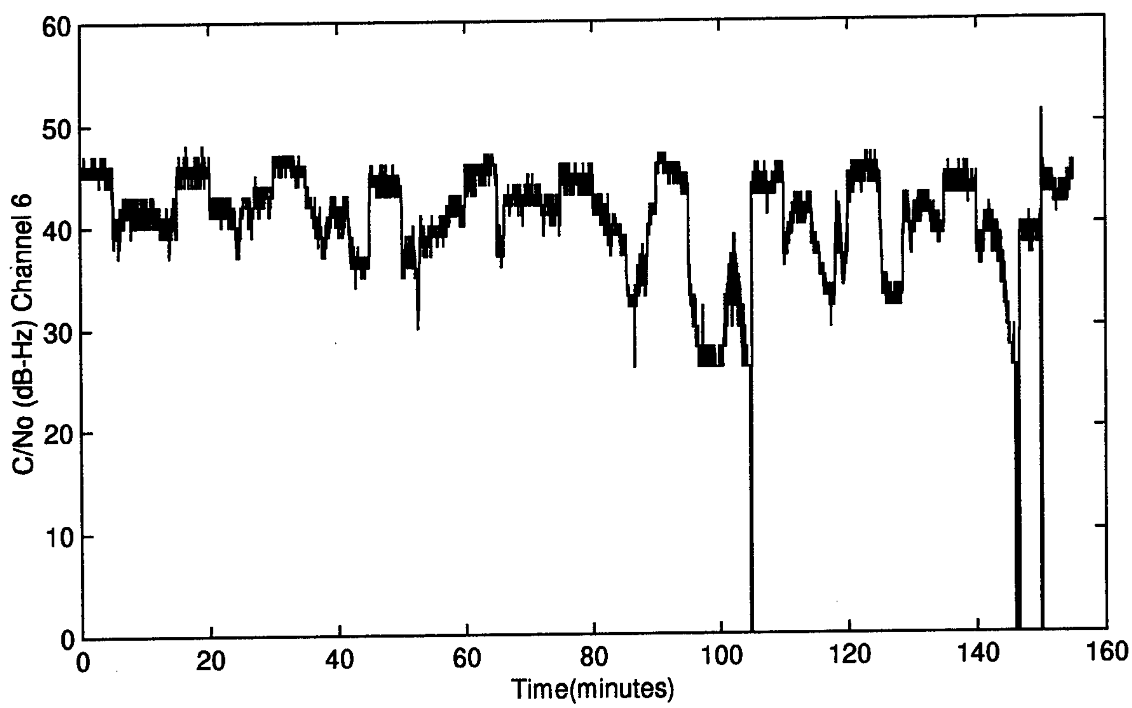

Figure T.18. C/No vs Time

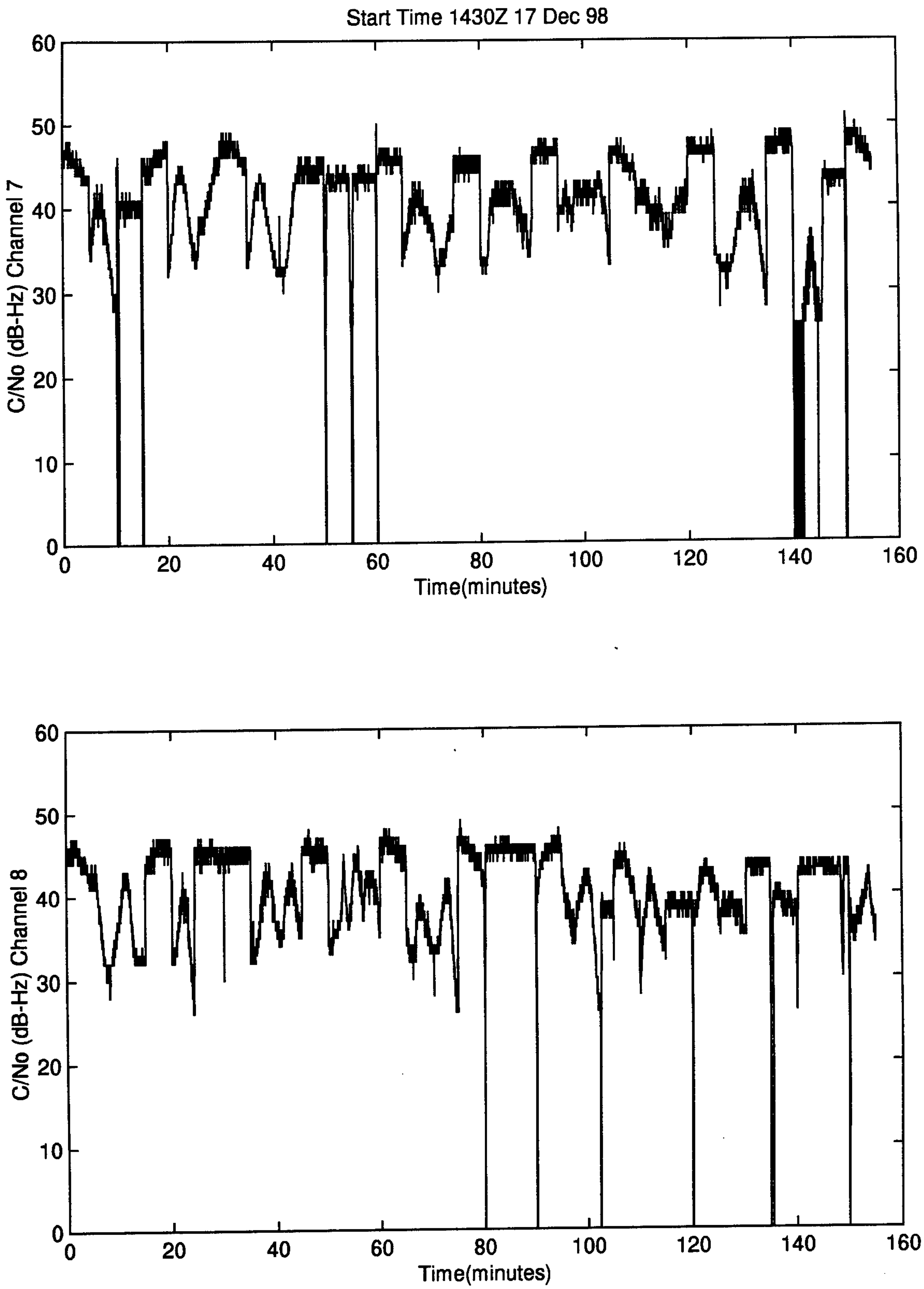

Figure T.19. C/No vs Time

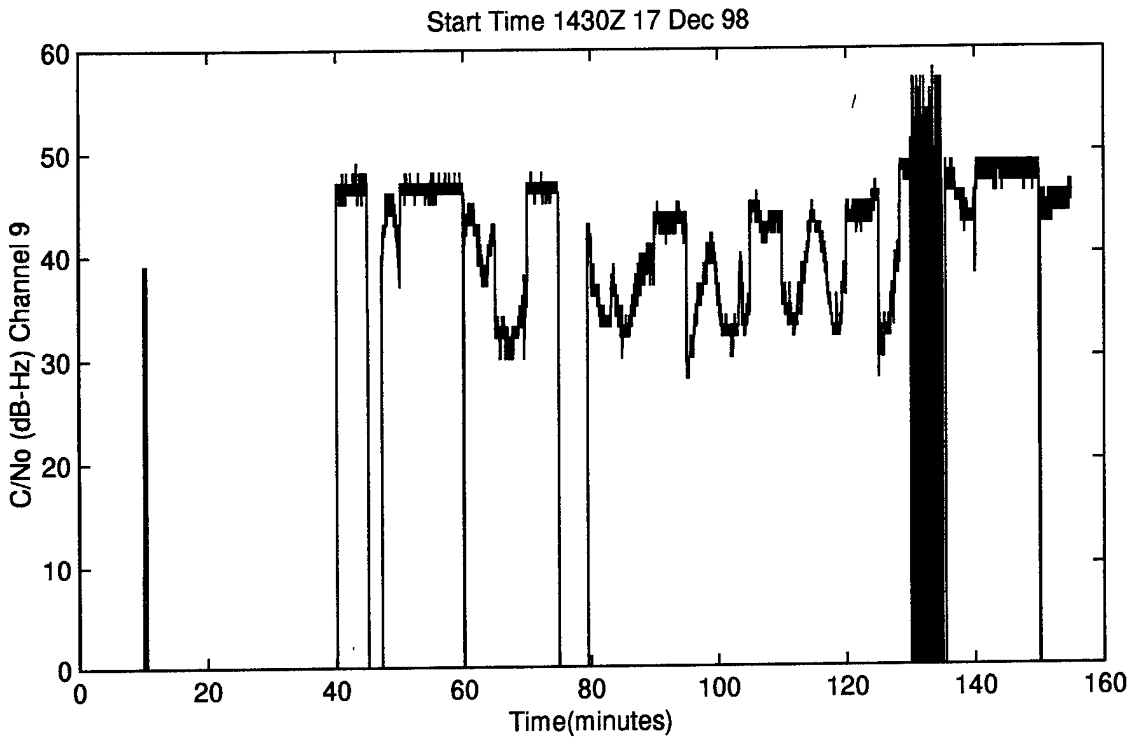

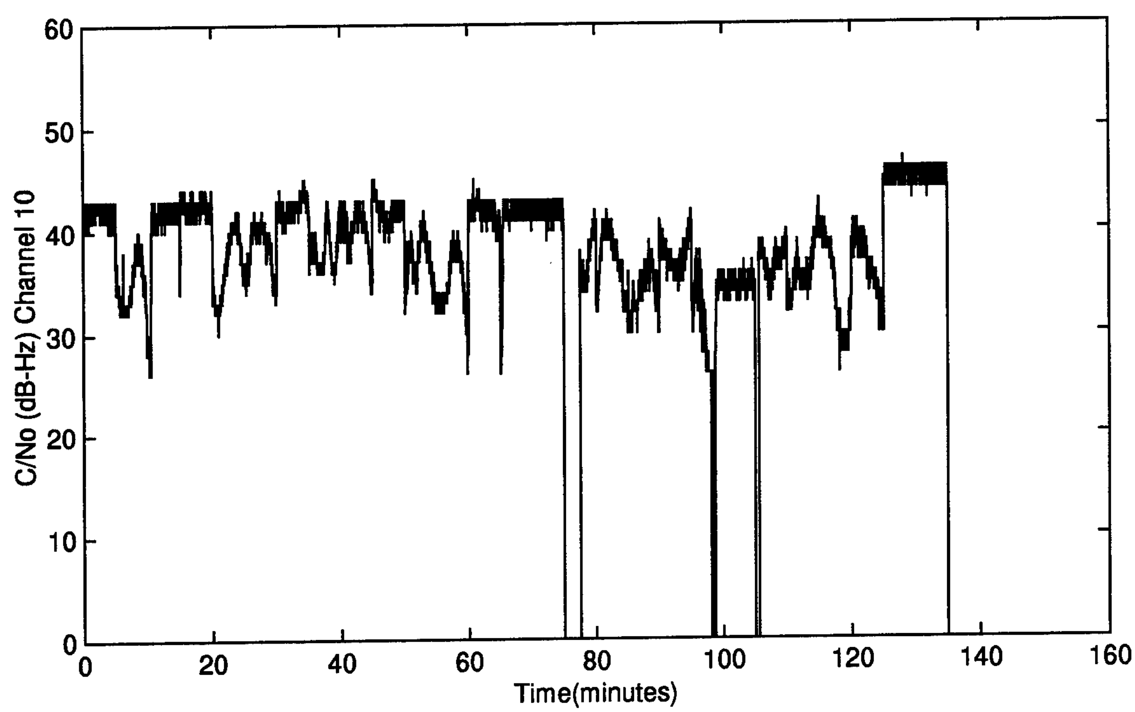

Figure T.20. C/No vs Time

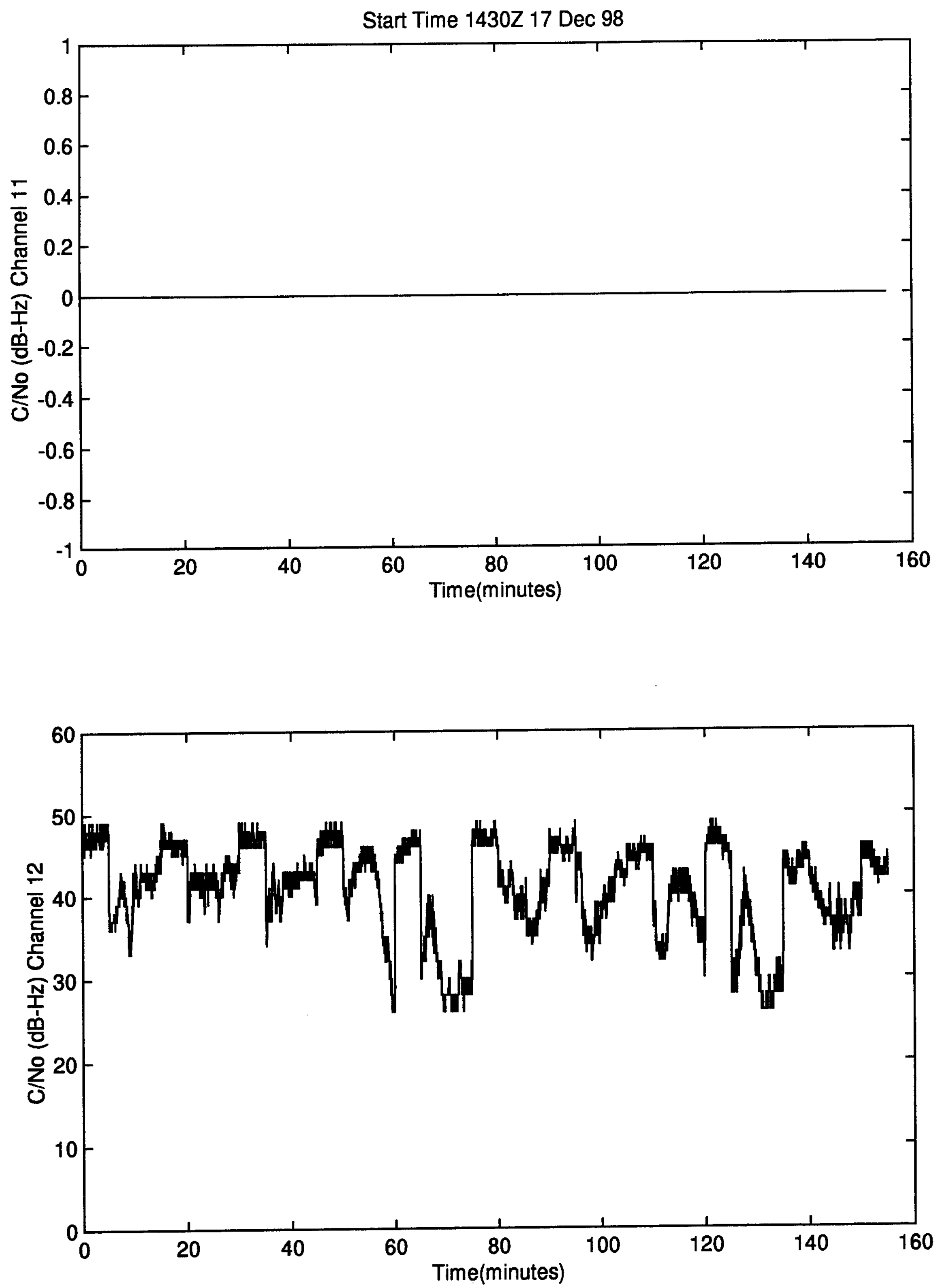

Figure T.21. C/No vs Time

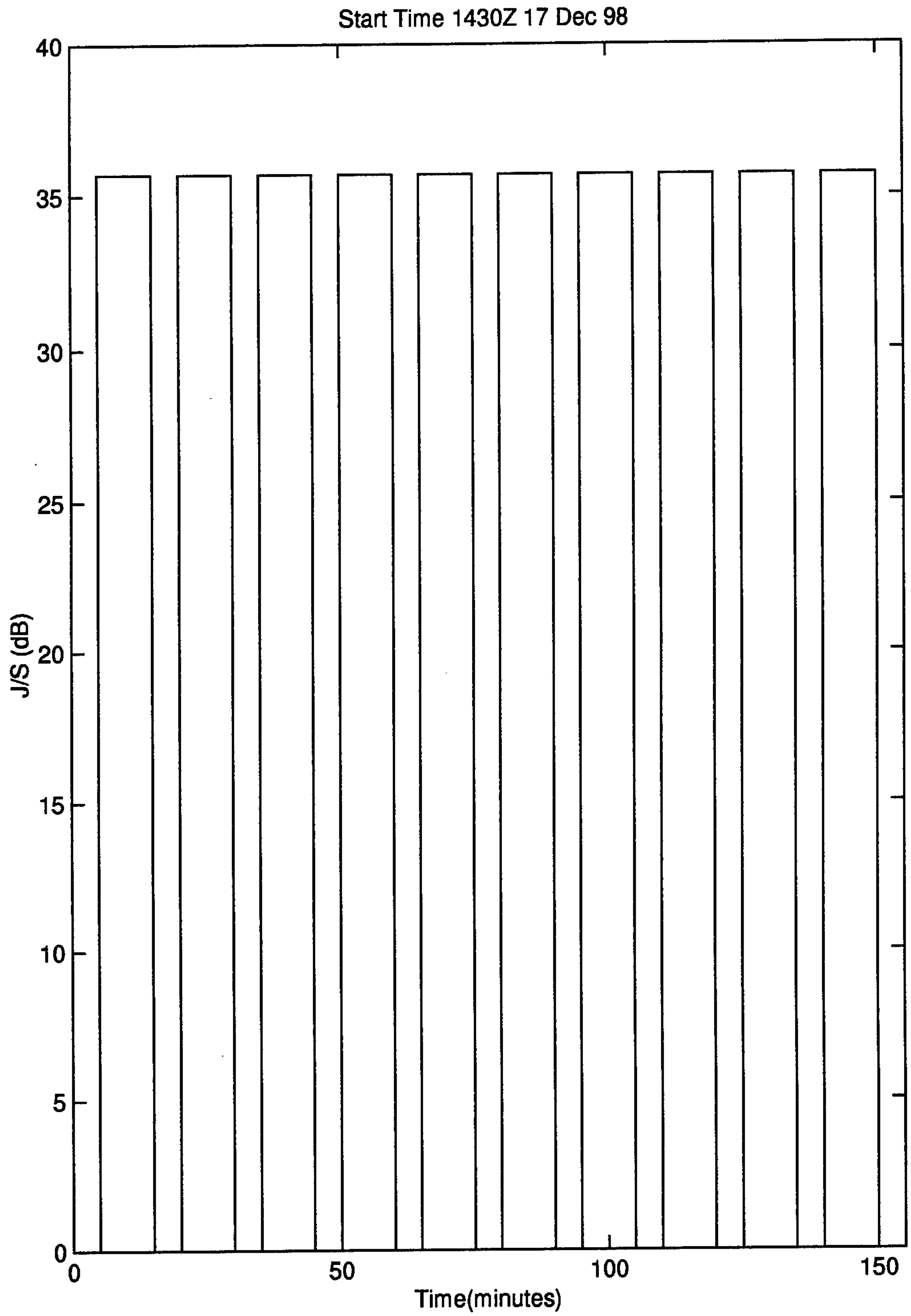

Figure T.22. Jamming Level J/S vs Time